

AD No. 32 513

ASTIA FILE COPY

FOURTH ANNUAL REPORT

ARC-CAS (MILITARY) - BASE ALLAYS

Contract No. 78701, Order Number 101
Project NR 039-002

to

Office of Naval Research
Naval Department

Prepared by
M. Semchyshen
and
R. Q. Barr

Chimex McHugh and Company, Mich.

195

THIS REPORT HAS BEEN DELIMITED
AND CLEARED FOR PUBLIC RELEASE
UNDER DOD DIRECTIVE 5200.20 AND
NO RESTRICTIONS ARE IMPOSED UPON
ITS USE AND DISCLOSURE.

DISTRIBUTION STATEMENT A

APPROVED FOR PUBLIC RELEASE;
DISTRIBUTION UNLIMITED.

DISTRIBUTION LIST

AIR FORCE

U. S. Air Forces
Research and Development Division
The Pentagon
Washington 25, D. C.

Chief of Metallurgical Group
Flight Research Laboratory
MCRR (MCPRXS5)
Wright-Patterson Air Force Base
Dayton, Ohio
Attn: Mr. J. B. Johnson

Metallurgical Branch
Materials Laboratory
Research Division
Wright Air Development Center
Dayton, Ohio
Attn: Mr. I. Perlmutter

Wright Air Development Command
Wright-Patterson Air Force Base
Dayton, Ohio
Attn: Materials Laboratory, MCREXM

Wright Air Development Command
Wright-Patterson Air Force Base
Dayton, Ohio
Attn: Power Plant Laboratory

ARMY

Chief of Staff, Department of the Army
The Pentagon
Washington 25, D. C.
Attn: Director of Research and
Development

Office of the Chief of Engineers
Department of the Army
The Pentagon
Washington 25, D. C.
Attn: Research and Development
Branch

Commanding Officer
Frankford Arsenal
Philadelphia, Pennsylvania
Attn: Laboratory Division

Office of Chief of Ordnance (ORDTB)
Department of the Army
The Pentagon
Washington 25, D. C.
Attn: E. L. Hollady (2)
Attn: ORDTB - Research
Coordination Branch (3)

Ordnance Department
Springfield Armory
Springfield, Massachusetts
Attn: Mr. H. P. Langston

Commanding Officer
Watertown Arsenal
Watertown, Massachusetts
Attn: Laboratory Division

ATOMIC ENERGY COMMISSION

Argonne National Laboratory
P. O. Box 5207
Chicago 80, Illinois
Attn: Dr. Hoylande D. Young

Brookhaven National Laboratory
Technical Information Division
Upton, Long Island, New York
Attn: Research Libr.

University of California
Radiation Laboratory
Information Division
Room 128, Building 50
Berkeley, California
Attn: Dr. R. K. Wehner

DISTRIBUTION LIST (cont'd)

ATOMIC ENERGY COMMISSION (cont'd)

General Electric Company
Technical Services Division
Technical Information Group
P. O. Box 100
Richland, Washington
Attn: Miss M. J. Friedank

Iowa State College
P. O. Box 14A, Station A
Ames, Iowa
Attn: Dr. F. H. Spedding

Illinois Atomic Power Laboratory
P. O. Box 1072
Schenectady, New York
Attn: Document Librarian

Los Alamos Scientific Laboratory
P. O. Box 1663
Los Alamos, New Mexico
Attn: Document Custodian

Mound Laboratory
U. S. Atomic Energy Commission
P. O. Box 32
Miamisburg, Ohio
Attn: Dr. M. M. Haring

U. S. Atomic Energy Commission
New York Operations Office
P. O. Box 30, Ansonia Station
New York 23, New York
Attn: Division of Technical Information
and Declassification Service

Carbide and Carbon Chemicals Division
Plant Records Department, Central
Files (K-25)
P. O. Box P
Oak Ridge, Tennessee

Carbide and Carbon Chemicals Division
Central Reports and Information Office
(Y-12)
P. O. Box P
Oak Ridge, Tennessee

Oak Ridge National Laboratory
P. O. Box P
Oak Ridge, Tennessee
Attn: Central Files

General Electric Company
P. O. Box 125
A.N.P. Project
Oak Ridge, Tennessee
Attn: Dr. Arthur E. Focke
Lead, Materials Division
Nuclear Aircraft Project

Oak Ridge National Laboratory
Oak Ridge, Tennessee
Attn: Metallurgical Division
W. D. Manly

U. S. Atomic Energy Commission
Library Branch, Technical Information
Service, ORE
P. O. Box E
Oak Ridge, Tennessee

Sandia Corporation
Sandia Base
Classified Document Division
Albuquerque, New Mexico
Attn: Mr. Dale H. Evans

U. S. Atomic Energy Commission
1901 Constitution Avenue, N. W.
Washington 25, D. C.
Attn: B. M. Fry

(2)

U. S. Atomic Energy Commission
Production Division
Defense Requirements Branch
Washington 25, D. C.
Attn: Mr. J. J. Perella

U. S. Atomic Energy Commission
Division of Research
Metallurgical Branch
Washington 25, D. C.

Westinghouse Electric Corporation
Atomic Power Division
P. O. Box 1468
Pittsburgh 30, Pennsylvania
Attn: Librarian

DISTRIBUTION LIST (cont'd)

NAVY

Post Graduate School
U. S. Naval Academy
Monterey, California
Attn: Department of Metallurgy

U. S. Naval Engineering Experiment
Station
Annapolis, Maryland
Attn: Metals Laboratory

Bureau of Aeronautics
Navy Department
Washington 25, D. C.
Attn: N. E. Promisel, AE-41
(Room 1W68)
Attn: Technical Library, TD-41

Superintendent
Naval Gun Factory
Washington 20, D. C.
Attn: Metallurgical Lab., De713

Commanding Officer
Naval Air Materiel Center
Naval Base Station
Philadelphia, Pennsylvania
Attn: Aeronautical Materials Lab.

Chief, Bureau of Ordnance
Navy Department
Washington 25, D. C.
Attn: Re5

Bureau of Ordnance
Navy Department
Washington 25, D. C.
Attn: Re9a (John S. Nachtman)

Bureau of Ordnance
Navy Department
Washington 25, D. C.
Attn: Re
Attn: Technical Library Ad3

Commanding Officer
U. S. Naval Ordnance Laboratory
White Oaks, Maryland

Commanding Officer
U. S. Naval Ordnance Test Station
Inyokern, California

Officer in Charge
Office of Naval Research
Navy No. 100
Fleet Post Office
New York, New York (5)

Director
Office of Naval Research
Branch Office
The John Crerar Library Building
10th Floor
86 E. Randolph Street
Chicago 1, Illinois (2)

Director
Office of Naval Research
Branch Office
346 Broadway
New York 13, New York

Director
Office of Naval Research
Branch Office
1030 E. Green Street
Pasadena, California

Chief of Naval Research
Department of the Navy
Washington 25, D. C.
Attn: Code 423 (2)

Office of Technical Services
Department of Commerce
Washington 25, D. C.

Director, Naval Research Laboratory
Washington 25, D. C.
Attn: Code 3500, Metallurgy Division
Attn: Code 2020, Technical Library (2)

Director, Naval Research Laboratory
Washington 25, D. C.
Attn: Tech. Information Officer (6)

DISTRIBUTION LIST (cont'd)

NAVY (cont'd)

Bureau of Ships
Navy Department
Washington 25, D. C.

Attn: Code 390
Attn: Code 343
Attn: Code 337L, Technical
Library

Director, Materials Laboratory
Building 291
New York Naval Shipyard
Brooklyn 1, New York
Attn: Code 907

Chief, Bureau of Yards and Docks
Navy Department
Washington 25, D. C.
Attn: Research and Standards Div.

Navy Liaison Officer for Guided Missiles
Jet Propulsion Laboratory
California Institute of Technology
Pasadena, California

CNR London, c/o Fleet P.O.
Navy 100, New York, N. Y.
For transmittal to
Armament Research Establishment
Metallurgical Branch
Ministry of Supply
Woolwich S.E. 18, ENGLAND

Commander NAMIC
Pt. Mugu, California
Attn: Engineering Department

Director
Office of Naval Research
Branch Office
1000 Geary Street
San Francisco 9, California

MISCELLANEOUS

Aerojet Engineering Corporation
Azusa, California
Via: Bureau of Aeronautics Representative
1534th Raymond Avenue
Pasadena, California

Allegheny Ballistics Laboratory
Cumberland, Maryland

(3) American Electro Metal Corporation
320 Yorkers Avenue
Yonkers 2, New York
Attn: R. P. Seelig

Battelle Memorial Institute
505 Kim Avenue
Columbus 4, Ohio
Attn: Mr. Harry T. McCann

Bendix Products Division
Bendix Aviation Corporation
401 Bendix Drive
South Bend 20, Indiana

Pittsburgh Steel Company
Pittsburgh, Pennsylvania
Attn: Dr. John Marsh

British Joint Service Mission
P. O. Box 165
Ben Franklin Station
Washington, D. C.
Attn: Navy Staff

National Bureau of Standards
Washington 25, D. C.
Attn: Physical Metallurgy Div.
Attn: Dr. A. Brenner, Chem. Div.

California Institute of Technology
Pasadena 4, California
Attn: Professor Pat Dunne
Department of Metallurgy

Metals Research Laboratory
Carnegie Institute of Technology
Pittsburgh, Pennsylvania
Attn: Professor R. E. Aehl

Metals Research Laboratory
Case Institute of Technology
Cleveland, Ohio
Attn: Professor W. M. Baldwin

DISTRIBUTION LIST (cont'd)

MISCELLANEOUS (cont'd)

Chimax Molybdenum Company of Michigan
14410 Woodrow Wilson Avenue
Detroit 3, Michigan
Attn: Mr. A. J. Herzig

Consolidated-Vultee Aircraft Corporation
San Diego 12, California
Via: Bureau of Aeronautics Representative
Consolidated-Vultee Aircraft Corp.
San Diego 12, California

Fansteel Metallurgical Company
North Chicago, Illinois
Attn: Dr. F. H. Driggs, President

General Electric Research Laboratory
at the Knolls
Schenectady, New York
Attn: Mr. Robert M. Parke

Horizons, Incorporated
1718 H Street, N. W.
Washington, D. C.
Attn: Dr. I. R. Kramer

Johns Hopkins University
Applied Physics Laboratory
Silver Springs, Maryland
Attn: Dr. W. H. Bray

Johns Hopkins University
Baltimore 18, Maryland
Attn: Dr. Robert Maddin
Dept. of Mechanical Engineering

M. W. Kellogg Company
Foot of Danforth Avenue
Jersey City 3, New Jersey
Attn: Special Projects Dept.

Lukens Steel Company
Coatesville, Pennsylvania
Attn: Mr. T. T. Watson
Director of Research

Massachusetts Institute of Technology
Department of Metallurgy
Cambridge 39, Massachusetts
Attn: Professor N. J. Grant
Attn: Professor John Wulff

Massachusetts Institute of Technology
Project Meteor
Cambridge 39, Massachusetts
Attn: Guided Missiles Library
Room 22-001

National Advisory Committee for
Aeronautics
Lewis Flight Propulsion Laboratory
Cleveland, Ohio

National Advisory Committee for
Aeronautics
1724 F Street, N. W.
Washington 25, D. C.

Chief, Office of Aeronautical Intelligence
National Advisory Committee for
Aeronautics
Washington 25, D. C.
Attn: Mr. Eugene B. Jackson

Ohio State University
Department of Metallurgy
Columbus 10, Ohio
Attn: Dr. Rudolph Speiser

Technical Library
Project Squid
Princeton University
Princeton, New Jersey

Raytheon Manufacturing Company
Waltham, Massachusetts
Attn: Mr. Leo Myer

Rensselaer Polytechnic Institute
Department of Metallurgy
Troy, New York
Attn: Dr. W. F. Hess

Sylvania Electric Products, Inc.
P. O. Box 6
Bayside
Long Island, New York
Attn: Miss Eileen Fishberg

Thompson Products, Inc.
2196 Clarkwood Road
Cleveland 3, Ohio
Attn: Director of Research

DISTRIBUTION LIST (cont'd)

MISCELLANEOUS (cont'd)

Westinghouse Electric Company Lamp Division, Research Laboratory Bloomfield, New Jersey Attn: Dr. J. W. Marden	Lockheed Aircraft Burbank, California
Westinghouse Electric Corporation Atomic Power Division Bettis Field Pittsburgh, Pennsylvania Attn: Mr. W. E. Shoupp	North American Aviation, Inc. Inglewood, California
Westinghouse Research Laboratories Metallurgical Department East Pittsburgh, Pennsylvania Attn: Howard Scott Manager, Metallurgical and Ceramic Department	Douglas Aircraft Corporation El Segundo, California
Westinghouse Electric Corporation Special Products Engineering 3 N. East Pittsburgh, Pennsylvania Attn: Dr. W. H. Brandt	Glenn L. Martin Co. Baltimore, Maryland
Bureau of Mines Albany, Oregon Attn: Dr. S. M. Shelton	Grumman Aircraft Engineering Corporation Bethpage, New York
Commanding Officer Office of Ordnance Research Duke University Durham, North Carolina Attn: Dr. A. Guy	McDonnell Aircraft Corporation St. Louis, Missouri
John L. Ham Director, Metallurgical Department National Research Corporation 70 Memorial Drive Cambridge 42, Massachusetts	Curtiss-Wright Corporation Columbus, Ohio
A. M. Bounds Chief Metallurgist Superior Tube Company Norristown, Pennsylvania	Piasecki Helicopter Corporation Morton, Pennsylvania
Bureau of Aeronautics Representative Cornell Aeronautical Laboratory Buffalo 21, New York	Sikorski Division United Aircraft Corporation Bridgeport, Connecticut
	Allison Division General Motors Corporation Indianapolis, Indiana
	Gas Turbine Division General Electric Company East Lynn, Massachusetts
	Curtiss-Wright Corporation Wright Aeronautical Division Wood-Ridge, New Jersey Attn: H. Hanink
	W. W. Dyrkacz Associate Director of Research Allegheny Ludlum Steel Corporation Pittsburgh 22, Pennsylvania
	Gas Turbine Division Westinghouse Electric Manufacturing Co. Essington, Pennsylvania

DISTRIBUTION LIST (cont'd)

MISCELLANEOUS (cont'd)

Pratt and Whitney Aircraft Division
United Aircraft Corporation
East Hartford, Connecticut

Recooled Motors, Inc.
Syracuse, New York

Lycoming Division, AVCO
Williamsport, Pennsylvania

Ranger Aircraft Engineering Division
Farmingdale, New York

Continental Aviation Engineering
Corporation
Detroit, Michigan

Solar Aircraft Company
San Diego, California

Ryan Aeronautical Company
San Diego, California

Air Research Corporation
Los Angeles, California

McCulloch Motors
Los Angeles, California

Kiekhoefer Corporation
Cedarsburg, Wisconsin

Marquardt Aircraft Corporation
Los Angeles, California

Boeing Aircraft
Seattle, Washington

Reaction Motors, Inc.
Rockaway, New Jersey

Commanding Officer
Naval Air Rocket Test Station
Lake Denmark
Dover, New Jersey

Armed Services Technical Information
Agency
Documents Service Center
Knott Building
Dayton 2, Ohio

Aero Product Division
General Motors Corporation
Dayton, Ohio

Curtiss-Wright Corporation
Propeller Division
Caldwell, New Jersey

G. M. Giannini and Company
San Francisco, California

Hamilton Standard Division
United Aircraft Corporation
East Hartford, Connecticut

Mr. W. L. Badger
General Electric Company
River Works
920 Western Avenue
West Lynn, Massachusetts

Climax Molybdenum Company
500 Fifth Avenue
New York 36, New York
Attn: Mr. Carl M. Loeb, Jr.
Vice President

Mr. R. B. Johnson
Aircraft Gas Turbine Division
General Electric Company
Evendale, Ohio

TABLE OF CONTENTS

	<u>PAGE</u>
FOREWORD	x
SUMMARY	1
INTRODUCTION	2
Equipment and Experimental Procedures	3
MECHANICAL PROPERTIES OF BINARY ALLOYS	4
Properties As Cast	7
Hardness	7
Macrostructure	10
Microstructure	10
Forging, Extrusion and Rolling of the Alloys	25
Forging and Rolling of Four-Inch-Diameter Ingots	25
Extrusion of Large Ingots	28
Extrusions from Four-Inch-Diameter Ingots	38
Strain Hardening and Recrystallization	38
Grain Size and Grain Growth	50
Mechanical Properties of Wrought Alloys	53
Hardness	53
Tensile Strength	57
Notched Bar (Impact) Transition Temperature	69
Creep-Rupture Properties	72
Oxidation	84
Summary	86
STUDIES OF DEOXIDATION	88
Melting	92
Hardness As Cast	93
Macrostructure	94
Microstructure	98
Bend Ductility	100
Forgeability	110
Exploratory Heats	110
Forging of 40- and 100-Pound Heats	114
Ring Bursting Tests	122
Summary	122
EMBRITTLEMENT	124

TABLE OF CONTENTS (continued)

	<u>PAGE</u>
TERNARY MOLYBDENUM-BASE ALLOYS	131
Molybdenum-Aluminum-Cobalt Alloys	133
Molybdenum-Aluminum-Niobium Alloys	135
Molybdenum-Aluminum-Titanium Alloys	137
Molybdenum-Aluminum-Vanadium Alloys	139
Molybdenum-Aluminum-Zirconium Alloys	141
Molybdenum-Cobalt-Aluminum Alloys	143
Molybdenum-Cobalt-Niobium Alloys	145
Molybdenum-Cobalt-Titanium Alloys	147
Molybdenum-Cobalt-Vanadium Alloys	149
Molybdenum-Cobalt-Zirconium Alloys	151
Molybdenum-Niobium-Aluminum Alloys	153
Molybdenum-Niobium-Cobalt Alloys	155
Molybdenum-Niobium-Titanium Alloys	157
Molybdenum-Niobium-Zirconium Alloys	159
Molybdenum-Titanium-Aluminum Alloys	161
Molybdenum-Titanium-Cobalt Alloys	163
Molybdenum-Titanium-Niobium Alloys	165
Molybdenum-Titanium-Vanadium Alloys	167
Molybdenum-Titanium-Zirconium Alloys	169
Molybdenum-Vanadium-Aluminum Alloys	171
Molybdenum-Vanadium-Cobalt Alloys	173
Molybdenum-Vanadium-Titanium Alloys	175
Molybdenum-Vanadium-Zirconium Alloys	177
Summary	179
ACKNOWLEDGMENT	179
REFERENCES	180
APPENDIX	187
A. Procedures for Chemical Analysis of Molybdenum-Base Alloys	190
B. Dynamic Hardness Tests	208
C. Mechanical Properties of Molybdenum and Molybdenum-Base Alloys	225

FOREWORD

Granting an abundant supply of raw material, the evolution of a new engineering material invariably requires the simultaneous solution of several problems which are not necessarily technologically interdependent from a research point of view. Molybdenum is abundant in the western hemisphere, and the evolution of molybdenum and molybdenum-base alloys as engineering materials involves the development of four major aspects of the overall problem. These are: First, the establishment of the properties obtainable in the new materials. Second, development of commercial methods of producing and fabricating the new materials. Third, the discovery of methods of protecting the new materials from oxidation at elevated temperatures. Fourth, the design of machines and equipment to use the new materials in our complicated technology.

The status of arc-cast molybdenum and its alloys on these four counts may be summarized as of this date, as follows:

1. The metallurgical foundation for the technological development of a new series of metallic alloys is virtually assured under the research program sponsored by the Office of Naval Research and for which this report is a significant part. Wrought alloys amenable to many of the current fabrication processes and having strengths at elevated temperature well above those of the present so-called "superalloys" have been produced and are becoming available.
2. Pilot operations at the Climax Molybdenum Company of Michigan over a period of three years have confirmed that the commercial production of molybdenum and molybdenum-base alloys by the arc-casting process is feasible. For large sections of materials and for material having special requirements, molybdenum produced by the arc-cast process is preferred to that currently produced by the processes of powder metallurgy.
3. The difficult problem of protecting molybdenum from oxidation has been receiving the attention of many well qualified investigators, both at the fundamental and the practical levels. This problem has already been reduced to a question of feasibility rather than possibility. Although a universally applicable method of protection may still be a long way off, results of research at this time suggest that the solution to the problem for special strategic applications is probably not far away.
4. Substantial quantities of the alloys are being made available for experimentation and for limited production where oxidation resistance is not a prerequisite to performance. Most, if not all, of the applications require developments in design to derive full benefit from the new material. It is to be expected that with the solution of the problem of oxidation resistance revolutionary engineering developments will be forthcoming.

Alvin J. Herzig
President
Climax Molybdenum Company of Michigan

FOURTH ANNUAL REPORT

ARC-CAST MOLYBDENUM-BASE ALLOYS

Contract N8onr-78700, Task Order N8onr-78701
Project NR 039-002

SUMMARY

One of the principal objectives of the fourth year program was to obtain mechanical property data for some of the arc-cast binary molybdenum-base alloys previously developed and shown to possess satisfactory forgeability and properties superior to unalloyed molybdenum. Twenty-two different alloys representative of five different binary systems have been produced on a pilot plant scale and have been fabricated by conventional commercial methods. Creep-rupture tests have shown that unalloyed molybdenum and all the alloys exhibit 100-hour creep-rupture strengths at 1800 F more than three times the strengths developed by the now widely used cobalt- and nickel-base alloys. Strain hardened sections of the alloys were superior in creep-rupture strength to recrystallized sections of the same materials at all temperatures, but the advantage was greater at 1600 and 1800 F than at 2000 F. Four binary alloys, Mo - 0.45% Ti, Mo - 1.25% Ti, Mo - 0.75% Nb, and Mo - 0.09% Zr, exhibited 100-hour creep-rupture strengths in the range 22,000-25,500 psi at 2000 F with the minimum elongation value of 10%. In general, the alloys were superior to unalloyed molybdenum at all test temperatures; there were a few exceptions.

A second objective was to produce carbon-free alloys or at least to reduce the residual carbon content to 0.01% maximum to improve ductility. Carbon-free molybdenum-vanadium and molybdenum-titanium alloys have been produced by deoxidation with rare earth metals in vacuum and have been hot worked successfully. Titanium and zirconium have been used as supplementary deoxidizers to produce forgeable ingots with low residual carbon contents (0.010-0.015%) by vacuum melting.

Elimination of the embrittlement of wrought molybdenum upon exposure to temperatures above 2000 F comprised a third objective. The addition of titanium to molybdenum and molybdenum-base alloys has been shown to minimize, and in some cases to prevent, elevated temperature embrittlement when deoxidation during melting was accomplished with carbon (vacuum melting), with aluminum (argon melting) or rare earth metals (either argon or vacuum melting).

The fourth year program has included the exploration of a series of graded castings of solid solution, molybdenum-rich, ternary alloys, each of which was composed of a different combination of two elements from the following group: aluminum, cobalt, niobium, titanium, vanadium, and zirconium. The test castings were made by melting bars of a binary alloy and adding the third element in increasing quantities as melting progressed. Ternary molybdenum-base alloys containing small amounts of aluminum or cobalt generally have lower hardness at room temperature than corresponding binary molybdenum-base alloys free from the aluminum or cobalt. This is similar to the effect of adding small amounts of aluminum or cobalt to unalloyed molybdenum. At 1600 F, all of the ternary alloys were harder than the corresponding binary alloys. In general, the hardening effects of addition of two alloying elements to molybdenum are additive.

ARC-CAST MOLYBDENUM-BASE ALLOYS

INTRODUCTION

Research on arc-cast molybdenum-base alloys has been sponsored by the Office of Naval Research under Contract N8onr-78700 at the Climax Molybdenum Company of Michigan since February, 1949. The bases for placing this contract were: (1) the desire to increase the rate of research on molybdenum-base alloys because of their potentialities as structural materials for high temperature applications, and (2) the prior development by Climax Molybdenum Company of Michigan of equipment and processes for producing forgeable, arc-cast ingots of molybdenum and molybdenum-base alloys.

Research accomplished under the contract by July 31, 1952, was described in the first three annual reports and may be summarized as follows:

1. Classification of the alloy systems according to solid solubility and the nature of the first excess phase developed in molybdenum-rich compositions.
2. Discovery of a number of very promising alloys exhibiting strengths higher than expected.
3. Measurement of the rates of increase of room-temperature and elevated-temperature hardness with increasing concentrations of alloying elements.
4. Preparation of tentative phase diagrams of molybdenum-beryllium, molybdenum-boron, molybdenum-aluminum, and molybdenum-silicon alloys.
5. Investigation of the effects of added elements on the control of oxygen in molybdenum produced by the arc-cast process and the indirect effect of each element on the hot working characteristics of molybdenum.
6. Investigation of the effects of variations in processing the cast metal on hot plasticity.
7. Evaluation of room-temperature ductility of molybdenum and molybdenum-base alloys as cast and after mechanical working.
8. The discovery of binary alloy systems of molybdenum which are amenable to heat treatment for the control of mechanical properties.
9. Development of heat treatments for precipitation hardening molybdenum-beryllium alloys.
10. An initial appraisal of the extrusion process for hot working alloy ingots and an investigation of some of the properties of a few alloys which were hot worked in this manner.

11. Determination of mechanical properties at room and elevated temperatures of a number of wrought, arc-cast molybdenum-base alloys.
12. Investigation of the embrittlement resulting from exposure to high temperatures.

This report covers the work done on Contract N8onr-78700 in the period August 1, 1952, through July 31, 1953. During this period the major fields of investigation were as follows:

1. Mechanical properties at room and elevated temperatures of a number of wrought arc-cast molybdenum-base alloys.
2. Deoxidation and forging practices.
3. Embrittlement of molybdenum resulting from exposure to high temperatures.
4. Preliminary appraisal of ternary molybdenum-base alloys, through metallographic examination, measurement of hardness at room and elevated temperatures, and measurement of lattice parameters.

Equipment and Experimental Procedures

Most of the equipment and experimental procedures employed in the investigation of molybdenum-base alloys have been described in previous annual reports. Two types of melting furnace have been used: a bar machine^{1*}, in which the consumable electrode is a preformed bar, and powder machines (PSM-3 and PSM-4)^{2,3} in which the charge comprises powder and in which pressing, sintering, and melting are continuous within the furnace. An induction furnace² was used for heat treating small samples at temperatures up to 4100 F in vacuum or argon atmosphere. This furnace permits oil quenching without exposure to air. A 1000-pound air hammer³ was used for initial breakdown of some small ingots prior to rolling.

During the fourth year of the contract, the metallographic procedure previously described^{1,2} was followed without change. The methods of mechanical testing, such as Vickers hardness, ring bursting, beam bending, impact, and tensile tests, were likewise unchanged. The strain rates and temperatures used for impact and tensile tests are given with the impact and tensile data in the section on mechanical properties of binary alloys. The dynamic hardness test was studied in greater detail, since an anomalous rise in dynamic hardness number was observed in most of the alloys at 2200 to 2800 F. The dynamic hot hardness testing apparatus and experiments to trace the cause of the anomalous hardness are described in Appendix B.

* The superscripts pertain to references appended to this report.

MECHANICAL PROPERTIES OF BINARY ALLOYS

During the past year, the study of molybdenum-base binary alloys has centered on two main objectives: (1) the feasibility of producing and processing large sections of 47 ingots prepared in the alloy systems of aluminum, cobalt, nickel, niobium, silicon, titanium, vanadium, and zirconium, and (2) evaluation of the variables of composition and fabrication in terms of mechanical properties. Some of the cobalt, niobium, titanium, and vanadium alloys were in test during the third year of the program; others were made and tested during the fourth year. The molybdenum-aluminum and molybdenum-zirconium alloys have now been studied extensively for the first time, while the molybdenum-nickel and molybdenum-silicon alloys have been investigated in an exploratory manner only.

Two vacuum-arc cast, carbon-deoxidized, unalloyed molybdenum ingots (937 and 1159*) were included in this study to provide a datum plane for measuring the effects of alloying elements. In this section the expression "unalloyed molybdenum" refers to these ingots. A third ingot (1053), deoxidized with aluminum and melted in argon, contained enough aluminum to accomplish deoxidation but not enough to be considered an alloy. This ingot, therefore, has been classed with unalloyed molybdenum. The mechanical properties of three heats deoxidized with rare earth metals--one unalloyed molybdenum, one molybdenum-vanadium alloy, and one molybdenum-titanium alloy--have also been determined.

At the outset of the program for the fourth year, experimental ingots of the alloys were four inches in diameter and weighed about 100 pounds; they were produced in the smaller powder machine. After extrusion of molybdenum proved to be feasible, and also more economical than hammer forging, larger alloy ingots were cast and extruded. These ingots were 7-1/2 to 8 inches in diameter, weighed about 300 pounds, and were produced in the larger powder machine.

Identifications of the alloy ingots, their chemical analyses and cast sizes are given in Table 1. All the alloys listed were produced from powder charges in PSM equipment without difficulty.

Most of the heats were deoxidized with carbon and melted in vacuum. In the molybdenum-aluminum series, aluminum served as the deoxidizer; therefore, carbon was not added, and the heats were melted in argon. Several heats were deoxidized by other procedures that had shown promise in earlier experiments. Three heats, deoxidized with rare earth metals under the deoxidation program (1045, 1048, 1049), were large enough to provide stock for mechanical testing as well as for the deoxidation studies. Titanium was used as an auxiliary deoxidizer in two alloy heats (1001, 1217), since it had been found earlier that molybdenum-titanium alloy heats deoxidized with carbon were characterized by an absence of speckling at the grain boundary and a strong resistance to intergranular fracture. Both of these characteristics have been associated with improved deoxidation.

* Laboratory heat numbers

TABLE 1

INGOTS FOR MECHANICAL PROPERTY STUDIES

Ingot	Mold Dia In.	Additions, %		Form and Supplier of Alloy Added	Analysis, %	
		Carbon	Alloy		Carbon	Alloy
937	6	0.042			0.015	
1159	7.5	0.047			0.040	
1045	4	(0.3 LCA)			0.003	0.005 Ce, 0.007 RE
1063	8		0.20 Al	atomized, Alcoa	0.003	0.17 Al
1058	8		0.60 Al	No. 101	0.006	0.49 Al
987	4		0.60 Al		0.003	0.53 Al
1059	8		1.00 Al		0.004	0.81 Al
983	4		1.00 Al		0.004	0.88 Al
1155	7.5		1.25 Al			
1154	7.5		1.37 Al			
1176	4		1.70 Al			1.43 Al
1144	7.5	0.040	0.12 Co	vacuum melted,	0.020	0.074 Co
1217	7.5	0.034	0.247 Co	National Re- search Corp.	0.030	0.11 Co, 0.18 Ti
			0.20 Ti			
1145	7.5	0.040	0.25 Co		0.022	0.123 Co
1146	7.5	0.040	0.37 Co		0.018	0.165 Co
1173	4	0.046	0.50 Co		0.017	0.19 Co
1153	7.5	0.040	0.11 Ni	powder, Metals Disintegrating Co.	0.008	0.044 Ni
988	4	0.035	0.25 Nb	powder, Fansteel	0.019	0.24 Nb
1082	8	0.051	0.30 Nb	Metallurgical	0.032	0.31 Nb
1001	8	0.043	0.30 Nb	Company	0.032	0.31 Nb, 0.16 Ti
			0.19 Ti			
978	4	0.036	0.50 Nb		0.019	0.52 Nb
979	4	0.036	0.75 Nb		0.022	0.76 Nb
1057	8	0.052	0.78 Nb		0.033	0.75 Nb
1147	7.5	0.033	1.04 Nb		0.012	1.10 Nb
1148	7.5	0.033	1.30 Nb		0.013	1.36 Nb
1152	7.5	0.040	0.10 Si	high purity powder	0.011	0.088 Si
1132	7.5	0.035	0.51 Ti	sponge, DuPont	0.024	0.45 Ti
1008	4	0.040	0.64 Ti	crystal bar	0.034	0.65 Ti
1048	4	(0.3 LCA)	1.00 Ti	sponge, DuPont	0.028	0.69 Ti, 0.12 RE
1133	7.5	0.038	1.03 Ti	sponge, DuPont	0.014	0.85 Ti
1134	7.5	0.038	1.29 Ti	sponge, DuPont	0.010	1.05 Ti
1138	7.5	0.038	1.55 Ti	sponge, DuPont	0.014	1.22 Ti
1009	4	0.040	1.28 Ti	crystal bar	0.036	1.26 Ti
1143	7.5	0.042	2.06 Ti	sponge, DuPont	0.018	1.66 Ti
1010	4	0.040	1.92 Ti	crystal bar		
1174	4	0.043	4.20 Ti	sponge, DuPont	0.027	3.59 Ti
1051	8	0.047	0.60 V	vacuum fusion,	0.027	0.54 V
1012	4	0.043	0.60 V	Electrometal-	0.030	0.56 V
1049	4	(0.3 LCA)	1.00 V	lurgical Corp.	0.001	0.85 V
						0.003 Ce, 0.003 RE
1052	8	0.047	1.20 V		0.029	1.00 V
1013	4	0.043	1.20 V		0.035	1.14 V
1053	8	0.047	1.50 V		0.032	1.24 V
1151	7.5	0.040	1.25 V		0.006	1.25 V
1014	4	0.043	1.50 V		0.032	1.39 V
1175	4	0.043	1.62 V		0.033	1.46 V
1207	7.5	0.036	0.09 Zr	sponge, A.E.C.	0.019	0.09 Zr
1062	8	0.052	0.10 Zr		0.036	0.11 Zr
1041	4	0.040	0.20 Zr		0.021	0.21 Zr
1149	7.5	0.033	0.20 Zr		0.013	0.22 Zr
1150	7.5	0.033	0.40 Zr		0.015	0.43 Zr

As cast most of the ingots had rough porous surfaces which were machined off prior to working. The larger ingots were machined to 6-1/2 inch diameter and were extruded at Babcock and Wilcox Tubular Products Division. Machining to this diameter removed all surface defects of these ingots.

Most of the four-inch-diameter ingots were turned to remove 1/4 inch on a radius, to produce cylindrical surfaces free from defects, and were forged on the hammer or the hydraulic press. Four of the smaller castings (1173, 1174, 1175, 1176) were quartered and extruded at Thompson Products Company, Tapco Division.

All of the ingots were analyzed chemically. The material for chemical analyses was obtained from two positions in the casting: from a cross section one or two inches from the top of the ingot, and from the last cut on the cylindrical surface. The analyses at the two positions agreed within the limits of accuracy of wet chemical analysis, and this agreement is presented as evidence of uniformity of composition of the casting. The unusually high hardness at the original surface of some ingots, particularly in the molybdenum-cobalt and molybdenum-nickel system, suggested greater concentrations of alloying elements at the surface, but these surface layers were removed by machining. The recoveries of cobalt and nickel were the poorest of the group of alloying elements studied, Table 2. There is evidence that cobalt and

TABLE 2
RECOVERY OF ALLOYING ELEMENTS

<u>Alloying Element</u>	<u>Recovery, %</u>
Aluminum	85
Cobalt	48
Nickel	40
Niobium	100
Silicon	88
Titanium, crystal bar	100
Du Pont sponge	82
Vanadium	90
Zirconium	100

nickel, because of their relatively high vapor pressures, evaporated from the melt and condensed upon the walls of the mold. As the bath rose in the mold, the molten metal solidified when it contacted the water-cooled mold wall so quickly that time was not available to effect solution and diffusion of the condensed metals. They therefore remained at the surface of the casting and were "lost" when the castings were machined. The remainder of the alloying element charged stayed in the melt and was assumed to be uniformly distributed throughout the machined section that was wrought to final shape.

Properties as Cast

Hardness

A slice one inch thick was prepared from the mid-length of the four-inch diameter ingots for determination of mechanical properties as cast. The slice from the larger ingots was taken from the top, as the major portion of the ingot in one section was required for the extrusion blank. Vickers hardness (10 kg load) of 30 alloys in the cast condition was determined; a summary of hardnesses at room temperature and 1600 F is given in the form of a bar graph in Figure 1. Curves of hardness as a function of testing temperature from room temperature to 1600 F for each alloy appear in Appendix C, Figures C1 to C7.

The Vickers hardness of unalloyed molybdenum is about 180 at room temperature and 60 at 1600 F. All the alloys except those containing 0.17% aluminum, 0.07% cobalt, 0.123% cobalt, and 0.044% nickel were harder than unalloyed molybdenum at room temperature. At 1600 F the alloy ingots, without exception, were harder than unalloyed molybdenum. Unalloyed molybdenum deoxidized with 0.3% rare earth metal, although only slightly harder at room temperature than molybdenum deoxidized with carbon, was appreciably harder at 1600 F.

Aluminum in amounts greater than necessary for deoxidation alone increased the hardness of molybdenum. This increase in hardness became progressively greater with increasing aluminum content, especially at the higher temperatures; in general, the change in hardness with increasing temperature was less for molybdenum-aluminum alloys than for unalloyed molybdenum and many of the other alloys.

The hot hardness curves for the three molybdenum-cobalt alloys were similar to those for the molybdenum-aluminum alloys, but at a lower hardness level.

The hardening effect of niobium on molybdenum was much less than that of aluminum if the two alloying elements are compared on the basis of weight per cent. The ingot containing 0.24% niobium was not significantly harder than unalloyed molybdenum. The curves for the family of molybdenum-niobium alloys were similar in shape to those for unalloyed molybdenum; the hardness dropped rapidly with increasing temperature in the range from room temperature to 600 F and remained fairly constant at higher temperatures.

The curves for molybdenum-titanium alloys likewise followed the general pattern established for unalloyed molybdenum. The elevated temperature hardness increased with increase in titanium content. The ingot containing 0.69% titanium and deoxidized with rare earth metals (1048) was harder at 1600 F than a molybdenum-titanium alloy containing 0.90% titanium and deoxidized with carbon.

Vickers hot hardness data for the group of molybdenum-vanadium alloys agreed well with the data previously obtained for this system, cf. third annual report. It is evident from the data that vanadium in solid solution has a greater effect upon the hardness of molybdenum at 1600 F than upon its hardness at room temperature. The hardness of the heat deoxidized with rare earth metals

CLIMAX MOLYBDENUM CO. 292

MARCH 2, 1953

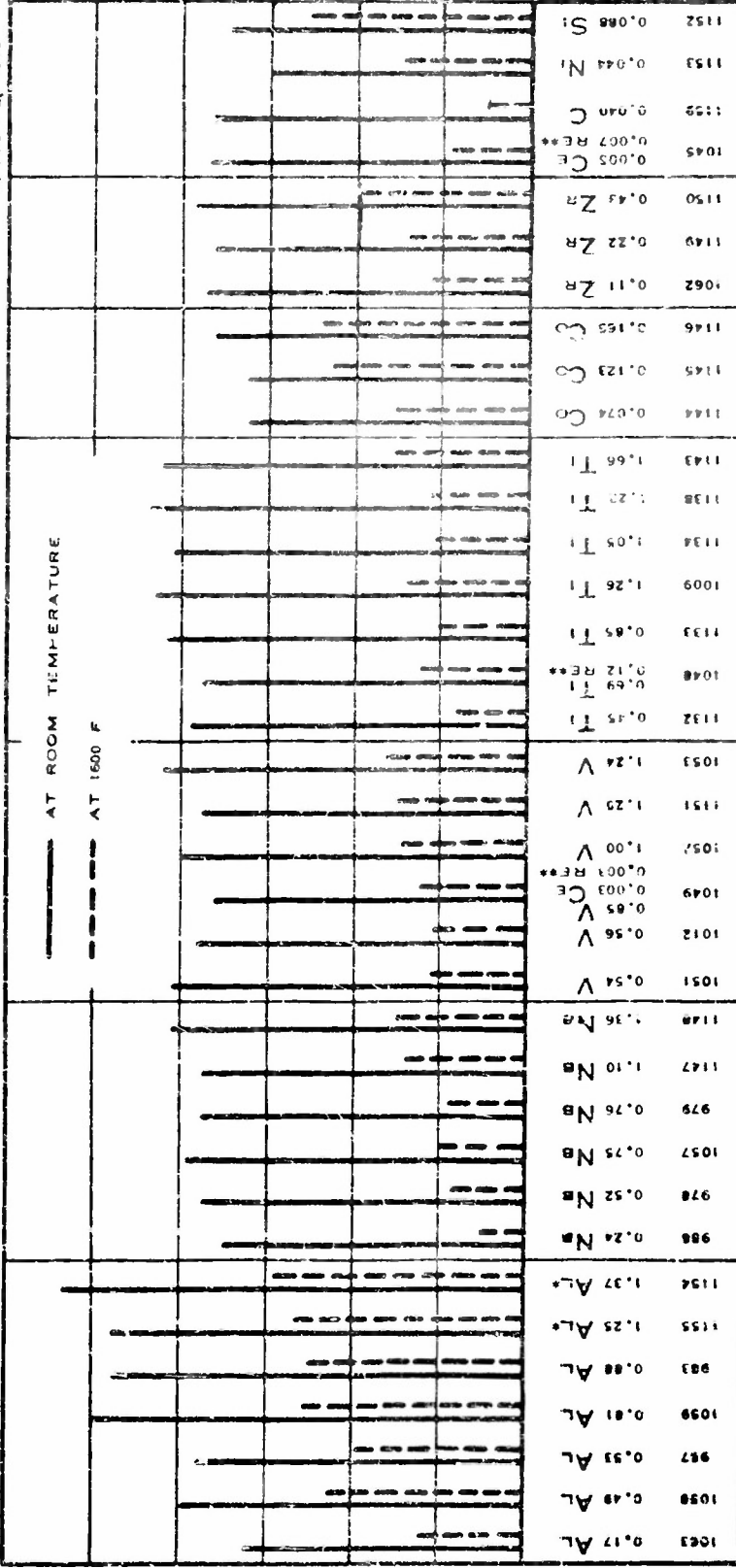
280

240

HARDNESS, VHN

AT ROOM TEMPERATURE

AT 1600 F



* ADDED ** OTHER RARE EARTH METALS

FIGURE 1 - HARDNESS AT ROOM TEMPERATURE AND 1600 F OF MOLYBDENUM - BASE ALLOYS AS CAST

was slightly lower than that of a carbon-deoxidized ingot of similar vanadium content reported earlier. The hardening effect of vanadium, on the basis of weight per cent, was only slightly superior to that of niobium.

Like aluminum and cobalt, but in somewhat lesser degree, zirconium flattened the hardness-temperature curve. On the basis of weight per cent, the relative hardening effect of zirconium at 1600 F was in the same range as that of aluminum.

The addition of 0.044% nickel and 0.088% silicon markedly raised the hardness of molybdenum at 1600 F. The decrease in hardness of the silicon alloy from room temperature to 1600 F was less than for any other alloys studied.

The relative hardening effects of the alloying elements discussed above are consistent with those published in the second annual report. The elements are listed below in order of decreasing hardening effect, on the bases of both weight and atomic per cent.

<u>Hardening Effect of Alloying Elements</u>		
	<u>Weight Per Cent</u>	<u>Atomic Per Cent</u>
greatest effect	silicon	silicon
	nickel	nickel
	cobalt	cobalt
	zirconium	zirconium
	aluminum	aluminum
	vanadium-titanium	niobium
	niobium	vanadium
least effect		titanium

As an illustration, it can be seen from Table 1 that at 1600 F, 0.07% cobalt, by weight, has approximately the same hardening effect as 1.7% titanium, 1.2% vanadium, and somewhat more than 1.3% niobium.

Additions of vanadium, titanium, or niobium do not significantly change the shape of the hardness-temperature curve established for unalloyed molybdenum. The rapid decrease in hardness as a function of increasing temperature occurs from room temperature to 800 F; between 800 F and 1600 F there is little change. Additions of aluminum, cobalt, zirconium, and silicon produce a more gradual decrease in hardness through the range from room temperature to 1000 F. Furthermore, for all the alloys studied, the room temperature hardness does not increase as rapidly with increasing alloy content as the hardness at 1600 F. This is fortunate because higher elevated temperature hardness is obtained without a proportional increase in room temperature hardness. Significant increase in room temperature hardness increases the difficulties of sawing, machining, or turning the alloys.

Macrostructure

The as-cast grain size and the macrostructure of a given alloy changed insignificantly when the casting diameter was increased from four inches to eight inches. All of the ingots filled the mold well and were devoid of macroporosity. Of the large ingots, only one (1132) was sectioned for examination of the macrostructure near the center of the ingot, Figure 2. This ingot contained 0.45% titanium and had essentially the same macrostructure as an ingot (1008) containing 0.65% titanium and cast in a four-inch-diameter mold.

The grain size and macrostructure of the two unalloyed ingots deoxidized with carbon (937, 1159) were the same as those of the 0.45% titanium ingot. The grains were columnar and were about 0.1 inch in diameter and 0.7 inch long. The grains of the ingot deoxidized with rare earth metals (1045) were finer, more like those of the 3.59% titanium ingot (1174). The ingot containing 0.17% aluminum was coarser grained than the unalloyed molybdenum, but as the aluminum content increased, the grains were progressively finer, Figure 3. A relatively small amount of cobalt (0.19%) not only raised the hardness of molybdenum but also refined the grain, Figure 3.

Niobium in amounts up to 0.78% had no effect upon grain size; the macrostructures of the molybdenum-niobium alloys were essentially the same as that shown for Ingot 1132, Figure 2. The addition of 0.1% nickel refined the grain considerably. The macrostructure of an ingot containing nickel (1209) is shown in the section on deoxidation, Figure 67. The macrostructure of the 0.088% silicon alloy was like that of the 3.59% titanium alloy. In the titanium series, the grain size decreased as the titanium content increased, from 0.45% to 0.65% and 3.59%, Figure 2. Vanadium up to 1.46% refined the grain slightly, Figure 3; zirconium up to 0.1% had no grain-refining effect, and the ingots containing zirconium exhibited a macrostructure similar to that of Ingot 1132, Figure 2.

Microstructure

Unalloyed molybdenum made in the large powder machine usually contains a small amount of carbide and speckling. Figure 4 is typical of the microstructure and fracture. The matter of speckling was discussed in detail in the third annual report, page 114. In brief, a platelike oxide is observed upon the intergranular fractures of poorly deoxidized molybdenum. As the degree of deoxidation is improved, the platelike oxide diminishes in amount and in form and eventually appears as fine dots on the intergranular fracture surfaces and disappears entirely in well-deoxidized molybdenum. The phase appearing as fine dots or specks is called "speckling". Upon metallographic examination of electropolished specimens, it was found that when speckling appeared on the fractures it also appeared in the microstructure of polished sections in the form of minute, black or gray dots, predominantly at the grain boundaries and visible at magnifications of 1500X and greater. Since the speckles are extremely small, it is difficult to reproduce them in photographs. Without question, speckling is more clearly revealed in the fractographs than in the photomicrographs of polished sections; hence, fractography has been relied upon as the principal procedure for evaluating the degree of deoxidation.



(B) MID CROSS-SECTION OF 4" DIAMETER INGOTS

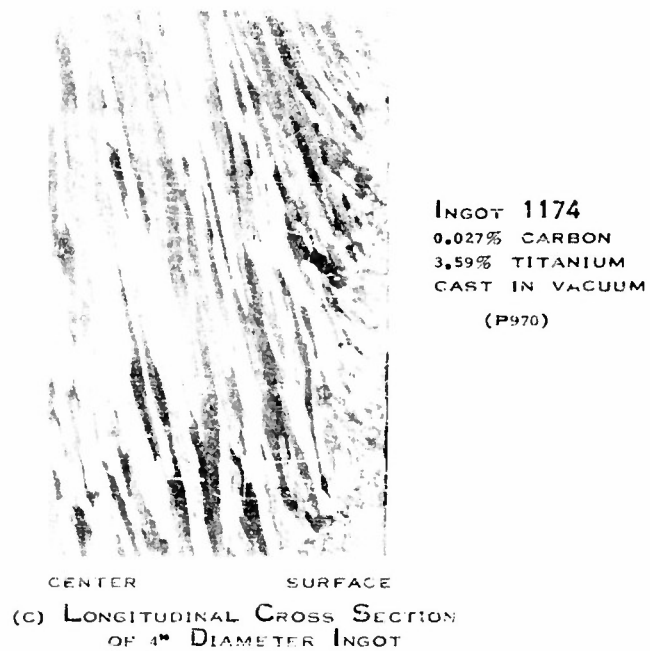
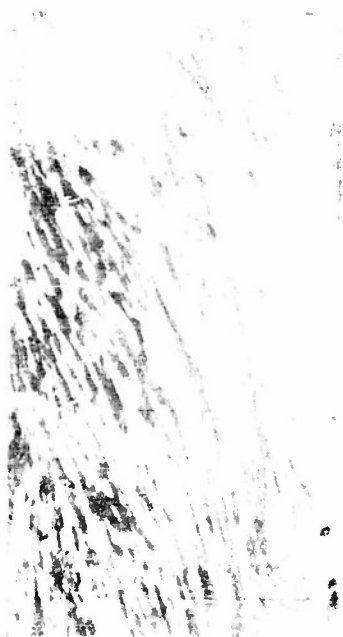


FIGURE 2 — MACROSTRUCTURES OF ARC-CAST MOLYBDENUM-TITANIUM ALLOYS, X1



INGOT 1176
1.43% ALUMINUM
CAST IN ARGON
(P970)



INGOT 1173
0.037% CARBON
0.19% COBALT
CAST IN VACUUM
(P970)



INGOT 1175
0.033% CARBON
1.46% VANADIUM
CAST IN VACUUM
(P970)



INGOT 1013
0.035% CARBON
1.14% VANADIUM
CAST IN VACUUM
(P905)

FIGURE 3 — MACROSTRUCTURES OF ARC-CAST MOLYBDENUM-BASE ALLOYS, X1
FOUR-INCH-DIAMETER INGOTS

The molybdenum-aluminum alloys were devoid of oxide at the grain boundaries and all exhibited a small amount of microporosity. No satisfactory intergranular fracture facets could be obtained for metallographic examination--an indication of relatively high intergranular strength and successful deoxidation. Figure 5 shows the microstructure typical of this group.

All of the molybdenum-cobalt ingots made in the large powder machine and deoxidized with carbon contained carbide and speckling, of which Figure 6 is typical. These ingots contained between 0.018 and 0.022% residual carbon. One heat made in the large machine with titanium as an auxiliary deoxidizer (1217) exhibited practically no speckling, Figure 7. An ingot deoxidized only with carbon in vacuum and made in the small powder machine contained 0.037% carbon and was devoid of speckling, Figure 8.

The molybdenum-nickel and molybdenum-silicon ingots (1153, 1152) were inadequately deoxidized. An excessive amount of speckling appeared in both; platelike oxide occurred in the nickel heat, Figures 9-10.

All the molybdenum-niobium alloys contained residual carbide and a moderate amount of speckling. As the niobium content increased from 0.52% to 1.36%, the amount of speckling increased slightly, Figures 11-12. When titanium was added as an auxiliary deoxidizer (1001), no speckling was observed.

The molybdenum-titanium ingots deoxidized with carbon exhibited clean grain boundaries and were devoid of speckling. Figures 13a and 13b show typical fracture and microstructure. It was very difficult to obtain intergranular fracture facets for metallographic examination--always an indication of high intergranular strength. The cleanliness and lack of speckling were consistent throughout the series; there was a progressive change in microstructure, however, as the titanium content increased. At 0.45% titanium massive carbide was readily recognized at the grain boundaries and within the grains, Figure 13c. When the titanium content was increased to 0.65%, a fine precipitate began to appear within the grains, which increased in amount as the titanium content was increased. Figures 14a and 14b show the carbide in alloys containing 1.22% and 3.59% titanium. The massive carbide had entirely disappeared from the grains of the 3.59% titanium alloy and was replaced by the finely dispersed carbide. At the grain boundaries the carbide had become thinner and more continuous, Figure 16b. The fine dispersion is thought to be carbide, since in amount it appeared to be a function of carbon content. A heat deoxidized with aluminum, containing no carbon and 1.65% titanium, Figure 15a, was devoid of the fine dispersion, whereas the 1.22% titanium alloy with 0.014% carbon, Figure 14a, contained a considerable amount of the dispersion. An excessive amount of the dispersion was also observed in an alloy containing appreciably more titanium and 0.027% carbon, Figure 15b. And finally, the ingot containing less titanium (2.66%) and more carbon (0.048%) exhibited by far the greatest amount of the dispersion, Figure 16.



(A) FRACTOGRAPH, X2000 (M3347)

(B) ELECTROPOLISHED, X2000 (M3334)

FIGURE 4 — MICROSTRUCTURE OF CAST UNALLOYED MOLYBDENUM

INGOT 1159, 0.040% CARBON, CAST IN VACUUM



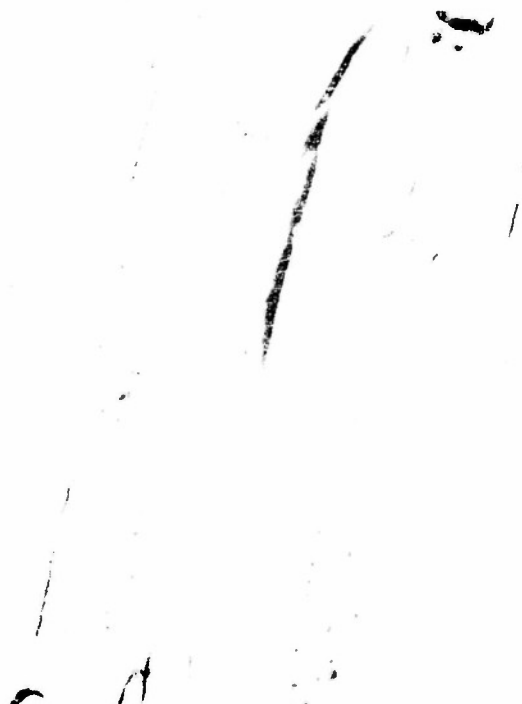
(A) ELECTROPOLISHED, LIGHTLY ETCHED IN SODIUM HYDROXIDE, X100 (M3345)



(B) ELECTROPOLISHED, ETCHED 5 SEC IN WEAK SODIUM HYDROXIDE + POTASSIUM FERRICYANIDE SOLUTION, X2000 (M1974)

FIGURE 5 — MICROSTRUCTURE TYPICAL OF CAST MOLYBDENUM-ALUMINUM ALLOYS

INGOT 983, 0.004% CARBON, 0.88% ALUMINUM, CAST IN ARGON



(A) FRACTOGRAPH, X2000 (M2416)

(B) ELECTROPOLISHED, X2000 (M2434)

FIGURE 6 — MICROSTRUCTURE OF MOLYBDENUM CONTAINING 0.123% COBALT,
AS CAST

INGOT 1145, 0.022% CARBON, CAST IN VACUUM



(A) FRACTOGRAPH, X2000 (M3221)

(B) ELECTROPOLISHED, X2000 (M3222)

FIGURE 7 — MICROSTRUCTURE OF MOLYBDENUM CONTAINING 0.11% COBALT
AND 0.9% TITANIUM, AS CAST

INGOT 1217, 0.030% CARBON, CAST IN VACUUM



(A) FRACTOGRAPH, X2000 (M2618)

(B) ELECTROPOLISHED, X2000 (M2690)

FIGURE 8 — MICROSTRUCTURE OF MOLYBDENUM CONTAINING 0.19% COBALT,
AS CAST

INGOT 1173, 0.037% CARBON, CAST IN VACUUM, PSM 3



(A) FRACTOGRAPH, X2000 (M2441)

(B) ELECTROPOLISHED, X2000 (M2496)

FIGURE 9 — MICROSTRUCTURE OF MOLYBDENUM CONTAINING 0.044% NICKEL,
AS CAST

INGOT 1153, 0.008% CARBON, CAST IN VACUUM



(A) FRACTOGRAPH, X2000 (M2440)

(B) ELECTROPOLISHED, X2000 (M2495)

FIGURE 10 — MICROSTRUCTURE OF MOLYBDENUM CONTAINING
0.10% SILICON, AS CAST

INGOT 1152, 0.011% CARBON, CAST IN VACUUM



(A) FRACTOGRAPH, X2000 (M2415)

(B) ELECTROPOLISHED, X2000 (M2411)

(C) ELECTROPOLISHED, X500 (M1239)

FIGURE 13 — MICROSTRUCTURE OF MOLYBDENUM CONTAINING
0.45% TITANIUM, AS CAST

INGOT 1132, 0.024% CARBON, CAST IN VACUUM

(A) INGOT 1138, 0.014% CARBON, 1.22% TITANIUM
ELECTROPOLISHED, X2000 (M3237)

(B) INGOT 1174, 0.027% CARBON, 3.59% TITANIUM
ELECTROPOLISHED, ETCHED IN SODIUM
HYDROXIDE + POTASSIUM FERRICYANIDE
SOLUTION, X250 (M2678)

FIGURE 14 — FINELY DISPERSED CARBIDES IN MOLYBDENUM-TITANIUM ALLOYS

(A) INGOT 947, 0.060% CARBON, 1.65% TITANIUM
0.23 ALUMINUM, CAST IN ARGON
ELECTROPOLISHED, X2000 (M2469)

(B) INGOT 1174, 0.027% CARBON, 3.59% TITANIUM
ELECTROPOLISHED, X2000 (M2679)

FIGURE 15 — FINELY DISPERSED CARBIDES IN MOLYBDENUM-TITANIUM ALLOYS



(A) ELECTROPOLISHED, ETCHED IN SODIUM HYDROXIDE + POTASSIUM FERRICYANIDE SOLUTION, X2600 (M2471)



(B) ELECTROPOLISHED, ETCHED IN SODIUM HYDROXIDE + POTASSIUM FERRICYANIDE SOLUTION, X100 (M2470)

FIGURE 16 - CARBIDE DISTRIBUTION IN MOLYBDENUM CONTAINING 2.66% TITANIUM, AS CAST

INGOT 4-887, 0.048% CARBON, CAST IN VACUUM



(A) FRACTOGRAPH, X2000 (M2023)

(B) ELECTROPOLISHED, X2000 (M2024)

**FIGURE 17 -- MICROSTRUCTURE OF MOLYBDENUM CONTAINING
1.39% VANADIUM, AS CAST**

INGOT 1014, 0.032% CARBON, CAST IN VACUUM

ELECTROPOLISHED, X2000 (M2114)

**FIGURE 18 -- MICROSTRUCTURE OF MOLYBDENUM CONTAINING
0.85% VANADIUM, AS CAST, DEOXIDIZED WITH
RARE EARTH METALS**

INGOT 1049, 0.001% CARBON, 0.003% CERIUM, 0.003% OTHER RARE EARTH METALS
CAST IN VACUUM




(A) FRACTOGRAPH, X2000 (M2623)

(B) ELECTROPOLISHED, X2000 (M2697)

(C) ELECTROPOLISHED, X500 (M3240)

FIGURE 19 — MICROSTRUCTURE OF MOLYBDENUM CONTAINING
0.09% ZIRCONIUM, AS CAST
INGOT 12-7, 0.019% CARBON, CAST IN VACUUM



(A) INGOT 1149, 0.013% CARBON, 0.22% ZIRCONIUM (B) INGOT 1150, 0.015% CARBON, 0.43% ZIRCONIUM
ELECTROPOLISHED, X2000 (M3241) ELECTROPOLISHED, X2000 (M3242)

**FIGURE 20 — FINELY DISPERSED CARBIDES IN MOLYBDENUM-ZIRCONIUM ALLOYS,
AS CAST**

All of the ingots in the molybdenum-vanadium system contained speckling. The photomicrographs of Figure 17 are representative of the series of alloys, regardless of vanadium content. Intergranular fracture for facet examination could not be obtained from the ingot deoxidized with rare earth metals (1049), but its microstructure is shown in Figure 18. Although the grain boundary contains some extraneous phase, the fact that intergranular fracture could not be obtained is evidence that deoxidation was more satisfactory than in the corresponding ingots deoxidized with carbon.

The molybdenum-zirconium alloys were similar to the molybdenum-titanium alloys in many respects. Ingots containing as little as 0.09% zirconium and deoxidized with carbon in vacuum were free from speckling and were difficult to fracture intergranularly. The carbide distribution changed with increasing zirconium content. Typical fracture and microstructure are shown in Figures 19a and 19b. The massive carbide at the grain boundaries and a small amount of finely dispersed precipitate are shown to better advantage at lower magnification, Figure 19c. The amount of fine carbide increased as the zirconium content increased from 0.22% to 0.43%, Figure 20.

Forging, Extrusion and Rolling of the Alloys

Forging and Rolling of Four-Inch-Diameter Ingots

Castings weighing about 100 pounds each were made in a four-inch-diameter mold. These were cut into two 12-inch lengths, then machined to 3-1/2 inch diameter for forging. The machined castings were heated in hydrogen for forging. They were then forged to about 2-1/4 inch diameter by somewhat over 20 inches long (20 inches was the minimum length acceptable for rolling on the commercial mill engaged). A 600-ton forging press with 60°-V die was used for forging. Prior to rolling the billets were annealed for one hour at 3000 F, cropped, and machined to remove surface defects. The bulk of the machining loss occurred at this stage of the processing. The billets were rolled to 1-inch and 5/8-inch diameter bar stock at Universal-Cyclops Steel Corporation on a commercial tool steel rolling mill at 2200-1900 F. A flow sheet showing the processing of the ingot containing 0.52% niobium, Figure 21, is typical of the four-inch-diameter ingots subjected to forging and rolling. The stock obtained by this procedure is listed in Table 3.

In forging molybdenum and molybdenum-base alloys, two factors seem to be the source of most of the difficulties. The first is the high resistance of molybdenum to plastic deformation at the forging temperatures available (up to 3000 F). This resistance increases with increase in alloy content, and satisfactory recovery was not obtained on forging billets containing more than 0.53% aluminum, 0.52% niobium, 1.26% titanium, or 0.85% vanadium in the equipment available. Moreover, the forging equipment available was too small to accomplish deformation of the center of the ingot without numerous reheatings. The necessity for frequent reheating made the second difficulty encountered in working (namely, the high rate of oxidation of molybdenum) of greater importance. Even though the billets were protected by hydrogen atmosphere

CLIMAX MOLYBDENUM CO. 247
DECEMBER 1, 1952

FIGURE 21
FORGING SCHEDULE
INGOT 978

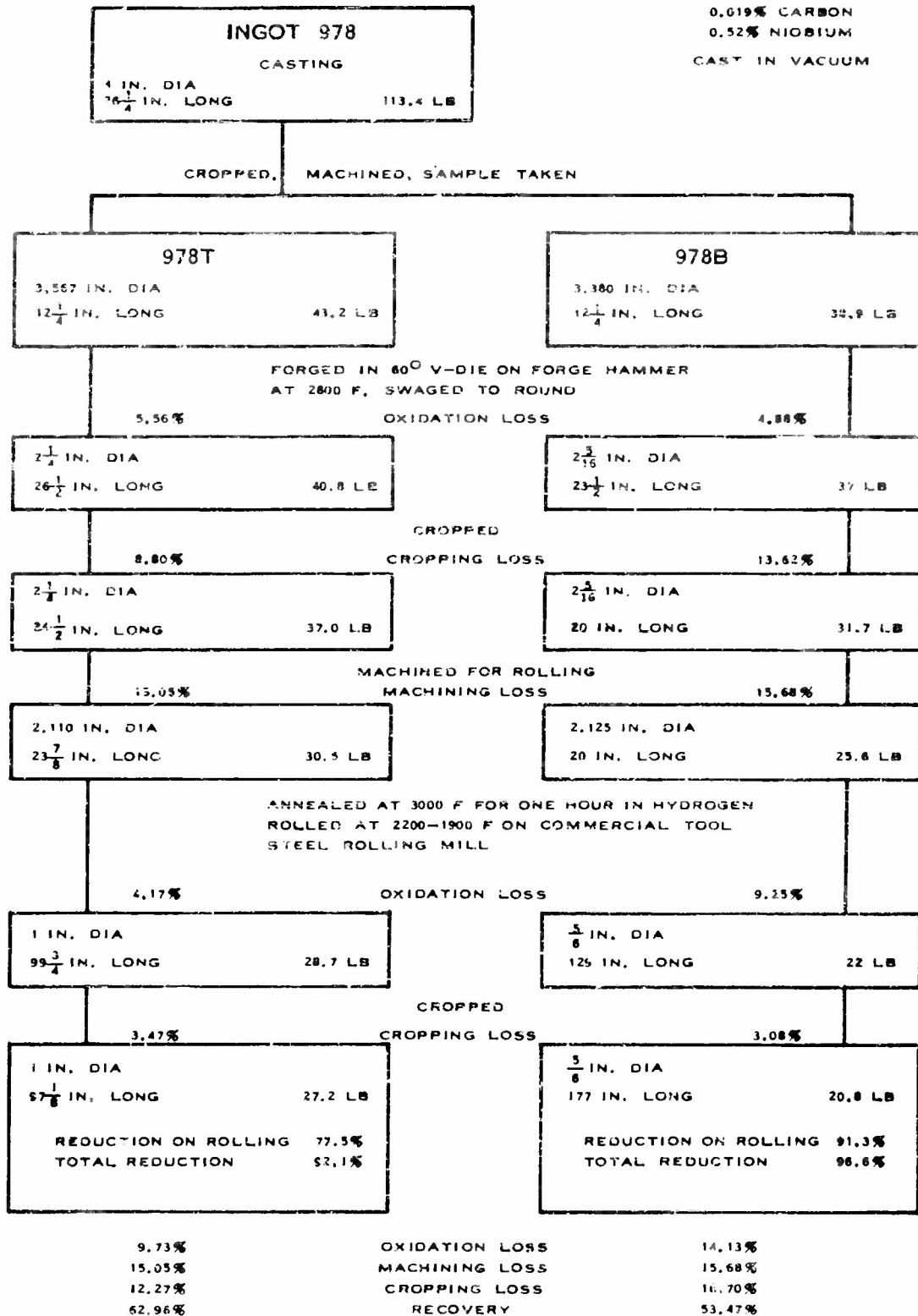


TABLE 3
4" DIAMETER INGOTS FORGED TO 2-1/4" DIAMETER AND ROLLED TO 1" AND 5/8" DIAMETER

Heat	Alloy, %	Forging Temp, F	Forging			Recovery on Forging, %	Rolling				Total Recovery, %
			Oxida- tion Loss, %	Crop- ping Loss, %	Machin- ing Loss, %		Rolled Dia, in.	Oxida- tion Loss, %	Crop- ping Loss, %	Machin- ing Loss, %	
987T	0.53 Al	2300-2600	cracked on forging								
987B		2600	6.79	3.29	12.96	76.95	5/8	14.2	8.23	12.95	64.61
983T	0.88 Al	3000	cracked on forging								
983B		3100	cracked on forging								
988T	0.24 Nb	2800	8.04	5.80	12.95	73.21	5/8	10.72	10.93	12.95	65.4
988B		2800	4.68	4.00	17.58	73.74	1	10.62	5.14	17.58	66.67
978T	0.52 Nb	2800	5.56	8.80	15.05	70.60	1	9.73	12.27	15.05	62.96
978B		2800	4.88	13.62	15.66	65.81	5/8	14.13	16.70	15.68	53.47
979T	0.75 Nb	3000	cracked on forging								
979B		3000	cracked on forging								
1008T	0.65 Ti	3000	cracked on forging								
1008B		2600-3000	cracked on forging								
1009T	1.26 Ti	2600	5.00	13.34	26.30	55.36	5/8	3.46	25.26	26.30	51.21
1009B		3000	cracked on forging								
1010B	1.92 Ti*	2600	cracked on forging								
1012T	0.56 V	2600	13.10	5.24	21.90	59.76	5/8	18.58	5.95	21.90	53.57
1012B		2600	6.16	9.55	25.28	58.60	1	7.42	10.66	25.28	56.64
1013T	1.14 V	2400	cracked on forging								
1013B		2400	cracked on forging								
1014B	1.39 V	2400	cracked on forging								

* added

Note: Heats 1045, 1048, and 1049 were 4" dia ingots forged to 1-1/4" dia and then rolled to 5/8" dia. Processing is shown in Flow Sheets, Figures 89-91.

during heating, forging was conducted in air. There is some evidence that internal oxidation of molybdenum and molybdenum-base alloys proceeds by means of preferential grain-boundary penetration. The process is accelerated by the formation of fine cracks on the surface during forging, and the penetration of oxide into the grain boundaries results in hot shortness.

About 50% recovery from the machined ingots is necessary if sufficient rolled stock is to be obtained for determination of the desired mechanical properties, when using the procedure outlined above. If the rolled stock is to be of uniform quality, the greater portion of hot working should be accomplished by rolling rather than by forging. If transverse cracks arise during the early stages of forging, the billet must be cut into short pieces and almost all of the subsequent reduction must be done by forging to produce the 20-inch-long blanks for rolling. Stock so produced is less uniform than that hot worked with a greater percentage of rolling.

Extrusion of Large Ingots

The Sejournet-Ugine extrusion process⁴ has been proved feasible for initial breakdown of large sections of vacuum-cast, unalloyed molybdenum and mild molybdenum-base alloys and yielded substantially greater recovery of sound metal than methods previously used. A series of ingots 7-1/2 to 8 inches in diameter was prepared for extrusion at Babcock and Wilcox Tube Company by the Sejournet-Ugine method. The ingots were machined to 6-1/2 inch diameter in preparation for extrusion.

A unique feature of the Sejournet-Ugine method is the use of glass as the lubricant for billet and die. In the method as it was conducted at Babcock and Wilcox, the hot billets were wrapped in fiber glass cloth and extruded through a die lubricated with wads of molten fiber glass in a horizontal hydraulic press limited to a force of 2400 tons. The 3-3/4 to 4-1/4 inch diameter dies were cleaned, sandblasted, and ground after each extrusion and then re-used. The diameter of the container was 6-3/4 inch. Force measurements were made with a Brush Recorder connected to SR-4 strain gages mounted on the tie rods of the press.

Extrusion data for 24 alloy ingots are presented in Table 4, and a typical flow sheet in Figure 22. The billets of the first group were preheated in a Salem furnace at 1600 F and then in a Selas gas-fired furnace at 2600 F. The time at 2600 F was 15 to 20 minutes. Two sheets of fiber glass were used as billet lubricant and three wads of fiber glass, three pieces of 1/8-inch-thick plate glass, and molybdenum disulfide were used between the die and the billet.

Because of the high extrusion pressures encountered in the first group, the billets of the second group were held for 30 to 45 minutes, which resulted in lowering of the pressures necessary for extrusion. As indicated in Table 4, the lubricants were different for the second group of billets. The die lubricant for the second group consisted of two wads of fiber glass and two plates 1/8 inch thick. One sheet of fiber glass equivalent in thickness to two of the sheets used for the first group was tried as the lubricant. This glass sheet was too heavy to be picked up easily by the billets heated to 2600 F in the gas-fired furnace. Barium chloride sprinkled on the fiber glass improved

TABLE 4
EXTRUSION DATA FOR MOLYBDENUM-BASE ALLOYS
6-1/2" Diameter Blanks

Group 1 - Billet lubricant: two sheets of fiber glass Die lubricant: 3 wads, 3 plates, and MoS ₂									
Heat	Alloy Content %	Length in.	Wt. lb.	Time at 2600 F, min.	Die Dia. in.	Pressure, tons		Dial	
						Brush Recorder Start	Run	Start	Run
1051	0.54 V	14-1/4	172	18	4	1780	1400		
1052	1.00 V	14-3/4	175	17	4	1830	1410	1800	1400
1053	1.24 V	9	106	15	4.25	1820	1520	1800	1400
1057	0.75 Nb	15-3/8	186	15	4	1600	1580		
1058	0.49 Al	13-1/8	157	25	4.25	1120	1120	1200	1200
1062	0.11 Zr	14	169	15	4	1600	1600		
1063	0.17 Al	18-3/8	222	15	4	1220	1160		
Group 2 - Billet lubricant: one sheet of fiber glass + BaCl ₂ Die lubricant: 2 wads, 2 plates Die diameter: 4"									
Heat	Alloy Content %	Length in.	Wt. lb.	Time at 2600F, min.	Ingot in Furn. at Temp.	Pressure, tons		Resistance to Deformation, psi	
						Brush Recorder Start	Run	Peak	Aver.
*1059	0.81 Al	15-3/16	172	54	44	1610	1430	69,000	61,200
1132B	0.47 Ti	12-1/4	149	90	55				
1133	0.90 Ti	15	159	73	59	1670	1670	71,500	71,500
1134	1.05 Ti	15	180	30	15	2280	1750	97,500	76,500
1138	1.27 Ti	15	179	38	25	1880	1880	80,800	80,800
1143	1.66 Ti	15	182	54	42	1800	1600	77,000	68,500
1144	0.07 Co	14-7/8	182	43	27	1670	1670	71,400	71,400
1145	0.12 Co	12-1/4	150	40	27	1930	1820	85,000	80,000
1146	0.17 Co	14-3/4	182	43	29	1930	1670	82,500	71,400
1147	1.10 Nb	14-1/2	172	49	32			sticker**	
1148	1.36 Nb	14-1/4	177	49	40	1790	1680	77,200	72,500
1149	0.22 Zr	13-1/4	162	45	35	2030	2030	88,600	88,600
1150	0.43 Zr	13-1/2	167	42	32	2400+		sticker***	
1151	1.25 V	13-5/8	165	54	43	1680	1570	73,400	68,500
1152	0.10 Si	14	171	50	40	1920	1710	83,000	74,000
1154	1.25 Al	12-3/4	152	46	36	1850	1570	79,000	69,000
1155	1.10 Al	13	155	54	43	1420	1580	69,500	62,300

* billet diameter was 6-3/8" instead of 6-1/2"

** insufficient billet lubrication

*** alloy too hard at 2600 F for extrusion on this press

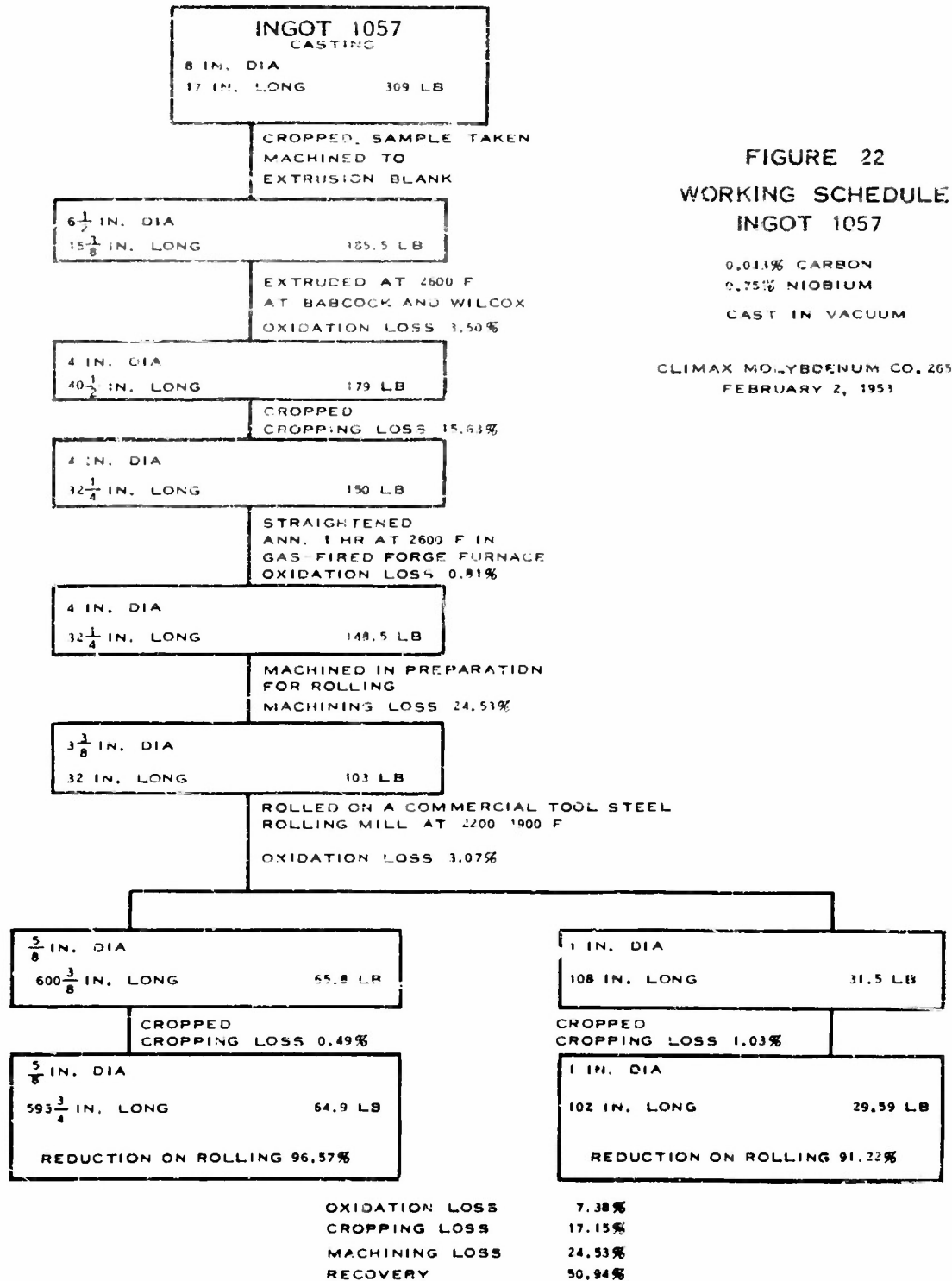


FIGURE 22
WORKING SCHEDULE
INGOT 1057

0.011% CARBON
0.75% NIOBIUM
CAST IN VACUUM

CLIMAX MOLYBDENUM CO., 265
FEBRUARY 2, 1953

the adherence of the cold glass blanket to the hot billet. The advantage of using barium chloride is obvious from the fact that the only reason for failure to extrude Billet 1147 was that inadvertently barium chloride had not been sprinkled on the fiber glass sheet. The fiber glass did not adhere to the billet, hence there was no lubrication for extrusion. The failure had nothing to do with alloy content or size of the billet. A second attempt to extrude this billet failed when the billet cracked severely. Ordinarily, if a billet fails to go through the press on the first attempt--whatever the reason--microcracks arise, which are rapidly propagated upon the second attempt at extrusion. In the present instance, cracking was not attributed to high alloy content but rather to the fact that re-extrusion was attempted. The difference in lubricating techniques between the two groups made little difference in extrusion pressure (compare the pressures for the 1.25% vanadium alloys).

Table 5 indicates the losses sustained during processing of the 6-1/2 inch diameter billets during extrusion and rolling. The greatest loss occurred on initial breakdown of the casting. The recovery of sound metal after extrusion was in the order of 65%. The loss during the first stage of working was due to the necessity of machining the surface to remove cracks, shown as machining loss in Table 5, prior to further working. The second large loss was due to cropping to remove end bursts--a loss which would be less, percentagewise, if longer billets were extruded. Typical end bursts are shown in Figure 23, and surface defects in Figures 24-27.

In general, as the concentration of a given alloying element was increased, the recovery of sound, extruded stock decreased. The addition of 0.81% aluminum, 0.11% cobalt, 0.75% niobium, 1.22% titanium, or 0.11% zirconium to molybdenum produced ingots that were extruded satisfactorily. The molybdenum-nickel alloy was not submitted for extrusion because it had been found to be incompletely deoxidized. The molybdenum-silicon alloy cracked on extrusion. The recovery of molybdenum-titanium alloys was erratic: the 1.22% titanium alloy extruded well, but the 1.05% titanium alloy cracked. The 0.43% zirconium alloy stopped the press. Failure to extrude was attributed to the high resistance of this alloy to deformation at 2600 F. Apparently, the upper limit of zirconium content for satisfactory extrusion at 2600 F on the 2400-ton press lies between 0.2 and 0.4%.

The extrusions were machined to remove surface defects and annealed for one hour at 2600-2800 F before being reduced further in cross section by rolling to 2 inches in diameter. Rolling was done at Universal-Cyclops Steel Corporation on a tool steel, hand round, rolling mill. From 2 inches in diameter the billets were rolled to 1 inch and 5/8 inch in diameter in a guide mill. As nearly as could be estimated, the furnace temperature was 2200 F. The bars were heated for rolling in a gas-fired furnace, and the number of passes between reheatings depended upon the resistance of the bar to rolling and "on-the-spot" decisions of the operators. The average reduction by rolling for the one-inch-diameter bars was 92.14% and for the 5/8-inch-diameter bars 97.78%. The loss due to rolling alone (oxidation and cracking) was about 12%. Only two bars which appeared to have extruded well failed on rolling, the 0.81% aluminum (1059) and the 0.11% zirconium (1062).

TABLE 5
RECOVERY ON EXTRUSION AND ROLLING OF 6-1/2" DIAMETER BILLETS

Heat	Alloy, %	Extrusion				Extrusion and Rolling			Total Recovery, %
		Oxidation Loss, %	Crop-ping Loss, %	Machining Loss, %	Recovery %	Oxidation Loss, %	Crop-ping Loss, %	Machining Loss, %	
937		5.80	7.03	23.03	64.13	8.32	11.93	23.03	56.71
1159			18.18	10.67	71.15		25.43	10.67	63.90
1063	0.17 Al	4.14	8.55	13.95	73.36	9.68	10.00	13.95	66.39
1058	0.49 Al	7.35	12.78	13.42	66.45	12.35	30.79	13.42	43.45
1059	0.81 Al	0.70	13.18	11.21	56.91	cracked on rolling			
1155	1.25 Al*	cracked on extrusion							
1154	1.37 Al*	cracked on extrusion							
1144	0.074 Co	1.59	15.02	31.30	52.08	1.59	28.01	31.30	39.09
1217	0.11 Co	1.14	21.83	31.77	45.26	1.14	37.77	31.77	29.31
	0.18 Ti								
1145	0.123 Co	cracked on extrusion							
1146	0.165 Co	cracked on extrusion							
1153	0.044 Ni	not extruded							
1001	0.31 Nb								
	0.16 Ti								
1057	0.75 Nb	4.31	15.63	24.53	55.53	7.38	17.15	24.53	50.94
1147	1.10 Nb	cracked on extrusion owing to lack of lubrication							
1148	1.36 Nb	cracked on extrusion							
1152	0.088 Si	cracked on extrusion							
1132	0.45 Ti	2.36	16.31	16.12	65.23	2.35	28.39	16.12	53.15
1133	0.85 Ti	1.89	21.38	16.60	60.13	1.89	36.23	16.60	45.28
1134	1.05 Ti	cracked on extrusion							
1138	1.22 Ti	1.68	12.10	21.23	64.99	1.68	26.21	21.23	50.87
1143	1.66 Ti	cracked on extrusion							
1051	0.54 V	6.39	13.37	12.50	67.73	11.39	22.26	12.50	53.84
1052	1.00 V	5.14	14.29	13.14	67.43	10.14	24.10	13.14	52.63
1053	1.24 V	cracked on extrusion							
1151	1.25 V	1.40	9.09	26.06	63.45	1.40	18.42	26.06	54.12
1207	0.09 Zr	1.94	21.67	29.28	47.11	1.94	32.61	29.28	36.17
1062	0.11 Zr	3.91	18.39	26.10	51.60	cracked on rolling			
1149	0.22 Zr	cracked on extrusion							
1150	0.43 Zr	stopped the extrusion press							

* added



FIGURE 23 -- CROPPED ENDS OF MOLYBDENUM-BASE ALLOY EXTRUSIONS, $\times \frac{1}{2}$
(P383)



FIGURE 24 — SURFACE OF EXTRUDED BILLET, X1
(P940)

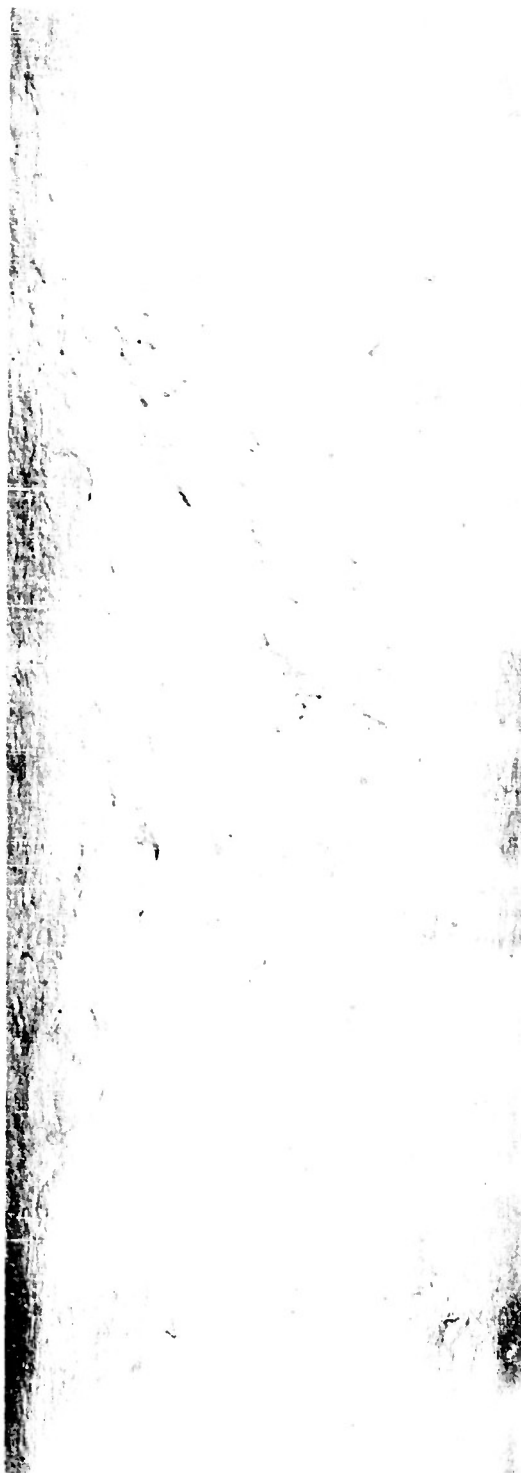


FIGURE 25 - SURFACE OF EXTRUDED BILLET, X1

(P938)

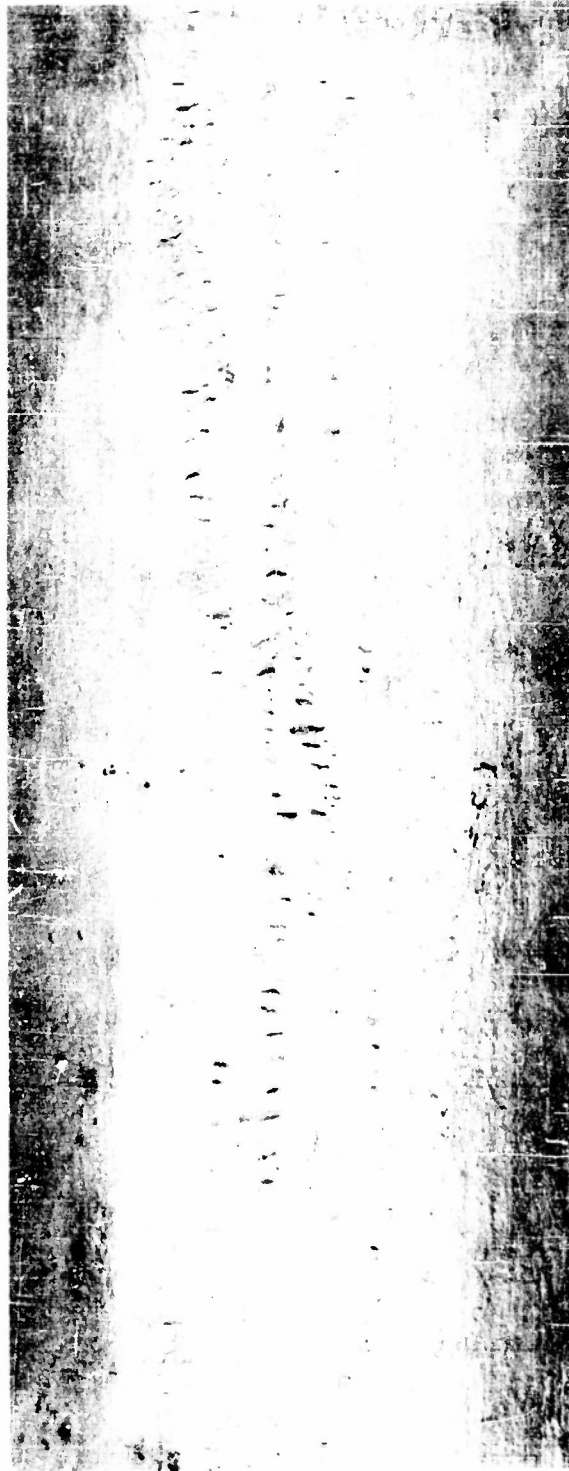


FIGURE 26 — SURFACE OF EXTRUDED BILLET, X1

(P939)

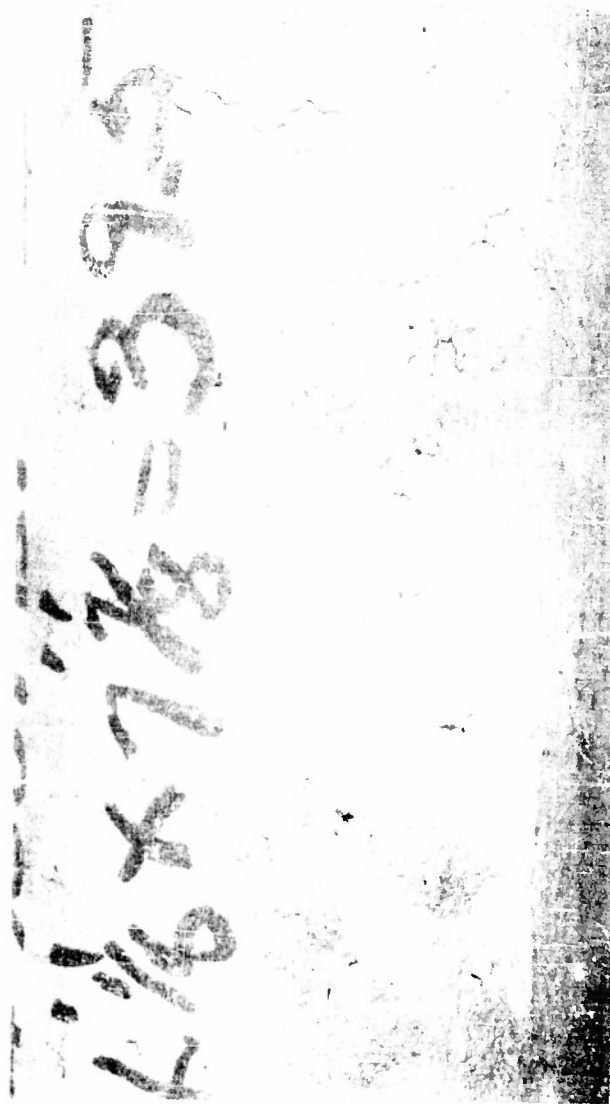


FIGURE 27 - SURFACE OF EXTRUDED BILLET, X1
(F941)

Extrusions from Four-Inch Diameter Ingots

In order to investigate the extrusion of smaller castings, several 1-1/4 inch diameter blanks were machined from 4-inch diameter castings and extruded on a full eccentric, 750-ton press designed for valve extrusion, at Thompson Products Company, Tapco Division. Glass lubrication was used on both billet and die--a fiber glass blanket 1/4 x 3-1/4 x 10 inches for the billet, and for the die a disk of plate glass 1/8 inch thick by 1-1/4 inch diameter with two wads of fiber glass cemented to each side with sodium silicate. The blanks were heated in a Globar furnace in argon to a maximum of 2650 F.

Four heats of moderately high alloy content were included in this group: 0.19% cobalt (1173), 3.59% titanium (1174), 1.46% vanadium (1175), and 1.43% aluminum (1176). In addition, two alloys were included for comparison of deoxidation practice and variation in rolling schedule: 0.31% niobium (1082) and 0.31% niobium - 0.16% titanium (1001). These last had been extruded previously at Babcock and Wilcox. Blanks 1-1/4 inch in diameter were machined directly from the Babcock and Wilcox extrusion of Ingot 1001, whereas the extrusion from Ingot 1082 was rolled to 1-1/4 inch diameter.

The ingot containing 1.43% aluminum was extruded, but the extrusion had a poor surface and some surface cracks. The other alloys extruded at Thompson Products were sound. In order to obtain more suitable stock for testing and to work the metal further, the bars extruded at Thompson Products were rolled at 2450 F to 1/2-inch diameter at the University of Michigan on a slow-speed, two-high rolling mill with square, oval, and round passes. The distance between the rolls could be varied, and rolling was more like hand-round than guide-mill rolling. A gas-fired furnace was used for heating the work to the rolling temperature. In these operations each bar was given two passes per heating; the reduction per heat was considerably less in these experimental operations than in the commercial rolling operations at Universal Cyclops.

Strain Hardening and Recrystallization

The potentialities of molybdenum-base alloys as structural materials for high-temperature applications make it imperative to determine quantitatively their mechanical properties at elevated temperatures and to investigate the significance of strain hardening and recrystallization processes on the mechanical properties at elevated temperatures. The binary molybdenum-base alloys under investigation are all terminal solid solutions in which an excess phase is regarded as an impurity. Two metallurgical methods of altering the mechanical properties of a single-phase solid solution are available, changing the concentration of alloying element and changing the degree of strain hardening. The addition of alloying elements which produce solid solutions develops small changes in mechanical properties, which gradually increase as the amount of alloy increases. The maximum amount of alloying element added to molybdenum is restricted by the difficulty in obtaining a product capable of beneficial plastic deformation. Strain hardening, on the other hand, brings about a marked change in mechanical properties, and these properties can be modified

by subsequent stress relieving and recrystallization. To retain the benefits obtained by strain hardening, however, the service temperature must be below the recrystallization temperature of the material in question.

Evaluation of the mechanical properties of wrought molybdenum-base, binary alloys must take into consideration not only composition changes, but also the structural condition of the material. The development of methods for working large bodies of molybdenum and molybdenum-base alloys is still in its infancy, and working schedules are dictated by existing equipment and the working temperatures available for other metals, particularly steel. These were used as a matter of expediency in producing wrought molybdenum and molybdenum-base alloys. In spite of the desirability of quantitative control of work hardening, such control was not attainable at this stage of the investigation.

The working of molybdenum and molybdenum-base alloys has been described in an earlier section. The temperature used for initial breakdown of the castings by extrusion (2600 F) produced a work-hardened structure. Annealing of the extruded billets in the temperature range 2800 to 3000 F was sufficient to accomplish at least partial recrystallization. The billets were then rolled in the temperature range 2200 to 1900 F. This temperature range was high enough that partial recrystallization could occur during rolling. Furthermore, such factors as number of passes per heating and finishing temperature could not be controlled; thus, the as-rolled bars were received in a variety of degrees of strain hardening. In view of these circumstances, determination of mechanical properties was conducted on specimens of a specific microstructure; that is, they were tested in the as-rolled, stress-relieved, and fully recrystallized conditions. These microstructures are defined as follows:

As Rolled - Grains elongated in the direction of working, obliterated grain boundaries, evidence of slip lines. Specimens were tested as received from the rolling mill, the bars were not reheated after the final pass.

Stress Relieved - Microstructure of essentially the same appearance as "as rolled". Specimens were held one hour at 1800 F. The beginning of recrystallization of the bulk of the alloys was observed in the temperature range 1900-2000 F. Therefore, 1800 F was arbitrarily selected as the stress-relieving temperature. In one instance, where recrystallization was observed at 1800 F, 1700 F was selected as the stress-relieving temperature.

Fully Recrystallized - New, unstrained grains supplant the cold worked structure. The annealing temperature was the minimum temperature to develop 100% recrystallization in one hour.

In the determination of recrystallization temperatures of wrought molybdenum-base alloys, the primary objective, then, was to establish the structural transition of the individual alloys. The recrystallization temperatures were determined to the nearest 50 degrees Fahrenheit by heating small samples for one hour, each at a different temperature, in hydrogen. The degree of recrystallization was determined by metallographic examination of each sample. Vickers hardness (10-kilogram load) was determined at room temperature on each sample after metallographic examination. Estimation of the temperature of complete recrystallization was based upon metallographic examination rather than upon hardness. It was found that in some cases the variations in degree of strain hardening overshadowed the effects of chemical composition. In spite of the limitations imposed by inability to control degree of cold work precisely, certain useful generalizations were derived from the recrystallization behavior of the bars in this investigation.

Table 6 presents recrystallization temperatures for virtually all of the bars tested to date under this contract. Figures C8-C16, Appendix C, are plots of hardness against annealing temperature for bars tested during the past year. The terminus of each line in the plots is intended to represent the temperature for complete recrystallization determined metallographically after an anneal of one hour.

The 1/2-inch diameter bars listed in Table 6 were rolled at 2300-2400 F at the University of Michigan from 3/4-inch diameter extrusions and sustained 33% hot cold-work on rolling. The 5/8- and 1-inch diameter bars were rolled at Universal-Cyclops from 3-inch to 4-inch diameter extrusions, and were reduced 97% by rolling at 2200-1900 F. Since cold working was less severe for the 1/2-inch diameter bars than for the 5/8-inch diameter bars, for comparable compositions the 1/2-inch bars recrystallized at a higher temperature than the 5/8-inch diameter bar stock. The 1-inch diameter bars, like the 1/2-inch bars, sustained less reduction on rolling than the 5/8-inch bars and consequently had higher recrystallization temperatures. This increase in recrystallization temperature was erratic, being only 50 degrees Fahrenheit for some of the bars and as much as 400 degrees for others. This undoubtedly reflects the variation in processing which was difficult to control.

Additions of aluminum to molybdenum in the range studied did not materially alter the recrystallization temperature of molybdenum. Cobalt alone among the alloying elements added resulted in recrystallization temperatures below that of unalloyed molybdenum. Niobium raised the recrystallization temperature slightly. Molybdenum-titanium alloys exhibited recrystallization temperatures from 2450 to 3000 F, significant increases over the recrystallization temperature of unalloyed molybdenum. The increases were proportional to titanium content only in the broadest sense. These data offer a good example of the dependence of recrystallization temperature on factors other than composition.

The recrystallization temperatures of molybdenum-vanadium alloys were only slightly higher, if at all, than those of unalloyed molybdenum.

TABLE 6

RECRYSTALLIZATION TEMPERATURES FOR MOLYBDENUM AND MOLYBDENUM-BASE ALLOYS

Bar	Composition %	Minimum Temperature, F, for Complete Recrystallization in 1 Hour for Bars of Indicated Diameter		
		1/2"	5/8"	1"
937	0.015 C		2150	
1159	0.040 C			2200
1045	LCA		2400	
1063	0.17 Al		2200	2250
1058	0.49 Al		2150	2300
987	0.53 Al		2200	
677	0.05 Co		2150	
1144	0.074 Co		2000	2150
1173	0.19 Co	2100		
988	0.24 Nb		2200	2500
1082	0.31 Nb	2300		
660	0.34 Nb		2150	
978	0.52 Nb		2200	2450
1057	0.75 Nb		2250	2300
1100	0.21 Ti	2700		
1132	0.45 Ti		2450	2600
1048	0.69 Ti (LCA)		2500	
1133	0.85 Ti		2500	2650
1138	1.22 Ti		2500	2600
1009	1.26 Ti		2900	
1080	1.41 Ti	2800		
651	2.29 Ti		2800	
885	2.46 Ti		2700	
1174	3.59 Ti	3000		
1051	0.54 V		2100	2500
1012	0.56 V		2150	2200
667	0.66 V		2150	
1049	0.85 V (LCA)		2500	
669	0.87 V		2250	
672	0.88 V	2500		
1052	1.00 V		2150	2350
1151	1.25 V		2200	2600
1175	1.46 V	2600		
1207	0.09 Zr		2750	2900
1217	0.18 Ti, 0.11 Co		2100	
1001	0.16 Ti, 0.31 Nb	2700		
1137	0.44 Ti, 0.23 Al	2700		

On the basis of weight percent, zirconium, of all of the alloying elements studied, exerted the most profound influence on recrystallization of molybdenum; the alloy containing 0.09% zirconium required a temperature 600 degrees Fahrenheit above the recrystallization temperature of unalloyed molybdenum to produce complete recrystallization.

Study of Figures C8-C16, Appendix C, shows that some of the bars tested attained the minimum hardness at temperatures significantly below those required for complete recrystallization as determined by metallographic inspection. The difference in temperatures is particularly marked in the molybdenum-titanium alloys, which recrystallize at temperatures between 2800 and 3000 F, and the 0.54% vanadium alloy (see Figure C13, Heat 1051, 1-inch diameter). It has been observed that the alloys are 95 to 99% recrystallized at the lowest temperature corresponding to minimum hardness but that temperatures several hundred degrees higher are required to remove the last remnants of worked structure. It is evident that for bars exhibiting this type of behavior, values reported for recrystallization temperature would be misleading if it were not noted that softening and loss of strength had occurred at a lower temperature. The molybdenum-zirconium alloy (1207) did not behave in this manner; attainment of minimum hardness corresponded with full recrystallization.

Lack of time prevented a complete treatment of all the alloys, but a quantitative evaluation of the effect of cold work on recrystallization temperature was conducted on a 0.66% vanadium alloy. Rolled stock 5/8 inch in diameter was fully recrystallized by heating one hour at 2150 F. Specimens one inch long from the recrystallized stock were upset at 1700 F in such a way as to obtain 5, 10, 25, 50, 75, and 90% "cold reduction". The degree of strain hardening as a function of percent reduction is shown in Figure 28. The minimum recrystallization temperature (nearest 50 F) for one-hour anneal is also shown as a function of the degree of cold work. Table 7 presents the grain size developed on full recrystallization after various degrees of cold work. The grain boundary intercept method was used to obtain a numerical representation of grain size. This method involved magnifying a polished and etched specimen 500 times and counting the number of grain boundaries intercepting a line five inches long. The numerical average of twenty such readings obtained at random positions on each specimen was taken as the grain size. By this method, the larger the reported number, the finer the grain size. Table 7 also shows the lowering of recrystallization temperature for 50% and 90% reduction when the annealing time at temperature is increased from one hour to 100 hours, as well as the corresponding grain size after annealing. These data indicate that molybdenum alloys behave as other metals in that the less the amount of cold work, the higher the recrystallization temperature and the coarser the grain upon complete recrystallization. Furthermore, recrystallization temperature falls rapidly as the amount of reduction increases to 25%. When the amount of cold work exceeds 25%, however, there is little change in recrystallization temperature.

In the process of examination of the progress of recrystallization in molybdenum and molybdenum-base alloys, it was evident that molybdenum behaved in the classical manner², that is, by means of recovery, primary recrystallization, grain growth, and secondary recrystallization. To illustrate the

CLIMAX MOLYBDENUM CO. 474

NOVEMBER 3, 1953

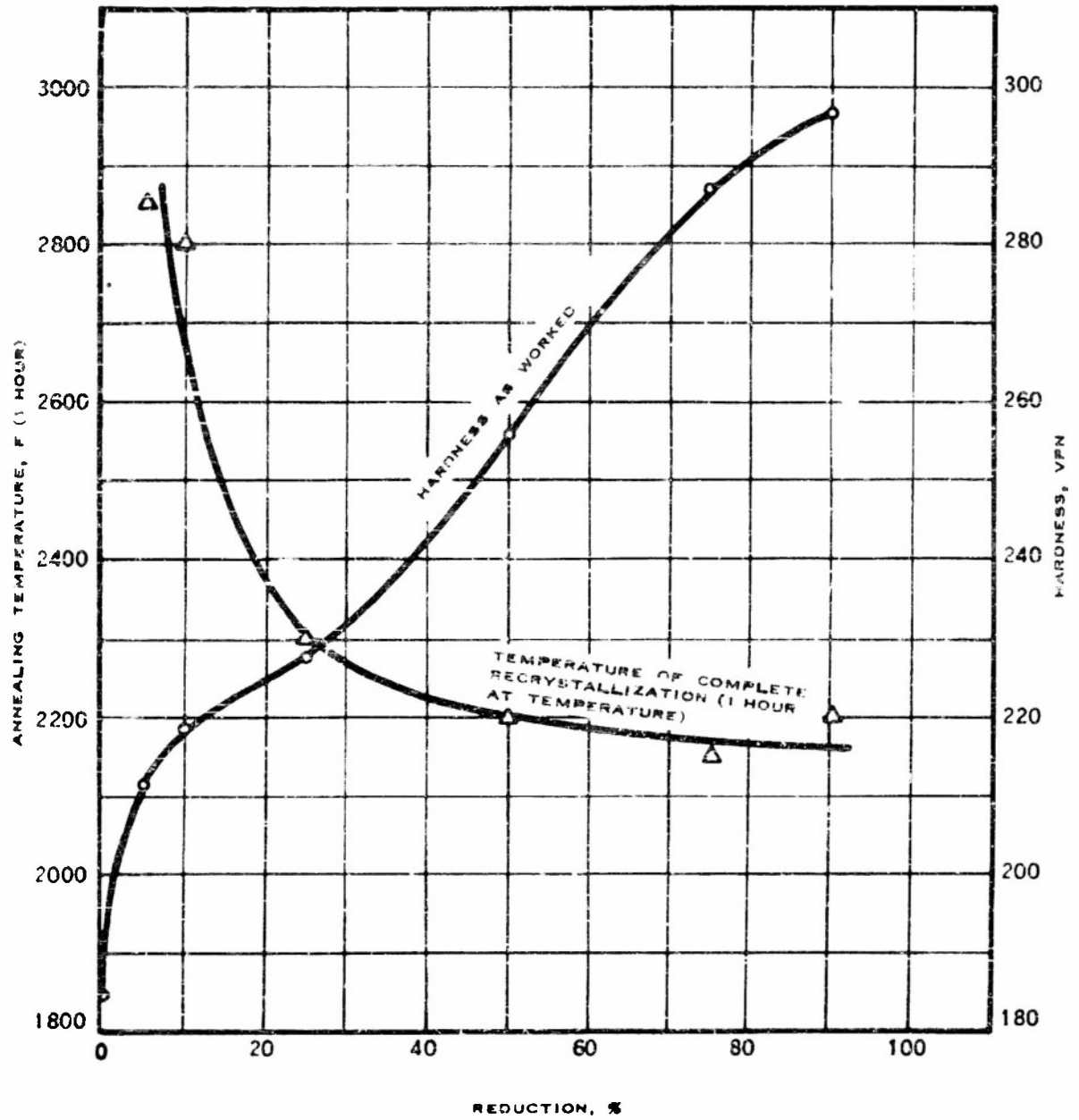


FIGURE 28 - HARDNESS AND RECRYSTALLIZATION TEMPERATURE AS A FUNCTION OF AMOUNT OF REDUCTION FOR 0.66% VANADIUM-MOLYBDENUM ALLOY

TABLE 7

GRAIN SIZE AND RECRYSTALLIZATION TEMPERATURE OF A
0.66% VANADIUM - MOLYBDENUM ALLOY AS A FUNCTION OF
AMOUNT OF COLD WORK

Reduction %	Recrystallization Temperature, F	Grain Boundaries Per 0.01 In.
1 hour at temperature		
5	2850	1.6
10	2800	3.9
25	2300	8.0
50	2200	12.9
75	2150	16.0
90	2200	17.1
100 hours at temperature		
50	2000	9.2
90	1800	15.0

changes in structure of deformed molybdenum upon heating, the following experiments were performed: a selected area of cold-worked molybdenum was examined after various heat treatments in a protective atmosphere. Inasmuch as the annealing treatments were carried out in a reducing atmosphere (in purified hydrogen) which removed the oxide produced by etching, it was necessary to re-etch the surfaces under study after each heat treatment. It was not necessary, however, to repolish the specimen after each heat treatment. This method permitted close scrutiny of the changes that occurred in specific types of structures and, consequently, some insight into the recrystallization process.

Figure 29 is a photomicrograph at 1000 diameters of 5/8-inch-diameter Bar 937 (0.015% carbon) as rolled. The elongation of the original grains and intragranular fragmentation are typical of molybdenum and molybdenum-base alloys that have not sustained extreme cold work, that is, where cold work was conducted at sufficiently elevated temperature or where the amount of plastic deformation was low.

Figure 30 shows the structure of the same bar, but not the same area, after an anneal of one hour at 2000 F. Several nearly equiaxed, recrystallized grains formed and the subgrain boundaries became more distinct. The sharpening of subgrain boundaries occurred as a result of heat treatment in the temperature range where recovery takes place. The subgrains evident in Figure 30 and in subsequent photomicrographs are thought to be representative of the reorientation-domain type of structure.

Figures 31-40 reveal the same area after indicated periods of exposure at 2100 F in an atmosphere of purified hydrogen. The formation of a stress-free grain at a reorientation-domain boundary may be observed in the area marked "1" on the photomicrographs. After one hour at 2000 F, Figure 30, Area "1" appears only as a reorientation-domain boundary somewhat more distinct than most of its neighbors. The area was not materially altered by heating 10 or 20 minutes at 2100 F, Figures 31-32, but after a total exposure of 60 minutes the boundary was noticeably broadened. Repolishing the specimen, removing a minimum of surface, revealed that a clear etching grain had formed in this area. Subsequent heating of the specimen resulted in growth of the newly formed grain to the large size shown in Figure 36.

Figures 30-36 illustrate the continual shifting and changing in shape with increasing time at temperature of the grain marked "2", even though recrystallization was not complete. Figures 37-40 illustrate additional changes in Grain 2 after recrystallization in the immediate area was complete. The behavior of Grain 2 in these photomicrographs is illustrative of several axioms concerning grain growth⁶:

1. Grain growth occurs by grain boundary migration, not by coalescence of adjacent grains.
2. A curved boundary migrates toward its center of curvature.
3. Grain boundary migration may be retarded by inclusions or voids.
4. Where grain boundaries meet at angles different from 120 degrees, the grain included by the more acute angle will be consumed, so that all angles approach 120 degrees.

The validity of the grain boundary migration theory is confirmed in Figure 39, where the shadows (lines remaining on the surface under study resulting from previous etchings of the sample) clearly indicate the migration of the boundary. The shadows in this case also illustrate the movement of curved grain boundaries toward their centers of curvature. The retardation of grain boundary migration is clearly evident in Figures 31-35. In Figure 31, a small spherical void is observed just below Grain 2. The boundary of this grain migrated until it touched the void after 40 minutes at 2100 F, Figure 33. In subsequent heatings, the boundary curved around the void, suggesting that the void retarded migration.

In Figure 37, the angle formed by the boundaries at the upper left of Grain 2 is less than 120 degrees. Migrations upon subsequent heatings seem to confirm the theory that grains of this geometry tend to be consumed during grain growth.

In order to show the process of recrystallization in a less severely worked sample, a second series of photomicrographs was made, Figures 41-43. The sample used for this series was taken from a completed stress-rupture specimen from Bar 937 (unalloyed molybdenum). The stress-rupture specimen



FIGURE 29 — AS ROLLED, ELECTRO-POLISHED (M2825)



FIGURE 30 — ANNEALED 1 HOUR AT 2000 F, ELECTROPOLISHED (M2839)



FIGURE 31 — ANNEALED 1 HOUR AT 2000 F + 10 MIN. AT 2100 F (M2840)



FIGURE 32 — ANNEALED 1 HOUR AT 2000 F + 20 MIN. AT 2100 F (M2864)

PROGRESS OF RECRYSTALLIZATION IN UNALLOYED MOLYBDENUM

HEAT 937, 0.015% CARBON, 5 R IN. DIA ROLLED BAR, ETCHED IN SODIUM HYDROXIDE + POTASSIUM FERRICYANIDE SOLUTION, X1000



FIGURE 33 — ANNEALED 1 HOUR AT 2000 F
+ 10 MIN. AT 2100 F (M2873)



FIGURE 34 — ANNEALED 1 HOUR AT 2000 F
+ 60 MIN. AT 2100 F (M2875)



FIGURE 35 — ANNEALED 1 HOUR AT 2000 F
+ 100 MIN. AT 2100 F (M2877)

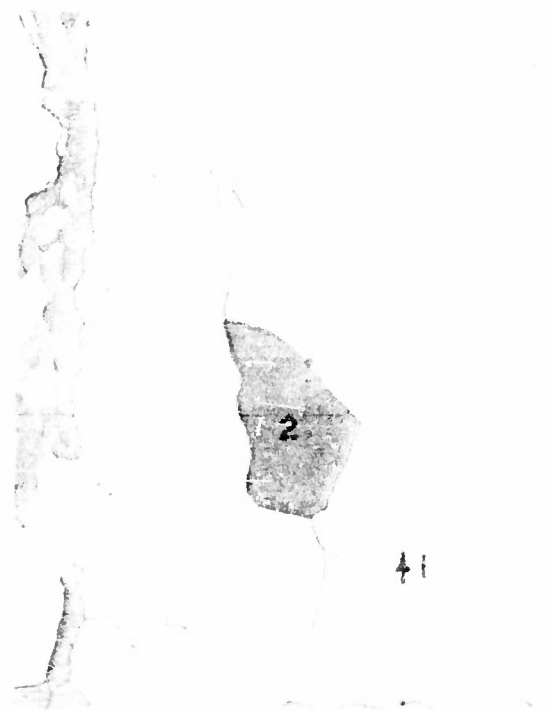


FIGURE 36 — ANNEALED 1 HOUR AT 2000 F +
100 MIN. AT 2100 F, REPOLISHED
15 SEC. AND ETCHED (M2878)

PROGRESS OF RECRYSTALLIZATION IN UNALLOYED MOLYBDENUM
(CONTINUED)

ETCHED IN SODIUM HYDROXIDE + POTASSIUM FERRICYANIDE SOLUTION, X1000



FIGURE 37 — ANNEALED 1 HOUR AT 2000 F
+ 160 MIN. AT 2100 F (M2879)

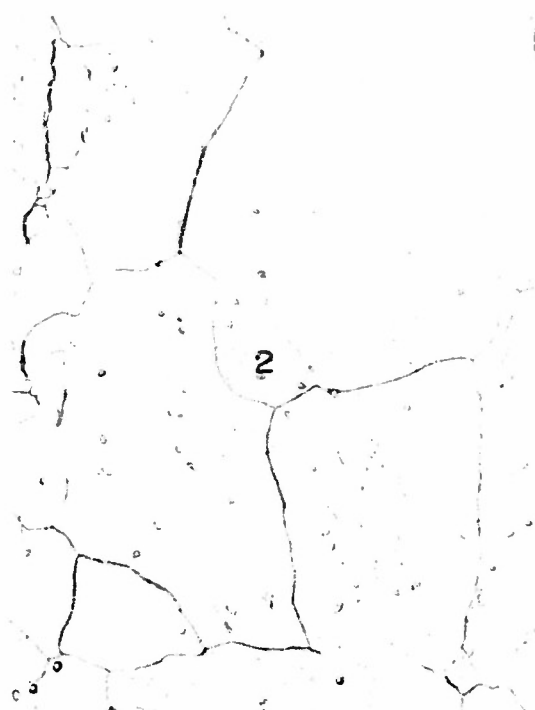


FIGURE 38 — ANNEALED 1 HOUR AT 2000 F
+ 250 MIN. AT 2100 F (M2890)



FIGURE 39 — ANNEALED 1 HOUR AT 2000 F
+ 370 MIN. AT 2100 F (M2968)

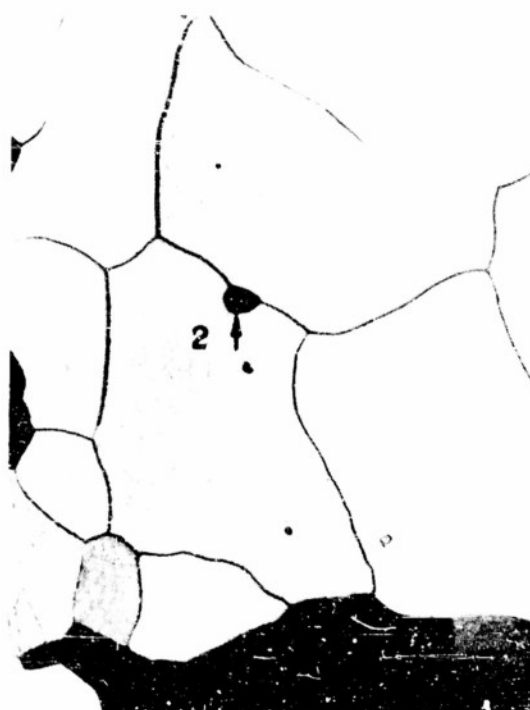


FIGURE 40 — ANNEALED 1 HOUR AT 2000 F +
370 MIN. AT 2100 F, REPOLISHED
15 SEC. AND ETCHED (M2969)

PROGRESS OF RECRYSTALLIZATION IN UNALLOYED MOLYBDENUM
(CONTINUED)

ETCHED IN SODIUM HYDROXIDE + POTASSIUM FERRICYANIDE SOLUTION, X1000



FIGURE 41 — AS TESTED IN STRESS
RUPTURE, ELECTROPOLISHED
(M3199)



FIGURE 42 — ANNEALED 1 HOUR AT 2200 F
AFTER STRESS-RUPTURE TEST
(M3201)



FIGURE 43 — ANNEALED 1 HOUR AT 2300 F
AFTER STRESS-RUPTURE TEST
(M3202)

RECRYSTALLIZATION OF STRESS-RUPTURE SPECIMEN 937

RUPTURE IN 2 HOURS AT 1600 F AND 22,300 PSI, ETCHED IN SODIUM
HYDROXIDE + POTASSIUM FERRICYANIDE SOLUTION, X1000

was fully recrystallized and then tested in stress rupture, sustaining a load of 22,300 psi for two hours at 1600 F. The amount of work hardening in this specimen was maximum at the location of the fracture and gradually decreased as the distance from the fracture increased, until it was essentially nil in the threaded portion. Figure 41 is a photomicrograph of the specimen after stress-rupture testing and shows the strain hardened structure. There is no evidence of recrystallization. The structural changes shown in Figures 42-43 occurred upon heating the specimen for one hour at 2200 and 2300 F, respectively. The shapes of the grains and appearance of the network within the grains changed upon recrystallization. High energy areas, and hence the first evidences of recrystallization, would be expected at intersections of the original grain boundaries. Several such areas, marked "X" in the large grain of Figure 41, are sites of new grains after a one-hour anneal at 2200 F. One hour at 2300 F, Figure 43, resulted in growth of these new grains, as well as a sharper delineation of the subgrain structure.

Virtually complete recrystallization with a large, yet heterogeneous grain size accompanied an anneal of one hour at 2400 F for the structure under observation. The coarse recrystallized grain size was undoubtedly associated with the low level of cold work at this position on the rupture sample.

The techniques used in this study are subject to three shortcomings:

1. Strains may be superimposed upon existing strains by heating and cooling the specimen between room temperature and the annealing temperature.
2. The etching treatment per se might modify the subsequent course of recrystallization.
3. Energy requirements for structural changes in two dimensions probably differ from those of unrestricted three-dimensional changes.

Grain Size and Grain Growth

Grain size determinations were made on samples of all of the wrought materials studied after heat treatment at the lowest temperature required to produce complete recrystallization. The grain boundary intercept method already described was used to obtain a numerical representation of grain size.

Table 8 lists grain sizes of wrought and recrystallized molybdenum and molybdenum-base alloys. From examination of the data, no generalizations can be drawn regarding type or amount of alloy and recrystallized grain size. Furthermore, there is no correlation between grain size and carbon content. Like other metals, however, molybdenum and molybdenum-base alloys have finer grains, the greater the amount of prior deformation. The general relationship is shown in Figure 44, where the hardness as rolled (a measure of prior deformation) is plotted against size of the recrystallized grains. The higher the hardness as worked, again the finer the size of the recrystallized grains. The 1/2-inch diameter bars processed by extrusion of 1-1/4 inch

TABLE 8

GRAIN SIZE OF WROUGHT AND RECRYSTALLIZED MOLYBDENUM AND MOLYBDENUM-BASE ALLOYS

Heat	Carbon, %	Alloy, %	Grain Size, Grains per 0.01"			
			1/2" dia bar	5/8" dia bar	1" dia bar	3/8" flat
937	0.015			9.3		
1159	0.040				5.6	
1045	0.0026	LCA		4.4		
1063	0.003	0.17 Al		11.6	3.8	
1058	0.006	0.49 Al		9.4	5.9	
987	0.003	0.53 Al		9.9		
1144	0.020	0.074 Co		19.8	9.4	
1173	0.037	0.19 Co	9.3			
1274	0.031	0.12 Cr				7.1
1272	0.022	0.10 Fe				3.5
988	0.019	0.24 Nb		9.8	1.6	
1082	0.032	0.31 Nb	7.6			
978	0.019	0.52 Nb		11.1	2.8	
1057	0.033	0.75 Nb		12.4	7.5	
1269	0.017	0.04 Ni				3.5
1273	0.030	0.09 Si				8.7
1100	0.015	0.21 Ti	2.0			
1132	0.024	0.45 Ti		14.4	11.5	
1048	0.0028	0.69 Ti, LCA		7.0		
1133	0.014	0.85 Ti		10.9	7.7	
1138	0.014	1.22 Ti		10.9	5.7	
1009	0.036	1.26 Ti		9.6		
1080	0.036	1.41 Ti	9.0			
1174	0.027	3.59 Ti	5.8			
1051	0.027	0.54 V		13.4	8.5	
1012	0.030	0.56 V		12.9	7.2	
1049	0.0012	0.85 V, LCA		5.6		
672	0.057	0.88 V	4.9			
1052	0.029	1.00 V		12.1	10.4	
1151	0.006	1.25 V		17.4	4.4	
1175	0.033	1.46 V	5.3			
1205	0.010	0.056 Zr				6.4
1207	0.019	0.09 Zr		12.6	8.3	
1001	0.032	0.31 Nb, 0.16 Ti	13.0			
1137	0.003	0.44 Ti, 0.23 Al	2.5			
1217	0.030	0.11 Co, 0.18 Ti		17.6		

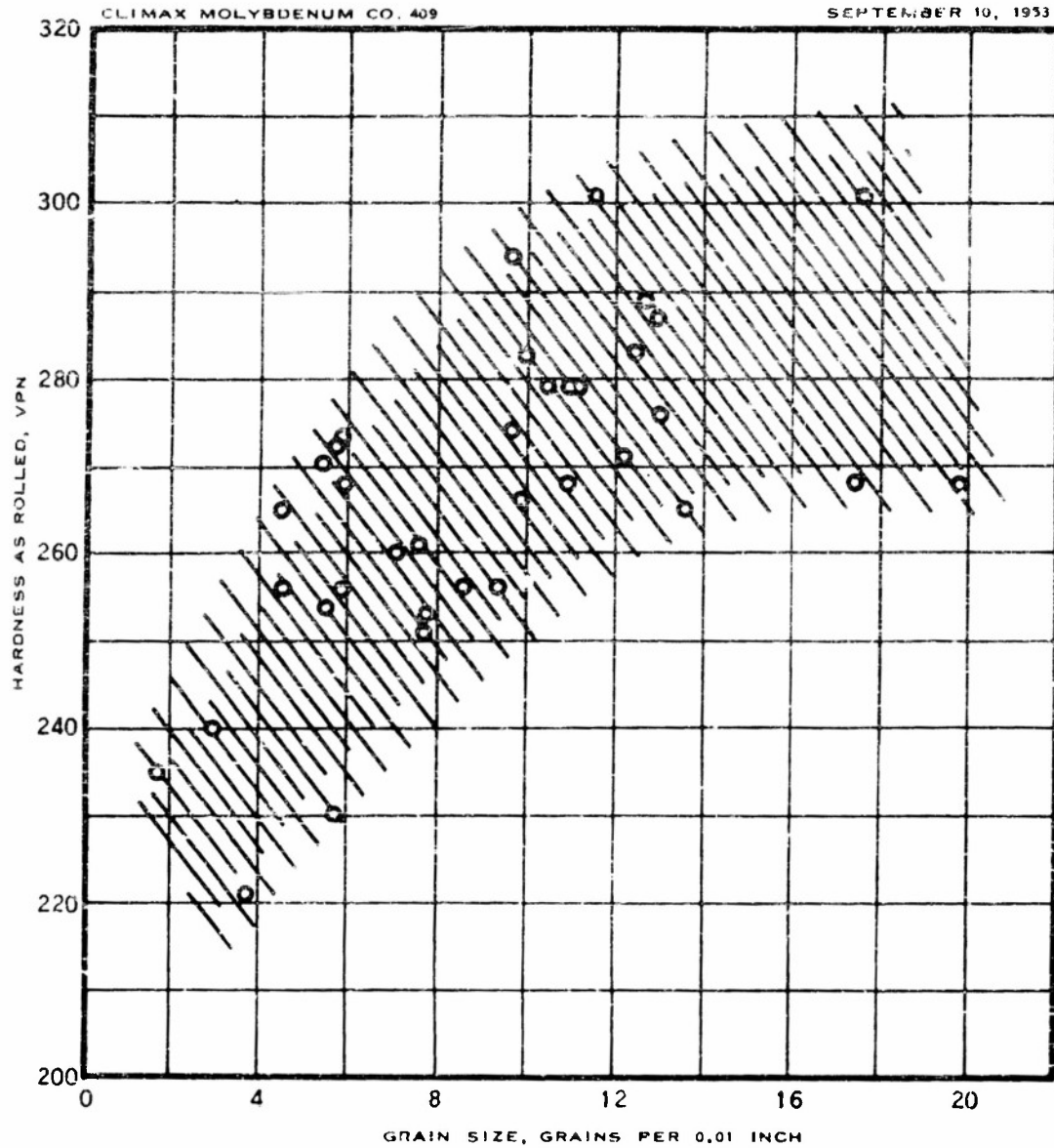


FIGURE 44 — RELATIONSHIP BETWEEN RECRYSTALLIZED GRAIN SIZE AND AS-ROLLED HARDNESS OF MOLYBDENUM AND MOLYBDENUM-BASE ALLOYS

diameter blanks to 3/4-inch diameter and then rolled to 1/2 inch at a higher temperature than for the 5/8-inch diameter bars were relatively coarse grained. As would be anticipated, the coarse grain size associated with smaller amounts of working and higher temperature of deformation of the 1/2-inch bars is consistent with accepted theory relating amount of cold work and recrystallized grain size.

One correlation seems consistent: the bars from heats deoxidized with rare earth metals are coarser grained after recrystallization than bars rolled from similar heats deoxidized with carbon.

The tendency toward grain coarsening of the alloys under consideration was investigated. Small samples from wrought sections of each alloy were heated for one-hour periods at temperatures up to 3900 F. The grain size was determined again by the grain boundary intercept method. The results are summarized in Figure 45, which is a plot of grain size against annealing temperature for one alloy from each system under study. Plots including all of the data obtained under this investigation may be found in Figures C17-C18, Appendix C.

The results of this work show that none of the alloying elements had a significant effect on grain size after one hour at 3700 F or above, all the alloys having grain sizes similar to the grain size of unalloyed molybdenum. Vanadium was the most effective in inhibiting grain growth at temperatures below 3700 F.

Mechanical Properties of Wrought Alloys

Hardness

Vickers hardness has been determined from room temperature to 1600 F on rolled bars 1/2, 5/8, and 1 inch in diameter, in three structural conditions, i.e., as rolled, stress relieved, and fully recrystallized. Plots of hardness as a function of testing temperature are contained in Figures C19-C46, Appendix C. Figures 46-47 summarize these data by comparing the hardness at 1600 F of all of the bars tested in the stress relieved and fully recrystallized conditions.

In general, the observations noted for hot hardness of cast alloys hold for wrought alloys of similar composition. On the basis of weight-percent of alloying element, cobalt appears to exert the most profound influence on elevated temperature hardness. Zirconium and aluminum follow in decreasing order with respect to relative hardening effect. Although the hardness of unalloyed molybdenum at 1600 F is enhanced by additions of niobium, titanium, and vanadium, these elements must be present in greater amount than cobalt to bring the hardness near that of the molybdenum-cobalt alloys. The greatest hardness at 1600 F for a stress-relieved specimen was exhibited by the 0.11%

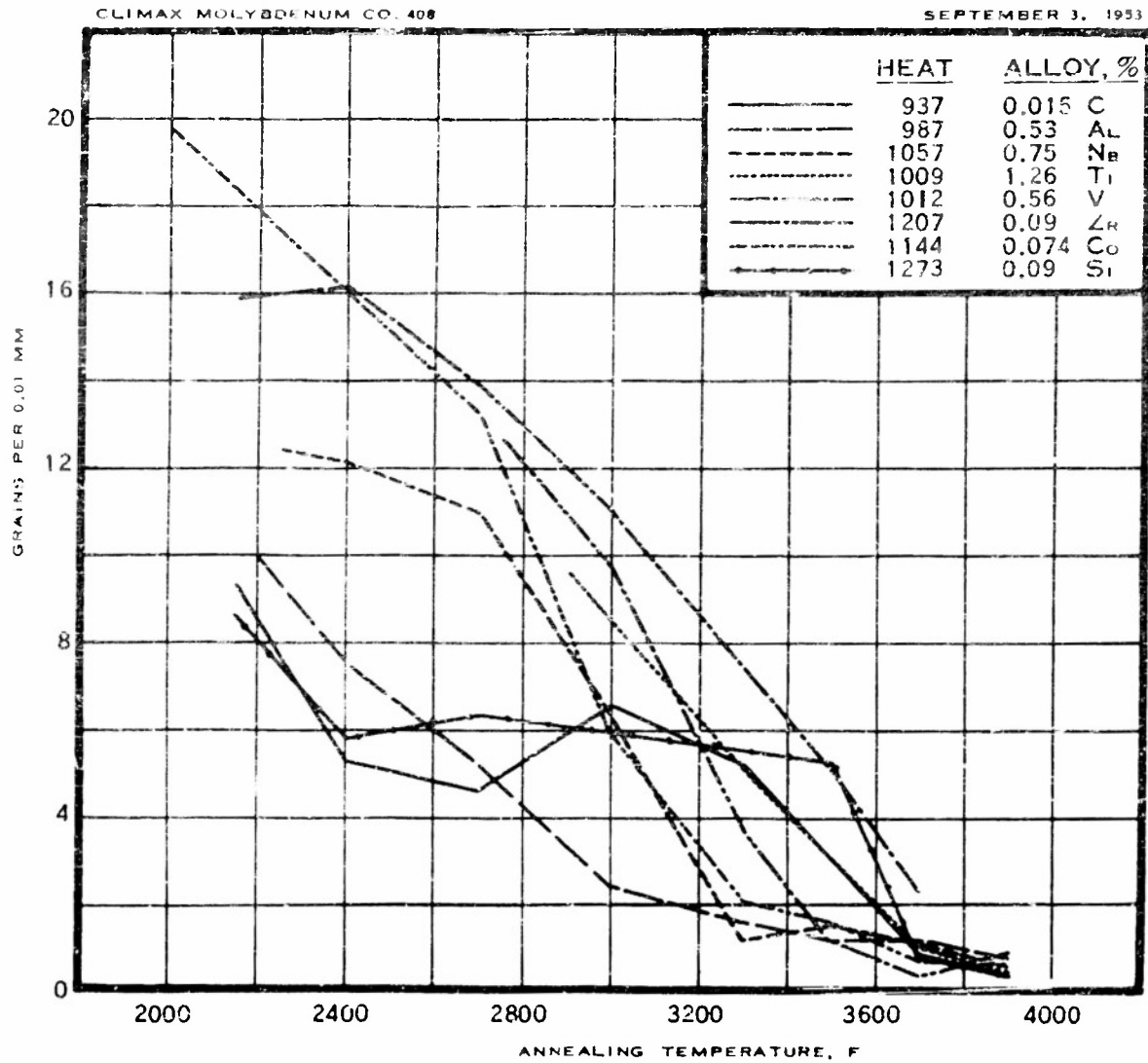


FIGURE 45 — EFFECT OF ANNEALING TEMPERATURE ON GRAIN SIZE OF INDICATED ALLOYS

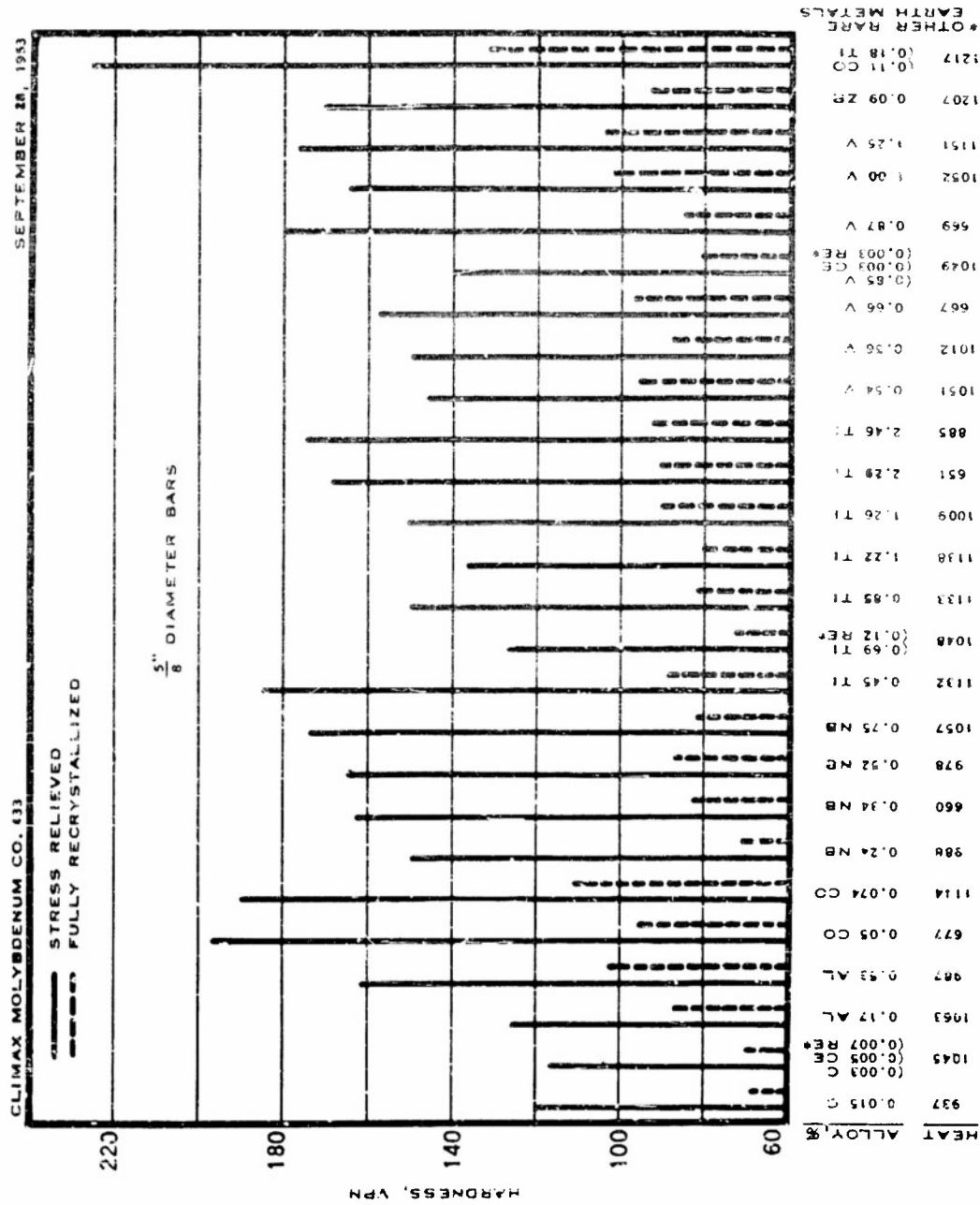


FIGURE 46 - HARDNESS AT 1600 F OF 5" DIAMETER MOLYBDE, 11M AND MOLYBDENUM-BASE ALLOYS

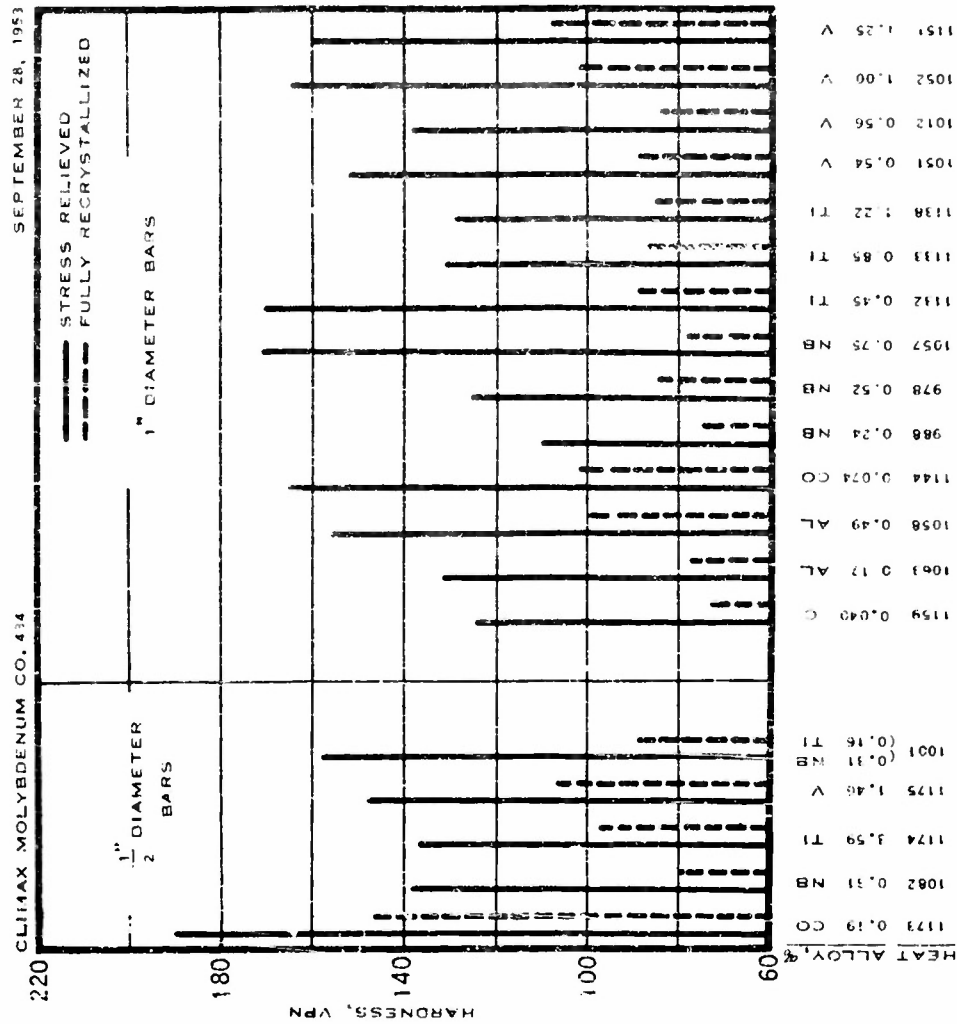


FIGURE 47 — HARDNESS AT 1600 F OF INDICATED $\frac{1}{2}$ " AND 1" DIAMETER MOLYBDENUM AND MOLYBDENUM-BASE ALLOYS

cobalt alloy containing 0.18% titanium (1173). The highest hardness for a fully recrystallized specimen at 1600 F was exhibited by the 0.19% cobalt alloy (1173), followed closely by the 0.11% cobalt-0.18% titanium alloy.

Deoxidation with rare earth metals did not noticeably alter the hot hardness of unalloyed molybdenum. The hardness of titanium and vanadium alloys deoxidized with rare earth metals was somewhat lower, however, than would be predicted on the basis of data on heats deoxidized with carbon.

The effect of bar size on hot hardness of fully recrystallized specimens was practically negligible. In the as-rolled or stress-relieved conditions, the 5/8-inch bars were slightly harder as a rule than the 1-inch bars from room temperature to 1600 F. The hardness differential between 5/8-inch and 1-inch diameter bars of like composition was not so great as the difference in tensile strength, as noted later in this report. Probably, in the case of the tensile tests, a specimen size factor was present in addition to the factor of amount of hot-cold work.

The drop in hardness from room temperature to 1600 F for a representative group of bars is presented in Table 9. Curves of hardness as a function of testing temperature for unalloyed molybdenum, Figures C19-C48, Appendix C, reveal a rapid decline in hardness from room temperature to about 400 F. Bars showing a high differential in hardness between room temperature and 1600 F behave in approximately the same manner as unalloyed molybdenum, with a rapid change in hardness from room temperature to 600 F. As the decline in hardness noted in Table 9 becomes smaller, however, the relationship of hardness to testing temperature approaches linearity.

Tensile Strength

Tensile tests at room temperature, 750, 1200, and 1600 F have been conducted on 5/8-inch and 1-inch-diameter stock. The structural conditions represented in these tests were as rolled, stress-relieved, and fully recrystallized. Unalloyed molybdenum bars in both sizes were included in the program to furnish datum points with which to compare binary molybdenum-base alloys containing aluminum, cobalt, niobium, titanium, vanadium, and zirconium, respectively.

In addition, tensile tests were conducted at room temperature on 1/2-inch diameter bar stock rolled at the University of Michigan from small extrusions made at Thompson Products Company.

Gage sections for specimens machined from 1/2- or 5/8-inch-diameter bars were 0.250 inch in diameter by 1-1/4 inch long; from 1-inch diameter bars, 0.475 inch in diameter by 2-3/8 inch long. All tests were run at strain rates of 3% per hour during elastic deformation and 60% per hour during plastic deformation. Stress-strain records were obtained for each test, and for specimens not exhibiting a drop in load at the yield 0.1% offset yield strengths were calculated.

TABLE 9

DECLINE IN HARDNESS BETWEEN ROOM TEMPERATURE AND 1600 F FOR
RECRYSTALLIZED MOLYBDENUM AND MOLYBDENUM-BASE ALLOY BARS

Ingot	Alloy, %	Bar Diameter	Decline in Hardness
		In.	Rm. Temp. to 1600 F, VFN
937	0.015 C	5/8	120
1159	0.040 C	1	124
1045	0.005 Ce 0.007 RE	5/8	124
1063	0.17 Al	5/8 1	76 88
1058	0.49 Al	1	81
1144	0.074 Co	5/8 1	69 62
1217	0.11 Co 0.18 Ti	5/8	56
1173	0.19 Co	1/2	47
988	0.24 Nb	5/8 1	121 115
1132	0.45 Ti	5/8 1	109 107
1138	1.22 Ti	5/8 1	124 116
1012	0.56 V	5/8 1	121 104
1151	1.25 V	5/8 1	89 70
1207	0.09 Zr	5/8	108

A partial pressure of argon was maintained within the furnace to minimize oxidation of specimens tested at 750 F and above. Periodic dimensional checks were made on the shoulders of specimens tested at elevated temperatures, and in no instance was the reduction in diameter due to oxidation in excess of 1%. Tensile transition tests run at temperatures from -30 to +250 F were conducted upon specimens immersed in suitable liquid media heated or cooled to the testing temperature.

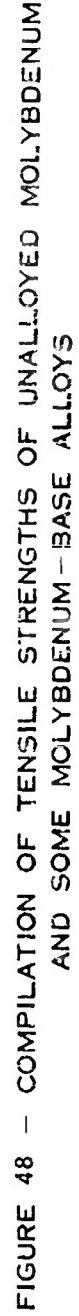
A tabulation of tensile test data may be found in Table C1, Appendix C. Charts of tensile strength as a function of testing temperature are also presented in Appendix C, Figures C47-C52. Figure 48 is a chart summarizing the tensile data.

The highest strength developed by any of the bars under test was 132,100 psi, displayed by the 5/8-inch diameter bar of 0.45% titanium alloy (1132) at room temperature after stress relief at 1800 F. The highest strength at 1600 F was 88,600 psi for the 1.25% vanadium alloy (1151) at 5/8-inch diameter. This was followed closely by the 0.45% titanium alloy, 88,300 psi at 1600 F. Both bars exhibited these properties after stress relief. The highest strength for 1-inch-diameter bars was 115,000 psi at room temperature and 78,400 psi at 1600 F, again for the 0.45% titanium alloy.

Analyses of the tensile property data reveal inconsistencies which at this stage of development cannot be explained. An example of such inconsistencies was the marked difference in tensile strength of 5/8-inch rolled bars from Heat 1012, alloyed with 0.56% vanadium, and Heat 1051, alloyed with 0.54% vanadium. A second example was the difference in tensile properties of 5/8-inch-diameter bars from Heat 1009, alloyed with 1.26% titanium, and Heat 1138, alloyed with 1.22% titanium. Owing to a meager background of experience with these compositions, the differences must be attributed to processing variables; it is impossible at this time to know which heats or bars of each pair are truly typical of the nominal composition. Further testing, development, and comprehensive studies of the effects of processing variables must be accomplished before the data can be fully weighed and interpreted.

There are other instances where uncontrolled variations in the rolling schedule resulted in scattered results for different bars from the same casting. For example, the room temperature tensile strength of 5/8-inch-diameter bar from Heat 1132, alloyed with 0.45% titanium, was 112,900 psi as rolled and 132,100 psi after stress relieving at 1800 F. From such data one can only conclude that the properties of parts fabricated from molybdenum-base alloys will be determined by the working schedule and that uniformity will be obtained only when the rolling and forging operations and annealing schedules are carefully controlled.

A large loss in strength always accompanies recrystallization of wrought molybdenum-base alloys. Moreover, recrystallization minimizes the effect of an alloy addition. This is evident in Figures C47-C52, Appendix C, where the curves of strength versus testing temperature are much more closely grouped for recrystallized bars than for the other two conditions studied. In considering applications at elevated temperature, greater significance is



therefore attached to elements that raise the recrystallization temperature of wrought molybdenum than to elements that produce high strength in any particular structural condition. Of the binary alloys studied to date, those with titanium and zirconium have exhibited the highest recrystallization temperatures. Relatively low concentrations of zirconium (0.1%) and titanium (0.5%) were sufficient to raise the recrystallization temperatures for 5/8-inch-diameter rolled bar stock to the range 2500-3000 F.

The effects of specific alloying elements and their concentrations on the tensile strength of 5/8-inch-diameter bars is shown in Figures 49-50. The cobalt and zirconium alloys provide an interesting contrast. Relatively small amounts of each of these elements have profound effects on tensile strength. As-rolled, 5/8-inch-diameter bars exhibited similar tensile strengths, but after complete recrystallization the bars containing cobalt exhibited substantially higher tensile strengths at room temperature and 1600 F; but complete recrystallization for the cobalt alloy was accomplished at 2000 F, whereas it was necessary to heat the zirconium alloy bars to 2750 F to accomplish complete recrystallization. The zirconium alloy, therefore, would be expected to retain its strength at much higher temperatures than the cobalt alloy. It will be noted later that the cobalt alloy also exhibited a higher temperature for the transition from ductile to brittle failures.

It will be observed that the 0.45% titanium alloy, because of high strength at 1600 F, develops a peak at 1600 F in the curve for tensile strength as a function of alloy content. It has not been determined whether 0.45% represents an optimum titanium concentration or whether unknown processing variables are responsible for the apparent maximum in the curve. Further tests will be run to establish the relationship between titanium content and tensile strength in the range of concentration where the maximum occurs.

In no case did specimens tested at 750 F or above exhibit brittle behavior in the tensile test, the lowest elongation figure for any such test being 11%.

The ductility, as indicated by elongation in the tensile test, of wrought molybdenum at room temperature normally undergoes an increase upon recrystallization. The work reported here has shown, however, that molybdenum deoxidized with rare earth metals or aluminum, and one alloy containing cobalt, suffer decided losses in elongation at room temperature after recrystallization. Inasmuch as the bars exhibiting low ductility at room temperature exhibited satisfactory ductility at 750 F, the room temperature brittleness was thought to indicate an upward shift in the tensile-transition relationship. This conclusion was verified in work reported in Table 10 and Figure 51, in which tests were run at temperatures from -30 to +250 F on bars representing either ductile or brittle behavior at room temperature.

It will be noted that molybdenum deoxidized with rare earth metals (1045) appears to have a transition temperature at approximately 400 F, yet the original room-temperature test on this bar yielded an elongation of only 2%.

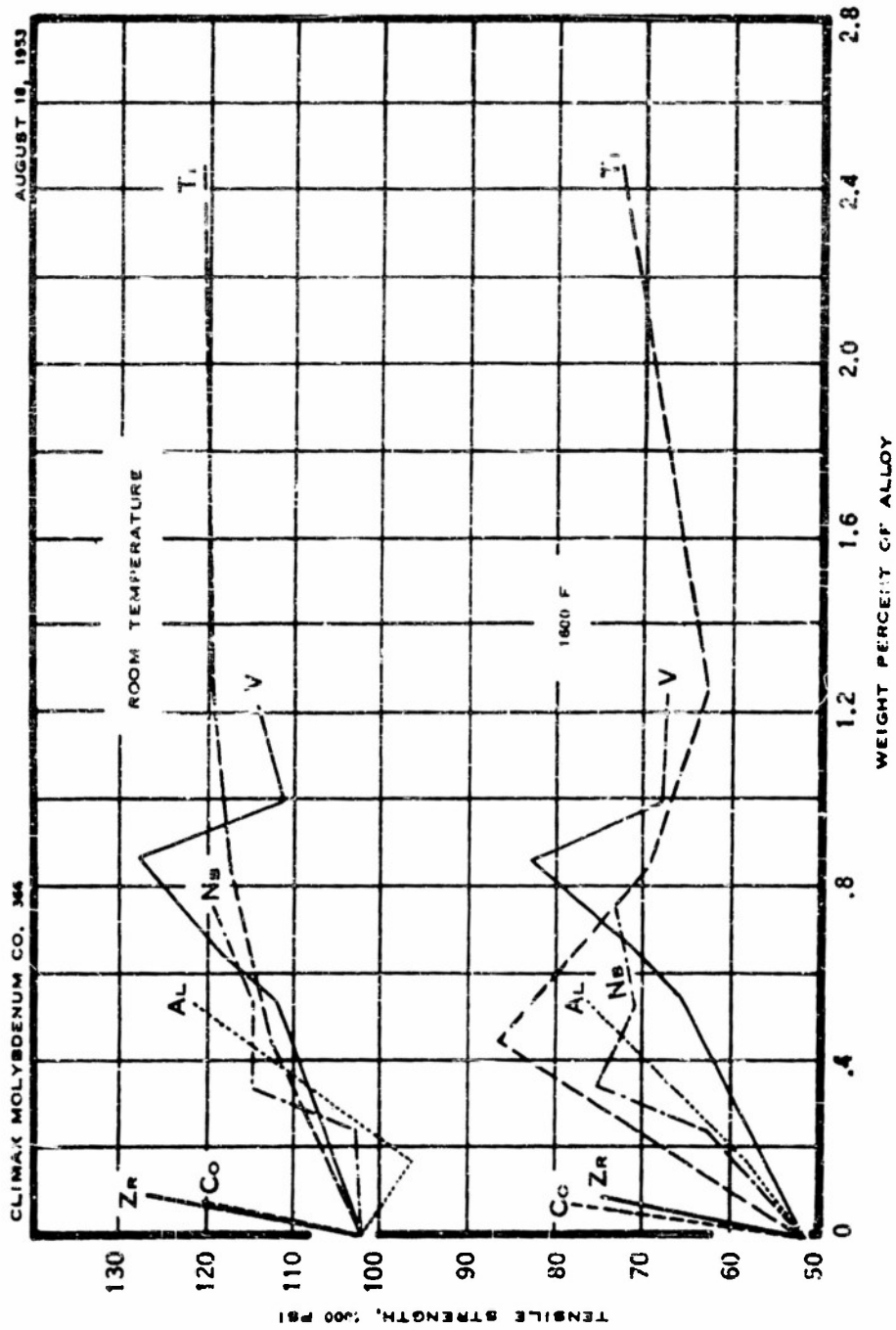


FIGURE 49 - TENSILE STRENGTH OF AS-ROLLED BARS
OF MOLYBDENUM-BASE ALLOYS
ROLLED TO $\frac{3}{8}$ DIAMETER

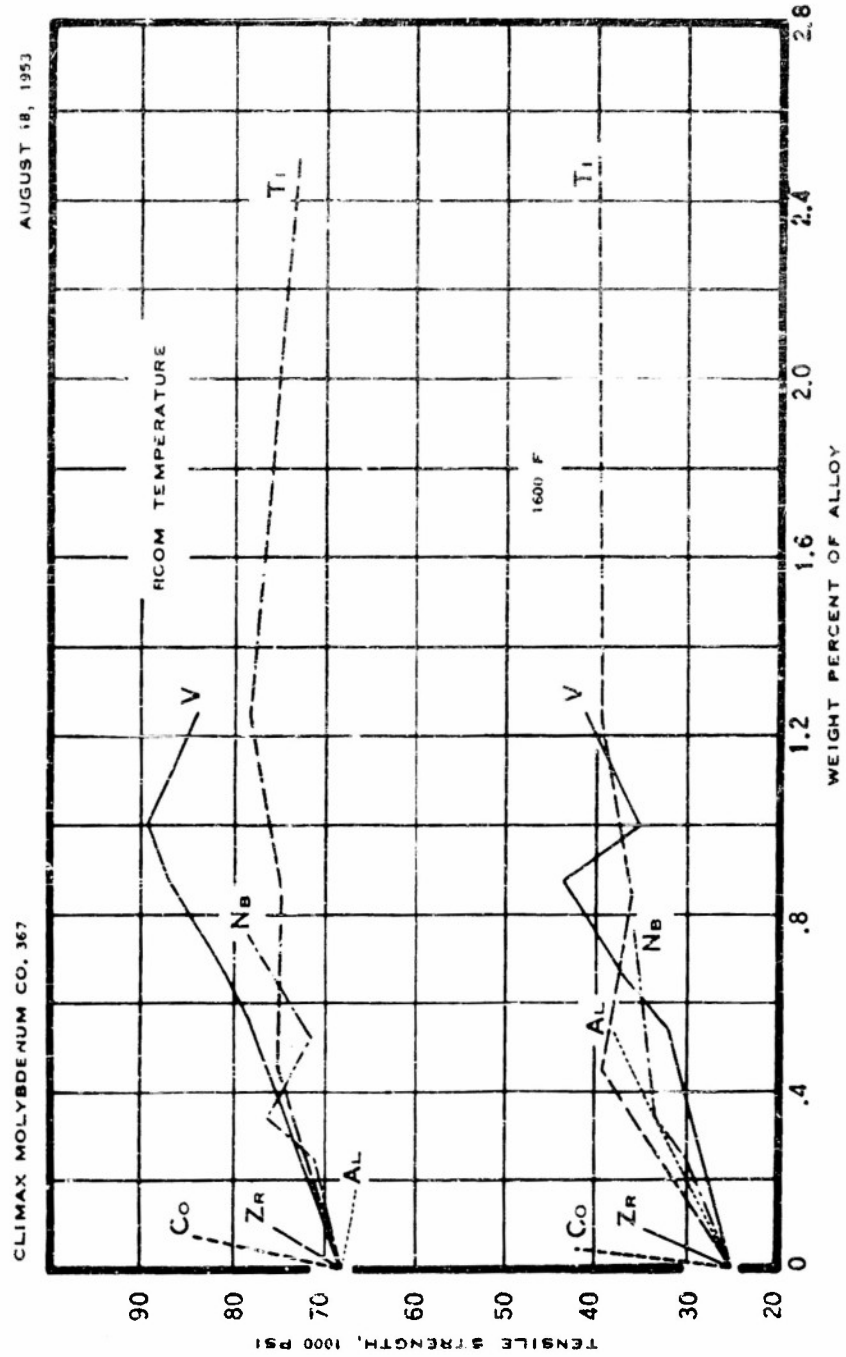


FIGURE 50 - TENSILE STRENGTH OF FULLY RECRYSTALLIZED
BARS OF MOLYBDENUM-BASE ALLOYS
ROLLED TO $\frac{1}{8}$ " DIAMETER

TABLE 10

TENSILE TRANSITION DATA ON 5/8" DIAMETER BARS

Heat	Composition %	Condition	Testing Temp, F	Yield Strength psi	Tensile Strength psi	El. %	R.A. %
937	0.015 C	as rolled	+ 10	82,500*	117,900	7	1.2
			20	84,200*	116,400	11	12.3
			32	77,900*	113,800	21	19.9
			50	66,100*	109,000	32	61.1
			81	78,800*	102,200	40	61.1
			180	59,400*	90,700	32	74.3
937	0.015 C	recryst. (2150 F)	- 4	84,000	84,000	2	3.2
			+ 14	79,400	79,400	3	3.2
			18	77,000	84,200	35	32.5
			23	80,100	82,600	38	34.2
			33	78,100	79,400	40	22.1
			61	55,900	68,200	42	37.8
1045	0.005 Ce 0.007 RE**	recryst. (2400 F)	+ 33	74,800	83,000	4	4.0
			50	58,000	72,000	45	45.5
			100	55,000	65,100	67	54.5
1058	0.49 Al	recryst. (2150 F)	+ 79	59,600	65,100	5	4.8
			120	61,200	77,100	15	12.7
			150	56,900	67,800	25	21.0
			180	54,900	74,400	26	21.2
			201	54,400	73,900	36	33.5
			250	56,500	69,800	34	31.6
1144	0.074 Co	recryst. (2000 F)	+ 80	66,900	66,900	5	4.4
			150	72,400	72,400	1	0.5
			180	63,500	71,000	19	16.8
			202	50,500	70,900	52	65.7
			250	63,100	68,100	50	56.5
1132	0.45 Ti	recryst. (2450 F)	- 30	102,500	105,000	12	9.7
			- 10	94,300	96,200	45	43.2
			+ 20	70,300	88,900	46	46.6
			81	60,000	75,500	55	38.0

* 0.1% offset yield strength

** other rare earth metals

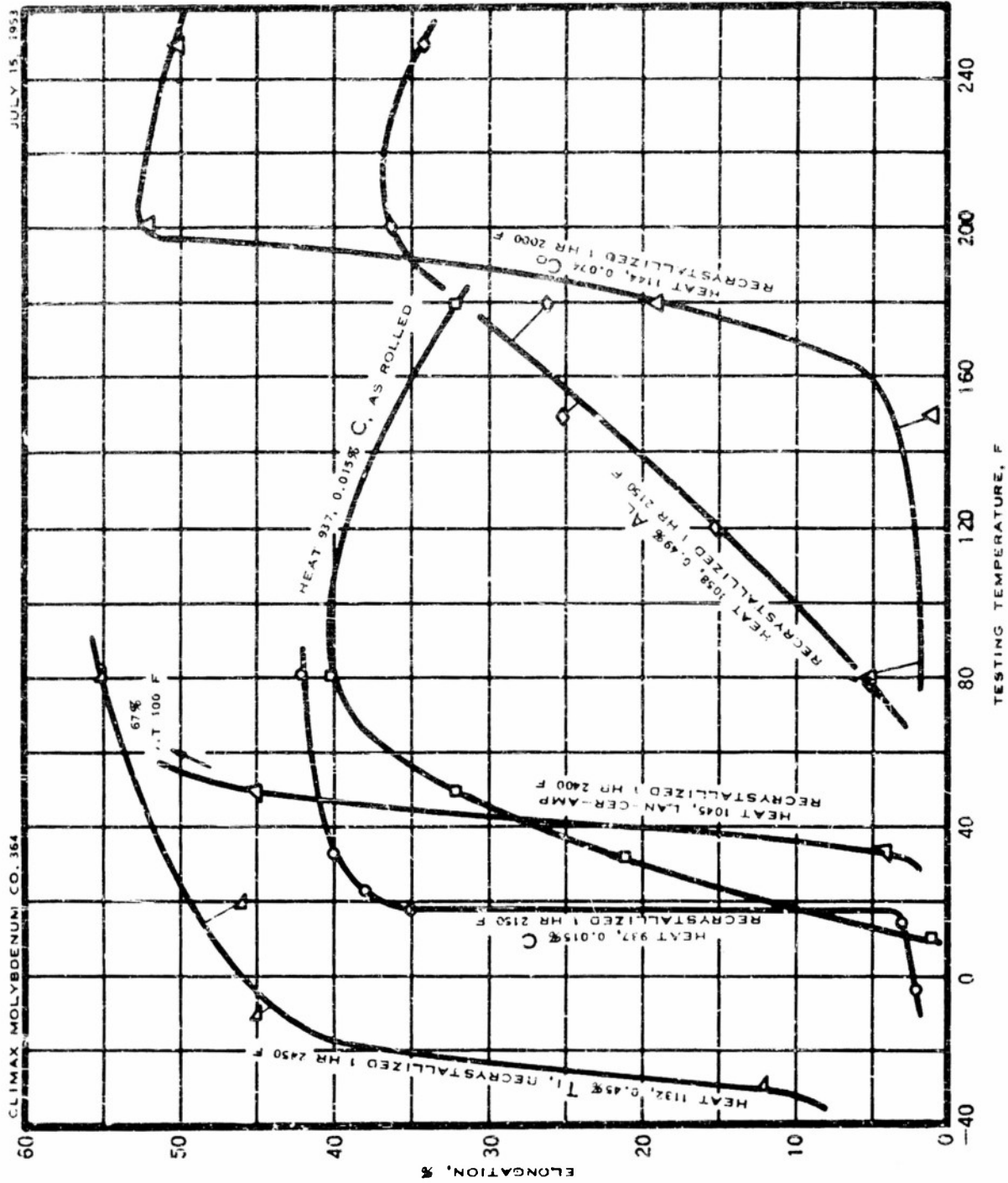


FIGURE 51 -- TENSILE TRANSITION CURVES FOR INDICATED MOLYBDENUM AND MOLYBDENUM-BASE ALLOY BARS (5/8" DIAMETER)

STRAIN RATE 3% PER HOUR IN THE ELASTIC RANGE, 60% PER HOUR IN THE PLASTIC RANGE

These apparently contradictory results are probably due to inhomogeneity of the bar and possibly to minute differences in heat treatment. Nonetheless, it may be concluded that the transition of this bar from brittle to ductile behavior under the conditions of the tensile test is not far from room temperature.

The molybdenum-aluminum alloy (1058) exhibited a relatively gradual transition from about room temperature to 200 F. The 0.074% cobalt alloy (1144) retained low ductility up to about 150 F.

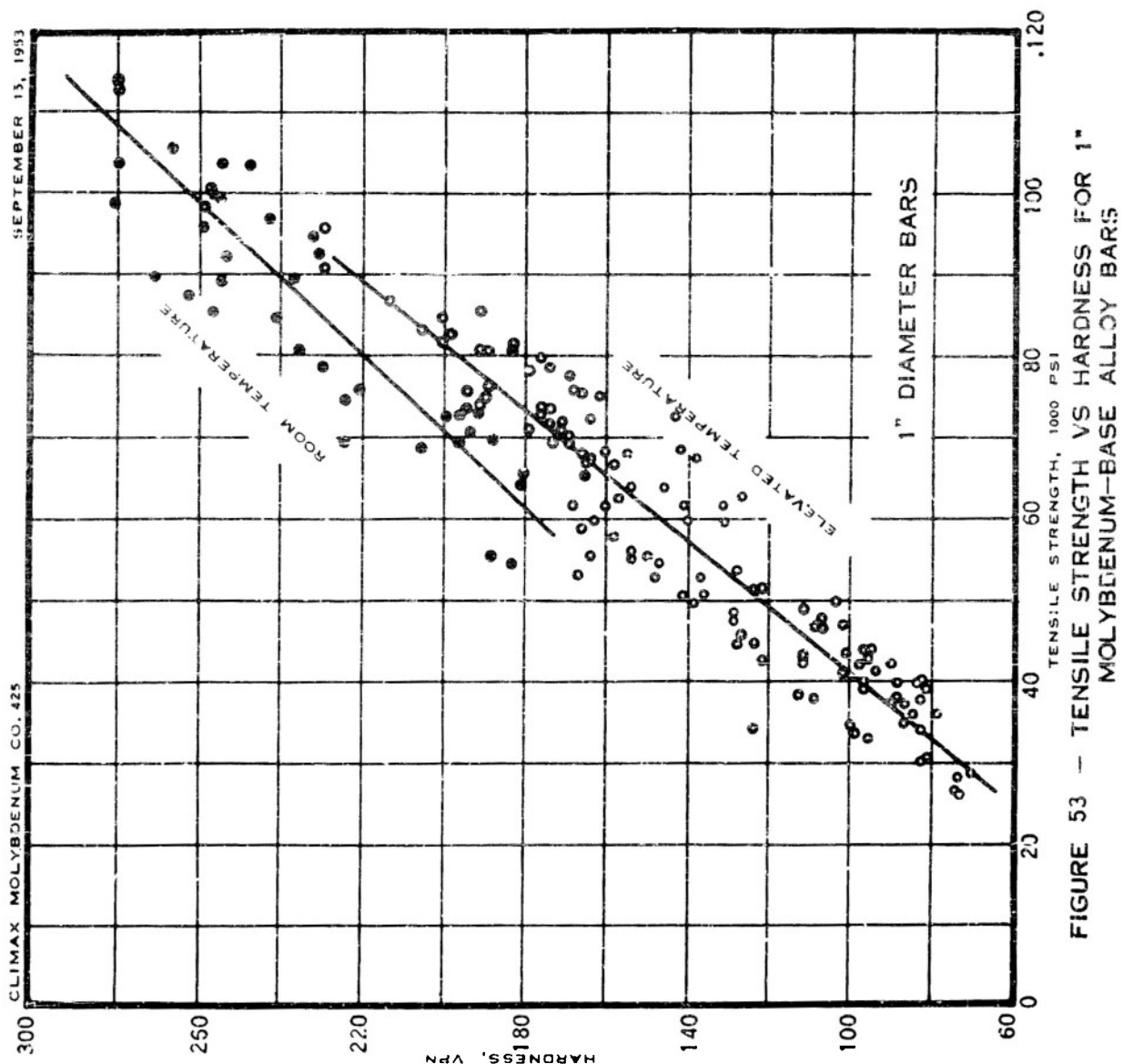
Heat 937 (unalloyed datum heat) was tested both as rolled and after recrystallization. As in the case of the V-notch impact transitions discussed in the next section, the tensile transition was more abrupt for the recrystallized condition than for the as-rolled condition. The 0.45% titanium alloy exhibited the lowest transition temperature of the entire group.

Returning to Figure 48, the 5/8-inch diameter bar stock, whether as rolled or stress relieved, generally exhibited higher tensile strength than 1-inch diameter stock of the same composition and thermal history. After recrystallization, the factor of amount of cold work assumed a position of secondary importance, and the tensile strengths of 5/8-inch and 1-inch diameter bars of comparable composition were much the same. Considering ductility as measured in the tensile test, elongation and reduction of area were usually higher for specimens from 5/8-inch bars than from comparable 1-inch bars. Three factors are thought to have affected tensile test ductility, namely, test specimen size, amount of cold work, and grain size. Tensile test gage diameters were 0.250 inch and 0.475 inch for the 5/8-inch and 1-inch diameter bars, respectively. Earlier, unpublished work at this laboratory has indicated that when tensile specimens of various gage diameter are taken from a homogeneous bar of molybdenum, an inverse relationship is obtained between specimen gage diameter and ductility values. The 5/8-inch bars, of course, had received more work than the 1-inch bars. A quantitative evaluation of this factor was not feasible inasmuch as that portion of the total reduction classifiable as "cold" work could not be determined, owing to the proximity of the working temperature to the temperature of recrystallization. Grain sizes for the 5/8-inch diameter bars in the recrystallized condition were consistently lower than for corresponding 1-inch diameter bars, and this structural difference also may have resulted in higher ductilities for the specimens from the 5/8-inch bars.

Some revision of the relationship between hardness and tensile strength of molybdenum and molybdenum-base alloys as given in the third annual report was necessary as a result of the large number of additional tests conducted during the past year. Figures 52-53 present tensile strength as a function of hardness for 5/8-inch and 1-inch diameter bars, respectively, regardless of structural condition or testing temperature. The lines for elevated temperature are similar to those reported earlier, but the data obtained at room temperature are better fitted by a line of somewhat different slope. For quick approximation of tensile strength when only the Vickers hardness number is available, a satisfactory formula is

$$\text{Tensile Strength, psi} = 400 \times \text{VPN}$$

FIGURE 52 -- TENSILE STRENGTH VS HARDNESS FOR 5/8" MOLYBDENUM-BASE ALLOY BARS



That factors other than hardness enter into determination of ultimate tensile strength is evidenced by the spread in data in Figures 52-53. The relationships presented in these figures, then, are of value only as general guides in predicting tensile strength at a given hardness.

Figures 52-53 show tensile strength as a function of hardness, and Figures C8-C16, Appendix C, show hardness versus annealing temperature. By combining these figures, estimates of tensile strength under intermediate conditions of annealing between stress relief and full recrystallization can be made. This analysis would, of course, be applicable only to bars having fabrication histories comparable to those of the materials used in the compilation of the aforementioned charts.

The results of tensile tests on 1/2-inch diameter bars rolled at the University of Michigan from bars extruded at Thompson Products Company are given at the end of Table C1, Appendix C. These values are significantly lower than those obtained on 5/8-inch diameter bars, Figures 49-50. The chief difference is, of course, in the method of fabrication. The majority of the 5/8-inch diameter bars were rolled from 4-inch diameter extrusions, while the 1/2-inch bars were rolled from extrusions approximately 3/4 inch in diameter, which in turn had been prepared from 1-1/4 inch diameter cast cylinders. Physically, these bars were low in strength and large grained, as noted earlier in this report. Hardness values of the 1/2-inch bars were comparable with results on 5/8-inch bars, however, so that if the hardness and tensile data are applied to Figure 52, they fall to the left of the line indicating room temperature.

Notched Bar (Impact) Transition Temperature

The objective of the notched bar transition testing program was to determine whether an alloy addition could lower the temperature at which the fracture of molybdenum changes from brittle to ductile, or in other words, to improve the ductility of arc-cast molybdenum.

Impact transition temperatures were determined for 5/8-inch and 1-inch diameter bars of unalloyed molybdenum and 23 molybdenum-base alloys in the as-rolled, stress-relieved, and fully recrystallized conditions. Standard V-notch Charpy test specimens were used. They were heated in air to the testing temperature and rapidly transferred to the Charpy machine for test.

Curves showing energy as a function of testing temperature for the alloys tested during the past year are given in Appendix C, Figures C37-C47. Summary curves showing transition temperature ranges for all of the 5/8-inch and 1-inch diameter bars tested during the past two years are given in Figures 54-55. Transition ranges have arbitrarily been taken as the temperature ranges limited by 20 and 120 foot-pounds of energy absorbed by the impact specimens.

The extent and general level of the transition temperature range was lower for 5/8-inch diameter bars than for 1-inch bars of similar composition in the as-rolled and stress-relieved conditions. Transition temperature ranges for fully recrystallized specimens from the two bar sizes were usually about the same.

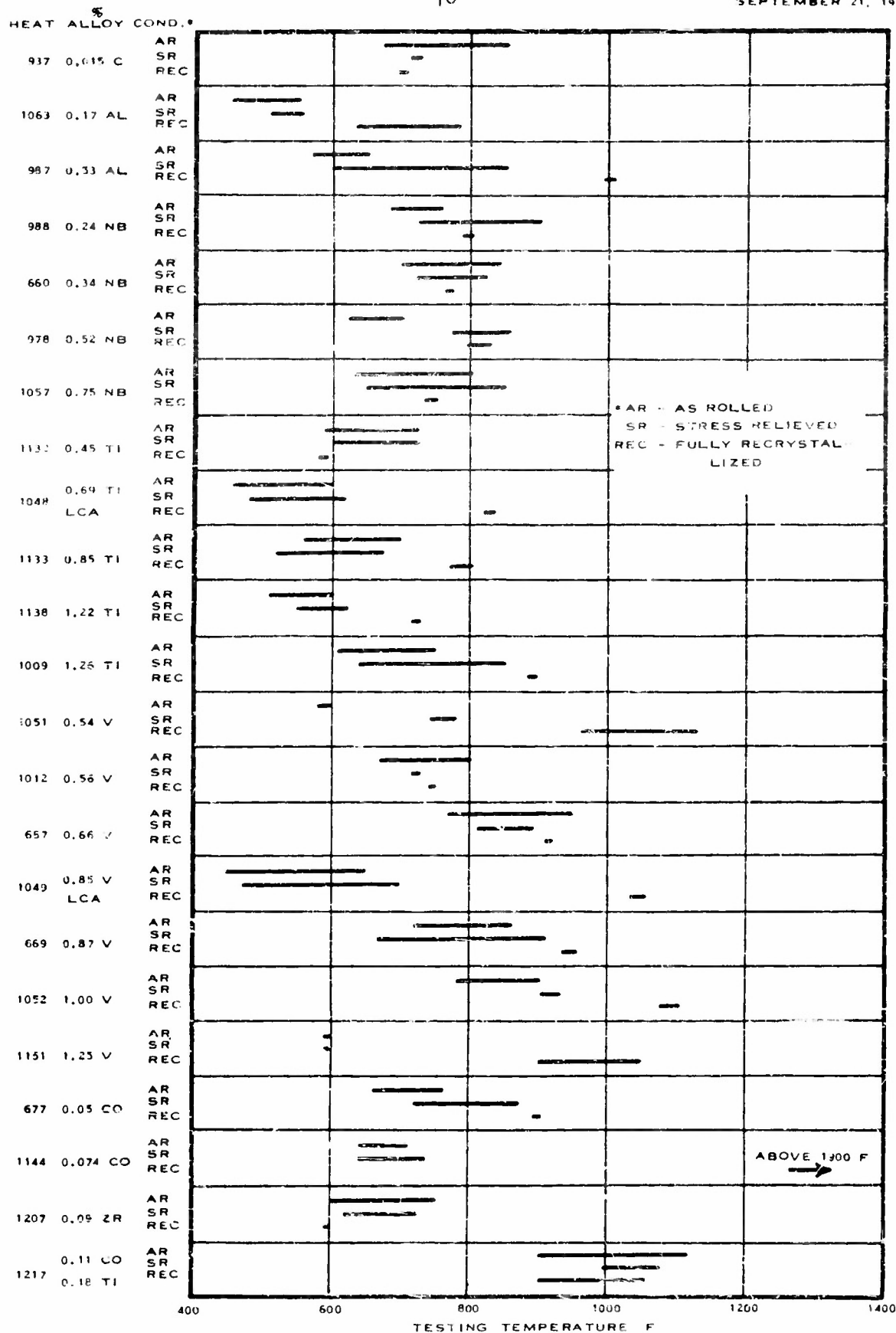
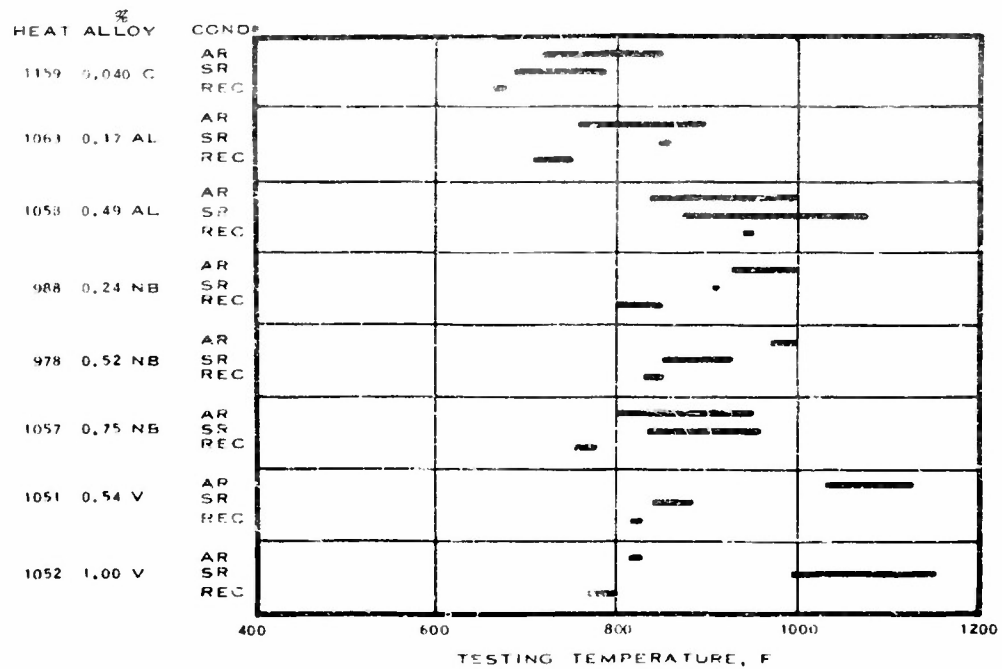


FIGURE 54 - V-NOTCH IMPACT TRANSITION TEMPERATURE RANGES FOR $\frac{5}{8}$ DIAMETER MOLYBDENUM AND MOLYBDENUM-BASE ALLOY BARS

CLIMAX MOLYBDENUM CO.

SEPTEMBER 21, 1953



• AR - AS ROLLED
 SR - STRESS RELIEVED
 REC - FULLY RECRYSTALLIZED

FIGURE 55 - V-NOTCH IMPACT TRANSITION TEMPERATURE RANGES
 FOR 1" DIAMETER MOLYBDENUM AND MOLYBDENUM--
 BASE ALLOY BARS

Transition temperature ranges for as-rolled and stress-relieved bars of the essentially carbon-free Heats 1063, 1048, and 1049 were significantly lower than that of unalloyed molybdenum deoxidized with carbon. It appears that as-rolled, unalloyed molybdenum containing an excess phase, such as molybdenum carbide, has a higher transition temperature than solid solution alloys of molybdenum containing no excess phase. After recrystallization, however, all of the carbon-free alloys exhibited a marked increase in notched bar transition temperature. This increase was also evident in the tensile transition temperature of molybdenum deoxidized with aluminum or rare earth metals, which lost room-temperature ductility (rise in transition temperature) after recrystallization.

It is evident from Figure 54 that an addition of niobium does not significantly alter the transition temperature of unalloyed molybdenum. Titanium lowers the transition range slightly for most of the alloys and structural conditions studied. Molybdenum-vanadium alloys deoxidized with carbon generally have higher Charpy transition temperatures than unalloyed molybdenum. Molybdenum-cobalt alloys in the as-rolled or stress-relieved conditions are comparable to unalloyed molybdenum, but undergo an increase in transition temperature after recrystallization. The transition temperature range for the 0.074% cobalt alloys, for example, was from 1300 to above 1900 F. The transition temperature ranges of the molybdenum-zirconium alloy were somewhat lower, and of the molybdenum-cobalt-titanium alloy significantly higher, than those of unalloyed molybdenum.

The 1-inch diameter bars of unalloyed molybdenum deoxidized with aluminum exhibited neither the low transition temperature in the worked condition nor the high transition temperature after recrystallization exhibited by 5/8-inch diameter bars of the same composition. None of the seven alloy bars tested in the 1-inch diameter size was superior to unalloyed molybdenum in respect to Charpy transition temperature.

Creep-Rupture Properties

One of the principal objectives of this project has been the development of molybdenum-base alloys for elevated temperature service. Load-carrying ability at elevated temperatures, then, is one of the most important considerations in rating the alloys developed to date.

Creep-rupture tests* have been run on nineteen compositions, including unalloyed molybdenum. Tests were conducted in vacuum at temperatures of 1600, 1800, and 2000 F on stress-relieved or fully recrystallized specimens. Rupture specimens were machined from 5/8-inch diameter bar stock. The gage dimensions of the specimens were 3/16-inch diameter by 1 inch long. In general, three tests were conducted at each testing temperature for each heat in each structural condition, aiming at rupture lives of one, ten, and one hundred hours duration. Tests lasting longer than an arbitrarily assigned limit (about 300 hours) were discontinued. Creep rates were calculated for all tests that sustained the applied loads long enough to yield time-deformation data.

* conducted by Battelle Memorial Institute

The results of the creep-rupture program are presented as plots of stress against rupture time in Figures 56-64. Table 11 lists the 100-hour rupture strengths for all the alloys tested under Contract N8onr-78700 in the last two years. A tabulation of rupture data may be found in Appendix C, Table C2.

In general, recrystallization lowered the 100-hour rupture strengths of the alloys tested at 1600 F about 40 to 50%. With increasing testing temperature, the differences between the two structural conditions lessened, so that for some of the alloys tested at 2000 F, only insignificant differences existed between rupture strengths of stress-relieved and recrystallized samples. This condition resulted from recrystallization in varying degrees of the stress-relieved specimens during testing, and again emphasizes the importance of alloy additions that increase the recrystallization temperature of molybdenum.

Most of the molybdenum-base alloys investigated under this project, even in the recrystallized condition, are superior in rupture-strength to all of the cobalt- and nickel-base alloys currently in use in high-temperature service. One of the best cobalt-base alloys, X-40 (cast), exhibits strengths at 100-hour life of 21,300 and 11,300 psi at 1600 and 1800 F, respectively. At 1600 F this material compares favorably with some of the low-alloy molybdenum-base compositions after recrystallization. At 1800 F, Alloy X-40 is inferior to unalloyed molybdenum. When tested in the stress-relieved condition, the best molybdenum alloy was over three times as strong at 1600 F and five times as strong at 1800 F as the cobalt-base alloy.

Creep rates obtained during the creep-rupture test for the higher strength molybdenum-base alloys at 2000 F in the stress-relieved condition or at 1600 F in the recrystallized condition were of the same order of magnitude as those published for the cobalt-base alloy S-816 tested at 1500 F.

The best of the alloys tested appear to be the 0.45% titanium, 1.26% titanium, 0.75% niobium, and 0.09% zirconium. At all three testing temperatures, unalloyed molybdenum exhibited the lowest rupture stress for 100-hour life of the group tested in the fully recrystallized condition. In the stress-relieved condition, the 0.17% aluminum heat was weakest at 1800 and 2000 F. Recrystallization during testing was undoubtedly a factor in the regrouping of the alloys tested at 1600 and 2000 F.

Comparison of elevated temperature tensile data with rupture life was feasible only at 1600 F, inasmuch as short-time tensile tests were not conducted at higher temperatures. Study of the data indicated no direct comparison between 100-hour rupture strength at 1600 F and short-time tensile data at the same temperature. The ratios of 100-hour rupture strength to tensile strength were compared for stress-relieved and for fully recrystallized specimens. These ratios varied from 0.54 to 0.97. The ratios were averaged for each alloy group. In order of decreasing ratio, the alloying elements rank as follows:

TABLE 11

CREEP-RUPTURE STRENGTH OF WROUGHT, ARC-CAST MOLYBDENUM AND MOLYBDENUM-BASE ALLOYS
100 Hours

1600 F		1800 F		2000 F	
		Stress Relieved			
31000 psi	Unalloyed Mo	18000 psi	0.17 Al	10000 psi	0.17 Al
36000	0.17 Al	19000	0.074 Co	11500	0.53 Al
37000	0.074 Co	22000	Unalloyed Mo	11500	0.54 V
41000	0.54 V	22000	0.56 V	11500	0.24 Nb
41000	0.56 V	24000	0.54 V	11500	1.00 V
41000	Mo + RE	27500	0.53 Al	13000	Unalloyed Mo
43000	1.22 Ti	28000	Mo + RE	13000	Mo + RE
44000	0.69 Ti + RE	28000	0.56 V	13000	0.56 V
45000	0.53 Al	29000	1.26 Ti	13500	0.34 Nb
46000	0.85 V + RE	31000	0.69 Ti + RE	14000	0.05 Co
47000	0.66 V	31000	1.00 V	15500	0.87 V
48000	0.85 Ti	31000	1.22 Ti	16000	0.52 Nb
49000	1.00 V	33000	0.05 Co	17000	0.69 Ti + RE
50000	1.26 Ti	33000	0.85 V + RE	19500	1.26 Ti
53000	0.24 Nb	34000	1.25 V	20500	0.85 V + RE
53000	0.87 V	36000	0.85 Ti	22000	0.75 Nb
55000	0.05 Co	37000	0.34 Nb	22000	2.46 Ti
58000	0.34 Nb	41000	0.87 V	22000	0.85 Ti
64000	0.52 Nb	41000	2.46 Ti	25000*	0.09 Zr
64000	0.09 Zr	43000	0.52 Nb	25500	0.45 Ti
66000	0.45 Ti	51000	0.75 Nb		
69000	0.75 Nb	53000	0.45 Ti		
		56000	0.09 Zr		
		Recrystallized			
16000	Unalloyed Mo	11500	Unalloyed Mo	9000	Unalloyed Mo
18500	0.17 Al	13000	0.17 Al	9200	0.17 Al
20000	Mo + RE	14000	Mo + RE	10000	0.53 Al
20000	0.85 V + RE	15000	0.54 V	10000	0.69 Ti + RE
21000	0.53 Al	15000	0.074 Co	10500	0.54 V
21000	0.54 V	15500	0.66 V	11000	0.24 Nb
22000	0.24 Nb	16000	0.53 Al	11500	0.66 V
23000	0.56 V	16000	0.85 V + RE	11500	0.85 V + RE
23000	0.69 Ti + RE	17000	0.24 Nb	12000	0.56 V
23500	1.22 Ti	17500	0.56 V	12500	Mo + RE
25000	0.34 Nb	17500	1.22 Ti	13000	1.00 V
25000	0.074 Co	18000	1.00 V	13500	0.34 Nb
26000	0.66 V	18500	0.69 Ti + RE	14000	0.87 V
26000	0.05 Co	19500	0.85 Ti	15000	0.52 Nb
27000	1.00 V	20000	0.34 Nb	15000	0.85 Ti
27500	0.85 Ti	21000	0.05 Co	15500	0.05 Co
29000	0.87 V	21500	0.87 V	18000	0.75 Nb
31000	0.52 Nb	25000	0.52 Nb	18500**	0.09 Zr
32000	0.09 Zr	27500	0.09 Zr	19500	0.45 Ti
34500	0.45 Ti	28000	0.45 Ti	22000	1.26 Ti
37000	0.75 Nb	38000	1.26 Ti		
40500	1.26 Ti				

* single test at 25,000 psi discontinued after 160.8 hours

** single test at 18,500 psi discontinued after 175.6 hours

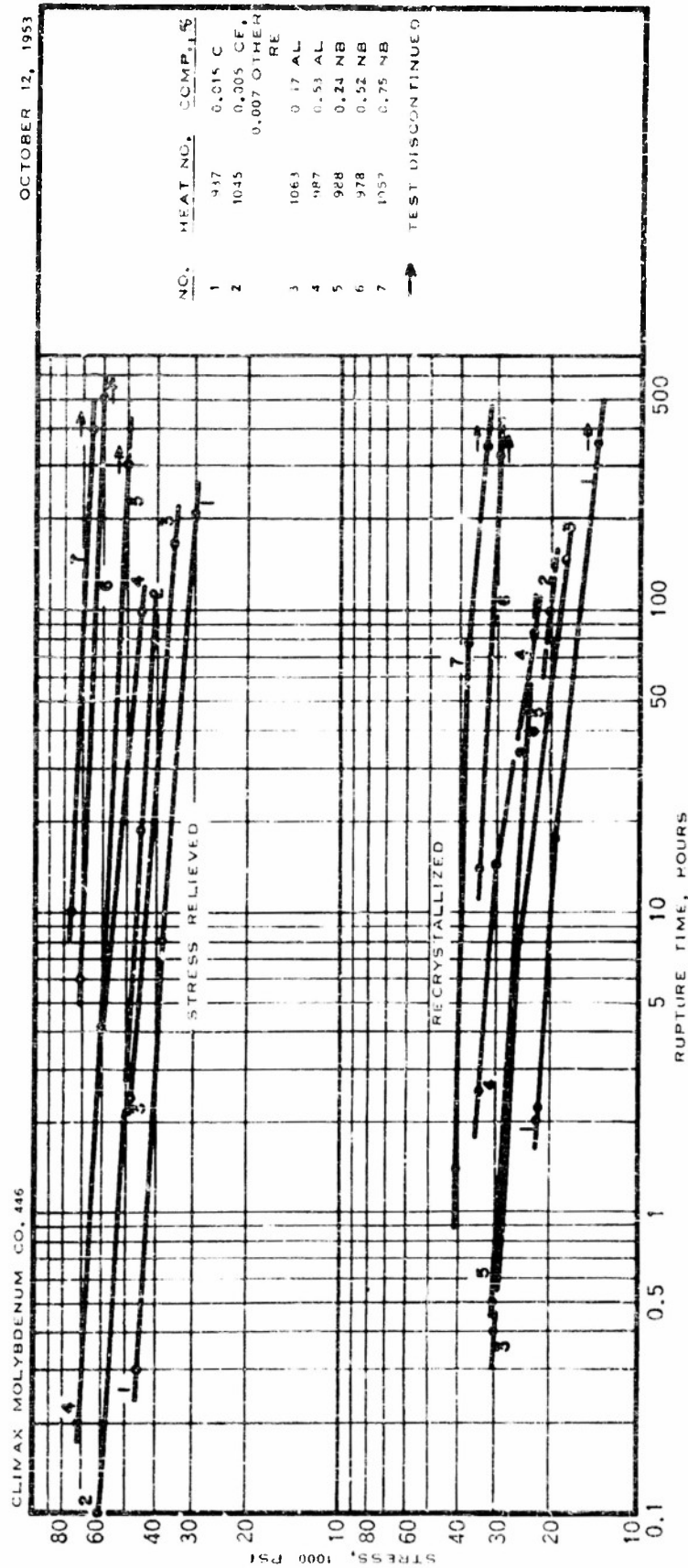


FIGURE 56 - CREEP RUPTURE STRENGTH OF MOLYBDENUM, ALUMINUM-MOLYBDENUM AND NIOBIUM-MOLYBDENUM ALLOY BARS TESTED IN VACUUM AT 1600 F

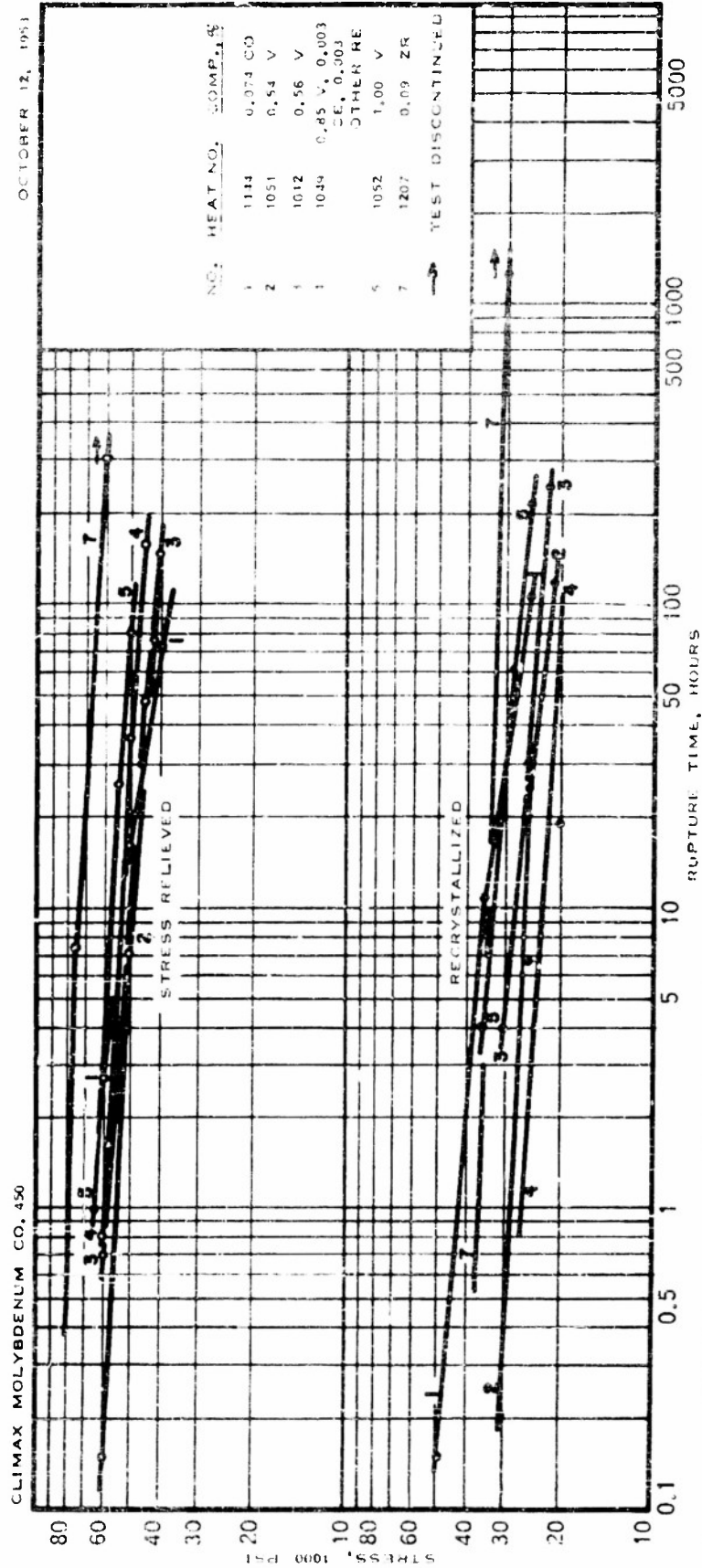


FIGURE 57 -- CREEP RUPTURE STRENGTH OF COBAL^T-MOLYBDENUM, VANADIUM-MOLYBDENUM AND ZIRCONIUM-MOLYBDENUM ALLOY BARS TESTED IN VACUUM AT 1500 F

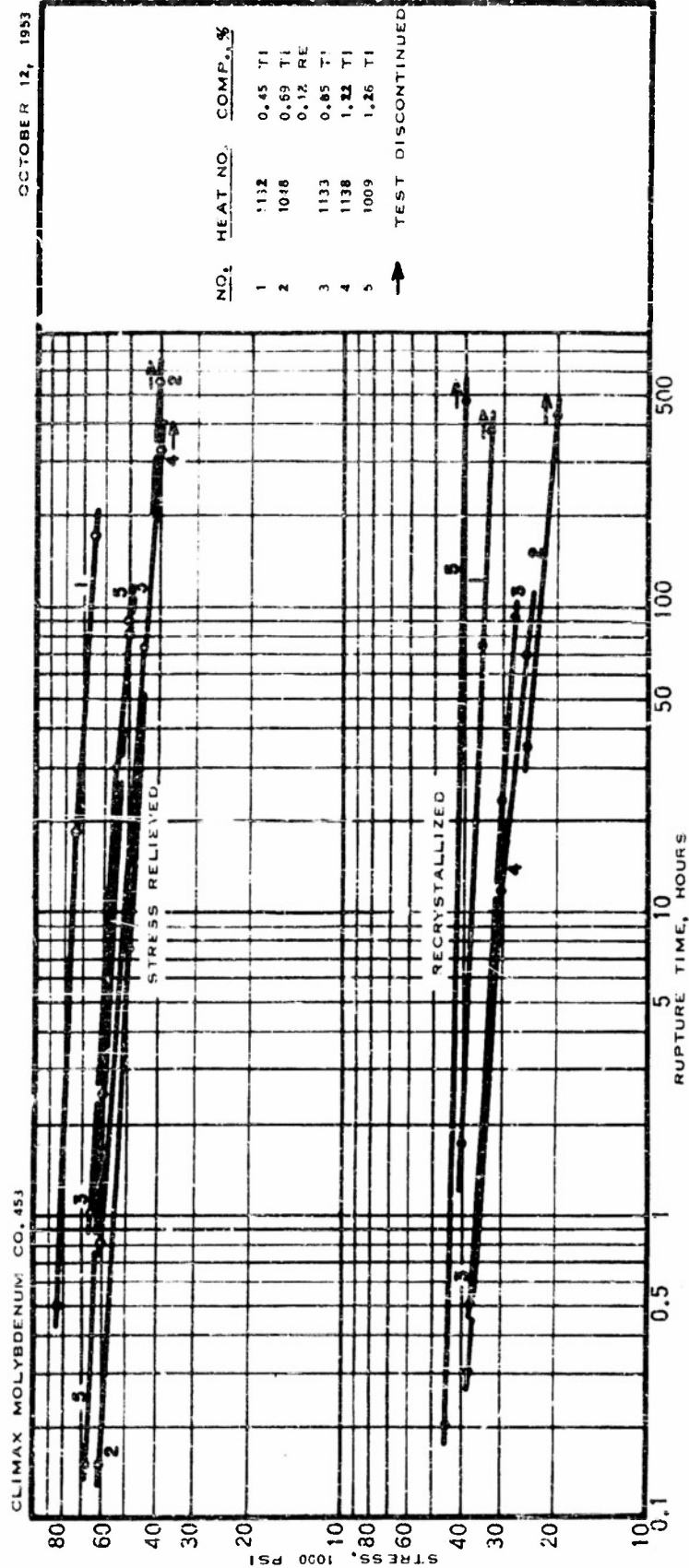


FIGURE 58 - CREEP RUPTURE STRENGTH OF TITANIUM-MOLYBDENUM ALLOY BARS TESTED IN VACUUM AT 1600 F

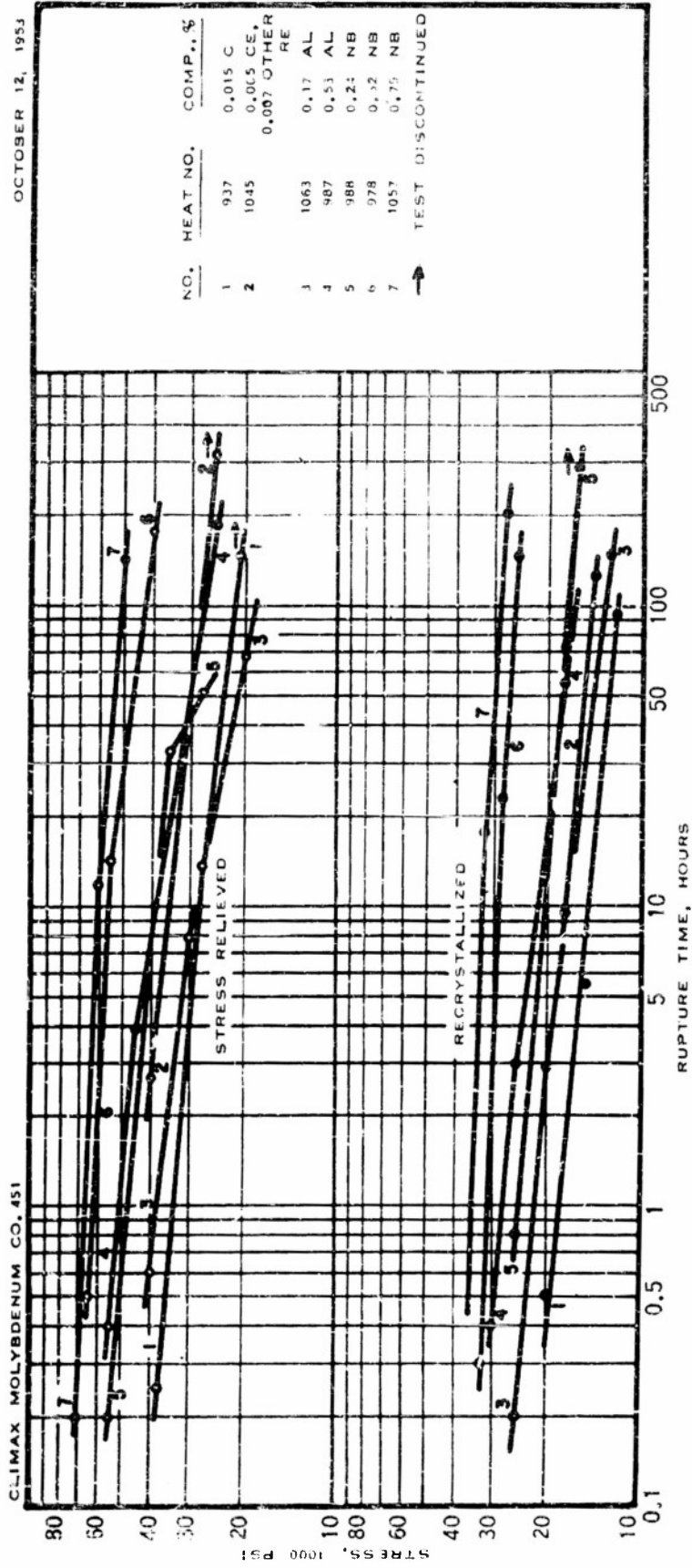


FIGURE 59 -- CREEP RUPTURE STRENGTH OF MOLYBDENUM, ALUMINUM-MOLYBDENUM AND NIOBIUM-MOLYBDENUM ALLOY BARS TESTED IN VACUUM AT 1800 F

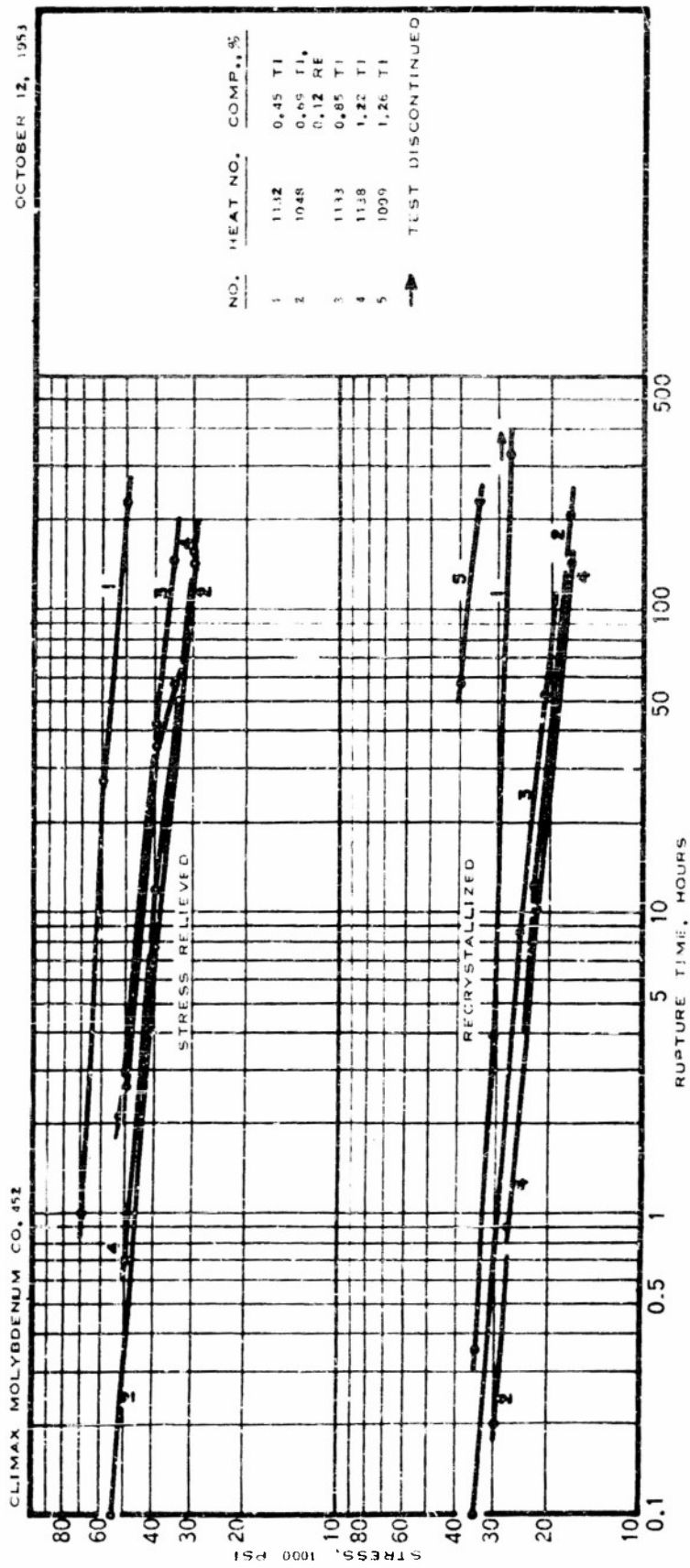


FIGURE 61 - CREEP RUPTURE STRENGTH OF TITANIUM-MOLYBDENUM ALLOY BARS TESTED IN VACUUM AT 1800 F

OCTOBER 12, 1953

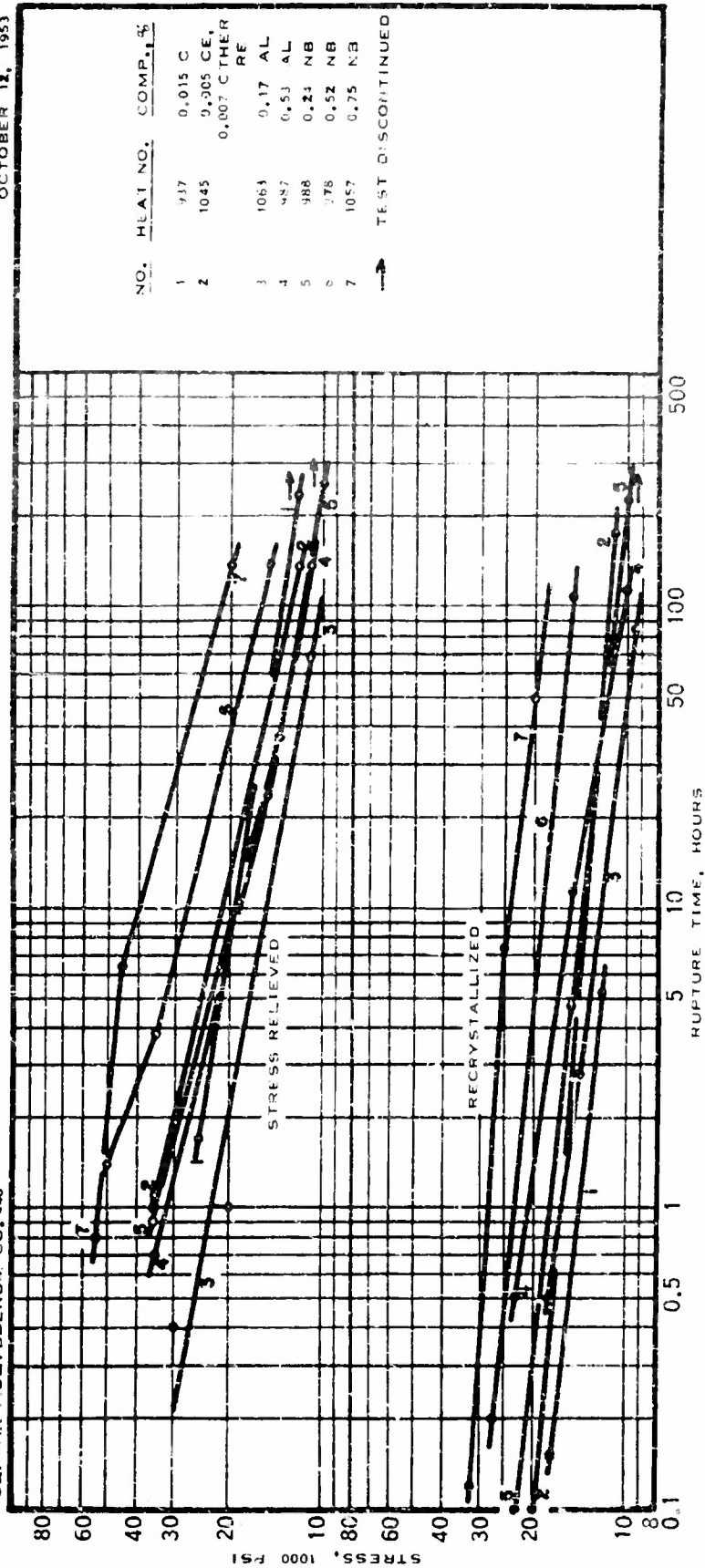


FIGURE 62 - CREEP RUPTURE STRENGTH OF MOLYBDENUM, ALUMINUM-MOLYBDENUM AND NIOBIUM-MOLYBDENUM ALLOY BARS TESTED IN VACUUM AT 2000 F

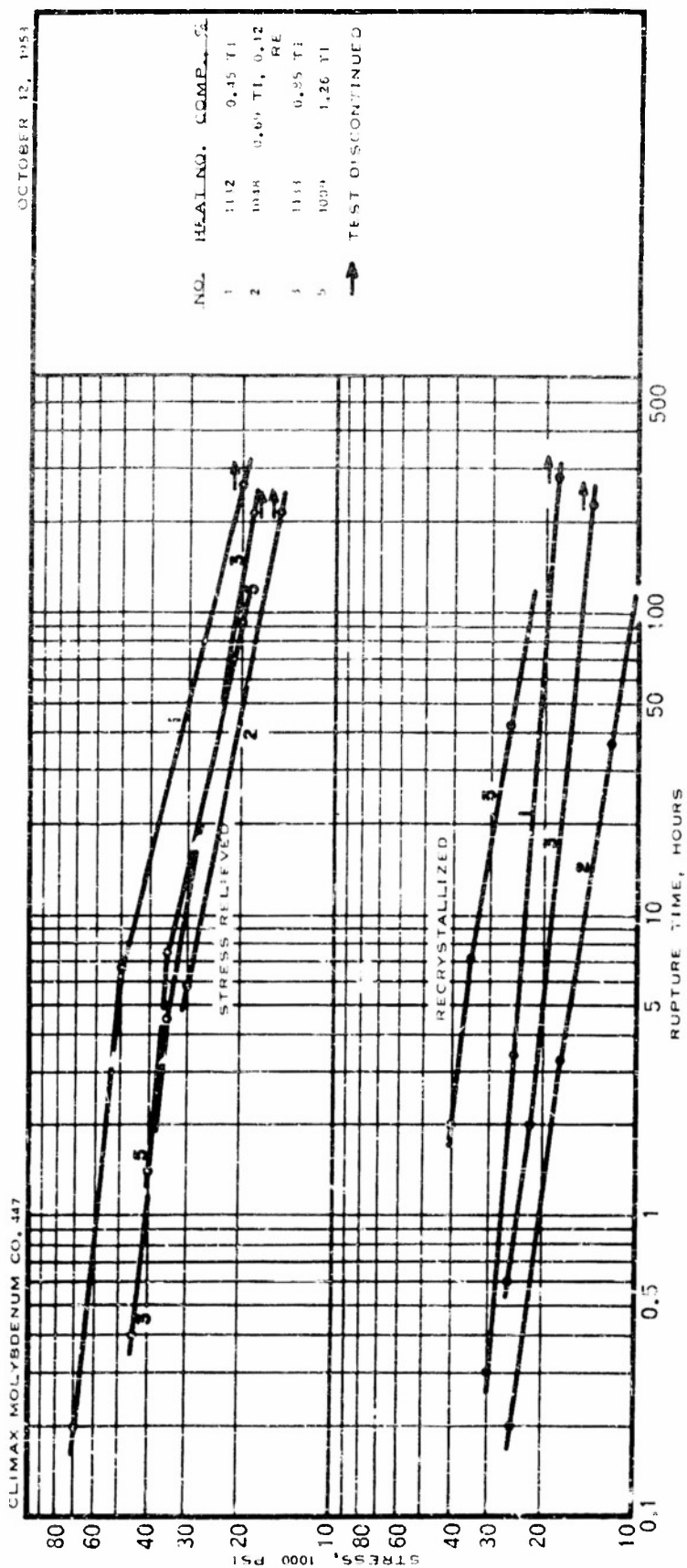


FIGURE 63 - CREEP RUPTURE STRENGTH OF TITANIUM-MOLYBDENUM ALLOY BARS TESTED IN VACUUM AT 2000 F

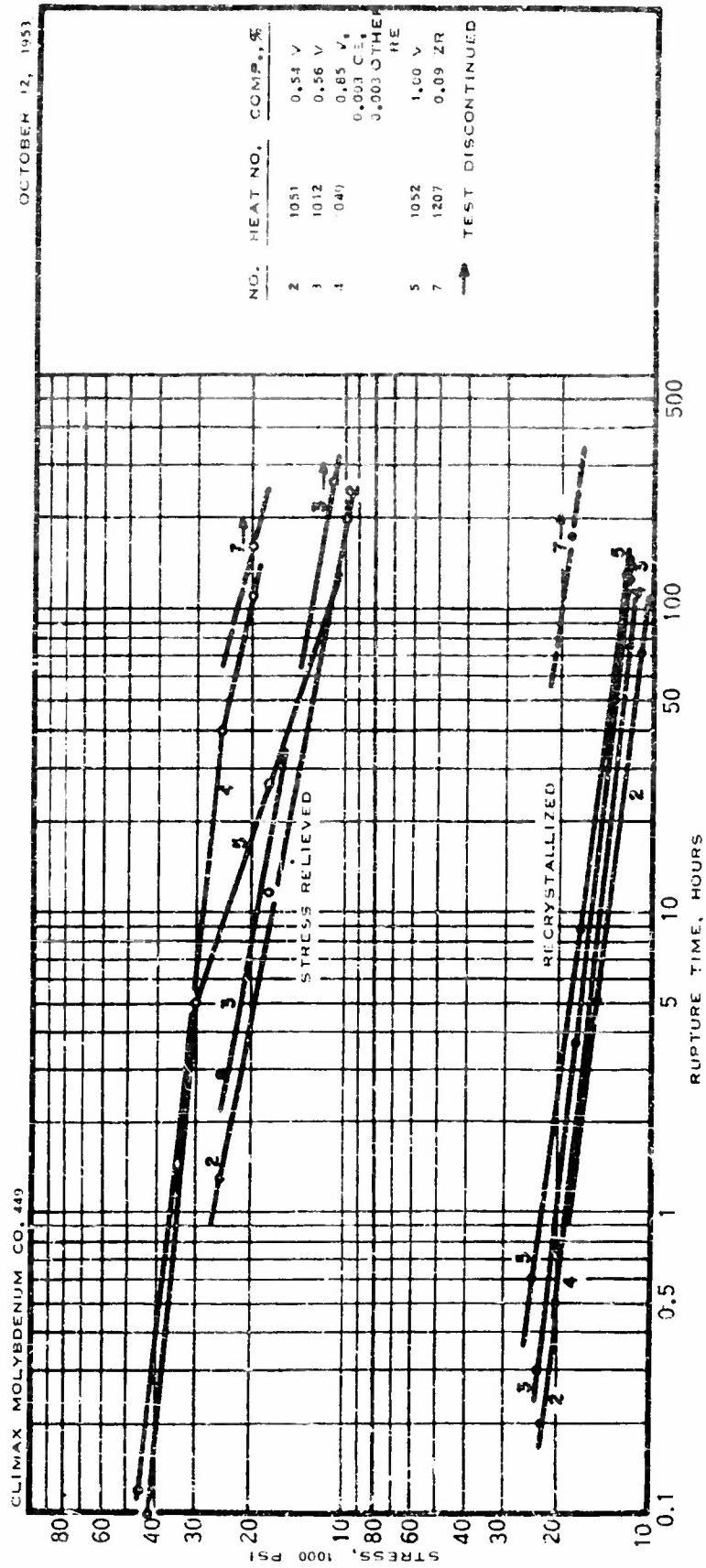


FIGURE 64 - CREEP RUPTURE STRENGTH OF VANADIUM-MOLYBDENUM, AND ZIRCONIUM-MOLYBDENUM ALLOY BARS TESTED IN VACUUM AT 2000 F

Average Ratio of Stress
to Rupture in 100 Hours
to Tensile Strength

Niobium	0.88
Zirconium	0.87
Titanium	0.77
Vanadium	0.70
Unalloyed Molybdenum	0.51
Aluminum	0.61
Cobalt	0.55

The 0.45% titanium alloy (1132) was superior in stress-rupture strength to the 0.85% titanium (1133) and 1.22% titanium (1138) alloys. A similar relationship was noted for elevated-temperature tensile properties. As indicated in a previous section of this report, the metallography of the molybdenum-titanium system changed as the titanium content increased from 0.45% to 0.85%, in that at the higher level a fine precipitate appeared within the grains. The amount of this precipitate increased with increasing titanium content. It is possible that the absence of direct correlation between titanium content and high-temperature properties is attributable to this structural change. The 1.26% titanium alloy (1009) had significantly higher stress-rupture strength than the 1.22% titanium alloy, regardless of testing temperature or structural condition. This apparent discrepancy may have been due to the fact that the 1.26% titanium alloy was prepared from crystal bar titanium, whereas the remaining molybdenum-titanium alloys of this phase of the program were prepared from Du Pont sponge titanium.

Ductility as measured by final elongation of virtually all of the rupture tests on stress-relieved molybdenum-base alloys was in excess of 10%. Corresponding values were two to three times greater for fully recrystallized specimens. Average elongation values, considering all the creep-rupture tests conducted, were 18.2% for specimens in the stress-relieved condition and 43.1% for specimens in the fully recrystallized condition. Reduction of area values were generally high, attesting to substantial localized deformation under the conditions of rupture testing. The tendency of molybdenum deoxidized with aluminum or rare earth metals to be less ductile after recrystallization was manifested in the rupture tests only by values for reduction of area somewhat lower than those for molybdenum deoxidized with carbon. Reduction of area figures were less dependent upon structural condition of the test specimen than the figures for elongation. Average values for reduction of area of bars deoxidized with carbon was 86.3% and of bars deoxidized by other means, 71.8%. The average values for reduction of area for all tests conducted at 2000 F were approximately 8% below those for tests conducted at 1600 and 1800 F.

Oxidation

Oxidation tests at 1750 F in moving air were conducted on 20 molybdenum-base alloys containing aluminum, cobalt, niobium, titanium, vanadium, or zirconium, some deoxidized with carbon, some with rare earth metals. A summary chart, Figure 65, relates alloy content and rate of oxidation for all the materials tested. Plots of loss in weight as a function of time may be found in Appendix C, Figures C74-C75.

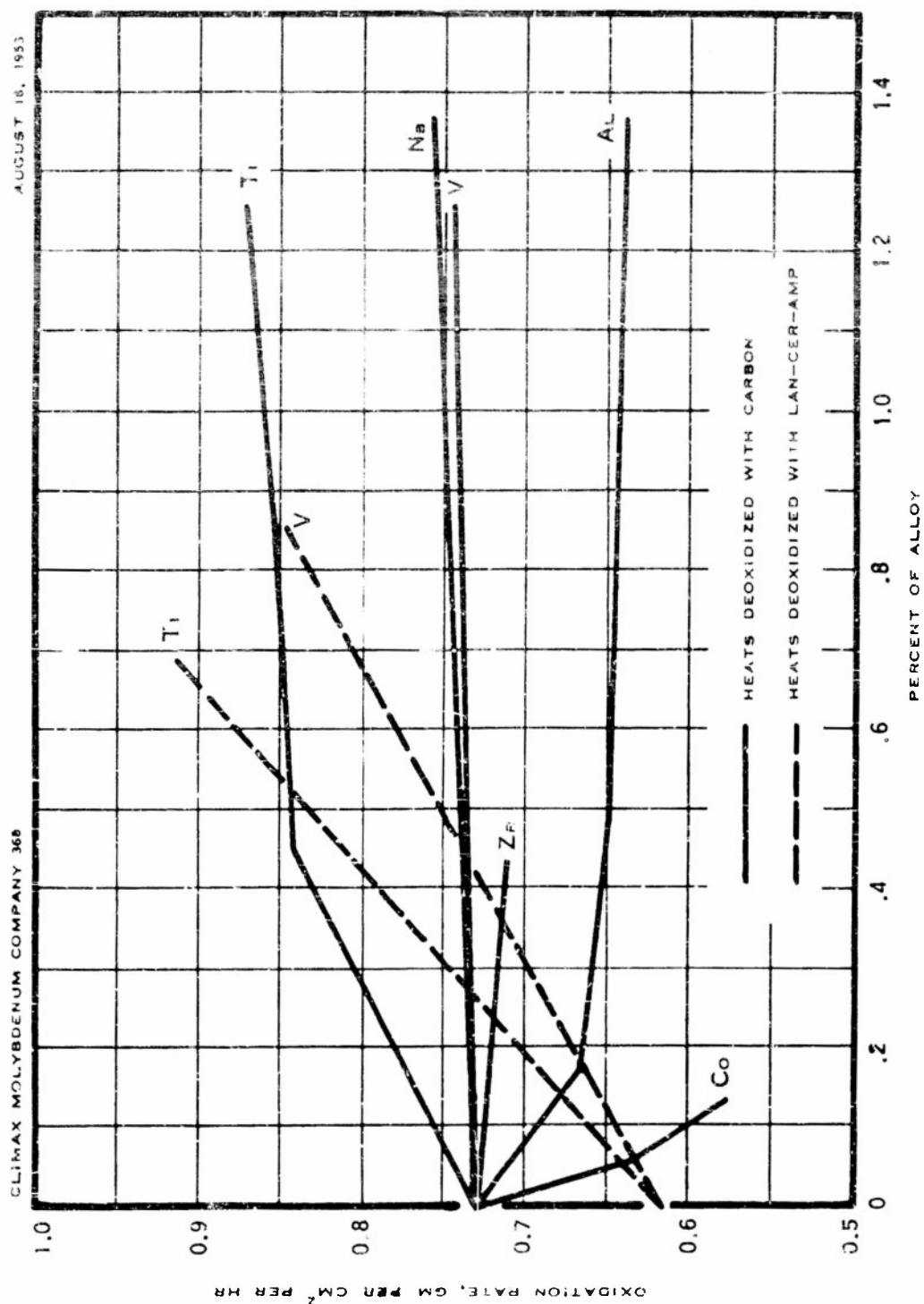


FIGURE 65 - RATES OF OXIDATION OF SOME MOLYBDENUM-BASE ALLOYS
AS A FUNCTION OF ALLOY CONTENT

OXIDATION TESTS IN FLOWING AIR AT 1750 F

It should be realized, in considering these data, that the oxidation rates indicated in Figure 65 are very high, reflecting the volatile nature of the molybdenum oxide formed under test conditions. For example, oxidation rates for Armco iron and SAE 1045 steel determined under approximately the same conditions are 0.070 and 0.049 grams per square centimeter per hour, respectively. It is evident that a decrease in oxidation rate such as that accompanying an increase in cobalt content does not result in an oxidation-resistant material but merely establishes a trend for the alloy system.

Niobium, vanadium, and zirconium exercised only a slight influence on the rate of oxidation of molybdenum within the range of compositions studied. Titanium produced a measurable increase in oxidation. Aluminum lowered the rate of oxidation but the effect was most pronounced between 0 and 0.17% aluminum. It will be noted that the pronounced effect of titanium on oxidation rate was also at the low end of the composition range. Inasmuch as aluminum and titanium contents of this low magnitude are considered primarily as deoxidizing agents and inasmuch as the unalloyed molybdenum deoxidized with rare earth metals, Figure 65, was markedly superior to carbon-deoxidized molybdenum in oxidation resistance, it is postulated that some relationship exists between deoxidation during melting and oxidation.

Cobalt additions enhanced the resistance of molybdenum to oxidation. Were it not for the limiting effects of cobalt additions on workability, it is possible that significant reductions in oxidation rate could be realized within the molybdenum-cobalt system.

In general, molybdenum-base alloys which were deoxidized with rare earth metals oxidized at a somewhat slower rate than the same alloys deoxidized with carbon only; titanium- and vanadium-containing alloys deoxidized with rare earth metals, however, oxidized at slightly faster rates than the same alloys deoxidized with carbon only.

Summary

Binary molybdenum-base alloys containing aluminum, cobalt, niobium, titanium, vanadium, and zirconium have been cast into ingots and worked into rolled bar stock. The size of the ingots processed was about the size that would be used if these materials were in commercial production. The upper limits of alloy content compatible with good recovery were raised by using the Sejournet-Ugine extrusion process for initial breakdown of the castings, but some of the alloys sustained high losses even when the cast sections were extruded. The properties of these alloys are sufficiently interesting for elevated temperature service to justify further study of the factors which affect their fabrication behaviors to determine whether they will be amenable to commercial production. Such factors as oxidation of the extrusion blanks during heating, lubrication, amount of upsetting of the blanks during the initial stages of extrusion, and extrusion ratios require further study. While extrusion temperature may be the most important factor, little can be done about it at present. The recovery of sound metal would be greater if the extrusion temperature could be raised far enough above the present 2600 F limit to allow true hot working.

For the alloys studied, the room-temperature hardness did not increase as rapidly with increasing alloy content as the hardness at 1600 F. The room-temperature hardness values for all of the alloys was low enough to permit secondary mechanical working without difficulty.

Addition of titanium or zirconium raised the temperature of recrystallization of wrought molybdenum significantly. All other additions studied had only minor effects upon recrystallization temperature. Since molybdenum-base alloys develop their highest rupture and creep strength when they are in the strain-hardened condition, a high recrystallization temperature is an important attribute, and metals which markedly raise the recrystallization temperature deserve the greatest amount of consideration for commercial development. Preliminary ventures into the theoretical aspects of recrystallization of arc-cast molybdenum indicate no drastic departure from classical concepts.

Tensile tests conducted at room and elevated temperatures revealed that substantial benefits result from alloying. These benefits were less pronounced for specimens in the recrystallized condition than for those in the as-rolled or stress-relieved conditions. In general, of all the alloys studied, the 0.45% titanium exhibited the highest strength. Bars prepared from castings deoxidized with aluminum or rare earth metals suffered loss in room-temperature elongation, as measured in the tensile test, upon recrystallization. Tensile-transition tests indicated a shift of the transition-temperature zone for these materials to levels above room temperature. The lowest transition temperature under the conditions of the tensile test was -30 F, exhibited by the 0.45% titanium alloy.

Studies of Charpy transition temperatures corroborated the findings of the tensile-transition tests. The impact-transition range of bars deoxidized with materials other than carbon was higher after recrystallization. The notched-bar tests also indicated that these same carbon-free materials had the lowest transition temperatures of all the bars tested prior to recrystallization. None of the alloy additions studied had a marked effect upon the notched-bar transition.

Creep-rupture values significantly in excess of those of the cobalt- and nickel-base superalloys were exhibited by all of the compositions tested. The superiority was more evident as testing temperature increased. The highest strengths were exhibited by the 0.45% and 1.26% titanium, 0.75% niobium, and 0.09% zirconium alloys. For example, the 0.45% titanium alloy, for 100-hour life at 2000 F, sustained a load of 25,500 psi in the stress-relieved condition and 19,500 psi in the recrystallized condition. The minimum elongation was 10% and the average was appreciably above this.

Cobalt and aluminum exerted a beneficial influence upon the resistance of molybdenum to oxidation. In the ranges of composition studied (limited by the factor of workability) the alloy additions did not render the metal sufficiently resistant to oxidation to justify consideration of alloying as a means of protection during exposure at elevated temperature.

STUDIES OF DEOXIDATION

The studies of deoxidation as outlined and pursued during the second and third years of the contract^{2,3} have been continued. The aims of this phase of the research are, in brief, to increase the room-temperature ductility of molybdenum as cast and after working, to increase resistance to high temperature embrittlement, and to improve the recovery of sound, usable, wrought material from a given weight of casting. The experimental work centered upon variations in methods of deoxidation, and during the current year was designed to fill in the gaps in the overall investigation and to enlarge upon the more promising methods developed in the preceding year.

Strictly speaking, deoxidation of molybdenum means the removal of oxygen from molybdenum. However, the term "deoxidation" is here used in a broad sense and covers processes which reduce oxygen content, eliminate gases, and combine residual oxygen in its least detrimental form to yield a workable material. This process is defined as "neutralization" rather than "deoxidation" by some investigators.

Variations in deoxidation have been evaluated on the basis of their effects upon intergranular inclusions on fractured surfaces, room-temperature ductility of cast metal as measured by bend tests, forgeability, transverse strength of wrought sections as measured by ring bursting tests, and high-temperature embrittlement as measured by bend tests after annealing wrought sections at a temperature considerably above the recrystallization temperature.

The methods of deoxidation under study have been divided into four classes, the first of which is the present basic process of arc casting molybdenum in vacuum using carbon as the principal deoxidizer and sometimes using other elements as auxiliary deoxidizers. The use of vacuum prevents the molybdenum from oxidizing during melting and promotes deoxidation by removing gaseous products of reaction. The second class comprises methods of deoxidation in vacuum without the use of added carbon. The titanium, vanadium, zirconium, thorium, and rare earth metals used as deoxidants in this class may or may not remain in the cast metal. Classes 3 and 4 comprise methods of deoxidation with and without carbon, respectively, in an atmosphere of argon instead of vacuum.

The effect of variation in deoxidation procedures upon macrostructure, microstructure, hardness, forgeability, and bend ductility were first investigated in small (6-10 pounds) exploratory ingots. Ingots weighing from 30 to 80 pounds were subsequently prepared by the most promising procedures. The larger ingots provided stock for more extensive forging tests and for a study of ductility of the material in both the cast and the worked conditions. The additions, analyses, hardness as cast, bend angles, and forgeability ratings of experimental ingots are given in Table 12. (The methods of chemical analysis of rare earth metals in molybdenum are described in Appendix A.)

TABLE 12
COMPOSITION, HARDNESS, AND BEND DUCTILITY OF ARC-CAST MOLYBDENUM
DEOXIDIZED IN VARIOUS WAYS

Ingot	Additions, %*	Analyses, %*	Hardness	Bend Angle		Forgeability Rating		
			As Cast	Degrees	When Forged at			
			VPN	Long.	Trans.	2000	2300	2600 F
Class 1 - Melted in Vacuum, Carbon Added								
1078	0.031 C, 0.2 Ti	0.005 C, 0.18 Ti	186		41			
1100	0.041 C, 0.21 Ti	0.015 C, 0.21 Ti	188					
1111	0.027 C, 0.1 LCA	0.007 C, 0.004 RE	181	48	19			
1112	0.030 C, 0.52 Ti	0.015 C, 0.49 Ti	191	44	23			
1205	0.027 C, 0.05 Zr	0.010 C, 0.056 Zr	179	68	33	1	1	2
1209	0.042 C, 0.15 Ni	0.025 C	167		-		porous	
B184	0.033 C, 0.07 Th	0.033 C, 0.091 Th	183		-	2	2	
B197	0.033 C, 0.30 Th		179		0	5	6	
Class 2 - Melted in Vacuum, No Carbon Added								
1045	0.3 LCA	0.003 C, 0.005 Ce 0.007 RE	187	66	51.5			
1048	0.3 LCA, 1.0 Ti	0.003 C, 0.69 Ti no Ce found, 0.12 RE	190	78	100**			
1049	0.3 LCA, 1.0 V	0.001 C, 0.85 V 0.003 Ce, 0.003 RE	184	110**	56			
1061	2.0 LCA		166		1.3	4	6	6
1073	0.1 Ce	0.003 C, 0.003 Ce	183		0		6	
1079	0.3 Al as Mo-Al alloy	0.001 C, 0.018 Al	168		1			
1114	0.5 Ce		161	78	9	2	1	2
1139	0.3 Al as MoAl ₂		172	15	1	5	5	
1141	0.5 Ce	0.006 C, 0.05 Ce	162					
B183	0.004 C, 0.18 Al	0.005 Al	176		0	5	4	5

* RE = total of other rare earth metals. LCA = Lan-Cer-Amp, 50% min. lanthanum, 45-50% cerium, 20-24% "didymium" and yttrium, 1% max iron and unreduced salts.
** did not break

TABLE 12 (continued)

COMPOSITION, HARDNESS, AND BEND DUCTILITY OF ARC-CAST MOLYBDENUM
DEOXIDIZED IN VARIOUS WAYS

Ingot	Additions, %*	Analyses, %*	Hardness	Bend Angle		Forgeability Rating		
			As Cast VPN	Degrees		When Forged at		
				Long.	Trans.	2000	2300	2600 F
Class 3 - Melted in Argon, Carbon Added								
1110	0.027 C, 0.1 LCA							
		(interrupted melt, small ingot)						
B173	0.033 C, 0.05 Th	0.035 C, 0.01 Th	194		8.9		1	1
B174	0.033 C, 5.0 Th	0.036 C, 1.15 Th	202		1	4	6	
B185	0.033 C, 0.07 Th	0.031 C, 0.004 Th	189		-	1	2	1
B196	0.033 C, 0.10 Th		181		0	5	6	
Class 4 - Melted in argon, No Carbon Added								
1064	5.0 LCA	0.075 C, 1.69 Ce 1.99 RE	168		4	6	6	6
1074	0.25 Ce	0.005 C, 0.03 Ce	188	2.7	1.5	4	6	6
1101	0.5 LCA	0.003 C, 0.015 Ce 0.026 RE	171	80	2.6	1	4	4
1102	0.1 Al	0.002 C, 0.096 Al	167	40	14	1	1	1
1105	0.2 LCA, 0.05 Al		175	36	2.3	3	2	6
1106	0.2 LCA		166	20	1	6	4	6
1115	0.5 Ce		163	58	31	1	1	1
1135	0.2 Al, 0.5 V	0.002 C, 0.17 Al 0.48 V	172	38	10	1	1	4
1136	0.2 Al, 0.3 Nb	0.007 C, 0.17 Al 0.32 Nb	160		9	3	2	2
1137	0.2 Al, 0.5 Ti	0.003 C, 0.23 Al 0.44 Ti	168					
1140	0.3 Al as MoAl ₂	0.005 C, 0.30 Al	155	46	30	1	1	1
1142	0.5 Ce	0.008 C, 0.11 Ce	157	69	10			
1201	0.03 Al	0.002 C, 0.012 Al	185	0	0	6	6	6
1202	0.05 Al	0.002 C, 0.027 Al	185	1.2	0	6		
1203	0.10 Al	0.002 C, 0.076 Al	152	39	4	1	1	2
1204	0.15 Al	0.003 C, 0.12 Al	163	27	5	2	2	
1210	0.2 Al, 0.15 Ni	0.003 C, 0.16 Al	181	7	0			

* RE = total of other rare earth metals. LCA = Lan-Cer-Amp, 30% min. lanthanum, 45-50% cerium, 20-24% "didymium" and yttrium, 1% max iron and unreduced salts.

** did not break

In Class 1, Ingots 1078, 1100, 1111, 1112, and 1205 were carbon-vacuum heats to which less carbon was added than is normally required for full de-oxidation, and an additional deoxidizer of some other type was added to supplement the carbon so that the residual carbon content of arc-cast molybdenum alloys could be reduced. The supplementary deoxidizers were titanium, zirconium, and rare earth metals. Titanium and zirconium were chosen because it had been noted in earlier heats that little or no speckling was evident on the fracture surfaces or in the microstructure when titanium or zirconium were added to carbon-vacuum molybdenum. Ingot 1209 was made to gain additional experience in deoxidizing molybdenum-nickel alloys before producing large ingots for mechanical property studies. Heats B184 and B197 (the prefix B indicates a bar machine heat cast in 2" diameter mold) were parts of a series of heats deoxidized with thorium, which was added to the first heat in the form of powder and to the last in the form of chips from thorium sheet. The heats of Class 3 form the remainder of the series de-oxidized with thorium.

In Class 2, Heat 1045 was a heat deoxidized with rare earth metal alone and was large enough to provide stock for extensive forging experiments. Heats 1048 and 1049 were also large heats deoxidized with rare earth metal, but contained titanium and vanadium as alloying elements. Heat 1061 was made with sufficient excess of rare earth metal for alloying. Heat 1073 was made with the addition of cerium equivalent to the amount of cerium in Lan-Cer-Amp. This amount of cerium proved to be insufficient for deoxidation; accordingly, a greater amount of cerium was added to Heat 1114. Ingot 1141 was a 40-pound ingot to provide more stock of the type studied in Heat 1114. For further study of deoxidation with aluminum in vacuum, aluminum was added to Heat 1139 in the form of MoAl_2 and to Heat 1079 as a molybdenum-aluminum alloy containing 1% aluminum. Heat B183 was made from molybdenum-aluminum bar stock that had been melted in argon and subsequently worked. The bar stock was remelted in vacuum, in an attempt to remove the residual aluminum and aluminum oxide by vaporization and thus obtain carbon-free unalloyed molybdenum of high purity.

The bar machine heats of Class 3, along with Heats B184 and B197 of Class 1, form a series for study of the deoxidizing and alloying effects of thorium. Thorium was added to Heat B185 in the form of powder and to B196 in the form of chips from thorium sheet. Heat 1110 was similar to Heat 1111 (Class 1) but was melted in argon.

In Class 4, Heats 1064 and 1074 were companion heats to 1061 and 1073 but were melted in argon rather than in vacuum. In earlier work it had been found that an ingot made with 0.5% misch metal (1005) forged well whereas one made with 0.5% Lan-Cer-Amp (1030) forged poorly³. It seemed unlikely that the difference in forgeability could be entirely the result of difference in the form of rare earth metal addition. To test this point, 0.5% Lan-Cer-Amp was added to Heat 1101. Heats 1105 and 1106 were companion heats made for determining whether forgeability could be improved by simultaneous deoxidation with aluminum and rare earth metal. Heat 1106, to which a small amount of rare earth metal was added, was aluminum-free. Heat 1105 was similar in composition but contained an additional 0.05% aluminum.

Heat 1115 was the companion to Heat 1114 of Class 2, and Heat 1142 was a large heat of the same type for additional stock. Heats 1135, 1136, and 1137 were alloy heats containing 0.5% vanadium, 0.3% niobium, and 0.5% titanium, respectively, and deoxidized with aluminum in argon with the aim of lowering residual carbon content and at the same time producing a forgeable product. Aluminum was added to Heat 1140 in the form of MoAl_2 for comparison with Heat 1139, Class 2. Heat 1210 was the exploratory nickel-alloy heat melted in argon.

Since excess aluminum affects the properties of arc-cast molybdenum, experiments were run to determine the minimum aluminum addition required to effect adequate deoxidation of a powder charge melted in argon. The oxygen contents of different lots of "acceptable" molybdenum powder vary from 0.010 to 0.04%, as determined by the loss of weight in dry hydrogen at 1950 F, and it would be expected that the minimum aluminum addition would depend upon the oxygen content of the powder. Four powder machine heats, 1201, 1202, 1203, and 1204 were melted from a single lot of powder which had a loss of weight in dry hydrogen equal to 0.023%. The amounts of aluminum added were 0.03, 0.05, 0.10, and 0.15%, respectively.

Melting

The heats prefixed with the letter "B" were bar machine heats cast in two-inch diameter molds and were approximately six inches long.

Ten-pound ingots were made in PSM 3 and were three inches in diameter by approximately four inches long. They were quartered lengthwise, and a longitudinal face of one of the quarters was ground, polished, and macro-etched. From examination of this surface, the ingot was judged on the basis of mold filling, general quality, and macro grain size. Later, bend-test specimens, both parallel and normal to the major axes of the grains, were machined from this segment, because of the ease with which the grains could be seen on the polished and etched surface. Sections $1/4$ inch thick were cut from the mid cross section of the second quarter for fractographic and micrographic examination and for hardness measurements. The two remaining quarters were machined to cylinders one inch in diameter to be used for forging tests.

The three large ingots, weighing 40 to 100 pounds, were also melted in PSM 3 in three-inch and four-inch diameter molds. After casting, a transverse slice one inch thick was cut from the mid-section for metallographic examination and determination of hardness and bend ductility. The remaining pieces were forged.

Special precautions were taken to prevent oxidation of the rare earth metals used for deoxidizing molybdenum and molybdenum-base alloys. The rare earth metals oxidize readily in air, especially when in the form of fine chips or powder. Since they are available in lumps only, chips were machined from the lumps for addition in the powder machine. Machining was conducted under kerosene and the chips were washed in carbon tetrachloride several times and sealed in vacuum until used.

Except for a few heats, all of the ingots of Table 12 were melted without difficulty. Thorium, because of its high emissivity, reduces the voltage for a given arc gap with a given arc current, which in turn reduces the power input. As a result, in the earlier heats containing thorium superheating was inadequate and the ingots did not fill the mold. In making later heats melting was governed, not by the current-voltage relationship, as normally, but by setting the feed on the bar machine at a given rate. The current registered by the meters was allowed to rise to a much higher level than usual. This resulted in much sounder ingots and better filling of the mold and was an expedient solution to the problem. At best, arc control with thorium is difficult, and commercial production is not yet feasible. It is possible that voltage-current relationships can be developed which will permit instrument-control of the D.C. arc in heats containing thorium.

Arc control was erratic in the heats to which nickel was added, whether in vacuum with carbon (1209) or in argon with aluminum (1210). This is attributed to lack of experience in melting nickel alloys in PSM 3. Difficulty was also experienced in melting the heat to which aluminum was added in the form of MoAl_2 in vacuum (1139), because the electrode broke repeatedly.

Hardness As Cast

The room-temperature hardness of the ingots, Table 12, was measured on electrolytically polished surfaces. The as-cast hardness of unalloyed molybdenum deoxidized with carbon in vacuum is in the range 176 to 184 VPN, which was established on the basis of hardness determinations made upon a large number of castings. In the series of ingots representing various methods of deoxidation, the hardness of castings was in the range 152 to 202 VPN. In general, the hardness of heats deoxidized with aluminum in argon is less than that of carbon-vacuum molybdenum, and in the present series varied from 152 to 167 VPN. The hardness of the heat containing 0.30% aluminum (1140) was 155 VPN. The heats to which only 0.03 and 0.05% aluminum was added were harder, 185 VPN; they were incompletely deoxidized and contained grain boundary inclusions. Molybdenum alloys containing vanadium or titanium and deoxidized with aluminum were also lower in hardness than comparable alloys deoxidized with carbon in vacuum; for example, compare Heat 1112 with Heat 1137 and Heat 1012 with Heat 1135:

Heat 1112	0.49% Ti	carbon-vacuum	191 VPN
Heat 1137	0.44% Ti	aluminum-argon	168 VPN
Heat 1012	0.56% V	carbon-vacuum	193 VPN
Heat 1135	0.48% V	aluminum-argon	172 VPN

In general, the hardness of alloys deoxidized with rare earth metals lies between that of comparable alloys deoxidized with carbon and those deoxidized with aluminum in argon. Molybdenum-titanium and molybdenum-vanadium alloys deoxidized with rare earth metals (1048, 1049) were not as hard as equivalent heats deoxidized with carbon.

The vacuum-melted heats to which small amounts of thorium as well as carbon were added were of about the same hardness as vacuum-melted, carbon-deoxidized unalloyed molybdenum. The hardness of a heat containing 1.15% thorium and melted in argon (B174), however, was 202 VPN, which reflects solid solution hardening caused by thorium.

The rise in hardness caused by an addition of titanium as a supplementary deoxidizer (1078, 1100) was commensurate with the amount of titanium added, whereas there was no change in hardness when 0.05% zirconium was added to unalloyed carbon-vacuum molybdenum.

Macrostructure

The macrostructures of representative ingots for the study of methods of deoxidation are shown in Figures 66-70. Figure 67 is typical of the heats to which auxiliary deoxidizers, such as titanium and zirconium, were added (1100, 1112, 1078, 1205), all of which filled the mold well. In macrostructure, these heats were comparable to unalloyed, carbon-vacuum molybdenum. The two molybdenum-nickel alloy heats (1209, 1210) did not fill the mold well; the heat deoxidized with carbon in vacuum (1209, Figure 68) exhibited slightly finer grain structure than unalloyed molybdenum and was porous.

The heats deoxidized with 0.01 to 0.30% aluminum and melted in argon, exhibited coarser grain, Figure 69, than comparable heats deoxidized with carbon in vacuum. Heats deoxidized with aluminum and melted in vacuum (1139, Figure 69, and 1079) were comparable in macrostructure to unalloyed, carbon-vacuum molybdenum; almost all of the aluminum addition had been removed during melting.

The argon-melted heats containing more than 0.08% aluminum (1102, 1140, 1204) filled the mold well and had macrostructures similar to that of Ingot 1140, Figure 69. The heats containing less than 0.08% aluminum (1201, 1202, 1203), on the other hand, filled the mold poorly. The macrostructures of Ingots 1201 and 1203 are shown in Figure 69; the macrostructure of Ingot 1202 is similar to these.

The vanadium (1135) and niobium (1136) alloy heats deoxidized with aluminum were similar in macrostructure and mold filling to Ingot 1140, Figure 69. The ingot deoxidized with aluminum and containing titanium (1137) was finer grained than carbon-vacuum ingots of similar titanium content. Ordinarily, coarse grain size is associated with low carbon content (cf. Ingot 1205, Figure 67), but in Ingot 1137 the titanium addition refined the grain in spite of the low carbon content. Titanium may prove to be valuable for refining the grain of future heats of molybdenum deoxidized with aluminum.

Rare earth additions up to 0.5%, whether made in vacuum or in argon, produce essentially the same grain size and macrostructure as that exhibited by Ingot 1105, Figure 70. Greater additions of rare earth metals, 2% (1061) and 5% (1064), produce marked grain refinement. In general, mold filling for all of the heats in the rare earth deoxidation series was not as good as in carbon-vacuum heats, the ingot to which 5% rare earth metals was added being the poorest in this respect.

The grain structure of the heats deoxidized with thorium was much the same whether in Class 1 or Class 3. Increase in thorium content from 0.01% to 1.15% refined the grain, Figure 66. The original diameter of the ingots containing thorium was two inches. Because of poor filling of the mold, the ingots shown in Figure 66 were machined to the size shown in the figure. The macrostructures of Ingots B184, B185, B196, and B197 were similar to that of Ingot B173, Figure 66.

INGOT B173

0.035% CARBON
0.01% THORIUM

CAST IN ARGON
(P917)

INGOT B174

0.035% CARBON
1.15% THORIUM

CAST IN ARGON
(P917)

FIGURE 66 — MACROSTRUCTURES OF INGOTS DEOXIDIZED
WITH CARBON AND THORIUM, X1



INGOT 1205

0.010% CARBON
0.05% ZIRCONIUM

CAST IN VACUUM
(P972)

FIGURE 67 — MACROSTRUCTURE
OF INGOT DEOXIDIZED
WITH ZIRCONIUM, X1



INGOT 1209

0.025% CARBON
0.15% NICKEL ADDED

CAST IN VACUUM
(P972)

FIGURE 68 — MACROSTRUCTURE
OF MOLYBDENUM-NICKEL
ALLOY DEOXIDIZED WITH
CARBON, X1

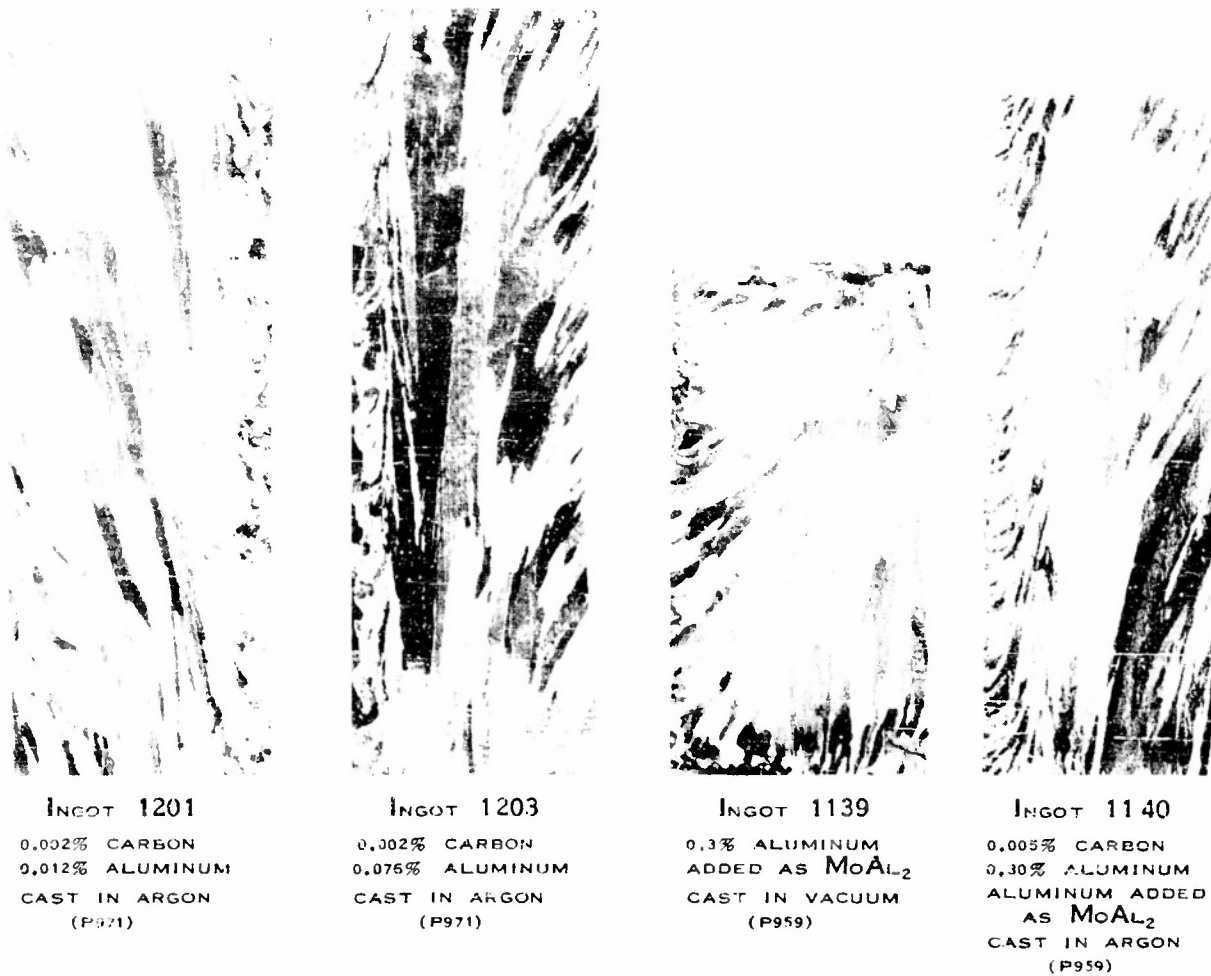
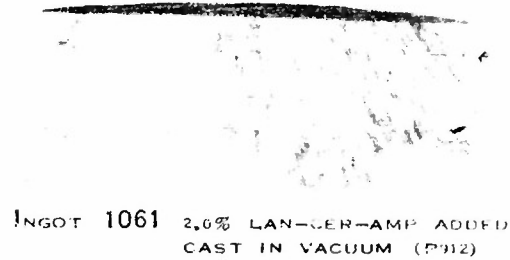


FIGURE 69 — MACROSTRUCTURES OF INGOTS DEOXIDIZED WITH ALUMINUM, X1



INGOT 1061 2.0% LAN-CER-AMP ADDED
CAST IN VACUUM (P912)



INGOT 1064
5.0% LAN-CER-AMP ADDED
0.075% CARBON
1.69% CERIUM
1.99% OTHER RARE EARTH
METALS
CAST IN ARGON (P912)



INGOT 1105
0.2% LAN-CER-AMP
AND 0.05% ALUMINUM
ADDED
CAST IN ARGON (P935)

FIGURE 70 — MACROSTRUCTURES OF INGOTS DEOXYGENIZED
WITH RARE EARTH METALS, X1

Microstructure

Metallographic examination of molybdenum and its alloys, especially examination of the intergranular fracture surfaces, has proved to be a useful tool for estimating degree of deoxidation³. The significance of "speckling" detected by fractography was discussed on page 10 of this report and will be evident in the micrographs presented here.

Titanium and zirconium were added as auxiliary deoxidizers in several unalloyed molybdenum heats. The 0.05% zirconium added to Heat 1205 apparently aided deoxidation. A little speckling was evident on the fracture but not in the microstructure. There was less speckling or oxide than would be expected in a corresponding carbon-vacuum ingot made without the addition of zirconium, Figure 71. Titanium was used as an auxiliary deoxidizer in conjunction with carbon in Heats 1078, 1100 and 1112. Here, the 0.005% residual carbon and the speckling observed on the grain boundary surfaces and in the microstructure, Figure 72, indicate that 0.2% titanium was inadequate for full deoxidation. Increasing the residual carbon to 0.015% and again adding 0.2% titanium, Figure 73, yielded a materially cleaner ingot, although some residual speckling was still visible. When the residual carbon was maintained at 0.015% but the titanium addition was increased to 0.5% (1112), the ingot was devoid of oxide; it was difficult to obtain an intergranular fracture of this ingot, Figure 74. The nickel-alloy heat deoxidized with carbon (1209) in vacuum was devoid of speckling and oxide. The carbide present was commensurate with the carbon content of the heat.

The heat which was melted in argon and to which 0.03% aluminum was added contained an excessive amount of molybdenum oxide and speckling, Figure 75. As the aluminum content was increased, the oxide and speckling decreased progressively. Less oxide and speckling appeared in heats deoxidized with 0.05% aluminum, Figure 76. Addition of 0.10% aluminum was sufficient for full deoxidation, Figure 77; speckling and grain boundary impurities were eliminated. When 0.3% aluminum was added in the form of MoAl_2 in argon (1140), the microstructure was similar to that of Ingot 1204, Figure 77. All the heats deoxidized with aluminum and melted in vacuum contained excessive speckling and oxide at the grain boundaries, whether the aluminum was added as MoAl_2 or as a master-alloy solid solution of aluminum in molybdenum (1079, 1139, B183). These heats were similar in microstructure to Ingot 1202, Figure 76. Poor deoxidation by aluminum in vacuum is not surprising in view of the high partial pressure of aluminum at the melting point of the solid solution, in the order of magnitude of 530 mm mercury; whereas, the operating pressure of the arc furnace was less than 0.1 mm. Analysis for residual aluminum in Ingot 1139 was not made, but there is no reason to suspect that it would be different from that of the aluminum-vacuum ingots previously reported (B183, 0.005% aluminum; 1079, 0.018% aluminum), especially in view of the similarity in microstructure.

Microporosity was observed in all of the molybdenum-base alloy ingots deoxidized with aluminum. The microstructures of the heats containing vanadium (1135), niobium (1136), and nickel (1210) were similar in appearance to that of Ingot 1204, Figure 77. The 0.5% titanium ingot deoxidized with aluminum in argon (1137, Figure 78) was cleaner than a comparable ingot made

previously (936)³. In both the fracture and microstructure, the extraneous constituent has the feathery appearance of carbide. Upon dissolving the sample from Ingot 1137 for chemical analysis, a black residue remained rather than the white residue of aluminum oxide usually obtained from this type of ingot. A black residue suggests the presence of carbide.

Heats deoxidized with less than 0.25% rare earth metals (1073, 1074, 1106), whether melted in argon or in vacuum, were incompletely deoxidized. Throughout the series of heats deoxidized with rare earth metals, the amount of oxide in the microstructure gradually decreased as the amount of rare earth metal was increased. The microstructure of the heat to which 0.1% cerium was added in vacuum contained sheetlike molybdenum oxide on the fracture, Figure 79, an indication of very poor deoxidation. Upon increasing the cerium addition to 0.2% (1106) deoxidation was more effective and only remnants of the oxide were observed in the microstructure. Deoxidation was complete in the 40-pound heat to which 0.3% rare earth metal was added (1045); there was no evidence of molybdenum oxide phase in the grain boundaries, Figure 80. The 0.69% titanium (1048) and 0.85% vanadium (1049) alloy heats deoxidized with 0.3% rare earth metals were similar in microstructure and fracture to Ingot 1045.

The sheetlike oxide was entirely absent from the heat deoxidized with 0.5% rare earth metals and the grain boundaries were clean, Figure 82. The formation of a second phase was first observed with further additions of rare earth metals. It appeared to make little difference whether the addition was cerium alone, or misch metal, or Lan-Cer-Amp. The resulting microstructures were much the same. The heats to which 0.5% cerium (1114, 1115, 1141, 1142) and 0.5% Lan-Cer-Amp (1101) were added were similar in microstructure. What might be second phase was observed in the microstructure of Ingot 1142 at the grain boundaries, Figure 82. On the fracture, more of this "second phase" appeared in Ingots 1115 and 1142 than in Ingots 1114 and 1141 because of the higher residual rare earth content of the ingots melted in argon (0.11% cerium in 1142, 0.05% rare earth metals in 1141). As the amount of rare earth metal added was increased to 2% (1061) and 5% (1064), the amount of second phase increased, Figure 83.

Metallographic techniques for revealing the structure of molybdenum to which rare earth metals have been added are not yet fully developed, especially for the higher concentrations of rare earth metal. It has not been established, therefore, whether the dark areas shown in the photomicrographs, Figure 81, of some of the alloys are a second phase or voids (perhaps remaining after a phase has been torn out in polishing). The amount of dark area increased with increasing amount of rare earth metal added.

Two additional experiments were performed with rare earth metal additions: First, a heat (1111) was made with insufficient carbon for complete deoxidation and insufficient Lan-Cer-Amp, if used alone, in vacuum. The combination produced a clean ingot with low residual carbon, 0.007%, Figure 84. Second, since it had previously been observed that either rare earth metal additions of less than 0.25% or aluminum additions of less than 0.05% were not sufficient for complete deoxidation, two heats were melted in argon with the addition of 0.2% Lan-Cer-Amp, one with 0.05% aluminum (1105) and one without

aluminum (1106). The heat to which no aluminum was added contained massive oxide, whereas the one to which a small amount of aluminum was added was free from oxide. The effects of aluminum and rare earth metals in deoxidizing Heat 1106 appear to be additive.

In the series of heats containing thorium, when the thorium content was about 0.01% or less (B173, B185) the heats were extremely clean and free from speckling, Figure 85. As the thorium content was raised (B174, B184, B196, B197), an oxide phase unlike molybdenum oxide in appearance was observed on the fractures and in the grain boundaries, Figure 86. The heat containing 0.004% thorium (B185) contained less of this phase than the other three heats. As the amount of thorium powder added was increased the amount of oxide increased. Thorium was added to two heats (B196, B197) in the form of sheet rather than powder, but without beneficial effect. The cleanliness of these heats was not improved in spite of the fact that the thorium sheet had been cleaned in nitric acid and hydrofluoric acid prior to introduction into the furnace; they contained large amounts of what is believed (on the basis of observation of unetched specimens) to be thorium oxide on the fractures and in the grain boundaries. Apparently, the thorium sheet contained a considerable amount of oxygen, since a large amount of oxide remained in the heats to which it was added. It has not been established whether the oxide in the molybdenum-thorium ingots was introduced by oxide in the thorium charged or whether the argon used as a protective atmosphere was insufficiently purified to protect thorium.

Bend Ductility

Ductility is generally considered to be a function of purity, the higher the degree of purity the greater the plasticity. In evaluating deoxidation practice, it was believed that ductility would be indicative of the degree of deoxidation and the effect of the deoxidizing agent on grain boundary strength. A simple beam bending test was used for measuring ductility. In adopting this test as a measure of ductility, it was recognized that factors such as rate of strain, temperature of testing and grain size and orientation were especially critical factors with respect to ductility and type of fracture. These factors were, therefore, maintained as constant as possible so that the only variable would be the deoxidation practice, but in some cases there was a sufficient excess of deoxidation agent to produce a significant alloying effect. The deoxidizing agents exerted their most important effects upon the amount, size, shape, and distribution of the excess phases such as oxides and carbides.

Because of lack of sufficient material for thorough investigation of transition from brittle to ductile failure as a function of temperature at a constant strain rate, bend tests were made at room temperature only and the bend angle obtained was used as a measure of the degree of deoxidation attained.

A complete description of the bend test may be found in the third annual report³, page 8. Specimens were cut in such a way that the columnar, as-cast grains of the castings were either longitudinal or transverse with respect to the major axes of the specimens. The surfaces of the specimens were prepared



(A) FRACTOGRAPH, X2000 (M2622)

(B) ELECTROPOLISHED, X2000 (M2680)

FIGURE 71 — MICROSTRUCTURE OF INGOT 1205

0,010% CARBON, 0,056% ZIRCONIUM, CAST IN VACUUM



(A) FRACTOGRAPH, X2000 (M2215)

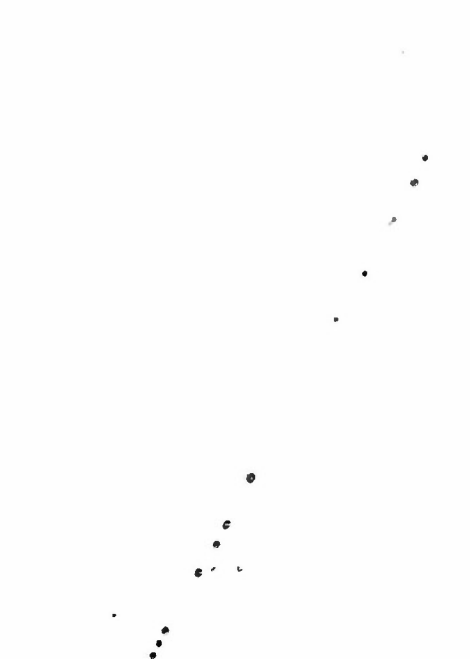
(B) ELECTROPOLISHED, X2000 (M2267)

FIGURE 72 — MICROSTRUCTURE OF INGOT 1078

0,005% CARBON, 0,18% TITANIUM, CAST IN VACUUM



(A) FRACTOGRAPH, X2000 (M2279)



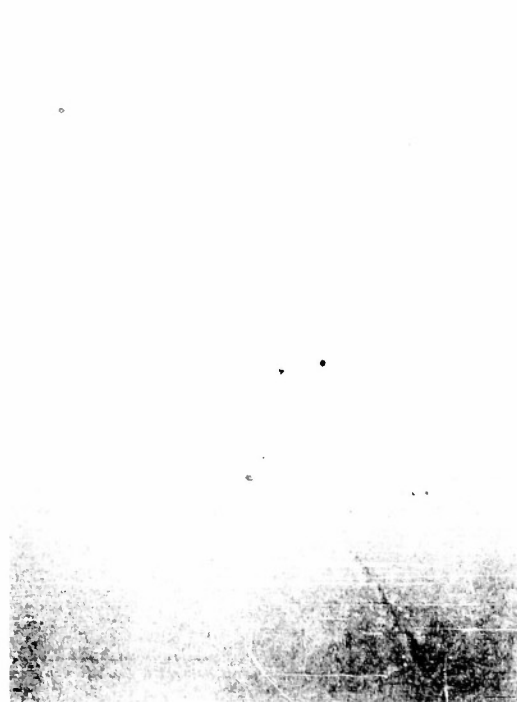
(B) ELECTROPOLISHED, X2000 (M2280)

FIGURE 73 — MICROSTRUCTURE OF INGOT 1100

0.015% CARBON, 0.21% TITANIUM, CAST IN VACUUM



(A) FRACTOGRAPH, X2000 (M2365)



(B) ELECTROPOLISHED, X2000 (M2366)

FIGURE 74 — MICROSTRUCTURE OF INGOT 1112

0.015% CARBON, 0.49% TITANIUM, CAST IN VACUUM

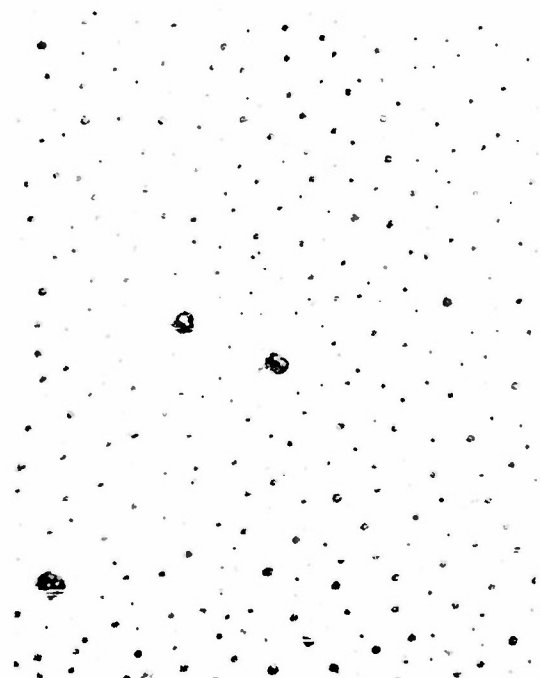


(A) FRACTOGRAPH, X2000 (M2619)

(B) ELECTROPOLISHED, X2000 (M2694)

FIGURE 75 — MICROSTRUCTURE OF INGOT 1201

0.002% CARBON, 0.012% ALUMINUM, CAST IN ARGON
(0.03% ALUMINUM ADDED)



(A) FRACTOGRAPH, X2000 (M2659)

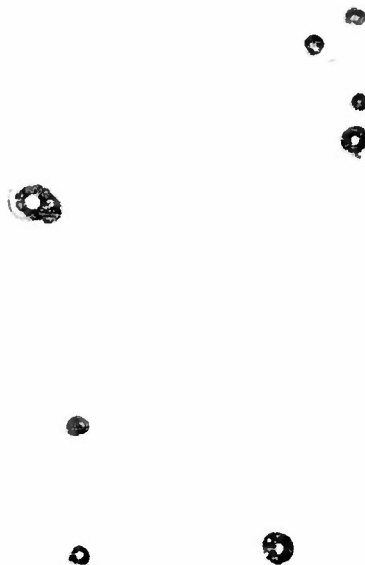
(B) ELECTROPOLISHED, X2000 (M2681)

FIGURE 76 — MICROSTRUCTURE OF INGOT 1202

0.002% CARBON, 0.027% ALUMINUM, CAST IN ARGON
(0.05% ALUMINUM ADDED)



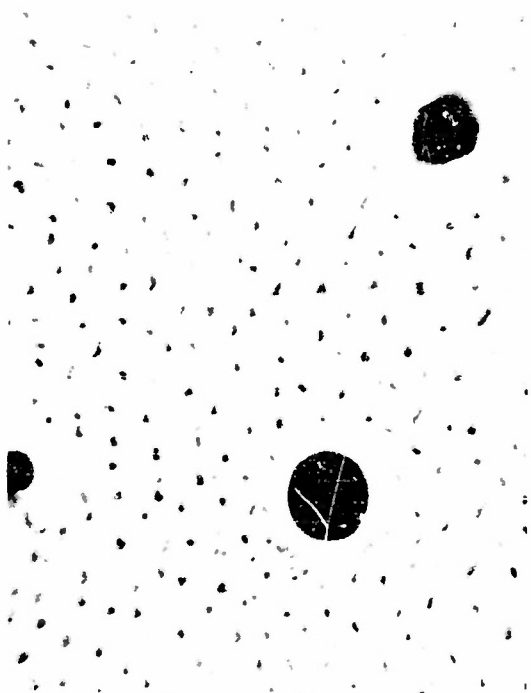
(A) FRACTOGRAPH, X2000 (M2621)



(B) ELECTROPOLISHED, X2000 (M2696)

FIGURE 77 — MICROSTRUCTURE OF INGOT 1204

0.003% CARBON, 0.12% ALUMINUM, CAST IN ARGON
(0.15% ALUMINUM ADDED)



(A) FRACTOGRAPH, X2000 (M2424)



(B) ELECTROPOLISHED, X2000 (M2504)

FIGURE 78 — MICROSTRUCTURE OF INGOT 1137

0.003% CARBON, 0.23% ALUMINUM, 0.44% TITANIUM, CAST IN ARGON



FRACTOGRAPH, X2000 (M2168)

FIGURE 79 — MICROSTRUCTURE OF INGOT 1073

0.1% CERIUM ADDED, CAST IN VACUUM
0.003% CARBON, 0.003% CERIUM



(A) FRACTOGRAPH, X2000 (M2108)

(B) ELECTROPOLISHED, X2000 (M2112)

FIGURE 80 — MICROSTRUCTURE OF INGOT 1045

0.3% LAN-CER-AMP ADDED, CAST IN VACUUM
0.003% CARBON, 0.005% CERIUM, 0.007% OTHER RARE EARTH METALS



(A) FRACTOGRAPH, X2000 (M2318)

(B) ELECTROPOLISHED, X2000 (M2319)

FIGURE 81 — MICROSTRUCTURE OF INGOT 1101

0.5% LAN-CER-AMP ADDED

0.003% CARBON, 0.015% CERIUM, 0.025% OTHER RARE EARTH METALS, CAST IN ARGON



(A) FRACTOGRAPH, X2000 (M2417)

(B) ELECTROPOLISHED, X2000 (M2496)

FIGURE 82 — MICROSTRUCTURE OF INGOT 1142

0.5% CERIUM ADDED

0.008% CARBON, 0.11% CERIUM, CAST IN ARGON



(A) FRACTOGRAPH, X2000 (M2122)



(B) POLISH-ETCH BUFF, X2000 (M2127)

FIGURE 83 — MICROSTRUCTURE OF INGOT 1064

0.0% LAN-CER-AMP ADDED

0.075% CARBON, 1.69% CERIUM, 1.99% OTHER RARE EARTH METALS, CAST IN ARGON



(A) FRACTOGRAPH, X2000 (M2354)

(B) ELECTROPOLISHED, X2000 (M2355)

FIGURE 84 — MICROSTRUCTURE OF INGOT 1111

0.007% CARBON, 0.004% RARE EARTH METALS, CAST IN VACUUM



(A) FRACTOGRAPH, X2000 (M2675)

(B) ELECTROPOLISHED, X2000 (M2699)

FIGURE 85 — MICROSTRUCTURE OF INGOT B185

0.031% CARBON, 0.004% THORIUM, CAST IN ARGON



(A) FRACTOGRAPH, X2000 (M2660)

INGOT B186, 0.033% CARBON, 0.011%
THORIUM ADDED, CAST IN VACUUM

(B) ELECTROPOLISHED, X2000 (M2687)

INGOT B186, 0.033% CARBON, 0.10%
THORIUM ADDED, CAST IN VACUUM**FIGURE 86 — MICROSTRUCTURE OF INGOTS DEOXIDIZED WITH THORIUM**

by polishing through 000 metallographic paper. A deflection rate of 0.005 inch per minute (a tension strain rate of approximately 0.0002 inch per inch per second on the tension side of the specimen) was used throughout.

Experience has shown that when molybdenum ingots are examined metallographically and evidence of oxide appears at the grain boundaries, either in the form of gross speckling or sheetlike oxide, the bend ductility, especially in the transverse direction, will be zero. However, if the specimen is well deoxidized, that is, no evidence of oxide on the fracture and microstructure, a minimum bend angle of 2° may be expected at room temperature in transverse specimens at a deflection rate of 0.005 inch per minute. Transverse bend ductility is more critical than longitudinal ductility.

Although the metallographic examination seems to correlate well with the minimum bend ductility obtained, the maximum bend ductility cannot be predicted from appearance of the microstructure. The maximum bend ductility is of especial interest, however, for two reasons: (1) it is an indication of lower transition temperature, and (2) it indicates that the material shows promise of resistance to high temperature embrittlement and might thus be more suitable for welding. The matter of embrittlement is discussed in a later section of this report. The bulk of the data on carbon-vacuum molybdenum show the bend ductility as determined in this bending test to be from about 2 to 12° prior to fracture. The average is about 4°.

The results obtained from the simple beam bending test are given in Table 12. In all but isolated instances they are the average of two tests. Where no bend ductility values are given, no test was made because of poor metallographic appearance (oxide) or because the material had already been tested in an earlier, duplicate heat. When the oxide content was not great and there was doubt about bend ductility, the test was made.

The high values of transverse bend ductility of the carbon-vacuum ingots containing a small amount of zirconium (1205) or titanium (1078, 1112) as auxiliary deoxidizers are noteworthy and confirm data published in the third annual report regarding improved ductility in the presence of zirconium and titanium. This high bend ductility is manifested in Ingot 1078 in spite of the incomplete deoxidation indicated by the microstructure.

The bend ductility of the nickel alloy heat deoxidized with aluminum (1210) was zero, in spite of metallographic evidence of good deoxidation. The nickel alloy heat deoxidized with carbon (1209) was very porous; therefore, no specimen was machined for bend test.

The transverse bend ductility of argon-melted heats to which aluminum was added in amounts up to 0.05% (1201, 1202) was zero. Aluminum contents sufficient to produce microstructures free from nonmetallic inclusions in the grain boundaries (1102, 1140, 1203, 1204) resulted in bend angles varying from 4° to 40°. The heats which were melted in vacuum and to which only aluminum was added for deoxidation (1079, 1139, B183) contained sheet-type oxides in the grain boundaries and exhibited poor bend ductility (1°, 1°, and 0°, respectively). The molybdenum-vanadium (1135) and molybdenum-niobium (1136) alloys melted in argon and deoxidized with aluminum had transverse

bend angles of 9° and 10°, respectively. A prior, 0.3% titanium alloy (946) melted in argon and deoxidized with 0.25% aluminum (discussed in the third annual report) also exhibited good bend ductility (19°).

Bend angles of heats made with additions of up to 0.25% rare earth metals (1073, 1074, 1106) were less than 2°. One heat vacuum melted with additions of 0.027% carbon and 0.10% Lan-Cer-Amp had a clean microstructure and a transverse bend angle of 19°. Heats deoxidized with 0.3% Lan-Cer-Amp and melted in vacuum (1045, 1048, 1049) exhibited higher transverse bend angles (51°, 100°+, and 56°, respectively) than any other castings with which the present year's investigation has been concerned. The titanium-bearing alloy (1048) casting had the highest bend angle ever observed in the performance of this project. When rare earth metal additions were increased to 0.5% (1101, 1114, 1115, 1142) the bend angles obtained were 2.6°, 9°, 10°, and 31°. Ingot 1141 was a duplicate of Ingot 1114 and was not tested. When the rare earth metal additions were further increased to 2% and 5%, bend angles were 1° and 4°, respectively. The grain sizes of these heats were markedly finer than in heats melted with less of the rare earth metals, and a second metallic phase was observed in the matrix and in the grain boundaries.

Although an addition of 0.2% Lan-Cer-Amp to an argon-melted heat gave a bend angle of 1° and an addition of 0.05% aluminum gave a bend angle of 0°, the combined additions of 0.2% Lan-Cer-Amp and 0.05% aluminum (1105) produced a bend angle of 2.3°.

To sum up the rare earth metal series, although the bend angles are scattered because the transition for the specimen occurs near room temperature, deoxidation with these elements, whether melting is accomplished in vacuum or in an argon atmosphere, has produced some of the best bend ductility values developed during the performance of this contract. There is evidence that Lan-Cer-Amp, misch metal, and pure cerium will produce comparable results.

In the thorium series, only four heats were tested by the bend ductility test. Heat B173, to which 0.05% thorium was added along with 0.033% carbon and which was melted in argon, sustained a bend angle of 8.9° before fracture; this heat exhibited grain boundaries free from nonmetallic inclusions. Of the other three heats, two were melted in argon with thorium additions of 5.0% (B174) and 0.10% (B196), and one was melted in vacuum (B197) with the addition of 0.3% thorium; bend angles for these heats were 1°, 0°, and 0°, respectively. All three of these heats contained an abundant amount of oxide in the grain boundaries.

Forgeability

Exploratory Heats. One of the most important criteria of the effectiveness of a deoxidizer, for the purposes of the present work, was forgeability. The forgeability of the 6 to 10-pound ingots of this series was measured by upsetting cylinders one inch in diameter by one inch long, machined with axes parallel to the ingot axes. Sufficient sound stock was available from some of the ingots only for cylinders 3/4 inch in diameter by 3/4 inch long.

The cylinders were upset 50% in 1/8-inch steps and were reheated between each step. Forging tests were made at 2000, 2300, and 2600 F. All of the specimens were heated in a hydrogen atmosphere for forging. Forgeability was rated according to the appearance of the upset cylinders on the scale shown in Figure 88. The data obtained from the forging test are given in Table 12. They correlate well with metallographic structure and transverse ductility determined in the bend test, Figure 87. Considering the data of Table 12, it appears that forging at 2600 F is a much more severe and selective test than forging at 2000 F.

Forging of the specimens from the series of heats deoxidized with increasing amounts of aluminum was about as expected from examination of the cast microstructure. All specimens from the ingot deoxidized with 0.03% aluminum (1201) cracked. The ingot deoxidized with 0.05% aluminum (1202) cracked upon forging at 2300 F but forged satisfactorily at 2000 F. The specimens from ingots deoxidized with 0.10% (1203, 1102) and 0.15% (1204) aluminum forged well at all three forging temperatures. The ingot to which 0.3% aluminum was added in the form of MoAl_2 (1140) also forged well. The heats deoxidized with aluminum in vacuum (B183, 1139) did not forge. The ingot deoxidized with 0.05% aluminum and 0.2% rare earth metal (1105) cracked less than the ingot deoxidized with 0.05% aluminum alone.

Ingot to which up to 0.25% rare earth metals were added (1073, 1074, 1106) were not forgeable, the upset cylinders contained large cracks. Likewise, the ingots to which 2% (1061) and 5% (1064) rare earth metals were added did not forge. Failure to forge the first group is attributed to insufficient deoxidation, whereas failure to forge the latter is undoubtedly due to the excessive amount of extraneous phase in the grain boundaries.

The ingots to which 0.5% rare earth metals was added (1101, 1114, 1115) were forgeable and warranted the production of additional stock for further study. The addition of 0.5% cerium produced an ingot of better forgeability than 0.5% Lan-Cer-Amp, especially when added in argon (1115).

In the series of alloys containing thorium, Heats B173, B184, and B185 forged satisfactorily without developing small bursts or cracks; whereas, Heats B174, B196, and B197 were unforgeable. The results of the forging tests agree well with observed microstructures. Of the heats to which thorium was added in the form of powder (B184, B185), the ingot melted in argon forged better than the ingot melted in vacuum. The heats made with chips from thorium sheet were unforgeable, undoubtedly because of the high oxide content at the grain boundaries, Figure 85a.

The ingot deoxidized with carbon and zirconium (1205) forged satisfactorily. Contrary to expectation after examination of the microstructure, the molybdenum-base nickel alloys did not forge well. It is possible that they could have been forged at a higher temperature. Because of their porosity, the ingots to which 0.15% nickel was added (1209, 1210) were not forged. Inasmuch as the two ingots containing nickel were comparatively new alloys from the point of view of melting in the powder machine, the defects in these heats

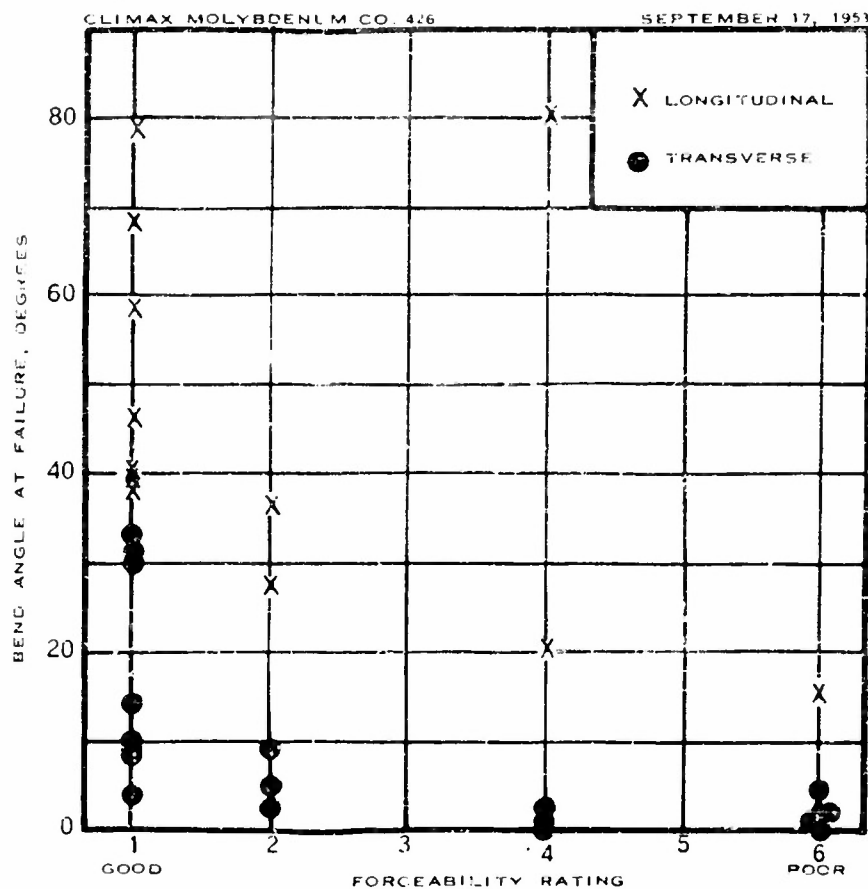


FIGURE 87 -- RELATIONSHIP BETWEEN BEND DUCTILITY AND FORGEABILITY OF MOLYBDENUM-BASE ALLOYS

1. NO DETECTABLE
SURFACE RUPTURES

2. SHORT CRACKS

3. MEDIUM LENGTH
INTERGRANULAR CRACKS

4. SMALL BURSTS

5. ONE LARGE BURST

6. GROSS RUPTURE



FIGURE 88 — SCALE FOR RATING FORGEABILITY OF UPSET CYLINDERS

(P902)

are thought to have been due more to inexperience in melting than to improper deoxidation. Further experience in handling and melting these alloys is expected to result in ingots of better quality.

The vanadium (1135) and niobium (1136) alloy heats deoxidized with aluminum forged satisfactorily.

Forging of 40- and 100-Pound Heats. The 40- and 100-pound ingots were made for more extensive forging tests. Ingots 1045, 1048 and 1049 were four inches in diameter and weighed about 100 pounds each. The others were three inches in diameter and weighed about 40 pounds. The ingots of these groups were cut in half crosswise, and a mid-section slice one inch thick was removed for determination of properties as cast. The two remaining pieces were machined to remove surface imperfections and submitted for forging, either under a hammer or on the forging press, between a 60°-V bottom die and a flat, top die. All specimens were heated in hydrogen. Previous experience indicated that the optimum temperature range for forging was 2300 to 2600 F. Therefore, an attempt was made to forge at least one half of each ingot in this range. If resistance to deformation was high, the forging temperature was raised.

The ingots to which 0.2% titanium (1078) and 0.3% aluminum (1079) were added cracked during early stages of forging. This behavior was predicted from the large amount of oxide observed on the fractures and at the grain boundaries. The ingot deoxidized with 0.1% lan-cer-amp and 0.027% carbon and cast in vacuum (1111) and that containing 0.5% titanium (1112) cracked badly on forging at 2600 and 3000 F. It is difficult to reconcile the poor forgeability of these ingots with what has so far been regarded as favorable appearance of fracture and microstructure.

Forging of the remaining ingots (1045, 1048, 1049, 1100, 1137, 1141, 1142) was satisfactory. Flow sheets showing the forging schedules are given in Figures 89-95. The ingots deoxidized with 0.5% cerium in argon or vacuum forged well and yielded satisfactory recovery, with one exception, Ingot 1141, forged at 2300 F. The percentage recovery from the three heats deoxidized with rare earth metals was low. This was not cause for immediate concern, however, since these not only were the first attempts to forge molybdenum-base alloys deoxidized with rare earth metals, but also were among the first attempts to forge molybdenum-base alloys in the 600-ton hydraulic forging press recently acquired. After Ingots 1045, 1048, and 1049 were forged, they were rolled in a commercial tool steel mill to 5/8-inch diameter and reserved for the study of mechanical properties recorded in an earlier section of this report.

The emphasis of further studies of forging molybdenum should be placed on the initial breakdown of the coarse, columnar, cast structure, as this is the critical operation. Generally speaking, if a billet survives the first few passes in the forging press without cracking, the total recovery upon completion of hot-cold working will be high. Sparse information at hand indicates that when coarse, columnar structure is present, intergranular oxidation of the surface layers easily occurs during initial forging and is responsible for hot shortness.

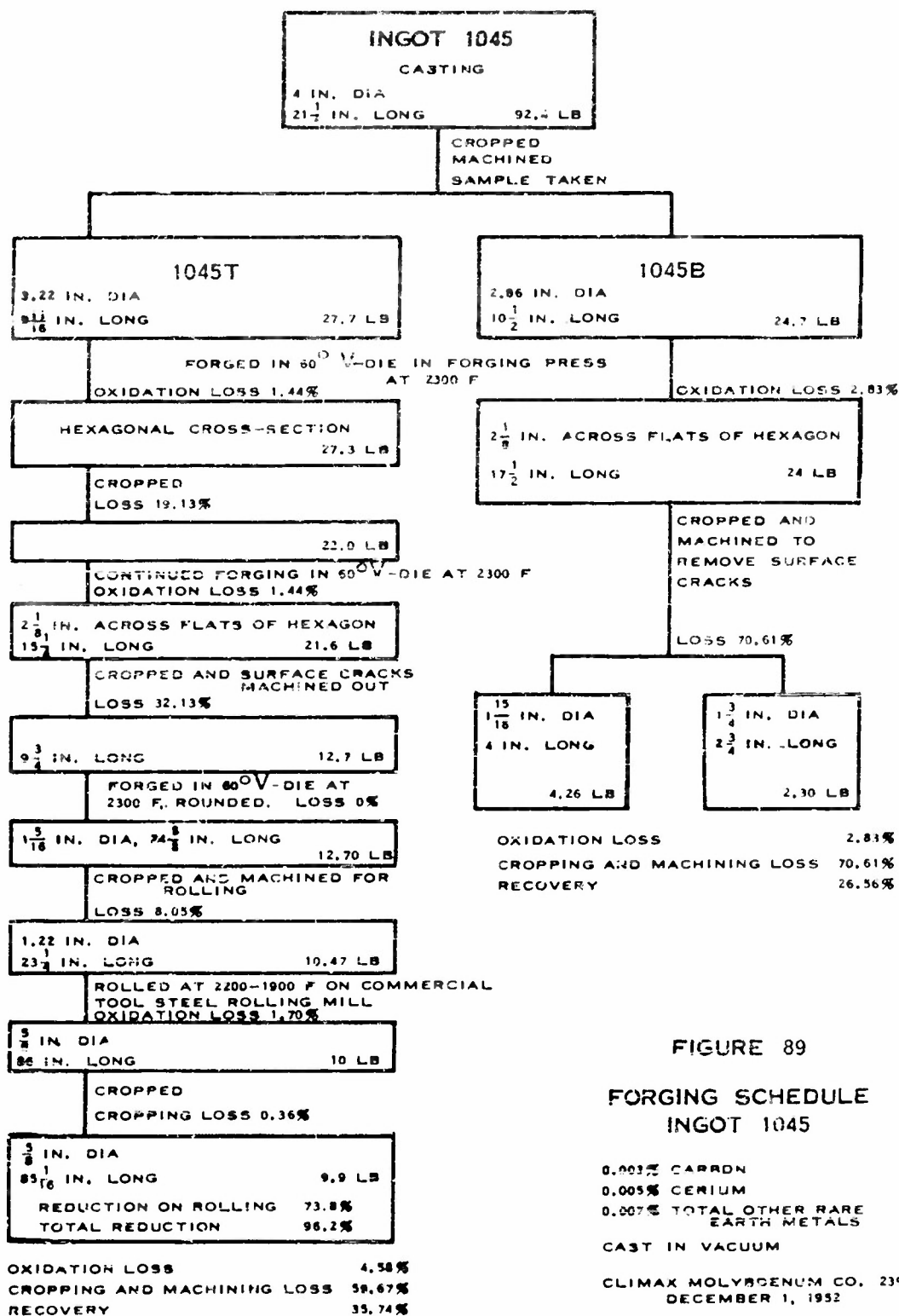
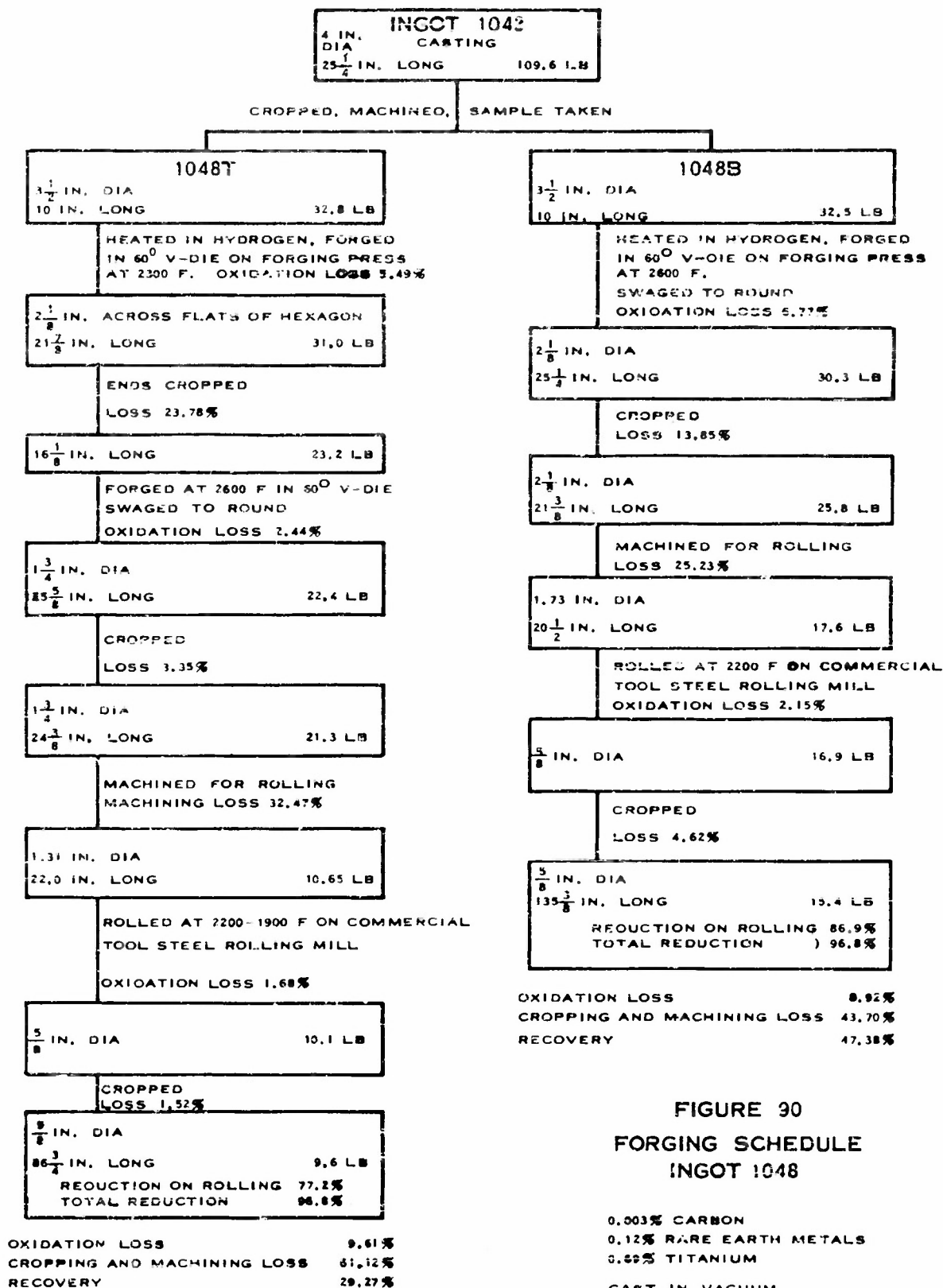


FIGURE 89

FORGING SCHEDULE INGOT 1045

0.003% CARBON
0.005% CERIUM
0.007% TOTAL OTHER RARE
EARTH METALS
CAST IN VACUUM

CLIMAX MOLYBDENUM CO. 239
DECEMBER 1, 1952



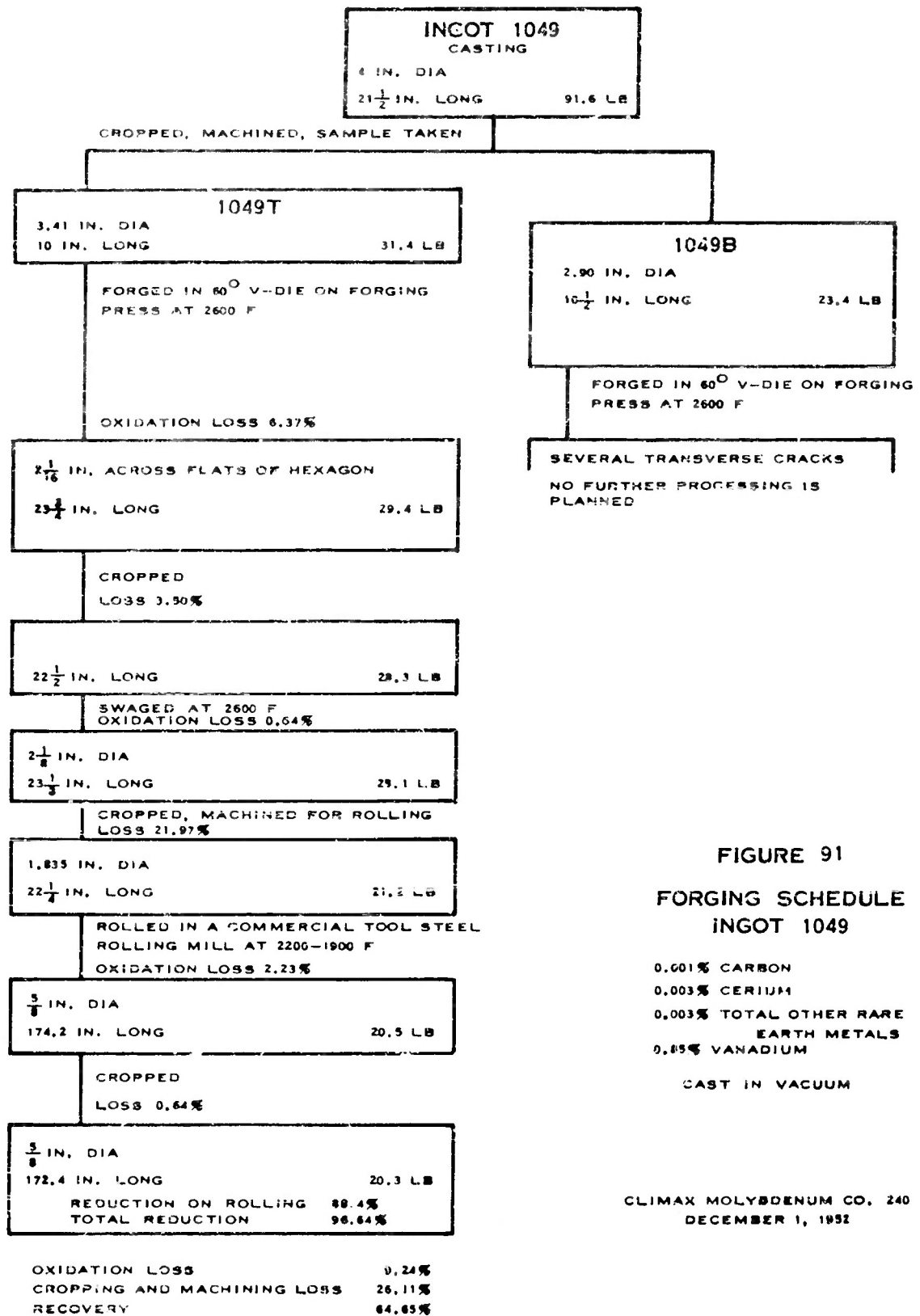


FIGURE 91
FORGING SCHEDULE
INGOT 1049

0.001% CARBON
0.003% CERIUM
0.003% TOTAL OTHER RARE
EARTH METALS
0.85% VANADIUM

CAST IN VACUUM

CLIMAX MOLYBDENUM CO. 240
DECEMBER 1, 1952

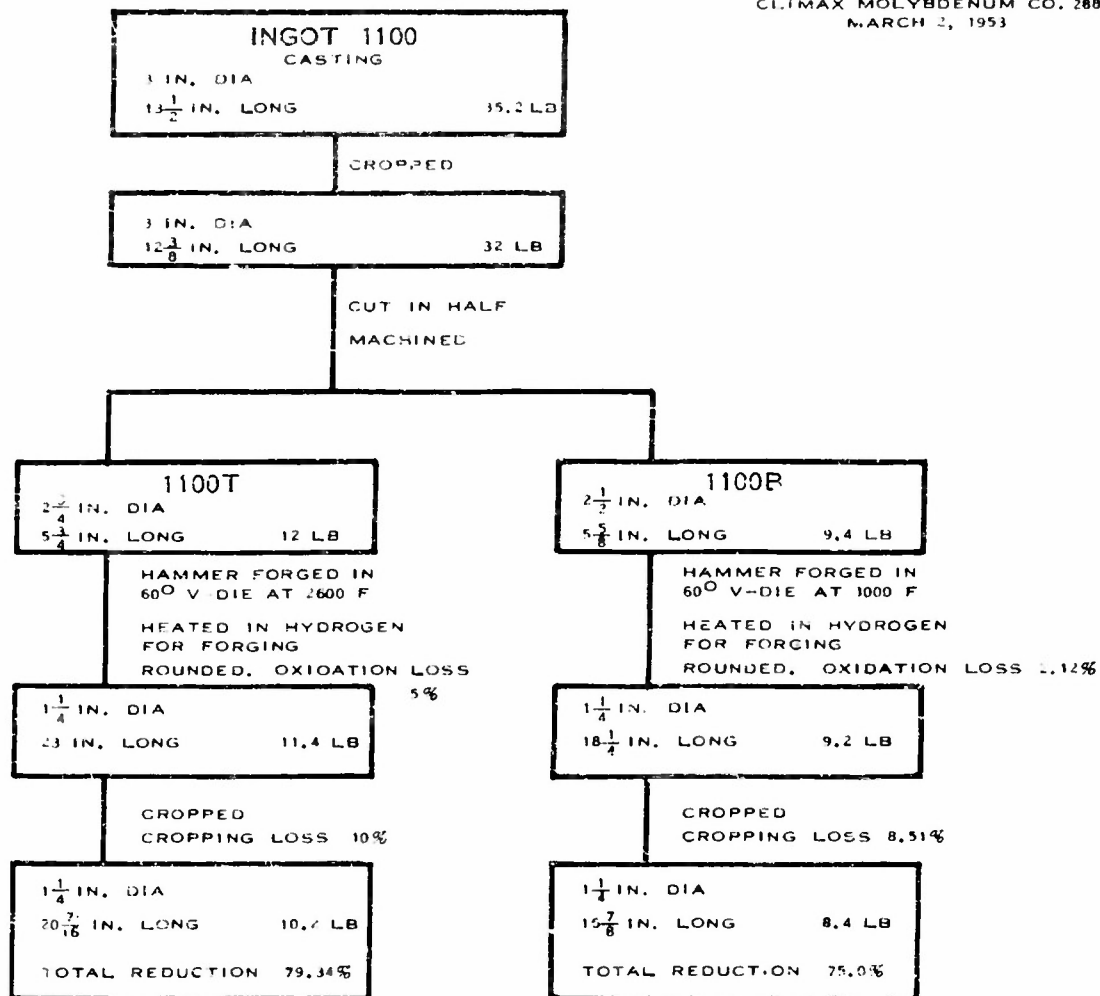
FIGURE 92

WORKING SCHEDULE INGOT 1100

0.015% CARBON
0.21% TITANIUM

CAST IN VACUUM

CLIMAX MOLYBDENUM CO. 288
MARCH 2, 1953



5%
10%
85%

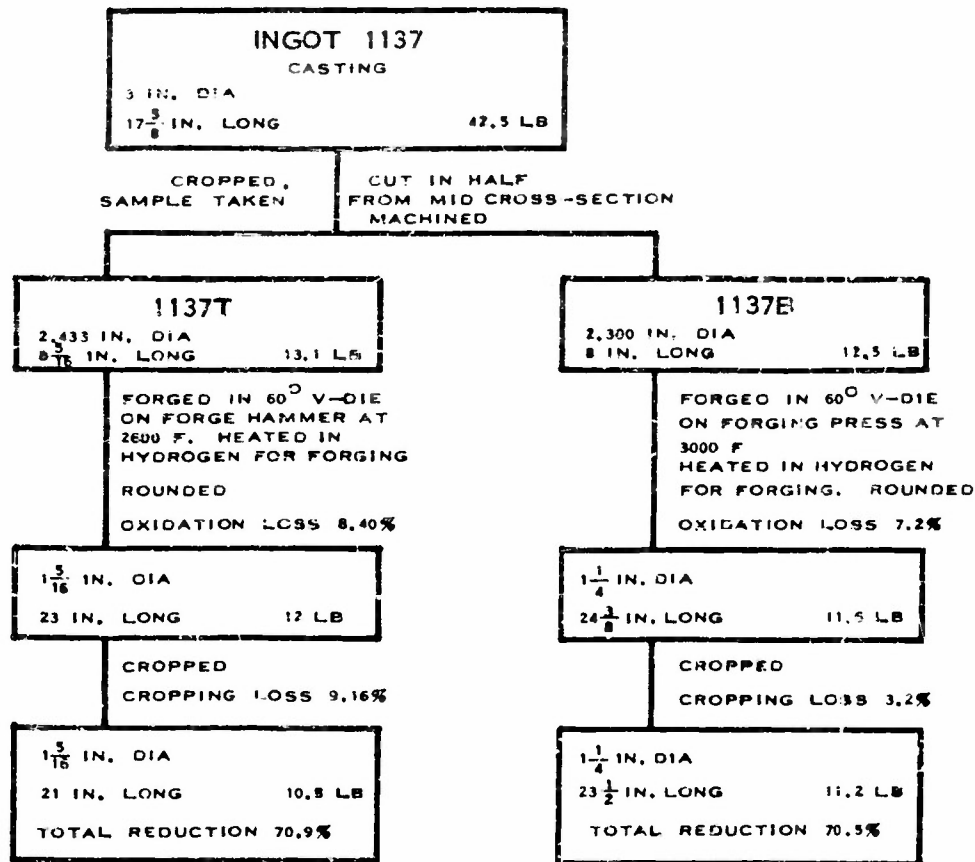
OXIDATION LOSS
CROPPING LOSS
RECOVERY

2.12%
8.51%
89.36%

FIGURE 93
WORKING SCHEDULE
INGOT 1137

0.003% CARBON
0.23% ALUMINUM
0.40% TITANIUM

CAST IN ARGON
CLIMAX MOLYBDENUM CO. 291
MARCH 2, 1953



8.40%
9.16%
82.44%

OXIDATION LOSS
CROPPING LOSS
RECOVERY

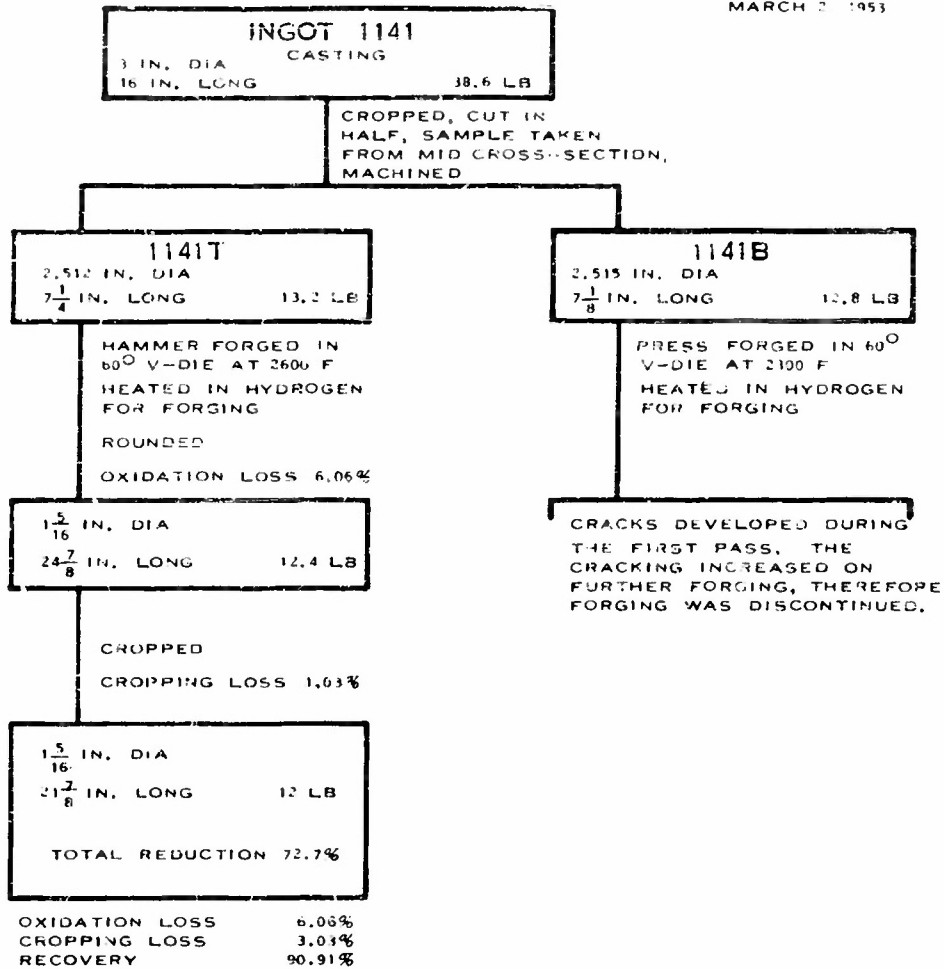
7.2%
3.2%
89.6%

FIGURE 94
WORKING SCHEDULE
INGOT 1141

0.006% CARBON
0.05% CERIUM

CAST IN VACUUM

CLIMAX MOLYBDENUM CO., 269
MARCH 2, 1953



CLIMAX MOLYBDENUM CO., 250
MARCH 2, 1953

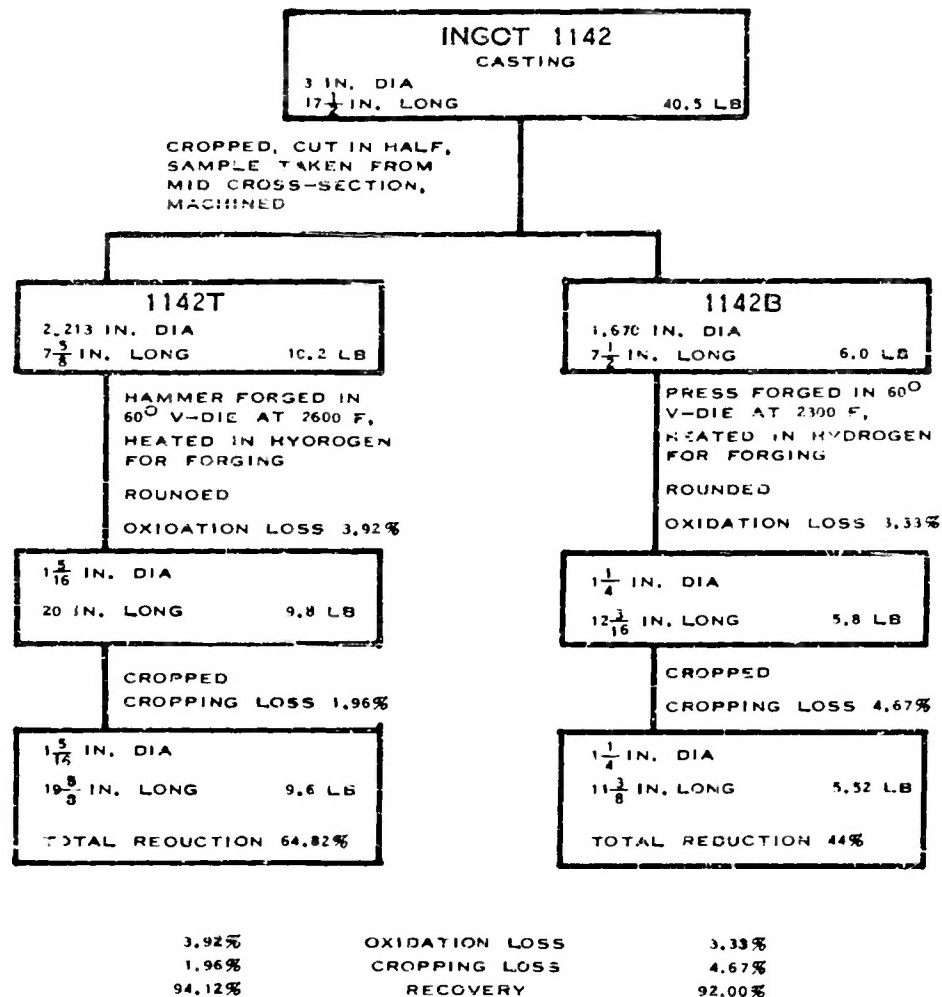
FIGURE 95

WORKING SCHEDULE

INGOT 1142

0.008% CARBON
0.11% CERIUM

CAST IN ARGON



Ring Bursting Tests

Transverse ductility was measured by the ring bursting test described in the third annual report. Bursting stress was computed according to the formula

$$f = \frac{2L}{dt\pi}$$

where t = thickness, d = inside diameter of the specimen and L = load at bursting. The purpose in making the test was to correlate transverse ductility with variations in deoxidation, forging practice, and heat treatment. The bars were heat treated over a range of temperatures to produce stress-relieved, partially recrystallized, and fully recrystallized structures, with and without subsequent grain growth. The ring bursting test was selected because it was the most convenient method of determining transverse strength and ductility on a limited amount of material. All of the data obtained by this test on the molybdenum-base alloys studied are given in Table 13.

Summary

1. Addition of supplementary deoxidizers, such as titanium and zirconium, to molybdenum ingots cast in vacuum and utilizing carbon as the primary deoxidizer, produces a workable ingot with low residual carbon content.
2. If aluminum alone is used for deoxidation, melting must be done in argon and an addition of at least 0.10% aluminum is necessary to accomplish adequate deoxidation and produce a workable ingot from molybdenum powders of commercial purity.
3. Workable, molybdenum-base, binary alloys of niobium, titanium, and vanadium have been produced by deoxidation with aluminum.
4. Workable, molybdenum-base binary alloys of titanium and vanadium have been produced by deoxidation with rare earth metals in vacuum.
5. The effects of variation in deoxidation practice on mechanical properties were discussed in the preceding section.

TABLE 13
RESULTS OF RING BURSTING TESTS

Ingot	Forging and Annealing Temperatures, F	Bursting Stress psi	Elongation %
1141T	forged at 2600	56,100	2.37
	ann. 1 hr at 2000	51,900	1.74
	2200	50,400	2.38
	2400	52,000	2.05
	2600	38,400	3.47
	2800	29,700	1.69
	3000	23,900	0.96
1142T	forged at 2600	49,000	1.97
	ann. 1 hr at 2000	46,900	0.75
	2200	46,100	1.31
	2400	48,500	3.93
	3000	29,500	2.06
1142B	ann. 1 hr at 2000	46,700	1.10
	2200	37,100	1.10
	2600	29,300	1.00
	2800	32,300	1.80
	3000	31,100	0.50
1045E	forged at 2300	59,400	2.40
	ann. 1 hr at 2200	57,600	2.00
	2400	50,100	1.50
	2600	43,100	2.90
	2800	41,800	3.30
1100T	forged at 2000	71,600	0.20
	ann. 1 hr at 2000	64,500	0.50
	2200	42,300	0.30
	2400	44,900	0.30
	2600	60,300	1.80
	2800	52,400	2.20
	3000	51,200	1.20
1100B	forged at 3000	71,300	1.60
	ann. 1 hr at 2000	69,600	1.70
	2200	68,000	1.40
	2400	61,000	1.40
	2600	56,200	2.60
	2800	46,200	1.10
1137T	forged at 2300	12,000	0.40
	ann. 1 hr at 2200	45,700	1.10
	2600	25,800	1.10
	2800	6,900	1.00
1137B	forged at 3000	20,100	0.70
	ann. 1 hr at 2000	25,000	1.20
	2200	22,000	1.00
	2400	16,300	1.10
	2600	11,100	0.90
	2800	27,400	1.20
	3000	21,300	0.80

EMBRITTLMENT

An empirical approach was made to the problem of loss of ductility of wrought molybdenum and molybdenum-base alloys after exposure to elevated temperatures. Thirty new compositions in addition to those described in the third annual report were investigated by submitting samples to one-hour annealing treatments in purified argon at temperatures up to and including 3900 F, and by preparing and testing beam bending specimens therefrom. The methods of sample preparation and testing technique were described in the third annual report.

In considering experiments of the type recorded here, it must be remembered that the ductility of any test specimen is a function not only of the material being tested, but also of the testing temperature, rate of application of strain, and mode of stressing. Stated somewhat differently, a critical temperature--or temperature range--exists for a given material, specimen geometry, and strain rate above which ductile behavior and below which brittle behavior is experienced. In a similar manner, critical strain rates are observed for isothermal tests conducted on specimens of like design. From these statements it follows that the term embrittlement implies a deleterious shift in the critical ranges of factors such as temperature and strain rate such that under the specific conditions of test, low ductility is obtained. It also follows that the term embrittlement is ambiguous unless all of the conditions under which an embrittlement test is made are reported. The results reported in this section represent embrittlement as indicated by beam bending tests run at uniform strain rate at room temperature.

Table 14 lists the compositions of the heats studied. Several heats in Table 14 are carried over from the previous year, including the unalloyed datum heat (739).

Inasmuch as all of the test specimens were wrought materials and were annealed at temperatures well above the recrystallization temperature, the variation in fabrication histories from heat to heat was not considered to be significant. In brief, however, specimens from heats used in the physical properties program were machined directly from rolled bar stock. All other specimens were taken from 1/4" thick plates flattened at approximately 1800 F.

Plots of bend ductility against annealing temperature are included as Figures 96 through 99. The curve for Heat 739 (0.045% carbon) has been reproduced on each chart as a means of evaluating effects of alloying and changes in deoxidation.

Unalloyed molybdenum deoxidized with carbon in vacuum (739) is observed to retain its ductility after heat treatment for one hour at 3100 F; higher temperatures, however, result in embrittlement under the conditions of strain rate and temperature of the bend test.

It was noted in the third annual report that aluminum-deoxidized molybdenum exhibited much greater resistance to elevated temperature embrittlement than carbon-deoxidized heats. The superiority was more pronounced for materials

TABLE 14

HEATS FOR EMBRITTLEMENT STUDY

Heat	Carbon, %	Others, %
739	0.045	
814	0.005	0.20 Al
987	0.003	0.53 Al
1135	0.002	0.17 Al, 0.48 V
1136	0.007	0.17 Al, 0.32 Nb
1137	0.003	0.23 Al, 0.44 Ti
1045	0.003	0.005 Ce, 0.007 RE*
1141	0.006	0.05 Ce
1142	0.008	0.11 Ce
1101	0.003	0.015 Ce, 0.026 RE*
1048	0.003	0.69 Ti, 0.12 RE*
1049	0.01	0.85 V, 0.003 Ce, 0.003 RE*
1144	0.020	0.074 Co
1274	0.031	0.12 Cr
1272	0.022	0.10 Fe
978	0.019	0.52 Nb
1057	0.033	0.75 Nb
1269	0.017	0.04 Ni
1273	0.030	0.09 Si
1100	0.015	0.21 Ti
1132	0.024	0.45 Ti
1133	0.014	0.85 Ti
1138	0.014	1.22 Ti
1009	0.036	1.26 Ti
1174	0.027	3.59 Ti
B185	0.031	0.004 Th
B173	0.035	0.01 Th
B125	0.035	0.03 Th
B184	0.033	0.091 Th
B174	0.036	1.15 Th
1151	0.006	1.25 V
1205	0.010	0.056 Zr
1207	0.019	0.09 Zr
* other rare earth metals		

containing aluminum in the range of 0.15 to 0.25% than for those with higher aluminum contents. These findings are corroborated by the data obtained during the past year to the extent that molybdenum containing 0.53% aluminum (987) is less resistant to loss of ductility upon heating than that containing 0.20% aluminum (814). These data may be found in the upper portion of Figure 96. Heats containing niobium or titanium and deoxidized with aluminum exhibited excellent resistance to embrittlement, while a vanadium alloy deoxidized with aluminum was only slightly superior to the datum heat.

Proceeding on the assumption that resistance to embrittlement was dependent upon methods of deoxidation (or more probably presence of a grain boundary phase such as molybdenum carbide), a series of rare-earth-deoxidized heats was studied. The results of tests on heats deoxidized with rare earth metals are plotted at the top of Figure 97.

The heat containing 0.59% titanium and deoxidized with rare earth metals (1048) showed excellent bend ductility, even after an anneal at 3900 F. The heats deoxidized with cerium alone (1141, 1142) were significantly inferior to those deoxidized with Lan-Cer-Amp (1045, 1101). There are certain discrepancies in the data for heats deoxidized with rare earth metals; for example, Heat 1045 was less resistant to embrittlement than Heat 1101, though similar in composition. Further study of the effects of deoxidation with rare earth metals will be necessary for a satisfactory understanding of embrittlement of this class of material.

In the early stages of the program on embrittlement, high hope was held for the molybdenum-thorium system on the basis of tests on a heat containing 0.03% thorium (B125). Repeated efforts to duplicate the results obtained on this heat were unsuccessful, as indicated in the graph in the lower half of Figure 96. It must be concluded now that the original heat was abnormal in some respect and that molybdenum-thorium alloys are no better than unalloyed molybdenum with respect to resistance to embrittlement, in the composition range studied.

Of the balance of the molybdenum-base alloys deoxidized with carbon, those containing cobalt, chromium, iron, nickel, niobium, silicon, vanadium, or zirconium were found to be neither superior nor inferior to unalloyed molybdenum within the range of composition studied. As indicated in the upper chart of Figure 98, molybdenum-titanium alloys, particularly those containing less than 1% titanium, were superior to unalloyed molybdenum. The benefit of titanium in reducing embrittlement is also evident from the results for the molybdenum-titanium heats deoxidized with aluminum (1137) and rare earth metals (1048), both of which were markedly superior to similarly deoxidized unalloyed molybdenum.

In conclusion, it would appear that resistance to embrittlement is in some way associated with deoxidation practice. Embrittlement starts at a lower temperature for heats deoxidized with carbon than for those deoxidized with aluminum or rare earth metals. The embrittlement of carbon-deoxidized molybdenum seems to be connected with the presence of excess carbide. Contrary to previous suppositions, thorium is no panacea for embrittlement. Titanium in the lower concentrations shows promise as far as alleviation of elevated temperature embrittlement is concerned, regardless of the method of deoxidation.

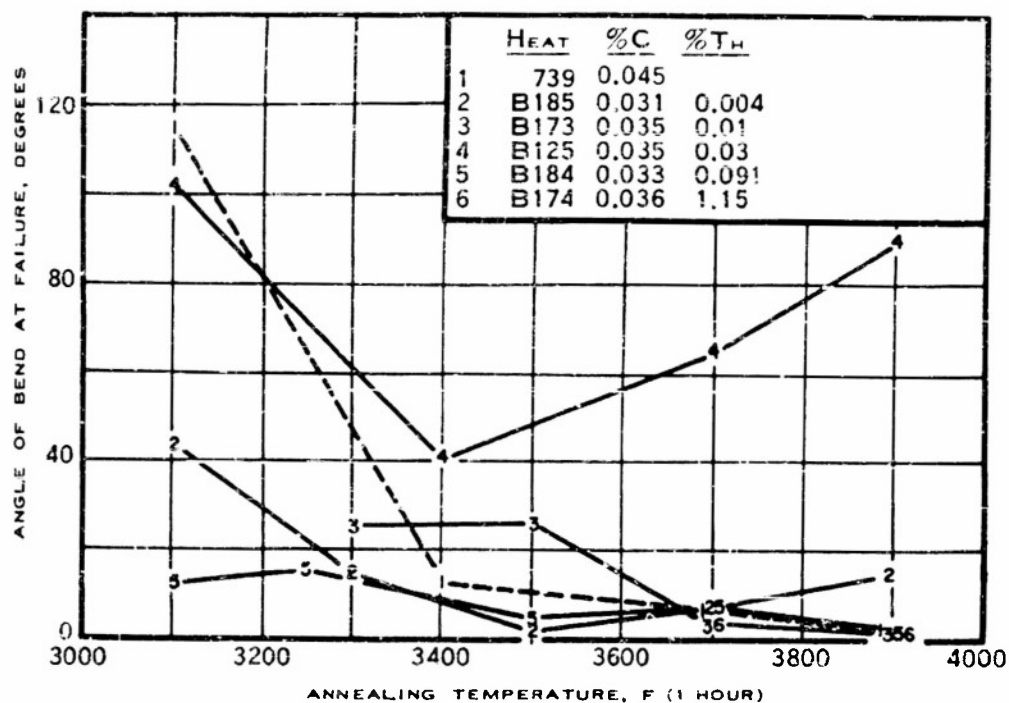
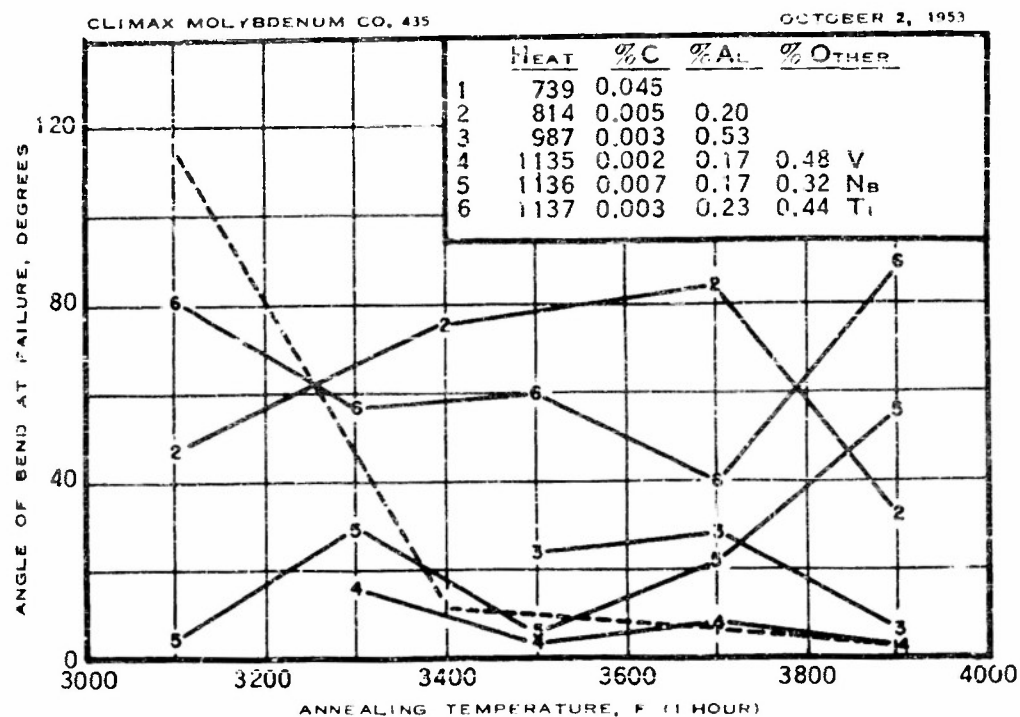


FIGURE 96 - BEND DUCTILITY OF MOLYBDENUM-ALUMINUM AND MOLYBDENUM-THORIUM ALLOYS AFTER ANNEALING ONE HOUR AT INDICATED TEMPERATURES

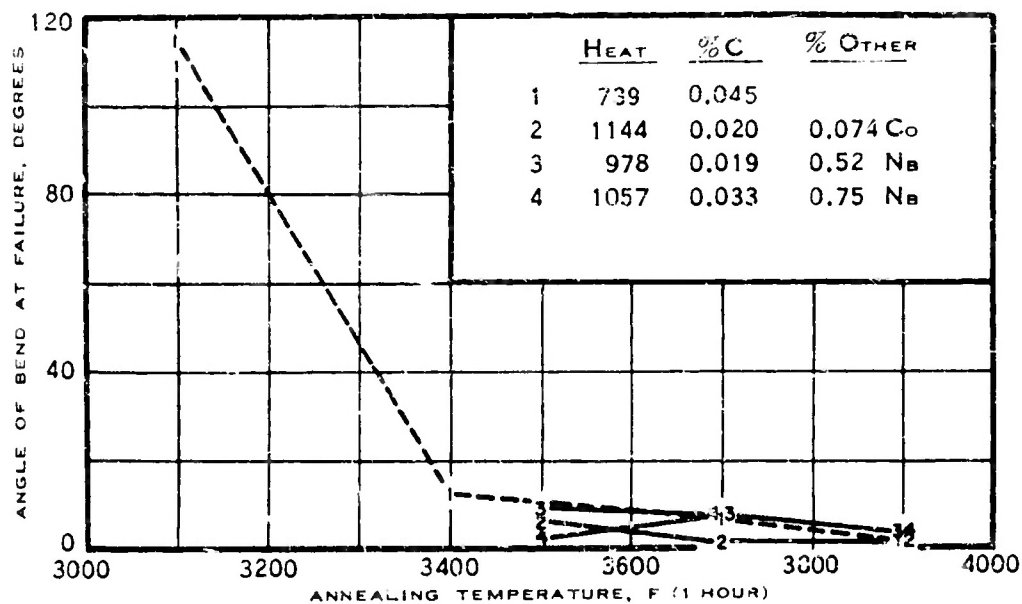
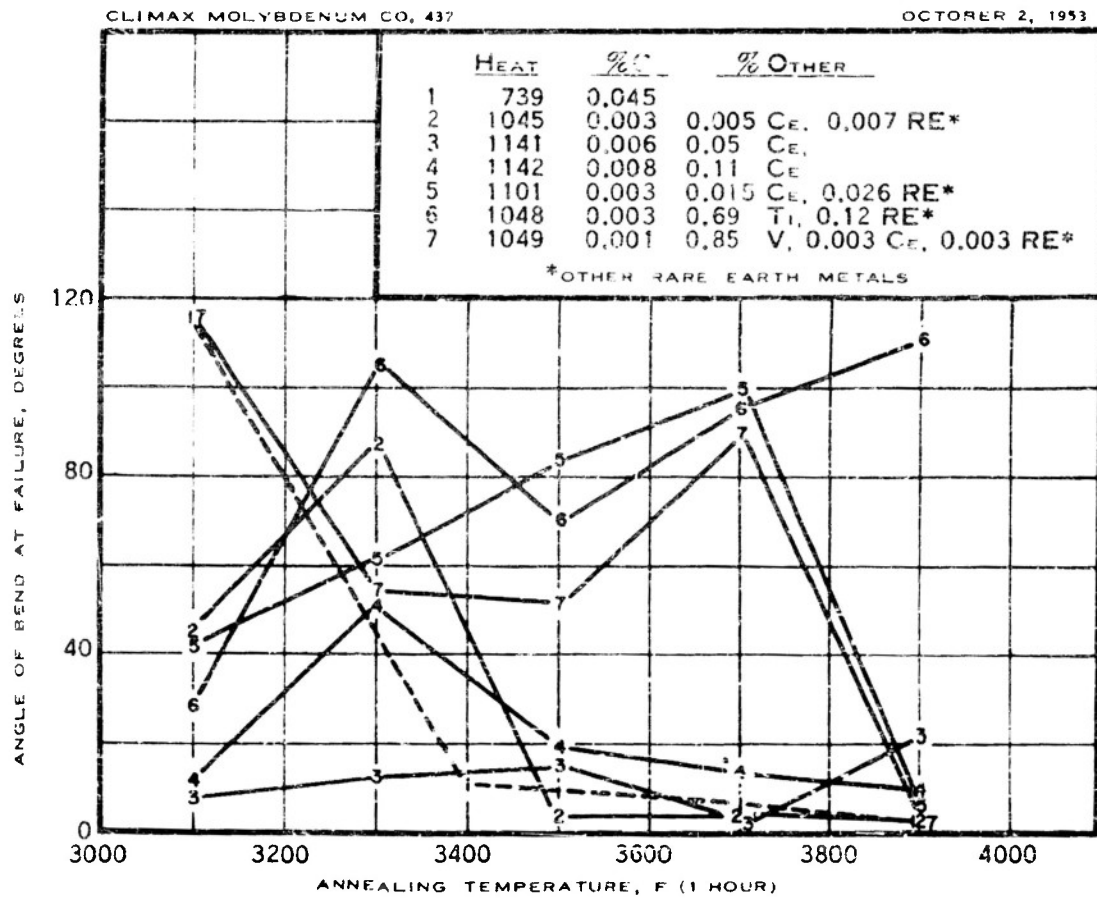


FIGURE 97 - BEND DUCTILITY OF MOLYBDENUM-BASE ALLOYS
AFTER ANNEALING ONE HOUR AT INDICATED
TEMPERATURES

CLIMAX MOLYBDENUM CO. 438

OCTOBER 2, 1953

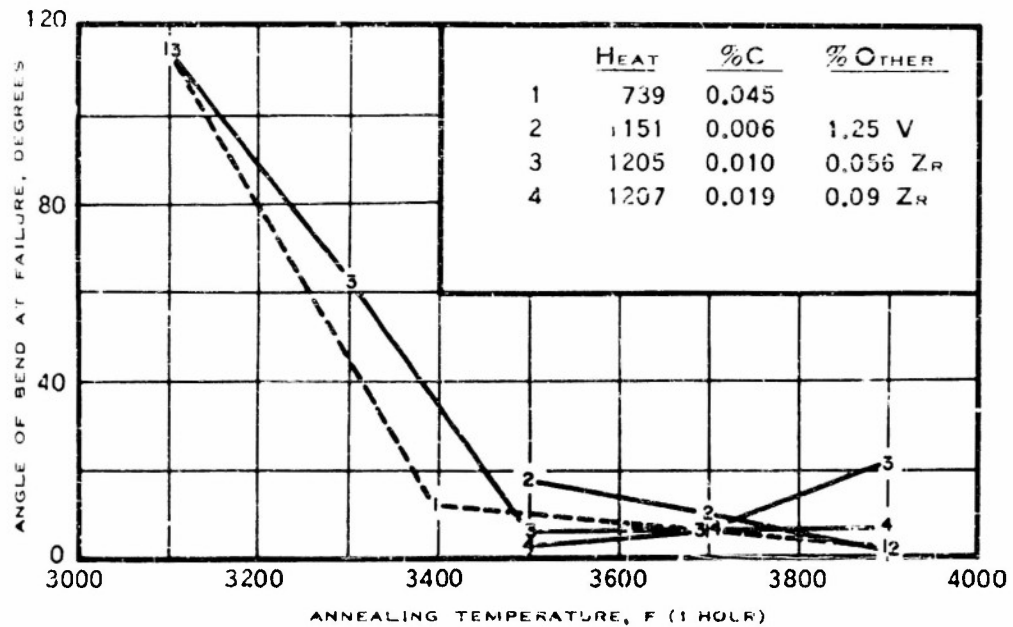
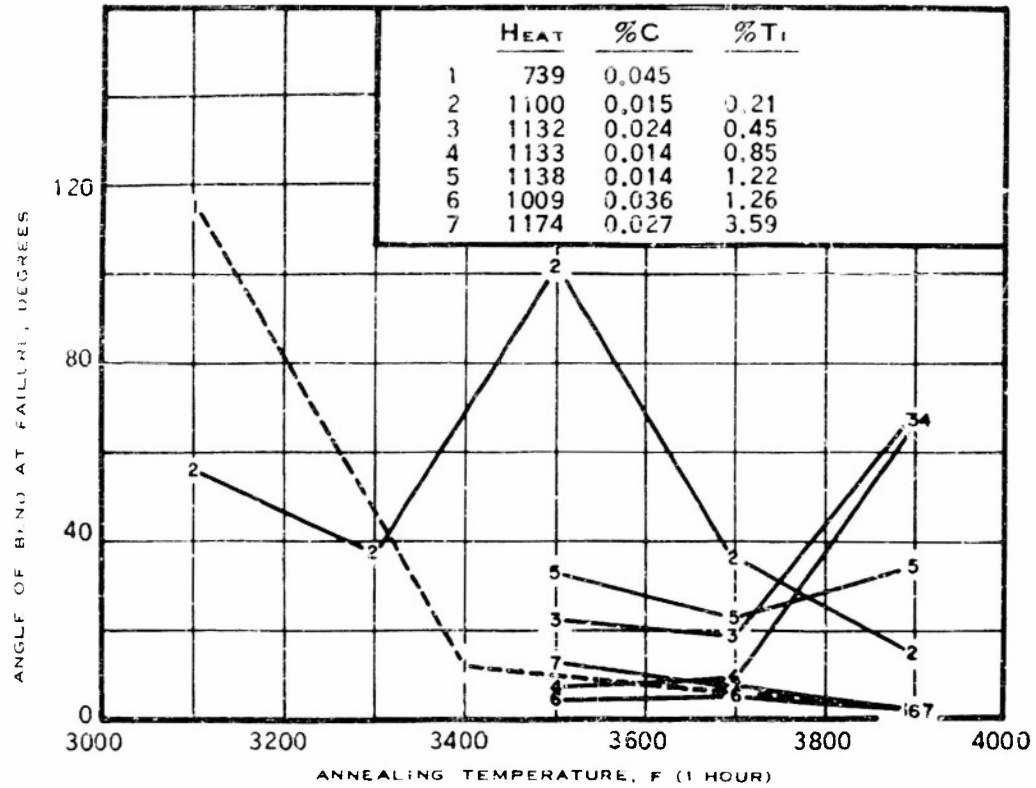


FIGURE 98 — BEND DUCTILITY OF MOLYBDENUM-BASE ALLOYS AFTER ANNEALING ONE HOUR AT INDICATED TEMPERATURES

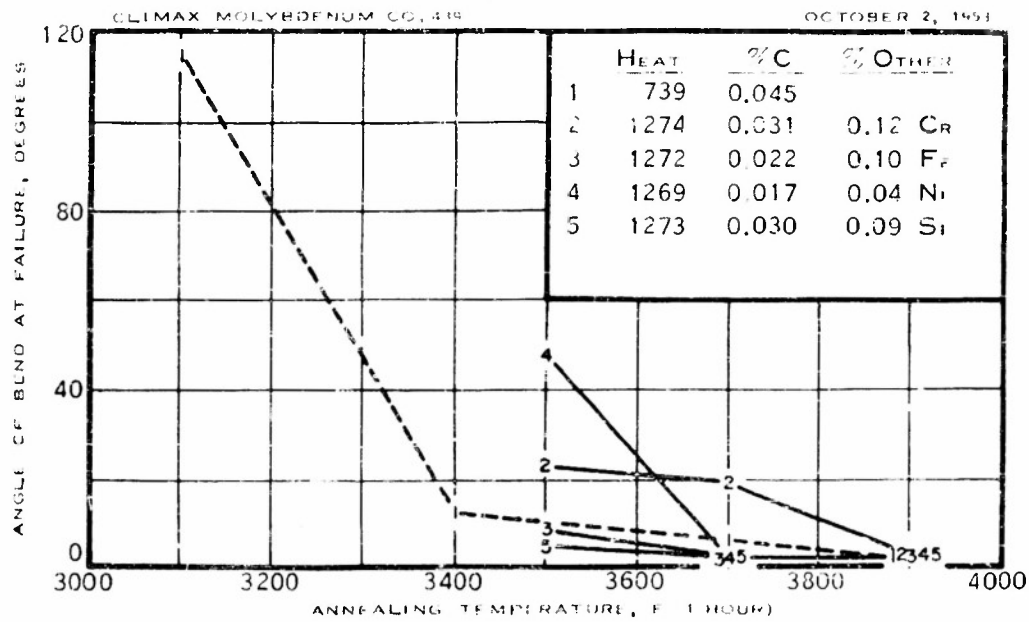


FIGURE 99 - BEND DUCTILITY OF MOLYBDENUM-BASE ALLOYS AFTER ANNEALING ONE HOUR AT INDICATED TEMPERATURES

TERNARY MOLYBDENUM-BASE ALLOYS

The object of this phase of the investigation was to conduct a preliminary survey of some ternary alloys of molybdenum to determine which alloys provided the greatest possibility of improving the mechanical properties of molybdenum for service as a structural material at elevated temperatures. The experimental work was planned to determine whether addition of two alloying elements would produce a combination of properties superior to those developed by only one alloying element.

The investigation was started on a series of graded ingots in which the concentration of one alloying element was a constant, arbitrarily selected so that the hardness of the binary alloy at 1600 F would be about 90 VPN, and in which the concentration of a second alloying element was gradually increased from zero to a percentage which would yield an alloy of about 200 VPN at 1600 F. By using a graded ingot, a series of alloys could be obtained from a single heat--alloys that otherwise would require the preparation of many heats involving considerable time, material, and effort.

The mechanical characteristics of the bar melting machine, described in the first annual report, are especially suited to the preparation of such ingots. The graded ingots were divided into small, homogeneous sections which were used for metallographic examination, x-ray diffraction studies, and hardness tests at room and elevated temperatures. The sections were also analyzed chemically, and the results of all tests and examinations were correlated with chemical composition. The aim of these correlations was to indicate the concentrations of alloying elements which warranted more extensive investigation on ternary ingots of uniform concentration.

The binary molybdenum-base alloys to which third elements were added were prepared specifically for the mechanical properties program described earlier in this report. Their heat numbers and alloy contents were as follows:

Heat 1063	0.17% Al	0.003% C
1144	0.07% Co	0.020% C
1057	0.75% Nb	0.033% C
1132	0.45% Ti	0.024% C
1051	0.54% V	0.027% C

These binary heats, except for 1063, were deoxidized with carbon in vacuum and contained residual carbon. This carbon was retained in the ternary alloys in the form of carbide, which is considered an impurity.

Bars 5/8 inch in diameter from the binary heats were used as the consumable electrode for making the ternary alloys. The ternary ingots were cast in a 2-inch diameter mold and weighed about six pounds each. The concentration of third element varied from zero at the bottom of the ingot to a maximum at the top. After casting, the ingots were soaked at 3000 F in hydrogen for 2 to 18 hours to minimize microscopic segregation. The ingots were split longitudinally for examination. Hardness surveys were made at room temperature with

Vickers impressions at 1/4-inch intervals over the entire longitudinal section. The hardness patterns indicated that there was no gross segregation of the alloys. Except for a hard outer shell 1/4-inch thick, the hardness was uniform across the ingots at any one plane perpendicular to the longitudinal axis.

A core 3/4-inch square, symmetrical about the axis and the full length of the ingot, was used for testing. This core was quartered lengthwise and one piece was reserved for determination of hardness at room and elevated temperatures. Another piece was used for chemical analysis, x-ray studies, and metallographic examination, care being taken to identify each sample by its position in the ingot so that the properties could be correlated with chemical composition. The data were plotted against composition.

Filings for x-ray studies were processed in the manner described in the first annual report. Procedures for quantitative analyses of ternary molybdenum-base alloys were developed as part of this investigation. These procedures are described in detail in Appendix A.

Molybdenum-Aluminum-Cobalt Alloys

Heat B181, 0.16% Al, 0-0.15% Co, 0.003% C. Cast in purified, re-circulated argon; heated three hours at 3000 F in hydrogen.

Macrostructure. Only the lower half of the ingot was used for physical property determinations, because, as is evident from the macrostructure, Figure 101, a filled-in shrink hole occupied the upper portion of the ingot. The grain size was the same as that of molybdenum-cobalt alloys of similar cobalt content.

Hardness. The hardness of these alloys was somewhat greater than that of comparable binary molybdenum-cobalt alloys, especially at 1600 F.

Lattice Parameter. Aluminum and cobalt each contract the lattice parameter of molybdenum. From the data at hand, the effects appear to be additive.

Microstructure. The coring shown in Figure 100 is evidence that three hours at 3000 F was insufficient for homogenization. The microporosity that appears at 100X seems to be closely related to the dendritic interstices. No second phase was found in the alloy concentrations covered in the graded heat. By chemical analysis it was determined that about 0.05% of the aluminum was present in the form of aluminum oxide. This suggests that some of the fine particles in the figure at 1000X were not voids but rather aluminum oxide. The presence of both voids and oxide was confirmed metallographically.

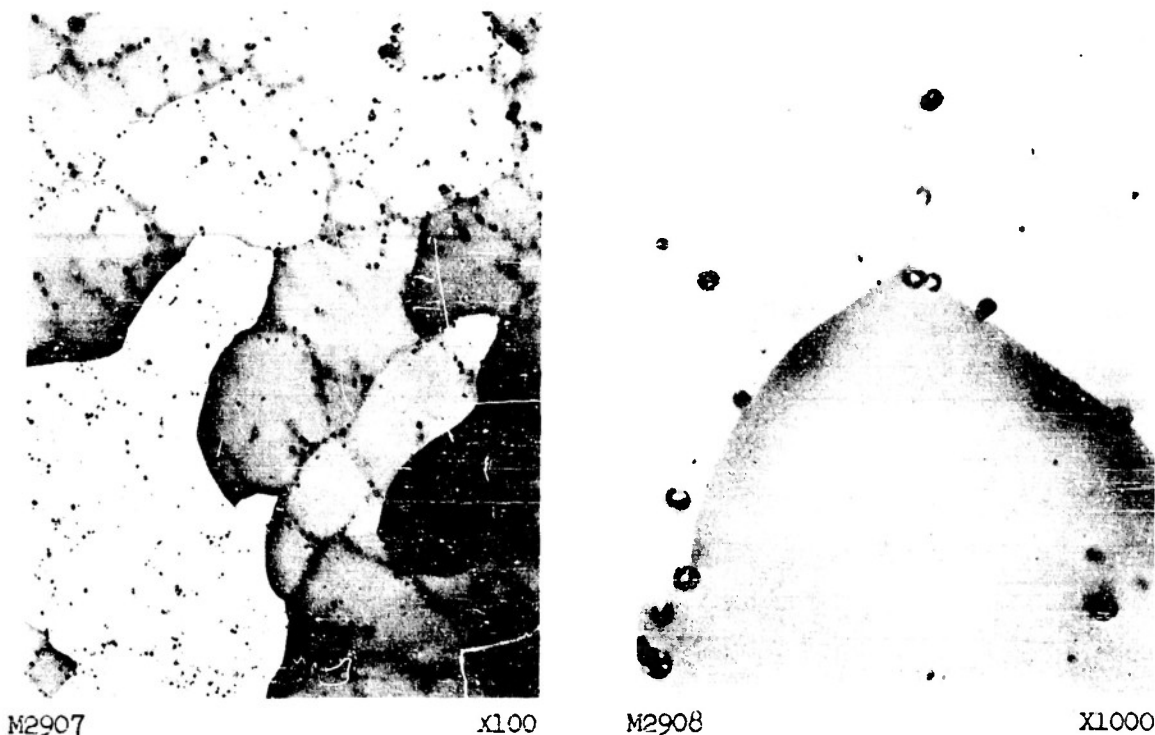


FIGURE 100 - MICROSTRUCTURE OF Mo-Al-Co ALLOY, HEAT B181
0.16% Al, 0.15% Co, 0.003% C, balance Mo,
cast in argon
Electropolished, etched in $\text{NaOH} + \text{K}_3\text{Fe}(\text{CN})_6$

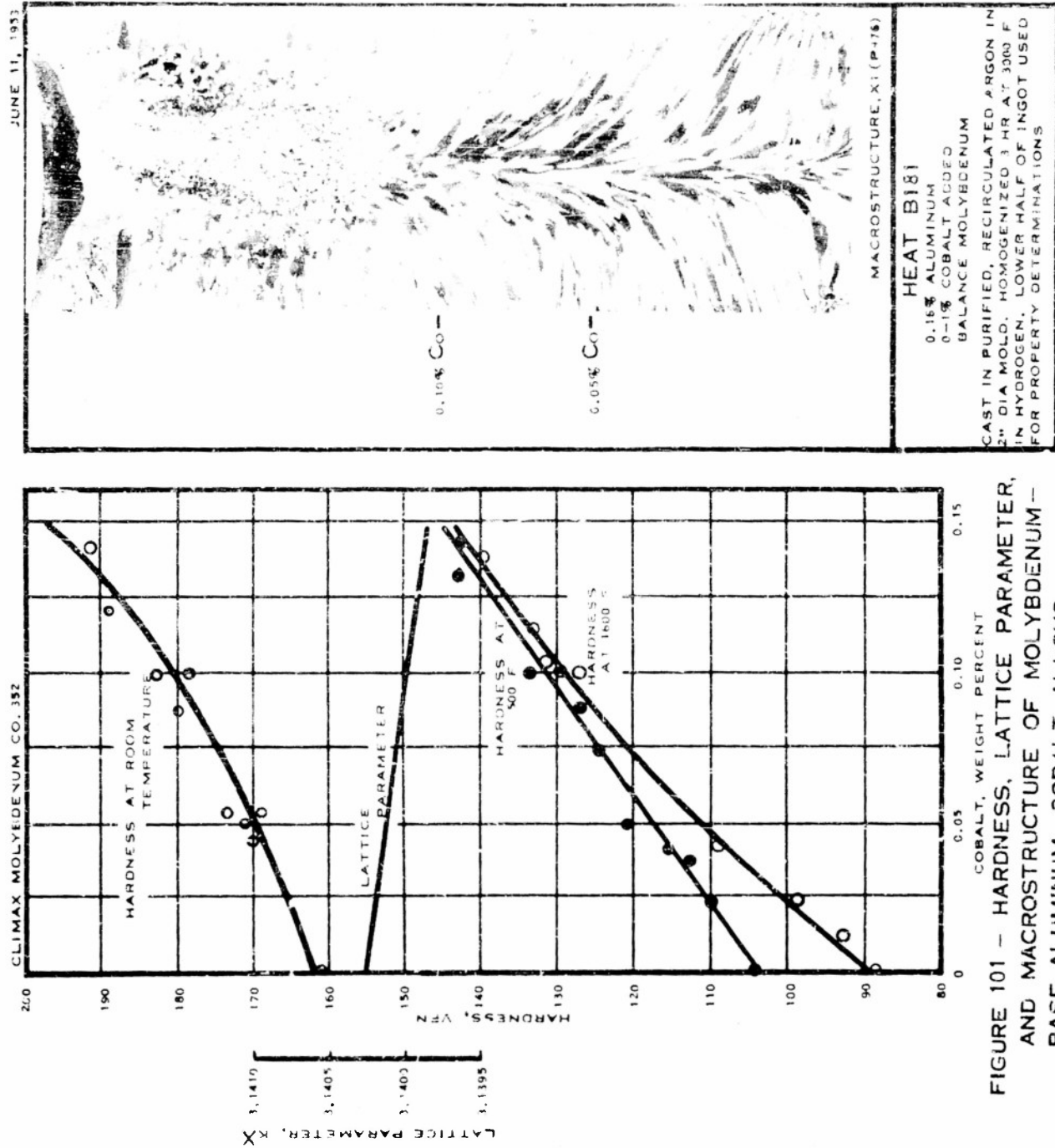


FIGURE 101 - HARDNESS, LATTICE PARAMETER,
AND MACROSTRUCTURE OF MOLYBDENUM -
BASE ALUMINUM-COBALT ALLOYS

Molybdenum-Aluminum-Niobium Alloys

Heat B179, 0.16% Al, 0-0.55% Nb, 0.003% C. Cast in purified, recirculated argon; heated two hours at 3000 F in hydrogen.

Macrostructure. The data were obtained upon the portion of the ingot below the filled-in shrink hole, Figure 103.

Hardness. The effect of aluminum in reducing room temperature hardness was evident in the alloys containing less than 0.03% niobium. The hardness of alloys containing more than 0.3% niobium was above that of binary molybdenum-niobium alloys. At 500 and 1600 F the hardness of the ternary alloys was appreciably higher than for corresponding molybdenum-niobium alloys. The hardness versus composition curves at 500 and 1600 F practically coincide above 0.3% niobium, indicating little change in hardness in that temperature range.

Lattice Parameter. The lattice parameter of the alloys increased with increasing niobium content, but not as much as in the binary molybdenum-niobium alloys, indicating the effect of aluminum in contracting the lattice parameter.

Microstructure. The microstructure of the alloy containing 0.5% niobium, Figure 102, shows a small amount of coring and interdendritic porosity.

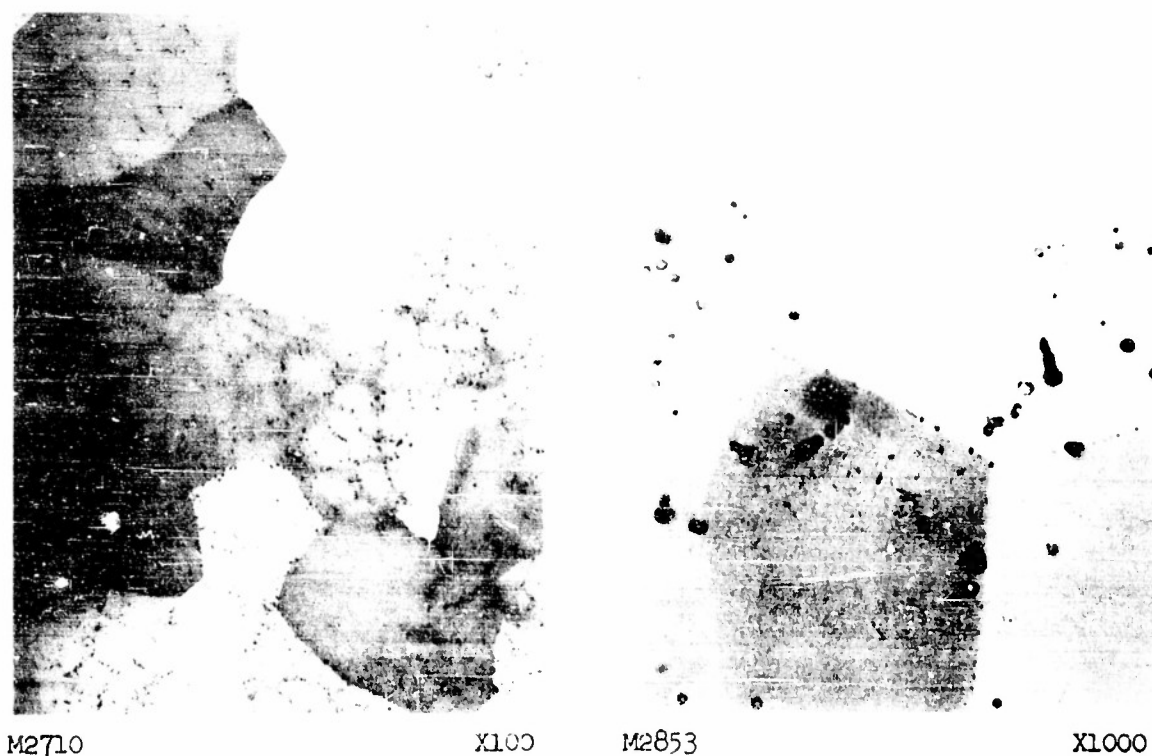


FIGURE 102 - MICROSTRUCTURE OF Mo-Al-Nb ALLOY, HEAT B179
0.16% Al, 0.5% Nb, 0.003% C, balance Mo,
cast in argon
Electropolished, etched in $\text{NaOH} + \text{K}_2\text{Fe}(\text{CN})_6$

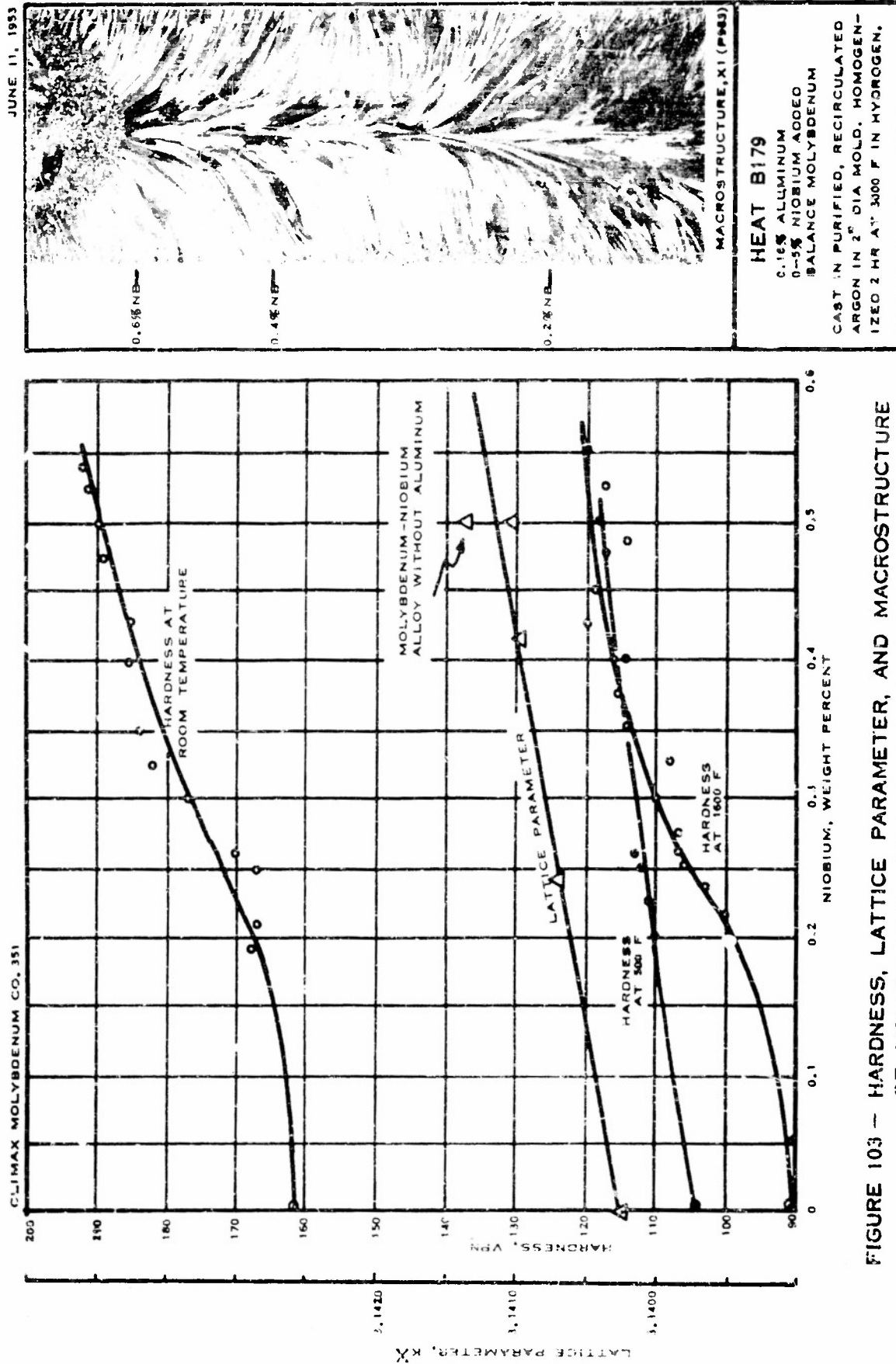


FIGURE 103 - HARDNESS, LATTICE PARAMETER, AND MACROSTRUCTURE OF MOLYBDENUM-BASE ALUMINUM-NIOBIUM ALLOYS

Molybdenum-Aluminum-Titanium Alloys

Heat B177, 0.16% Al, 0-4.3% Ti, 0.003% C. Cast in purified, re-circulated argon; heated two hours at 3000 F in hydrogen.

Macrostructure. During casting of the lower portion of the ingot (0-2.5% titanium) it was difficult to control the arc; therefore, this portion of the ingot was defective and was not used for determination of physical properties. The grain size of the alloys was the same as for comparably molybdenum-titanium binary alloys, Figure 105.

Hardness. In the satisfactory portion of the graded ingot where the concentration of titanium increased from 2.75 to 4.25%, there was a small, gradual increase in hardness with increasing titanium content. The room temperature hardness of the alloys containing 0.16% aluminum and 0-4% titanium was below that of binary molybdenum-titanium alloys in this range of titanium contents.

Microstructure. The microstructure of the 3% titanium-0.16% aluminum alloy is shown in Figure 104. The interdendritic segregation shown in the figure indicates that two hours at 3000 F was not sufficient for homogenization. The marked coring suggests that there had been a wide temperature range of solidification. At high magnification (not shown) yellowish inclusions, believed to be titanium oxide, were observed on unetched specimens.

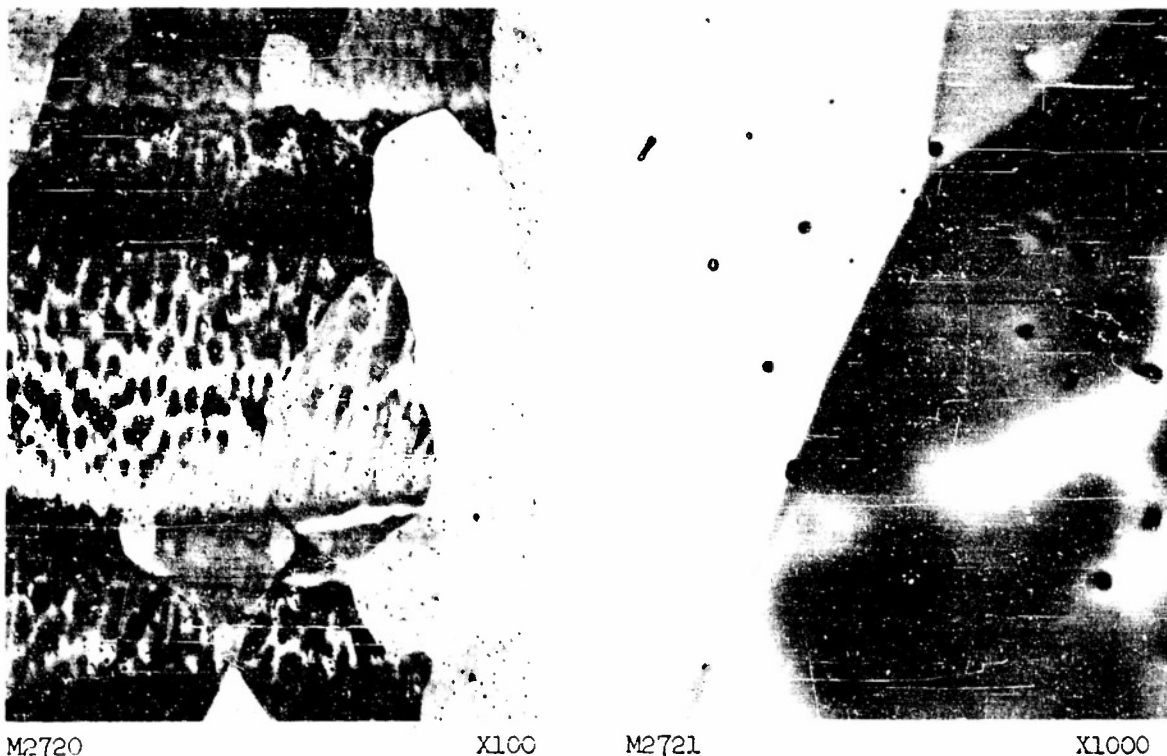


FIGURE 104 - MICROSTRUCTURE OF Mo-Al-Ti ALLOY, HEAT B177
0.16% Al, 3% Ti, 0.003% C, balance Mo, cast
in argon
Electropolished, etched in NaOH+K₃Fe(CN)₆

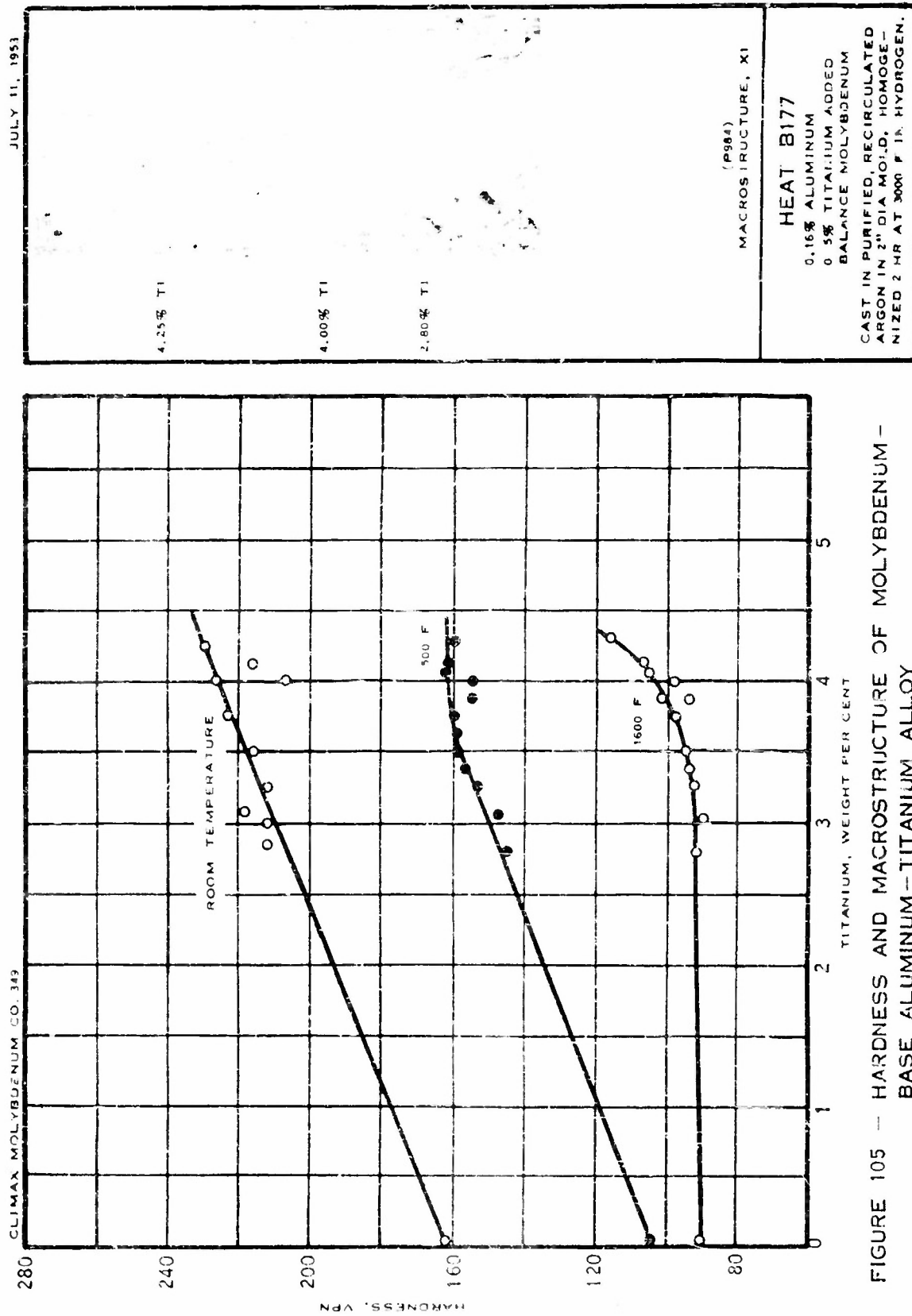


FIGURE 105 — HARDNESS AND MACROSTRUCTURE OF MOLYBDENUM —
BASE ALUMINUM — TITANIUM ALLOY

Molybdenum-Aluminum-Vanadium Alloys

Heat B178, 0.16% Al, 0-2.1% V, 0.003% C. Cast in purified, re-circulated argon; heated two hours at 3000 F in hydrogen.

Macrostructure. The grain size became markedly finer as the vanadium content increased above 2%, Figure 107.

Hardness. The hardness of the graded material at room temperature was appreciably lower than for corresponding binary molybdenum-vanadium alloys. At 500 and 1600 F, however, the hardness of the ternary alloys was considerably above that of the binary alloys. The hardness-versus-composition curves at 500 and 1600 F practically coincided above 0.8% vanadium, indicating little change in hardness in that temperature range.

Lattice Parameter. Both aluminum and vanadium contract the lattice parameter of molybdenum. In combination the effect is slightly more than that of vanadium alone.

Microstructure. Severe coring in the ternary alloy containing 2% vanadium and 0.16% aluminum is shown in Figure 106. Microporosity and aluminum oxide, but no intermetallic second phase, were visible in the structure at 1000X.

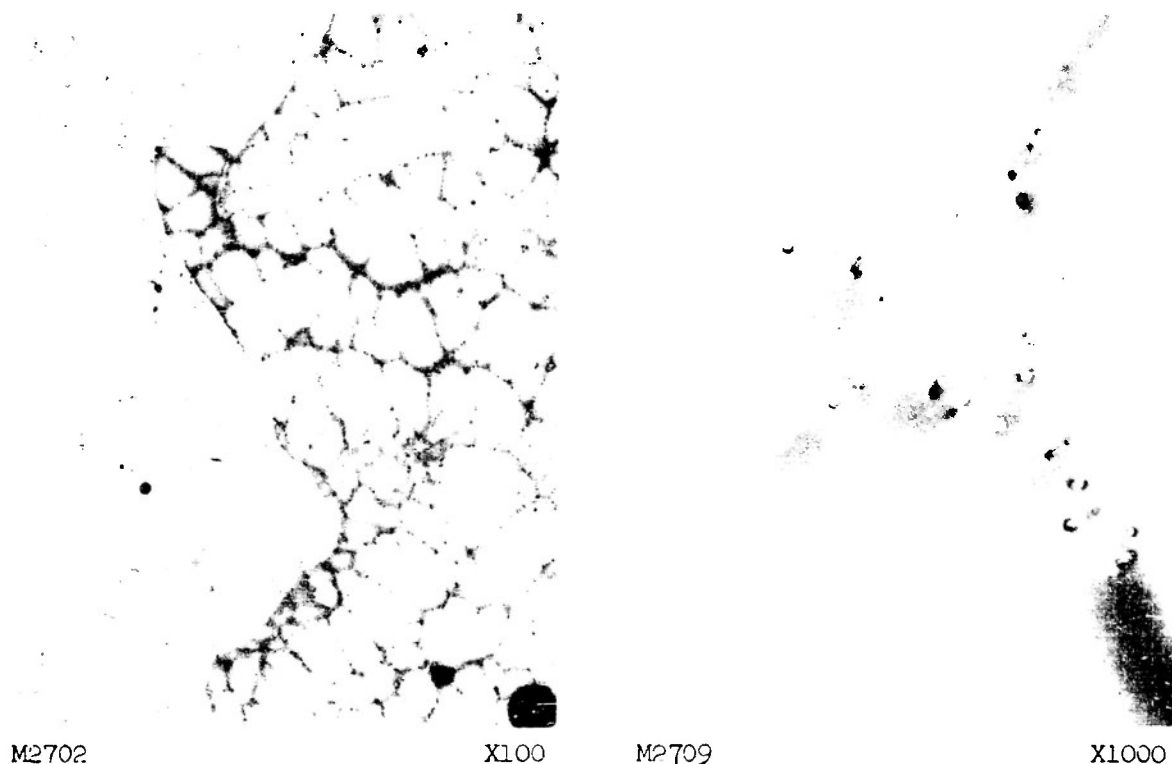


FIGURE 106 - MICROSTRUCTURE OF Mo-Al-V ALLOY, HEAT B178
0.16% Al, 2% V, 0.003% C, balance Mo, cast
in argon
Electropolished, etched in $\text{NaOH} + \text{K}_3\text{Fe}(\text{CN})_6$

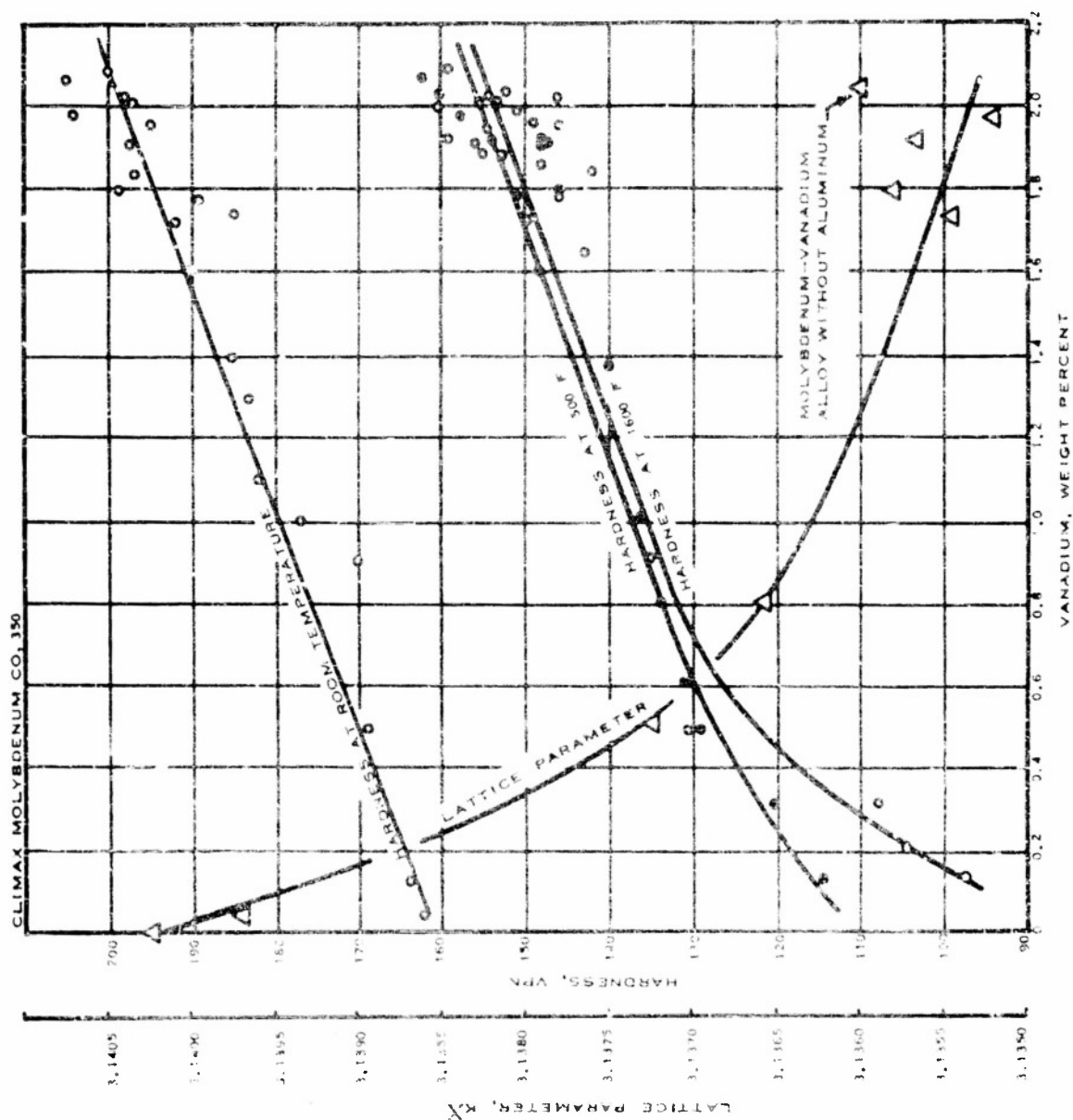


FIGURE 107 - HARDNESS, LATTICE PARAMETER, AND MICROSTRUCTURE OF MOLYBDENUM-BASE ALUMINUM-VANADIUM ALLOY

Molybdenum-Aluminum-Zirconium Alloys

Heat B182, 0.16% Al, 0-0.4% Zr, 0.003% C. Cast in purified, re-circulated argon; heated three hours at 3000 F in hydrogen.

Macrostructure. The grain size of the ternary alloys, Figure 109, was the same as that of corresponding binary molybdenum-zirconium alloys.

Hardness. The effect of aluminum in reducing room temperature hardness was manifested in the ternary alloys containing up to 0.2% zirconium. At 500 F the hardness of the ternary alloys was slightly higher than for the corresponding molybdenum-zirconium alloys without aluminum. At 1600 F, the Mo-Al-Zr alloys containing up to 0.2% zirconium were harder than the corresponding molybdenum-zirconium alloys, but above 0.2% zirconium the molybdenum zirconium alloys were harder.

Microstructure. Severe coring and porosity, as well as an interdendritic second phase, were observed in the microstructure of the ternary alloy containing 0.35% zirconium and 0.16% aluminum, Figure 108. The precipitate shown in the photomicrograph at 1000X was interpreted to be an aluminum-zirconium-oxygen compound.

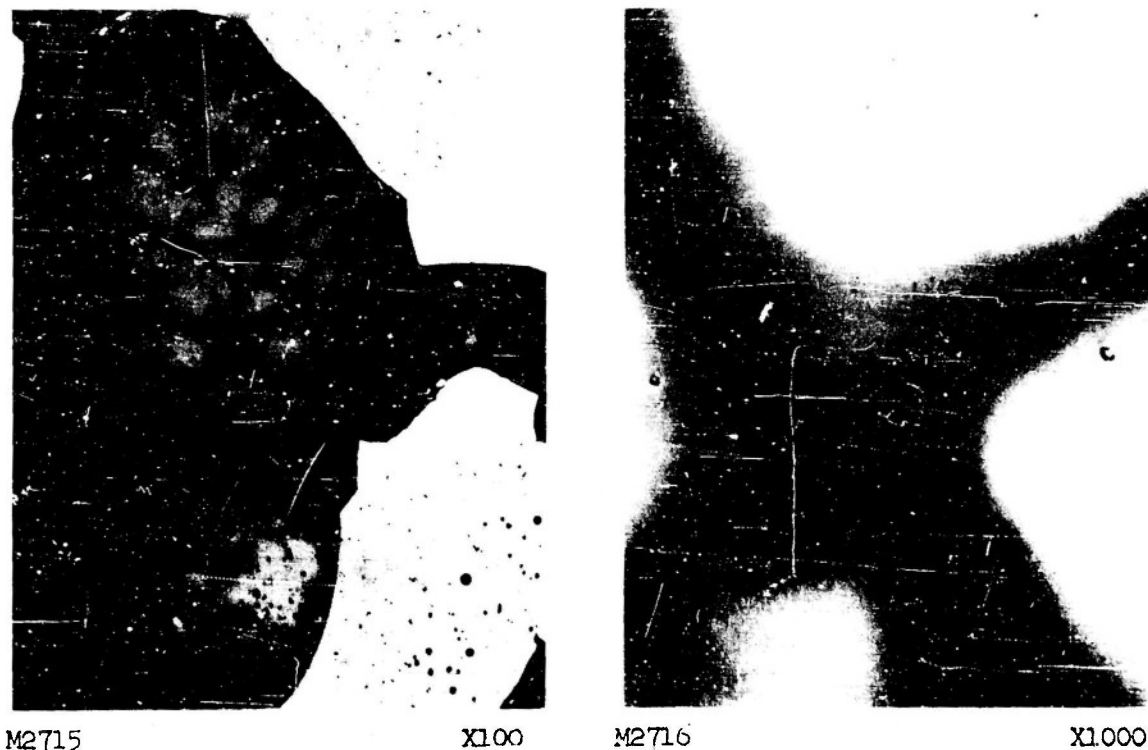


FIGURE 108 - MICROSTRUCTURE OF Mo-Al-Zr ALLOY, HEAT B182
0.16% Al, 0.35% Zr, 0.003% C, balance Mo,
cast in argon
Electropolished, etched in $\text{NaOH} + \text{K}_3\text{Fe}(\text{CN})_6$

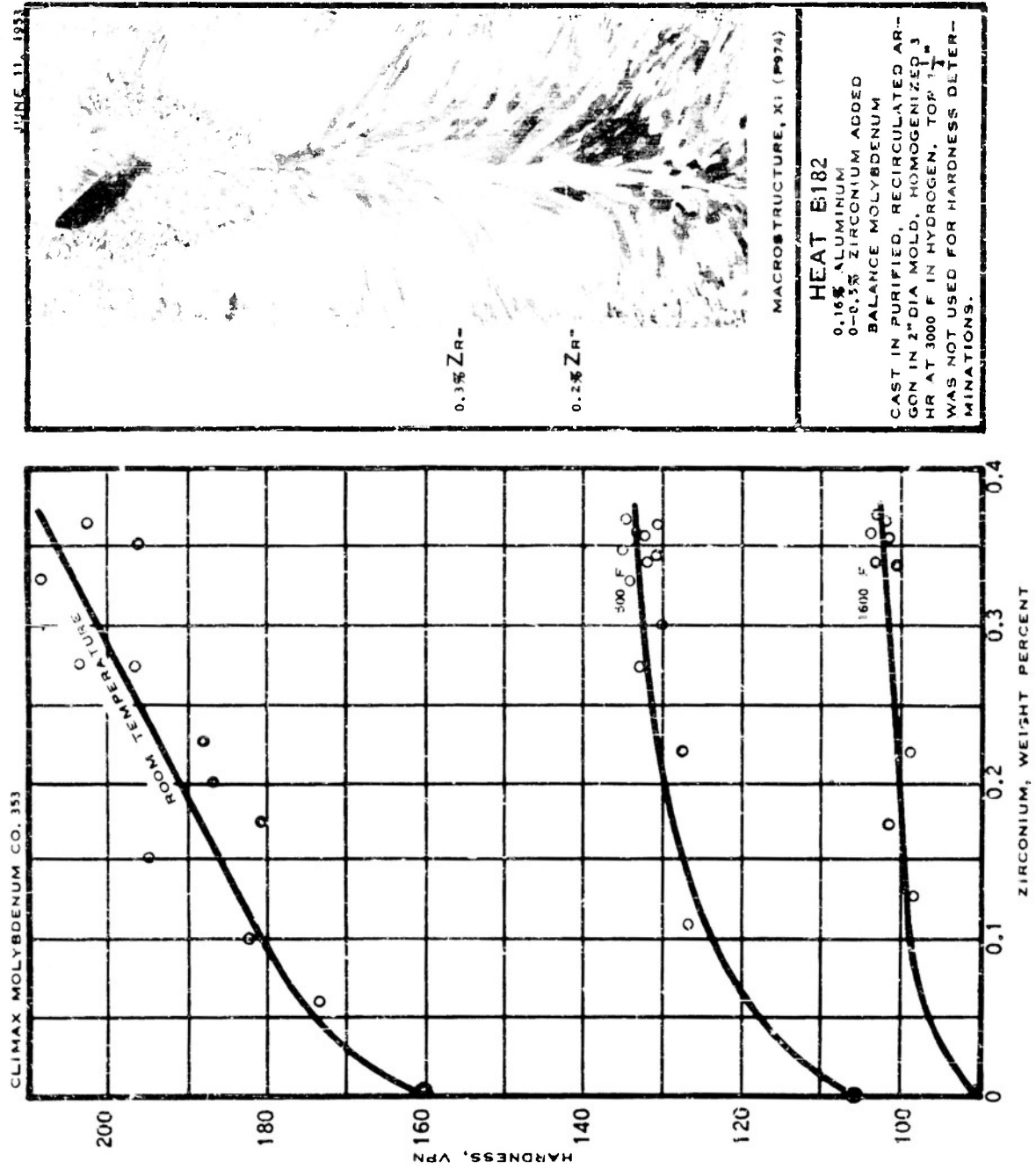


FIGURE 109 — HARDNESS AND MACROSTRUCTURE OF MOLYBDENUM-BASE ALUMINUM-ZIRCONIUM ALLOY

Molybdenum-Cobalt-Aluminum Alloys

Heat B213, 0.07% Co, 0-1.3% Al, 0.020% C. Cast in purified, re-circulated argon; heated 18 hours at 3000 F in hydrogen.

Macrostructure. The grain size shown in Figure 111 is somewhat finer than that of comparable binary molybdenum-aluminum alloys, cf. first annual report, page 40.

Hardness. The hardness of the ternary alloys, at both room temperature and elevated temperatures, was slightly higher than that of molybdenum-aluminum binary alloys. The drop in hardness with rising temperature was gradual at each aluminum level.

Microstructure. Except for a small amount of carbide, the alloy shown in Figure 110 was single phase. The presence of carbide was due to 0.02% carbon in the molybdenum-cobalt electrode used for making Heat B213. Less microporosity was observed than in carbon-free molybdenum-aluminum alloys produced in the powder machines.



M3053

X100

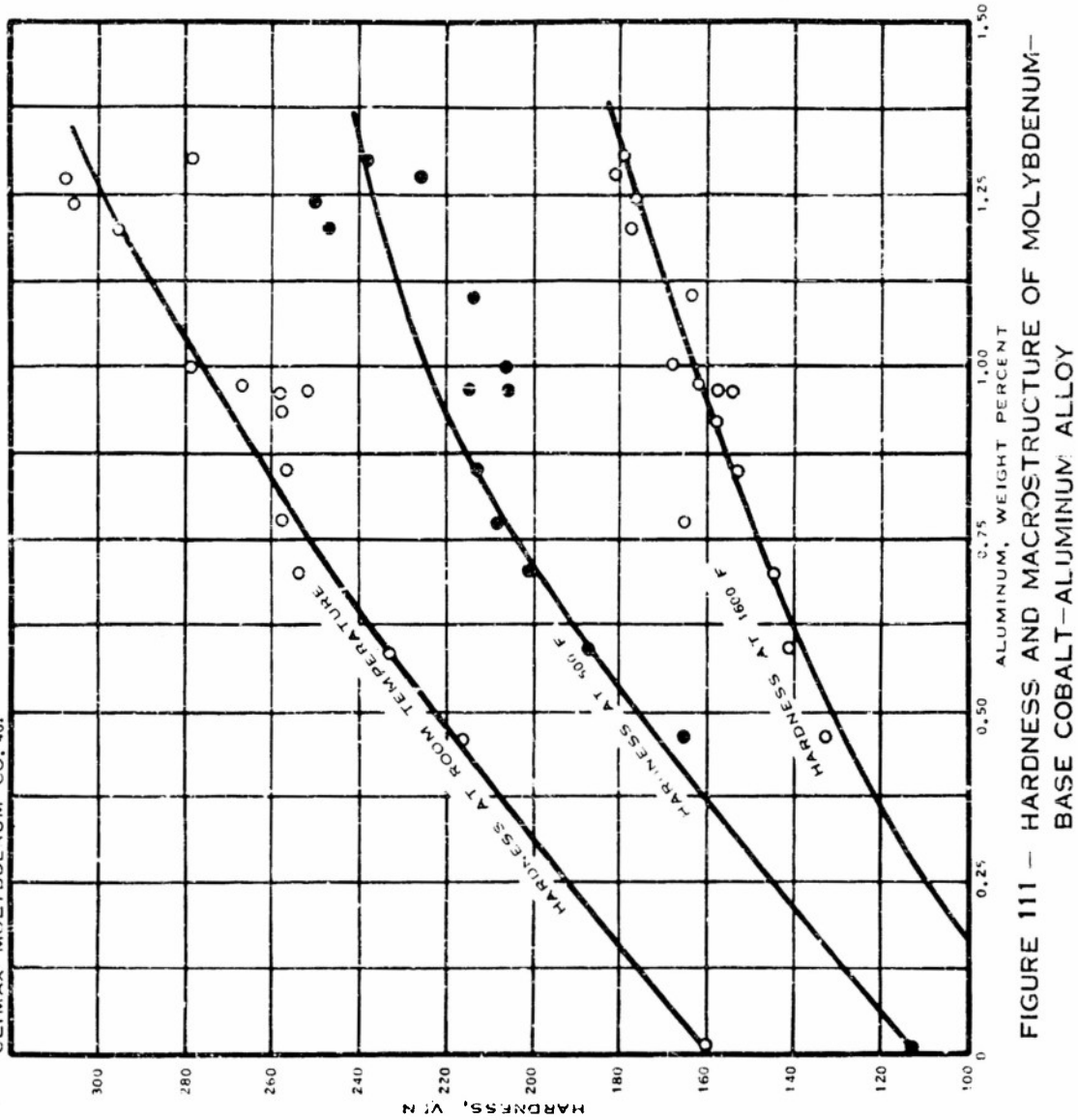


M3073

X1000

FIGURE 110 - MICROSTRUCTURE OF Mo-Co-Al ALLOY, HEAT B213
0.07% Co, 1.25% Al, 0.020% C, balance Mo,
cast in argon
Electropolished, etched in $\text{NaOH} + \text{K}_3\text{Fe}(\text{CN})_6$

OCTOBER 11, 1954



1.0% Al.

0.5% Al.

MACROSTRUCTURE, X1 (P1021)

HEAT B213

0.07% COBALT
0-2% ALUMINUM ADDED
BALANCE MOLYBDENUM

CAST IN PURIFIED RECIRCULATED
ARGON IN 2" DIA MCQ, HOMO-
GENIZED 18 HR AT 3000 F IN
HYDROGEN

Molybdenum-Cobalt-Niobium Alloys

Heat B210, 0.05% Co, 0-3.5% Nb, 0.020% C. Cast in vacuum, heated 18 hours at 3000 F in hydrogen.

Macrostructure. The macrostructure shown in Figure 113 is similar to that previously observed in molybdenum-niobium binary alloys of comparable niobium content.

Hardness. The hardness of the ternary alloys dropped rapidly between room temperature and 500 F, but changed very little between 500 and 1600 F. Although the hardness of the ternary alloys at room temperature was about the same as that of the molybdenum-niobium binary alloys, at 1600 F the ternary alloys were appreciably harder.

Microstructure. The microstructure of the alloy shown in Figure 112 is single phase, except for finely dispersed carbide within the grains.



M3057

X100

FIGURE 112 - MICROSTRUCTURE OF Mo-Co-Nb ALLOY, HEAT B210
0.05% Co, 3% Nb, 0.020% C, balance Mo, cast
in vacuum
Electropolished, etched in $\text{NaOH} + \text{K}_3\text{Fe}(\text{CN})_6$

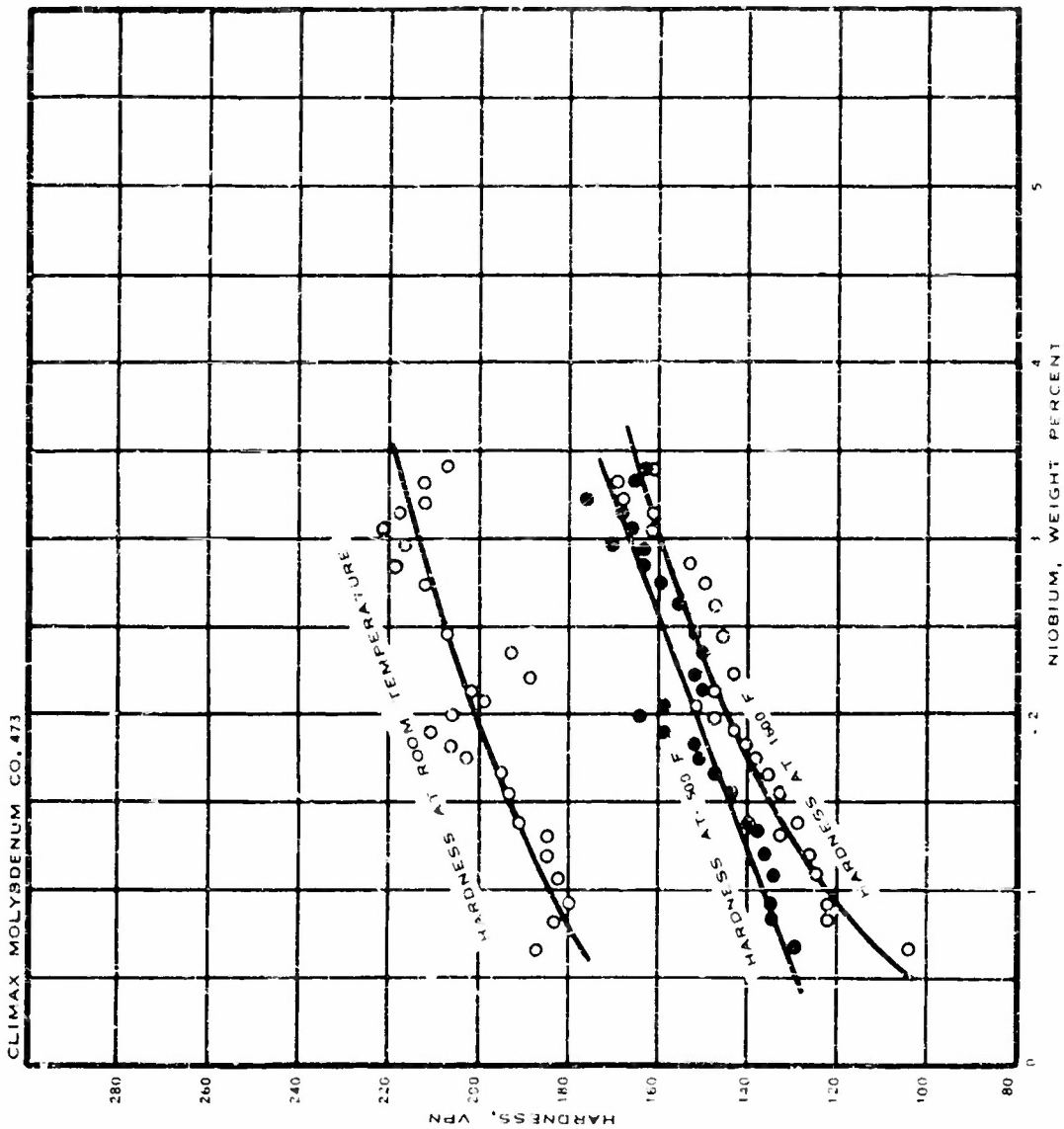
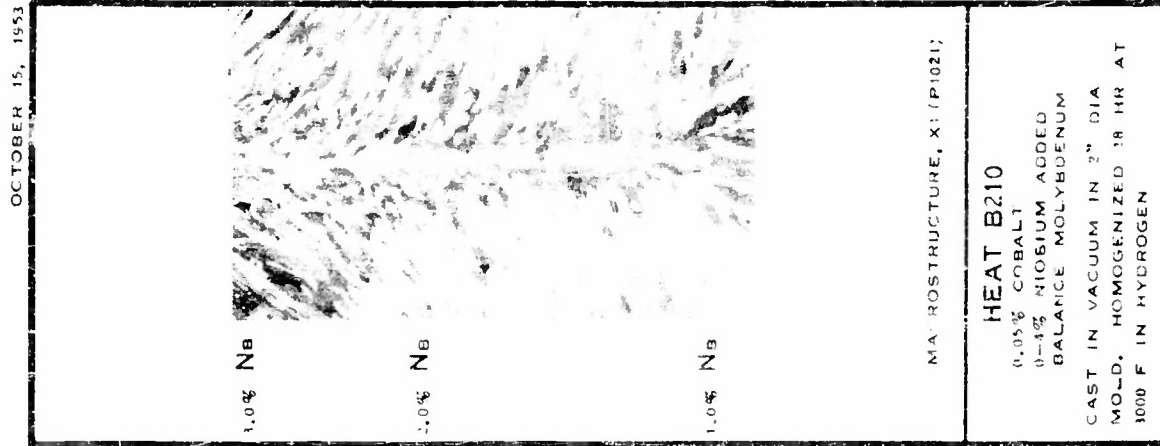


FIGURE 113 - HARDNESS AND MACROSTRUCTURE OF MOLYBDENUM-
BASE COBALT-NIOBIUM ALLOY

Molybdenum-Cobalt-Titanium Alloys

Heat B208, 0.06% Co, 0-0.75% Ti, 0.020% C. Cast in vacuum, heated 18 hours at 3000 F in hydrogen.

Macrostructure. The grain size, Figure 115, was the same as that of comparable molybdenum-titanium binary alloys or unalloyed molybdenum.

Hardness. A gradual drop in hardness of the ternary alloys occurred as the temperature rose from room temperature to 1600 F. At room temperature the ternary alloy was not as hard as a comparable molybdenum-titanium binary alloy; at 500 F and 1600 F the ternary alloy was harder.

Microstructure. The alloy whose microstructure is shown in Figure 114 was single phase except for the presence of carbide.

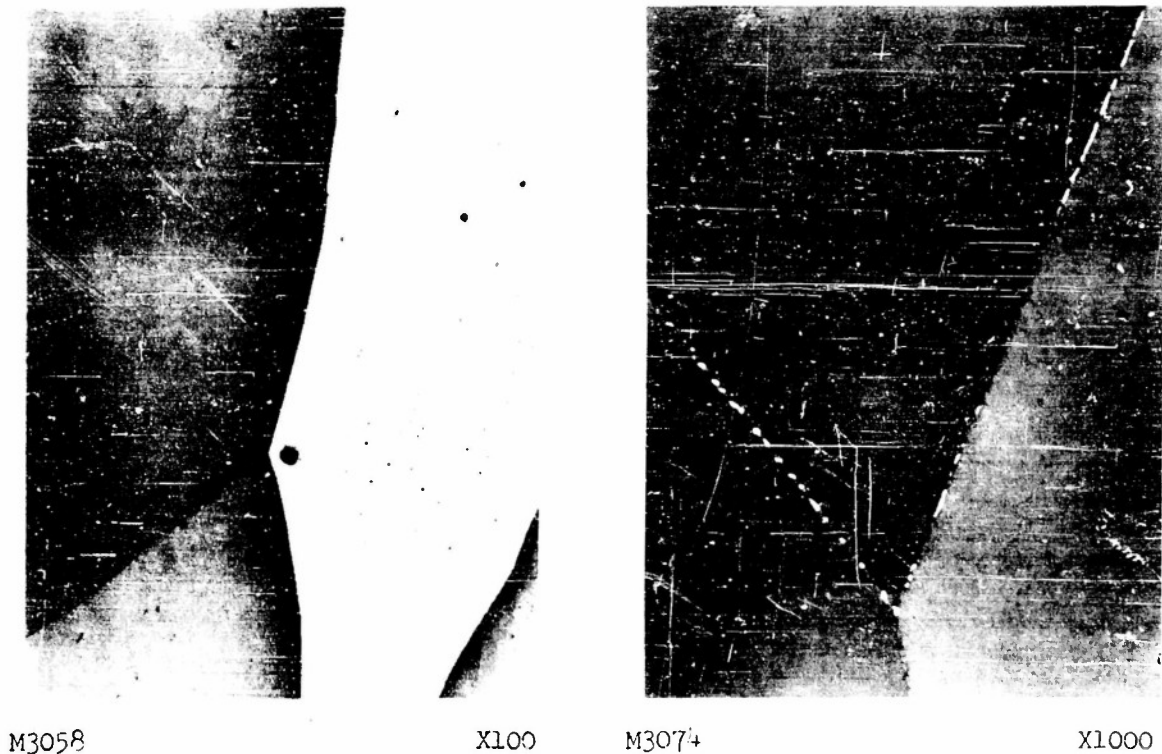


FIGURE 114 - MICROSTRUCTURE OF Mo-Co-Ti ALLOY, HEAT B208
0.06% Co, 0.70% Ti, 0.020% C, balance molybdenum,
cast in vacuum
Electropolished, etched in $\text{NaOH} + \text{K}_3\text{Fe}(\text{CN})_6$

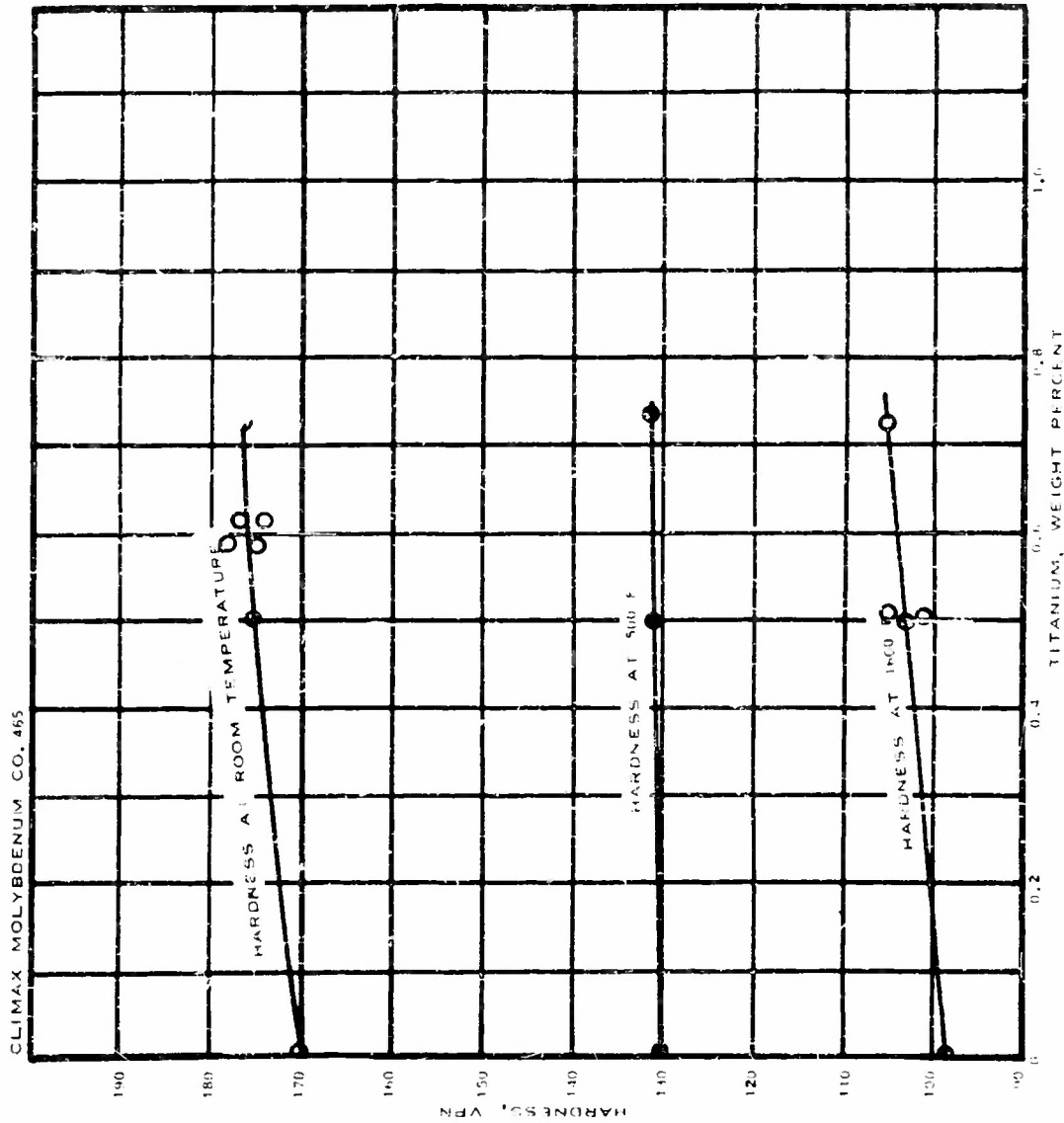


FIGURE 115 -- HARDNESS AND MACROSTRUCTURE OF MOLYBDENUM--
BASE COBALT-TITANIUM ALLOY

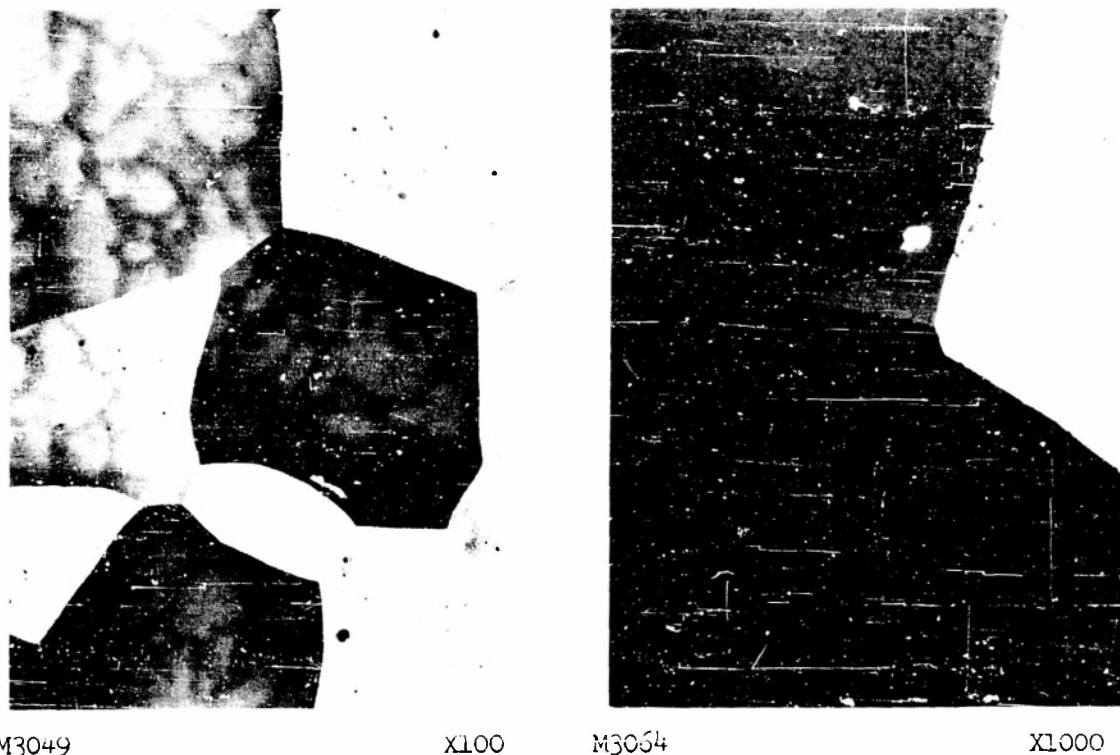
Molybdenum-Cobalt-Vanadium Alloys

Heat B207, 0.04% Co, 0-2.25% V, 0.020% C. Cast in vacuum, heated 18 hours at 3000 F in hydrogen.

Macrostructure. The grain size of the ternary alloy, Figure 117, is the same as that of a comparable molybdenum-vanadium binary alloy.

Hardness. The hardness of the ternary alloys dropped sharply from room temperature to 500 F, but only slightly from 500 F to 1600 F. The hardness of the ternary alloys at room temperature was lower than that of comparable molybdenum-vanadium alloys. At 1500 F, on the other hand, the ternary alloys had the higher hardness.

Microstructure. It can be observed, Figure 116, that the microstructure of the ternary alloy containing 2% vanadium was single phase.



M3049

X100

M3054

X1000

FIGURE 116 - MICROSTRUCTURE OF Mo-Co-V ALLOY, HEAT B207
0.04% Co, 2% V, 0.020% C, balance Mo, cast
in vacuum
Electropolished, etched in $\text{NaOH} + \text{K}_3\text{Fe}(\text{CN})_6$

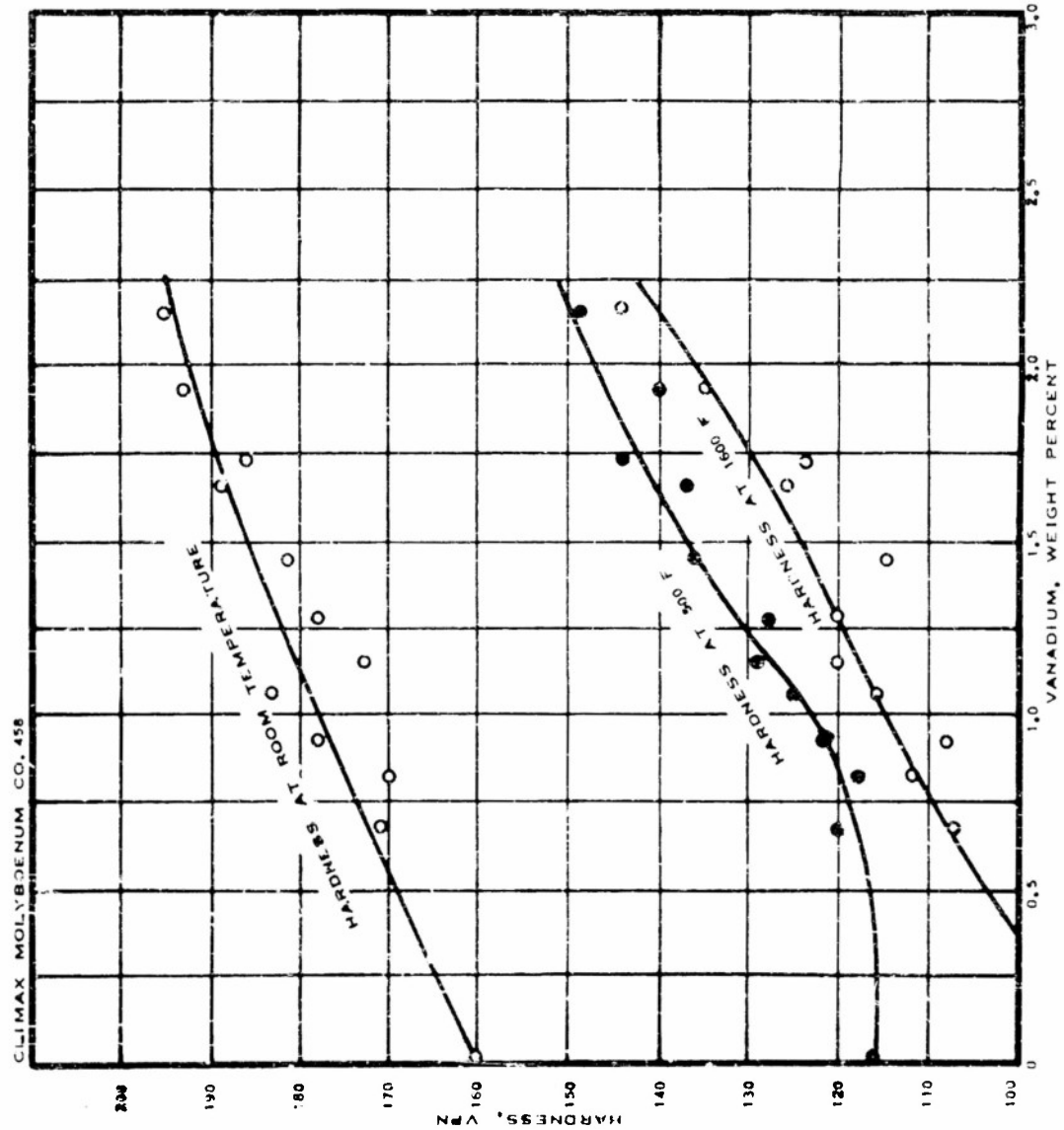
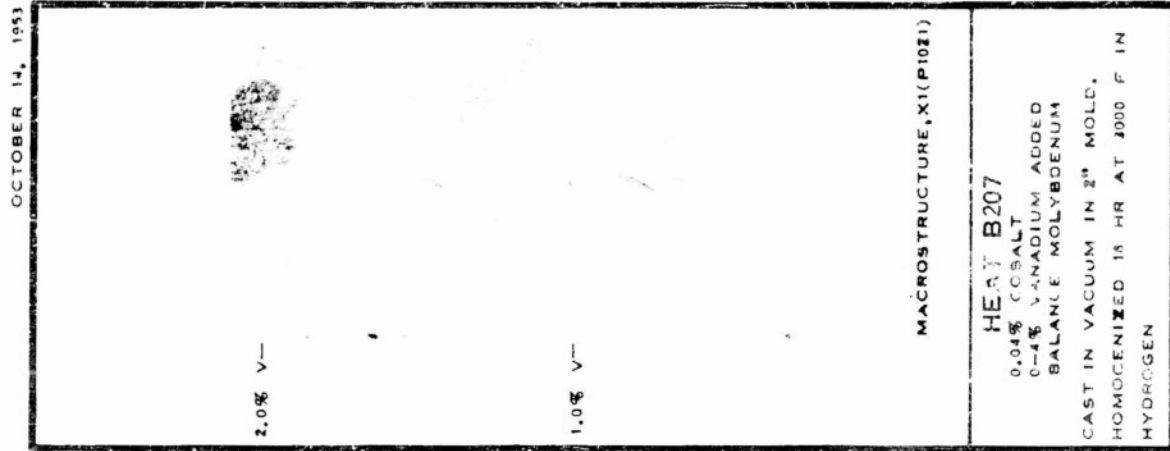


FIGURE 117— HARDNESS AND MACROSTRUCTURE OF MOLYBDENUM--
BASE COBALT-VANADIUM ALLOY

Molybdenum-Cobalt-Zirconium Alloys

Heat B209, 0.05% Co, 0-1.5% Zr, 0.020% C. Cast in vacuum, heated 18 hours at 3000 F in hydrogen.

Macrostructure. The grain size of the ternary alloys, Figure 119, was the same as that of corresponding binary molybdenum-zirconium alloys. Zirconium refines the molybdenum grains appreciably.

Hardness. The hardness of the ternary alloys dropped gradually as the testing temperature increased from room temperature to 500 F and 1600 F. The room-temperature hardness was below or about the same as that of comparable molybdenum-zirconium binary alloys. At 1600 F, however, the binary alloys were somewhat harder.

Microstructure. Heat treatment for 18 hours at 3000 F did not eliminate the extreme coring shown in Figure 118. Some carbide was present as a very fine precipitate within the grains.

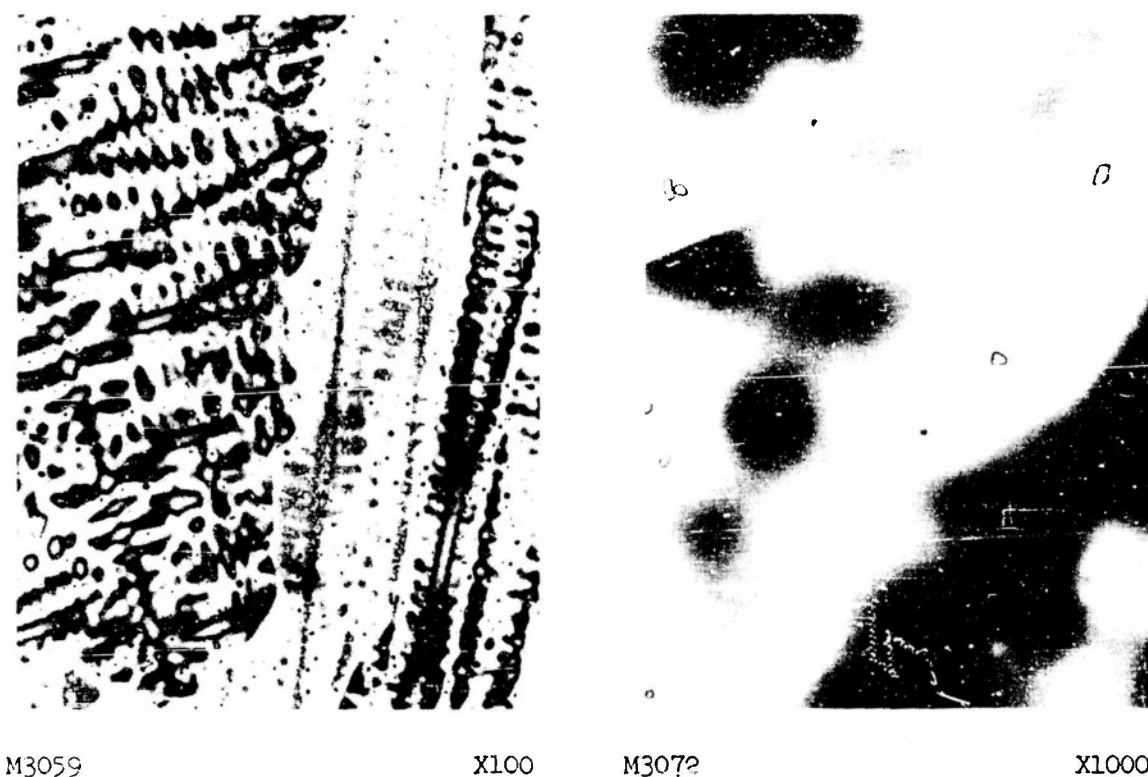


FIGURE 118 - MICROSTRUCTURE OF Mo-Co-Zr ALLOY, HEAT B209
0.05% Co, 1.5% Zr, 0.020% C, balance Mo, cast
in vacuum
Electropolished, etched in $\text{NaOH} + \text{K}_3\text{Fe}(\text{CN})_6$

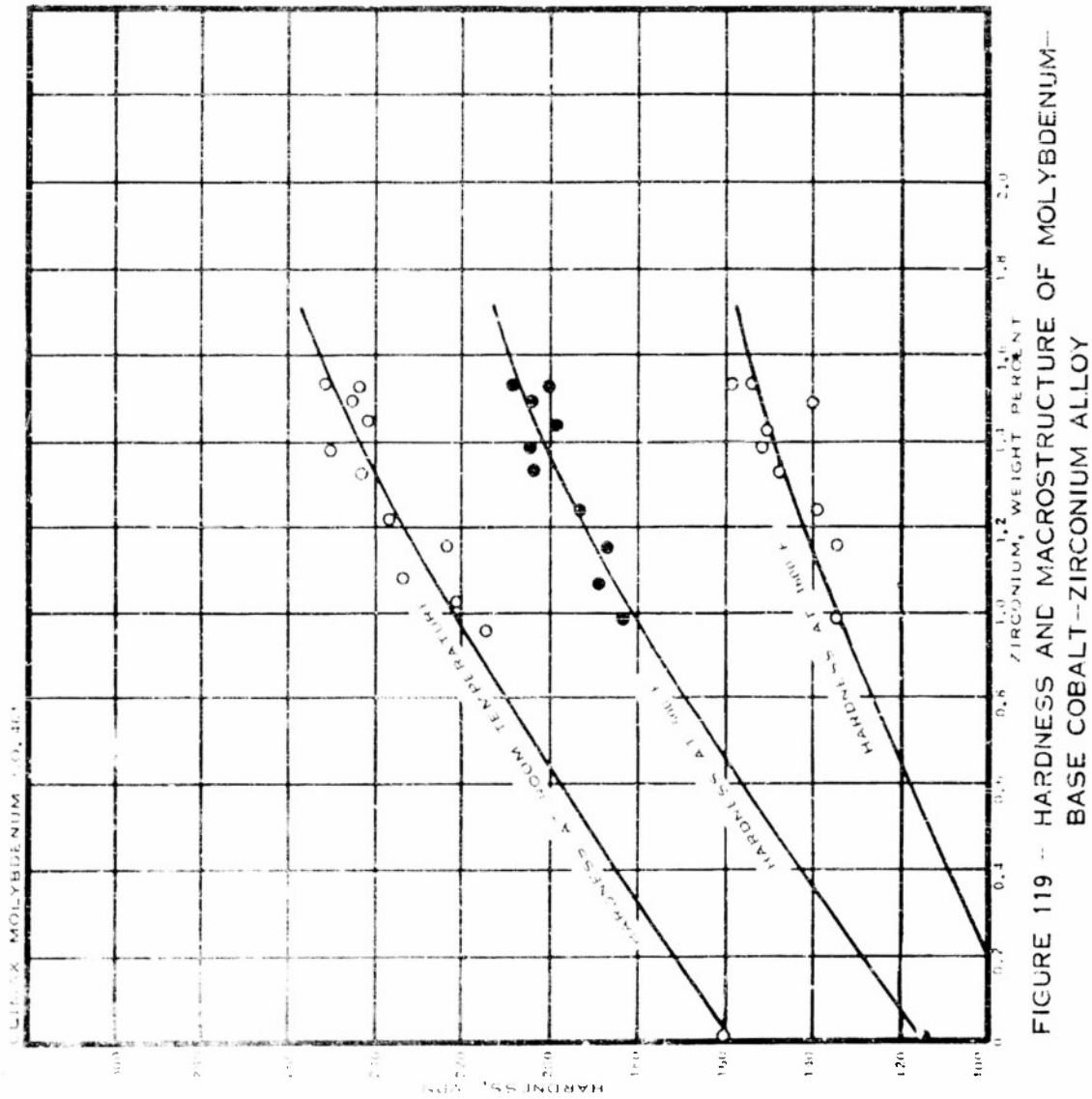
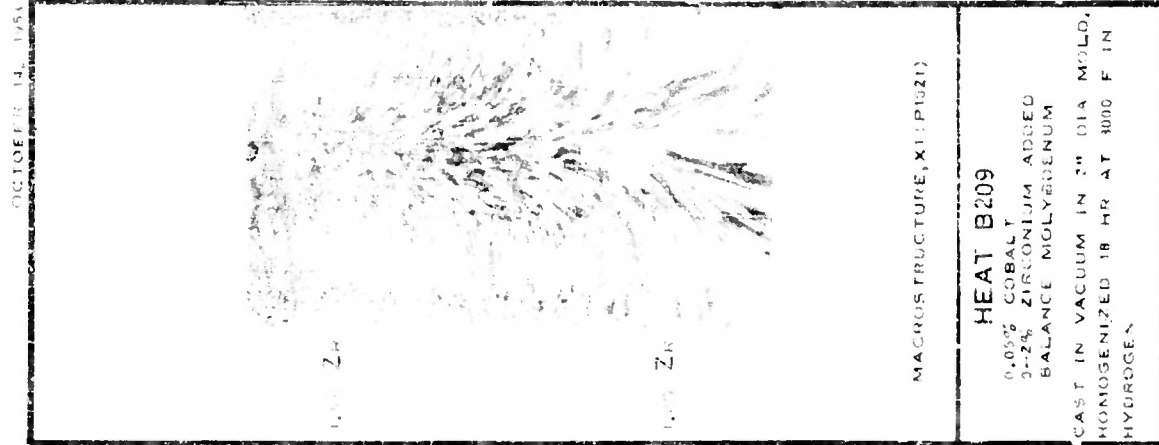


FIGURE 119 -- HARDNESS AND MACROSTRUCTURE OF MOLYBDENUM--
BASE COBALT--ZIRCONIUM ALLOY

Molybdenum-Niobium-Aluminum Alloys

Heat B195, 0.75% Nb, 0-1.75% Al, 0.033% C. Cast in purified, recirculated argon; heated 16 hours at 3000 F in hydrogen.

Macrostructure. Increasing the aluminum content above 0.5% brought about refinement of the grain in the same order of magnitude as in the binary molybdenum-aluminum alloys.

Hardness. The hardness changes in the ternary alloys were comparable to those of the binary molybdenum-aluminum alloys. Raising the aluminum content from 0 to 0.5% caused only a very small change in hardness at room temperature, whereas at 500 F and 1600 F the hardness increased at a uniform rate as the aluminum content increased from 0 to 1.75%.

Lattice Parameter. The decrease in lattice spacing with increasing aluminum content is more rapid in the ternary alloys than in the corresponding binary molybdenum-aluminum alloys.

Microstructure. The microstructure of the ternary alloy containing 1.55% aluminum and 0.75% niobium is shown in Figure 120. It is single phase with a fine dispersion of carbides at the grain boundaries and within the grains.



M3062

X100



M3067

X1000

FIGURE 120 - MICROSTRUCTURE OF Mo-Nb-Al ALLOY, HEAT B195
0.75% Nb, 1.55% Al, 0.033% C, balance Mo, cast
in argon
Electropolished, etched in $\text{NaOH} + \text{K}_3\text{Fe}(\text{CN})_6$

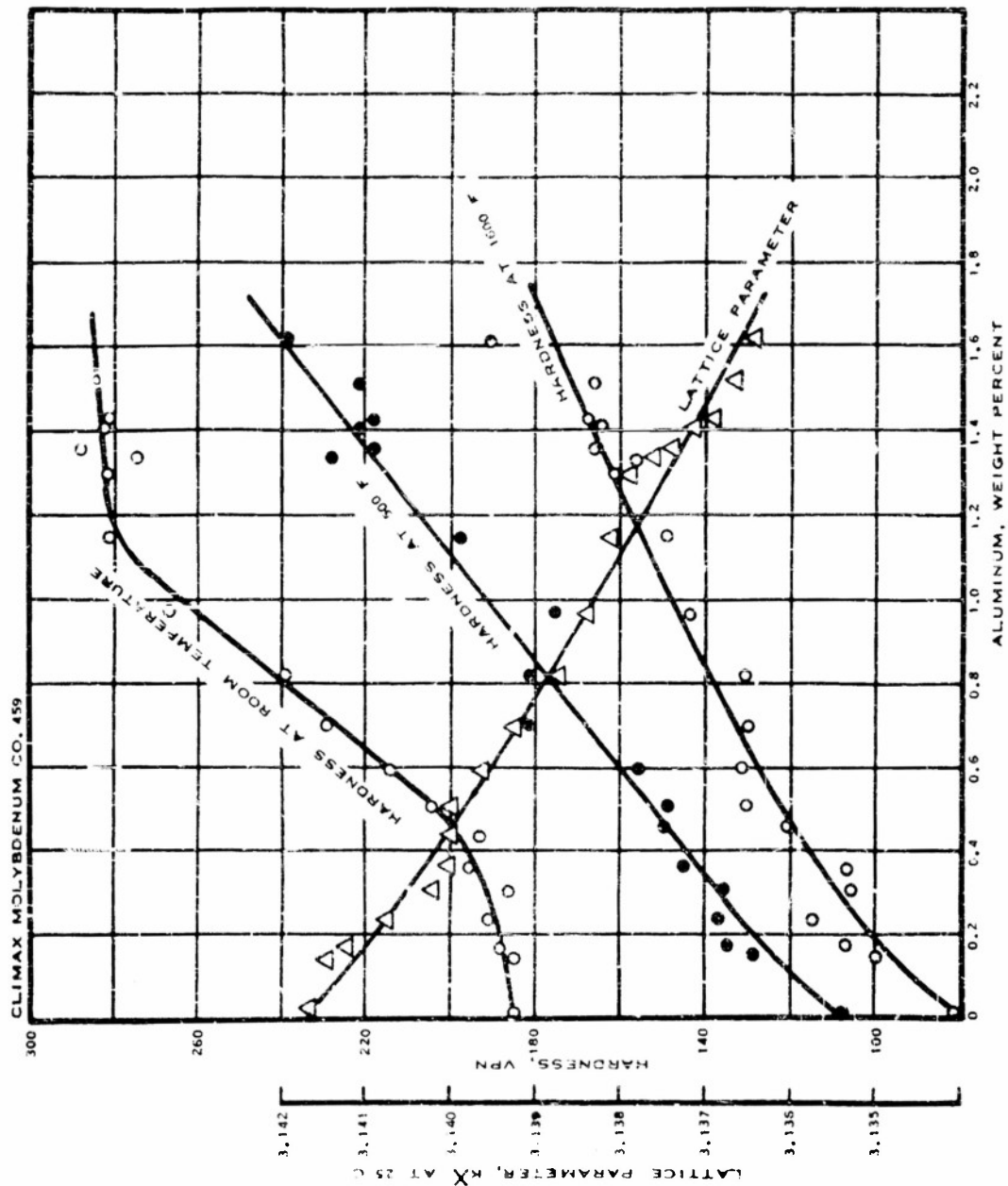
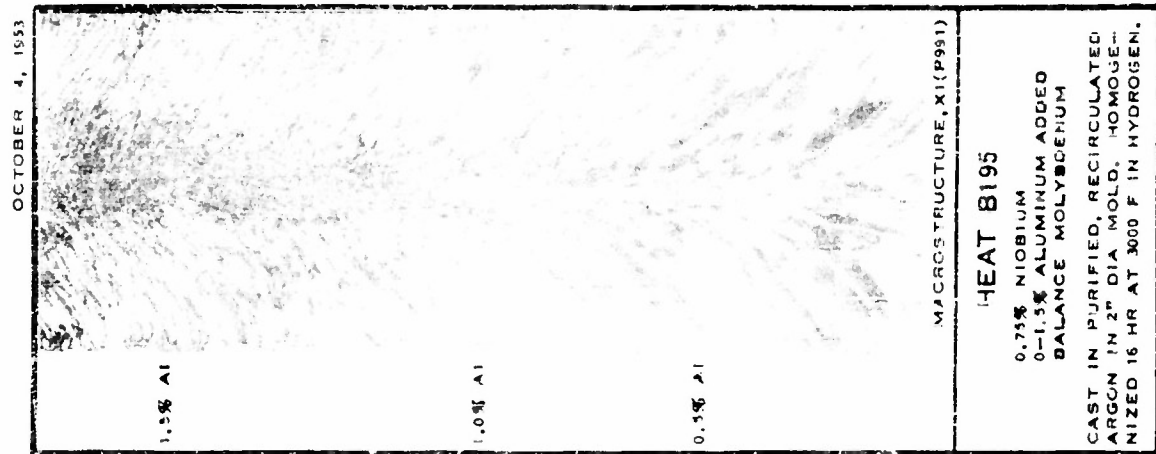


FIGURE 121 - HARDNESS, LATTICE PARAMETER, AND MACROSTRUCTURE OF MOLYBDENUM-BASE NIOBIUM-ALUMINUM ALLOYS

Molybdenum-Niobium-Cobalt Alloys

Heat B193, 0.75% Nb, 0-0.05% Co, 0.033% C. Cast in vacuum, heated 16 hours at 3000 F in hydrogen.

Macrostructure. The macrostructure of the ternary alloys, Figure 123, was the same as that of the corresponding molybdenum-cobalt binary alloys.

Hardness. The hardness of the ternary alloys gradually dropped as the testing temperature increased from room temperature to 500 F and 1600 F. The addition of niobium to molybdenum-cobalt alloys slightly increased the hardness at room temperature but raised it considerably at 500 F and 1600 F.

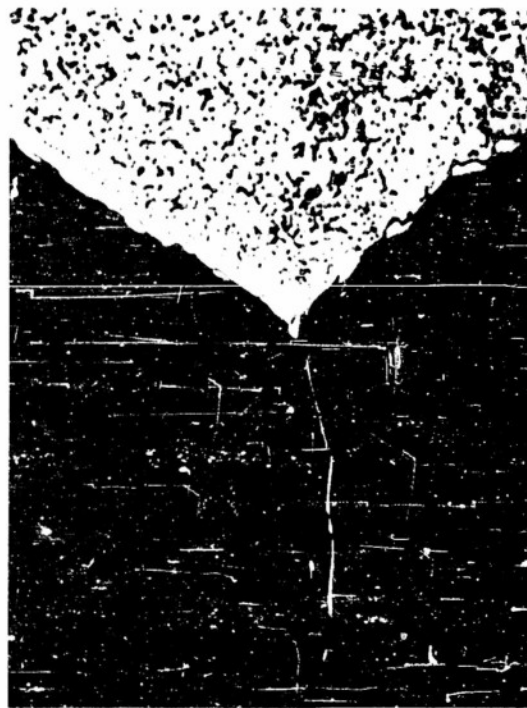
Lattice Parameter. The addition of niobium to molybdenum increases the lattice parameter spacing of molybdenum, whereas cobalt contracts it. The effect of the two alloying elements in combination is an algebraic summation of the effects of each element commensurate with the relative amount of each.

Microstructure. Coring is evident at low magnification in the microstructure of the ternary alloy containing 0.04% cobalt and 0.74% niobium, Figure 122. Carbide had precipitated at the interdendritic interstices as well as at the grain boundaries. What appears to be a precipitate within the white grain at the higher magnification is not a second phase but rather etching pits similar to those found in ferrite.



M3061

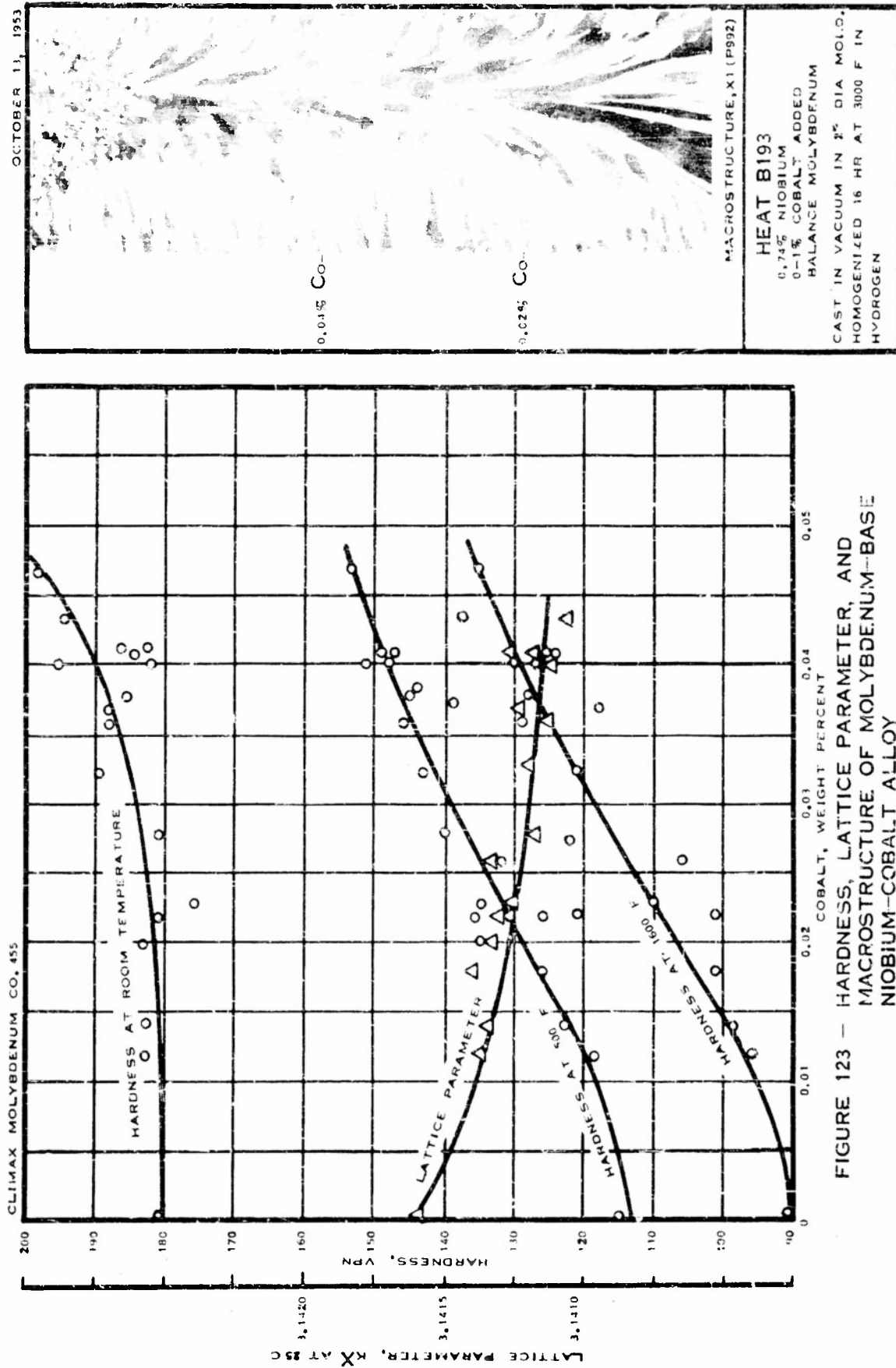
X100



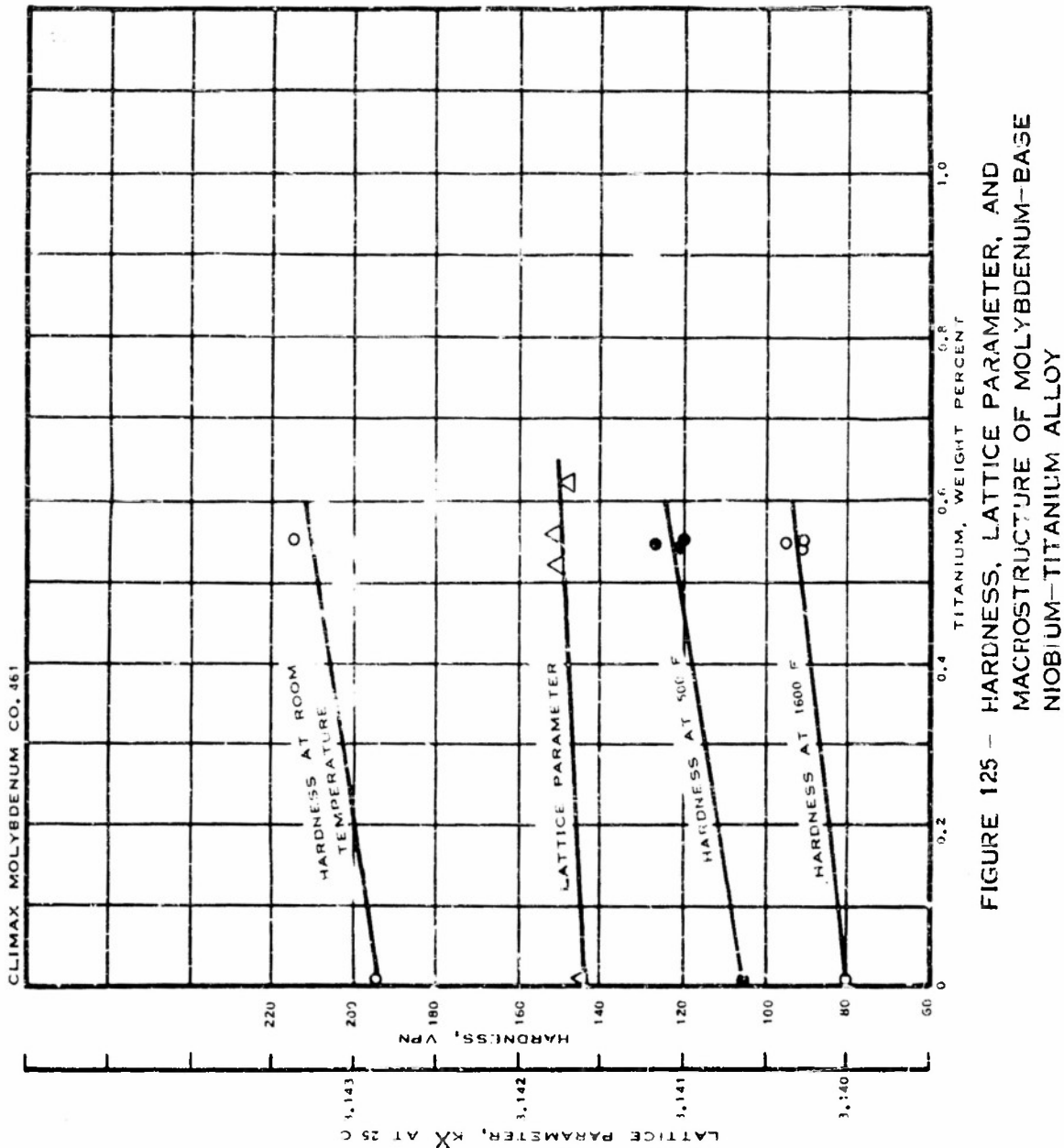
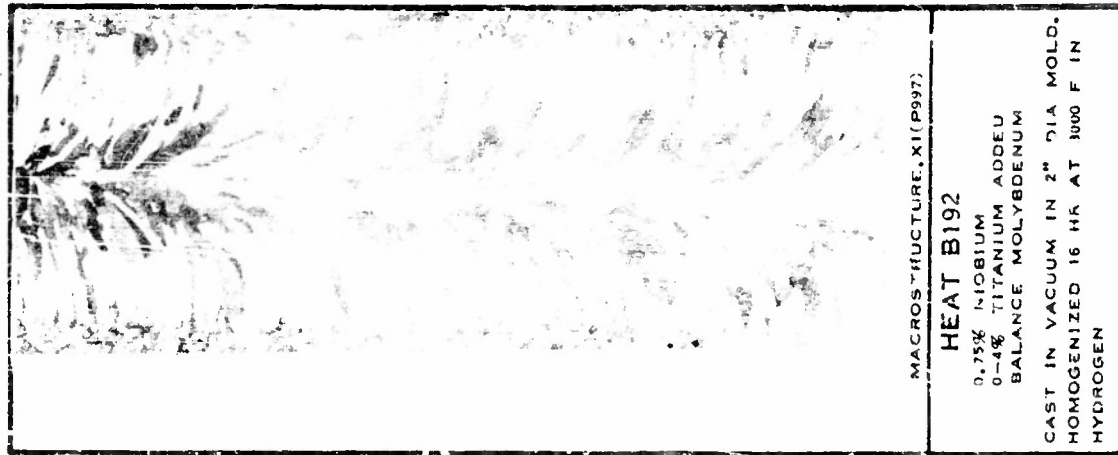
M3063

X1000

FIGURE 122 - MICROSTRUCTURE OF Mo-Nb-Co ALLOY, HEAT B193
0.74% Nb, 0.04% Co, 0.033% C, balance Mo, cast
in vacuum
Electropolished, etched in $\text{NaOH} + \text{K}_3\text{Fe}(\text{CN})_6$



OCTOBER 14, 1953



Molybdenum-Niobium-Zirconium Alloys

Heat B194, 0.75% Nb, 0-0.75% Zr added, 0.033% C. Cast in vacuum, heated 16 hours at 3000 F in hydrogen. A method for determining the amount of zirconium in molybdenum-base alloys in the presence of niobium has not yet been developed; therefore, zirconium analysis of this heat is not available. It has been determined, however, that zirconium added to other molybdenum-base alloys was fully recovered in the ingot.

Macrostructure. The macrostructure of the ternary alloys, shown in Figure 127, indicates a uniform decrease in grain size with increasing zirconium addition, which implies that the zirconium content of the ingot increased uniformly. The grain refining effect of zirconium is clearly shown.

Hardness. The hardness of the ternary alloys gradually decreased as the testing temperature was increased from room temperature to 500 F and 1600 F.

Microstructure. Figure 126 shows the microstructure at a point one inch from the top of the ingot. Marked interdendritic coring is shown at the lower magnification. A fine dispersion of carbide within the grains, but very little grain-boundary carbide, is shown at higher magnification.

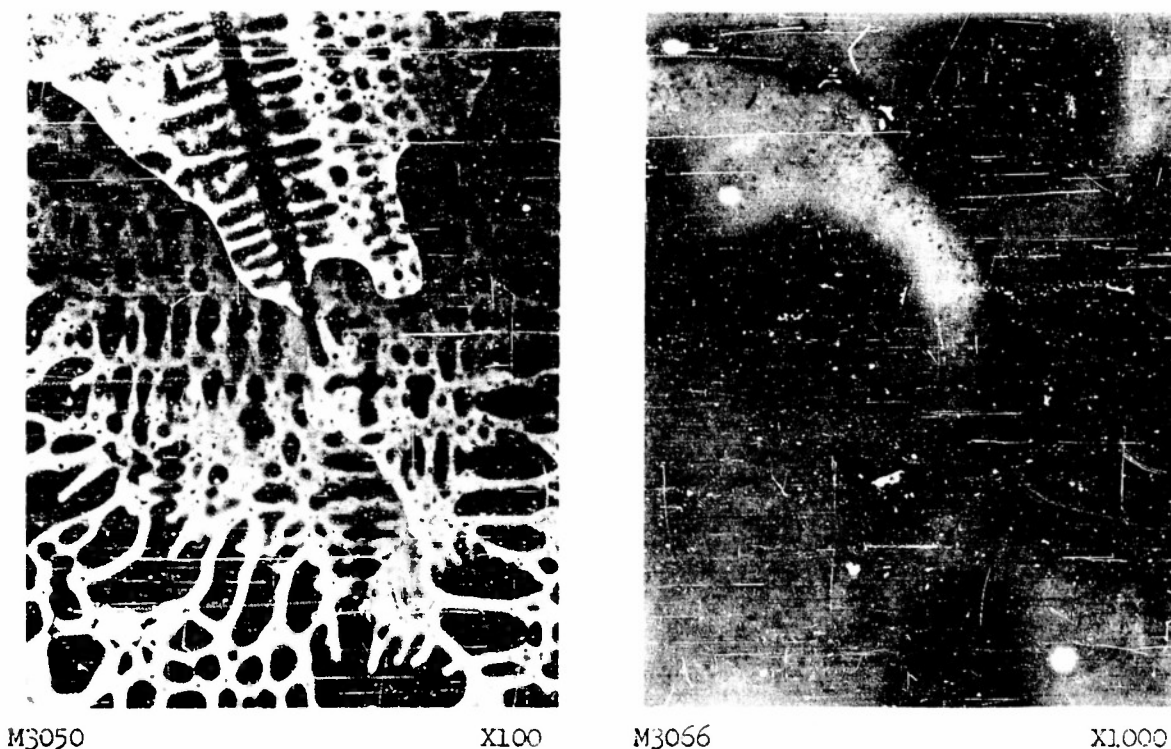


FIGURE 126 - MICROSTRUCTURE OF Mo-Nb-Zr ALLOY, HEAT B194
Structure one inch below top of ingot containing
not more than 0.75% Zr, 0.033% C, 0.75% Nb
Electropolished, etched in $\text{NaOH} + \text{K}_3\text{Fe}(\text{CN})_6$

OCTOBER 14, 1951



MACROSTRUCTURE, X1 (P1994)

HEAT B:94

0.75% NIOBIUM

0-75% ZIRCONIUM ADDED

BALANCE MOLYBDENUM

CAST IN VACUUM IN 2" DIA MOLD.

HOMOGENIZED 16 HR AT 3000 F IN HYDROGEN

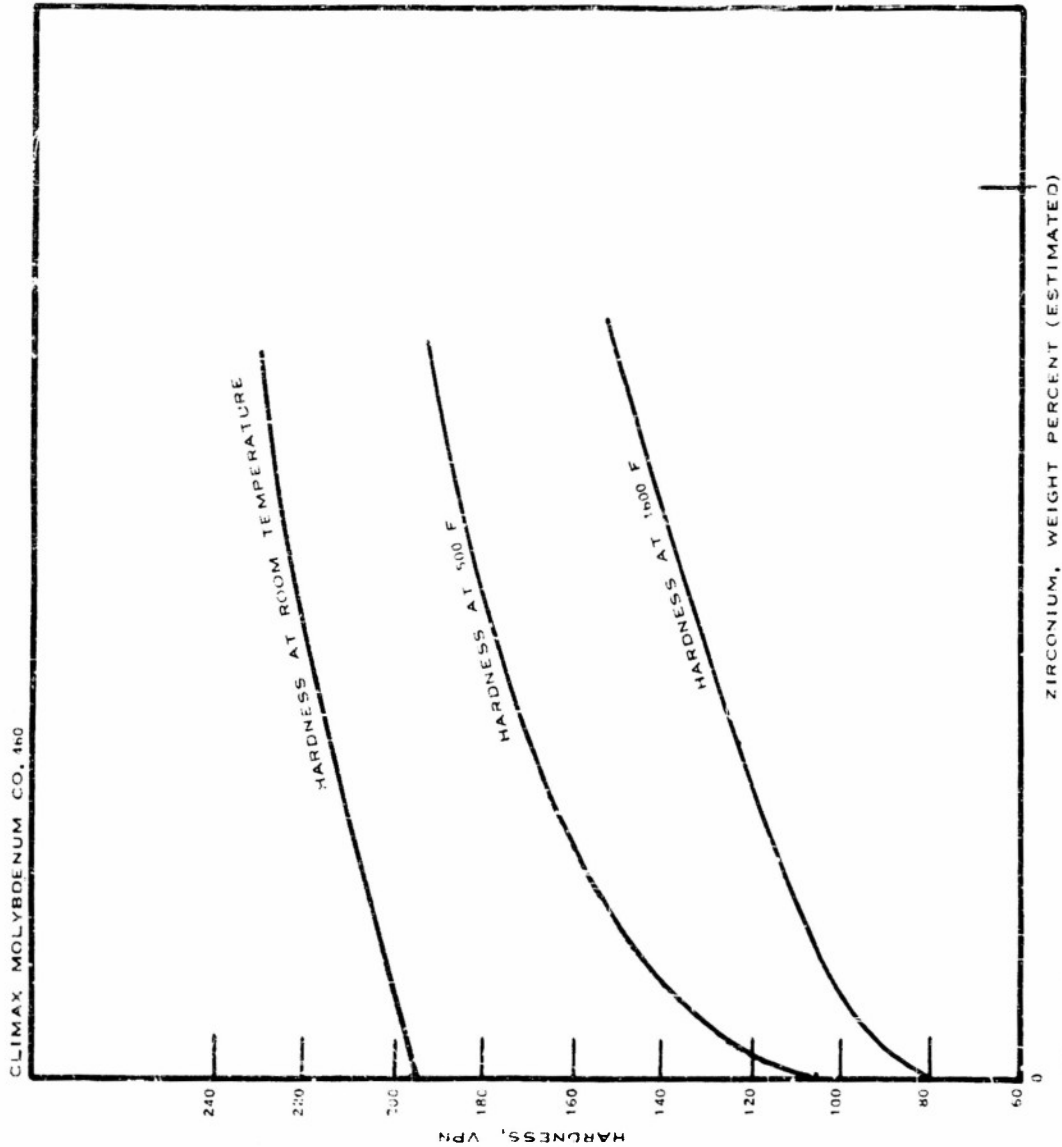


FIGURE 127 - HARDNESS AND MACROSTRUCTURE OF MOLYBDENUM-BASE NIOBIUM-ZIRCONIUM ALLOY

Molybdenum-Titanium-Aluminum Alloys

Heat B202, 0.47% Ti, 0-0.9% Al, 0.024% C. Cast in purified, re-circulated argon; heated 18 hours at 3000 F in hydrogen.

Macrostructure. The combination of 0.47% titanium and aluminum in excess of 0.3% refined the grain somewhat more than would be expected from each alloying element alone, Figure 129.

Hardness. The hardness of the ternary alloys gradually dropped as the testing temperature was raised from room temperature to 500 F and 1500 F. The addition of titanium increased the hardness of the molybdenum-aluminum alloys slightly.

Lattice Parameter. The change in lattice parameter of molybdenum-titanium-aluminum alloys with increasing aluminum content was practically the same as for the molybdenum-aluminum binary alloys, that is, it seems to be a function of aluminum content only.

Microstructure. Figure 128 shows the microstructure of the ternary alloy containing 0.90% aluminum and 0.47% titanium. It is a single-phase solid solution.

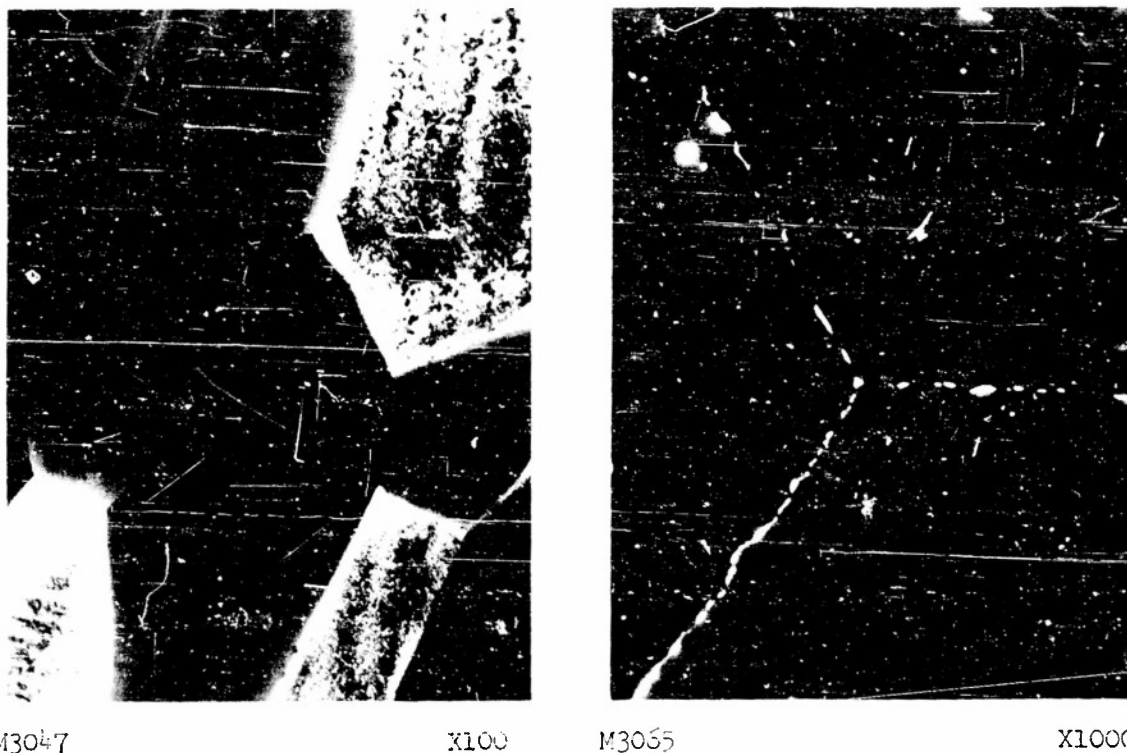
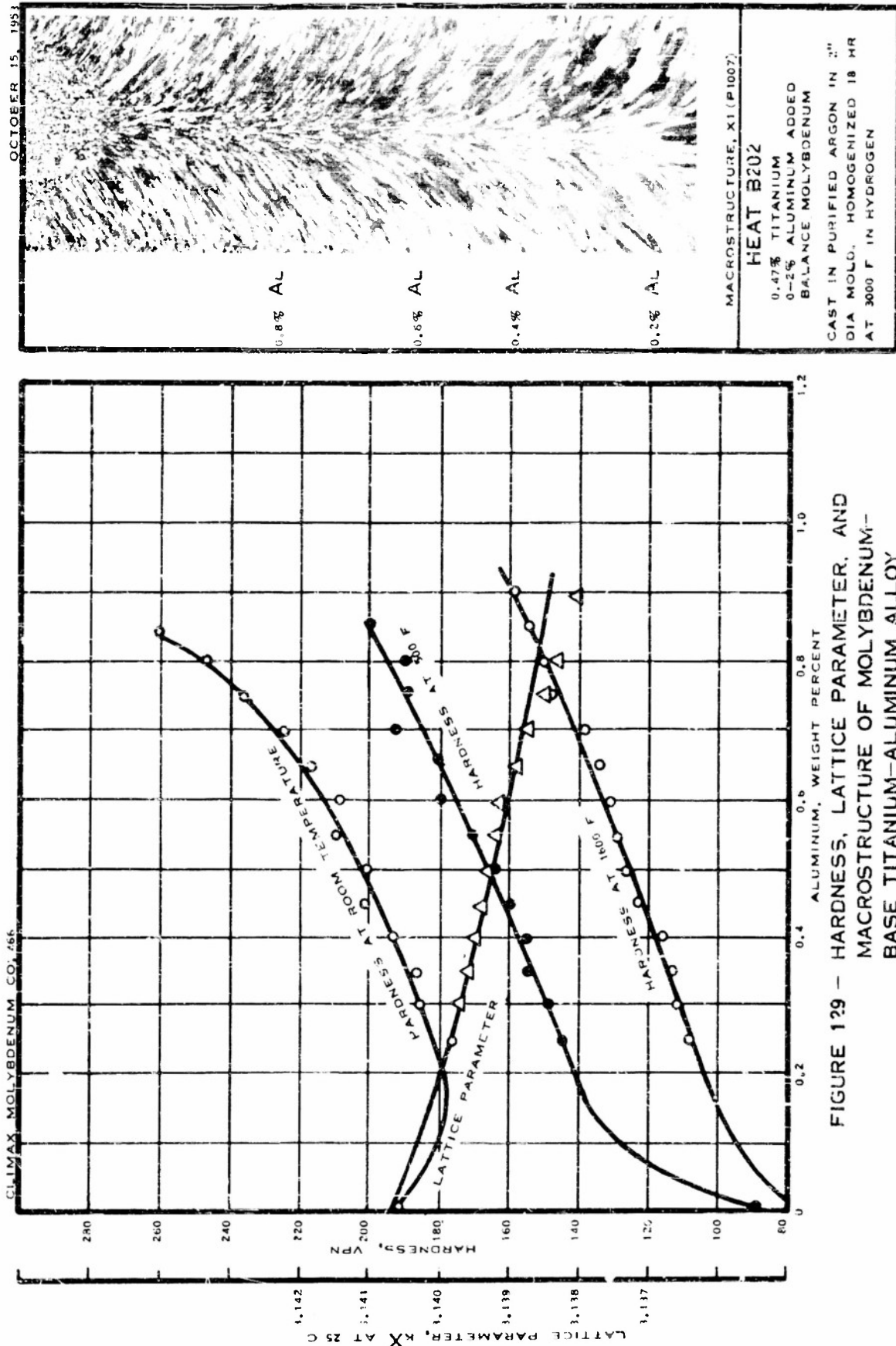


FIGURE 128 - MICROSTRUCTURE OF Mo-Ti-Al ALLOY, HEAT B202
0.47% Ti, 0.90% Al, 0.024% C, balance Mo,
cast in argon
Electropolished, etched in $\text{NaOH} + \text{K}_3\text{Fe}(\text{CN})_6$



Molybdenum-Titanium-Cobalt Alloys

Heat B201, 0.41% Ti, 0-0.12% Co, 0.024% C. Cast in vacuum, heated 18 hours at 3000 F in hydrogen.

Macrostructure. Within the range of composition of this ingot, the alloying elements exerted no grain refining effect. The grains tend to be equiaxed, Figure 131.

Hardness. Addition of up to 0.05% cobalt progressively decreased the hardness of the 0.41% titanium alloy at both room and elevated temperatures. Cobalt additions of 0.05 to 0.12%, however, raised the hardness slightly at room temperature, 500, and 1600 F.

Lattice Parameter. The decrease in lattice spacing of the molybdenum-titanium alloys was commensurate with amount of cobalt added.

Microstructure. The microstructure of the ternary alloy containing 0.41% titanium and 0.09% cobalt, Figure 130, is that of a single-phase solid solution. Carbides in very fine dispersion appear at the interdendritic interstices and at the grain boundaries.

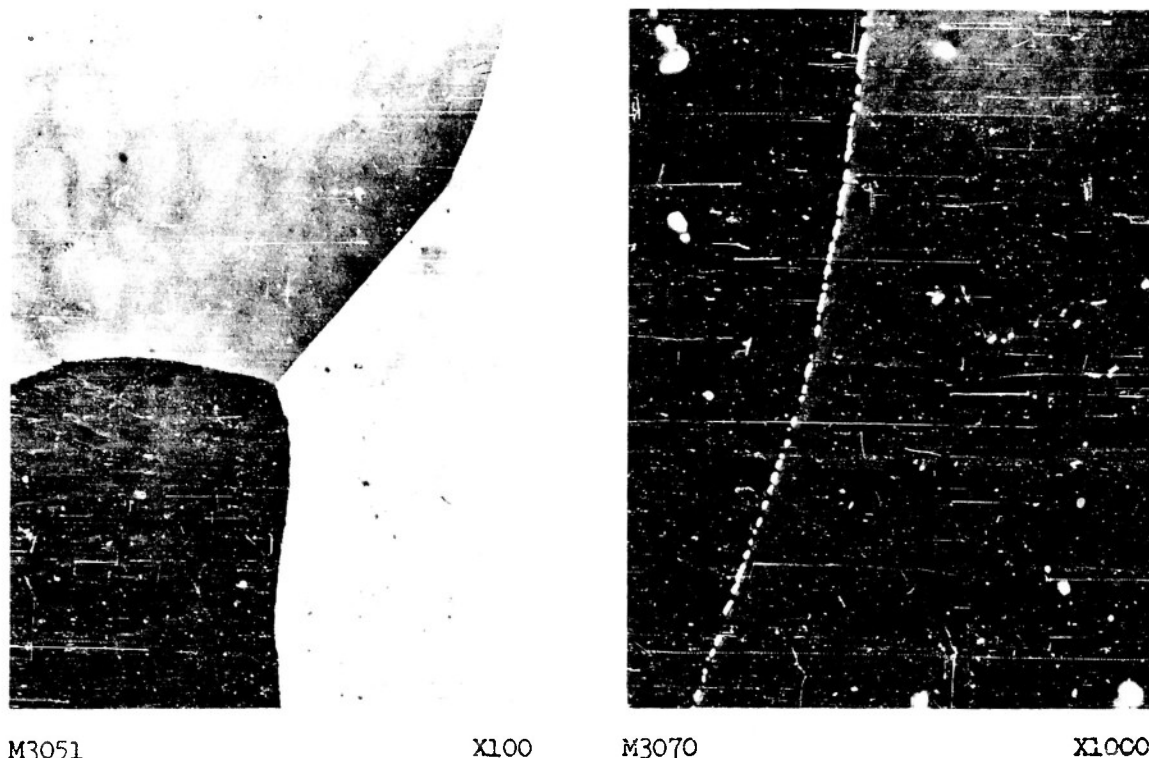


FIGURE 131 - MICROSTRUCTURE OF Mo-Ti-Co ALLOY, HEAT B201
0.41% Ti, 0.09% Co, 0.024% C, balance Mo,
cast in vacuum
Electropolished, etched in $\text{NaOH} + \text{K}_3\text{Fe}(\text{CN})_6$

Molybdenum-Titanium-Niobium Alloys

Heat B199, 0.27% Ti, 0-14% Nb, 0.024% C. Cast in vacuum, heated 18 hours at 3000 F in hydrogen.

Microstructure. Within the portion of the ingot containing 0 to 10% niobium, the size and shape of the grains, Figure 133, were essentially the same as for unalloyed molybdenum.

Hardness. The hardness of the ternary alloys gradually decreased as the testing temperature was raised from room temperature to 500 and 1600 F. The addition of 0.27% titanium to the alloys containing 0 to 14% niobium slightly increased the hardness at the three testing temperatures from that of comparable binary molybdenum-niobium alloys.

Microstructure. The microstructure of the alloy containing 0.27% titanium and 14% niobium is shown in Figure 132. It is a single-phase solid solution containing a very fine dispersion of carbide.



M3054

X100

FIGURE 132 - MICROSTRUCTURE OF Mo-Ti-Nb ALLOY, HEAT B199
0.27% Ti, 14% Nb, 0.024% C, balance Mo,
cast in vacuum
Electropolished, etched in $\text{NaOH} + \text{K}_3\text{Fe}(\text{CN})_6$

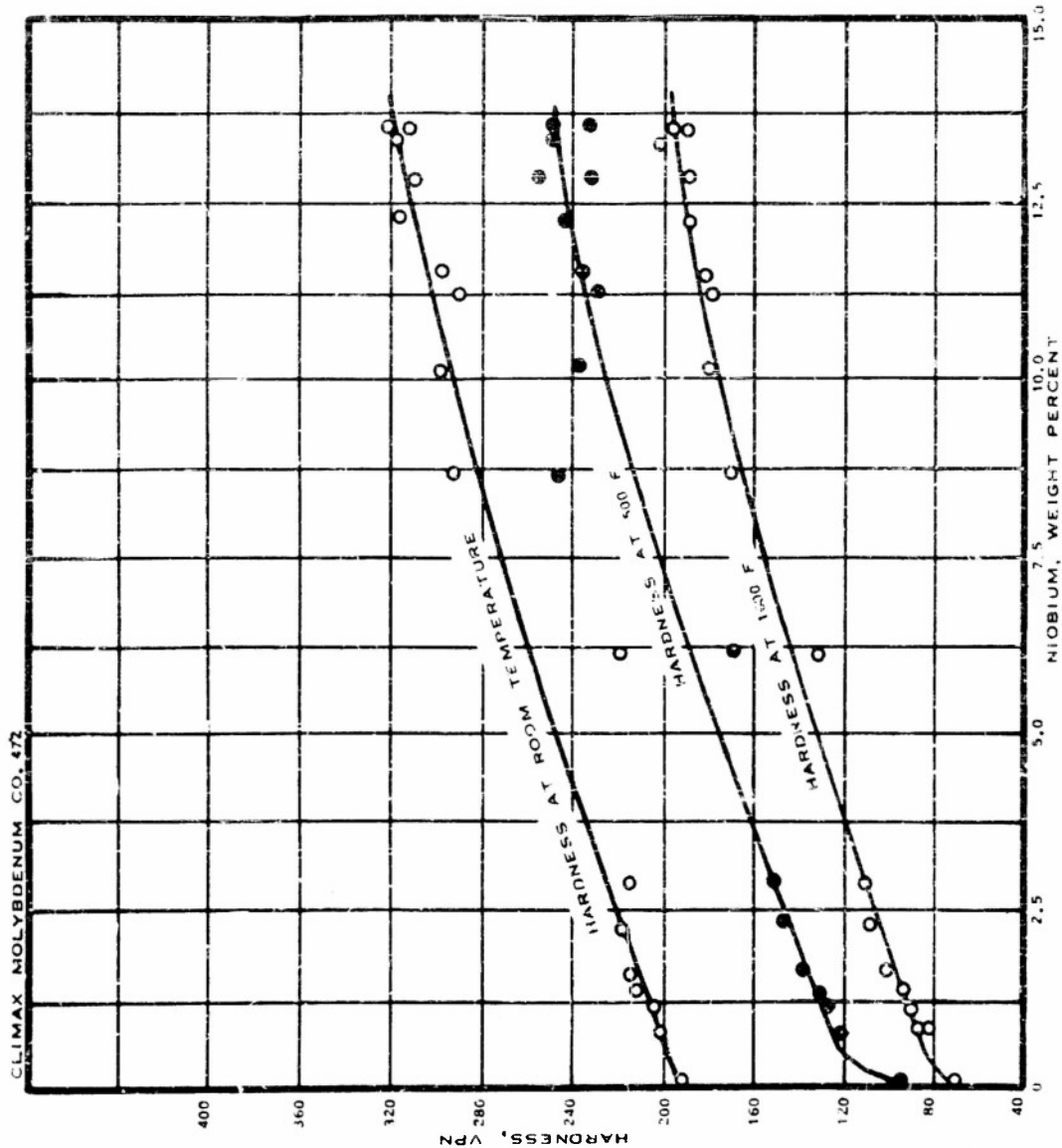
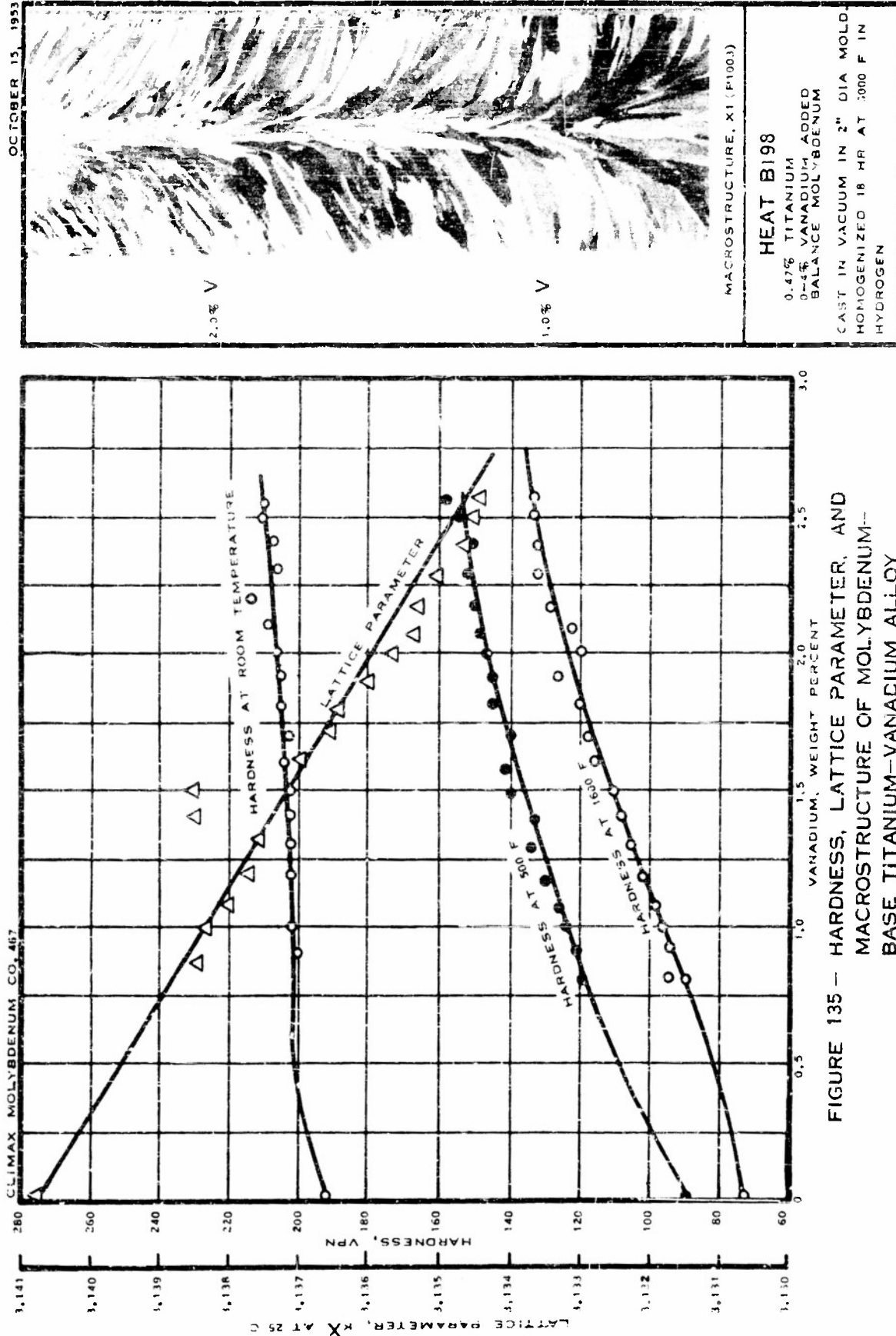


FIGURE 133 -- HARDNESS AND MACROSTRUCTURE OF MOLYBDENUM-BASE TITANIUM-NIOBIUM ALLOY



Molybdenum-Titanium-Zirconium Alloys

Heat B200, 0.42% Ti, 0-0.9% Zr, 0.024% C. Cast in vacuum, heated 18 hours at 3000 F in hydrogen.

Macrostructure. The grain size of the ternary alloys, Figure 137, was finer than that of molybdenum-zirconium binary alloys of similar zirconium content.

Hardness. There was a gradual decrease in hardness of the ternary alloys with increasing temperature from room temperature to 500 and 1600 F. The hardness at room temperature and 500 F was about the same as that of similar molybdenum-zirconium alloys at the same temperatures, but at 1600 F the ternary alloys were not as hard as the corresponding binary molybdenum-zirconium alloys.

Microstructure. Severe interdendritic coring of the solid solution is evident in Figure 136, which shows the structure of the ternary alloy containing 0.42% titanium and 0.78% zirconium. Carbide particles occur predominantly in the grains.



M3060

X100



M3069

X1000

FIGURE 136 - MICROSTRUCTURE OF Mo-Ti-Zr ALLOY, HEAT B200
0.42% Ti, 0.78% Zr, 0.024% C, balance Mo,
cast in vacuum
Electropolished, etched in $\text{NaOH} + \text{K}_3\text{Fe}(\text{CN})_6$

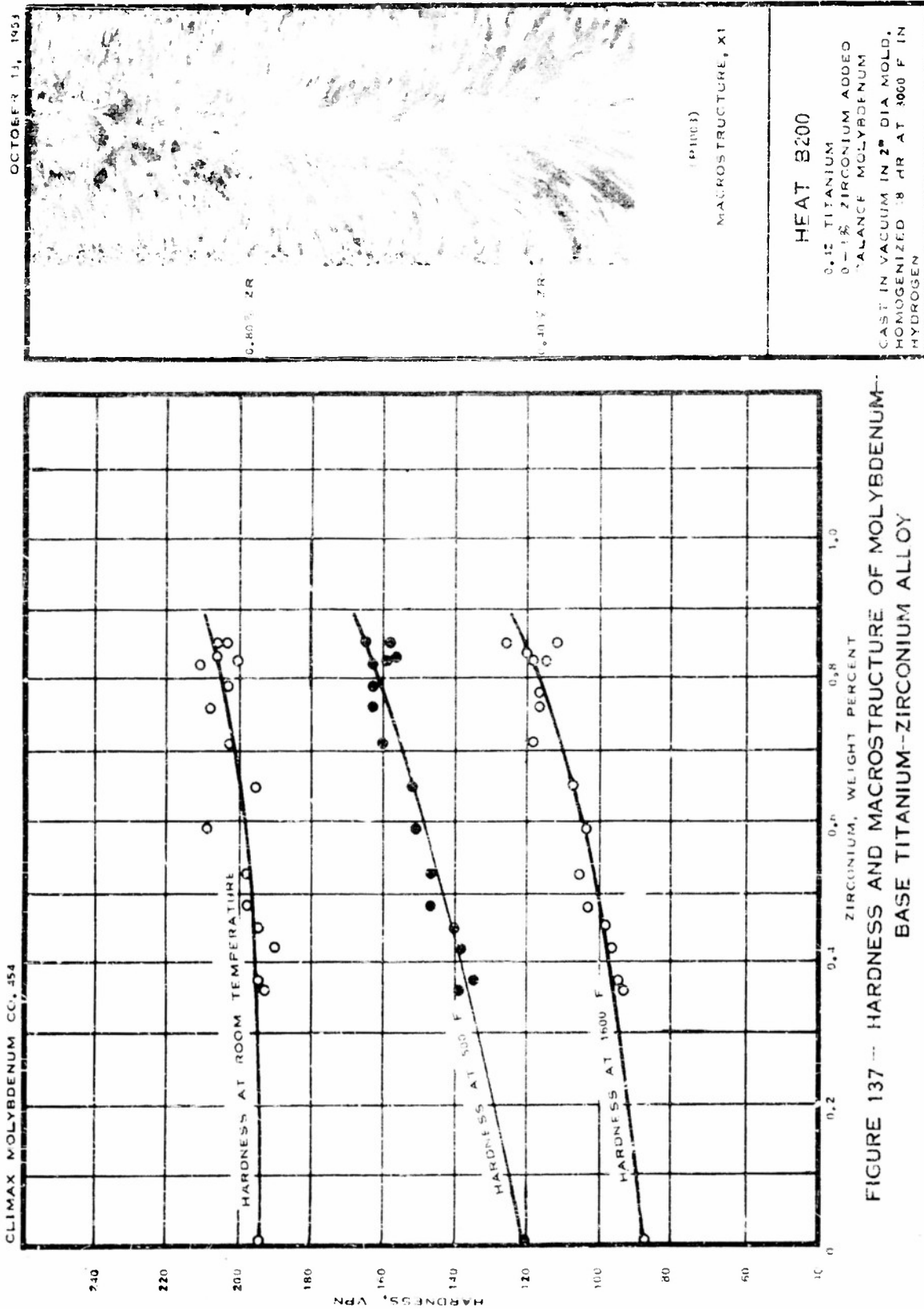


FIGURE 137 -- HARDNESS AND MACROSTRUCTURE OF MOLYBDENUM--
BASE TITANIUM--ZIRCONIUM ALLOY

Molybdenum-Vanadium-Aluminum Alloys

Heat B188, 0.54% V, 0-1.2% Al, 0.027% C. Cast in purified, recirculated argon; heated 18 hours at 3000 F in hydrogen.

Macrostructure. The refinement of grain with increasing aluminum content is similar to the behavior of binary molybdenum-aluminum alloys.

Hardness. The hardness of the ternary alloys gradually dropped as the testing temperature was raised from room temperature to 500 and 1600 F. Addition of up to 0.25% aluminum produced little change in the hardness of the 0.54% vanadium binary alloy at room temperature, whereas at 500 and 1600 F the hardness increased with increasing aluminum content.

Lattice Parameter. Both vanadium and aluminum contract the lattice spacing of molybdenum. In combination the effects are additive.

Microstructure. The microstructure of the ternary alloy containing 0.54% vanadium and 1.2% aluminum is shown in Figure 138. It consists of a single-phase solid solution with carbide clusters within the grains.



M3056

X100

FIGURE 138 - MICROSTRUCTURE OF Mo-V-Al ALLOY, HEAT B188
0.54% V, 1.2% Al, 0.027% C, balance Mo,
cast in argon
Electropolished, etched in $\text{NaOH} + \text{K}_3\text{Fe}(\text{CN})_6$

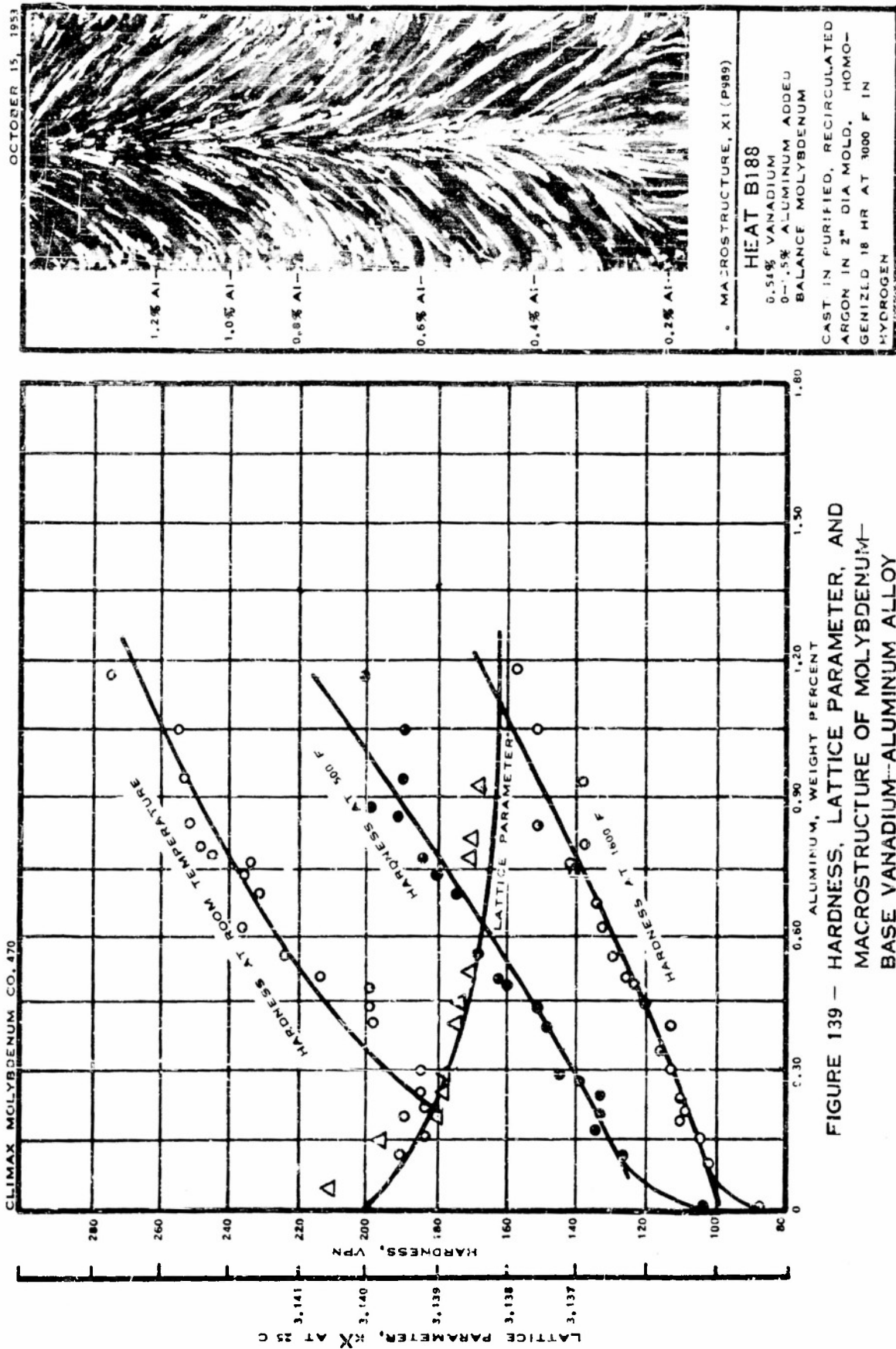


FIGURE 139 — HARDNESS, LATTICE PARAMETER, AND
MACROSTRUCTURE OF MOLYBDENUM-
BASE VANADIUM-ALUMINUM ALLOY

Molybdenum-Vanadium-Cobalt Alloys

Heat B189. 0.52% V, 0-0.25% Co, 0.027% C. Cast in vacuum, heated 18 hours at 3000 F in hydrogen.

Macrostructure. The grain size, Figure 141, was similar to that of binary molybdenum-cobalt and molybdenum-vanadium alloys within the same range of composition. The addition of cobalt tends to obliterate the columnar structure and to form equiaxed grains.

Hardness. The drop in hardness was greater from room temperature to 500 F than from 500 F to 1600 F. The addition of cobalt in amounts up to 0.05% to the 0.52% vanadium alloy caused a slight drop in room temperature hardness. Addition of 0.05 to 0.25% cobalt caused a slight change in hardness at room temperature but a substantial increase in hardness at 500 and 1600 F.

Microstructure. The microstructure of the ternary alloy containing 0.52% vanadium and 0.20% cobalt, Figure 140, consists of a single-phase solid solution containing a dispersion of coarser carbide than was found in the other ternary alloys. Some microporosity was observed.

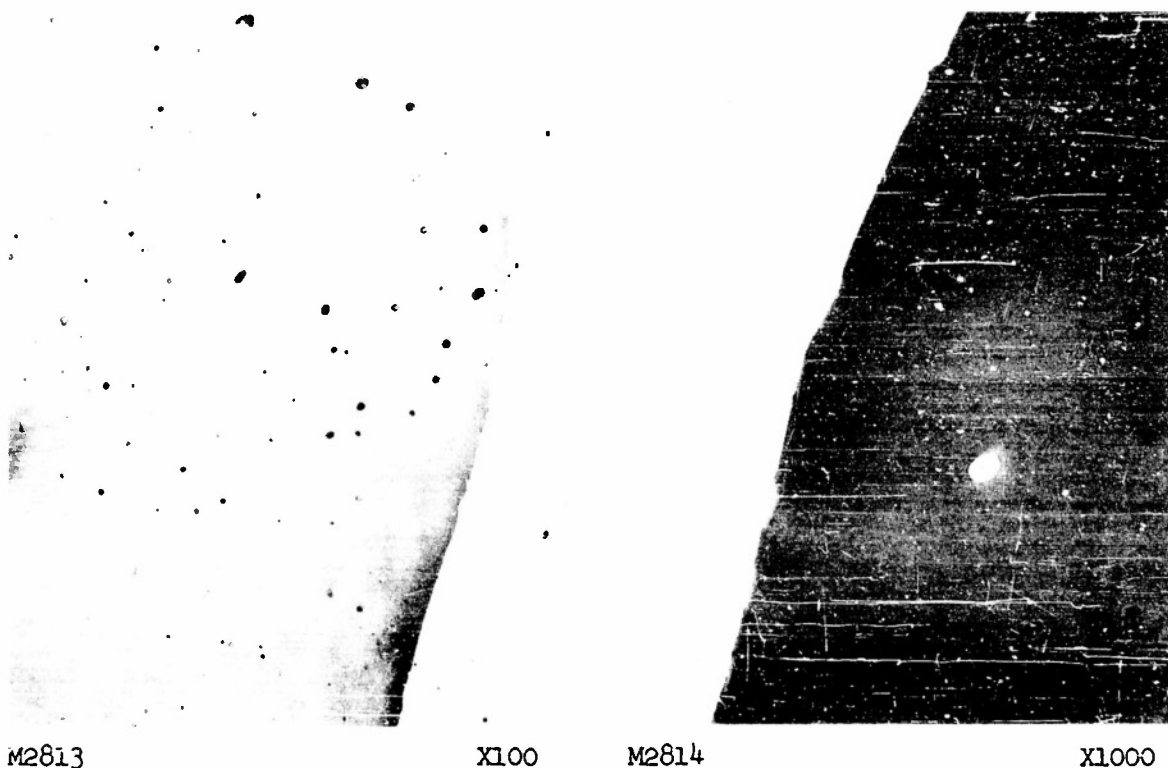


FIGURE 140 - MICROSTRUCTURE OF Mo-V-Co ALLOY, HEAT B189
0.52% V, 0.20% Co, 0.027% C, balance Mo, cast
in vacuum
Electropolished, etched in $\text{NaOH} + \text{K}_3\text{Fe}(\text{CN})_6$

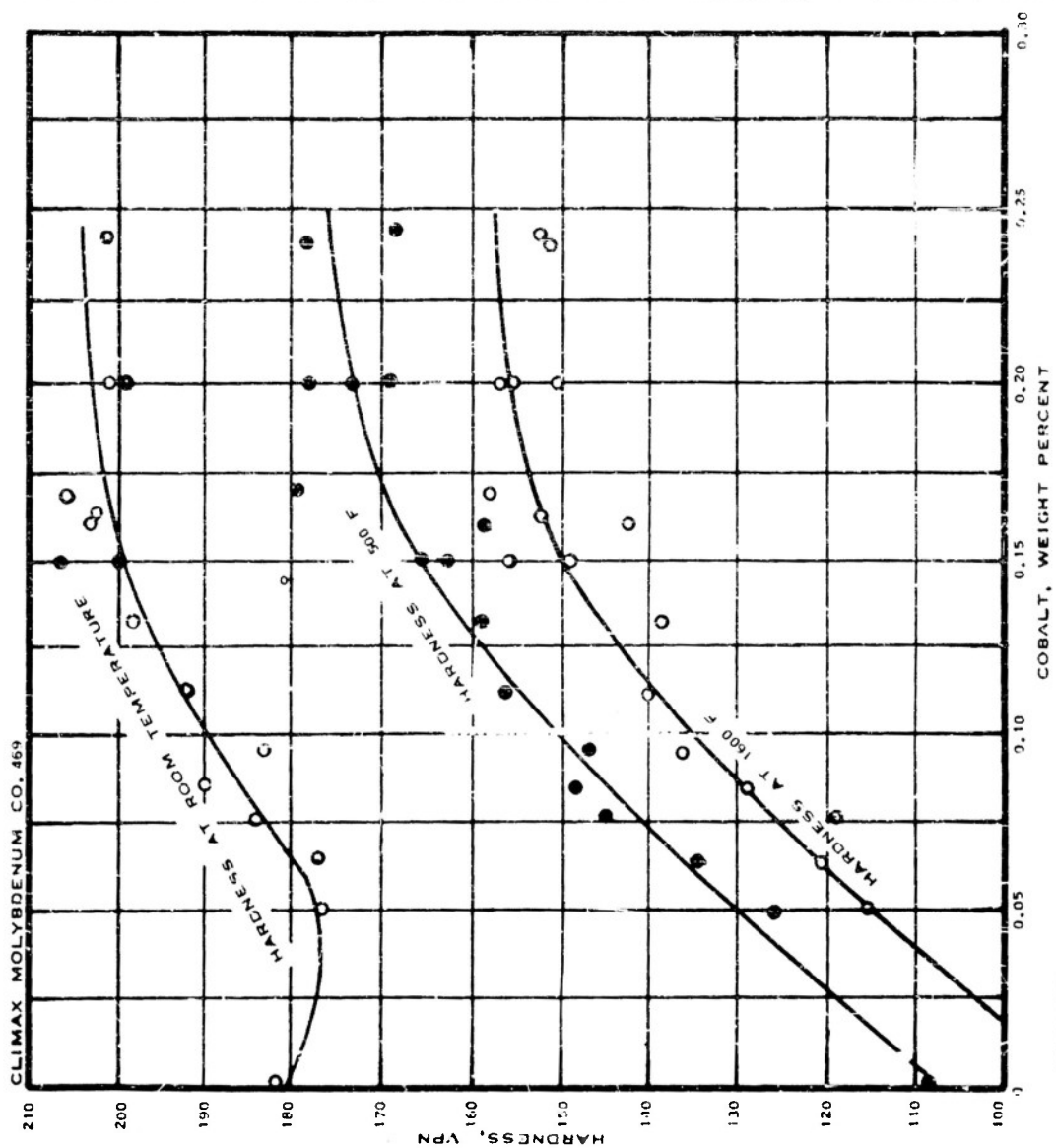
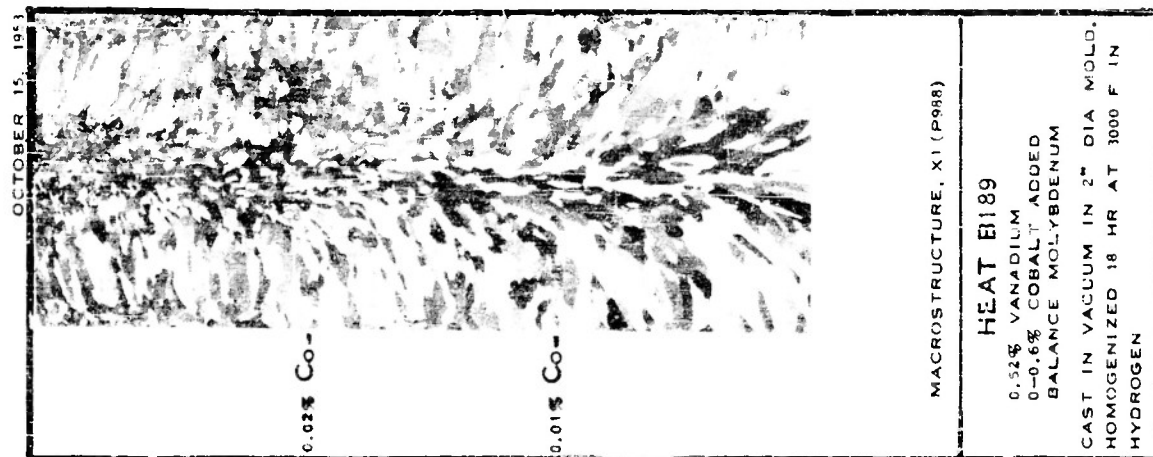


FIGURE 141 — HARDNESS AND MACROSTRUCTURE OF MOLYBDENUM—
BASE VANADIUM-COBALT ALLOY

Molybdenum-Vanadium-Titanium Alloys

Heat B187, 0.54% V, 0-0.7% Ti, 0.027% C. Cast in vacuum, heated 18 hours at 3000 F in hydrogen.

Macrostructure. The grain size of the ternary alloys was the same as that of molybdenum-titanium binary alloys of similar titanium content.

Hardness. The hardness of the ternary alloys dropped rapidly as the testing temperature was raised from room temperature to 500 F and dropped slowly as the temperature was raised from 500 to 1600 F. Addition of up to 0.7% titanium produced a small increase in hardness of the 0.54% vanadium alloy at room temperature and at 1600 F, but at 500 F it increased the hardness greatly.

Lattice Parameter. Titanium increases the lattice spacing of molybdenum and vanadium contracts it. The effect of combining the two alloying elements was that of algebraic addition.

Microstructure. The microstructure of the ternary alloy containing 0.54% vanadium and 0.67% titanium is shown in Figure 142. It consists of a single-phase solid solution. At lower concentrations of titanium, the carbide phase had coalesced at the grain boundaries. As the titanium content was increased, the carbide phase became more finely dispersed and appeared in clusters within the grains, as shown in the photomicrographs below.

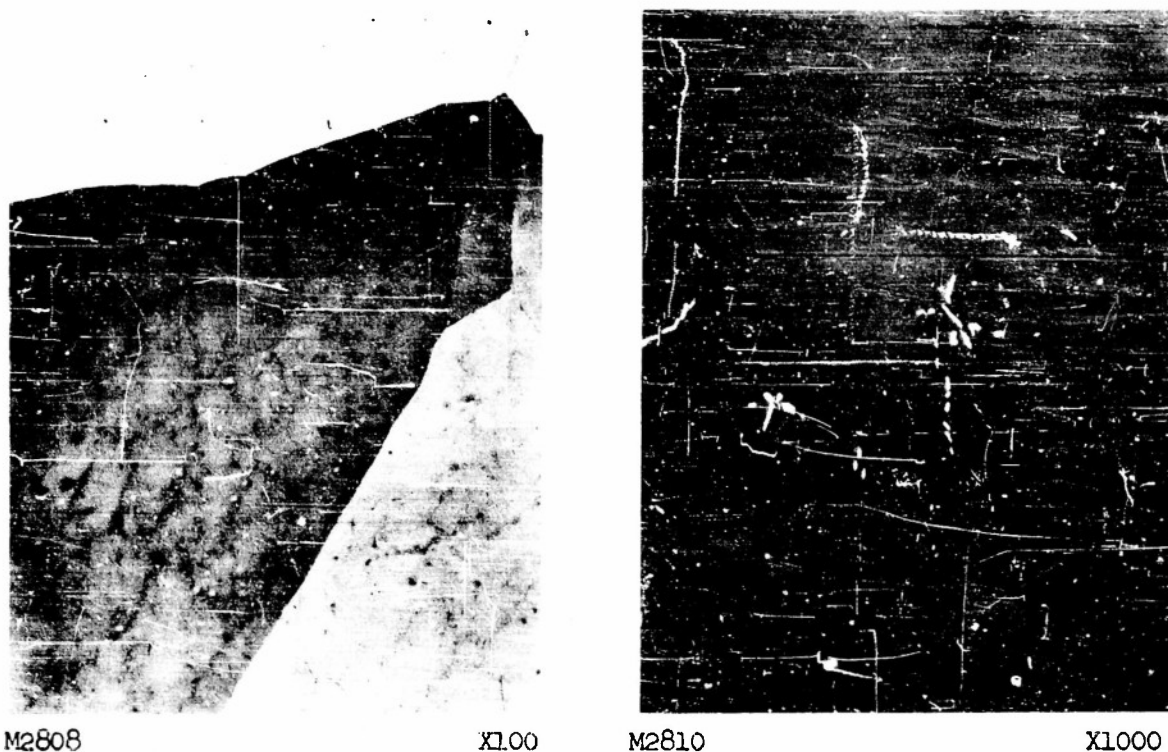
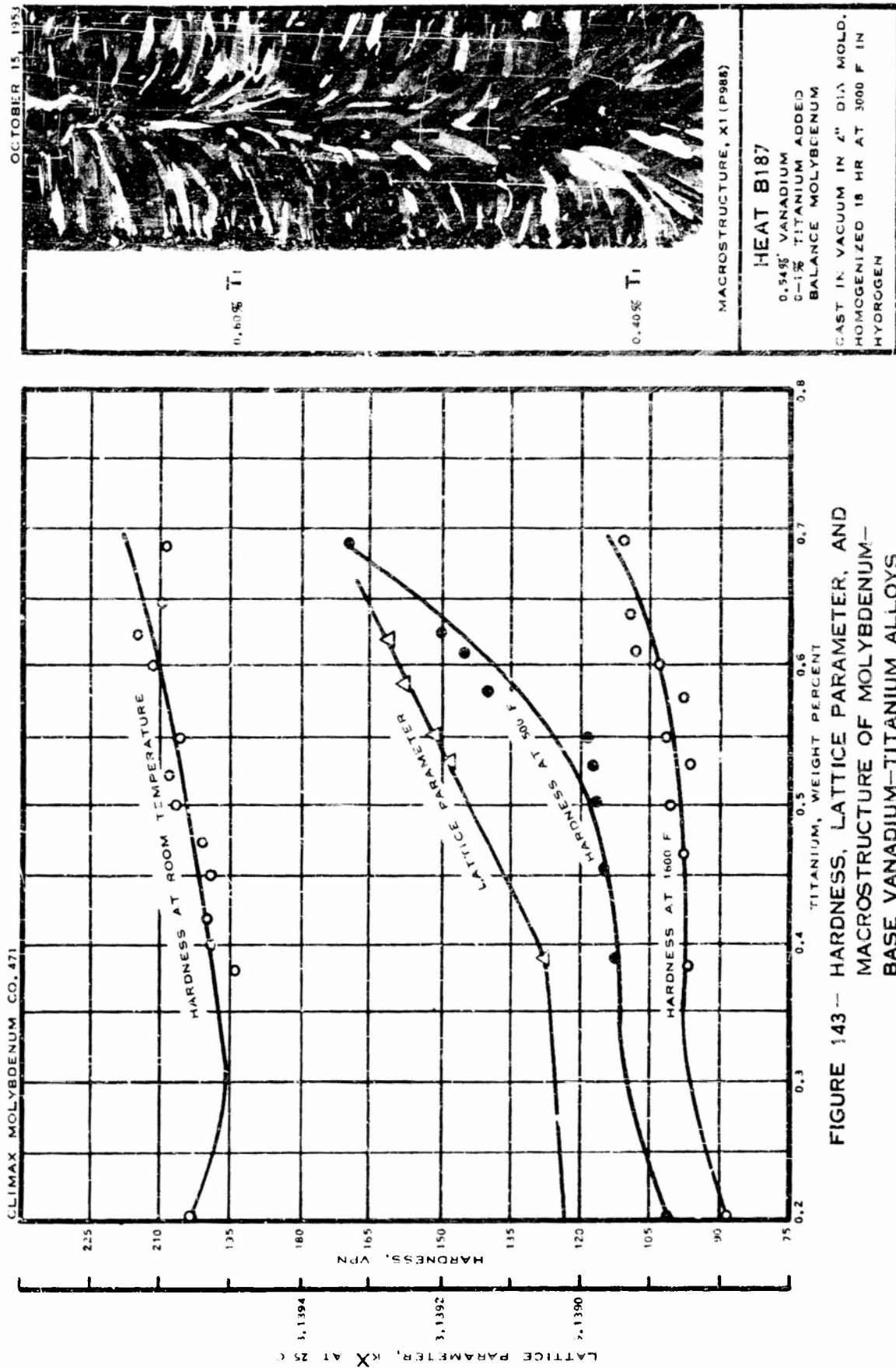


FIGURE 142 - MICROSTRUCTURE OF Mo-V-Ti ALLOY, HEAT B187
0.54% V, 0.57% Ti, 0.027% C, balance Mo, cast
in vacuum
Electropolished, etched in $\text{NaOH} + \text{K}_3\text{Fe}(\text{CN})_6$



Molybdenum-Vanadium-Zirconium Alloys

Heat B190, 0.51% V, 0-0.9% Zr, 0.027% C. Cast in vacuum, heated 16 hours at 3000 F in hydrogen.

Macrostructure. The photomicrograph, Figure 145, shows progressive grain refinement with increasing zirconium content, similar to that of the molybdenum-zirconium binary alloys.

Hardness. The hardness of the ternary alloys gradually dropped as the testing temperature was raised from room temperature to 500 and 1600 F. At room temperature the hardness of the ternary alloys was essentially the same as for the corresponding binary molybdenum-zirconium alloys. At 500 F the ternary alloys were slightly lower in hardness, and at 1600 F appreciably lower, than the corresponding binary molybdenum-zirconium alloys. This anomalous behavior of hardness is probably associated with the severely cored structure of the ternary alloys, see Figure 144.

Microstructure. The cored structure of the alloy containing 0.51% vanadium and 0.87% zirconium is shown in Figure 144. Finely dispersed carbide occurred in clusters within the grains, as it had in binary molybdenum-zirconium alloys containing 0.15% or more zirconium.

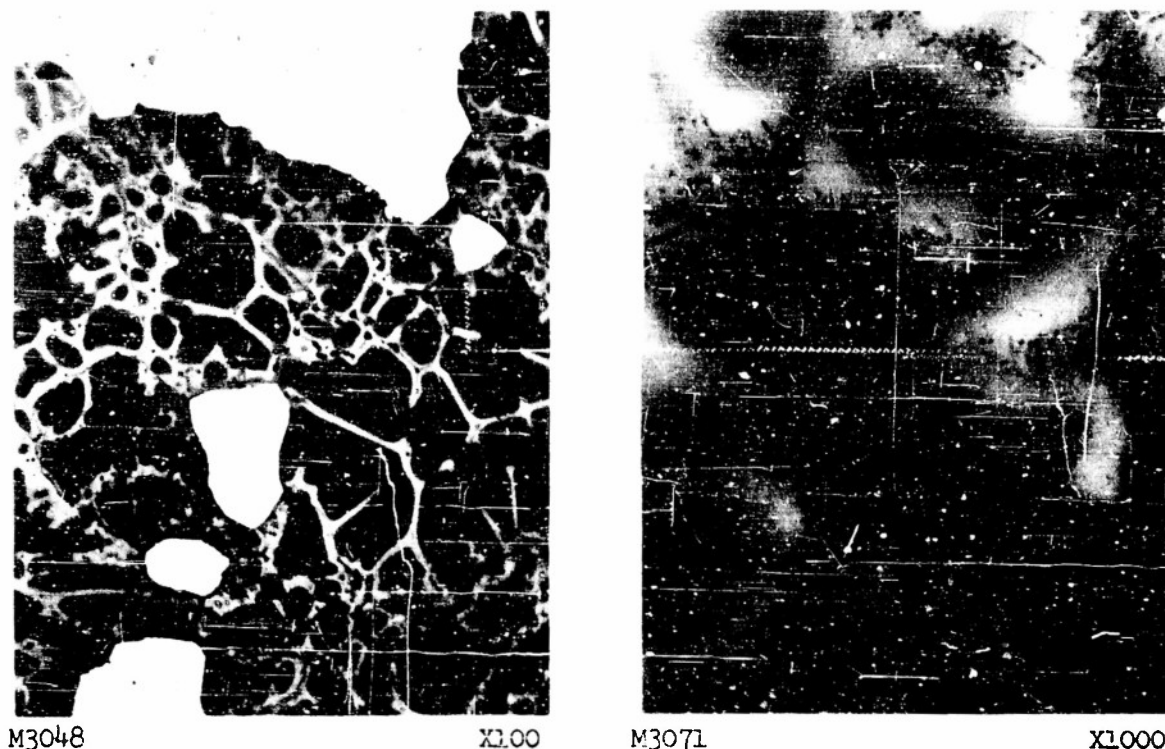


FIGURE 144 - MICROSTRUCTURE OF Mo-V-Zr ALLOY, HEAT B190
0.51% V, 0.87% Zr, 0.027% C, balance Mo, cast
in vacuum
Electropolished, etched in $\text{NaOH} + \text{K}_3\text{Fe}(\text{CN})_6$

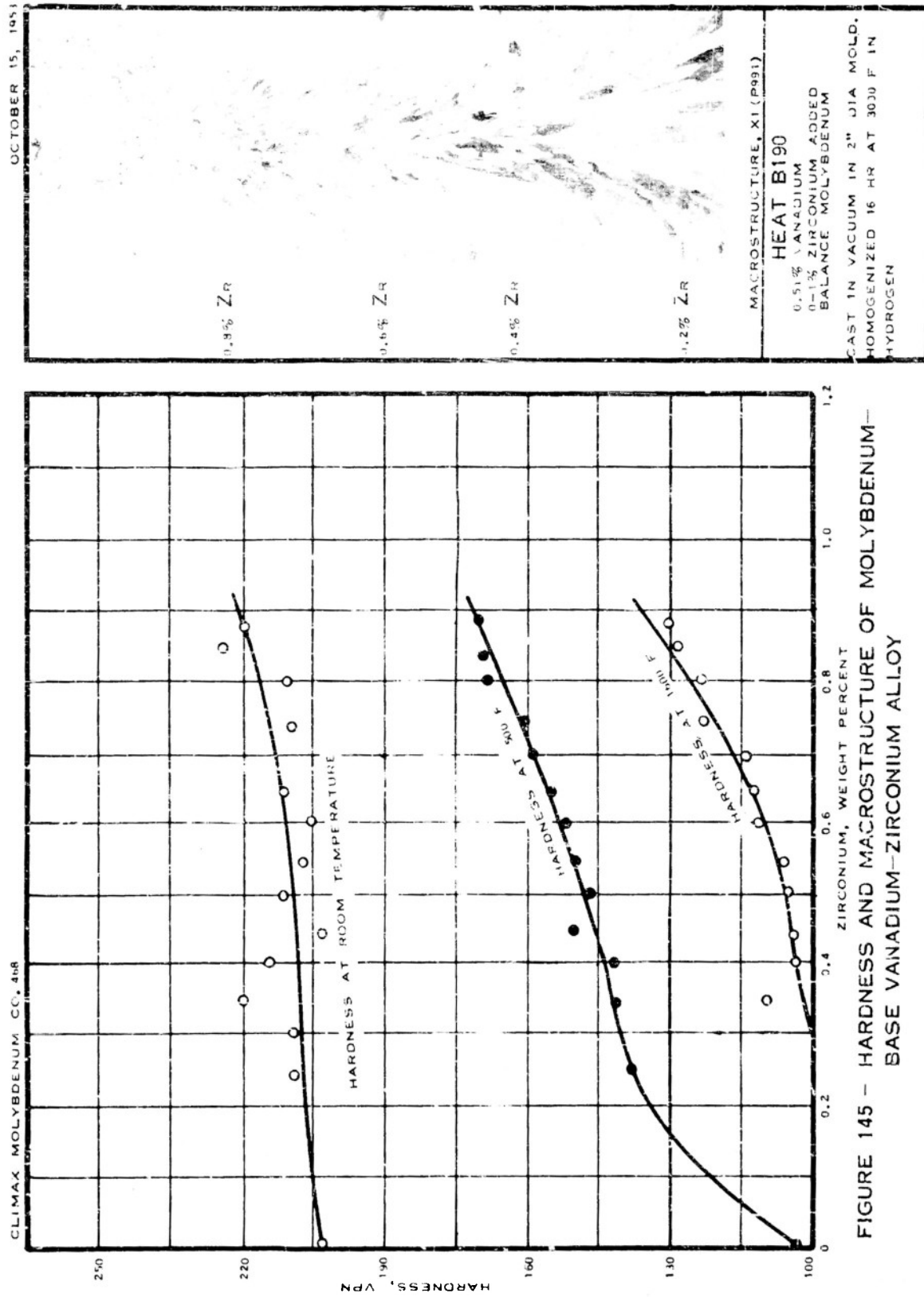


FIGURE 145 - HARDNESS AND MACROSTRUCTURE OF MOLYBDENUM-BASE VANADIUM-ZIRCONIUM ALLOY

Summary

1. No difficulty attributable to the alloying elements was encountered during melting of the ternary molybdenum-base alloys, either in maintaining the arc or in filling the mold.
2. All the ternary alloys consisted of terminal solid solutions, except for a small amount of carbide phase resulting from the method of deoxidation.
3. The carbide phase occurred in two characteristic forms. In ternary molybdenum-base alloys containing any two elements of the group aluminum, cobalt, niobium, and vanadium, the carbides occurred as coalesced particles within the grains and at the grain boundaries. Addition of zirconium or titanium to these alloys caused the carbide to precipitate in an extremely fine dispersion, principally within the grains at interdendritic interstices. The transition of the carbides from the coalesced type to the fine dispersion was a function of zirconium and/or titanium contents. To produce significant transition, about 0.15% zirconium or 0.50% titanium is required. The effect is similar to that observed in unalloyed molybdenum to which zirconium and titanium are added.
4. All of the alloys exhibited interdendritic segregation, an indication that solidification had occurred over a wide range of temperature. Coring was most pronounced in the ternary alloys containing zirconium. Heating the castings for 18 hours at 3000 F did not eliminate this microsegregation.
5. The lattice parameter of a ternary molybdenum-base alloy is a function of the amount of alloying element present. The effects of two alloying elements simultaneously present were algebraically additive.
6. Figures 146-151 summarize hardness data obtained in this investigation at room temperature and 1600 F for the molybdenum-base ternary alloys and for pertinent molybdenum-base binary alloys as a comparison. The effect of the third element upon the hardness of the binary alloys was erratic. Ternary molybdenum-base alloys containing small amounts of aluminum or cobalt generally have lower hardness at room temperature than corresponding binary molybdenum-base alloys free from the aluminum or cobalt. This is similar to the effect of adding small amounts of aluminum or cobalt to unalloyed molybdenum. At 1600 F, all of the ternary alloys were harder than the corresponding binary alloys. In general the hardening effects of addition of two alloying elements to molybdenum are additive.

ACKNOWLEDGMENT

The work described in this report represents the combined efforts of the Climax Molybdenum Company Research Laboratory personnel, with valued advice from its administrative and technical supervisory staff. This indispensable cooperation is herewith acknowledged. In particular, we wish to thank William C. Coons for metallographic examination, and Robert H. Maurer for chemical analysis, of the materials of this investigation.

* * *

This report covers work conducted at the Detroit Research Laboratory of the Climax Molybdenum Company. The developments disclosed have been or will be embodied in patent applications assigned to the Climax Molybdenum Company.

REFERENCES

1. Arc-Cast Molybdenum-Base Alloys, First Annual Report, Contract N8onr-78700, to Office of Naval Research, Navy Department, April 1, 1950. Climax Molybdenum Company of Michigan
2. The same, Second Annual Report, 1951
3. The same, Third Annual Report, 1952
4. U. S. Patents 2,538,917 and 2,630,220. Steel, vol 130, No. 22 (1952), 92
5. ASM Handbook, American Society for Metals, 1948, p 259
6. "Progress in Metal Physics", Bruce Chalmers, Editor, Interscience Publishers, Inc., New York, vol 3 (1952), 266, 274

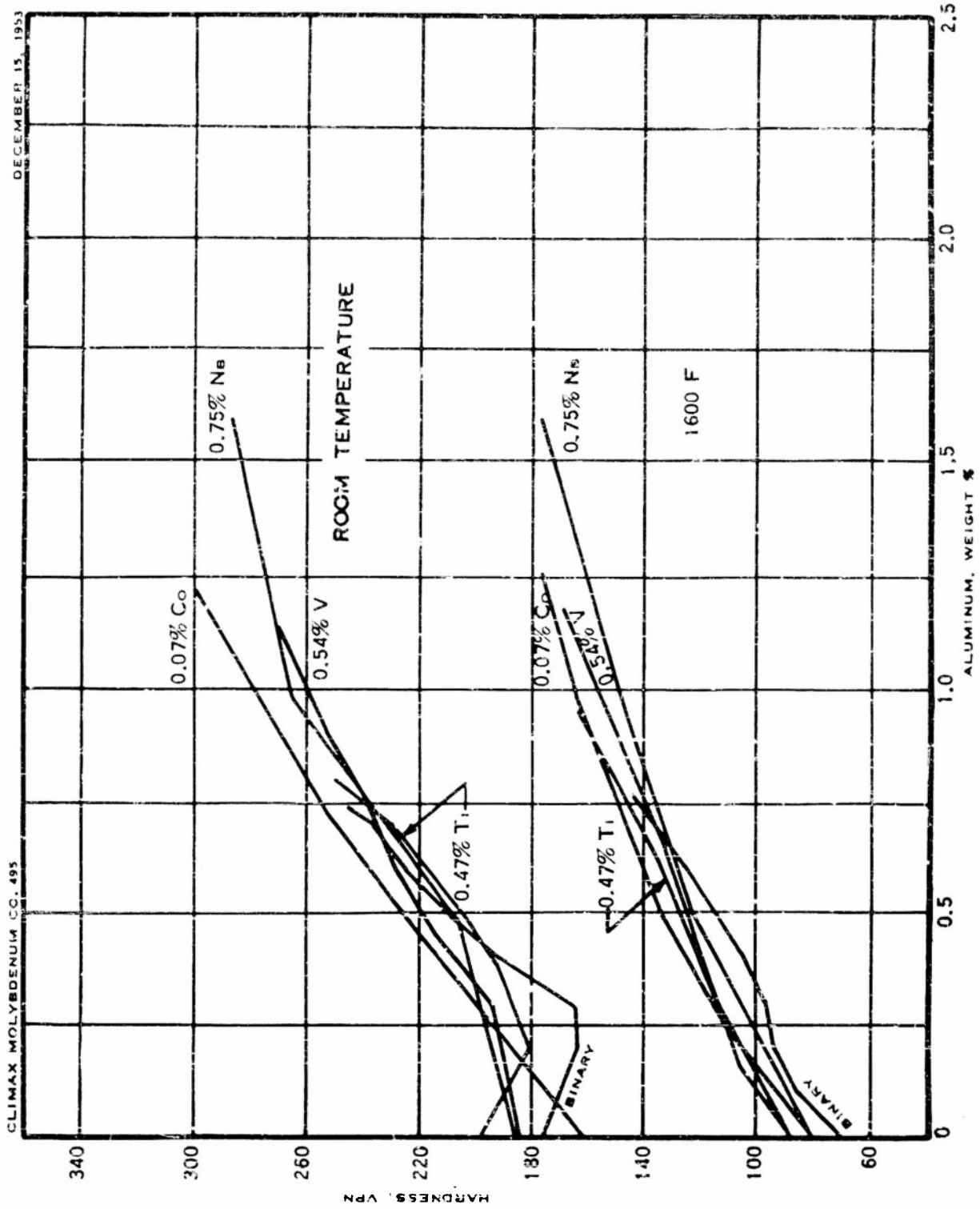


FIGURE 146 -- EFFECT OF ALUMINUM CONTENT UPON THE HARDNESS OF TERNARY MOLYBDENUM-BASE ALLOYS

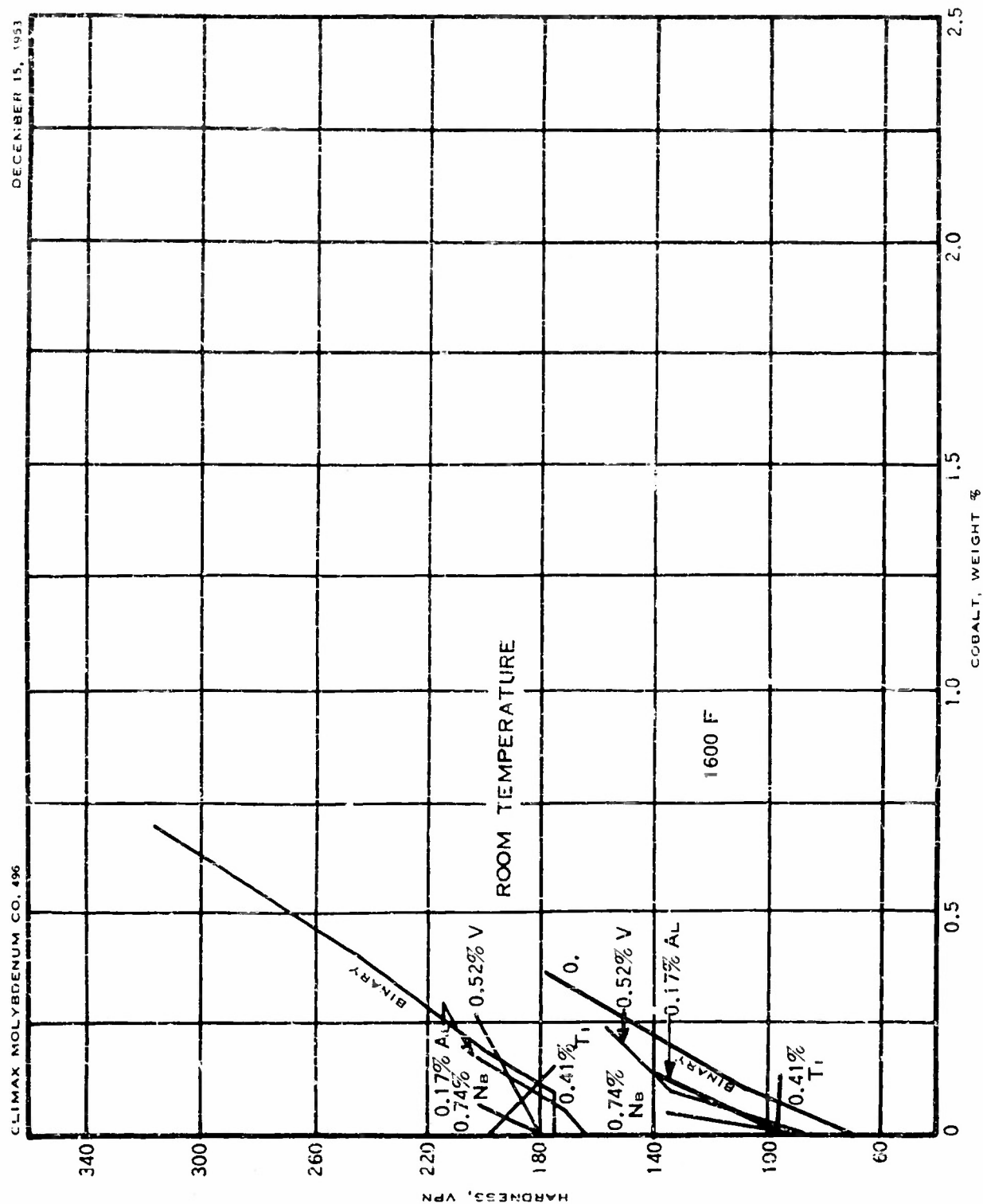


FIGURE 147 - EFFECT OF COBALT CONTENT UPON THE HARDNESS OF TERNARY MOLYBDENUM-BASE ALLOYS

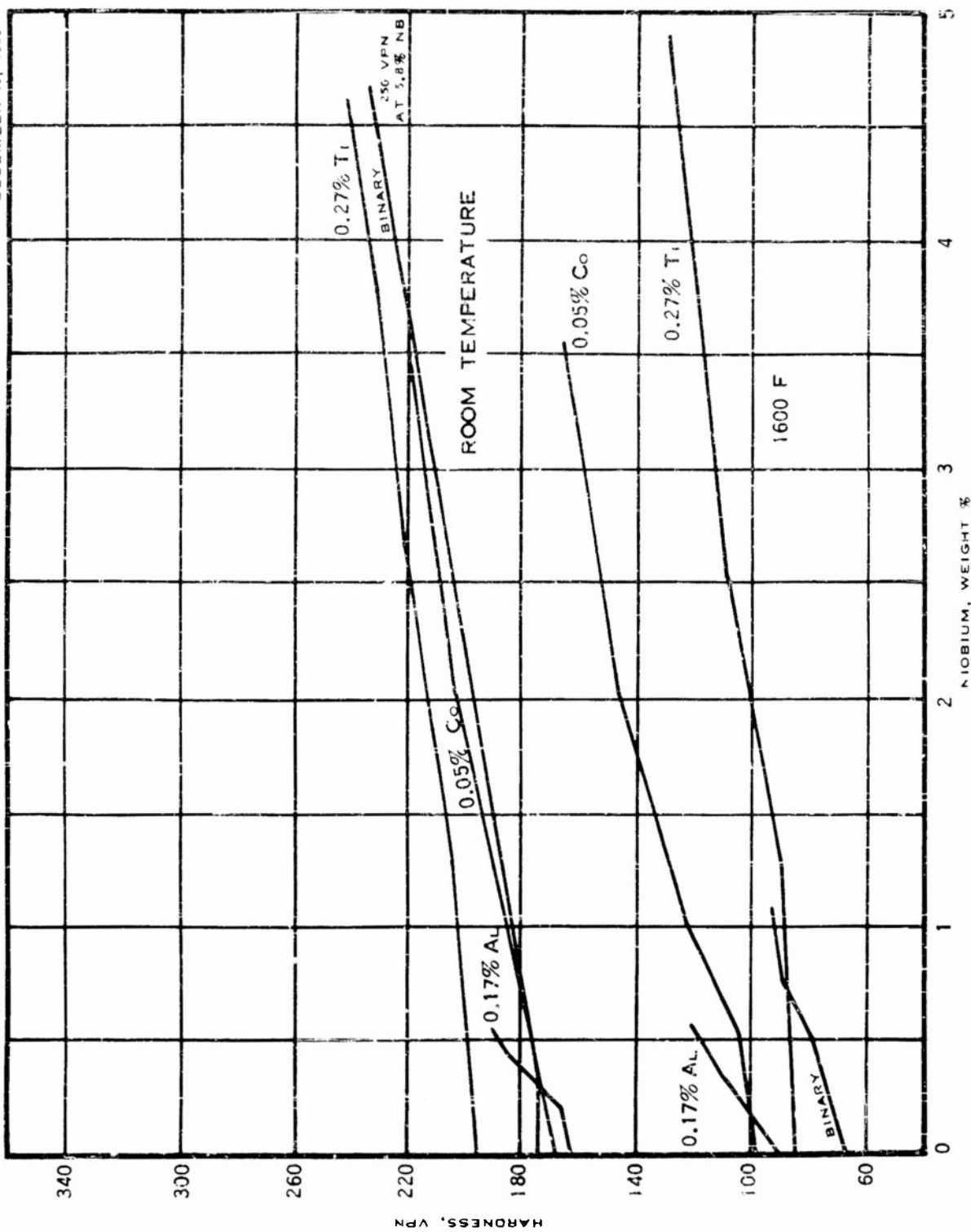


FIGURE 148 - EFFECT OF NIOBIUM CONTENT UPON THE HARDNESS OF TERNARY MOLYBDENUM-BASE ALLOYS

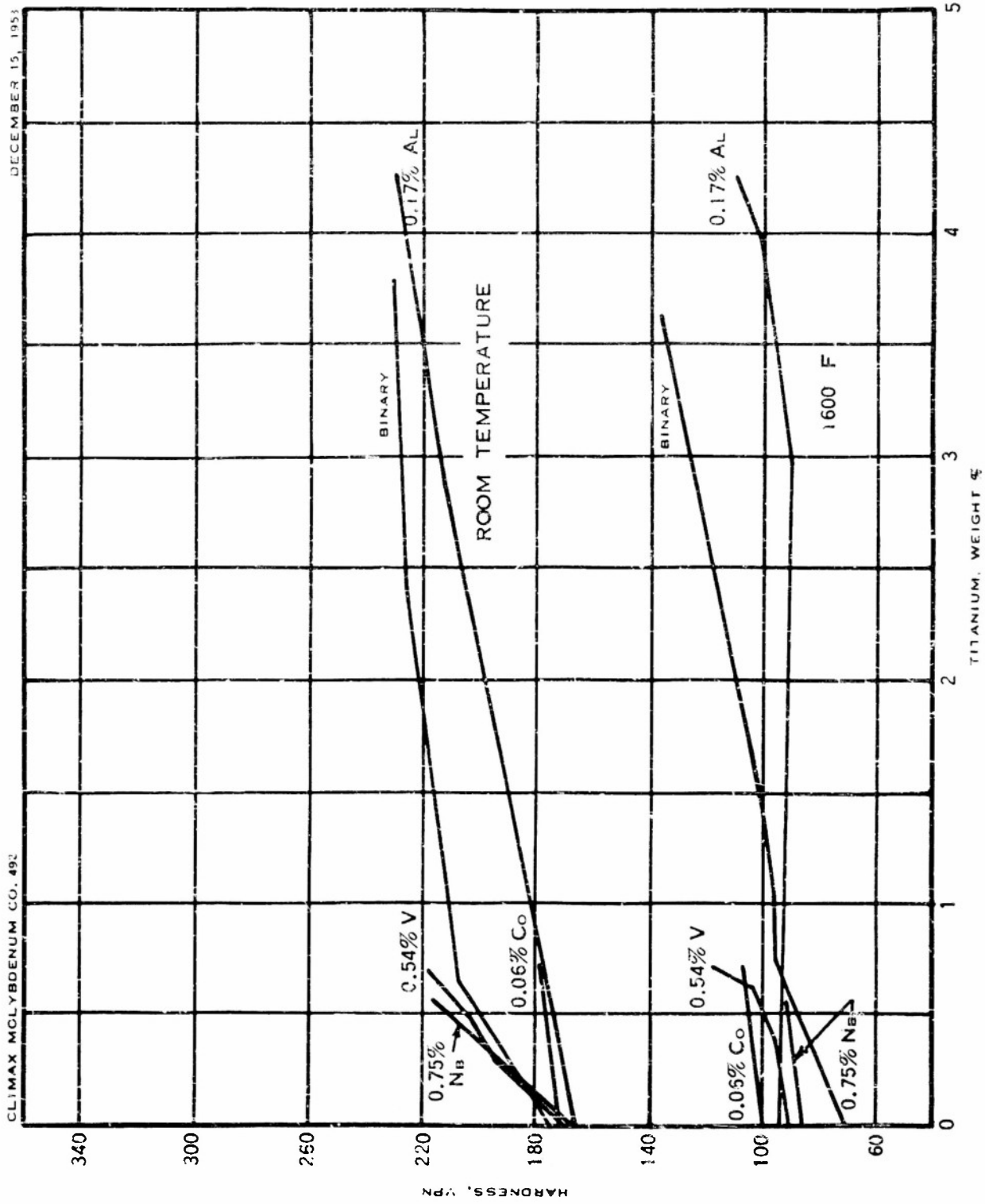


FIGURE 149 - EFFECT OF TITANIUM CONTENT UPON THE HARDNESS OF TERNARY MOLYBDENUM-BASE ALLOYS

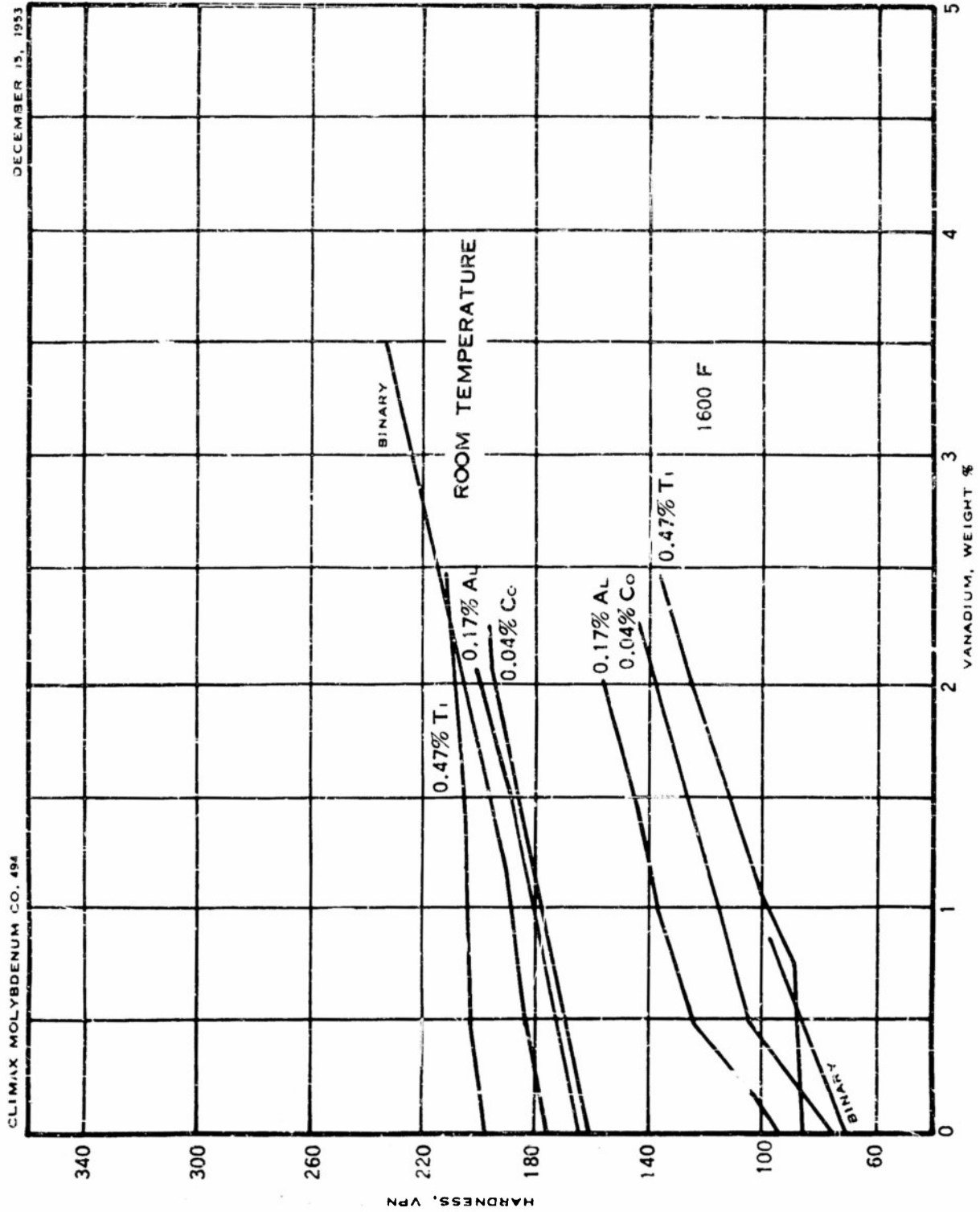


FIGURE 150 -- EFFECT OF VANADIUM CONTENT UPON THE HARDNESS
OF TERNARY MOLYBDENUM-BASE ALLOYS

APPENDIX

	<u>PAGE</u>
A. PROCEDURES FOR CHEMICAL ANALYSIS OF MOLYBDENUM-BASE ALLOYS	190
Rare Earth Metals	190
Al and Co in Mo-Al-Co Alloys	192
Al and Ni in Mo-Al-Ni Alloys	192
Al and Nb in Mo-Al-Nb Alloys	194
Al and Ti in Mo-Al-Ti Alloys	196
Al and V in Mo-Al-V Alloys	197
Al and Zr in Mo-Al-Zr Alloys	197
Co and Nb in Mo-Co-Nb Alloys	199
Co and Ti in Mo-Co-Ti Alloys	200
Co and V in Mo-Co-V Alloys	201
Co and Zr in Mo-Co-Zr Alloys	202
Nb and Ti in Mo-Nb-Ti Alloys	202
Ti and V in Mo-Ti-V Alloys	204
Ti and Zr in Mo-Ti-Zr Alloys	205
V and Zr in Mo-V-Zr Alloys	207
B. DYNAMIC HARDNESS TESTS	208
C. MECHANICAL PROPERTIES OF MOLYBDENUM AND MOLYBDENUM-BASE ALLOYS	225
Tensile Properties at Room and Elevated Temperatures of Rolled Molybdenum-Base Alloys, Table C1	225
Creep-Rupture Data on Arc-Cast Molybdenum-Base Alloys in Stress-Relieved and Recrystallized Conditions at 1600, 1800, and 2000 F, Table C2	239
Hot Hardness of Molybdenum and Molybdenum-Base Alloys as Cast	248
Molybdenum deoxidized with rare earth metals; Mo-Ni, and Mo-Si Alloys	248
Mo-Al Alloys	249
Mo-Co Alloys	250
Mo-Nb Alloys	251
Mo-Ti Alloys	252
Mo-V Alloys	253
Mo-Zr Alloys	254
Hardness vs Annealing Temperature of Molybdenum and Molybdenum- Base Alloy Bars	255
Unalloyed Molybdenum	255
Mo-Al Alloys	256
Mo-Nb Alloys	257
Mo-Ti Alloys	258-259
Mo-V Alloys	260-261
Mo-Co and Mo-Zr Alloys	262
Mo-Nb-Ti, Mo-Al-Ti, and Mo-Co-Ti Alloys	263

APPENDIX (continued)

	<u>HEAT</u>	<u>PAGE</u>
Effect of Annealing Temperature on the Grain Size of Molybdenum-Base Alloys		264-265
Hot Hardness of Wrought Molybdenum and Molybdenum-Base Alloys		266
Unalloyed Molybdenum		
0.015 C	937	266
0.040 C	1159	267
0.0026 C, 0.005 Ce, 0.007 other rare earth metals	1045	268
Molybdenum-Aluminum Alloys		
0.17 Al, 0.003 C	1063	269
0.49 Al, 0.006 C	1058	270
0.53 Al, 0.003 C	987	271
Molybdenum-Cobalt Alloys		
0.074 Co, 0.020 C	1144	272
0.11 Co, 0.18 Ti, 0.030 C	1217	273
0.19 Co, 0.037 C	1173	274
Molybdenum-Niobium Alloys		
0.24 Nb, 0.019 C	988	275
0.31 Nb, 0.032 C	1082	276
0.31 Nb, 0.032 C, 0.16 Ti	1001	277
0.52 Nb, 0.019 C	978	278
0.75 Nb, 0.033 C	1057	279
Molybdenum-Titanium Alloys		
0.45 Ti, 0.024 C	1132	280
0.69 Ti, 0.0028 C, 0.12 other rare earth metals	1048	281
0.85 Ti, 0.014 C	1133	282
1.22 Ti, 0.014 C	1138	283
1.26 Ti, 0.036 C	1009	284
3.59 Ti, 0.027 C	1174	285
Molybdenum-Vanadium Alloys		
0.54 V, 0.027 C	1051	286
0.56 V, 0.030 C	1021	287
0.85 V, 0.0012 C, 0.003 Ce, 0.003 other rare earth metals	1049	288
0.88 V, 0.057 C	672	289
1.02 V, 0.029 C	1052	290
1.25 V, 0.006 C	1151	291
1.46 V, 0.033 C	1175	292
Molybdenum-Zirconium Alloy		
0.09 Zr, 0.019 C	1207	293

APPENDIX (continued)

	HEAT	PAGE
Tensile Strength of 1" and 5/8" Diameter Bars		294
Unalloyed Molybdenum		294
Mo-Al Alloys		295
Mo-Co and Mo-Zr Alloys		296
Mo-Nb Alloys		297
Mo-Ti Alloys		298
Mo-V Alloys		299
Impact (V-Notch) Transition		300
Unalloyed Molybdenum		
0.015 C	937	300
0.040 C	1159	300
Molybdenum-Aluminum Alloys		
0.17 Al, 0.003 C	1063	301
0.49 Al, 0.006 C	1058	301
0.53 Al, 0.003 C	987	302
Molybdenum-Cobalt Alloys		
0.074 Co, 0.020 C	1144	310
0.11 Co, 0.03 C, 0.18 Ti	1217	309
Molybdenum-Niobium Alloys		
0.24 Nb, 0.019 C	988	302
0.52 Nb, 0.019 C	978	303
0.75 Nb, 0.033 C	1057	303
Molybdenum-Titanium Alloys		
0.45 Ti, 0.024 C	1132	304
0.69 Ti, 0.0028 C, 0.12 other rare earth metals	1048	304
0.85 Ti, 0.014 C	1133	305
1.22 Ti, 0.014 C	1138	305
1.26 Ti, 0.036 C	1009	306
Molybdenum-Vanadium Alloys		
0.54 V, 0.027 C	1051	306
0.56 V, 0.030 C	1012	307
0.85 V, 0.0012 C, 0.003 Ce, 0.003 other rare earth metals	1049	307
1.00 V, 0.029 C	1052	308
1.25 V, 0.006 C	1151	308
Molybdenum-Zirconium Alloy		
0.09 Zr, 0.019 C	1207	309
Oxidation of Molybdenum and Molybdenum-Base Alloys at 1750 F		311
Unalloyed Mo, Mo-Al, and Mo-Nb Alloys		311
Mo-Ti, Mo-V, Mo-Co, and Mo-Zr Alloys		312

APPENDIX A

PROCEDURES FOR CHEMICAL ANALYSIS
OF MOLYBDENUM-BASE ALLOYS

by

Robert H. Maurer

Determination of Rare Earth MetalsOutline of Method

The combined rare earths are separated from molybdenum by repeated precipitation with excess ammonium hydroxide. The combined hydroxides of the rare earths are converted to oxides by ignition at 650 C. The oxides are dissolved in concentrated hydrochloric acid and the solution evaporated just to dryness. The rare earth chlorides are redissolved in a little water and then precipitated as oxalates with oxalic acid. The oxalates are ignited to oxides and weighed as combined rare earth oxides. The oxides are redissolved by fusion with KHSO_4 and the cerium oxidized to the tetravalent state by ammonium persulphate in the presence of silver nitrate. Cerium is then determined by titration with standard ferrous ammonium sulphate solution. The cerium is calculated to the oxide and this weight deducted from the total weight of combined rare earth oxides. No chemical methods are known for the quantitative separation of the other rare earths. Spectroscopic or flame photometer methods are usually used for quantitative determinations of the rare earths.

Solutions Required

0.0125N $\text{Fe}(\text{NH}_4)_2(\text{SO}_4)_2 \cdot 6\text{H}_2\text{O}$ solution. Dissolve 4.902 g $\text{Fe}(\text{NH}_4)_2(\text{SO}_4)_2 \cdot 6\text{H}_2\text{O}$ in 200 ml H_2O containing 20 ml H_2SO_4 . Cool and dilute to 1 liter. Standardize against 0.0125N $\text{K}_2\text{Cr}_2\text{O}_7$ solution.

0.0125N $\text{K}_2\text{Cr}_2\text{O}_7$ solution. Dissolve 0.6129 g of the Bureau of Standards standard sample of $\text{K}_2\text{Cr}_2\text{O}_7$ in water and dilute to exactly 1000 ml. This is a primary standard.

Diphenylamine sulfonic acid: Dissolve 0.32 g of barium diphenylamine sulfonate in 100 ml H_2O . Add 3 ml H_2SO_4 , heat to boiling and digest for 10 minutes. Allow the BaSO_4 to settle and filter through Whatman No. 42 paper. Cool to room temperature.

Silver Nitrate: 1% solution.

Standardize the ferrous ammonium sulphate solution as follows: To 25 ml of the ferrous solution add 200 ml water, 10 ml H_2SO_4 (1-5), 5 ml H_3PO_4 and 12 drops diphenylamine sulphonic acid indicator. Titrate with the standard dichromate solution.

Procedure

Dissolve 5 g of sample in a 500 ml beaker with 75 ml HCl and 15 ml HNO₃. A blank containing 5 g of pure molybdenum is carried through the entire procedure. When solution is complete, add 100 ml H₂O and 4 or 5 drops of phenol red indicator solution (1% in 25% ethanol). Neutralize with NH₄OH, then add an excess of NH₄OH equal to about 10% of the total volume of solution, i.e., about 25 ml excess NH₄OH. Heat to boiling and boil for one minute. Allow to cool to room temperature, preferably over night. Filter through Whatman No. 42 filter paper containing a little ashless filter paper pulp. Wash with cold 5% NH₄Cl solution containing 100 ml NH₄OH per liter. Place the original beaker under the funnel and dissolve the precipitate by washing the paper at least three times with hot HCl (1-3). Wash the paper three times with hot water, then once with cold 3% NH₄OH. Reserve the filter paper. Repeat the NH₄OH precipitation exactly as before, cool and filter through the reserved filter paper. Wash with ammoniacal NH₄Cl solution as before. Dry the paper and residue in a platinum crucible, then ignite at 980 C. Cool, add 2 ml H₂SO₄, 5 ml HF and evaporate to fumes of SO₃.

Transfer the H₂SO₄ solution to a 250 ml beaker and dilute to 100 ml. Add phenol red indicator and neutralize with NH₄OH, then add an excess of 10% by volume. Boil for one minute, cool to room temperature and filter through No. 40 Whatman paper containing a little ashless filter paper pulp. Wash with 5% NH₄Cl solution containing 100 ml NH₄OH per liter. Dry and ignite the paper at 500 C. Cool, add 5 ml HCl, cover and warm the crucible until the residue is completely dissolved. Transfer the solution to a 50 ml beaker, rinsing the crucible with a little water. Evaporate just to dryness, cool, add 20 ml saturated oxalic acid solution and digest below boiling for 30 minutes. Let stand over night, filter through a 9 cm Whatman No. 42 paper and wash with 0.5% oxalic acid. Ignite in a weighed platinum crucible at 980 C, cool and weigh. Deduct the weight of the blank and the remainder is the weight of the rare earth oxides. Also included in this residue is any thorium, scandium, yttrium and lanthanum which may have been present originally.

Fuse the residue in 2-3 g KHSO₄ and dissolve the melt in 200 ml H₂O containing 10 ml H₂SO₄. Add 15 ml of the silver nitrate solution and 2 g of ammonium persulphate crystals. Boil gently for 10-15 minutes, then cool to room temperature. Add 2 drops of 0.025M ortho-phenanthroline ferrous complex and titrate with standard 0.0125 N ferrous ammonium sulphate solution. One ml 0.0125 N Fe (NH₄)₂ (SO₄)₂·6H₂O solution is equivalent to 0.0017517 g Ce or 0.0020518 g Ce₂O₃. Calculate the cerium to Ce₂O₃ and deduct this weight from the total weight of rare earth oxides. No satisfactory wet chemical methods are available for the quantitative separation of the other rare earths. The spectroscope and the flame photometer are used for the quantitative determination of the various rare earths, but neither of these instruments is available in this laboratory. As a reasonable approximation of the total rare earth metals present, other than cerium, a factor for the conversion of the oxide to the metal which is the mean of all the factors for the rare earths should be satisfactory. Using the mean value of 0.866, the result obtained for rare earths as metals would be close to the true value, regardless of the actual distribution of the rare earths in the mixture under consideration.

Spectrographic Analysis

Prior to the development of wet chemical methods of determining rare earth metals in molybdenum and molybdenum-base alloys, a number of spectrographic determinations were made. Specimens of alloys containing rare earth metals were sent to New England Spectrochemical Laboratories, Ipswich, Massachusetts, for analysis. A list of the alloys, melting atmospheres, additions, and spectrographic analyses is given in Table A1. Analyses made by the method of wet chemistry described above are also given. The correlation between the results of the two types of analysis is poor, particularly when the rare earth metal additions were high. It was judged advisable to rely upon the wet chemical analyses; therefore, only these are given for the heats of the deoxidation series containing rare earth metals, Table 12.

Determination of Aluminum and Cobalt in Molybdenum-Aluminum-Cobalt Alloys

Synthetic mixtures of these metals were prepared from solutions of pure molybdenum and from standard solutions of cobalt and aluminum. This synthetic solution was equivalent to a solution of a ternary alloy containing 99.65% molybdenum, 0.25% aluminum and 0.20% cobalt. Tests with this synthetic mixture gave the following results:

- (a) Complete recovery of aluminum was obtained by using the method given in the first annual report for the determination of aluminum in the binary alloy of molybdenum and aluminum.
- (b) Complete recovery of cobalt was also obtained by the method for its determination in the binary alloy of molybdenum and cobalt.

Determination of Aluminum and Nickel in Molybdenum-Aluminum-Nickel Alloys

A solution of a synthetic alloy of molybdenum, aluminum and nickel was prepared from solutions of pure molybdenum metal, pure aluminum metal and a standard solution of nickel prepared from reagent grade nickel nitrate. This solution was prepared to contain 5 g molybdenum, 0.0102 g nickel and 0.0125 g aluminum. Tests with this mixture gave the following results:

- (a) Complete recovery of aluminum was obtained by using the method given in the first annual report for the determination of aluminum in the binary alloy of molybdenum and aluminum.
- (b) Complete recovery of the added nickel was also obtained by the dimethylglyoxime method used for its determination in the binary molybdenum-nickel alloy, first annual report.

TABLE A1
SPECTROGRAPHIC DETERMINATION OF RARE EARTH METALS

Heat	Melting Atm.	Additions, %		Spectrographic Analyses, %				Wet Chemical Analyses, %		
		Rare Earth*	Other	Ce	La	Nd	Pr	Other	C	Other*
950	vacuum	0.1 M	0.04 C		0.045				0.033	
952	argon	0.2 M			0.045				0.003	
996	vacuum	0.2 M		0.02	0.040				0.002	
997	vacuum	0.5 M			0.055				0.002	
998	vacuum	0.5 M	0.025 C		0.042				0.014	
1002	vacuum	0.1 M	0.02 C		0.032				0.012	
1003	argon	0.1 M	0.05 Al		0.036			0.0033 Al	0.003	
1005	argon	0.5 M			0.030	0.045			0.005	
1006	argon	0.1 M	0.026 C		0.050	0.028			0.014	
1020	vacuum	0.2 LCA			0.090	0.032			0.004	
1024	vacuum	0.5 LCA			0.035	0.030			0.004	
1030	argon	0.5 LCA			0.028	0.035			0.003	
1045	vacuum	0.3 LCA			0.050	0.090			0.003	0.005 Ce, 0.007 RE
1048	vacuum	0.3 LCA	1.0 Ti		0.15	0.02	0.04	0.12 Ti	0.003	0.000 Ce, 0.12 RE
1049	vacuum	0.3 LCA	1.0 V		0.020	0.025			0.001	0.003 Ce, 0.003 RE
1061	vacuum	2.0 LCA			0.048	0.040				
					0.40	0.30				
1064	argon	5.0 LCA			0.14	0.055	0.03	0.075	0.075	1.69 Ce, 1.99 RE
					1.05	0.80	0.10	0.13		

* M - misch metal, LCA - Lan-Cer-Amp, RE - other rare earth metals

Determination of Aluminum and Niobium
in Molybdenum-Aluminum-Niobium Alloys

Outline of Method

Aluminum and niobium are determined on separate samples. Both elements are separated from molybdenum by precipitation with ammonium hydroxide. Aluminum requires careful control of the pH for its complete precipitation while a large excess of ammonium hydroxide is necessary for all of the niobium to be precipitated.

Some niobium always accompanies the aluminum hydroxide precipitate obtained by the ammonium hydroxide precipitation. The niobium is precipitated by hydrolysis in a dilute hydrochloric acid solution containing sulphurous acid. The hydrolyzed niobium is removed by filtration and aluminum determined gravimetrically on the filtrate.

The precipitation of niobium with excess ammonium hydroxide is contaminated with aluminum hydroxide. Aluminum is dissolved by boiling with 5% HCl. Boiling the dilute HCl solution with sulphurous acid completely precipitates the niobium by hydrolysis. The precipitate is filtered, ignited and silica removed with hydrofluoric acid.

Aluminum

Weigh a sample of such size as to contain not more than 0.05 g aluminum. Dissolve the chips with a mixture of concentrated HCl and HNO_3 containing 10 ml HCl and 3 ml HNO_3 for each gram of sample. Heat gently until the sample is decomposed. Add 100 ml H_2O and 5 or 6 drops of phenol red indicator (0.1 g dissolved in 100 ml of 25% ethanol). Add concentrated NH_4OH from a burette until the first permanent red color of the indicator appears, then add 0.7 ml excess. Add a little ashless filter paper pulp and heat the solution to boiling. Boil for one minute, remove from the hot plate and let stand until the solution is cool, or better, overnight. Filter through No. 42 Whatman paper or its equivalent, rinsing the beaker several times with cold 2% NH_4Cl , pouring the rinsings through the filter paper. Wash the precipitate on the filter paper four times with cold 2% NH_4Cl solution.

Place the original beaker under the funnel and, using a wash bottle, wash the paper and precipitate thoroughly with hot HCl (1-1). At least three washings are required to dissolve all of the soluble matter on the filter. Wash the paper twice with hot water and then once with cold 3% NH_4OH solution. Reserve the filter paper. Dilute the filtrate to 100 ml, add phenol red indicator and add NH_4OH until neutral, then add 0.7 ml excess. Add a little ashless filter paper pulp, heat to boiling and boil for one minute. Remove from the hot plate, let settle and then filter through the reserved filter paper. Wash with hot 2% NH_4Cl . Place the paper and precipitate in a platinum crucible and ignite until the paper is destroyed. Fuse the residue with 4 or 5 g KHSO_4^* . Dissolve the melt in 100 ml HCl (1-1) in a 250 ml beaker. Remove the crucible and rinse with water. Transfer the solution to a 600 ml beaker,

* See Note 1

dilute to 250 ml with water, and add 5 drops phenol red indicator. Neutralize with NH_4OH and add 0.7 ml excess. Add a little ashless filter paper pulp and heat to boiling for one minute. Let settle, filter through a No. 40 Whatman paper and wash with hot 2% NH_4Cl . Transfer the washed paper and residue to the original beaker and add 100 ml 5% HCl and 25 ml 6% H_2SO_3 . Macerate the paper to a pulp and boil for three minutes. Digest just below boiling for fifteen minutes. Filter through a 12.5 cm Whatman No. 42 paper and wash with hot 2% HCl . Discard the paper and any insoluble residue. To the filtrate add phenol red indicator and neutralize with NH_4OH , then add 0.7 ml excess. Add a little ashless paper pulp and boil one minute. Let settle, then filter through No. 40 Whatman paper and wash with hot 2% NH_4Cl . Dry and ignite the paper and residue in a weighed platinum crucible until all organic matter is decomposed. Add 3 or 4 drops of H_2SO_4 (1-1) and 5 ml HF . Evaporate to dryness, then ignite at 1800 F for 20 minutes. Cool and weigh.

A blank must be carried through the entire procedure, using a weight of pure molybdenum equal to the weight of sample used. The weight of the blank obtained is deducted from the weight of the oxide obtained in the sample.

Niobium

Dissolve a sample containing not more than 0.02 g Nb in a mixture of concentrated HCl and HNO_3 containing 10 ml HCl and 3 ml HNO_3 for each gram of sample. Heat gently until the sample is decomposed, add 200 ml H_2O and 4 or 5 drops of phenol red indicator. Neutralize with NH_4OH and add 10 ml in excess. Boil for 15 minutes, add a little ashless filter paper pulp and cool to room temperature. Digest at least one hour at room temperature. Filter through No. 42 Whatman paper or its equivalent, containing a little ashless pulp. Wash with hot 2% NH_4Cl containing 1 ml NH_4OH per liter of solution. Place the paper and precipitate in a platinum crucible and ignite until all the paper is destroyed*. Fuse the ignited residue with 4 or 5 g KHSO_4 and dissolve the melt in a 250 ml beaker with 100 ml HCl (1-1). Remove the crucible and rinse it with water. Transfer the solution to a 600 ml beaker, dilute to about 250 ml and add 5 drops phenol red indicator. Neutralize with NH_4OH , then add 10 ml excess. Boil for 15 minutes, add a little ashless filter paper pulp and digest at room temperature for one hour. Filter through a No. 42 Whatman paper containing a little ashless pulp. Wash with hot 2% NH_4Cl containing 1 ml NH_4OH per liter of solution.

Transfer the paper and precipitate to the original beaker and add 100 ml of 5% HCl and 25 ml of 6% H_2SO_3 . Macerate the paper to pulp and boil for 3 minutes. Digest just below the boiling point for 15 minutes. Filter through a 12.5 cm Whatman No. 42 paper containing a little ashless pulp and wash with hot 2% HCl . Ignite in a weighed platinum crucible, first at a low temperature to burn off the paper and finally for 15 minutes at 1800 F. Cool, add 2 ml H_2SO_4 (1-1) and 2 ml HF . Evaporate to dryness on the hot plate, then ignite at 1800 F for 30 minutes. Cool and weigh the Nb_2O_5 .

* See Note 2

Note 1. Some samples contain Al_2O_3 as nonmetallic inclusions. This Al_2O_3 remains insoluble during the attack with HCl-HNO_3 . If precautions were not taken to insure the solution of all the aluminum in the sample, the undissolved Al_2O_3 would remain with the Nb_2O_5 precipitate and yield apparently high values for niobium. Similarly, correspondingly low values would result in the aluminum determination. If the initial decomposition of the sample yields a perfectly clear solution, the ignition and fusion of the precipitate with KHSO_4 may be eliminated from both the determination of Al and Nb.

Note 2. It is not necessary to carry along a blank in the niobium determination. In a number of tests, the blank was found to be so small as to be of no consequence.

Determination of Aluminum and Titanium in Molybdenum-Aluminum-Titanium Alloys

The combined, impure Al_2O_3 and TiO_2 are obtained exactly as described in the method for the determination of aluminum or titanium in binary molybdenum-base alloys. A blank sample of pure molybdenum metal of the same weight as the sample to be analyzed is carried through the entire procedure.

After the weight of the combined oxides has been ascertained, fuse the residue with 1 to 2 grams of KHSO_4 . Dissolve the melt in 200 ml of 10% (by volume) sulphuric acid. Add a little ashless filter paper pulp to the solution and cool to 5 to 10 C. Precipitate the titanium by the addition of 15 ml of a cold, freshly prepared solution of 6 g Cupferron in 100 ml water. Add the reagent by allowing it to run slowly down the side of the beaker and stirring continuously during the addition. Let settle 2 or 3 minutes, then check for completeness of precipitation by adding a little more reagent. The formation of a white, crystalline precipitate indicates complete precipitation. The titanium precipitate of Cupferron is yellow.

Filter through No. 40 Whatman paper containing a little ashless filter paper pulp. Wash the paper and precipitate five times with cold 10% H_2SO_4 solution containing 25 ml of the 6% Cupferron reagent per liter of solution. Transfer the paper and precipitate to a weighed platinum crucible and dry for two hours at 110 C. Char the paper on an asbestos pad over a Fisher or Meker burner. Ignite carefully until organic matter is destroyed, then finally ignite at 1800 F for 30 minutes. Cool and weigh the ignited residues. Deduct the weight of the blank residue and the remainder is pure TiO_2 of which 59.95% is titanium.

Aluminum is determined by difference. Deduct the weight of blank originally obtained from the weight of combined, impure Al_2O_3 and TiO_2 . The weight obtained is pure $\text{Al}_2\text{O}_3 + \text{TiO}_2$. Now deduct the weight of TiO_2 obtained by the Cupferron method and the remainder is pure Al_2O_3 of which 52.91% is aluminum.

Determination of Aluminum and Vanadium
in Molybdenum-Aluminum-Vanadium Alloys

A synthetic mixture of molybdenum, aluminum and vanadium was prepared from a solution of pure molybdenum metal and from standard solutions of aluminum and vanadium. This synthetic solution was equivalent to a solution of a ternary alloy containing 99% molybdenum, 0.75% vanadium and 0.25% aluminum. Tests with this synthetic mixture gave the following results:

- (a) The method given in the first annual report for the determination of vanadium in a binary molybdenum-vanadium alloy was equally satisfactory for the ternary alloy containing aluminum.
- (b) Complete recovery of aluminum was obtained by using the method given in the first annual report for the determination of aluminum in the binary alloy of molybdenum and aluminum. When vanadium was present, a very dark colored solution was obtained as the neutral point approaches with the addition of ammonium hydroxide. The appearance of a purplish color was assumed to be the neutral point to the phenol red indicator. This was the point taken for the addition of the excess ammonium hydroxide. Boiling, followed by digestion below boiling caused the dark color to disappear and the normal red color of the indicator appeared. No dark color was observed in the subsequent precipitations with ammonium hydroxide.

Determination of Aluminum and Zirconium
in Molybdenum-Aluminum-Zirconium Alloys

Outline of Method

The combined hydroxides of aluminum and zirconium are separated from the bulk of the molybdenum by repeated precipitation with NH_4OH . The hydroxides are ignited to the oxides in a platinum crucible. These oxides are redissolved by fusion with KHSO_4 and the melt dissolved in dilute H_2SO_4 . Zirconium is then separated from aluminum by precipitation as phosphate. Zirconium is separated from phosphate by fusion with Na_2CO_3 and is then precipitated by NH_4OH and finally weighed as the oxide. Aluminum is determined in the filtrate from the zirconium phosphate precipitate. The solution is partially neutralized, an acetic acid solution of 8-hydroxyquinoline added, and aluminum oxyquinolate precipitated by making the solution ammoniacal. After filtration, the organic matter is destroyed by evaporation with H_2SO_4 and HNO_3 . Aluminum is then precipitated with NH_4OH and finally ignited and weighed as Al_2O_3 .

Procedure

Dissolve a suitable weight of sample with HCl and HNO_3 , using 10 ml HCl and 3 ml HNO_3 for each gram of sample. A blank containing an equal weight of pure molybdenum is carried through the entire procedure. When solution is complete, heat gently until most of the oxides of nitrogen are driven off. Add 100 ml H_2O , a little ashless filter paper pulp and five or six drops of phenol red indicator. Add NH_4OH until the first permanent red color of the indicator appears, then add a 0.7 ml excess. Heat to boiling and boil for one minute, remove from the hot plate and let stand until the solution is at room temperature. Filter through No. 42 Whatman paper and wash the precipitate with cold 2 or 3% NH_4NO_3 . Discard the filtrate and washings.

Place the original beaker under the funnel and dissolve the precipitate by washing with hot 1-1 HCl. Wash the paper twice with hot water and finally, once with cold 3% NH_4OH . Reserve the filter paper. Dilute the filtrate and washings to 100 ml and repeat the precipitation with NH_4OH . Boil one minute, let settle a few minutes, then filter through the reserved paper. Wash the precipitate with hot, dilute NH_4NO_3 . Discard the filtrate and washings. Place the original beaker under the funnel, redissolve the precipitate with HCl and make a third separation with NH_4OH . Dry and ignite the final precipitate at 1800 F in a platinum crucible.

Fuse the residue with 4 or 5 g KHSO_4 and dissolve the cooled melt in 100 ml of 10% H_2SO_4 . Cool to room temperature, add a little ashless filter paper pulp and 20 ml of a freshly prepared 25% solution of $(\text{NH}_4)_2\text{HPO}_4$. Digest for two hours at 40-50 C, then filter through No. 40 Whatman paper and wash four or five times with hot 2 or 3% NH_4NO_3 . Reserve the filtrate and washings for the determination of aluminum.

Ignite the zirconium phosphate precipitate very carefully until the paper is destroyed. Finally ignite at 1800 F. Now separate the zirconium from the phosphate by fusion with Na_2CO_3 , and complete the zirconium determination as described in "The Determination of Zirconium in Molybdenum-Base Alloys".

Evaporate the reserved filtrate to approximately 150 ml. Add two drops of methyl orange indicator solution and add concentrated NH_4OH until the solution is just slightly acid to the indicator. If too much NH_4OH is inadvertently added at this point (indicated by formation of a precipitate in the solution), add two or three drops of concentrated H_2SO_4 . Add 10 ml* 8-hydroxyquinoline solution (5 g dissolved in 100 ml 2N acetic acid), then add NH_4OH until alkaline, and finally an excess of 5 ml NH_4OH . Warm to 50-60 C and digest at this temperature until the precipitate becomes dense and crystalline. Cool and filter through No. 40 Whatman paper containing a little ashless paper pulp. Wash with a cold 3% NH_4OH containing 25 ml of the reagent previously neutralized with NH_4OH in one liter. Discard the filtrate.

* This amount of reagent is adequate to precipitate 50 mg of aluminum. An excess of reagent does no harm. In any event, sufficient reagent should be added to color the solution yellow.

Return the paper containing the precipitate to the original beaker, add 10 ml concentrated H_2SO_4 and macerate the paper. Add 15 ml HNO_3 , cover the beaker and heat until SO_3 fumes are evolved. Remove the beaker from the hot plate and cautiously add an additional 15 ml HNO_3 . Again evaporate to SO_3 fumes. All organic matter should now be destroyed. Cool, add 75 ml H_2O and five drops of phenol red indicator. Add concentrated NH_4OH until the first permanent red color appears, then add an excess of 0.7 ml. Add a little ashless paper pulp, boil for one minute and let settle. Filter through a No. 40 Whatman paper and wash with hot 3% NH_4NO_3 solution. Dry and ignite at a low temperature until the paper is destroyed, then heat for 30 minutes at 1800 F. Remove silica by treatment with HF and a few drops of 1-1 H_2SO_4 . Again ignite and weigh as Al_2O_3 .

Determination of Cobalt and Niobium in Molybdenum-Cobalt-Niobium Alloys

Outline of Method

Cobalt and niobium are determined on separate samples. Cobalt, together with at least part of the niobium is separated from molybdenum as the sulfide in an ammoniacal solution. After filtration, the cobalt and niobium sulfides are decomposed with acid and the niobium precipitated by hydrolysis with sulfuric acid. The niobium is removed by filtration and cobalt determined in the filtrate by electroplating.

Cobalt

Transfer a 2 gram sample to a 400 ml beaker and add 25 ml HCl and 10 ml HNO_3 . Heat gently until decomposition is complete. Dilute the solution to 100 ml, neutralize with NH_4OH and add 15 ml excess. Now add 25 ml of dark ammonium sulfide solution and digest below boiling for one hour. Filter through a No. 40 Whatman paper containing a little ashless paper pulp. Wash with a 2% solution of NH_4Cl containing 10 ml of the ammonium sulfide solution per liter. Discard the filtrate and washings. Transfer the paper and the insoluble residue to the original beaker, add 20 ml HCl (1-1) and 5 ml HNO_3 (Sp.Gr.-1.20). Digest below boiling until the sulfides are decomposed. Dilute to 200 ml with water, add 25 ml H_2SO_3 (6%) and boil 3 minutes. Digest below boiling for 15 minutes. Filter through No. 42 Whatman paper and wash with 2% HCl . Discard the paper and any insoluble matter. Add 10 ml H_2SO_4 (1-1) to the filtrate and evaporate to strong fumes of SO_3 . Cool slightly, add 5 ml HNO_3 and again evaporate to strong fumes. Cool, transfer the solution to a 250 ml beaker, rinsing the larger beaker thoroughly with water. Adjust the volume to about 75 ml, neutralize with NH_4OH , then add an excess of 35 ml. Add 2 g NaHSO_3 and cool the solution in running water.

Electrolyze for 1-1/2 hours using a current of 1 ampere. The electrodes should be made from platinum gauze and the solution stirred continuously during the electrolysis. Without interrupting the current, lower the beaker slowly while rinsing the cathode with distilled water. Remove the beaker, shut off the current and disconnect the electrode. Dissolve the deposit from the electrode with approximately 25 ml HNO₃. Add 10 ml H₂SO₄ (1-1) to the solution and evaporate to strong fumes of SO₃. Cool, add 50 ml H₂O, neutralize with NH₄OH and add an excess of 35 ml. Add 2 g NaHSO₃ and cool to room temperature. Electrolyze for 1 hour using a current of 1 ampere. Without interrupting the current, lower the beaker slowly while rinsing the cathode with distilled water. Remove the beaker, shut off the current and rinse the cathode with absolute ethyl alcohol. Dry at 105 C for 5 minutes, cool and weigh. The increase in weight of the cathode is cobalt.

$$\frac{\text{Weight of cobalt}}{\text{Weight of sample}} \times 100 = \% \text{ Cobalt}$$

Niobium

Tests with synthetic solutions show that niobium is quantitatively recovered without interference from cobalt by the standard tannic acid method, which is used for binary molybdenum-niobium alloys. The analyst is referred to the first annual report for details of the niobium determination.

Determination of Cobalt and Titanium in Molybdenum-Cobalt-Titanium Alloys

Outline of Method

Both titanium and cobalt are separated from molybdenum by repeated precipitation with sodium hydroxide. The combined cobalt and titanium are obtained in a sulfuric acid solution, and the titanium is precipitated by Cupferron. The Cupferron precipitate is ignited and weighed as titanium dioxide. Organic matter is destroyed in the filtrate from the Cupferron precipitate and the cobalt in this solution is determined electrolytically.

This method, applied to synthetic samples, yielded results slightly high for the titanium and correspondingly low for cobalt, indicating that a little cobalt is included with the Cupferron precipitate. The error is approximately 5% of the total cobalt and titanium present. Since other factors in the program are even less accurate, this discrepancy was considered acceptable.

Procedure

Transfer a suitable weight of sample to a 400 ml beaker and add 10 ml HCl and 4 ml HNO_3 for each gram of sample. Heat gently until solution is complete, then add 100 ml H_2O . Neutralize with a 25% solution of NaOH, using litmus indicator, then add an excess of 5 ml. Digest at 80-90 C for 20 minutes, then filter through a fritted glass filtering crucible of fine porosity (5 micron). Wash the precipitate thoroughly with hot water. Discard the filtrate and washings. Dissolve the precipitate by adding 25 ml of a hot mixture of 20 ml HCl (1-1) and 5 ml HNO_3 . After one minute apply suction until dry. Repeat the treatment with another 25 ml of the acid mixture and finally wash thoroughly with hot water. Transfer the solution to the original beaker and make two additional precipitations with 25% NaOH, filtering and washing after each precipitation exactly as just described.

Dissolve the precipitate finally obtained in the HCl- HNO_3 mixture as before. Transfer the solution to the original beaker and add 20 ml H_2SO_4 (1-1). Evaporate on the hot plate until dense fumes are evolved. Cool, add 200 ml H_2O and cool to 10 C. Add 15 ml of a freshly prepared, cold 6% aqueous solution of Cupferron, slowly with stirring. Add a little ashless filter paper pulp, let settle, then check for completeness of precipitation by adding a little more reagent. A white precipitate indicates complete precipitation. Filter through No. 40 Whatman paper and wash five times with cold 10% H_2SO_4 containing 25 ml Cupferron solution per liter. Reserve the filtrate and washings for the cobalt determination. Drain the precipitate as completely as possible and transfer the paper and precipitate to a platinum crucible. Cautiously dry and then heat gently until the paper begins to char. The precipitate tends to liquefy and heating must therefore be done carefully. Gradually increase the heat until carbon is destroyed and finally ignite at 1000 C for 20 minutes. Cool and weigh as TiO_2 .

Evaporate the reserved filtrate to a volume of about 100 ml. Add 25 ml HNO_3 and continue the evaporation to SO_3 fumes. Cover with a Speedy vap cover glass and, without cooling, cautiously add 10 ml HNO_3 from a pipette. Again evaporate to SO_3 fumes. If the presence of organic matter is still indicated, repeat the HNO_3 additions until all organic matter is destroyed. Cool, transfer the solution to a 400 ml beaker and dilute to 100 ml. Neutralize with concentrated NH_4OH , then add 35 ml excess. Cool to room temperature, add 2 g NaHSO_3 , then electrolyze for one hour at one ampere, using a weighed platinum gauze cathode. Cobalt is deposited as the metal on the cathode.

Determination of Cobalt and Vanadium in Molybdenum-Cobalt-Vanadium Alloys

Synthetic mixtures were prepared containing 4 grams molybdenum, 0.0222 grams vanadium and 0.0060 grams cobalt. Tests with these solutions indicated that:

(a) The method for the determination of vanadium in binary molybdenum-vanadium alloys, first annual report, is also applicable to this ternary system.

(b) Complete recovery of cobalt is obtained from this ternary alloy by the procedure used for the determination of cobalt in binary molybdenum-cobalt alloys, also given in the first annual report. During the first precipitation of cobalt with sodium hydroxide solution, a dark blue color caused by vanadium compounds interferes somewhat with the observation of the neutralization point. However, this point is not critical and if a strip of wet litmus paper is placed on the side of the beaker, partially submerged in the solution, the change in color of the paper can readily be observed. The blue color of the solution disappears during the hot digestion of the solution. No blue color develops during the subsequent precipitations.

Determination of Cobalt and Zirconium in Molybdenum-Cobalt-Zirconium Alloys

Synthetic mixtures were prepared containing 5 grams molybdenum, 0.0125 grams zirconium and 0.0059 grams cobalt. Tests with solutions of this mixture indicated that complete recovery of both cobalt and zirconium was obtained by the procedures for the determination of these metals in binary molybdenum-base alloys given in the first annual report.

Determination of Niobium and Titanium in Molybdenum-Niobium-Titanium Alloys*

Outline of Method

Titanium and niobium are separated from molybdenum by repeated precipitation with excess NH_4OH and weighed, after ignition, as the combined oxides, $\text{Nb}_2\text{O}_5 + \text{TiO}_2$. The oxides are redissolved by fusion in KHSO_4 and the titanium is determined spectrophotometrically. The transmittance of the yellow colored solution given by titanium in a sulfuric acid solution containing hydrogen peroxide is measured at 420 millimicrons. The niobium content is obtained by difference.

Procedure

Dissolve a 5 gram sample in a 500 ml beaker with 75 ml HCl and 15 ml HNO_3 . When action is complete, cool somewhat and add 100 ml H_2O . Add 5 drops of phenol red indicator (0.1 g in 100 ml 25% ethanol), neutralize with NH_4OH and add 10 ml excess. Add a little ashless paper pulp, heat to boiling and boil

* This method is not applicable if the titanium content is over 0.5%.

for one minute. Remove from the hot plate and allow to cool to room temperature. Filter through an 11 cm Whatman No. 40 filter paper and wash three or four times with hot 2% NH_4Cl solution. Discard the filtrate and washings. Place the original beaker under the funnel and dissolve the precipitate from the paper by repeated washing with hot 1-1 HCl . At least three washings are necessary. Now wash the paper three times with hot water and once with cold 3% NH_4OH . Reserve the filter paper and any insoluble residue it may contain.

Again add phenol red indicator and precipitate Nb and Ti with NH_4OH exactly as before. Add paper pulp, boil one minute, cool to room temperature and filter through the reserved No. 40 Whatman paper. Wash with hot 2% NH_4Cl and discard the filtrate and washings. Dry and ignite the paper and residue at 1800 F in a platinum crucible until all organic matter is destroyed. Cool, add 2 ml H_2SO_4 and 5 ml HF . Evaporate to strong fumes of SO_3 . Cool and transfer the H_2SO_4 solution to a 250 ml beaker. Dilute to 100 ml, add phenol red indicator and again precipitate Nb and Ti with NH_4OH , using 10 ml excess. Add a little ashless filter paper pulp, boil for one minute, then cool to room temperature. Filter through No. 40 Whatman paper and wash the precipitate with hot 2% NH_4Cl . Dry and ignite the paper and residue in a weighed platinum crucible at a low temperature until carbon is destroyed, then ignite for 20 minutes at 1800 F. Cool and weigh. A blank containing five grams of pure molybdenum is carried through the entire procedure thus far. Deduct the weight of the blank from the weight of residue obtained in the sample. The remainder then is the weight of combined oxides, $\text{Nb}_2\text{O}_5 + \text{TiO}_2$.

Fuse the residue containing the combined oxides with three or four grams of KHSO_4 . Dissolve the cooled melt in 100 ml of 10% H_2SO_4 . Transfer this solution to a 250 ml volumetric flask and dilute the solution to exactly 250 ml with 10% H_2SO_4 . Transfer an aliquot portion of this solution containing a maximum of approximately 1.0 mg of titanium to a 100 ml volumetric flask and dilute to the mark with 10% H_2SO_4 . Transfer a portion of this solution to the spectrophotometer cuvette and adjust the instrument to 100% transmission with the solution in the beam of light at a wave length of 420 millimicrons. Now take 10-15 ml of the solution in a 50 ml beaker and develop the yellow titanium color by the addition of three drops of 3% H_2O_2 . Measure the transmission of this solution in the spectrophotometer at 420 millimicrons* and obtain the weight of titanium present in the aliquot from the calibration curve.

Preparation of Calibration Curve

A standard solution of titanium containing 0.012 mg Ti/ml was prepared from reagent grade TiO_2 . Dilute 10, 20, 30, 40, 50, 75 and 100 ml of this solution with 10% H_2SO_4 to 100 ml in volumetric flasks. Now measure the transmission of portions of these solutions exactly as described in the procedure. The aliquots taken above contain, respectively, 0.12, 0.24, 0.36, 0.48, 0.60, 0.90 and 1.2 mg Ti. Plot the percent transmission against the weight of titanium on coordinate paper. The relationship is linear.

* According to Milner, Proctor and Weinberg (Ind. and Eng. Chem., Anal. Ed., vol 17, no. 3, p 142), maximum absorption for the titanium complex occurs at this wave length and therefore the greatest sensitivity.

Niobium is determined by difference. Find the total weight of titanium present in the five gram sample and multiply this weight by 1.6681 to convert it to TiO_2 . Now deduct the weight of TiO_2 from the weight of combined oxides, $\text{Nb}_2\text{O}_5 + \text{TiO}_2$, previously obtained. The difference is Nb_2O_5 of which 69.90% is niobium.

Determination of Titanium and Vanadium in Molybdenum-Titanium-Vanadium Alloys

Outline of Method

Vanadium and titanium are determined on separate samples. Vanadium is determined by the procedure developed for the determination of vanadium in the binary molybdenum-vanadium alloy, see first annual report. The presence of titanium causes no interference.

Titanium, together with some vanadium, is separated from molybdenum by repeated precipitation with ammonium hydroxide, and the combined oxides weighed. The vanadium in the combined oxides is then determined volumetrically and calculated to V_2O_5 which is deducted.

Procedure

Weigh a sample of such size that the titanium hydroxide precipitate can be conveniently handled. In general, 0.05 g titanium is the maximum weight for convenient manipulation. Carry along a blank of pure molybdenum metal of the same weight as the sample being analyzed. Dissolve the alloy in a mixture of HCl and HNO_3 containing 10 ml HCl and 3 ml HNO_3 for each gram of sample. Heat gently until the sample is decomposed. Add 100 ml H_2O and 5 drops of phenol red indicator (0.1 g dissolved in 100 ml of 25% alcohol). Now add concentrated NH_4OH from a burette until the first permanent red color of the indicator appears, then add 0.7 ml excess NH_4OH . Add a little ashless filter paper pulp and heat to boiling. Boil for one minute, then remove the solution from the hot plate and cool to room temperature. Filter through a No. 42 Whatman paper or its equivalent. Rinse the beaker several times with cold 2% NH_4Cl and pour the rinsings through the filter. Wash the paper and precipitate four times with cold 2% NH_4Cl . Discard the filtrate and washings.

Place the original beaker under the funnel and dissolve the precipitate by washing at least three times with hot 1-1 HCl . Wash the paper twice with hot water, then once with cold 3% NH_4OH . Reserve the filter paper. Dilute the filtrate and washings to 100 ml, add phenol red indicator, then add NH_4OH until the solution is neutral to the indicator. Add 0.7 ml excess NH_4OH , a little ashless filter paper pulp and heat to boiling. Boil for one minute, remove from the hot plate and allow the precipitate to settle. Filter through the reserved filter paper and wash four times with hot 2% NH_4Cl .

Transfer the paper and precipitate to a platinum crucible. Dry, then ignite at a low temperature until the paper is destroyed. Then ignite for ten minutes at 1800 F. Cool, add 2 ml H_2SO_4 and 5 ml HF. Evaporate on an asbestos pad on the hot plate until fumes of SO_3 are freely evolved. Cool, transfer the H_2SO_4 solution to a 250 ml beaker, rinsing the crucible thoroughly with water. Dilute the solution in the beaker to 100 ml with 10% H_2SO_4 , add 5-6 drops phenol red indicator and neutralize with concentrated NH_4OH . Add an excess of 0.7 ml NH_4OH , a little ashless filter paper pulp and heat to boiling. Boil for one minute, allow the precipitate to settle, then filter through No. 40 Whatman filter paper. Carefully police the beaker, then wash the precipitate on the paper four times with hot 2% NH_4Cl . Transfer the paper and precipitate to a weighed platinum crucible, dry, then ignite at a low temperature until the carbon is destroyed. Finally, ignite for 30 minutes at 1800 F. Cool and weigh. The residue obtained at this point contains all of the titanium as TiO_2 plus part of the vanadium which is present as V_2O_5 . Deduct the weight of the blank and the resulting weight is the combined weight of TiO_2 plus V_2O_5 .

Fuse the combined oxides with 5 g $\text{K}_2\text{S}_2\text{O}_7$ and dissolve the melt in 100 ml of solution containing 25 ml H_2SO_4 (1-1). Rinse and remove the crucible and transfer the solution to a 500 ml Soxhlet flask. Dilute to about 200 ml and cool the solution to room temperature. Add 10 ml of approximately 0.03N ferrous sulfate solution to reduce the vanadium. Now add 15 ml of a freshly prepared solution of 10% $(\text{NH}_4)_2\text{S}_2\text{O}_8$ solution and shake for at least one minute. Titrate the vanadium with standard 0.01 normal KMnO_4 . Calculate the vanadium to V_2O_5 and deduct this weight from the weight of combined V_2O_5 and TiO_2 . The remainder is TiO_2 .

Factors: 1 ml 0.01 normal KMnO_4 = 0.0009095 g V_2O_5
 TiO_2 Ti = 0.5995

Determination of Titanium and Zirconium in Molybdenum-Titanium-Zirconium Alloys

Outline of Method

Titanium and zirconium are determined on separate samples. In the titanium determination the titanium, together with the zirconium is separated from molybdenum by repeated precipitation with ammonium hydroxide. Titanium is then determined colorimetrically.

Zirconium is separated from molybdenum and most of the titanium by precipitation as phosphate from sulfuric acid solution. The phosphate is converted to carbonate by sodium carbonate fusion and the zirconium finally precipitated with ammonium hydroxide. A small amount of titanium which always accompanies the zirconium is determined colorimetrically and the weight of impure zirconium dioxide is corrected for the titanium.

Titanium

Dissolve a sample containing not more than 0.02 g titanium in a mixture of HCl and HNO_3 , using 10 ml HCl and 4 ml HNO_3 for each gram of sample. When action is complete, cool somewhat and add 100 ml H_2O . Add 5 drops of phenol red indicator (0.1 g in 100 ml 25% ethanol), neutralize with NH_4OH and add 0.7 ml excess. Add a little ashless filter paper pulp, heat to boiling and boil for one minute. Remove from the hot plate and allow to cool to room temperature. Filter through an 11 cm Whatman No. 42 filter paper and wash three times with cold 3% NH_4NO_3 solution. Discard the filtrate and washings. Place the original beaker under the funnel and dissolve the precipitate from the paper by repeated washing with hot 1-1 HCl. At least three washings are necessary. Now wash the paper three times with hot water, then once with cold 3% NH_4OH . Reserve the filter paper and any insoluble residue it may contain.

Again add phenol red indicator and precipitate the titanium together with the zirconium by addition of an excess of NH_4OH . Add a little ashless filter paper pulp, heat to boiling, let settle and filter while hot through the reserved filter paper. Wash as before, then redissolve with HCl, catching the filtrate in the original beaker. Wash with hot water, place the paper and any insoluble residue in a platinum crucible and reserve. Add phenol red indicator to the filtrate and make a third precipitation with NH_4OH exactly as before. Filter through No. 40 Whatman paper and wash with hot 3% NH_4NO_3 solution. Place the paper and precipitate in the platinum crucible containing the reserved filter paper, dry, then ignite at 1800 F until all carbon is destroyed.

Fuse the residue containing the combined oxides with three or four grams of KHSO_4 . Dissolve the cooled melt in 100 ml of 10% H_2SO_4 . Transfer this solution to a 250 ml volumetric flask and dilute the solution to exactly 250 ml with 10% H_2SO_4 . Transfer an aliquot portion of this solution containing a maximum of approximately 1.2 mg of titanium to a 100 ml volumetric flask and dilute to the mark with 10% H_2SO_4 . Transfer a portion of this solution to the spectrophotometer cuvette and adjust the instrument to 100% transmission with the solution in the beam of light at a wave length of 420 millimicrons. Now take 10-15 ml of the solution in a 50 ml beaker and develop the yellow titanium color by the addition of three drops of 3% H_2O_2 . Measure the transmission of this solution in the spectrophotometer at 420 millimicrons* and obtain the weight of titanium present in the aliquot from the calibration curve.

A standard solution of titanium containing 0.012 mg Ti/ml was prepared from reagent grade TiO_2 . Dilute 10, 20, 30, 40, 50, 75 and 100 ml of this solution with 10% H_2SO_4 to 100 ml in volumetric flasks. Now measure the transmission of portions of these solutions exactly as described in the procedure. The aliquots taken above contain, respectively, 0.12, 0.24, 0.36, 0.48, 0.60, 0.90 and 1.2 mg Ti. Plot the percent transmission against the weight of titanium on coordinate paper. The relationship is linear.

* According to Milner, Proctor and Weinberg (Ind. and Eng. Chem., Anal. Ed., vol 17, no. 3, p 142), maximum absorption for the titanium complex occurs at this wave length and therefore the greatest sensitivity.

Zirconium

Zirconium is separated from molybdenum by the same procedure which is used for the determination of zirconium in the binary zirconium-molybdenum alloy. However, some titanium always accompanies the zirconium in this procedure and the final weighed precipitate must be corrected for any TiO_2 present.

Fuse the ignited residue containing all of the zirconium together with a little titanium with 4 to 5 grams of $\text{K}_2\text{S}_2\text{O}_7$. Dissolve the melt in 100 ml of 10% H_2SO_4 . Transfer the solution to a 200 ml. volumetric flask and dilute to the mark with 10% H_2SO_4 . Mix thoroughly, take an aliquot portion containing a maximum of one milligram of titanium and transfer it to a 100 ml. volumetric flask. Dilute this solution to 100 ml. with 10% H_2SO_4 . Determine the titanium colorimetrically as described above under the method for titanium.

Calculate the total weight of titanium found in the zirconium precipitate to TiO_2 . The factor for converting Ti to TiO_2 is 1.6681. Deduct the blank plus the weight of TiO_2 found from the weight of impure ZrO_2 and the remainder is pure ZrO_2 .

Factor: ZrO_2 $\text{Zr} = 0.7403$

Determination of Vanadium and Zirconium in Molybdenum-Vanadium-Zirconium Alloys

Synthetic mixtures were prepared containing 3 grams molybdenum, 0.0133 grams vanadium and 0.0125 grams zirconium. Tests with these solutions indicated that

- (a) The method for the determination of vanadium in binary molybdenum-vanadium alloys given in the first annual report is also applicable to this ternary alloy.
- (b) Complete recovery of zirconium is obtained from this ternary alloy by the same method used for the determination of zirconium in the binary molybdenum-zirconium alloys, first annual report. The presence of vanadium causes no interference.

APPENDIX B

DYNAMIC HARDNESS TESTS

To evaluate the behavior of molybdenum and molybdenum-base alloys at elevated temperatures, a hardness test was devised for operation at temperatures up to 3000 F, as hardness was the mechanical property most easily determined and at the same time useful in the evaluation. The basis of the test was the making of an impression upon the surface of the specimen by dropping an indenter upon it at the desired testing temperature and measuring the depth of the impression. This test has been named the dynamic hot hardness test and was described in the first annual report. To review the operation of the test briefly, an indenter (7 in Figure B1) falls a distance of approximately 10 inches on to the specimen (8) thereby making a hardness impression. Two flanges on the rod to which the indenter is attached guide the assembly through the vertical tube above the furnace to the correct position on the specimen. The indenter assembly is maintained in the cocked position when not in use. In this position, the indenter rests well out of the heated zone of the furnace, actually about two inches above the top of the furnace shell.

Hardness was determined in an atmosphere of purified argon for the alloys prepared in the study of mechanical properties. The data obtained are shown in Figures B2-B8. Some useful and some anomalous data were obtained from this test. For example, unalloyed molybdenum and all of the alloys except the aluminum alloys exhibited a rise in dynamic hardness number in the temperature range 2200-2800 F. The hardness of the aluminum alloys increased slightly with increasing temperature in the range 1600-2000 F. These increases in hardness with rising temperature are not readily explained. The curves for the families of alloys indicate that there is no consistent correlation of dynamic hardness number with alloy content.

The hardness of unalloyed molybdenum at 3000 F was lower than that of all of the alloys studied except those containing up to 0.5% aluminum. On the whole, the vanadium alloys were not so hard as the other alloys.

Because of these discrepancies and inconsistencies, it was desired to ascertain the validity of the results obtained with the dynamic hardness testing apparatus.

Nonuniform behavior of the test equipment as the testing temperature was varied was thought to be a factor responsible for the anomalous hardness. It is obvious that if there were any increase in the friction between the flanges and the vertical tube, the vertical acceleration of the indenter would be decreased, the size of the impression would be small, and the indicated hardness would be high. It was postulated that at the temperatures at which the questionable increase in dynamic hardness number occurred, the lower guide became hot and expanded against the vertical tube, increasing the friction component of the system. To investigate this possibility, a movable shield was so placed within the furnace shell that the withdrawn indenter assembly was not subjected to direct radiation from the element or the specimen. A run was made with the indenter shielded after each impression. The results, Figure B9, indicate no significant difference between tests made with and without the shield.

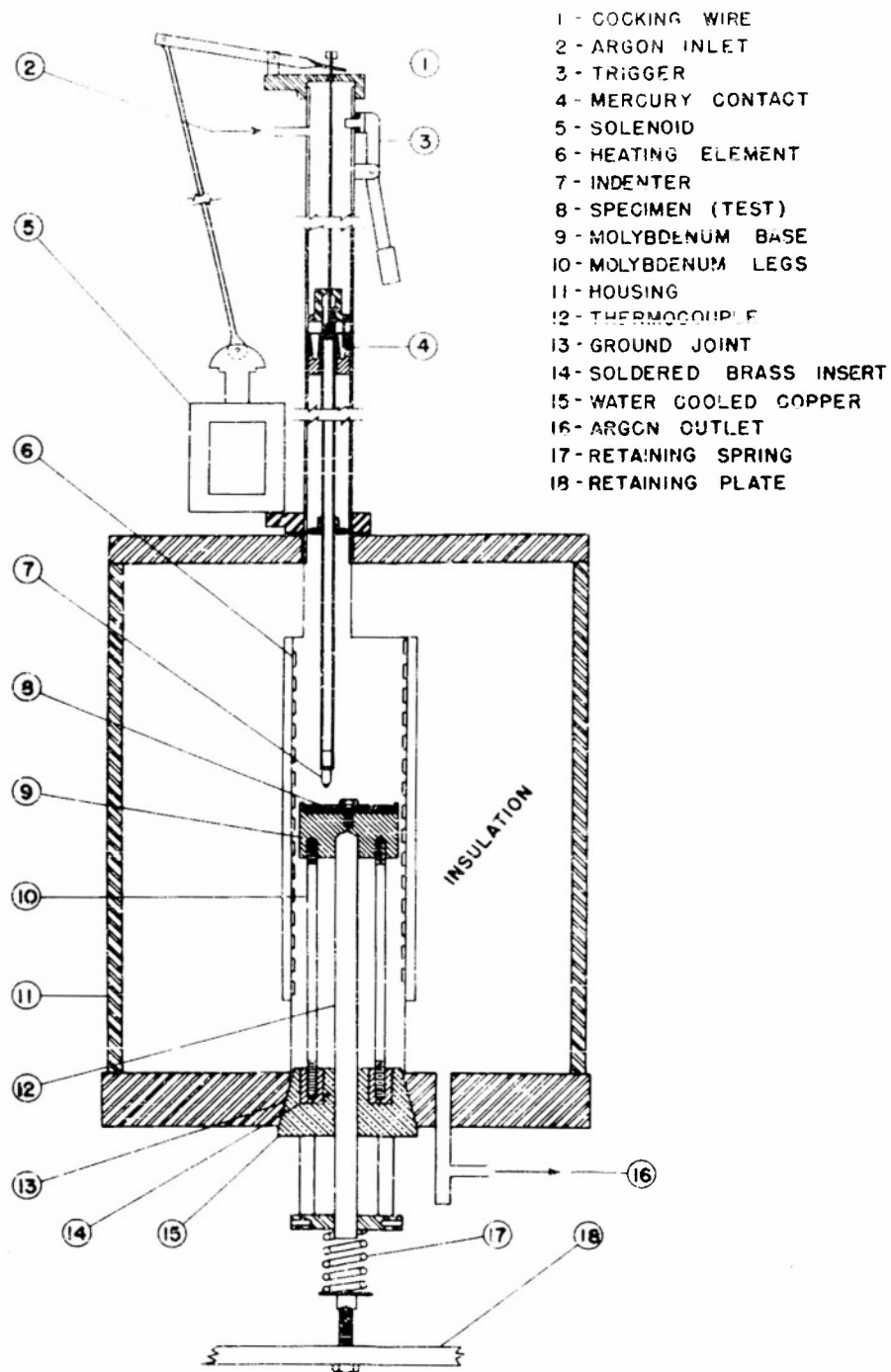


FIGURE B1 — DYNAMIC HOT HARDNESS TESTER

(P 739)

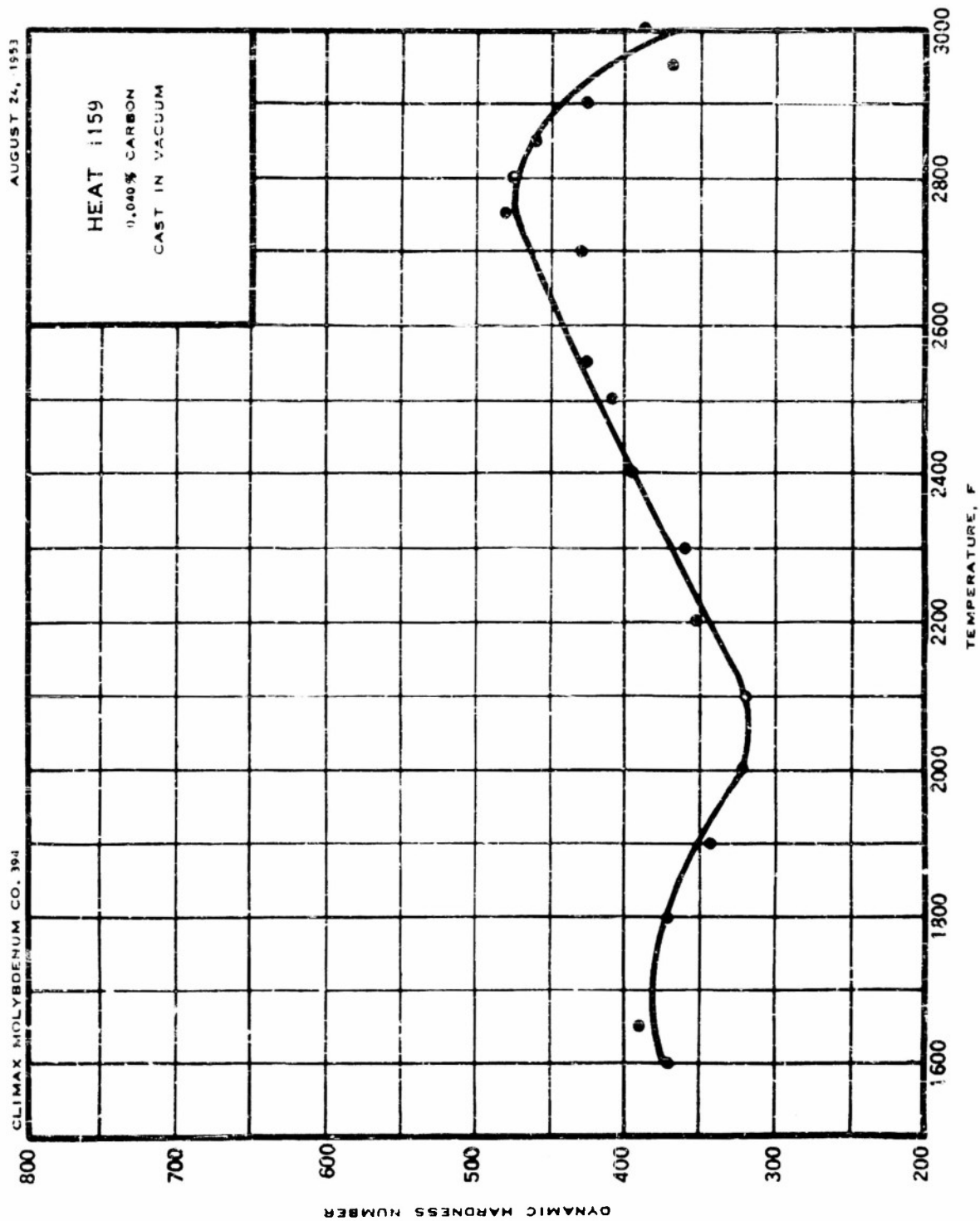


FIGURE B2 - DYNAMIC HOT HARDNESS OF UNALLOYED MOLYBDENUM AS CAST

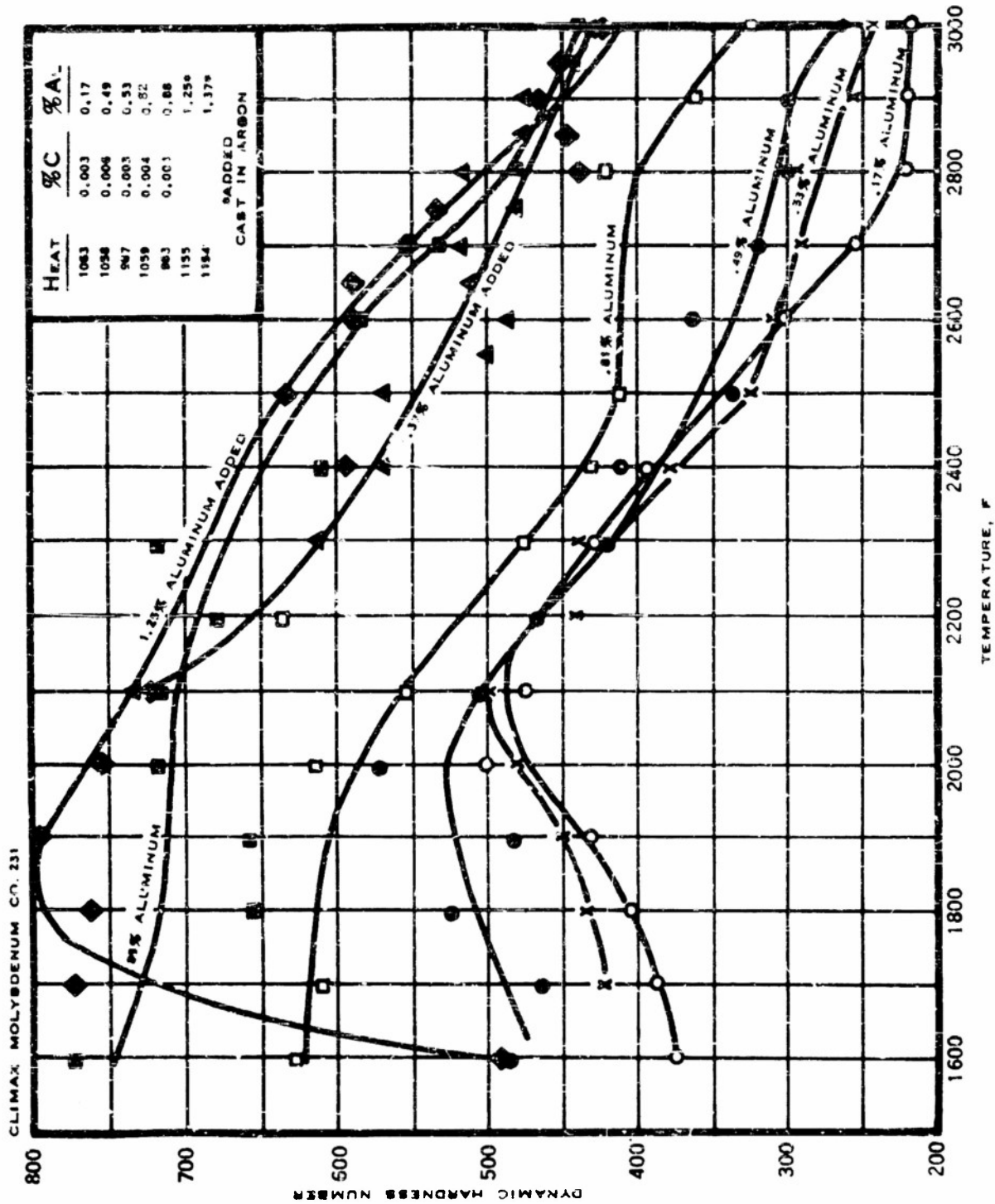


FIGURE B3 -- DYNAMIC HOT HARDNESS OF MOLYBDENUM-ALUMINUM ALLOYS AS CAST

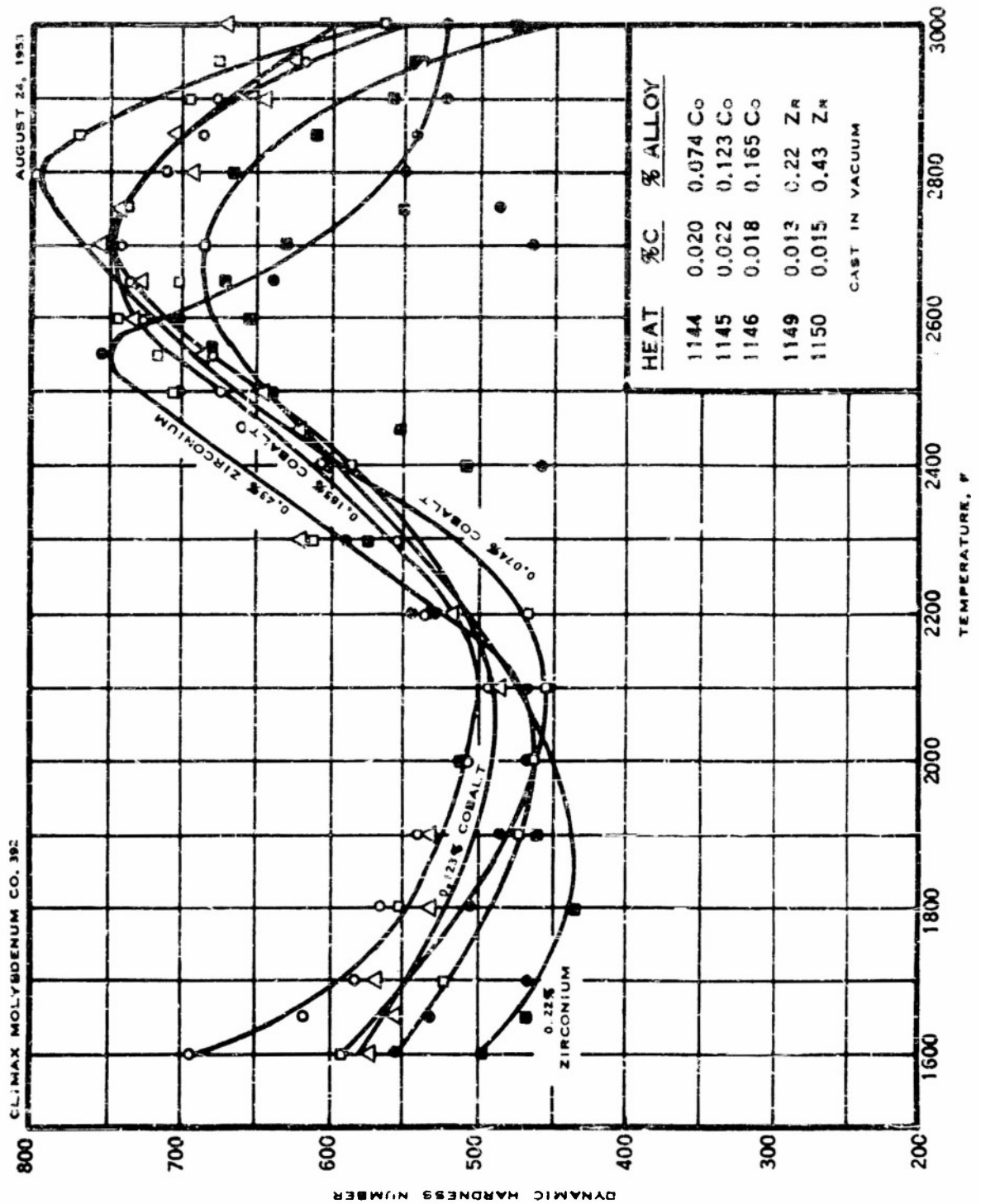


FIGURE B4 - DYNAMIC HOT HARDNESS OF MOLYBDENUM-COBALT AND MOLYBDENUM-ZIRCONIUM ALLOYS AS CAST

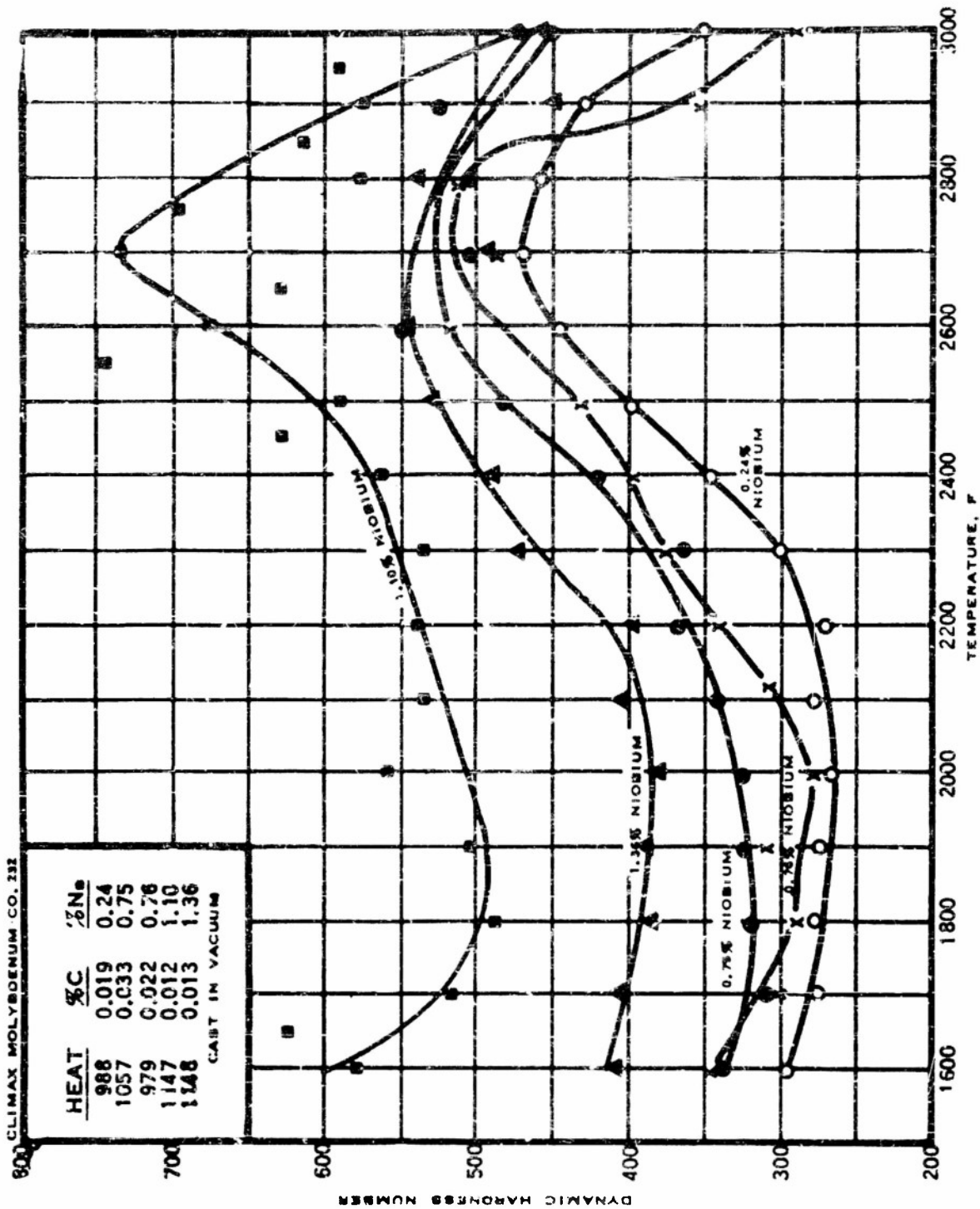


FIGURE B5 -- DYNAMIC HOT HARDNESS OF MOLYBDENUM-NIOBIUM ALLOYS AS CAST

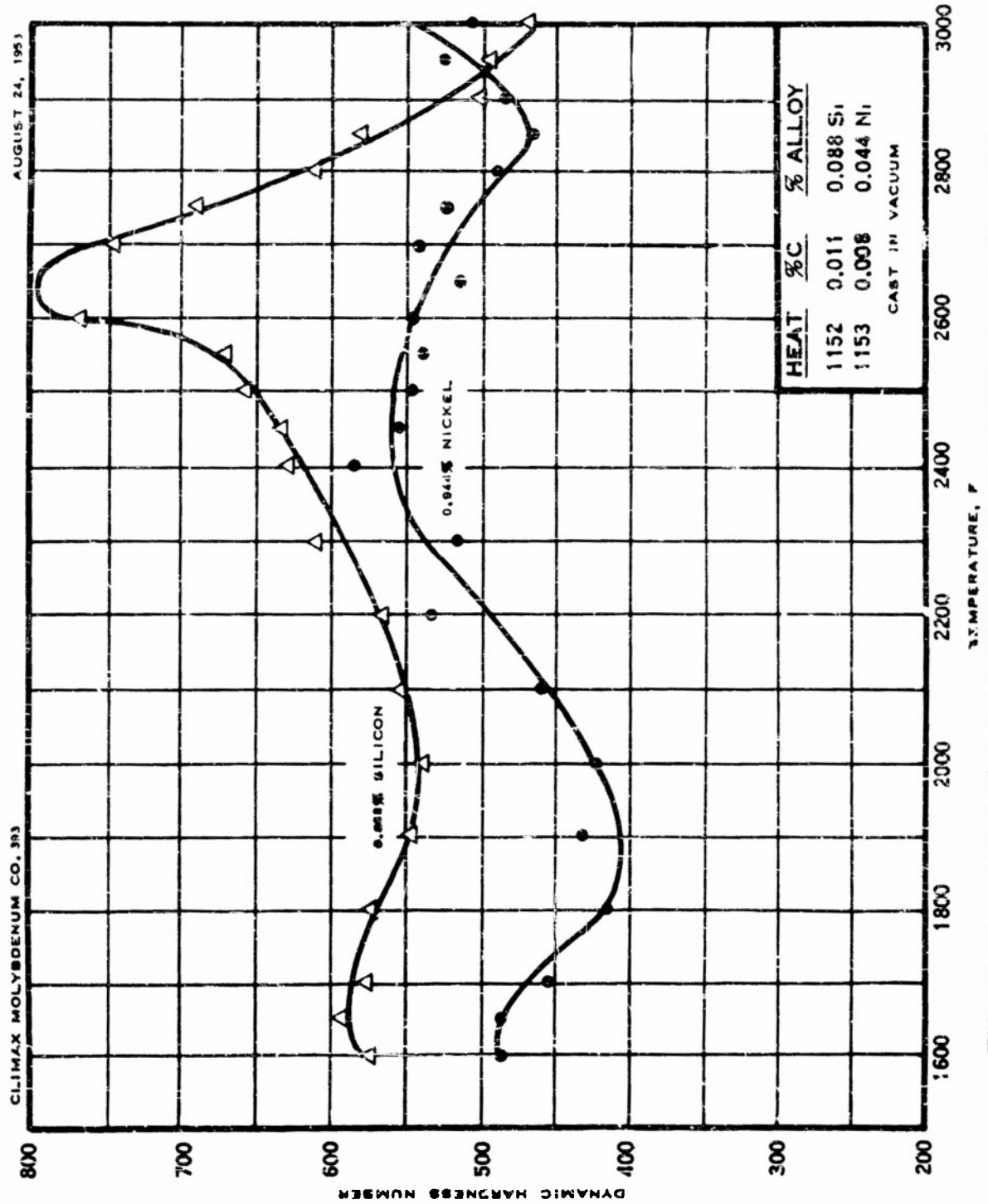


FIGURE B6 - DYNAMIC HOT HARDNESS OF MOLYBDENUM-NICKEL AND MOLYBDENUM-SILICON ALLOYS AS CAST

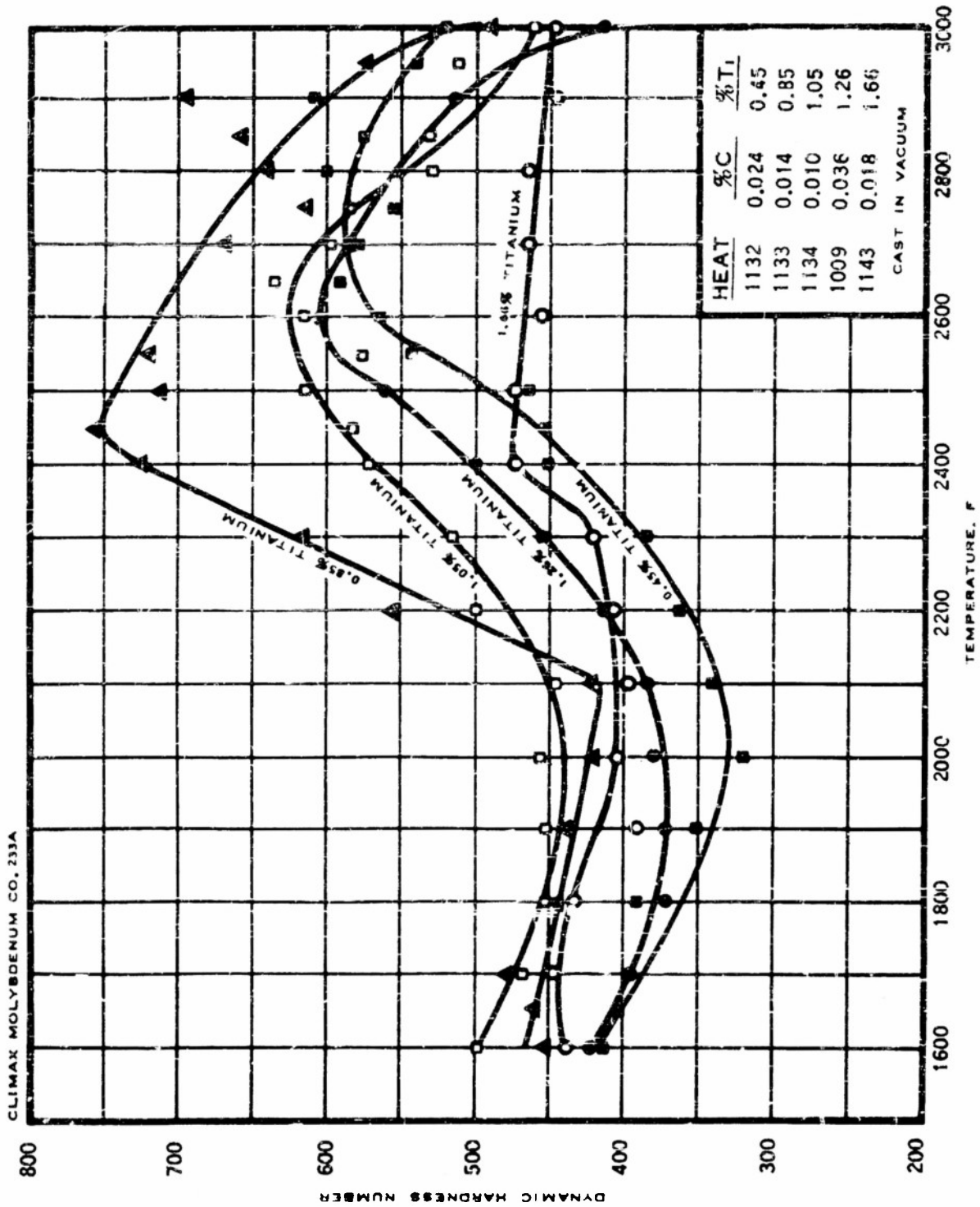


FIGURE B7 - DYNAMIC HOT HARDNESS OF A MOLYBDENUM - TITANIUM ALLOY AS CAST

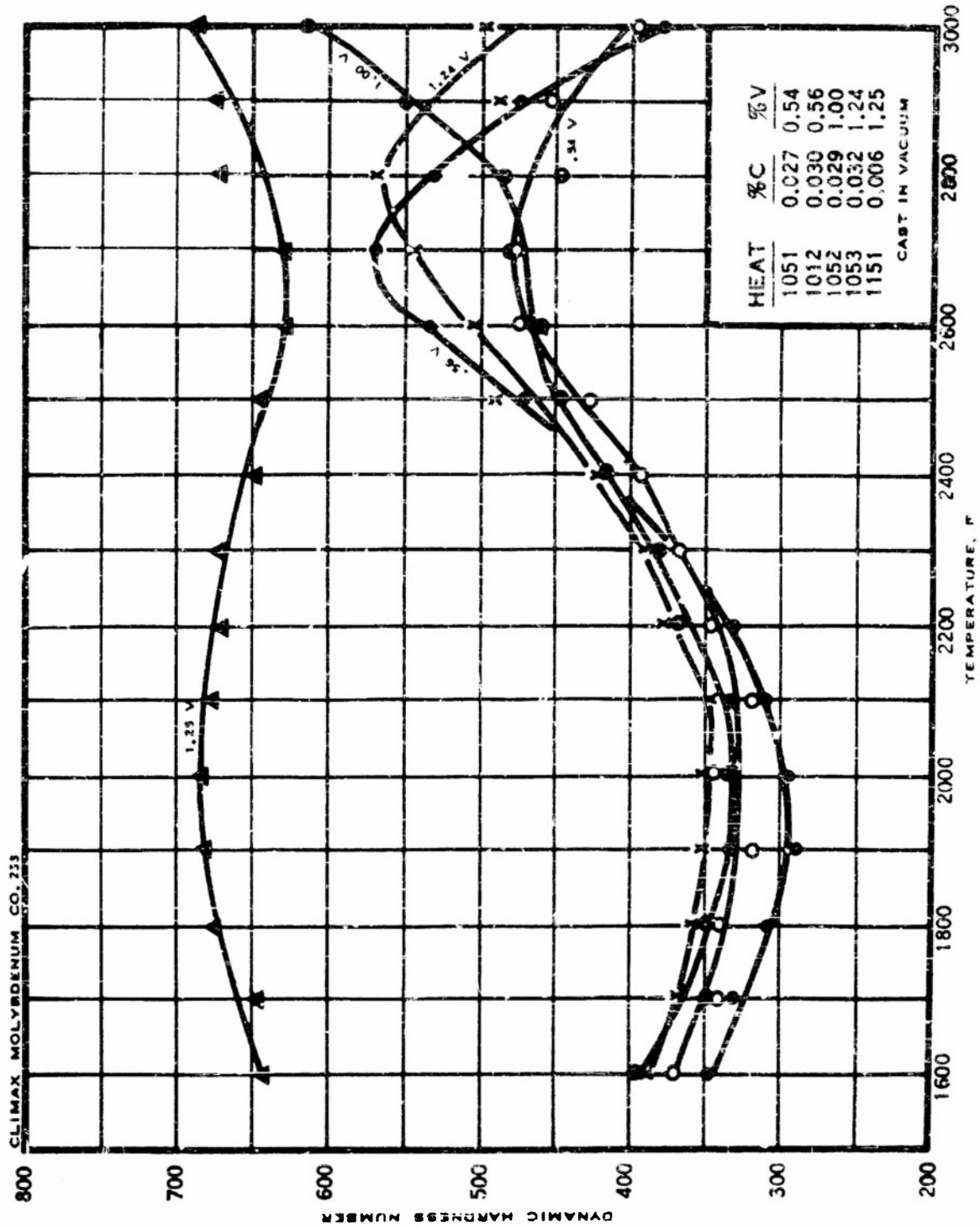


FIGURE B8 -- DYNAMIC HOT HARDNESS OF MOLYBDENUM-VANADIUM ALLOYS AS CAST

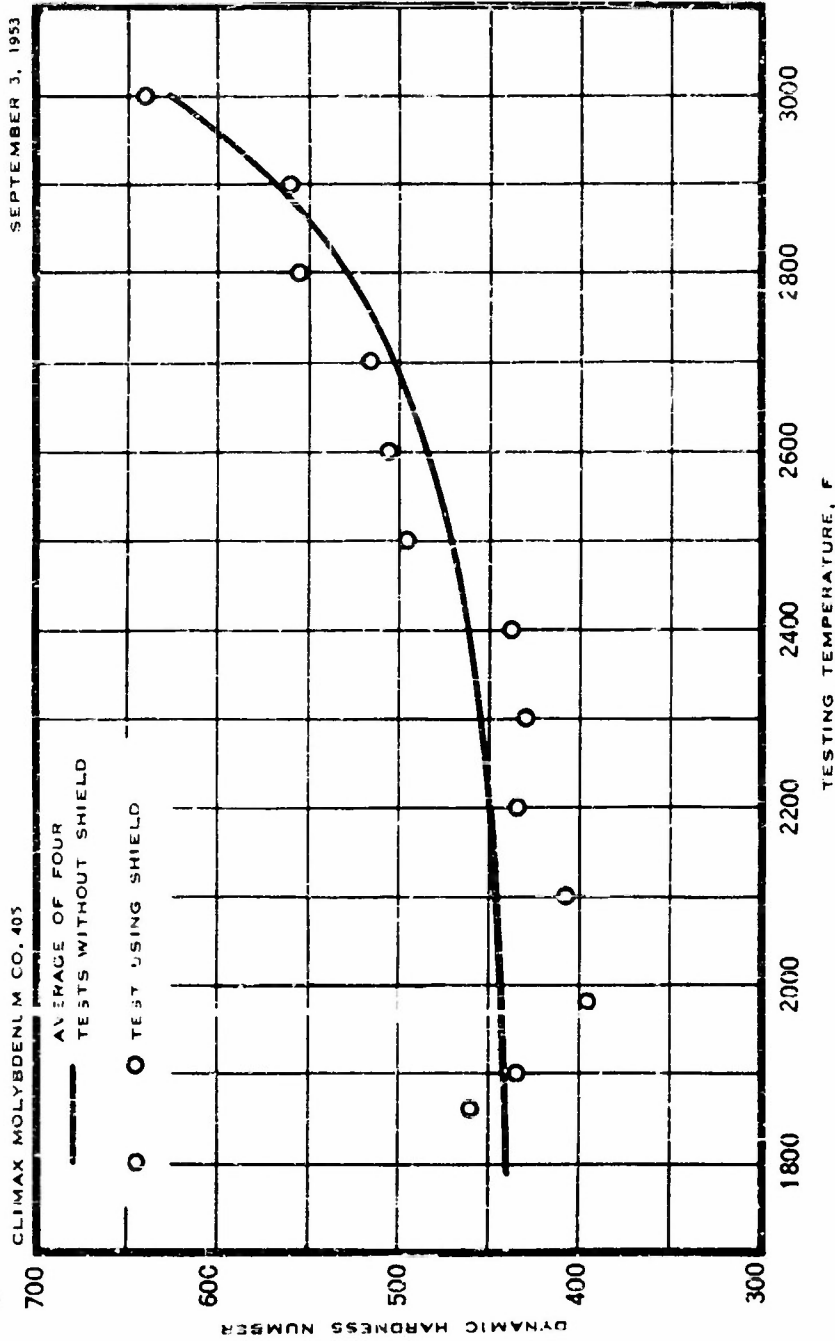


FIGURE B9 -- COMPARISON OF RESULTS OF DYNAMIC HARDNESS TESTS MADE WITH AND WITHOUT SHIELDING OF INDENTER ASSEMBLY

HEAT 669, 0.08% VANADIUM

In a second experiment, designed to measure the energy delivered by the apparatus at various temperatures, an electronic timer was incorporated into the system so that the time between the release of the trigger and contact with the specimen could be determined accurately. Results of the test are tabulated in Table B1.

TABLE B1

DURATION OF FALL OF INDENTER AT ELEVATED TEMPERATURES

<u>Testing Temp. F</u>	<u>Number of Readings</u>	<u>Average Time of Drop, Sec.</u>
78	23	0.271
1800	14	0.243
2200	16	0.240
2400	19	0.236
2600	16	0.230

The increase in dynamic hardness did not appear to be a function of movement of the indenter, in fact, the indenter traveled more rapidly at 2600 F than at room temperature, thereby delivering slightly more energy to the specimen at the higher temperature. It was concluded from these experiments that mechanical operation of the apparatus did not change with temperature.

The anomalous rise in hardness noted at elevated temperatures might be attributed to chemical and structural changes in the specimen. All of the alloys were single-phase solid solutions except for small amounts of excess carbide. If the rise in hardness with rising temperature were an actual property of the material, it must have been due to increased solubility of the carbide phase in the matrix. Experiments were designed to determine the solubility of the carbide at temperatures of the dynamic hardness test. Specimens were held for short times at temperatures up to 3000 F--times and temperatures comparable to those encountered in the hardness test--and drastically quenched. Metallographic examination and hardness determinations at room temperature indicated that no significant solution of carbide had occurred.

As to the matter of chemical changes of the specimen, it was possible that oxidation of the surface of the specimen was responsible for the anomalous hardness. In addition, it was noted that the room-temperature Vickers hardness of many specimens was significantly higher after dynamic hardness testing than before. These data are itemized in Table B2 for virtually all of the alloys tested under the present contract.

In order to study further the surface oxidation of hardness test specimens, a sample of 0.5% vanadium alloy (1015) as cast was chosen, as it had exhibited the characteristic increase in dynamic hardness number above about 2000 F as well as an increase of 76 VPI in room-temperature hardness after the

TABLE B2

ROOM-TEMPERATURE HARDNESS OF DYNAMIC HARDNESS SPECIMENS

Heat	Alloy Content %	Average Hardness, VFN		
		As Cast	After Dynamic Hardness Testing	Change
1159	0.040 C	187	178	- 9
1063	0.17 Al	169	198	+29
1058	0.49 Al	198	232	+34
987	0.53 Al	192	268	+76
1059	0.81 Al	240	283	+43
983	0.88 Al	229	304	+75
1155	1.25 Al*	231	251	+20
1154	1.36 Al*	255	269	+34
1144	0.074 Co	169	152	-17
1145	0.123 Co	170	156	-14
1146	0.165 Co	185	179	- 6
1153	0.044 Ni	160	158	- 2
988	0.24 Nb	180	196	+16
978	0.52 Nb	189	206	+17
1057	0.75 Nb	197	210	+13
1147	1.10 Nb	190	207	+17
1148	1.36 Nb	204	219	+15
1152	0.086 Si	178	222	+44
1132	0.45 Ti	195	241	+46
1133	0.85 Ti	206	243	+37
1134	1.05 Ti	204	256	+52
1009	1.26 Ti	212	285	+73
1143	1.66 Ti	209	232	+23
1051	0.54 V	203	221	+18
1012	0.56 V	192	270	+78
1052	1.00 V	200	203	+ 3
1053	1.24 V	208	235	+27
1151	1.25 V	190	206	+16
1062	0.11 Zr	189	264	+75
1149	0.22 Zr	186	276	+90
1150	0.43 Zr	194	342	+148

* added

dynamic hardness test. To ascertain the change in room temperature hardness of the specimen after exposure to elevated temperatures in the range 1600-3000 F, an interrupted test was made; that is, the dynamic hardness was determined at a given temperature, the specimen was allowed to cool to room temperature, and its room-temperature hardness was determined. Testing was continued alternately at progressively higher temperatures and at room temperature; the results of the test are plotted in Figure B10. The dynamic hardness data of this experiment closely paralleled those of the original standard dynamic hardness test for Ingot 1012. It is evident from Figure B10 that the room-temperature hardness increased and decreased in approximately the same manner as the dynamic hot hardness. It will be noted that the net increase in room-temperature Vickers hardness of the interrupted samples was 15 compared to 78 for the original sample from Heat 1012. This difference may have resulted from differences in the purity of the atmosphere or differences in the speed of testing, which would result in different depths of oxide penetration.

A sample was cut from the original dynamic hardness specimen from Heat 1012 and prepared for a microhardness survey on a plane perpendicular to the surface employed for the dynamic test. Results of the survey, Figure B11, indicated a very high hardness near the surface, but an affected depth of only about 0.004 inch.

In order to confirm the postulate that oxidation of the surface of the specimen took place in spite of the use of a protective atmosphere of purified argon, the dynamic hardness was determined on the same specimen in a reducing atmosphere, namely, hydrogen. The results of this experiment, Figure B12, were of interest in that no increase in room temperature hardness, and therefore insignificant oxidation, was noted after testing; yet the dynamic hardness exhibited the characteristic increase between 2000 and 2600 F, although it was of less magnitude than the increase obtained in argon. It must be assumed from these data that at least a portion of the rise in dynamic hardness near 2600 F was caused by factors other than oxidation of the surface.

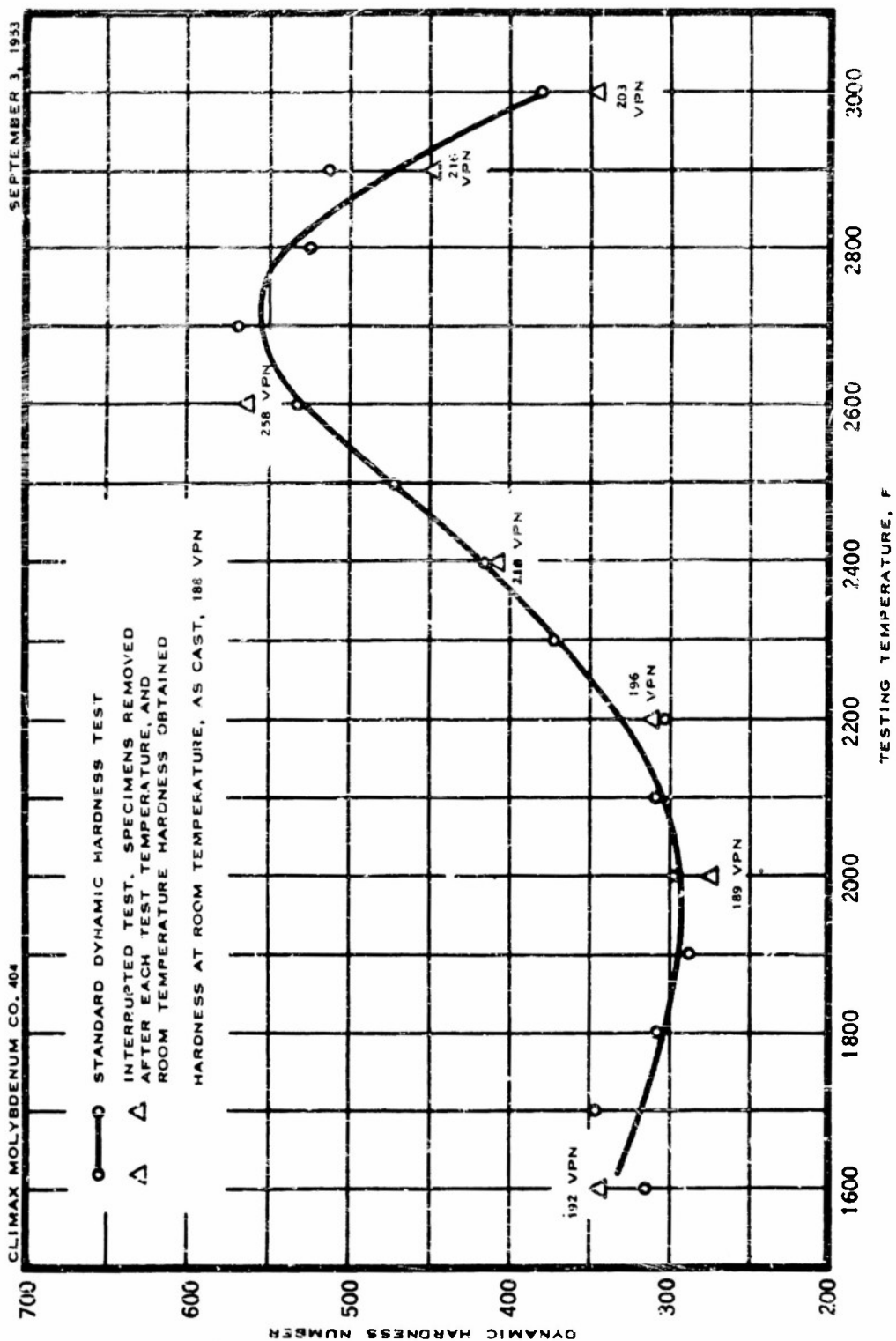


FIGURE B10— INTERRUPTED DYNAMIC HARDNESS TEST

HEAT 1012, 0.56% VANADIUM

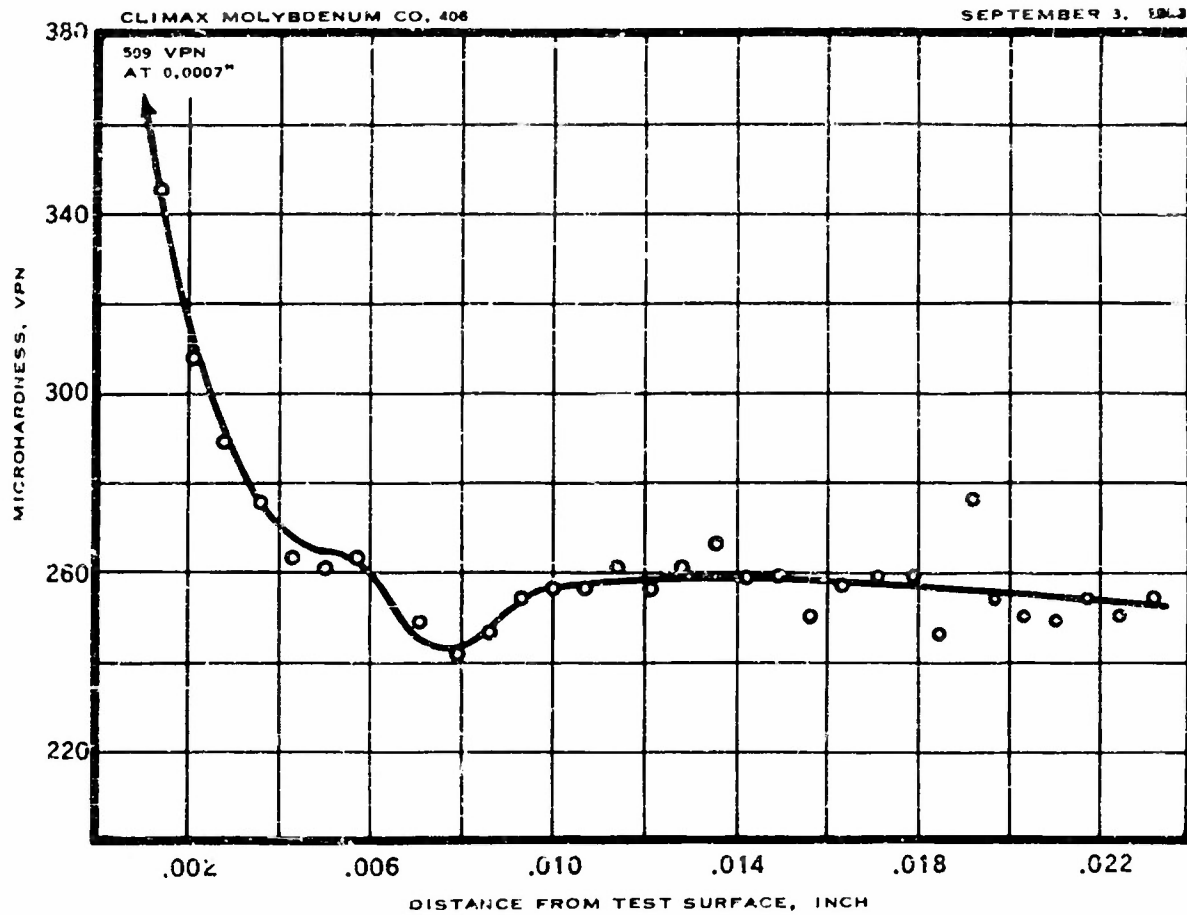


FIGURE B11 — COMPLETED DYNAMIC HARDNESS SPECIMEN, MICROHARDNESS TRAVERSE ON SURFACE PERPENDICULAR TO TEST SURFACE
HEAT 1012, 0.56% VANADIUM

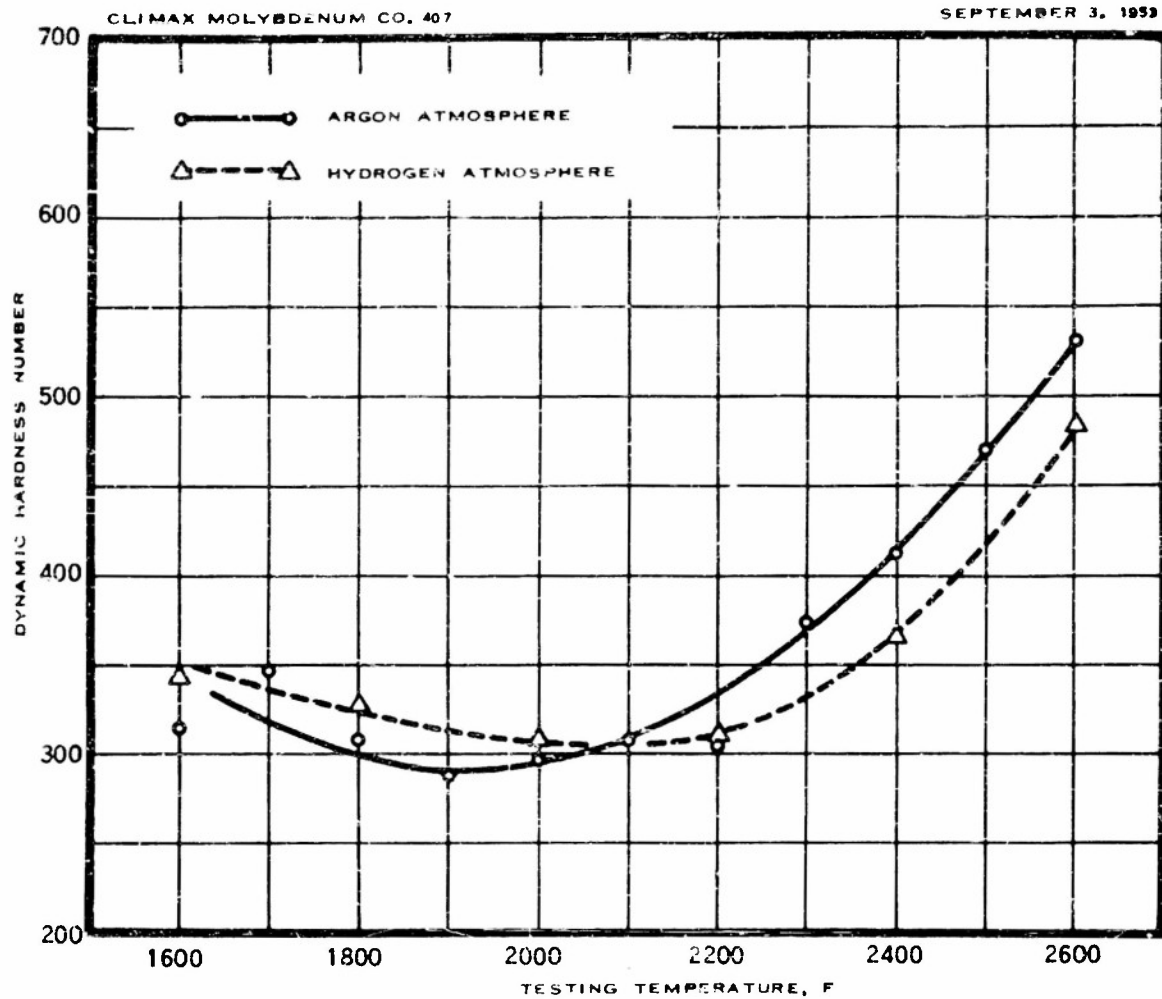


FIGURE B12— DYNAMIC HARDNESS TESTS CONDUCTED IN
ARGON AND IN HYDROGEN ATMOSPHERES

HEAT 1012, 0.56% VANADIUM

TABLE C1

TENSILE PROPERTIES AT ROOM AND ELEVATED TEMPERATURES
OF ROLLED MOLYBDENUM-BASE ALLOYS

Bar Dia In.	(1) Condition	Testing Temp, F	Yield Str. psi	Tensile Strength psi	(2) Elongation %	Reduction of Area %
<u>Bar 937 - Unalloyed Mo, 0.015% C</u>						
5/8	as rolled	81	78,800*	102,200	40	61.1
		750	53,400*	79,300	20	82.4
		1200	49,800*	69,600	18	84.2
		1600	37,000*	52,000	24	88.6
	str. relieved	81	82,900*	97,200	42	69.0
		750	57,200*	62,400	20	81.2
		1200	48,100*	65,200	22	86.1
		1600	33,400*	52,400	24	88.6
	recrystallized (2150 F)	81	55,900	68,200	42	37.8
		750	21,000	39,200	60	84.7
		1200	11,000	33,600	57	84.8
		1600	7,600*	25,100	60	84.6
<u>Bar 1159 - Unalloyed Mo, 0.040% C</u>						
1	as rolled	72	72,200*	92,400	30.5	35.5
		750	-	65,700	20	79.0
		1200	57,900*	72,500	16	79.0
		1600	41,900*	51,100	21	85.4
	str. relieved	81	75,400	89,600	29	37.9
		750	29,200	63,800	19.5	77.9
		1200	-	59,800	17.5	80.2
		1600	43,200*	51,000	20	83.6
	recrystallized (2250 F)	74	48,100	69,200	45	32.8
		750	16,600	38,600	51	83.2
		1200	10,300	34,300	48	87.5
		1600	-	27,400	49	89.9

(1) Stress relieved by heating 1 hr at 1600 F, fully recrystallized by heating 1 hr at the indicated temperature

(2) Percent elongation in 1 in. for specimens from 5/8 in. dia bars
percent elongation in 2 in. for specimens from 1 in. dia bars

* 0.1% offset yield strength taken from stress-strain plot; all other yield strength values from drop in load

TABLE C1 (continued)

TENSILE PROPERTIES AT ROOM AND ELEVATED TEMPERATURES
OF ROLLED MOLYBDENUM-BASE ALLOYS

Bar Dia In.	Condition	Testing Temp, F	Yield Str. psi	Tensile Strength psi	Elongation %	Reduction of Area %
<u>Bar 1045 - Unalloyed Mo Deoxidized with Rare Earth Metals</u>						
5/8	as rolled	78	83,300*	105,300	25	34.5
		1600	45,800*	55,000	11	51.3
	str. relieved	78	81,500*	100,900	9	13.8
		1600	43,400*	55,000	19	82.8
	recrystallized (2400 F)	78	46,600	62,500	2	12.3
		1600	11,300*	25,600	55	86.4
	<u>Bar 1063 - 0.17% Al</u>					
	as rolled	78	75,200*	96,300	36	57.1
		750	59,400*	76,400	19	70.6
		1200	56,100*	68,900	16	77.1
		1600	40,700	58,700	20	76.1
	str. relieved	78	72,400*	94,700	40	63.1
		750	54,600*	74,100	24	74.7
		1200	54,900*	66,400	18	71.3
		1600	45,200*	60,600	18	74.1
	recrystallized (2200 F)	78	41,300	66,700	18	14.4
		750	21,900	43,500	58	81.1
		1200	15,800	39,800	50	79.8
		1600	10,800	29,100	49	80.9
1	as rolled	78	-	75,600	2	1.7
		750	53,600*	61,400	20	75.1
		1200	-	55,600	17.5	76.1
		1600	39,400*	47,200	21.5	81.0
	str. relieved	78	64,500	74,600	1.5	1.1
		750	-	58,900	20.5	76.8
		1200	-	55,200	19	75.0
		1600	-	48,200	18.5	79.3
	recrystallized (2250 F)	79	34,200	65,200	21.5	18.8
		780	10,700	39,300	56	80.3
		1200	10,300	36,900	46.5	79.4
		1600	12,500	25,900	56.5	88.7

TABLE C1 (continued)

TENSILE PROPERTIES AT ROOM AND ELEVATED TEMPERATURES
OF ROLLED MOLYBDENUM-BASE ALLOYS

Bar Dia In.	Condition	Testing Temp, F	Yield Str. psi	Tensile Strength psi	Elongation %	Reduction of Area %
<u>Bar 1058 - 0.49% Al</u>						
1	as rolled	78	82,200*	89,200	1.5	0.6
		750	-	75,700	18.5	71.8
		1200	66,300*	71,700	17	71.9
		1600	55,300	61,500	17.5	76.0
	str. relieved	78	81,300	85,500	1	0.5
		750	67,700	74,100	19	72.3
		1200	65,500	70,800	16.5	69.5
		1600	-	62,300	18.5	78.8
	recrystallized (2300 F)	79	45,900	64,000	6	5.6
		750	26,200	42,200	40	73.1
		1200	25,500	46,600	41	81.4
		1600	13,700	34,100	50.5	83.2
<u>Bar 987 - 0.53% Al</u>						
5/8	as rolled	78	102,000*	121,200	2	0.2
		750	79,600*	101,900	14.5	57.5
		1200	74,700*	91,400	16	66.9
		1600	55,400*	76,800	18	63.7
	str. relieved	78	98,200	105,800	3	2.0
		750	79,000*	88,400	19	60.4
		1200	66,600*	82,900	18	82.1
		1600	55,300*	72,100	19	68.6
	recrystallized (2200 F)	78	none	46,100	0	0
		750	43,800	56,200	42	72.3
		1200	37,900	51,400	41	80.0
		1600	17,700*	38,100	42	54.7
<u>Bar 1144 - 0.074% Co</u>						
5/8	as rolled	78	110,900	113,300	35	70.0
		750	94,300	94,300	22	78.2
		1200	84,900	87,000	19	80.0
		1600	-	75,700	26	80.0

TABLE C1 (continued)

TENSILE PROPERTIES AT ROOM AND ELEVATED TEMPERATURES
OF ROLLED MOLYBDENUM-BASE ALLOYS

Bar Dia In.	Condition	Testing Temp, F	Yield Str. psi	Tensile Strength psi	Elongation %	Reduction of Area %
Bar 1144 - 0.074% Co (continued)						
5/8	str. relieved (1700 F)	80	111,500	111,500	36	68.3
		750	95,000	95,000	23	77.8
		1200	-	87,800	19	77.4
		1600	44,600*	68,000	25	93.6
	recrystallized (2000 F)	80	66,900	66,900	5	4.4
		1200	49,100	53,800	43	82.4
		1600	-	46,100	62	57.5
1	as rolled	79	78,700*	97,000	19.5	23.2
		750	38,000*	75,800	20	73.7
		1200	62,300*	73,200	16	80.0
		1600	53,500*	66,900	23	85.3
	str. relieved	80	82,500	94,900	20.5	19.9
		750	68,500	73,900	18.5	74.4
		1200	44,800*	70,900	16	78.9
		1600	57,000*	67,400	24	79.3
	recrystallized (2150 F)	83	60,800	67,100	10.5	9.8
		750	42,200	48,500	45	76.7
		1200	36,400	46,700	37.5	84.5
		1600	14,200	41,700	46	91.5

TABLE C1 (continued)

TENSILE PROPERTIES AT ROOM AND ELEVATED TEMPERATURES
OF ROLLED MOLYBDENUM-BASE ALLOYS

Bar Dia In.	Condition	Testing Temp, F	Yield Str. psi	Tensile Strength psi	Elongation %	Reduction of Area %
Bar 988 - 0.24% Nb (continued)						
1	as rolled	78	70,100*	80,600	1	0.6
		750	51,100*	52,600	20	80.0
		1200	48,100*	50,700	19	83.1
		1600	39,700	44,200	19	84.9
	str. relieved	78	62,200	69,300	1	0.5
		750	43,800*	45,600	23	81.4
		1200	40,000*	41,900	21	85.9
		1600	35,300*	37,300	21.5	87.7
	recrystallized (2500 F)	76	40,000	55,200	3	2.5
		750	13,100	33,400	57.5	76.7
		1200	9,300	28,100	49	84.4
		1600	8,500	25,600	73.5	93.2
Bar 978 - 0.52% Nb						
5/8	as rolled	78	92,600*	114,600	28	54.8
		750	71,500*	92,500	18	68.8
		1200	50,900*	80,800	16	78.9
		1600	51,100*	71,300	18	73.9
	str. relieved	78	94,300	109,400	29	59.4
		750	68,300*	89,400	17	70.7
		1200	67,200*	82,700	16	72.9
		1600	58,600*	72,200	16	72.3
	recrystallized (2200 F)	78	62,800	71,900	27	21.8
		750	32,100	42,600	60	85.3
		1200	17,500	39,500	48	85.5
		1600	-	34,900	52	88.8
1	as rolled	78	73,000*	84,600	1	0.6
		750	58,400*	59,600	21	83.2
		1200	48,000*	54,400	17.5	79.8
		1600	-	49,400	18.5	80.4
	str. relieved	78	68,000	78,600	1.5	0.5
		750	50,000*	55,100	20.5	81.8
		1200	47,400*	52,400	18	83.1
		1600	40,700	44,200	22	79.8

TABLE C1 (continued)

TENSILE PROPERTIES AT ROOM AND ELEVATED TEMPERATURES
OF ROLLED MOLYBDENUM-BASE ALLOYS

Bar Dia In.	Condition	Testing Temp, F	Yield Str. psi	Tensile Strength psi	Elongation %	Reduction of Area %
Bar 978 - 0.52% Nb (continued)						
1	recrystallized (2450 F)	80	42,300	65,500	10	8.5
		750	11,100	36,600	47	78.6
		1200	8,900	33,000	50.5	82.7
		1600	9,600*	30,000	40.5	86.9
Bar 1057 - 0.75% Nb						
5/8	as rolled	78	94,400*	118,300	32	62.5
		750	74,200*	96,600	17	73.8
		1200	-	89,000	17	77.3
		1600	41,400*	73,100	12	71.1
	str. relieved	78	96,000*	118,100	33	66.7
		750	73,700*	96,000	17	71.2
		1200	67,400*	88,400	16	73.7
		1600	48,700*	76,700	17	67.6
	recrystallized (2250 F)	78	66,400	78,400	53	70.1
		750	27,300	46,300	52	81.2
		1200	18,900	43,600	48	76.5
		1600	13,600	36,000	61	83.6
1	as rolled	78	none	87,400	0.5	0.2
		750	-	83,100	19	78.5
		1200	78,000	80,700	17	76.1
		1600	53,400*	72,100	16	72.9
	str. relieved	78	none	84,500	0.5	0.2
		750	74,500*	82,400	19	75.7
		1200	70,800*	78,100	16	76.8
		1600	59,300	69,100	18.5	71.0
	recrystallized (2300 F)	80	55,800	73,400	15.5	13.5
		750	15,200	43,400	53	83.8
		1200	13,800	38,700	47.5	85.1
		1600	-	35,100	49	83.7

TABLE C1 (continued)

TENSILE PROPERTIES AT ROOM AND ELEVATED TEMPERATURES
OF ROLLED MOLYBDENUM-BASE ALLOYS

Bar Dia In.	Condition	Testing Temp, F	Yield Str. psi	Tensile Strength psi	Elongation %	Reduction of Area %
<u>Bar 1132 - 0.45% Ti</u>						
5/8	as rolled	82	96,700*	112,900	29	59.7
		750	78,900*	100,400	18	76.1
		1200	80,600*	101,300	18	82.6
		1600	81,000*	86,900	17	84.0
	str. relieved	80	99,100*	132,100	31	70.0
		750	89,000*	110,000	18	72.8
		1200	84,000*	100,500	17	74.1
		1600	76,500*	88,300	15	71.1
	recrystallized (2450 F)	81	60,000	75,500	55	38.0
		750	30,200	45,600	47	86.4
		1200	-	43,700	45	86.2
		1600	15,400	39,900	47	88.4
1	as rolled	77	89,000*	115,100	30	46.8
		750	-	90,800	16	75.5
		1200	68,300*	84,900	15.5	74.5
		1600	64,800*	78,400	15.5	75.0
	str. relieved	83	87,900*	113,000	20	25.4
		750	71,300*	90,700	17	73.5
		1200	62,600*	84,700	16	71.9
		1600	62,800*	77,700	16	75.7
	recrystallized (2600 F)	74	53,900	72,500	22	18.7
		750	11,800	42,400	45	83.9
		1200	10,300	39,200	42.5	87.7
		1600	14,500	37,500	48.5	87.6
<u>Bar 1048 - 0.69% Ti, 0.12% R.E.</u>						
5/8	as rolled	80	91,000*	110,100	22	38.5
		750	66,200*	84,200	20	52.3
		1200	59,800*	73,800	18	82.3
		1600	47,500*	60,300	17	77.3
	str. relieved	80	82,400*	108,300	34	46.1
		750	61,500*	78,100	19	73.8
		1200	62,000*	69,400	18	81.5
		1600	-	60,700	17	76.6

TABLE C1 (continued)

TENSILE PROPERTIES AT ROOM AND ELEVATED TEMPERATURES
OF ROLLED MOLYBDENUM-BASE ALLOYS

Bar Dia In.	Condition	Testing Temp, F	Yield Str. psi	Tensile Strength psi	Elongation %	Reduction of Area %
<u>Bar 1048 - 0.69% Ti, 0.12% R.E. (continued)</u>						
5/8	recrystallized (2500 F)	80	53,700	68,400	8	6.3
		750	16,900	38,300	67	81.6
		1200	11,400	34,700	65	84.9
		1600	13,400*	33,800	41	84.8
<u>Bar 1133 - 0.85% Ti</u>						
5/8	as rolled	78	88,300*	117,800	36	60.5
		750	68,900*	92,700	20	81.7
		1200	62,900*	81,800	20	87.0
		1600	47,000*	69,600	24	90.1
	str. relieved	78	86,100*	117,200	32	63.4
		750	73,300*	89,600	19	84.1
		1200	60,100*	79,300	22	79.2
	recrystallized (2500 F)	82	66,800	74,900	44	35.9
		750	14,900	43,300	47	90.0
		1200	-	41,100	48	94.8
		1600	11,200	36,400	50	79.7
	1	as rolled	76	75,800*	103,800	19
750			75,000*	75,300	21	80.3
1200			58,100*	63,900	18.5	89.9
1600			49,200*	61,300	21.5	83.7
str. relieved		79	75,100*	103,600	26.5	28.4
		750	-	75,000	19.5	79.6
		1200	51,600*	68,100	17.5	85.0
		1600	45,100*	59,600	17.5	90.8
recrystallized (2650 F)		80	67,400	72,300	12.5	12.1
		750	19,400	43,000	44.5	84.9
		1200	14,400	39,200	40.5	92.9
		1600	11,400	39,500	45.5	87.0

TABLE C1 (continued)

TENSILE PROPERTIES AT ROOM AND ELEVATED TEMPERATURES
OF ROLLED MOLYBDENUM-BASE ALLOYS

Bar Dia In.	Condition	Testing Temp, F	Yield Str. psi	Tensile Strength psi	Elongation %	Reduction of Area %
<u>Bar 1138 - 1.22% Ti</u>						
5/8	as rolled	80	37,700*	114,100	37	66.1
		750	86,200*	91,500	18	85.6
		1200	63,100*	77,500	21	86.0
		1600	41,100*	56,500	17	83.3
	str. relieved	79	85,500*	112,900	37	65.9
		750	56,900*	84,400	21	82.4
		1200	56,100*	75,600	21	87.0
		1600	39,900*	58,400	25	83.8
	recrystallized (2500 F)	80	51,700	76,000	30	23.5
		750	-	43,300	45	86.2
		1200	-	38,300	45	87.0
		1600	23,100*	33,400	52	85.0
1	as rolled	76	75,000*	100,200	35.5	46.2
		1200	50,500*	62,600	17.5	88.3
		1600	47,900*	55,400	19	84.1
	str. relieved	78	73,800	99,000	31	33.5
		750	61,100*	67,900	14	53.4
		1200	58,100*	61,300	18	89.0
		1600	49,000*	53,500	22	98.1
	recrystallized (2600 F)	82	53,200	68,600	6.5	6.2
		750	23,900	40,900	46	79.3
		1200	13,400*	37,100	43	91.9
		1600	12,100	35,200	46	86.1
	<u>Bar 1009 - 1.26% Ti</u>					
5/8	as rolled	78	109,000*	124,200	4	1.6
		750	87,200*	92,600	19	79.8
		1200	64,900*	80,900	18	80.2
		1600	56,600*	69,100	20	82.2
	str. relieved	78	106,300*	125,500	20	24.6
		750	85,500*	95,500	18	77.8
		1200	71,000*	81,000	18	76.8
		1600	55,900	68,400	14	40.2

TABLE C1 (continued)

TENSILE PROPERTIES AT ROOM AND ELEVATED TEMPERATURES
OF ROLLED MOLYBDENUM-BASE ALLOYS

Bar Dia In.	Condition	Testing Temp. F	Yield Str. psi	Tensile Strength psi	Elongation %	Reduction of Area %
Bar 1009 - 1.26% Ti (continued)						
5/8	recrystallized (2900 F)	78	61,400	80,800	19	18.2
		750	33,100	44,000	55	76.3
		1200	22,800	43,300	42	91.7
		1600	14,900*	45,900	29	40.7
Bar 1051 - 0.54% V						
5/8	as rolled	78	90,300*	104,400	40	71.0
		750	37,900*	81,000	18	79.0
		1200	-	76,900	20	68.7
		1600	-	60,900	15	72.5
	str. relieved	78	93,400	103,600	38	72.2
		750	41,400*	79,100	19	78.6
		1200	35,800	75,000	18	76.9
		1600	45,700*	60,800	21	75.4
	recrystallized (2100 F)	78	70,400	74,400	40	37.1
		750	41,400	45,500	55	81.6
		1200	26,300	45,500	40	83.6
		1600	13,300	32,400	52	79.8
1	as rolled	78	95,300	100,000	4	2.3
		750	75,200	76,100	15.5	78.3
		1200	-	73,900	16.5	75.1
		1600	48,600*	57,600	20	78.5
	str. relieved	78	85,100	92,200	3.5	4.0
		750	65,900	72,700	19	76.8
		1200	64,300*	68,200	17	75.3
		1600	-	50,300	17	88.9
	recrystallized (2500 F)	80	56,300	69,700	20.5	18.1
		750	16,700	42,200	50	80.0
		1200	14,100	41,800	32	86.8
		1600	13,300	32,500	50	86.9

TABLE C1 (continued)

TENSILE PROPERTIES AT ROOM AND ELEVATED TEMPERATURES
OF ROLLED MOLYBDENUM-BASE ALLOYS

Bar Dia In.	Condition	Testing Temp, F	Yield Str. psi	Tensile Strength psi	Elongation %	Reduction of Area %
Bar 1012 - 0.56% V						
5/8	as rolled	78	98,000*	121,500	4	7.4
		720	81,200*	102,000	16	65.5
		1200	56,800*	90,100	18	73.1
		1600	44,800*	70,100	21	79.9
	str. relieved	78	76,600	122,200	26	39.2
		750	65,600*	90,600	9	69.6
		1200	-	83,000	16	74.5
		1600	60,200	65,400	23	75.9
	recrystallized (2150 F)	78	83,200	83,200	25	20.4
		750	34,700	45,900	53	79.9
		1200	24,200	45,400	39	80.2
		1600	14,400	33,100	41	79.3
1	as rolled	78	87,900	96,000	1	1.7
		750	72,300*	81,000	13	56.5
		1200	70,300*	75,600	16	75.7
		1600	-	59,600	19	80.2
	str. relieved	78	88,300	92,400	1.5	1.1
		750	67,800*	75,900	15	72.9
		1200	60,000*	71,900	16.5	78.7
		1600	55,500*	67,700	18.5	83.0
	recrystallized (2200 F)	79	61,900	70,600	19	15.9
		750	22,000	41,300	56.5	82.7
		1200	15,300	43,500	34	85.0
		1600	15,900	29,700	51	85.9
Bar 1049 - 0.85% V, 0.003% Ce, 0.003% R.E.						
5/8	as rolled	80	87,900*	112,500	16	24.6
		750	67,000*	90,500	15	71.9
		1200	67,400*	78,300	19	81.5
		1600	34,200*	62,600	19	76.7

TABLE C1 (continued)

TENSILE PROPERTIES AT ROOM AND ELEVATED TEMPERATURES
OF ROLLED MOLYBDENUM-BASE ALLOYS

Bar Dia In.	Condition	Testing Temp, F	Yield Str. psi	Tensile Strength psi	Elongation %	Reduction of Area %	
Bar 1049 - 0.85% V, 0.003% C ₂ , 0.003% R.E. (continued)							
5/8	str. relieved	80	79,400*	106,200	2	2.4	
		750	66,600*	85,200	17	71.8	
		1200	62,100*	75,900	19	77.7	
		1600	48,800*	63,100	21	81.7	
	recrystallized (2500 F)	80	53,700	53,700	1	0	
		750	23,300	39,900	57	83.1	
		1200	16,300	38,700	44	82.8	
		1600	11,600*	30,100	13	16.4	
	Bar 1052 - 1.00% V						
	5/8	as rolled	78	98,600	111,200	32	57.8
			750	72,200*	89,300	34	78.2
			1200	71,600*	86,400	15	69.5
1600			-	67,200	18	74.0	
str. relieved		78	95,200	100,000	29	54.5	
		750	68,500*	88,900	13	66.4	
		1200	55,200	35,400	15	67.5	
		1600	47,700	71,900	20	74.8	
recrystallized (2150 F)		80	89,700	89,700	28	21.6	
		750	39,500	50,000	55	81.6	
		1200	37,000	52,200	35.5	79.3	
		1600	14,600	35,500	58	83.6	
1	as rolled	78	96,500	103,600	2	1.1	
		750	84,500	87,000	16	73.4	
		1200	72,700*	85,500	13.5	69.1	
		1600	-	69,200	20	77.5	
	str. relieved	78	94,000	98,400	1.5	1.3	
		750	76,600*	81,800	16.5	71.8	
		1200	-	80,700	14.5	69.1	
		1600	51,900	52,900	17	12.9	
	recrystallized (2350 F)	80	70,200	72,900	24	20.8	
		750	35,000	46,100	45	78.0	
		1200	22,500	49,600	30	73.6	
		1600	10,600	33,900	43	88.0	

TABLE C1 (continued)

TENSILE PROPERTIES AT ROOM AND ELEVATED TEMPERATURES
OF ROLLED MOLYBDENUM-BASE ALLOYS

Bar Dia In.	Condition	Testing Temp, F	Yield Str. psi	Tensile Strength psi	Elongation %	Reduction of Area %
Bar 1151 - 1.25% V						
5/8	as rolled	80	105,000	114,500	34	59.7
		750	85,600*	92,700	20	81.0
		1200	63,800*	90,600	19	81.2
		1600	45,600*	67,600	16	92.3
	str. relieved	80	103,900	115,200	27	47.0
		750	59,700*	86,800	19	80.0
		1200	69,400*	84,300	15	82.6
		1600	64,400*	88,600	20	79.4
	recrystallized (2200 F)	80	84,300	84,300	2	6.2
		750	46,900	47,900	46	88.2
		1200	33,500	53,600	35	84.1
		1600	-	41,500	48	86.9
1	as rolled	73	88,200	105,700	9	9.0
		750	76,400*	82,500	15	73.8
		1200	63,900*	81,200	15	72.0
		1600	61,800*	69,900	16.5	81.7
	str. relieved	83	97,100	98,900	2	1.7
		750	75,500*	80,900	15.5	63.6
		1200	59,100*	79,900	14	74.2
		1600	60,800	68,000	17	80.0
	recrystallized (2600 F)	76	54,200	54,200	1	2.1
		1200	19,000	47,500	33.5	85.9
		1600	14,900	37,900	41	89.7
		Bar 1207 - 0.09% Zr				
5/8	as rolled	82	108,200*	126,700	30	55.5
		750	-	104,900	18	78.7
		1200	68,800*	96,400	19	72.5
		1600	59,000*	74,400	15	78.1

TABLE C1 (continued)

TENSILE PROPERTIES AT ROOM AND ELEVATED TEMPERATURES
OF ROLLED MOLYBDENUM-BASE ALLOYS

Bar Dia In.	Condition	Testing Temp, F	Yield Str. psi	Tensile Strength psi	Elongation %	Reduction of Area %
Bar 1207 - 0.09% Zr (continued)						
5/8	str. relieved	82	104,200*	125,900	29	40.0
		750	80,200*	102,900	19	71.1
		1200	72,300*	97,300	20	85.7
		1600	53,600*	79,000	18	86.1
	recrystallized (2750 F)	79	65,900	75,800	44	43.7
		750	21,100	48,700	44	91.1
		1200	19,400*	44,700	43	89.3
		1600	18,900	35,100	55	93.6
1	as rolled	87	92,600*	110,000	4.5	4.6
	str. relieved	87	91,600	105,700	4.5	3.7
	recrystallized (2900 F)	87	46,400	72,300	18	15.0
1/2" Dia Bars Tested at Room Temperature Only						
1082	0.31 Nb					
	str. relieved	79	74,600	88,700	16	38.3
	recryst (2300 F)	80	54,800	69,400	48	37.1
1001	0.31 Nb, 0.16 Ti					
	str. relieved	81	100,600*	111,500	2	0.1
	recryst (2700 F)	81	59,100	73,500	44	37.1
672	0.88 V					
	as rolled	79	74,100*	92,100	1	1.0
	recryst (2500 F)	81	46,700	70,600	7	4.1
1173	0.19 Co					
	recryst (2100 F)	82	69,500	77,900	5	5.6
1174	3.59 Ti					
	str. relieved	82	70,400*	92,300	4	3.2
	recryst (3000 F)	79	56,900	56,900	0	0
1175	1.46 V					
	as rolled	79	86,100	88,900	1	1.0
	recryst (2600 F)	80	46,900	52,600	3	1.6

TABLE 32

CREEP-RUPTURE DATA ON ARC-CAST MOLYBDENUM-BASE ALLOYS
IN STRESS-RELIEVED AND RECRYSTALLIZED CONDITIONS
AT 1600 F

Tests conducted by Battelle Memorial Institute

Heat	Alloy, %	Heat Treatment	Stress psi	Rupture Time, hr	Elong. %	Reduction of Area, %	Creep Rate % per hour
937	0.015 C	SR	45,000	0.3	17.4	92.0	-
		SR	37,500	8.0	17.8	92.9	1.7
		SR	30,000	206.3	18.0	93.4	0.012
		R2150	22,300	2.0	54.9	94.0	12.2
		R2150	22,000	2.2	64.2	93.1	10.5
		R2150	17,500	19.7	40.7	86.5	0.95
		R2150	14,000	353.5 ^a	34.2	-	0.067
1045	0.003 C 0.005 Ce 0.007 RE	SR	60,000	0.1	12.9	95.7	-
		SR	45,000	18.7	18.0	91.1	0.07
		R2400	30,000	on loading	51.6	96.0	-
		R2400	20,000	97.9	52.0	97.3	0.19
1063	0.17 Al	SR	60,000	on loading	13.8	79.0	-
		SR	48,000	2.4	15.6	75.9	0.70
		SR	35,000	163.5	16.1	86.3	0.011
		R2200	30,000	0.4	59.3	93.2	-
		R2200	25,000	7.9	78.6	86.1	2.50
		R2200	18,000	145.3	43.2	88.8	0.012
987	0.53 Al	SR	70,000	0.2	12.5	74.4	-
		SR	60,000	4.1	13.8	75.0	0.6
		SR	45,000	97.7	15.4	60.0	0.034
		R2200	34,000	2.5	49.5	64.6	-
		R2200	30,000	14.1	56.9	67.0	-
		R2200	22,500	82.5	26.5	51.4	0.12
1144	0.074 Co	SR ₁₇₀₀	60,000	2.7	22.4	93.8	1.3
		SR ₁₇₀₀	50,000	15.9	47.5	89.1	0.20
		SR ₁₇₀₀	39,000	72.6	27.6	91.1	0.044
		R ₂₀₀₀	50,000	0.15	41.8	87.9	-
		R ₂₀₀₀	35,000	10.9	78.6	92.8	3.0
		R ₂₀₀₀	25,000	106.5	91.7	92.9	0.23
988	0.24 Nb	SR	70,000	on loading	12.3	88.7	-
		SR	60,000	4.1	12.8	85.6	0.45
		SR	50,000	300.0 ^a	3.8	-	0.0046
		R2200	30,000	0.5	51.9	95.2	-
		R2200	25,000	34.0	44.8	91.4	0.70
		R2200	22,000	39.6	23.9	52.1	0.25

^adiscontinued

SR - stress relieved one hour at 1800 F unless otherwise indicated

R - recrystallized, held one hour at indicated temperature

TABLE C2 (continued)

CREEP-RUPTURE DATA ON APC-CAST MOLYBDENUM-BASE ALLOYS
IN STRESS-RELIEVED AND RECRYSTALLIZED CONDITIONS
AT 1600 F

Heat	Alloy, %	Heat Treatment	Stress psi	Rupture Time, hr	Elong. %	Reduction of Area, %	Creep Rate % per hour
978	0.52 Nb	SR	80,000	on loading	13.1	77.1	-
		SR	70,000	5.9	13.5	86.5	0.47
		SR	60,000	500.0 ^a	3.0	-	0.0065
		R2200	40,000	on loading	42.2	86.6	-
		R2200	34,000	13.8	36.9	87.3	1.05
		R2200	30,000	315.0 ^a	22.1	-	0.042
1057	0.75 Nb	SR	75,000	9.5	14.8	75.5	0.31
		SR	65,000	377.2 ^a	3.2	-	0.0056
		SR	50,000	424.9 ^a	0.8	-	0.0006
		R2250	40,000	1.4	43.2	89.4	-
		R2250	37,500	76.4	47.3	46.3	0.12
		R2250	32,800	341.6 ^a	13.9	-	0.004
1132	0.45 Ti	SR	65,000	0.5	14.9	86.8	4.0
		SR	75,000	18.2	17.4	88.3	0.22
		SR	65,000	171.0	17.5	77.5	0.03
		R2450	40,000	1.7	44.8	90.4	-
		R2450	35,000	74.9	32.8	86.4	0.19
		R2450	33,500	379.4 ^a	15.3	-	0.027
1048	0.69 Ti 0.12 RE	SR	60,000	0.15	12.1	90.5	-
		SR	50,000	7.6	13.6	78.4	0.21
		SR	40,000	547.6 ^a	2.4	-	0.0017
		R2500	35,000	on loading	34.7	82.2	-
		R2500	25,000	35.1	25.2	28.3	0.09
		R2500	20,000	411.9 ^a	4.1	-	0.023
1133	0.85 Ti	SR	65,000	1.0	16.8	88.0	2.2
		SR	55,000	29.9	18.3	72.8	0.094
		SR	50,000	82.2	10.6	86.1	0.044
		R2500	37,500	0.5	41.6	91.4	-
		R2500	30,000	23.2	43.2	92.7	0.56
		R2500	27,500	92.7	43.3	92.3	0.05
1138	1.22 Ti	SR	60,000	0.8	10.1	71.0	-
		SR	45,000	74.9	15.4	68.4	0.044
		SR	40,000	330.3 ^a	4.6	-	0.011
		R2500	38,000	0.3	42.7	96.0	-
		R2500	30,000	11.8	47.1	89.8	1.3
		R2500	25,000	69.5	60.8	95.3	0.3

^adiscontinued

TABLE C2 (continued)

CREEP-RUPTURE DATA ON ARC-CAST MOLYBDENUM-BASE ALLOYS
IN STRESS-RELIEVED AND RECRYSTALLIZED CONDITIONS
AT 1600 F

Heat	Alloy, %	Heat Treatment	Stress psi	Rupture Time, hr	Elong. %	Reduction of Area, %	Creep Rate % per hour
1009	1.26 Ti	SR	67,000	0.15	15.0	95.0	-
		SR	60,000	2.5	15.8	95.7	0.53
		SR	50,000	91.0	22.2	91.4	0.048
		R ₂₉₀₀	44,500	0.2	29.6	95.9	-
		R ₂₉₀₀	40,000	72.6 ^a	4.8	-	nil
		R ₂₉₀₀	30,000	258.6 ^{a,b}	-	-	nil
		R ₂₉₀₀	50,000	on loading	28.6	95.3	-
1051	0.54 V	SR	60,000	0.15	16.8	86.9	-
		SR	50,000	7.1	15.9	79.9	0.24
		SR	42,000	76.2	21.9	88.0	-
		R ₂₁₀₀	30,000	2.1	48.7	88.0	10.5
		R ₂₁₀₀	25,000	25.3	57.1	93.7	1.20
		R ₂₁₀₀	21,000	118.5	52.8	94.8	0.18
1012	0.56 V	SR	60,000	0.7	18.5	79.8	-
		SR	45,000	47.4	18.4	89.0	0.08
		SR	40,000	146.6	29.4	94.7	0.035
		R ₂₁₅₀	30,000	4.0	50.4	89.4	-
		R ₂₁₅₀	25,000	30.0	36.0	84.8	0.50
		R ₂₁₅₀	22,000	243.0	72.2	96.5	0.10
1049	0.85 V 0.003 Ce 0.003 RE	SR	60,000	0.8	13.7	74.4	1.3
		SR	50,000	36.1	18.5	86.0	0.11
		SR	45,000	158.0	20.8	89.7	0.027
		R ₂₅₀₀	32,500	0.05	20.0	31.8	-
		R ₂₅₀₀	25,000	6.6	17.6	34.1	1.15
		R ₂₅₀₀	20,000	18.2	4.8	6.6	0.18
1052	1.00 V	SR	65,000	1.0	13.6	84.0	2.2
		SR	55,000	25.5	14.5	84.8	0.12
		SR	50,000	81.6	16.9	86.9	0.048
		R ₂₁₅₀	35,000	4.0	45.2	88.9	4.6
		R ₂₁₅₀	28,000	61.7	45.2	85.3	0.33
		R ₂₁₅₀	25,000	220.4	53.7	85.3	0.091
1207	0.09 Zr	SR	85,000	0.05	13.6	88.4	-
		SR	75,000	7.4	13.7	87.3	0.32
		SR	60,000	305.0 ^a	2.0	-	0.0027
		R ₂₇₅₀	40,000	0.05	50.0	92.0	-
		R ₂₇₅₀	30,000	1266.2 ^a	13.8	-	0.0046

^adiscontinued^breloaded at a stress of 50,000 psi and failed when load was applied

TABLE C2 (continued)

CREEP-RUPTURE DATA ON ARC-CAST MOLYBDENUM-BASE ALLOYS
IN STRESS-RELIEVED AND RECRYSTALLIZED CONDITIONS
AT 1800 F

Tests conducted by Battelle Memorial Institute

Heat	Alloy, %	Heat Treatment	Stress psi	Rupture Time, hr	Elong. %	Reduction of Area, %	Creep Rate % per hour
937	0.015 C	SR	37,500	0.25	14.9	94.0	-
		SR	27,500	13.6	17.1	91.0	-
		SR	21,000	144.8 ^b	4.9	-	0.036
		R2150	20,000	0.5	48.8	95.7	-
		R2150	15,000	5.5	54.4	94.5	7.0
		R2150	12,000	93.3	75.2	93.2	0.28
1045	0.003 C 0.005 Ce 0.007 RE	SR	40,000	2.7	19.0	95.2	-
		SR	25,000	318.0 ^a	4.1	-	-
		R2400	17,500	9.5	47.1	94.9	2.2
		R2400	14,000	125.3	18.7	30.4	0.075
1063	0.17 Al	SR	40,000	0.6	18.6	83.6	2.4
		SR	30,000	8.0	16.0	87.6	0.31
		SR	20,000	67.9	32.8	91.4	0.026
		R2200	25,000	0.2	52.6	88.7	-
		R2200	20,000	2.9	67.9	92.3	8.0
		R2200	12,500	148.8	62.8	97.6	0.14
987	0.53 Al	SR	55,000	0.4	19.7	90.4	-
		SR	45,000	3.9	18.4	83.0	1.0
		SR	25,000	185.0	21.0	85.7	0.028
		R2200	30,000	0.4	57.3	91.7	-
		R2200	25,000	4.0	50.3	90.1	8.5
		R2200	17,500	54.9	39.6	92.1	0.34
1144	0.074 Co	SR1700	50,000	0.6	25.3	82.7	4.3
		SR1700	30,000	10.8	37.3	83.5	0.21
		SR1700	19,000	102.3	29.6	80.9	0.05
		R2000	32,500	0.5	66.9	87.7	-
		R2000	25,000	3.2	77.6	92.2	10.8
		R2000	15,000	110.9	30.2	79.0	0.07
988	0.24 Nb	SR	55,000	0.2	13.1	90.7	-
		SR	35,000	32.8	13.1	90.7	0.030
		SR	27,500	51.2	14.2	92.9	0.0001
		R2200	25,000	0.8	53.3	93.9	-
		R2200	17,500	71.6	50.0	94.0	0.32
		R2200	16,000	287.6 ^a	28.9	-	0.086

^adiscontinued

^btest discontinued because of furnace failure

TABLE C2 (continued)

CREEP-RUPTURE DATA ON ARC-CAST MOLYBDENUM-BASE ALLOYS
IN STRESS-RELIEVED AND RECRYSTALLIZED CONDITIONS
AT 1800 F

Heat	Alloy, %	Heat Treatment	Stress psi	Rupture Time, hr	Elong. %	Reduction of Area, %	Creep Rate % per hour
978	0.52 Nb	SR	65,000	0.5	12.4	80.2	-
		SR	55,000	14.2	14.4	86.1	0.23
		SR	40,000	175.3	7.7 ^c	7.8 ^c	-
		R ₂₂₀₀	32,500	0.3	48.9	92.0	-
		R ₂₂₀₀	28,000	23.0	49.2	86.5	0.90
		R ₂₂₀₀	25,000	145.5	51.9	91.4	0.20
1057	0.75 Nb	SR	70,000	0.2	12.5	86.2	-
		SR	60,000	11.9	15.8	84.5	0.33
		SR	50,000	140.5	15.6	82.7	0.03
		R ₂₂₅₀	40,000	2 min	47.6	90.4	-
		R ₂₂₅₀	32,500	17.7	48.8	80.5	1.35
		R ₂₂₅₀	27,500	200.2	37.0	86.1	0.048
1132	0.45 Ti	SR	70,000	1.0	16.5	83.2	3.2
		SR	60,000	27.5	18.5	88.0	0.21
		SR	50,000	227.9	16.3	61.8	0.012
		R ₂₄₅₀	35,000	0.35	50.5	92.3	-
		R ₂₄₅₀	31,000	3.9	45.6	89.7	5.8
		R ₂₄₅₀	27,500	328.7 ^a	22.4	-	0.014
1048	0.69 Ti 0.12 RE	SR	55,000	1/2 min	13.0	89.8	-
		SR	40,000	7.8	14.5	88.3	0.32
		SR	30,000	142.1	17.9	95.0	0.027
		R ₂₅₀₀	30,000	0.2	36.0	95.2	-
		R ₂₅₀₀	22,500	12.4	38.9	93.7	0.62
		R ₂₅₀₀	17,500	209.5	41.9	80.8	0.016
1133	0.85 Ti	SR	52,000	2.1	18.6	91.4	1.5
		SR	40,000	42.9	11.7	90.1	0.10
		SR	35,000	148.5	15.5	85.7	0.022
		R ₂₅₀₀	35,000	0.1	40.7	87.5	-
		R ₂₅₀₀	25,000	8.6	45.2	90.8	1.7
		R ₂₅₀₀	21,000	52.8	52.8	92.9	0.42
1138	1.22 Ti	SR	50,000	0.7	17.4	71.1	3.1
		SR	40,000	12.0	19.1	92.3	0.27
		SR	30,000	155.9	15.2	62.9	nil
		R ₂₅₀₀	27,500	0.9	45.1	94.5	-
		R ₂₅₀₀	22,000	10.1	46.6	94.8	2.2
		R ₂₅₀₀	17,000	142.7	79.2	95.7	0.25

^adiscontinued^clow values probably caused by loss of vacuum for short time

TABLE C2 (continued)

CREEP-RUPTURE DATA ON ARC-CAST MOLYBDENUM-BASE ALLOYS
IN STRESS-RELIEVED AND RECRYSTALLIZED CONDITIONS
AT 1800 F

Heat	Alloy, %	Heat Treatment	Stress psi	Rupture Time, hr	Elong. %	Reduction of Area, %	Creep Rate % per hour
1009	1.26 Ti	SR	50,000	2.7	18.3	94.0	11.0
		SR	40,000	35.9	26.2	92.9	0.15
		SR	35,000	56.7	21.1	92.3	0.089
		R ₂₉₀₀	47,000	on loading	38.9	95.4	-
		R ₂₉₀₀	40,000	57.9	24.2	94.7	0.02
		R ₂₉₀₀	35,000	231.0	17.3	91.4	0.002
1051	0.54 V	SR	50,000	0.1	16.0	90.1	-
		SR	38,000	4.4	18.7	88.3	-
		SR	28,000	38.0	20.7	90.0	0.11
		R ₂₁₀₀	30,000	0.2	62.8	91.0	-
		R ₂₁₀₀	20,000	11.6	66.5	90.8	2.4
		R ₂₁₀₀	15,000	108.9	58.3	90.7	0.26
1012	0.56 V	SR	42,000	1.4	14.5	92.9	-
		SR	35,000	6.9	17.5	90.8	0.34
		SR	25,000	50.8	19.7	92.6	0.12
		R ₂₁₅₀	32,000	0.1	58.1	89.4	-
		R ₂₁₅₀	25,000	2.1	57.4	93.7	12.5
		R ₂₁₅₀	17,500	120.6	77.3	94.1	0.24
1049	0.35 V 0.003 Ce 0.003 RE	SR	50,000	0.3	14.4	81.8	-
		SR	40,000	9.5	16.8	83.1	0.41
		SR	30,000	381.1 ^a	5.5	-	0.010
		R ₂₅₀₀	25,000	0.4	23.0	36.2	-
		R ₂₅₀₀	20,000	7.1	29.1	28.2	0.23
		R ₂₅₀₀	16,000	85.6	15.1	39.6	0.11
1052	1.00 V	SR	55,000	0.2	14.5	89.1	-
		SR	45,000	4.1	15.5	88.0	0.82
		SR	35,000	42.3	19.5	86.4	-
		R ₂₁₅₀	25,000	5.9	60.2	87.7	5.0
		R ₂₁₅₀	20,000	43.9	43.7	85.7	0.54
		R ₂₁₅₀	17,000	197.4	48.3	91.8	0.14
1151	1.25 V	SR	50,000	2.3	18.9	91.8	1.3
		SR	38,000	36.7	18.9	89.4	0.14
1207	0.09 Zr	SR	70,000	0.9	15.3	79.0	-
		SR	60,000	43.8	16.8	74.9	0.13
		SR	56,000	109.8	17.2	79.5	0.05
		R ₂₇₅₀	40,000	on loading	46.6	91.8	-
		R ₂₇₅₀	30,000	26.7	40.9	90.6	0.70
		R ₂₇₅₀	27,500	102.9	35.0	82.3	0.052

^adiscontinued

TABLE C2 (continued)

CREEP-RUPTURE DATA ON ARC-CAST MOLYBDENUM-BASE ALLOYS
IN STRESS-RELIEVED AND RECRYSTALLIZED CONDITIONS
AT 2000 F

Tests conducted by Battelle Memorial Institute

Heat	Alloy, %	Heat Treatment	Stress psi	Rupture Time, hr	Elong. %	Reduction of Area, %	Creep Rate % per hour
937	0.015 C	SR	25,000	1.7	19.5	92.3	-
		SR	17,500	10.0 ^c	16.0	33.5	-
		SR	12,000	232.1 ^a	6.4	-	0.023
		R ₂₁₅₀	17,500	0.15	60.1	83.1	-
		R ₂₁₅₀	12,000	5.3	41.3	63.0	3.0
1045	0.003 C 0.005 Ce 0.007 RE	SR	35,000	1.1	13.8	84.6	2.5
		SR	12,000	137.0	34.4	90.0	0.080
		R ₂₄₀₀	20,000	0.1	38.7	95.0	-
		R ₂₄₀₀	11,000	176.0	24.0	5.3	0.044
1063	0.17 Al	SR	30,000	0.4	21.6	89.2	6.0
		SR	20,000	1.0	41.6	84.0	2.0
		SR	11,000	69.7	25.6	15.2	0.084
		R ₂₂₀₀	18,000	0.5	64.7	83.6	-
		R ₂₂₀₀	14,000	2.8	50.9	40.1	4.5
		R ₂₂₀₀	9,500	85.2	46.6	82.0	0.20
987	0.53 Al	SR	35,000	0.7	25.0	83.0	2.8
		SR	14,000	37.0	38.7	84.2	0.15
		SR	11,000	136.9	23.6	80.5	0.04
		R ₂₂₀₀	23,000	0.5	67.8	97.1	-
		R ₂₂₀₀	15,000	11.2	70.2	91.9	2.0
		R ₂₂₀₀	10,000	112.8	51.5	83.8	0.095
988	0.24 Nb	SR	35,000	0.9	11.5	87.5	-
		SR	15,000	23.4	43.9	82.9	0.13
		SR	10,000	258.8 ^a	12.7	-	0.045
		R ₂₂₀₀	23,000	0.1	54.6	94.3	-
		R ₂₂₀₀	15,000	4.8	37.0	48.6	5.6
		R ₂₂₀₀	10,000	225.8 ^a	37.0	-	0.091
978	0.52 Nb	SR	50,000	1.4	15.1	82.6	-
		SR	35,000	3.8	14.1	87.4	-
		SR	15,000	139.8	39.4	72.2	0.04
		R ₂₂₀₀	27,500	0.2	44.4	88.1	-
		R ₂₂₀₀	17,500	32.8 ^a	-	-	0.84
		R ₂₂₀₀	15,000	109.3	44.1	86.8	0.18

^adiscontinued^cspecimen overheated, rupture time estimated

TABLE C2 (continued)

CREEP-RUPTURE DATA ON ARC-CAST MOLYBDENUM-BASE ALLOYS
IN STRESS-RELIEVED AND RECRYSTALLIZED CONDITIONS
AT 2000 F

Heat	Alloy, %	Heat Treatment	Stress psi	Rupture Time, hr	Elong. %	Reduction of Area, %	Creep Rate % per hour
1057	0.75 Nb	SR	55,000	0.8	19.7	84.9	-
		SR	45,000	6.5	16.8	84.2	0.33
		SR	20,000	139.2	48.0	46.4	0.13
		R2250	32,500	0.12	56.0	88.2	-
		R2250	25,000	7.4	48.4	79.3	0.40
		R2250	20,000	49.9	48.0	72.2	0.46
1132	0.45 Ti	SR	70,000	0.2	12.1	79.8	-
		SR	50,000	6.7	19.2	87.6	0.52
		SR	20,000	261.6 ^a	2.4	-	0.004
		R2450	30,000	0.3	48.3	79.7	-
		R2450	25,000	4.4	51.7	86.7	6.0
		R2450	18,000	280.0 ^a	12.6	-	0.023
1048	0.69 Ti 0.12 RE	SR	55,000	on loading	14.4	87.0	-
		SR	30,000	5.8	16.8	61.8	0.25
		SR	15,000	212.7 ^a	3.2	-	-
		R2500	25,000	0.2	34.8	72.3	-
		R2500	17,500	4.3	12.0	45.6	1.05
		R2500	12,000	36.7	3.9	4.6	0.037
1133	0.85 Ti	SR	45,000	0.4	16.6	92.1	-
		SR	35,000	4.5	17.6	88.2	0.50
		SR	18,600	214.0 ^a	5.7	-	0.0012
		R2500	26,000	0.6	40.6	84.3	-
		R2500	22,000	2.0	31.7	26.7	5.5
		R2500	14,000	228.8 ^a	10.9	-	-
1009	1.26 Ti	SR	40,000	1.4	19.5	96.0	1.3
		SR	35,000	7.5	22.6	89.2	0.60
		SR	20,000	93.3	21.6	84.0	0.044
		R2900	40,000	2.0	21.2	87.7	0.75
		R2900	35,000	7.2	22.8	86.1	0.18
		R2900	26,000	41.1	20.0	90.0	0.018
1051	0.54 V	SR	42,000	on loading	23.0	89.8	-
		SR	25,000	1.3	16.0	90.0	1.70
		SR	10,000	198.6	48.0	74.0	0.072
		R2100	22,000	0.2	62.6	91.6	-
		*R2100	11,000	75.0	50.0	87.2	0.21
		*R2100	11,000	72.3	49.5	87.9	0.21

^adiscontinued

*these two specimens were tested at the same stress by mistake

TABLE C2 (continued)

CREEP-RUPTURE DATA ON ARC-CAST MOLYBDENUM-BASE ALLOYS
IN STRESS-RELIEVED AND RECRYSTALLIZED CONDITIONS
AT 2000 F

Heat	Alloy, %	Heat Treatment	Stress psi	Rupture Time, hr	Elong. %	Reduction of Area, %	Creep Rate % per hour
1012	0.56 V	SR	25,000	2.2	35.0	88.2	1.10
		SR	17,500	11.6	84.8	84.3	0.70
		SR	11,000	265.0 ^a	10.3	-	0.018
		R ₂₁₅₀	23,000	0.3	58.4	90.0	-
		R ₂₁₅₀	17,500	3.7	52.8	89.0	4.8
		R ₂₁₅₀	12,000	125.0	44.8	85.5	0.002
1049	0.85 V 0.003 Ce 0.003 RE	SR	45,000	0.12	15.9	85.1	-
		SR	25,000	39.8	18.4	75.0	0.018
		SR	20,000	111.4	13.6	36.6	0.036
		R ₂₅₀₀	20,000	0.5	32.3	28.1	-
		R ₂₅₀₀	15,000	5.1	18.5	15.1	1.60
		R ₂₅₀₀	12,000	76.2	12.0	15.6	0.030
1052	1.00 V	SR	42,000	0.1	22.0	81.7	-
		SR	30,000	5.0	40.0	91.0	1.10
		SR	17,500	26.8	59.3	92.0	0.14
		R ₂₁₅₀	24,000	0.6	31.4	91.0	-
		R ₂₁₅₀	17,000	8.8	32.0	82.2	1.9
		R ₂₁₅₀	12,500	130.8	45.6	79.8	0.14
1207	0.09 Zr	SR	25,000	160.8 ^b	1.0	-	0.0028
		R ₂₇₅₀	18,500	175.6 ^a	4.1	-	0.006

^a discontinued^b failed in specimen holder

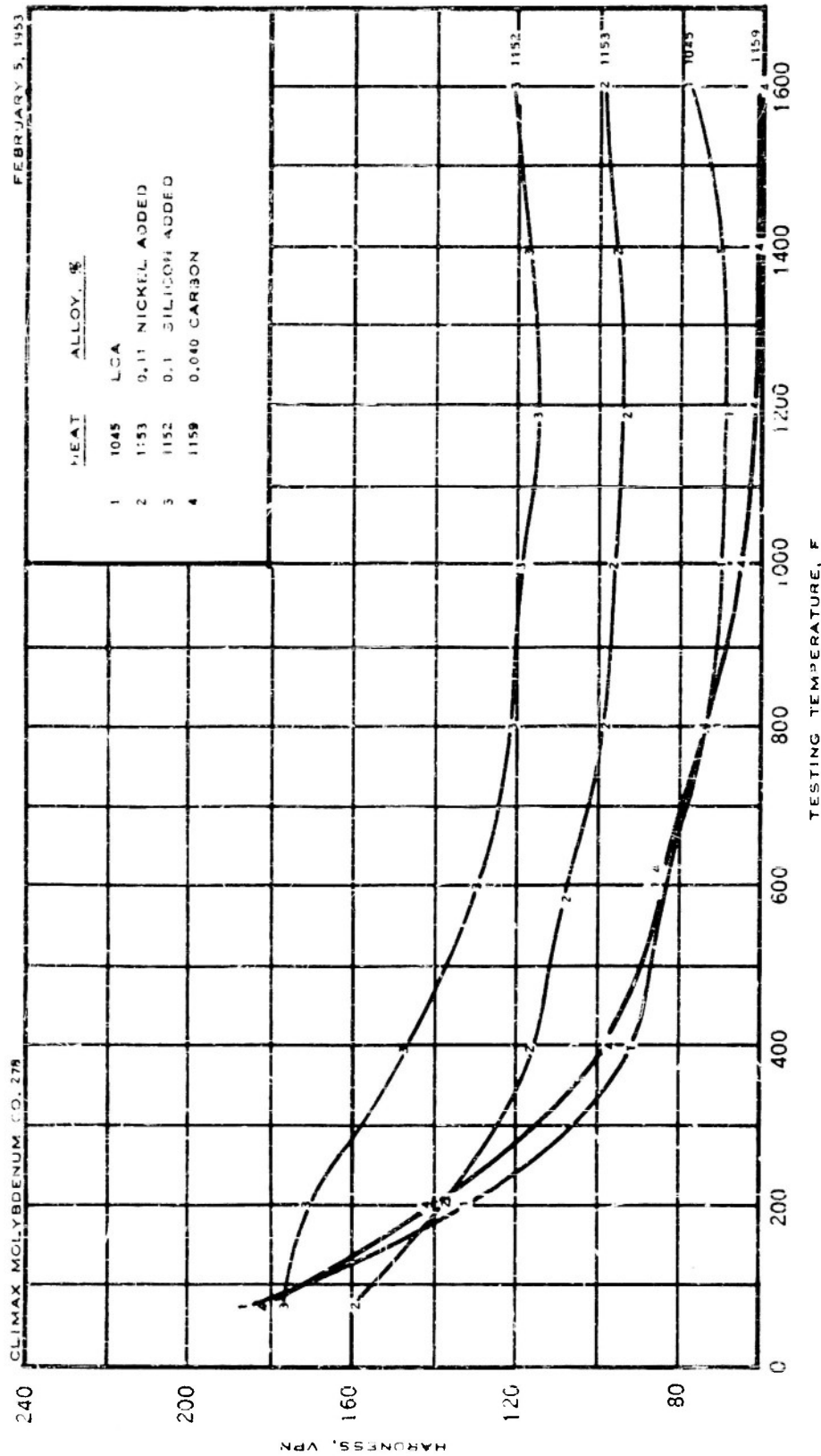


FIGURE C1 - HOT HARDNESS OF SOME MOLYBDENUM-BASE ALLOYS AS CAST

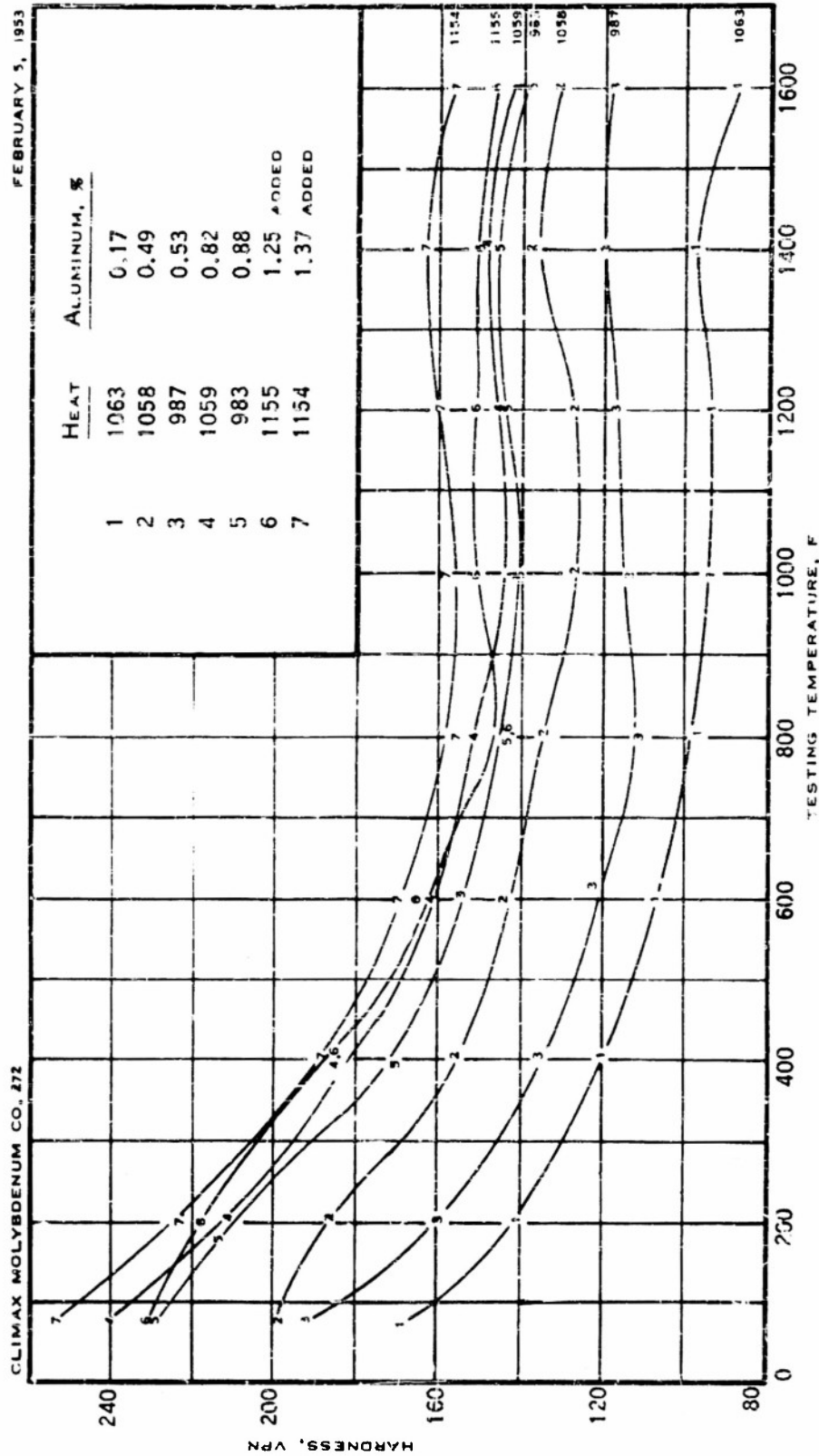


FIGURE C2 - HOT HARDNESS OF SOME MOLYBDENUM-ALUMINUM ALLOYS AS CAST

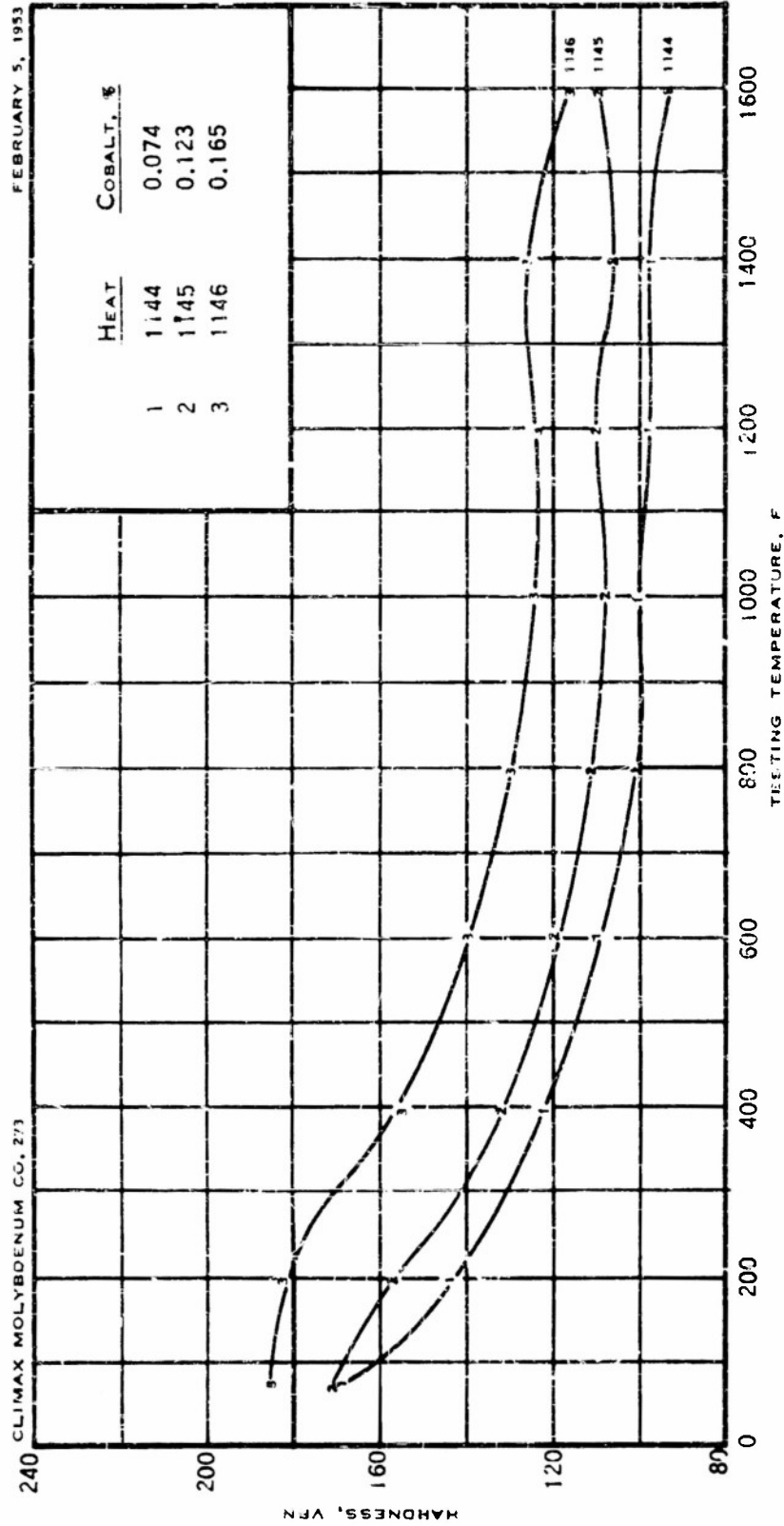


FIGURE C3 — HOT HARDNESS OF SOME MOLYBDENUM-COBALT ALLOYS AS CAST

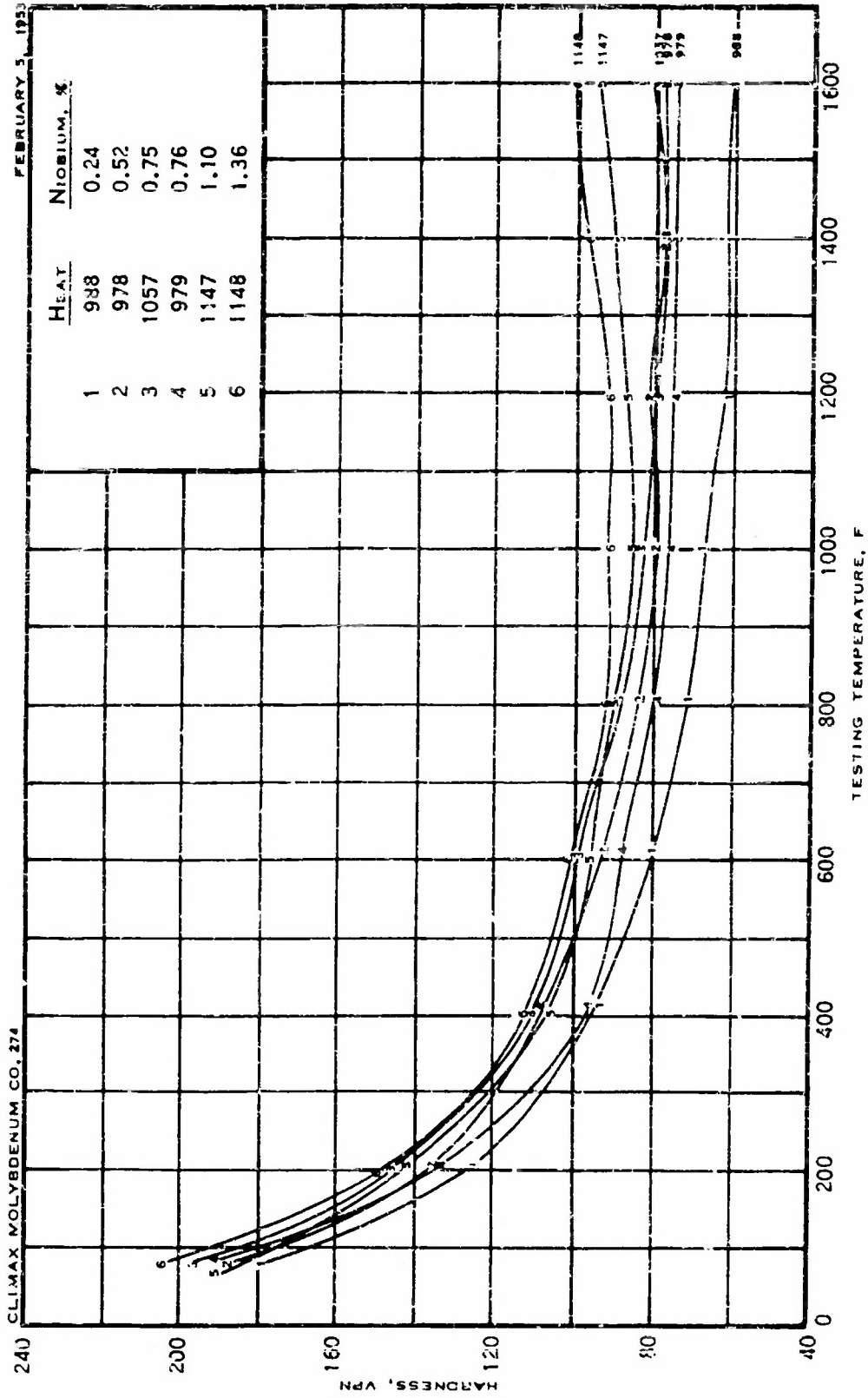


FIGURE C4 - HOT HARDNESS OF SOME MOLYBDENUM-NIOBIUM ALLOYS AS CAST

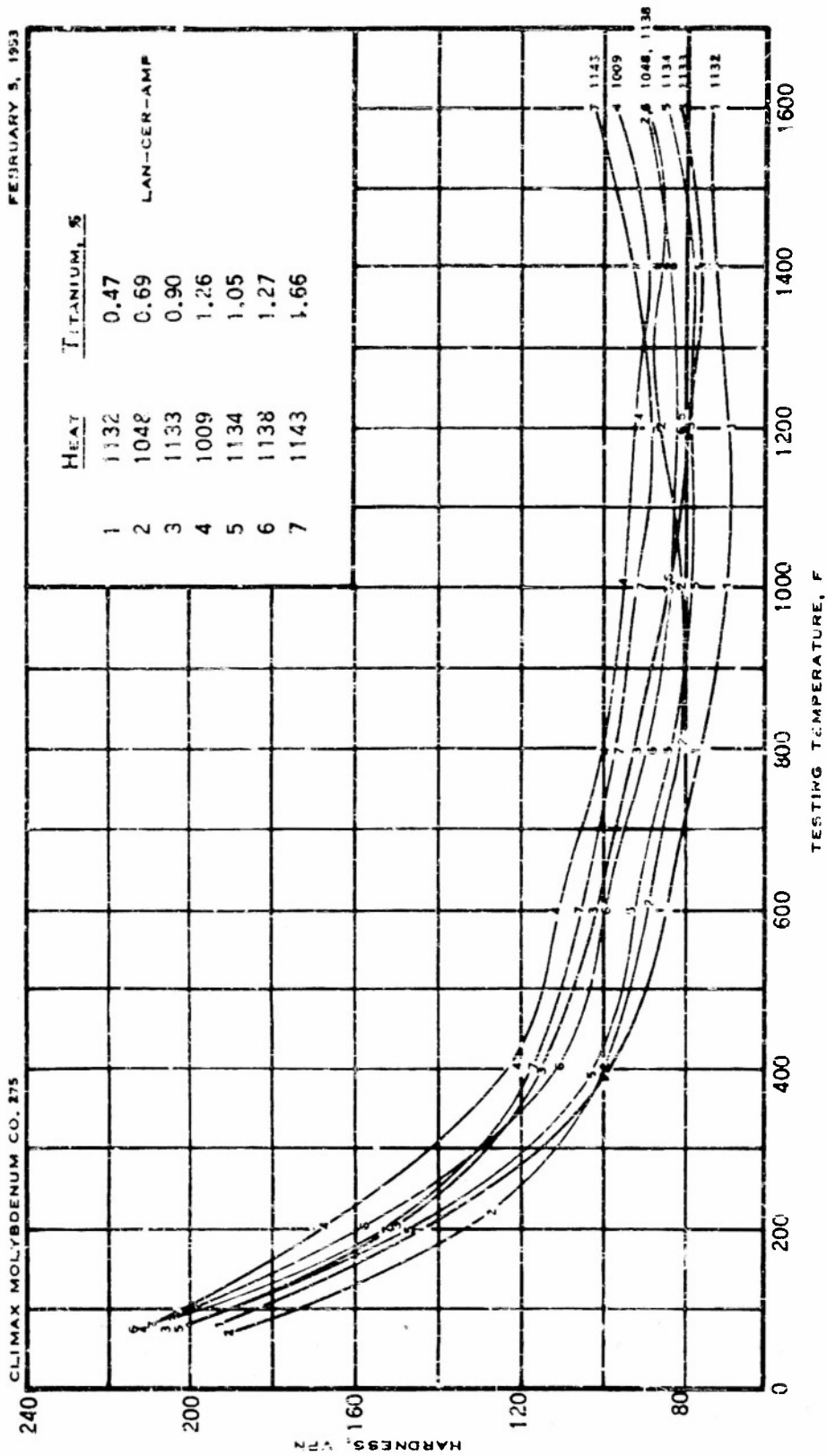


FIGURE C5 -- HOT HARDNESS OF SOME MOLYBDENUM-TITANIUM ALLOYS AS CAST

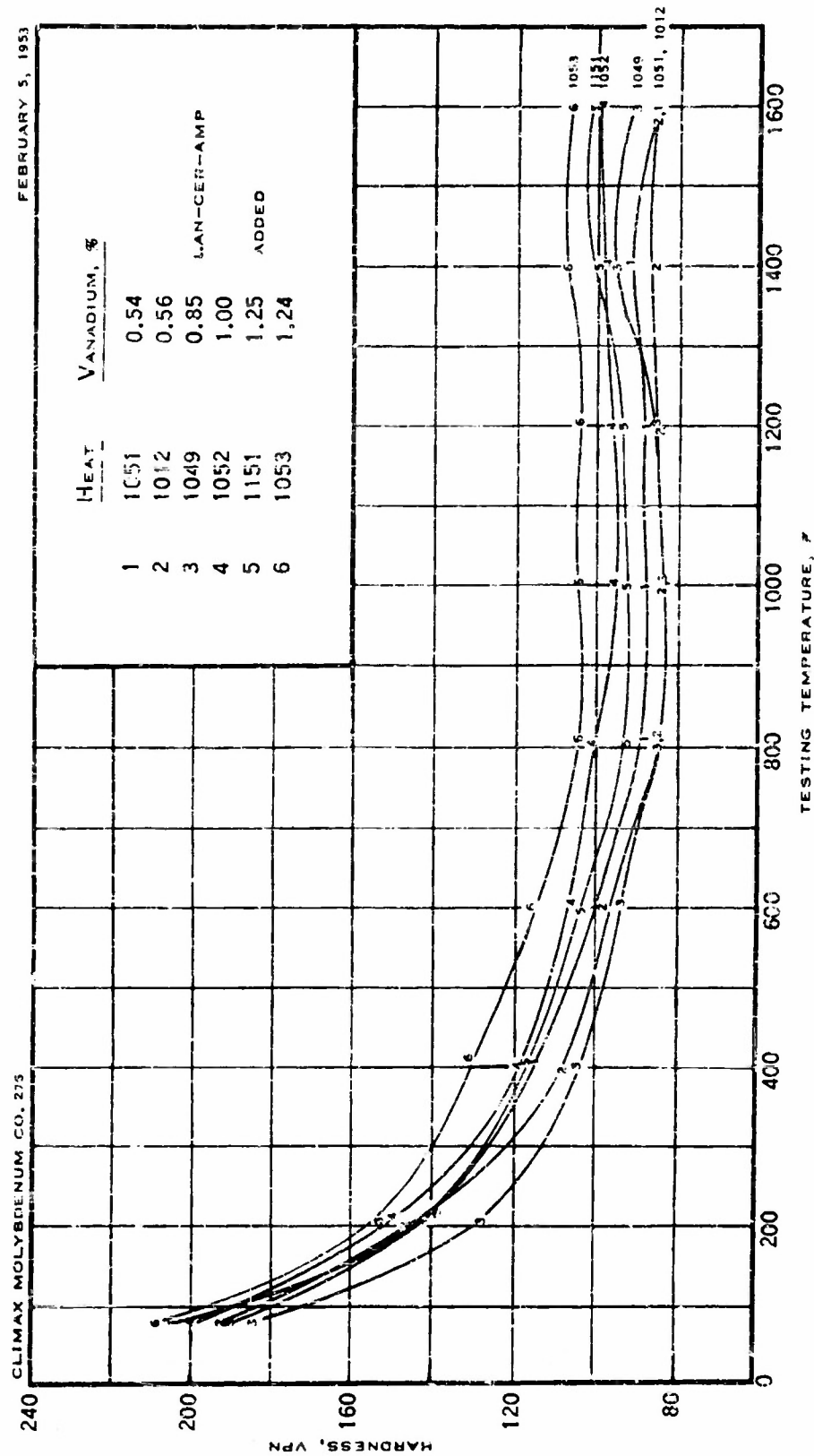


FIGURE C6 -- HOT HARDNESS OF SOME MOLYBDENUM-VANADIUM ALLOYS AS CAST

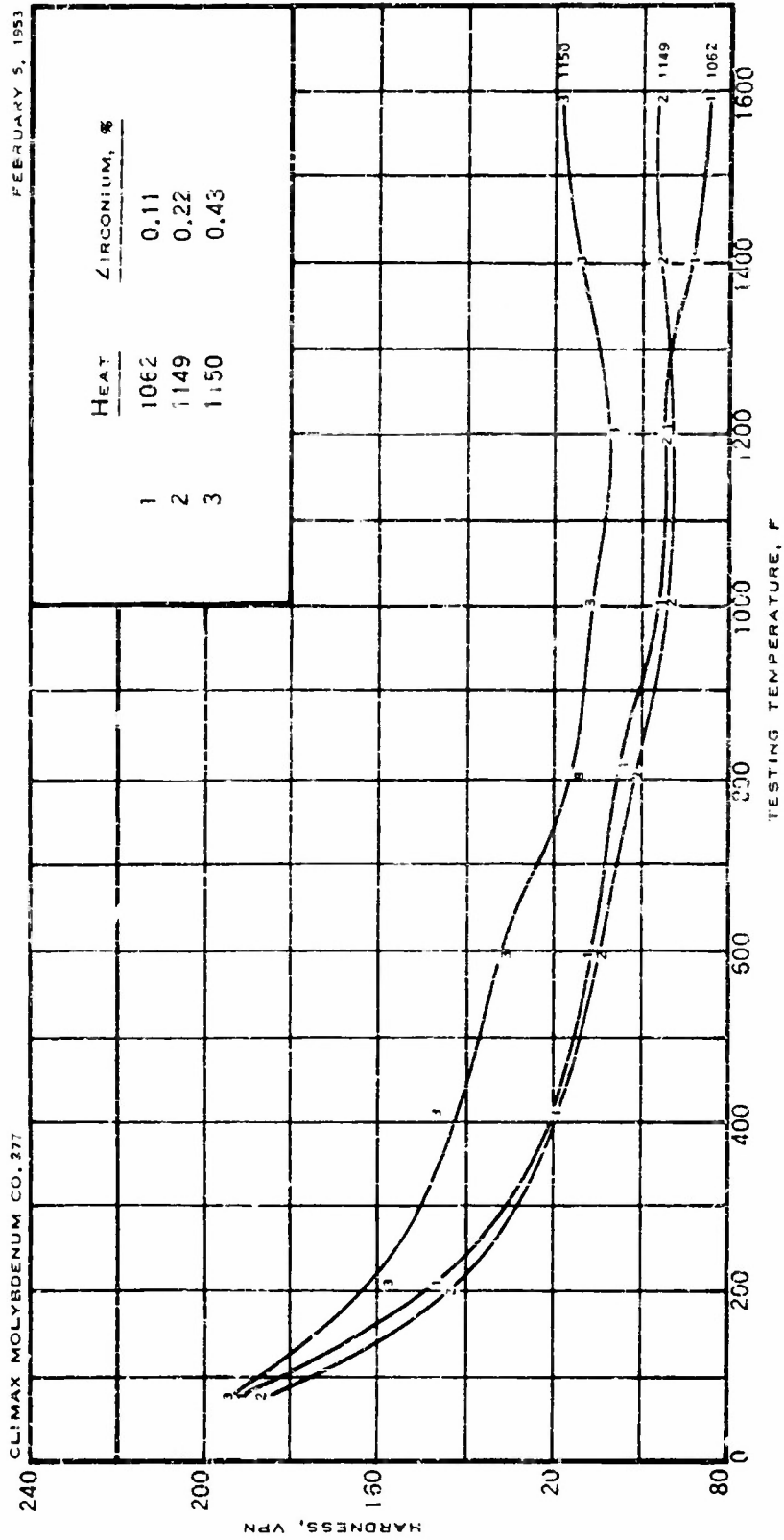


FIGURE C7 - HOT HARDNESS OF SOME MOLYBDENUM-ZIRCONIUM ALLOYS AS CAST

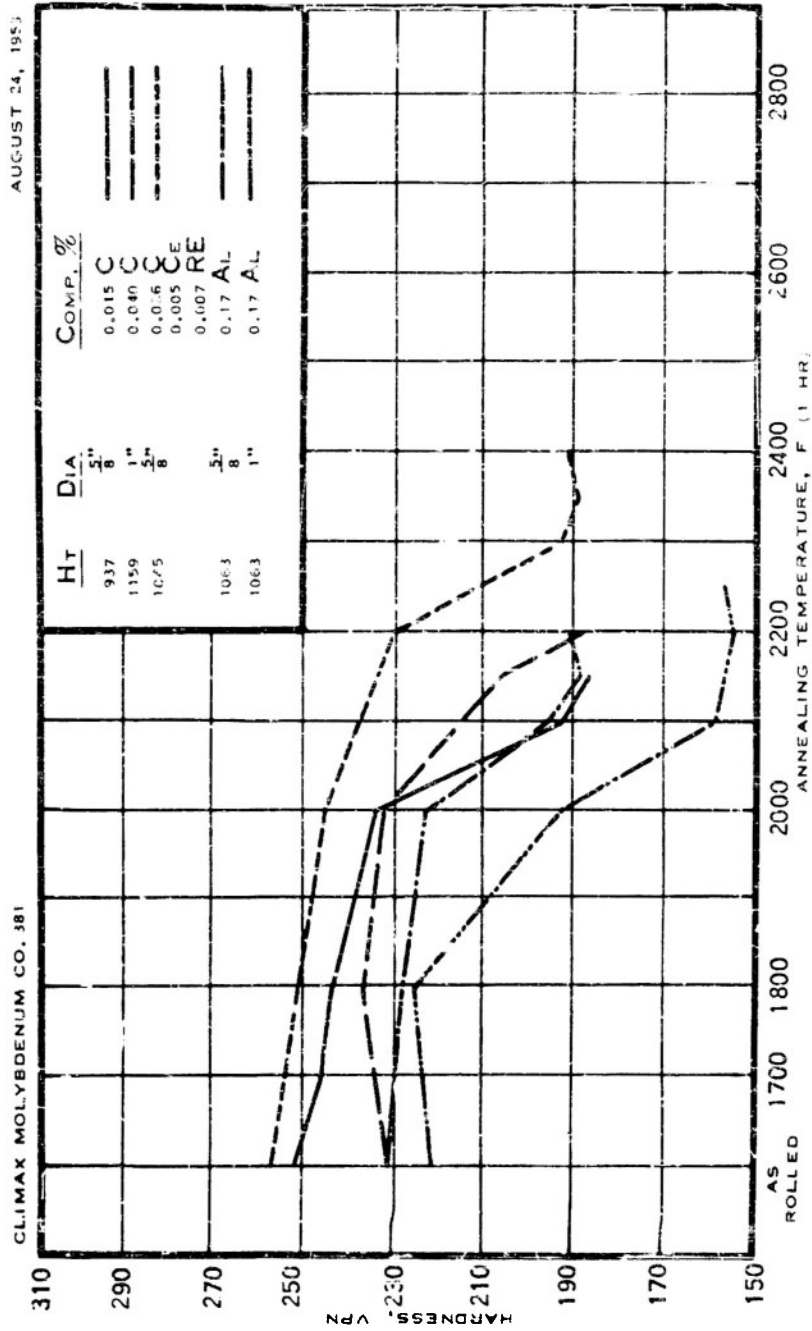


FIGURE C8 - HARDNESS VS ANNEALING TEMPERATURE FOR UNALLOYED MOLYBDENUM BARS

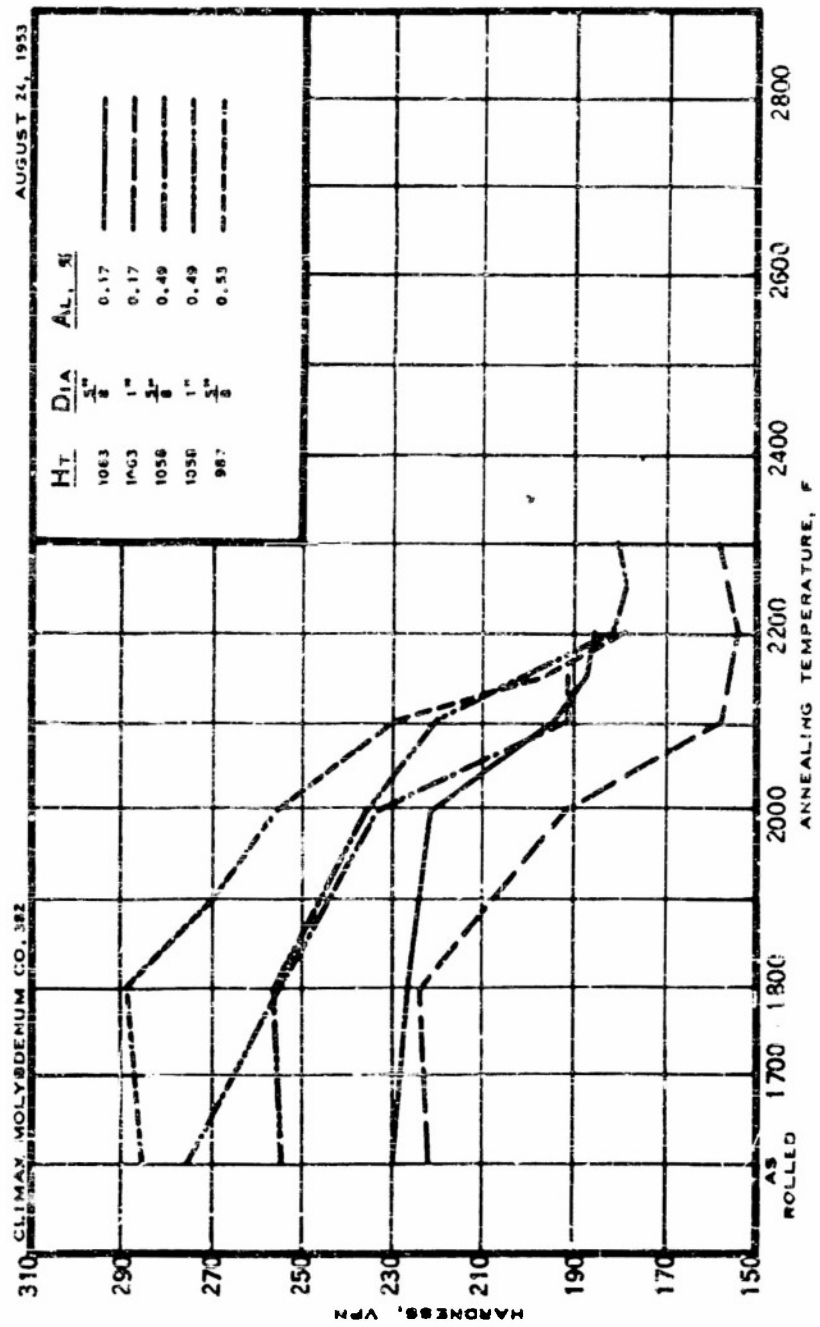


FIGURE C9 - HARDNESS VS ANNEALING TEMPERATURE FOR ALUMINUM - MOLYBDENUM ALLOY BARS

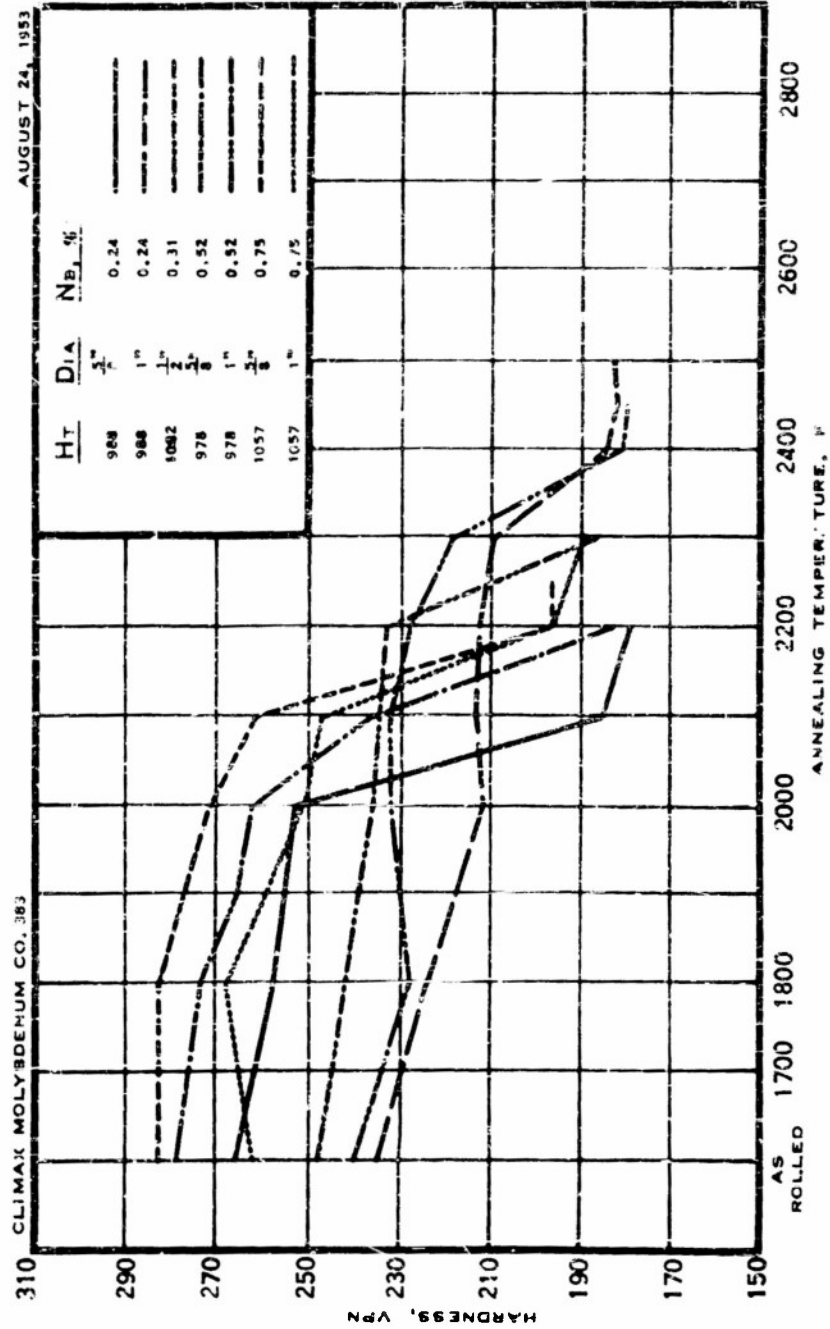
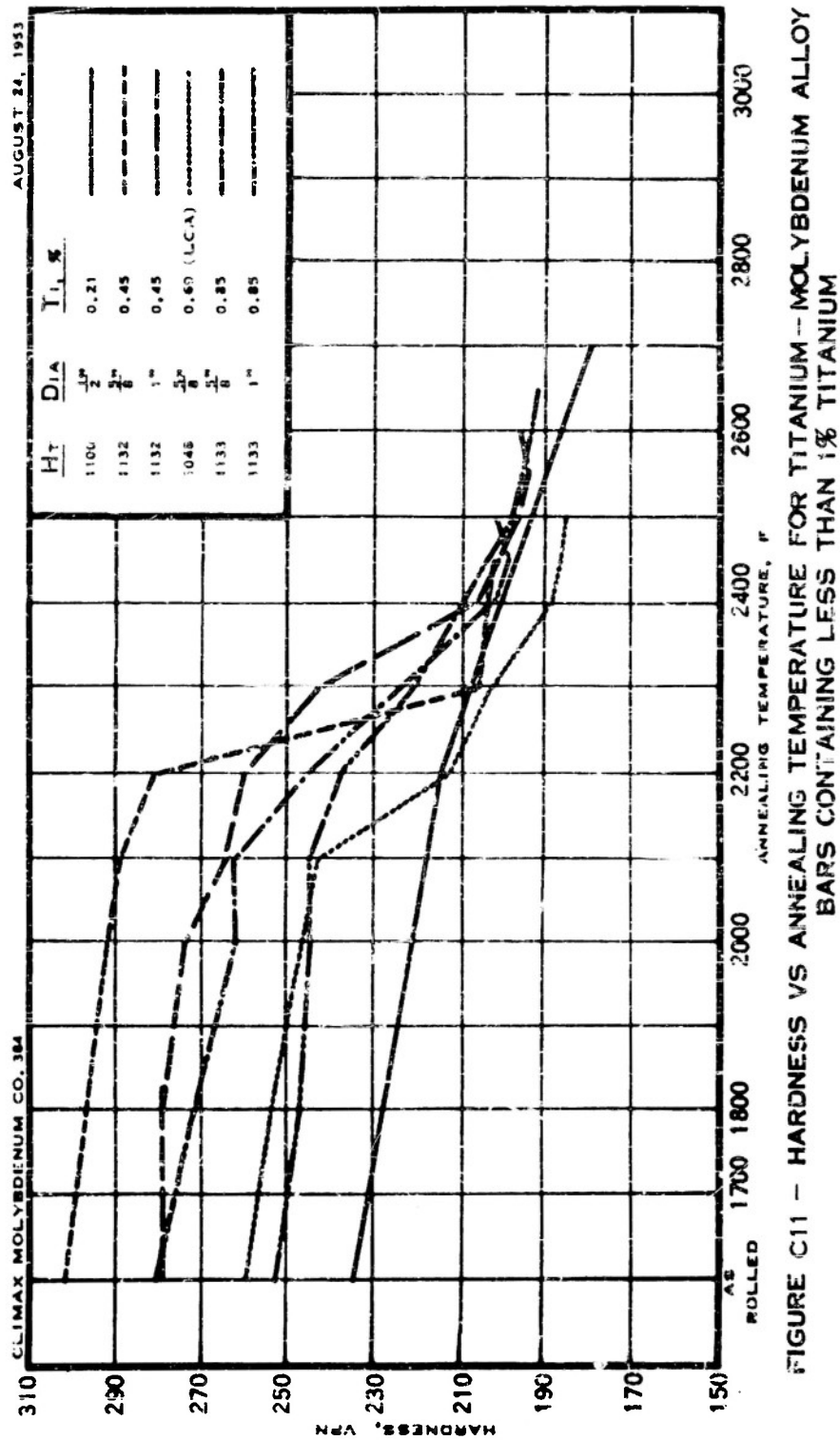


FIGURE C10 - HARDNESS VS ANNEALING TEMPERATURE FOR NIOBIUM - MOLYBDENUM ALLOY BARS



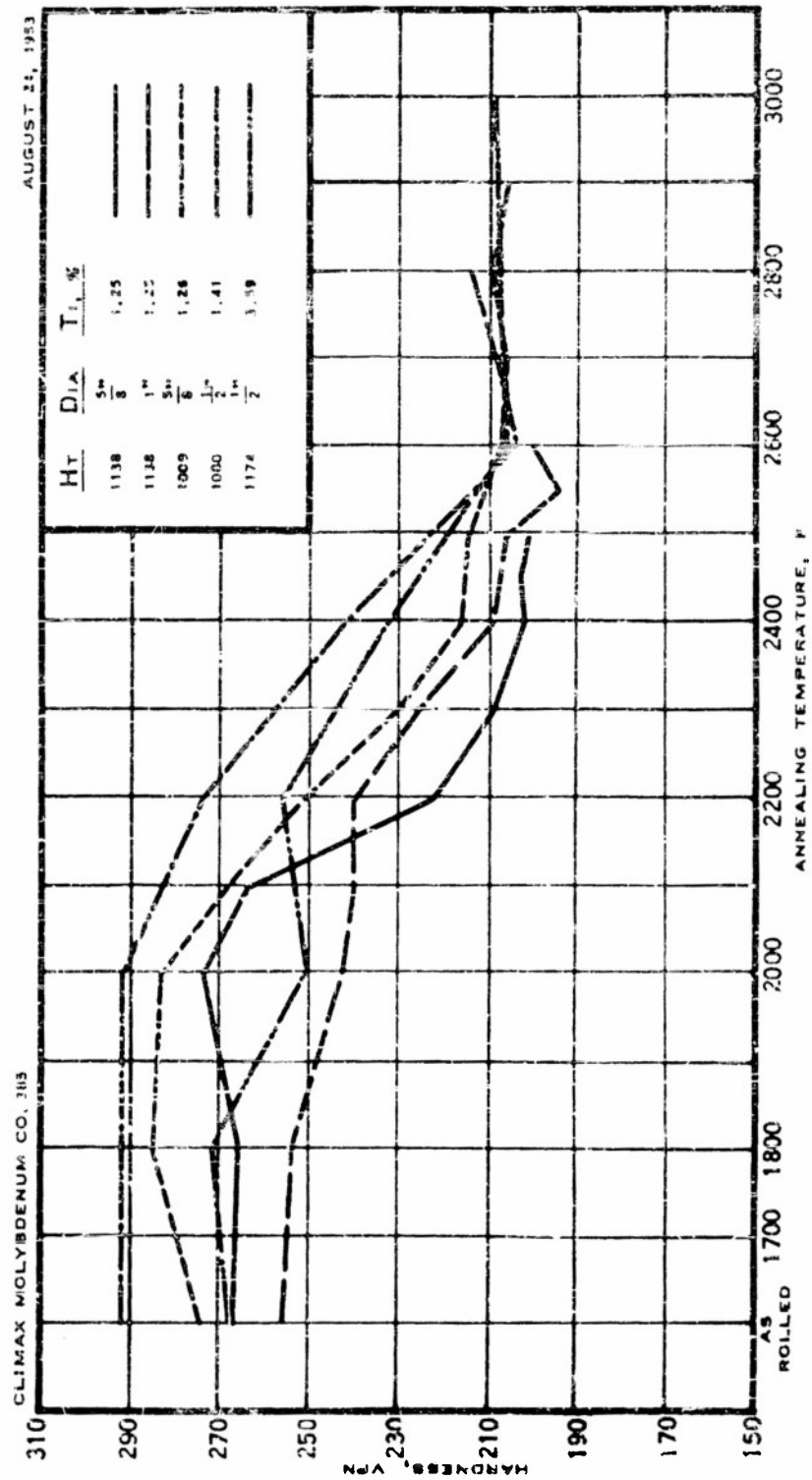


FIGURE C12 - HARDNESS VS ANNEALING TEMPERATURE FOR TITANIUM - MOLYBDENUM ALLOY
BARS CONTAINING IN EXCESS OF 1% TITANIUM

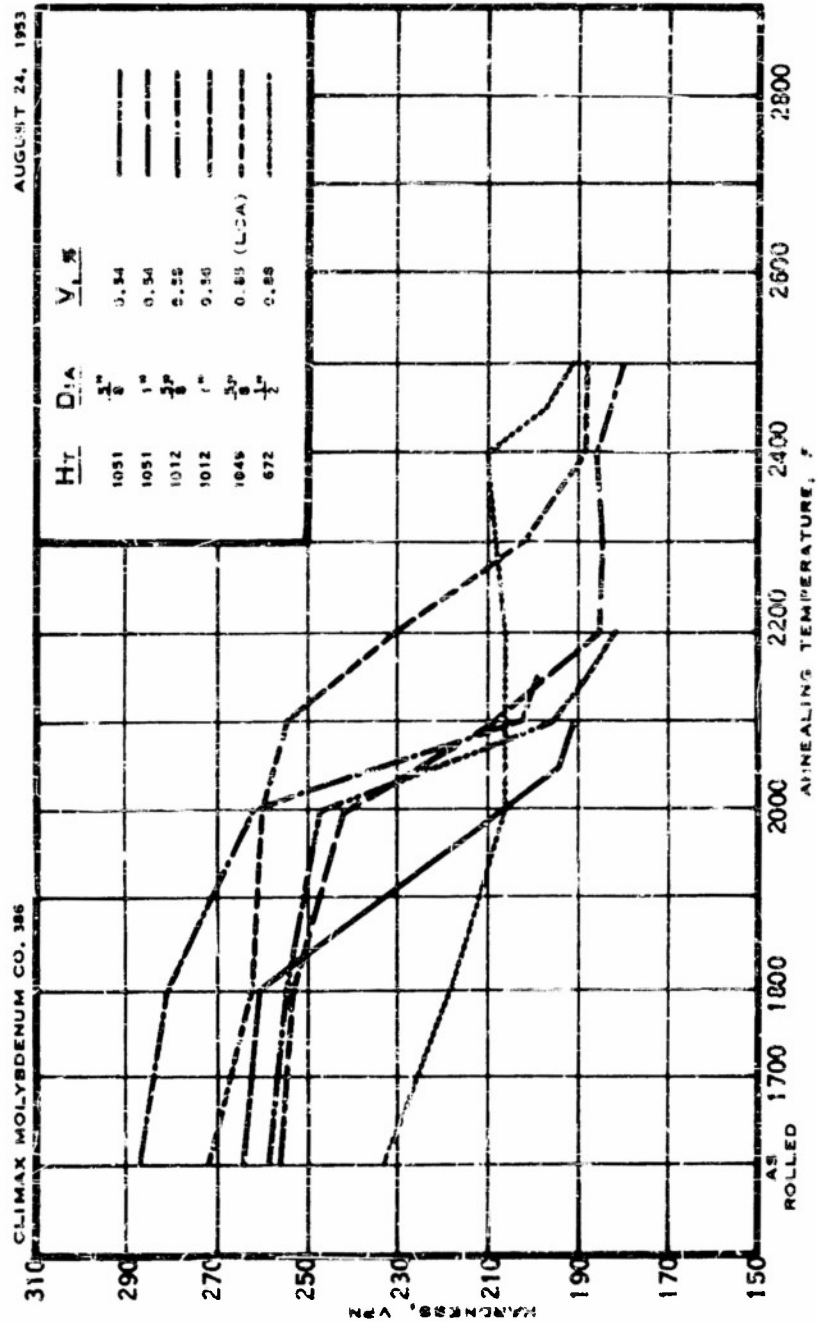


FIGURE C13-- HARDNESS VS ANNEALING TEMPERATURE FOR VANADIUM-MOLYBDENUM ALLOY BARS CONTAINING LESS THAN 1% VANADIUM

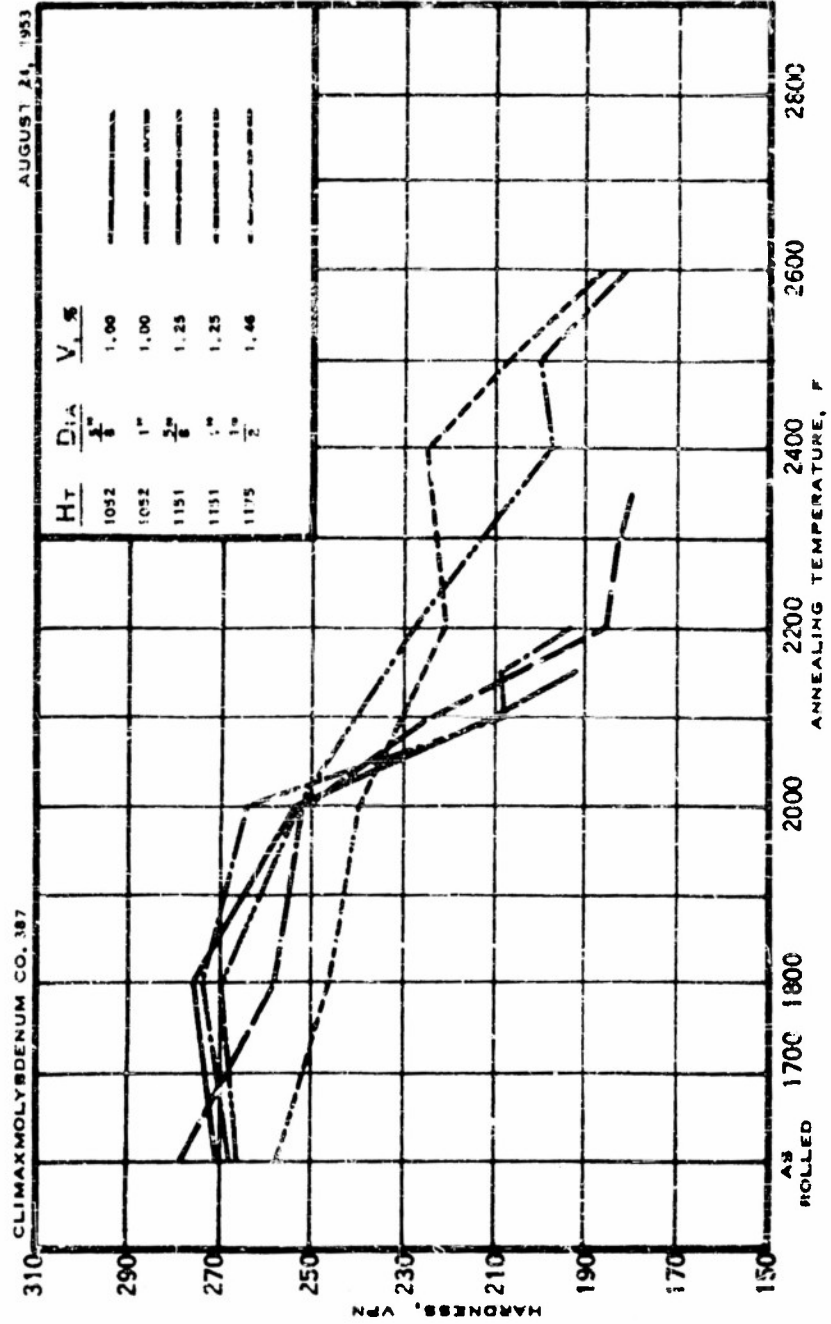


FIGURE C14 - HARDNESS VS ANNEALING TEMPERATURE FOR VANADIUM - MOLYBDENUM ALLOY
EARS CONTAINING IN EXCESS OF 1% VANADIUM

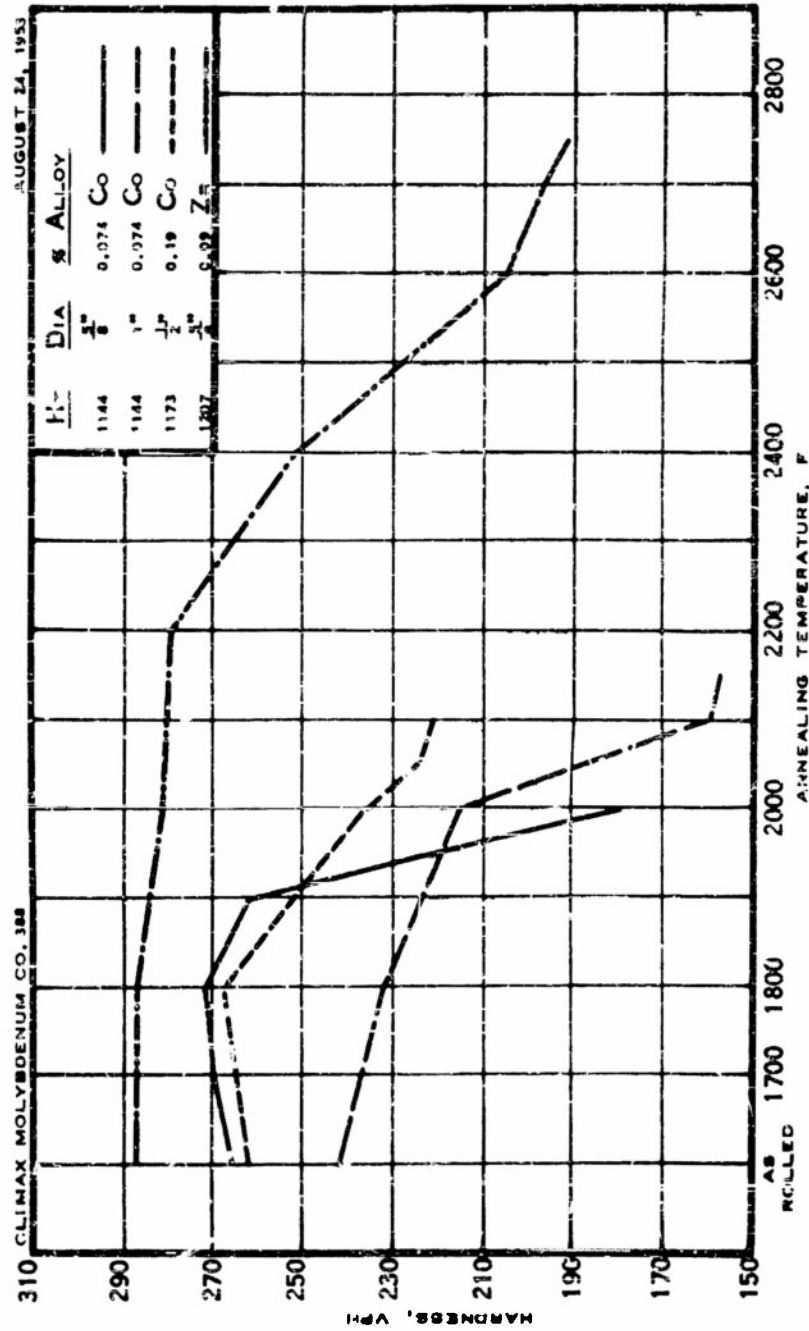


FIGURE C15 - HARDNESS VS ANNEALING TEMPERATURE FOR COBALT-MOLYBDENUM AND ZIRCONIUM-MOLYBDENUM ALLOY BARS

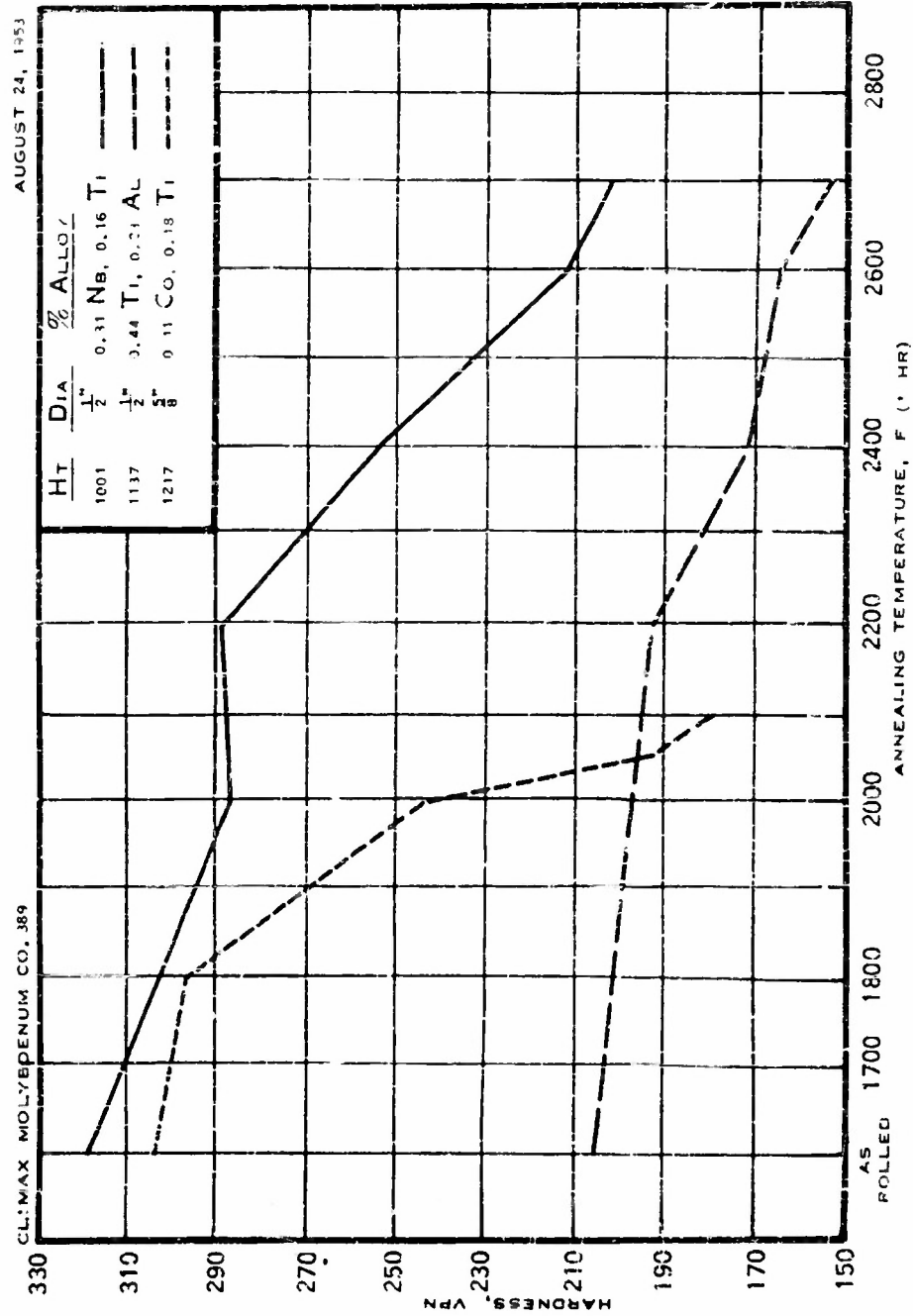


FIGURE C16 - HARDNESS VS ANNEALING TEMPERATURE FOR INDICATED MOLYBDENUM-BASE ALLOY BARS

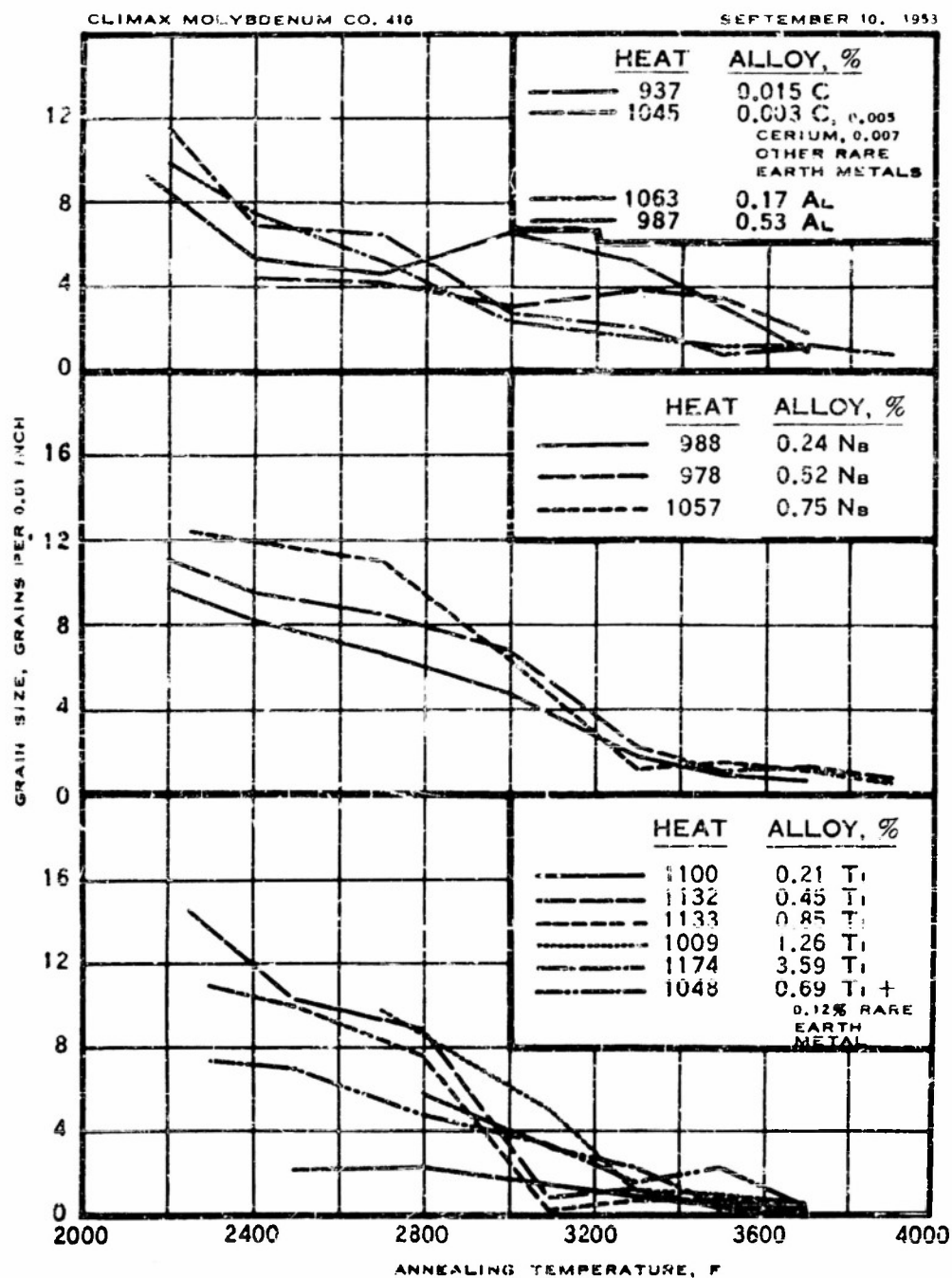


FIGURE C17 - EFFECT OF ANNEALING TEMPERATURE ON THE GRAIN SIZE OF INDICATED MOLYBDENUM-BASE ALLOYS

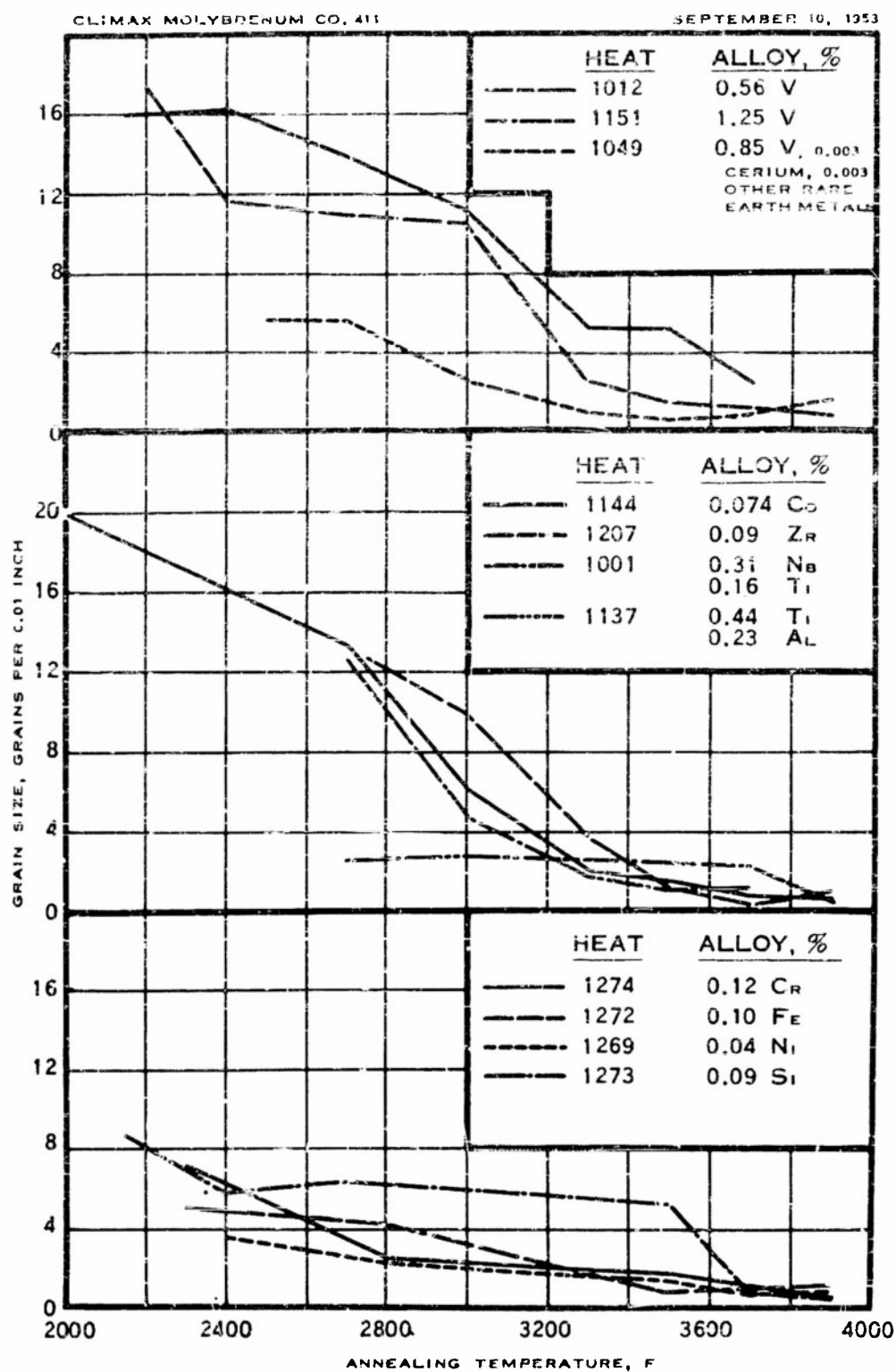


FIGURE C18 - EFFECT OF ANNEALING TEMPERATURE ON THE GRAIN SIZE OF INDICATED MOLYBDENUM-BASE ALLOYS

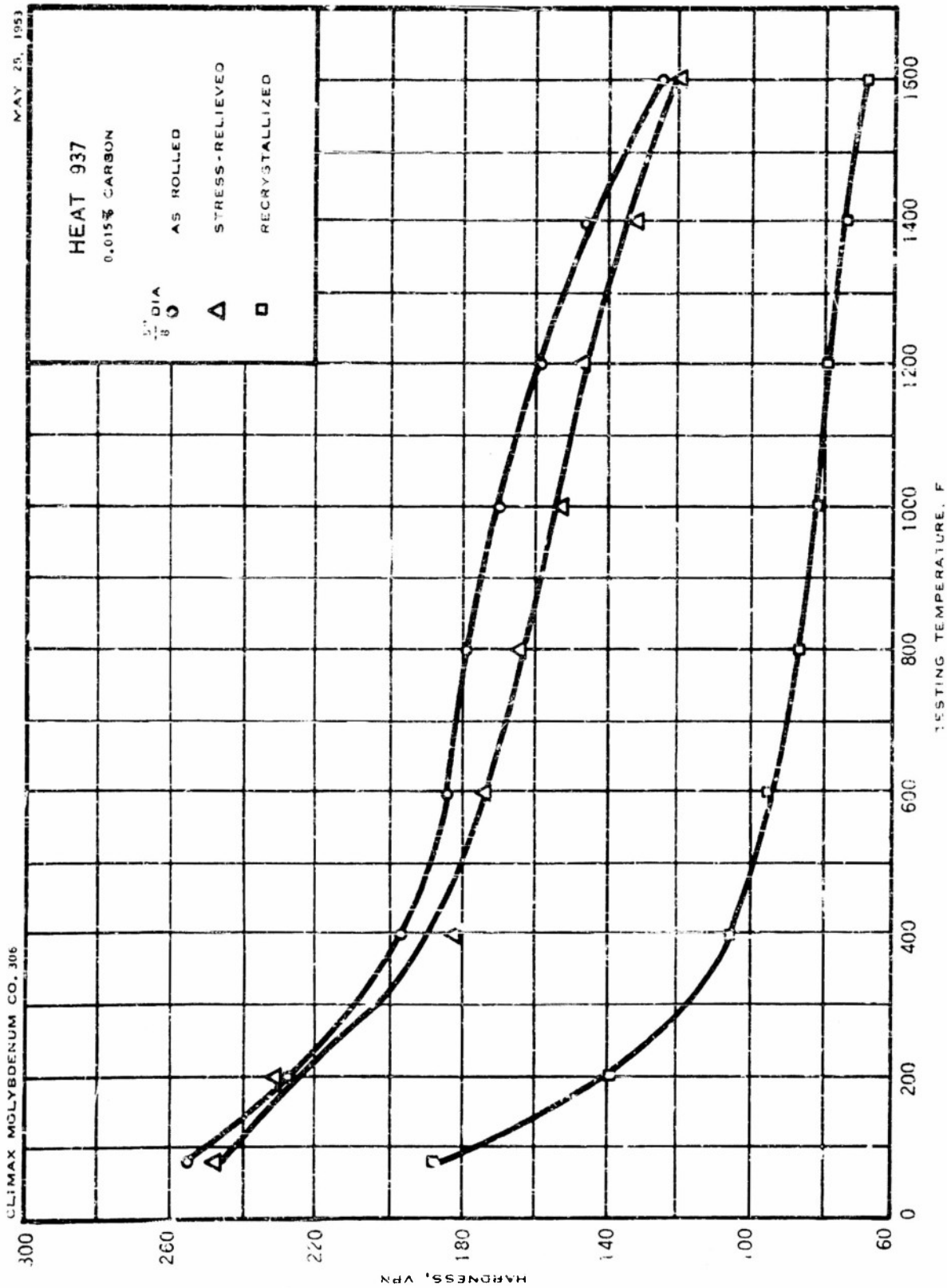


FIGURE C19 — HOT HARDNESS OF ROLLED BARS OF UNALLOYED MOLYBDENUM

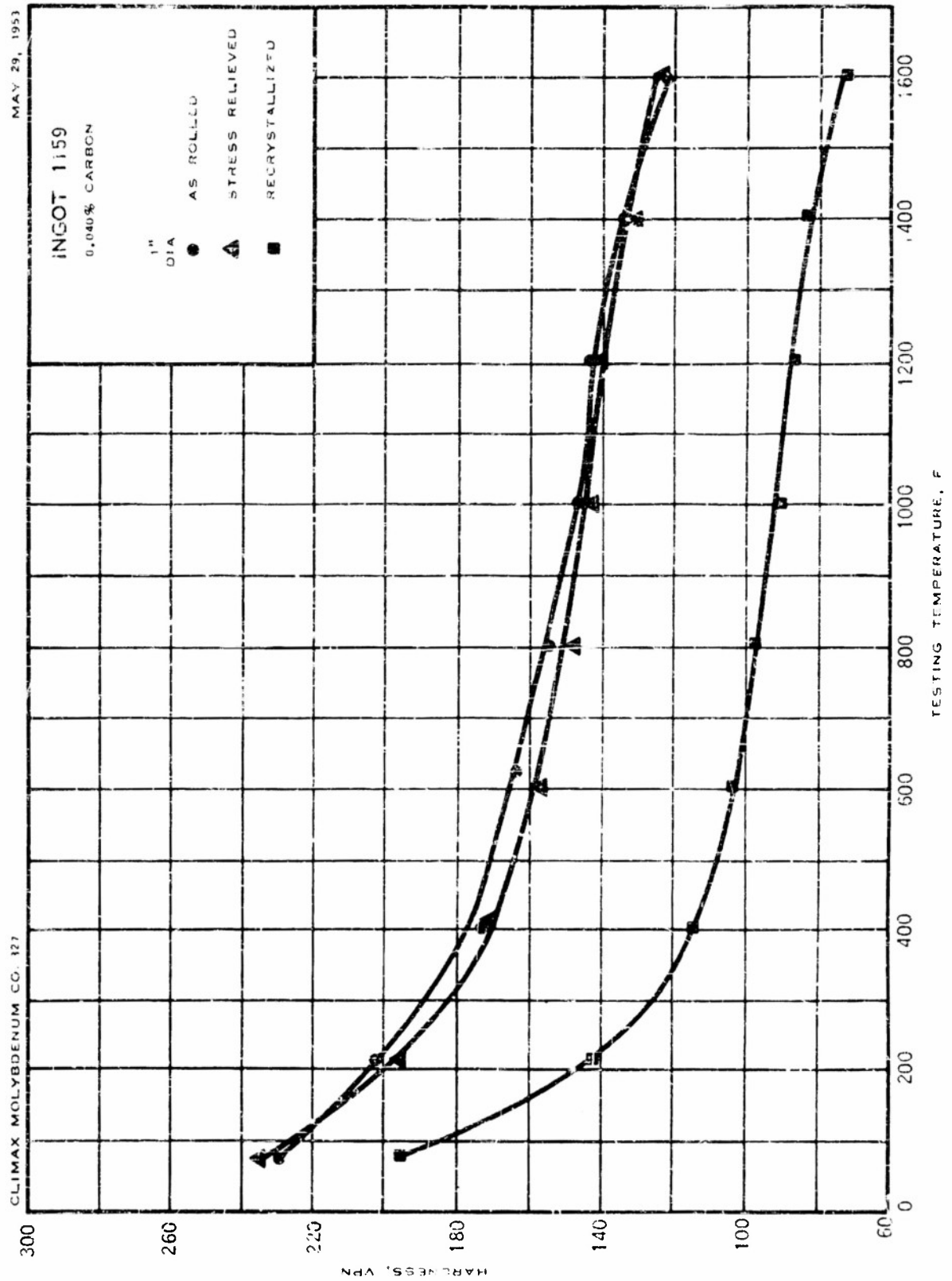


FIGURE C20 -- HOT HARDNESS OF ROLLED BARS OF UNALLOYED MOLYBDENUM

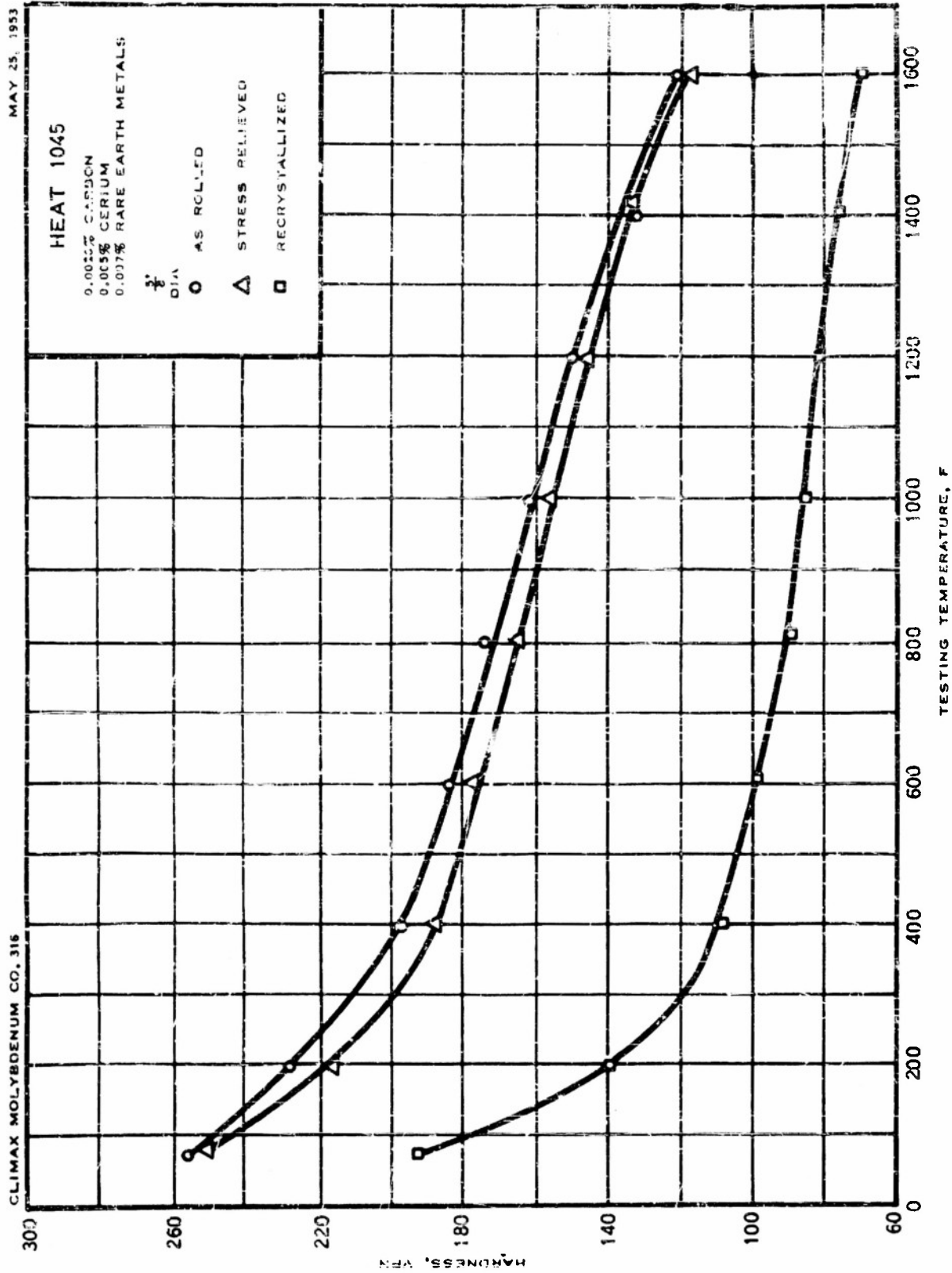


FIGURE C2.1 - HOT HARDNESS OF ROLLED BARS OF MOLYBDENUM DEOXIDIZED WITH RARE EARTH METALS

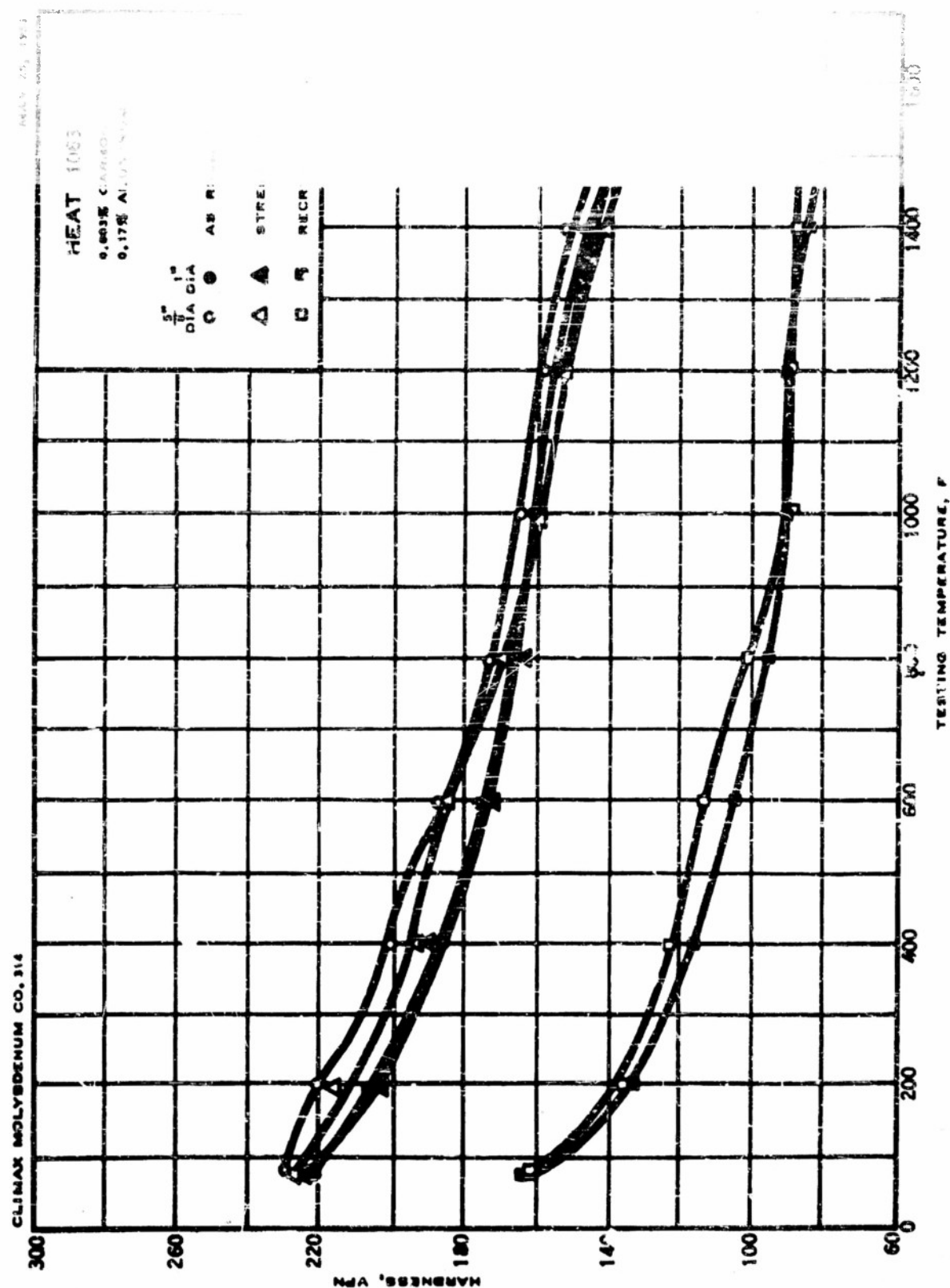


FIGURE C22 - HOT HARDNESS OF ROLLED BARS OF 0.17% ALUMINUM - MOLYBDENUM ALLOY

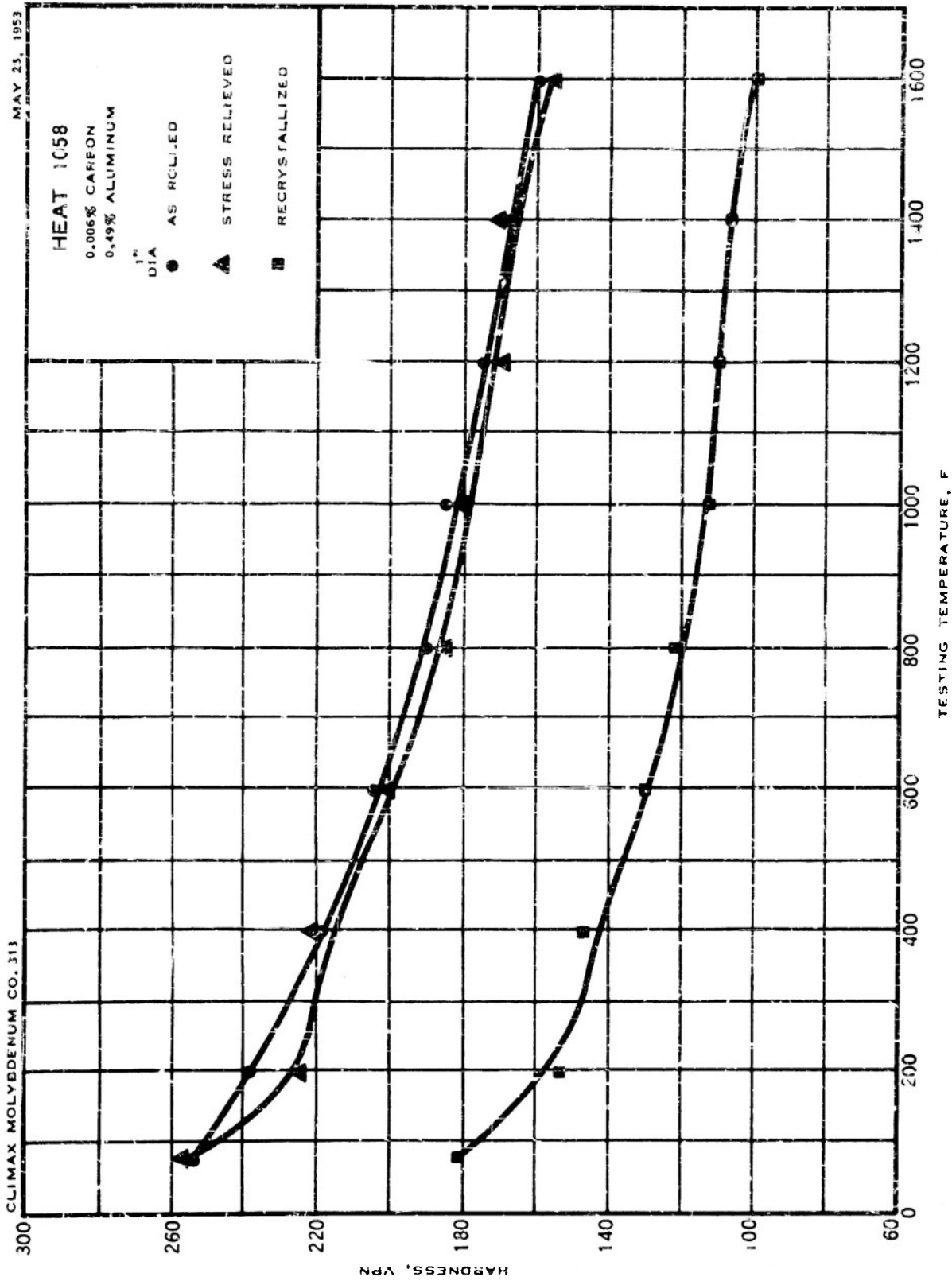


FIGURE C23— HOT HARDNESS OF ROLLED BARS OF 0.49% ALUMINUM— MOLYBDENUM ALLOY

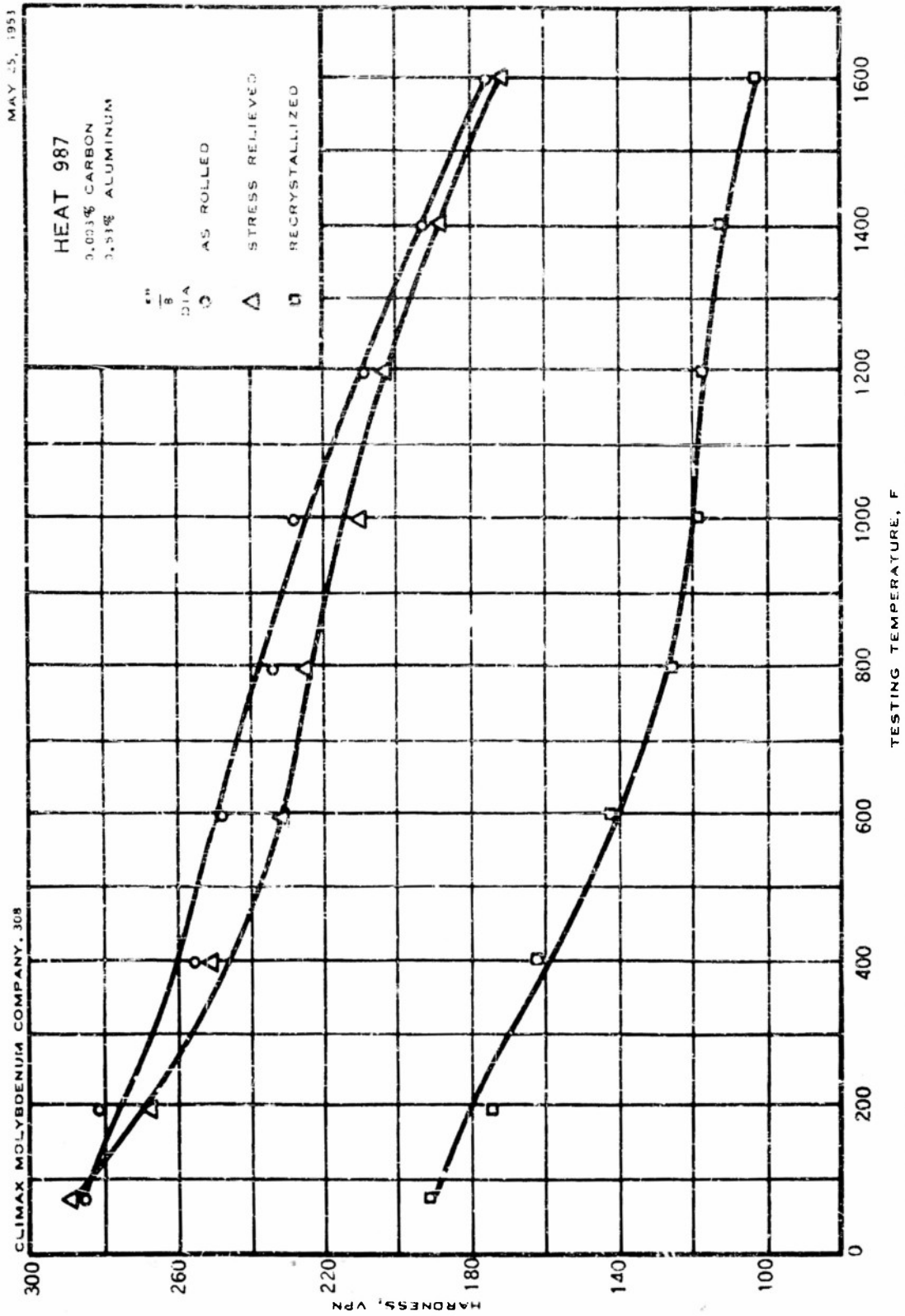


FIGURE C24 — HOT HARDNESS OF ROLLED BARS OF 0.53% ALUMINUM—MOLYBDENUM ALLOY

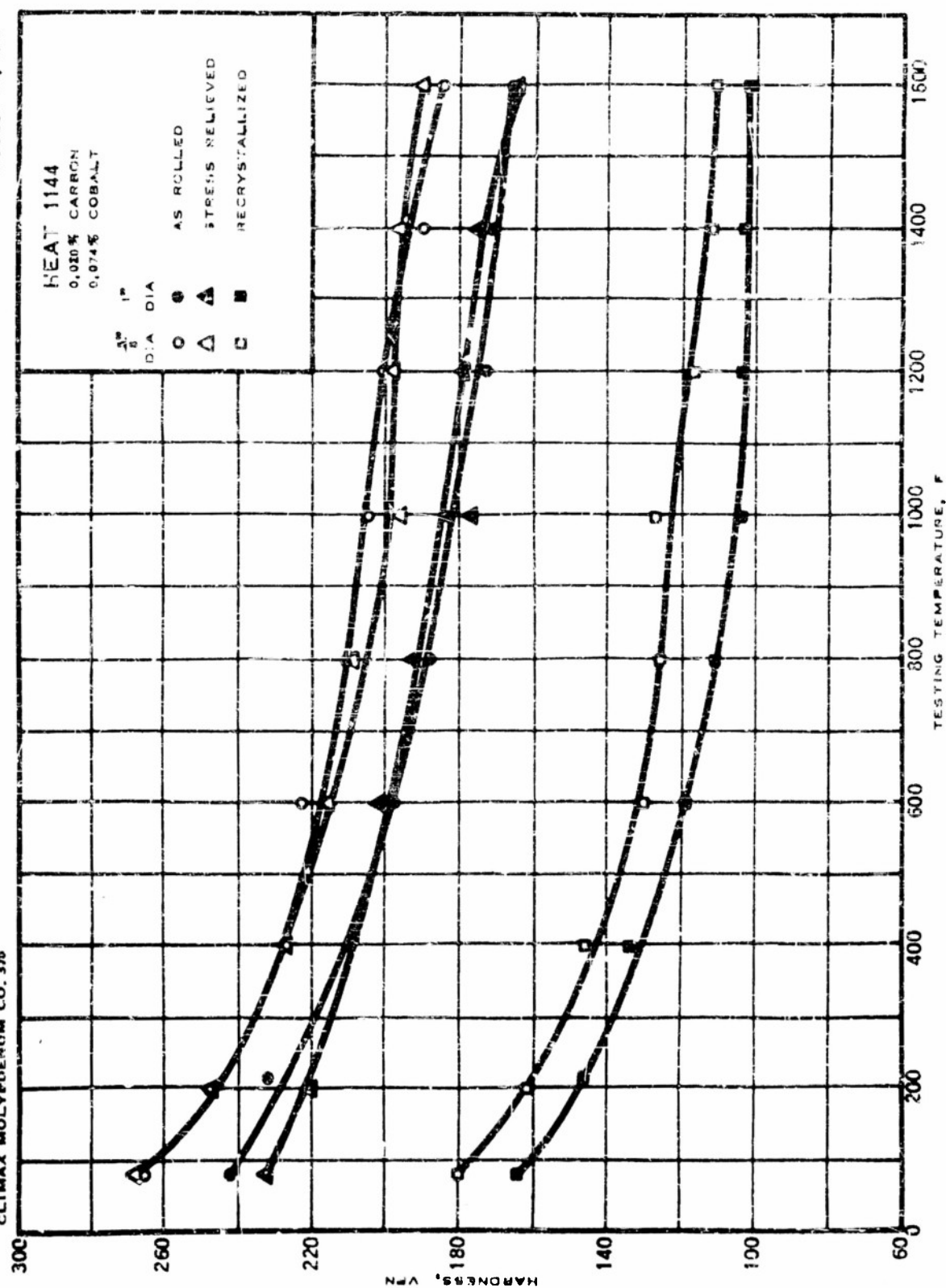


FIGURE C25—HOT HARDNESS OF ROLLED BARS OF 0.074% COBALT-MOLYBDENUM ALLOY

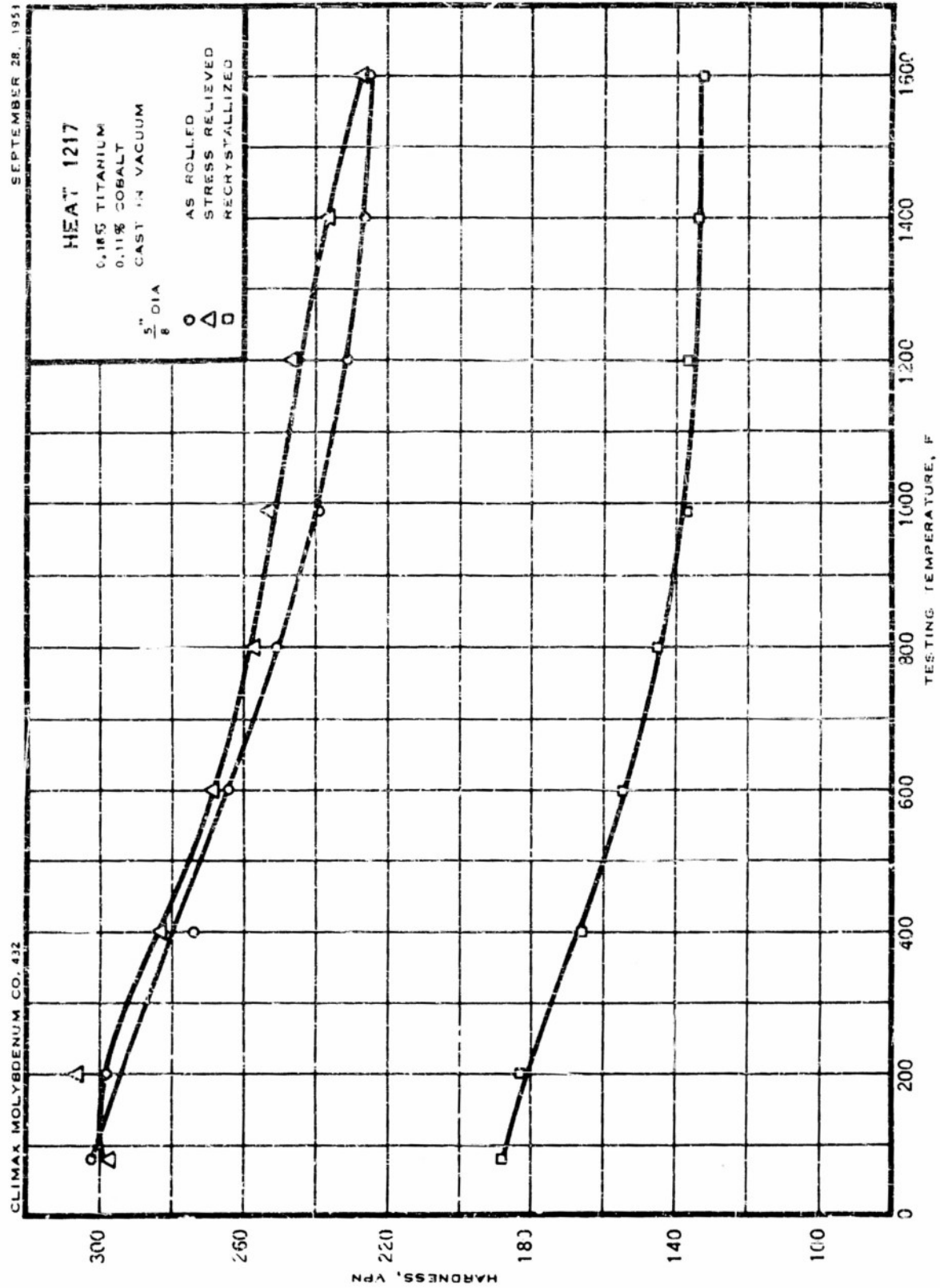


FIGURE C26 - HOT HARDNESS OF ROLLED BARS OF 0.18% TITANIUM, 0.11% COBALT, MOLYBDENUM ALLOY

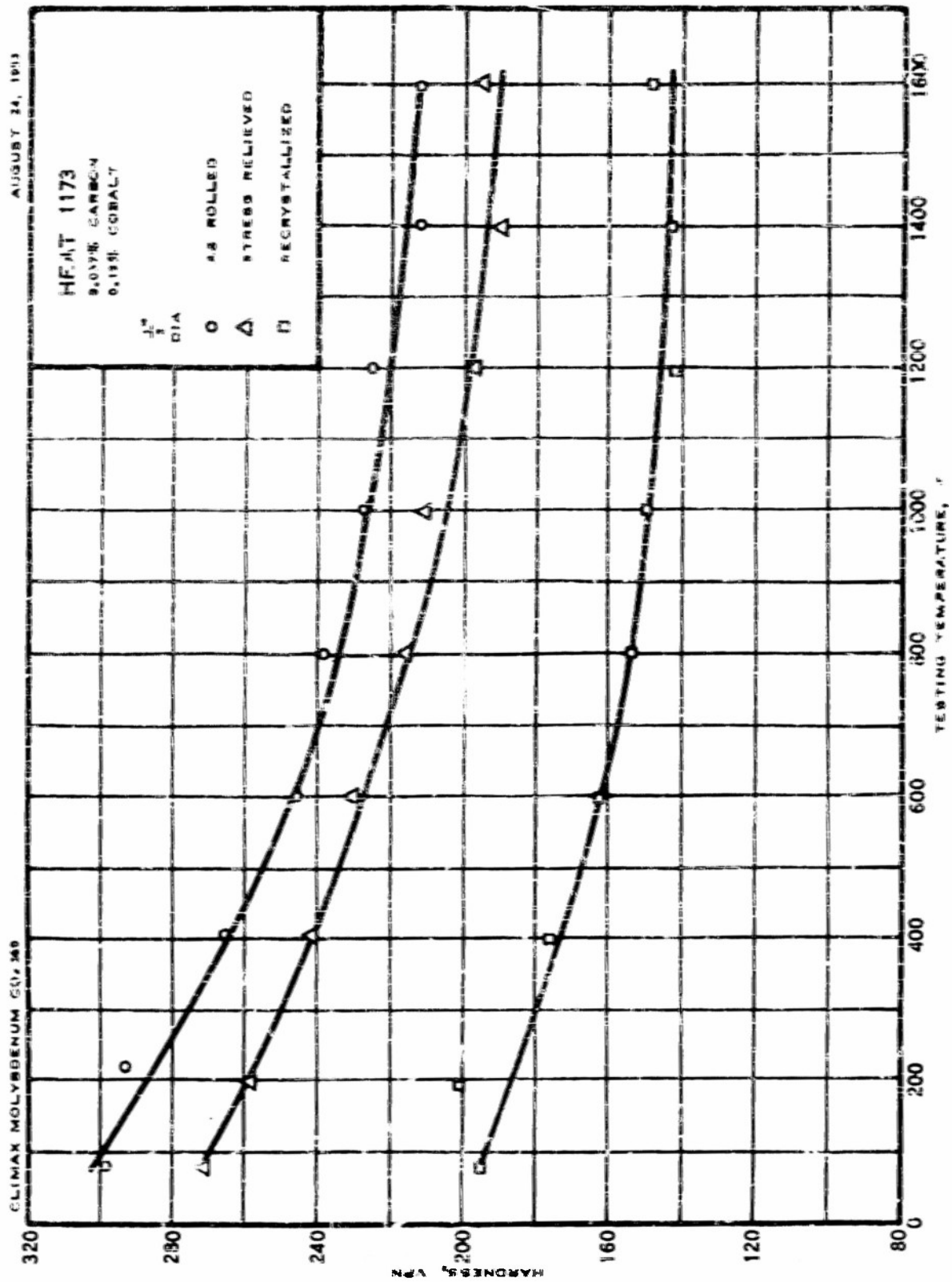


FIGURE C27 -- HOT HARDNESS OF ROLLED BARS OF 0.19% COBALT-MOLYBDENUM ALLOY

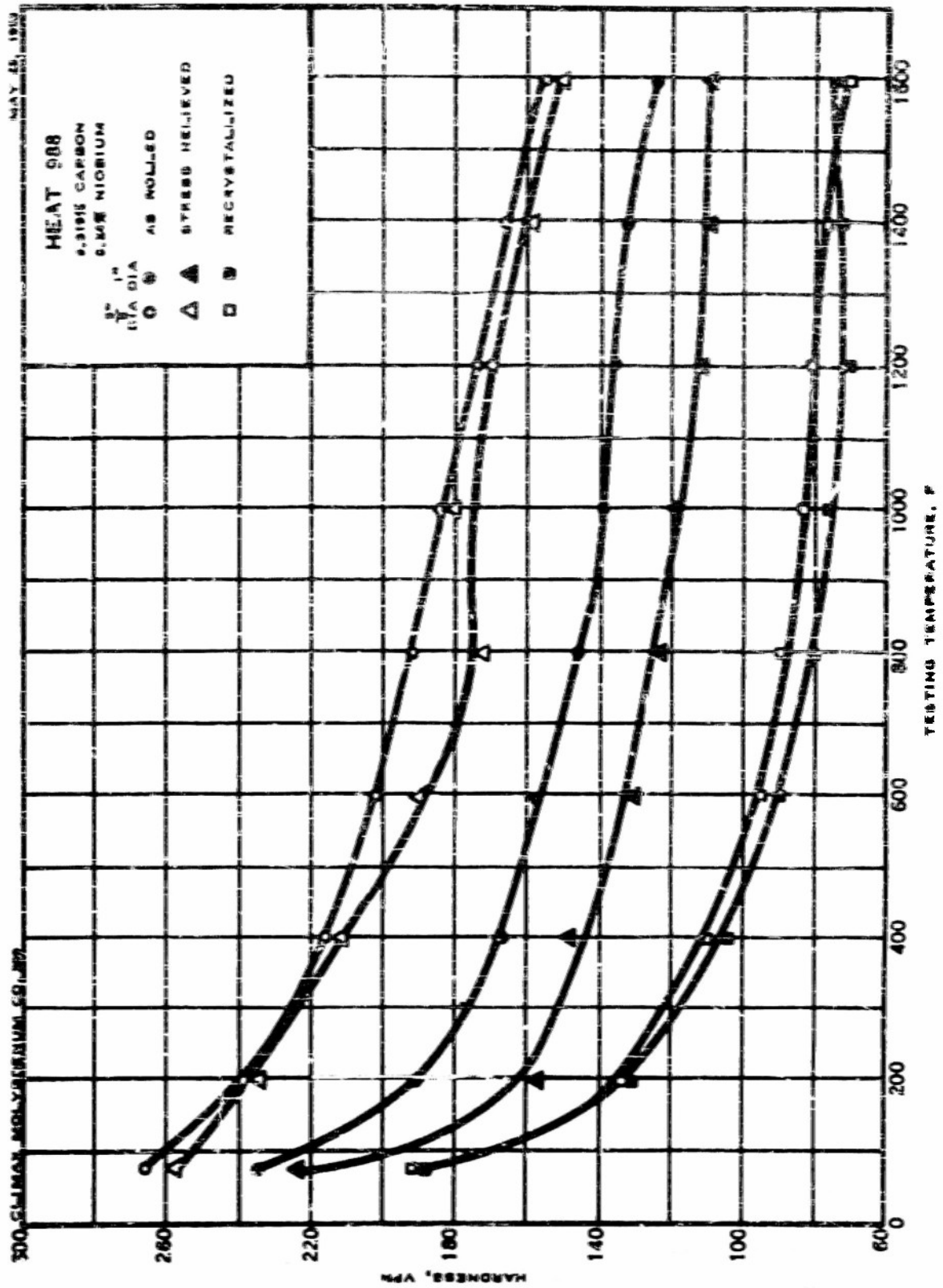


FIGURE C28 — HOT HARDNESS OF ROLLED BARS OF 0.24% NIOBIUM — MOLYBDENUM ALLOY

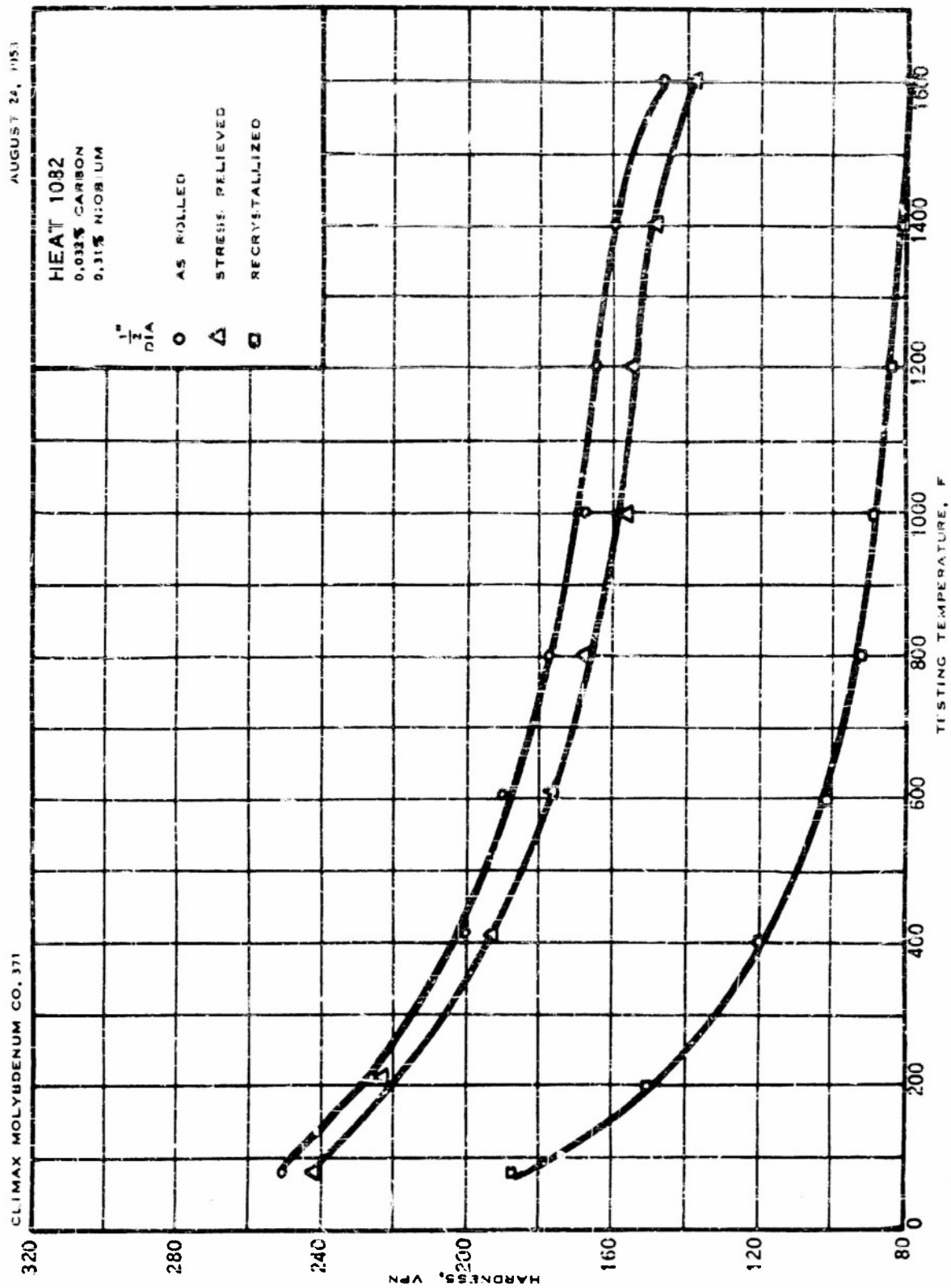
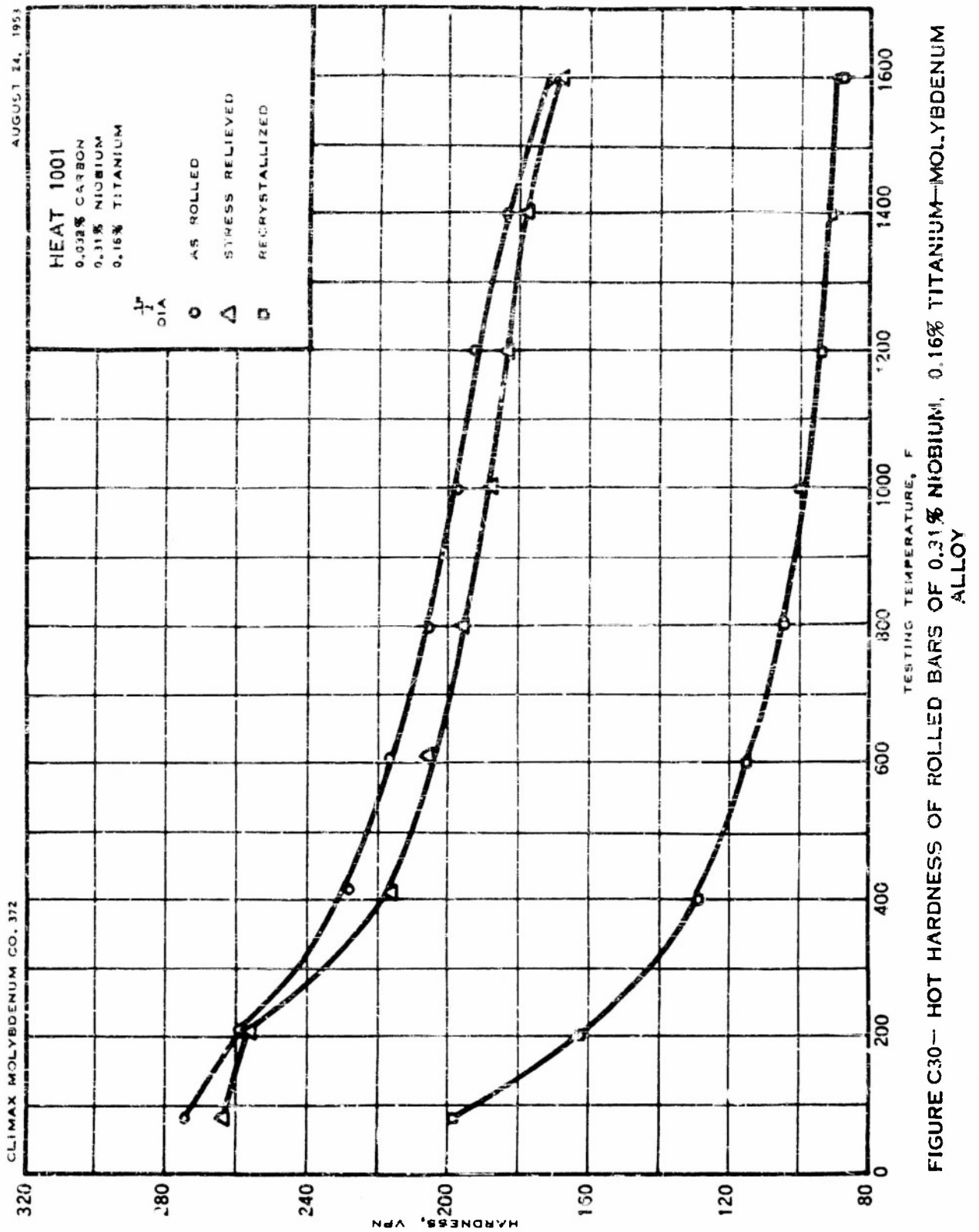


FIGURE C29—HOT HARDNESS OF ROLLED BARS OF 0.033% NIOBIUM—MOLYBDENUM ALLOY



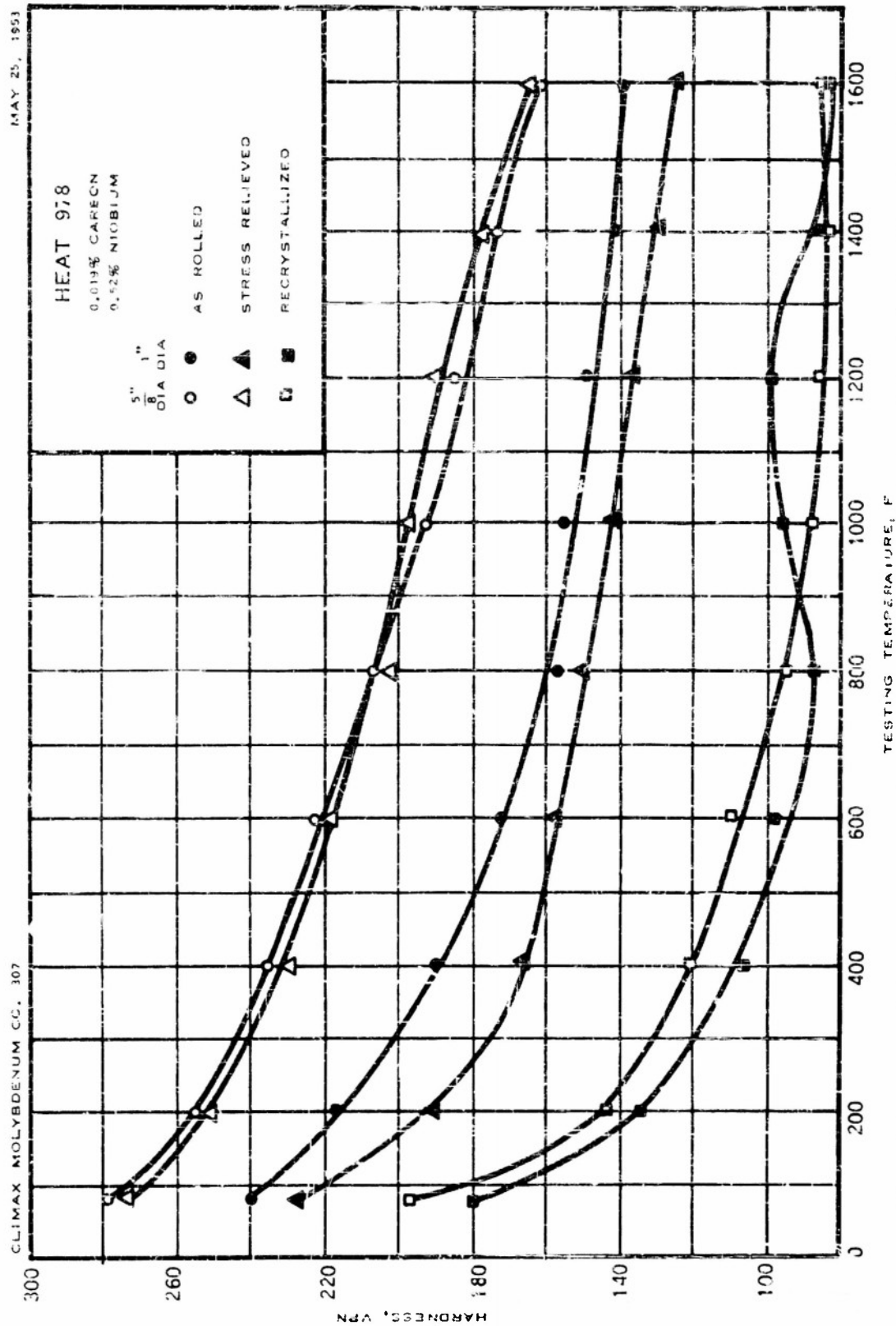


FIGURE C31 -- HOT HARDNESS OF ROLLED BARS OF 0.52% NIOBIUM-MOLYBDENUM ALLOY

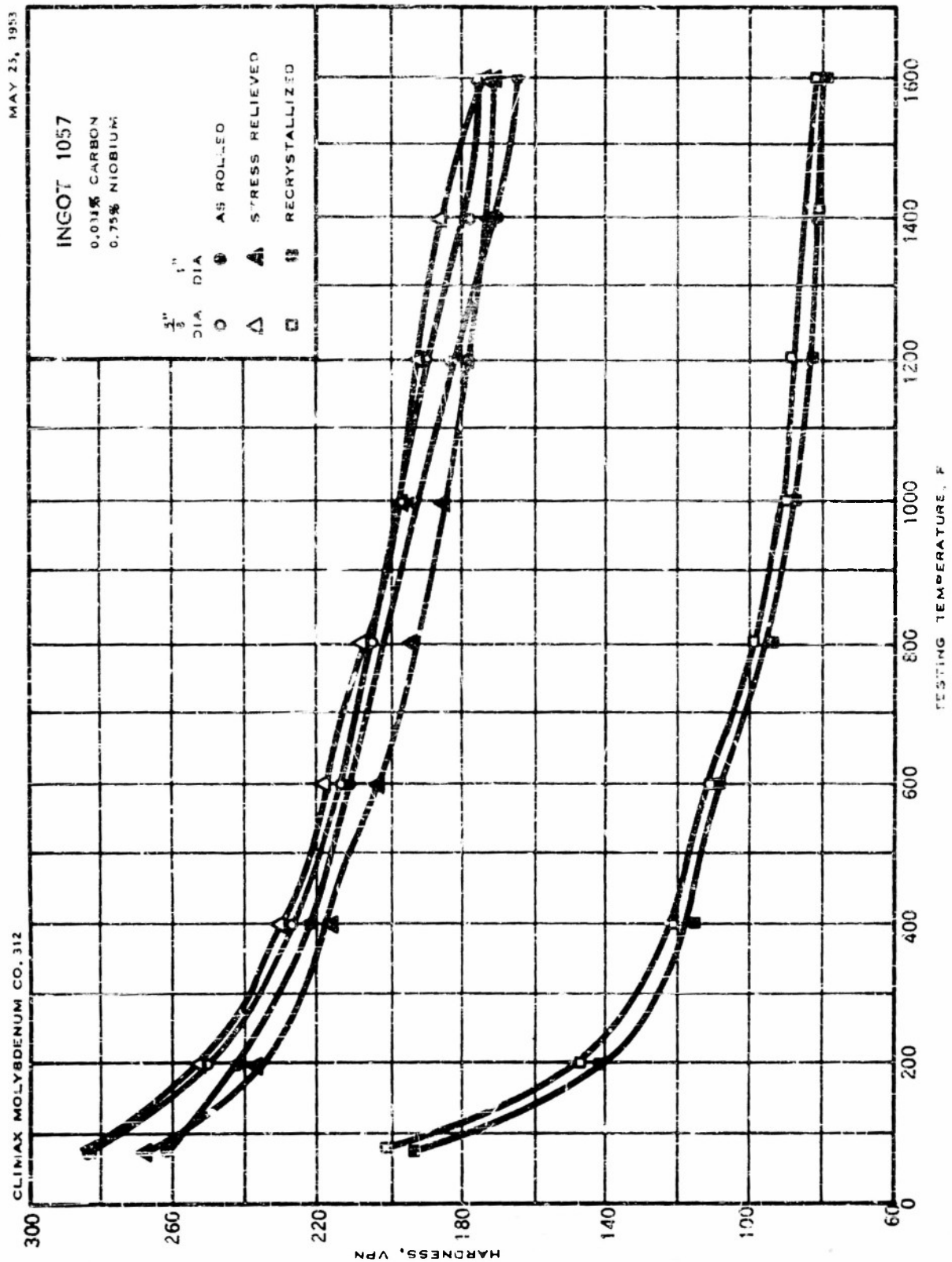
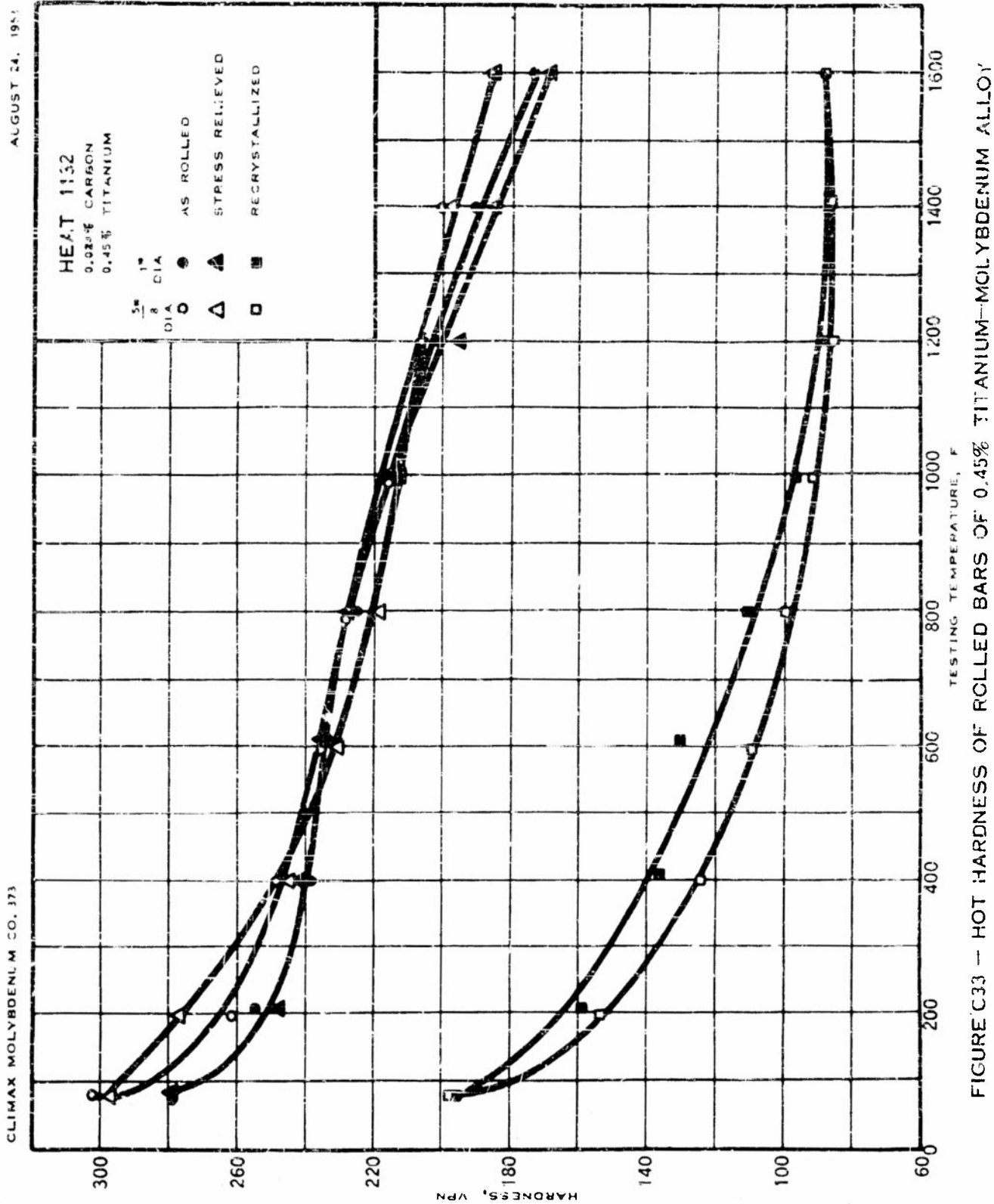


FIGURE C32 — HOT HARDNESS OF ROLLED BARS OF 0.75% NIOBIUM—MOLYBDENUM ALLOY



AUGUST 24, 1951

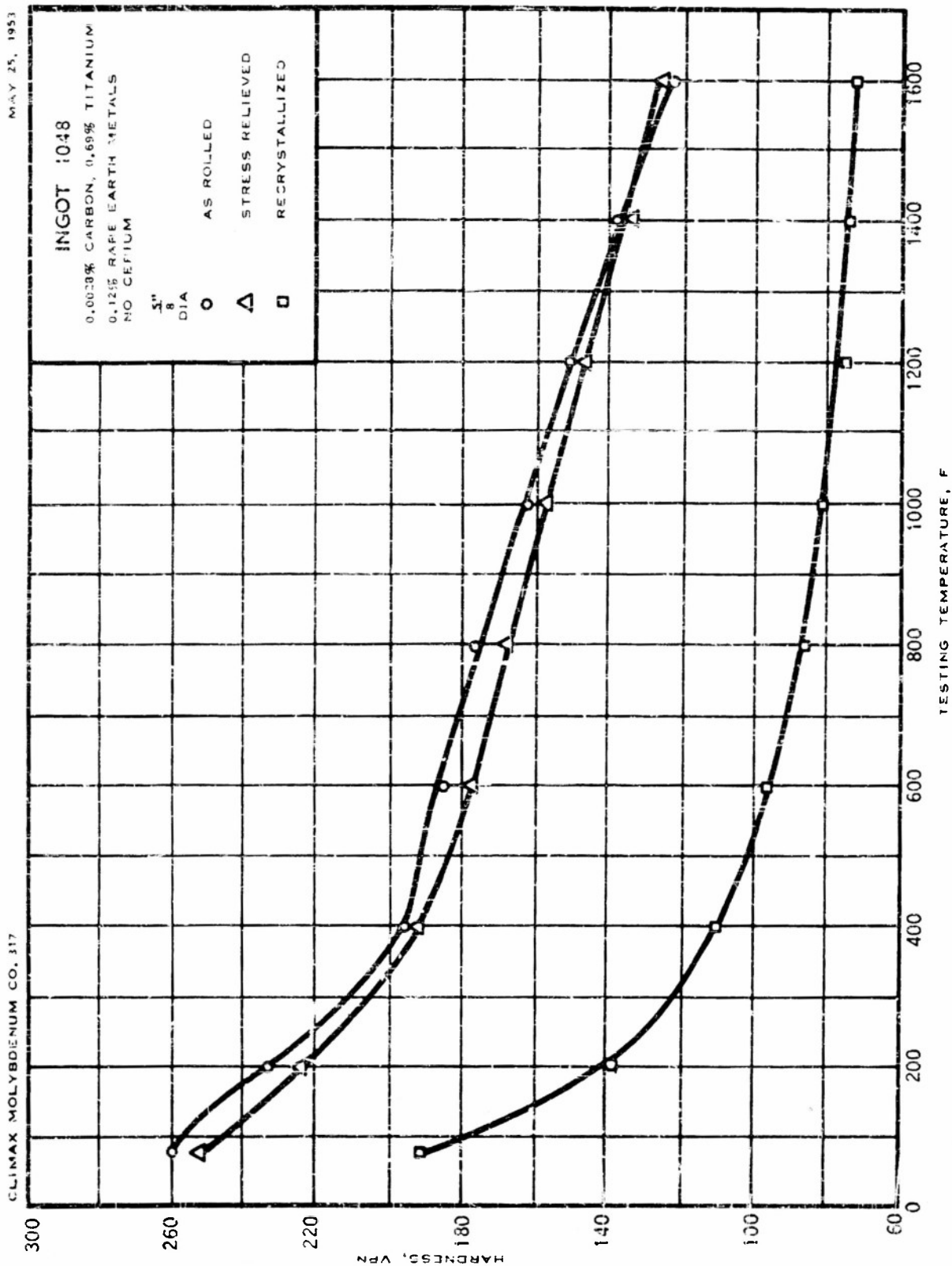


FIGURE C34 - HOT HARDNESS OF ROLLED BARS OF 0.69% TITANIUM-MOLYBDENUM ALLOY
DEOXYDIZED WITH RARE EARTH METALS

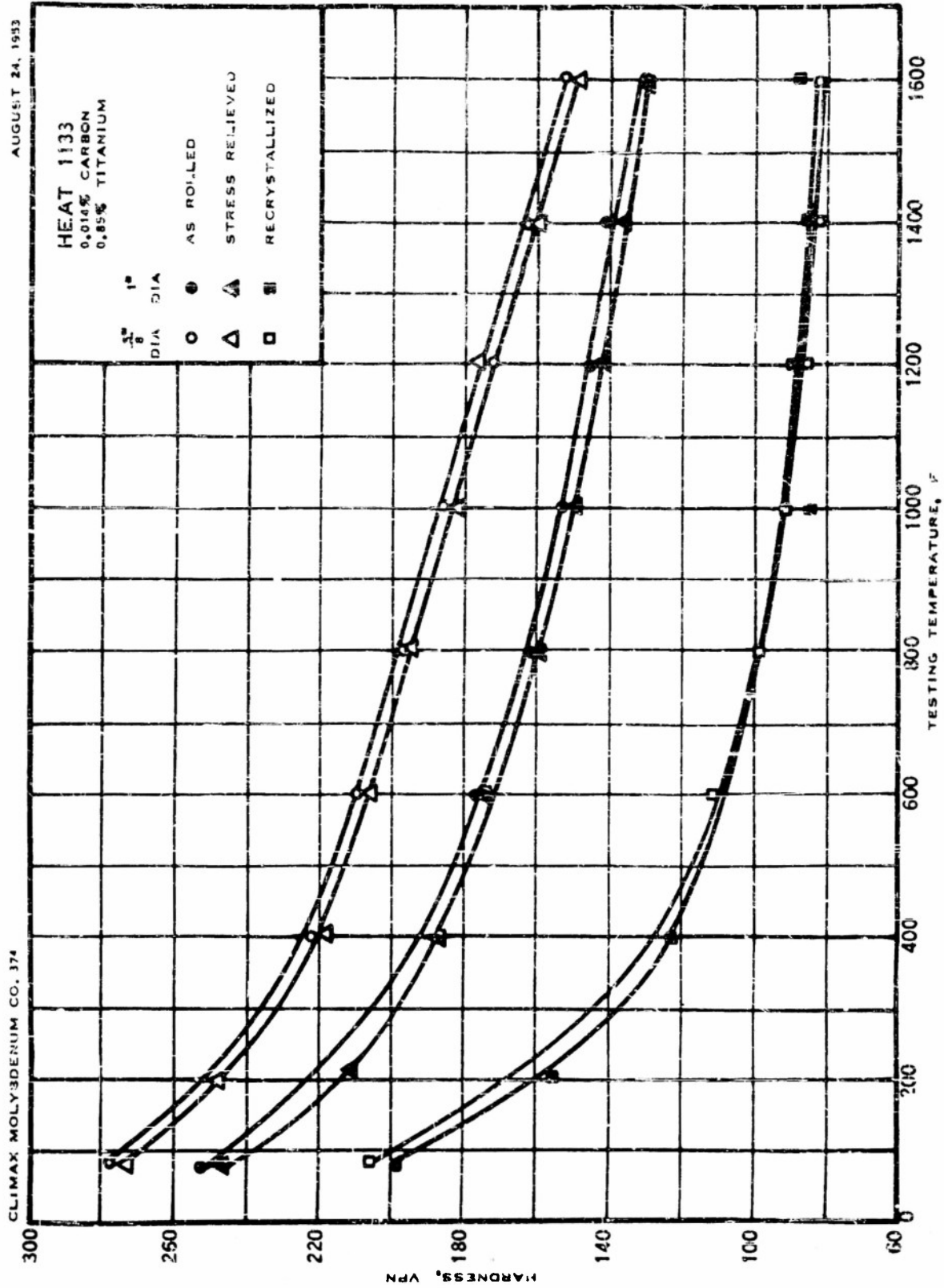


FIGURE C35—HOT HARDNESS OF ROLLED BARS OF 0.85% TITANIUM—MOLYBDENUM ALLOY

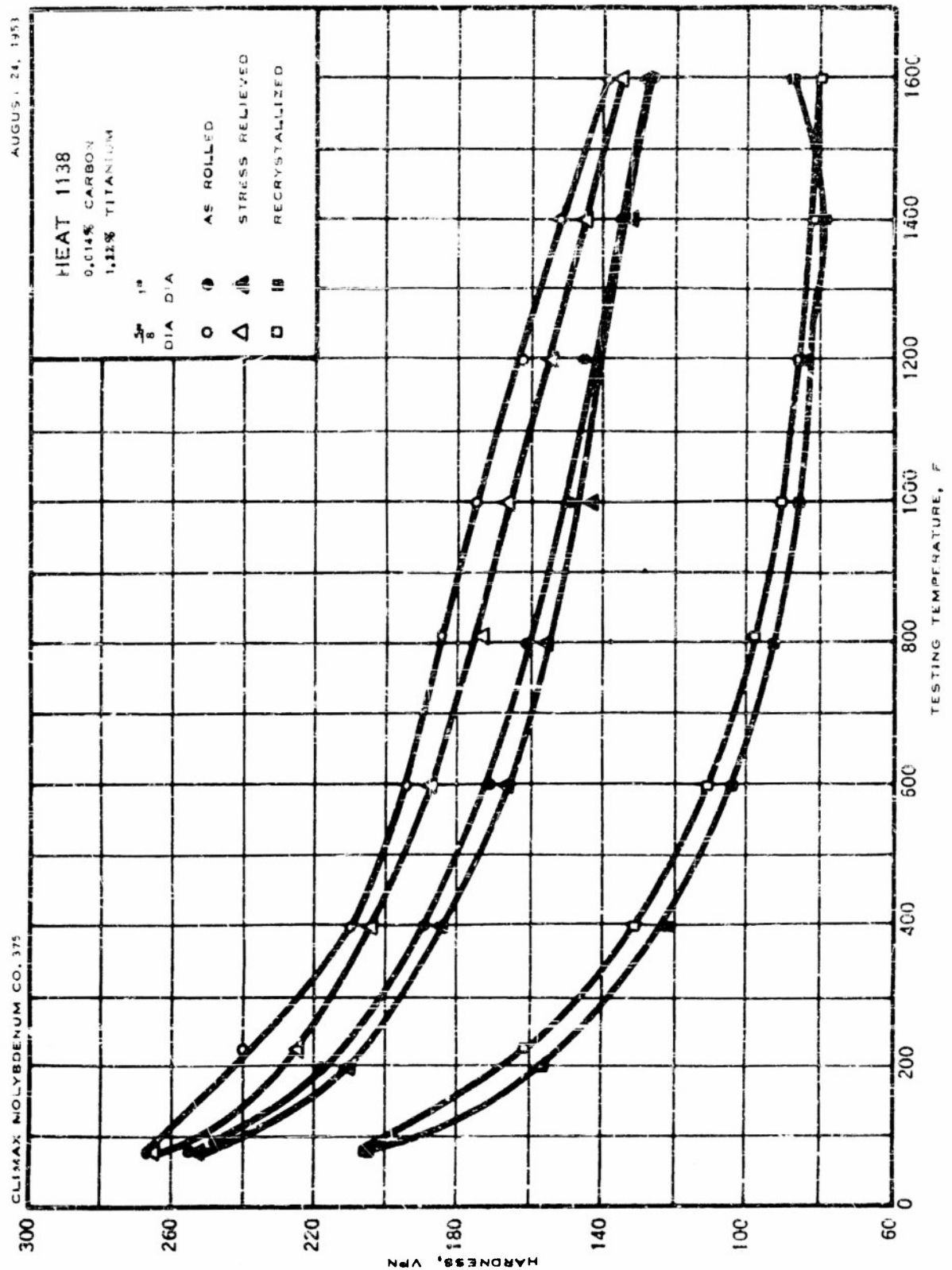


FIGURE C36 -- HOT HARDNESS OF ROLLED BARS OF 1.22% TITANIUM-MOLYBDENUM ALLOY

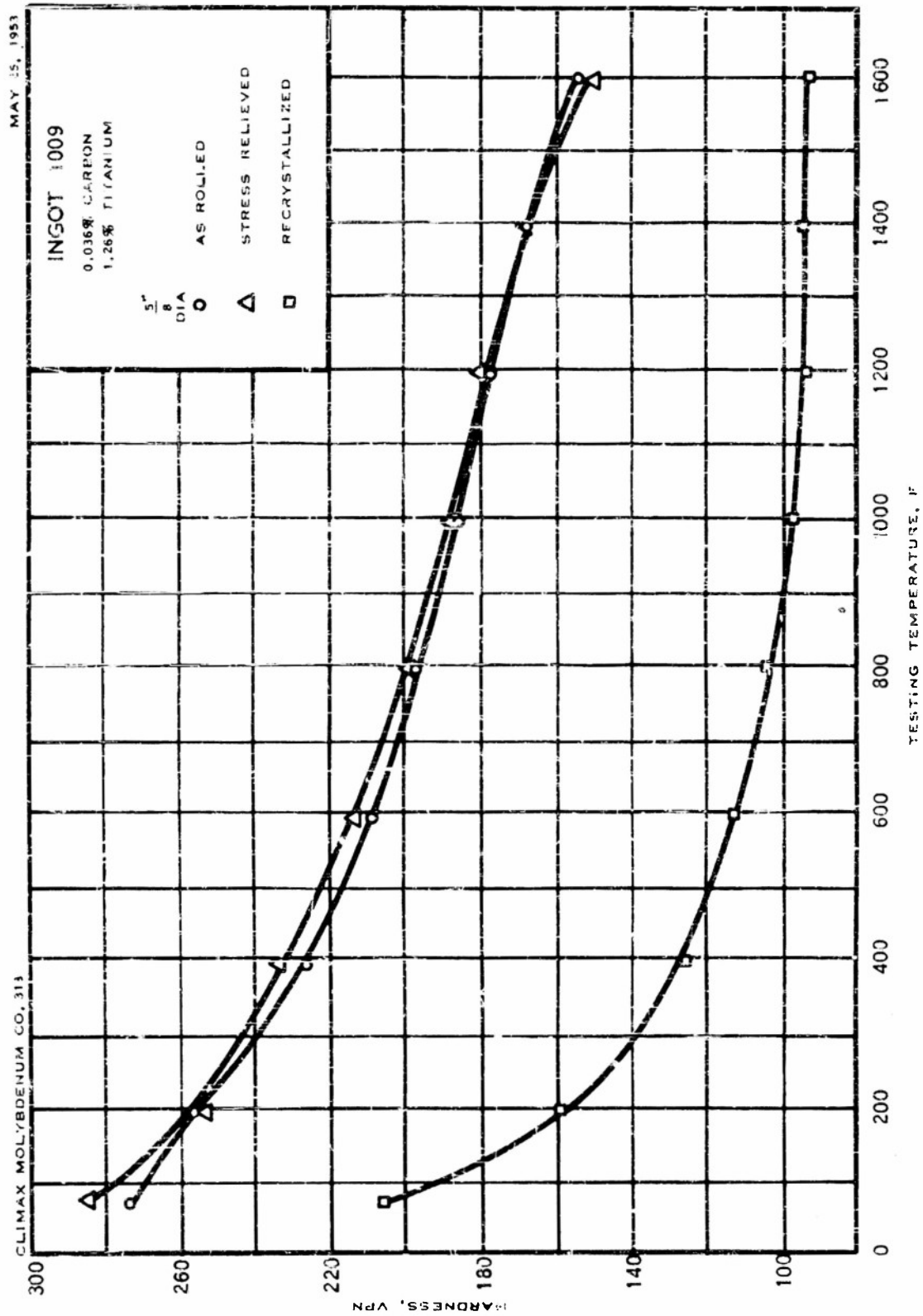


FIGURE C37 - HOT HARDNESS OF ROLLED BARS OF 1.25% TITANIUM--MOLYBDENUM ALLOY

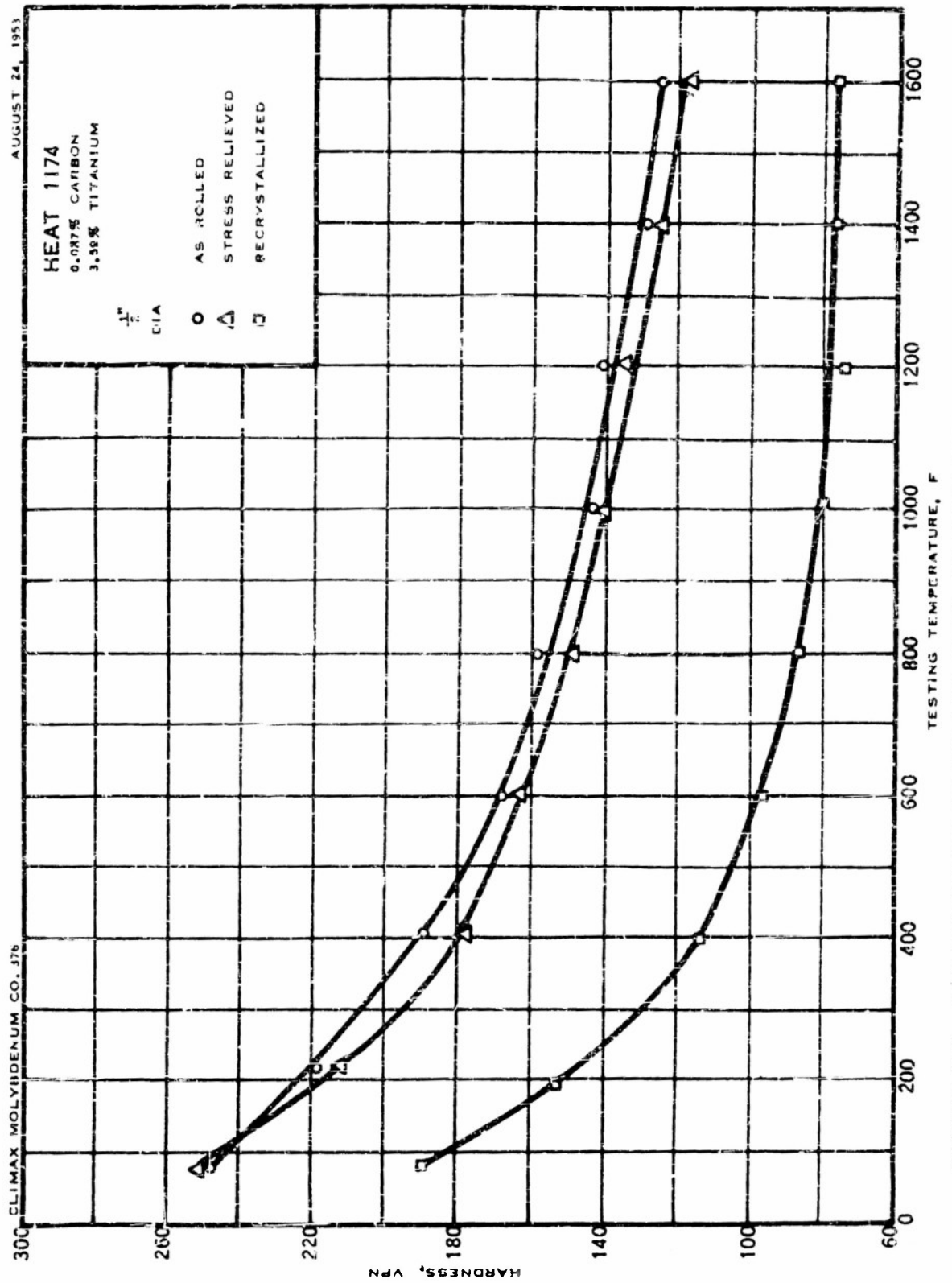


FIGURE C38— HOT HARDNESS OF ROLLED BARS OF 3.59% TITANIUM—MOLYBDENUM ALLOY

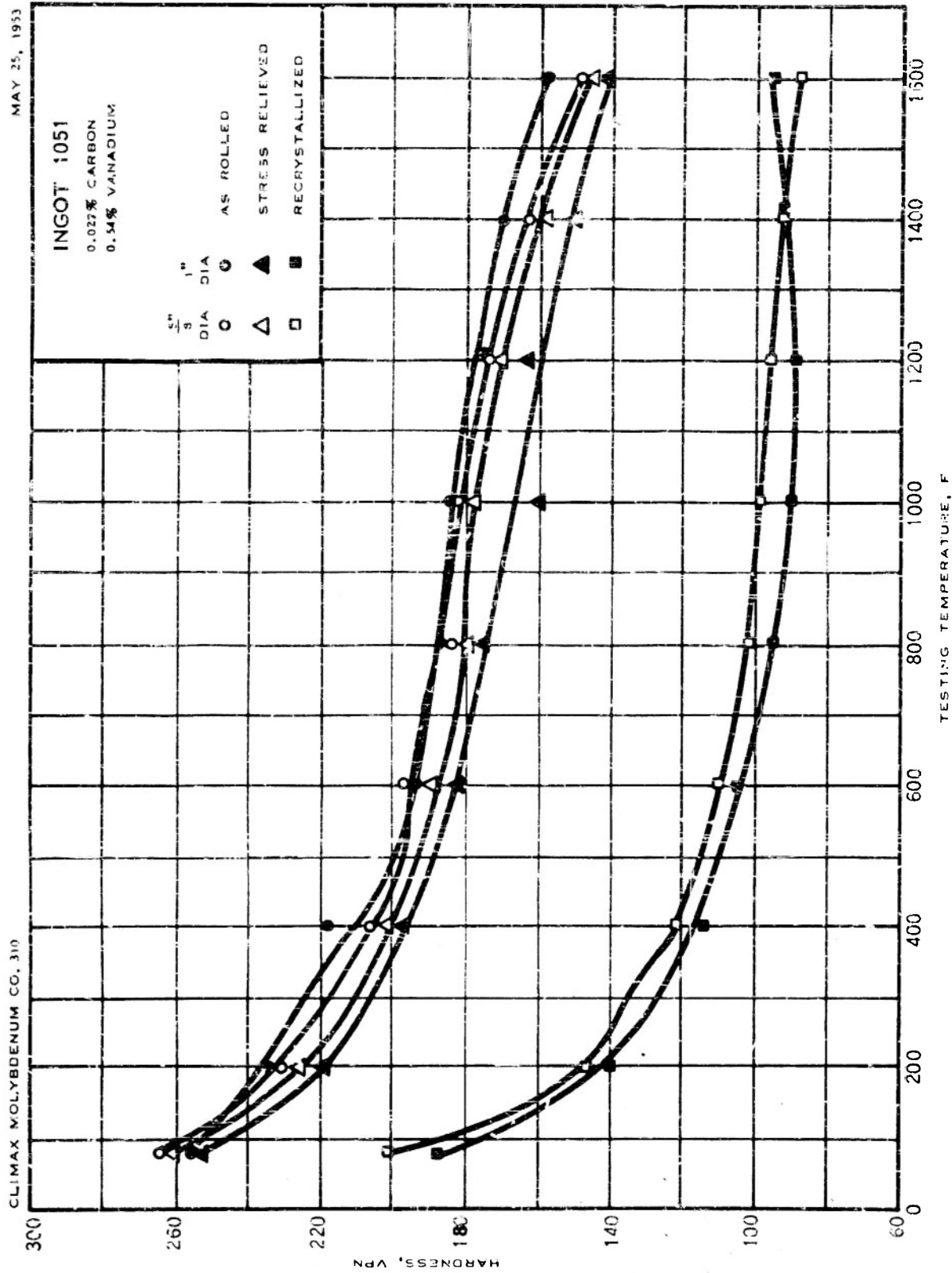


FIGURE C39 -- HOT HARDNESS OF ROLLED BARS OF 0.54% VANADIUM-MOLYBDENUM ALLOY

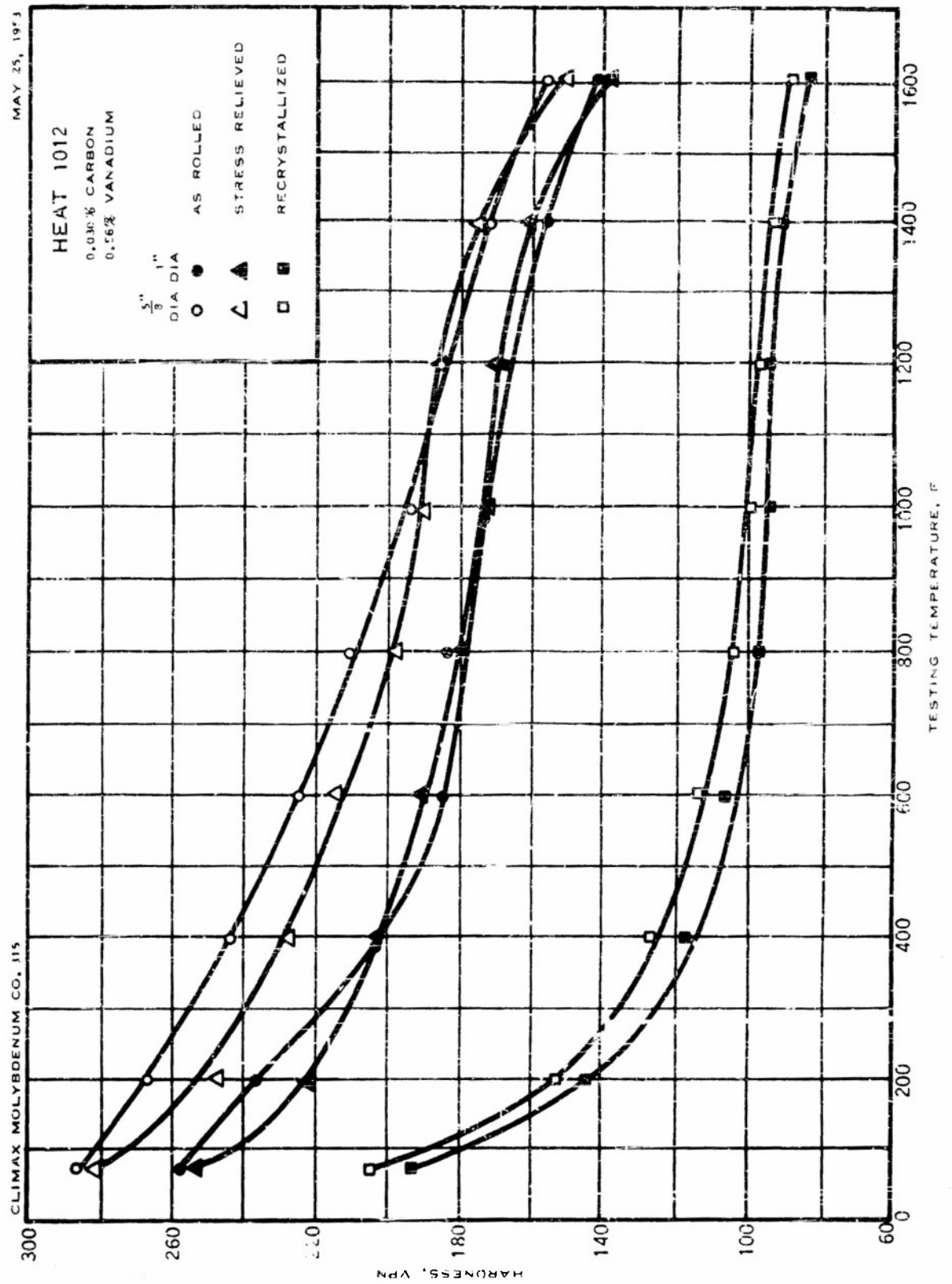


FIGURE C40 - HOT HARDNESS OF ROLLED BARS OF 0.56% VANADIUM - MOLYBDENUM ALLOY

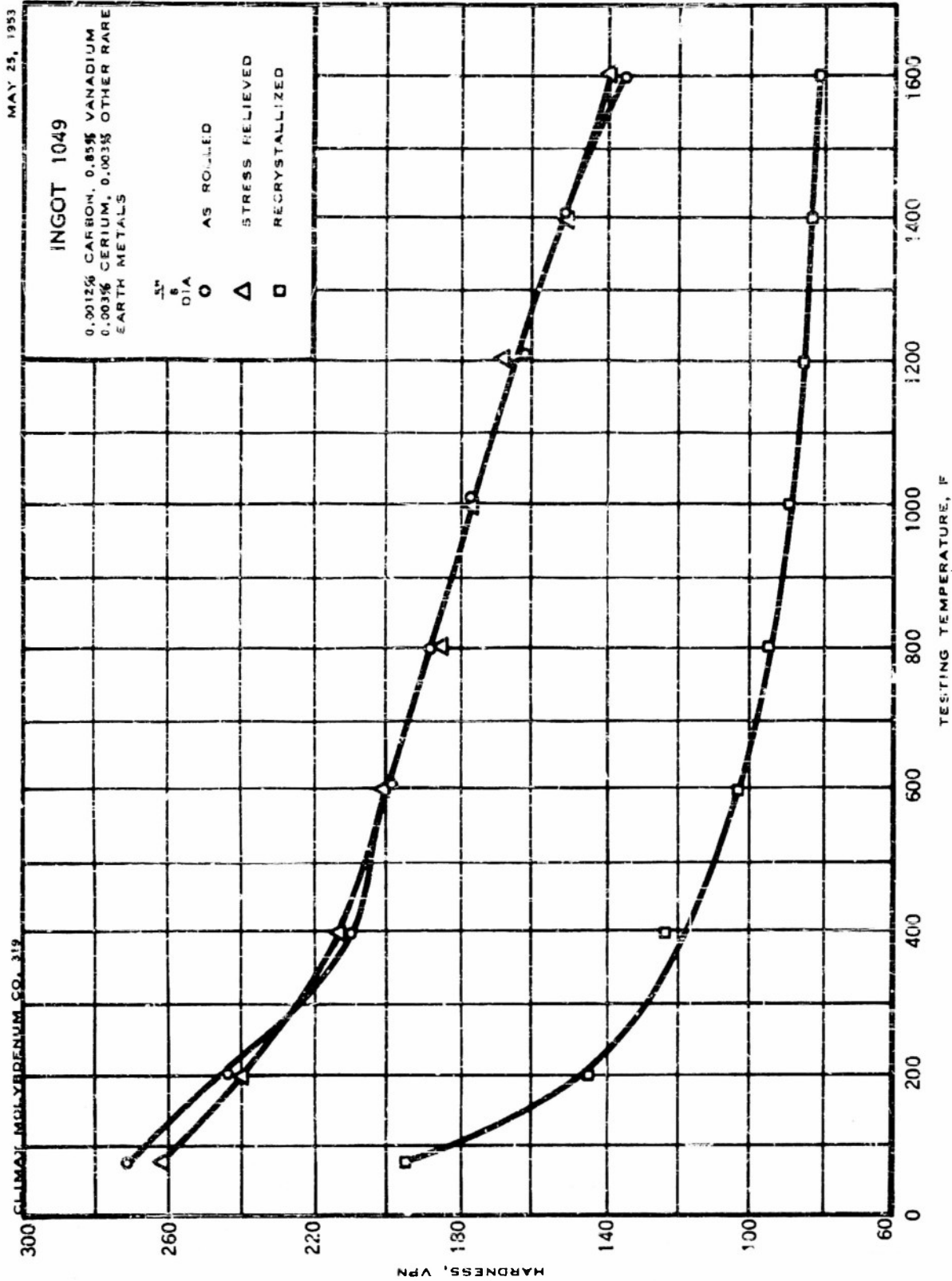


FIGURE C41 - HOT HARDNESS OF ROLLED BARS OF 0.85% VANADIUM--MOLYBDENUM ALLOY
DEOXIDIZED WITH RARE EARTH METALS

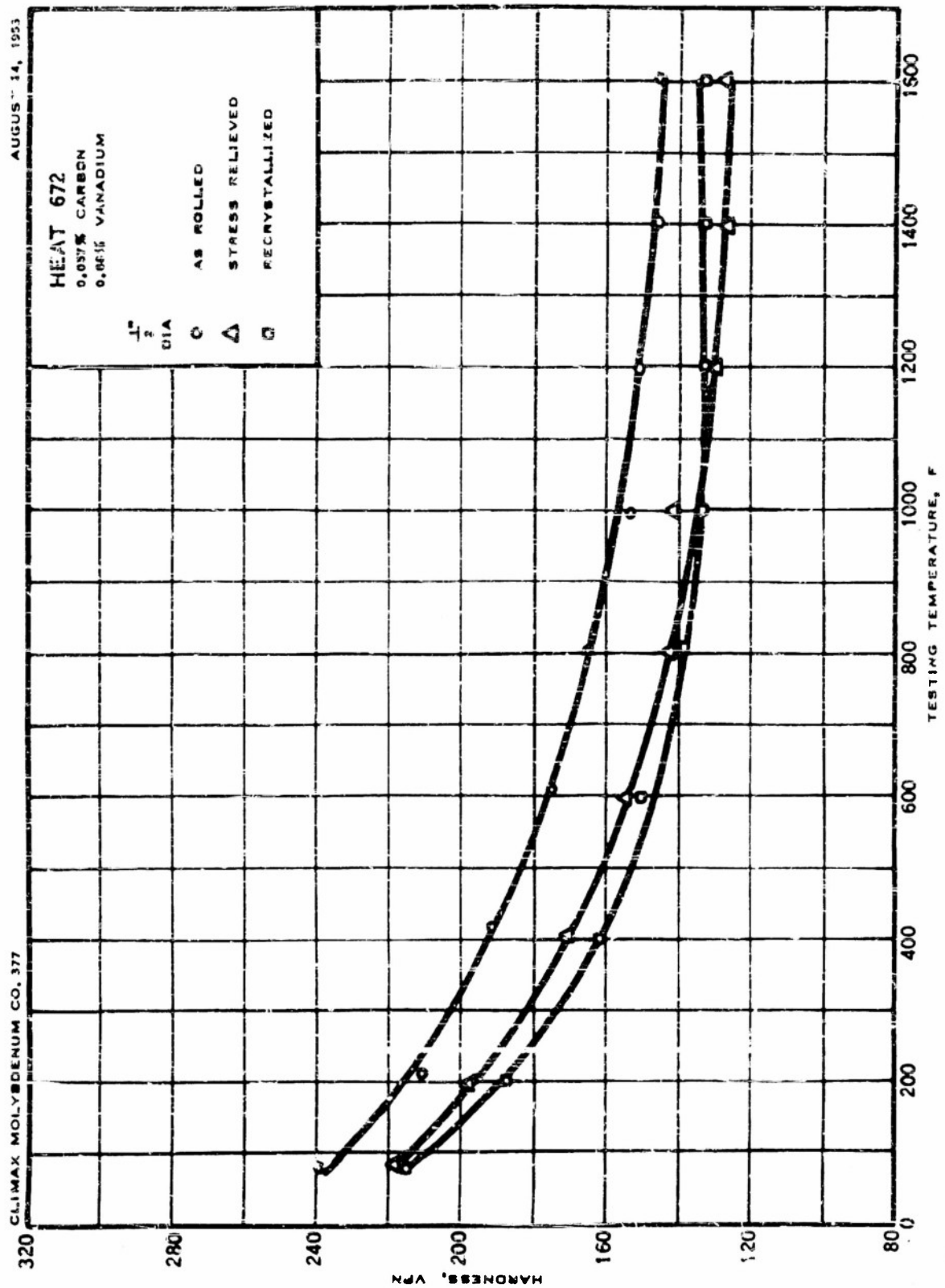


FIGURE C42 -- HOT HARDNESS OF ROLLED BARS OF 0.88% VANADIUM-MOLYBDENUM ALLOY

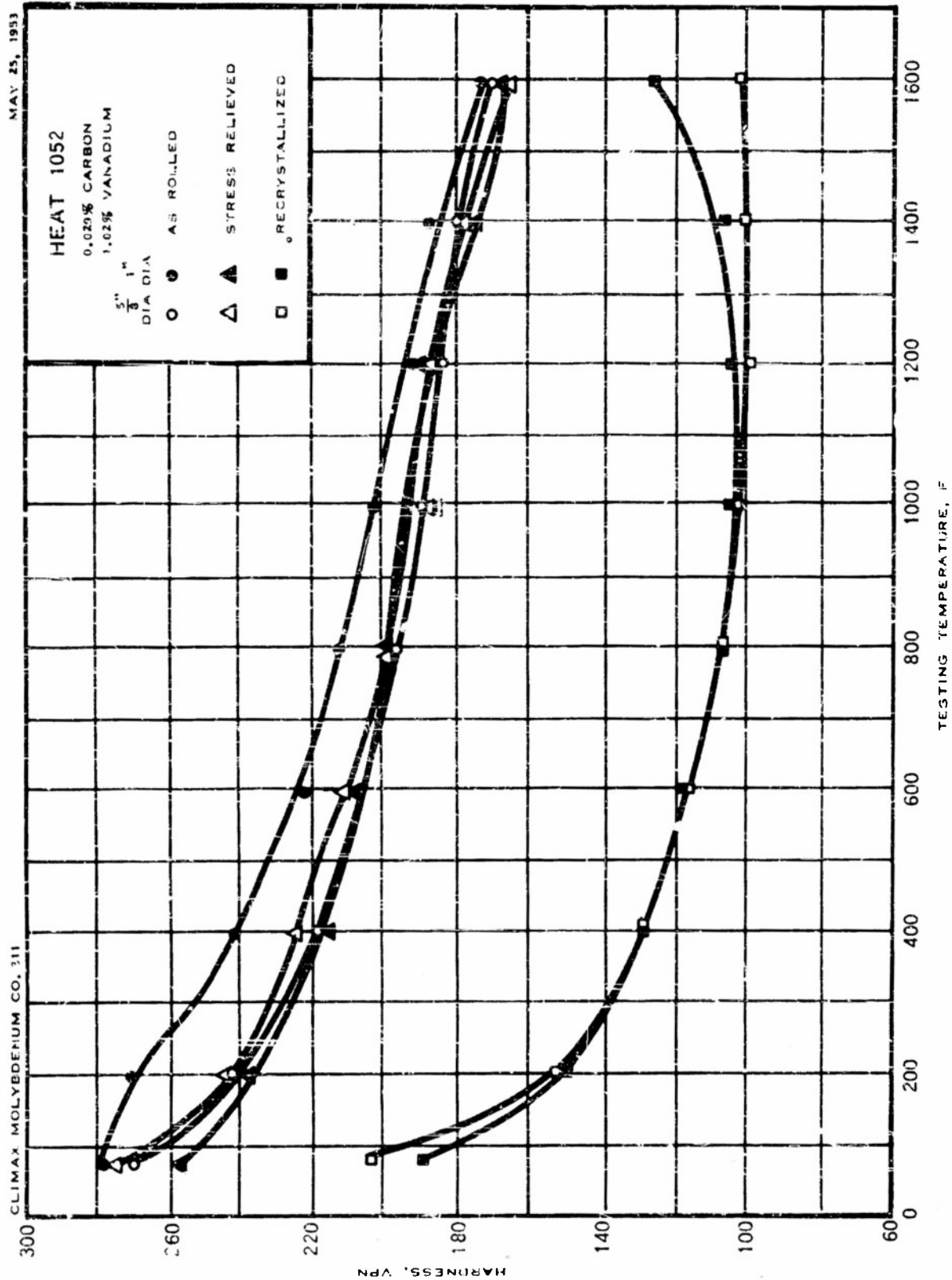


FIGURE C43 — HOT HARDNESS OF ROLLED BARS OF 1.02% VANADIUM—MOLYBDENUM ALLOY

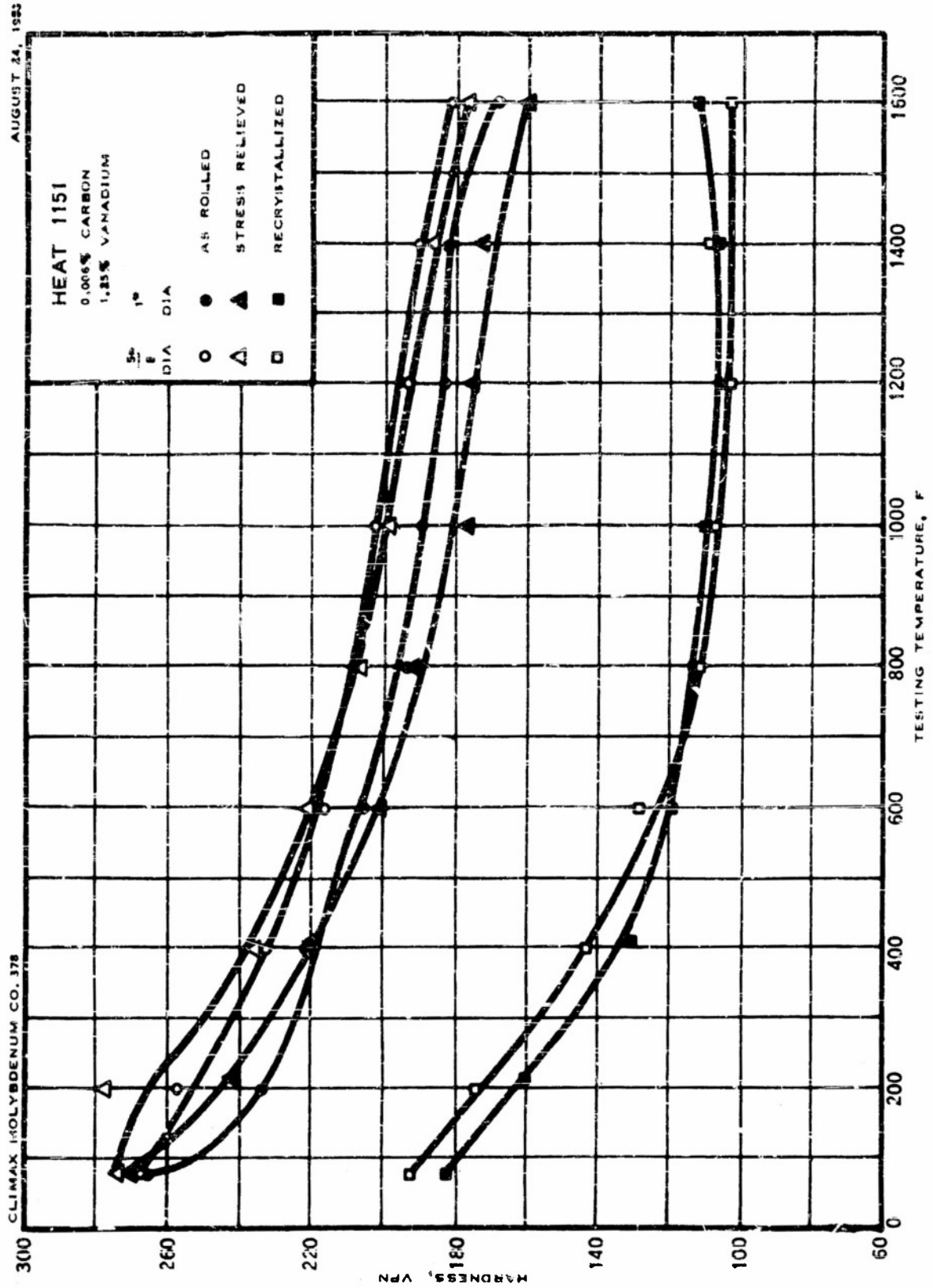


FIGURE C44— HOT HARDNESS OF ROLLED BARS OF 1.25% VANADIUM—MOLYBDENUM ALLOY

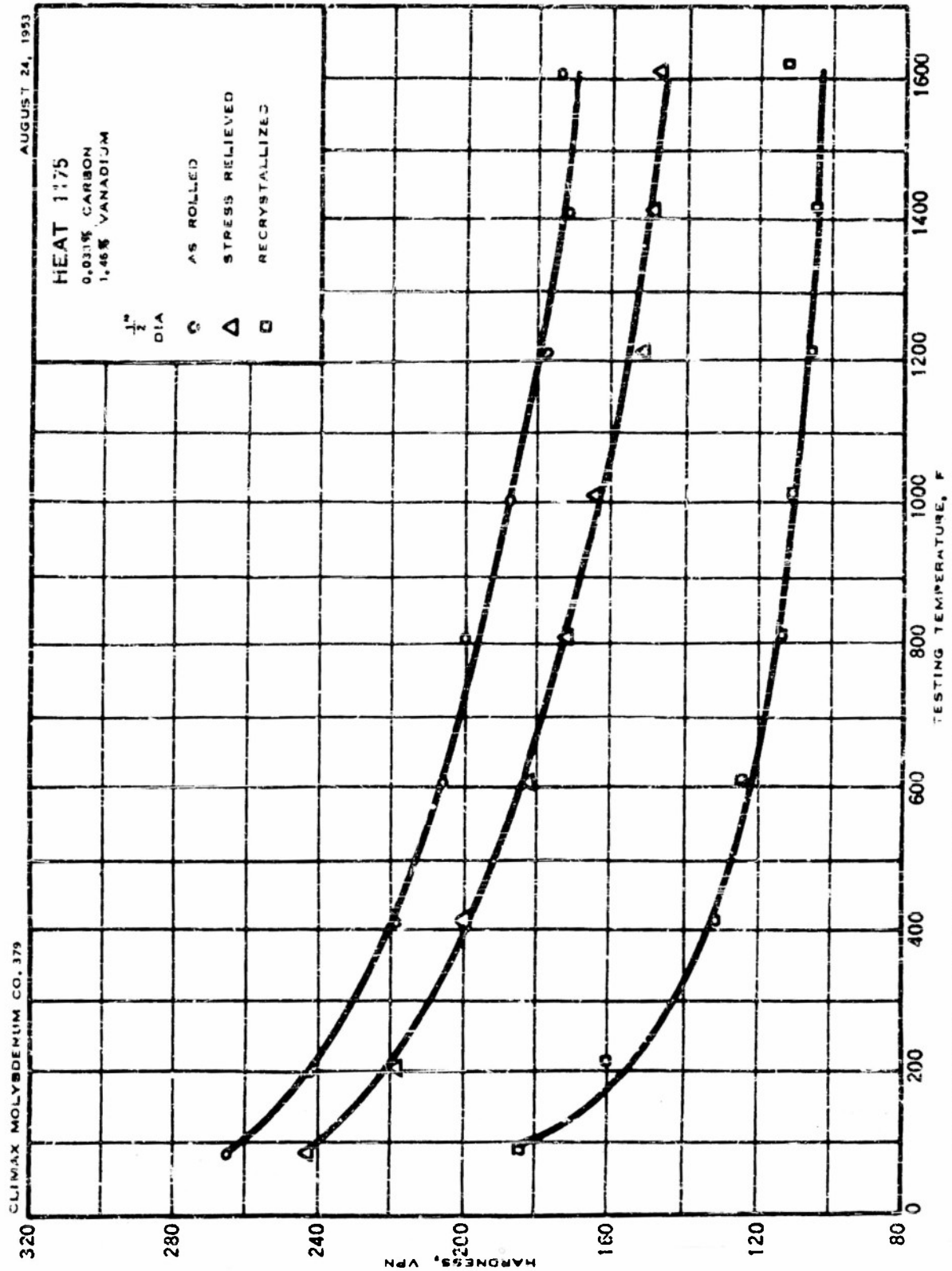


FIGURE C45 — HOT HARDNESS OF ROLLED BARS OF 1.46% VANADIUM-MOLYBDENUM ALLOY

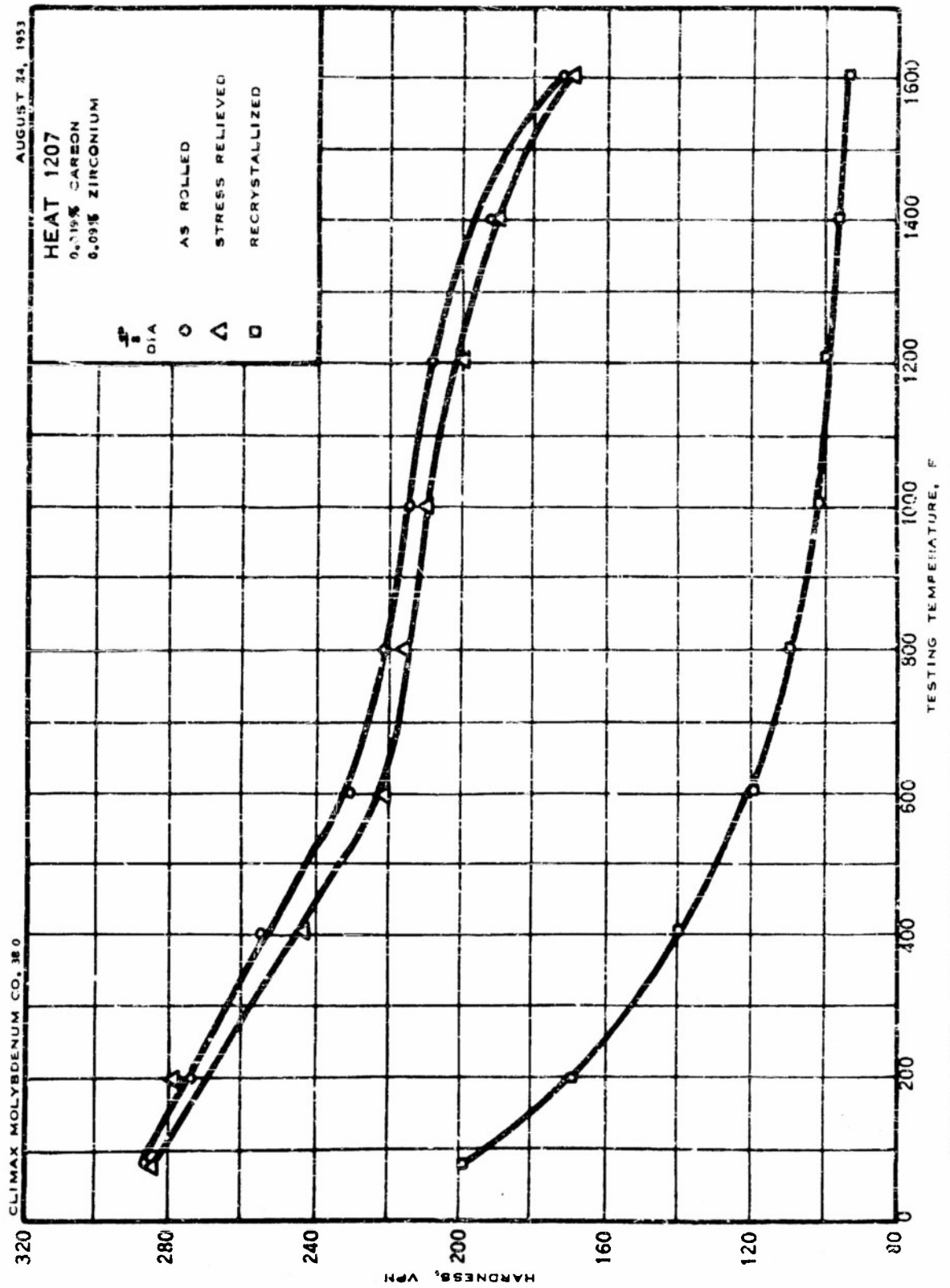


FIGURE C46—HOT HARDNESS OF ROLLED BARS OF 0.09% ZIRCONIUM-MOLYBDENUM ALLOY

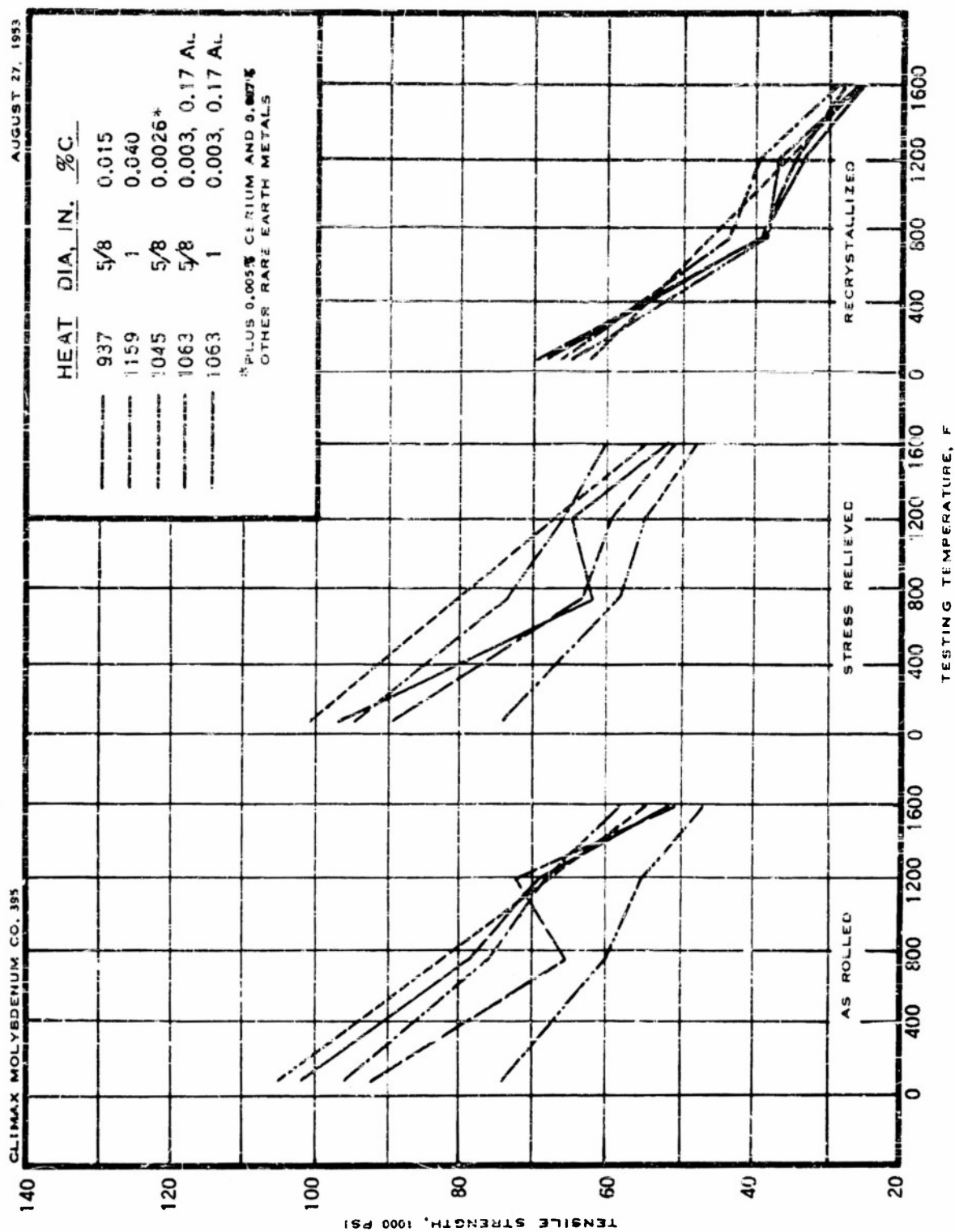


FIGURE C47 - TENSILE STRENGTH OF UNALLOYED MOLYBDENUM BARS

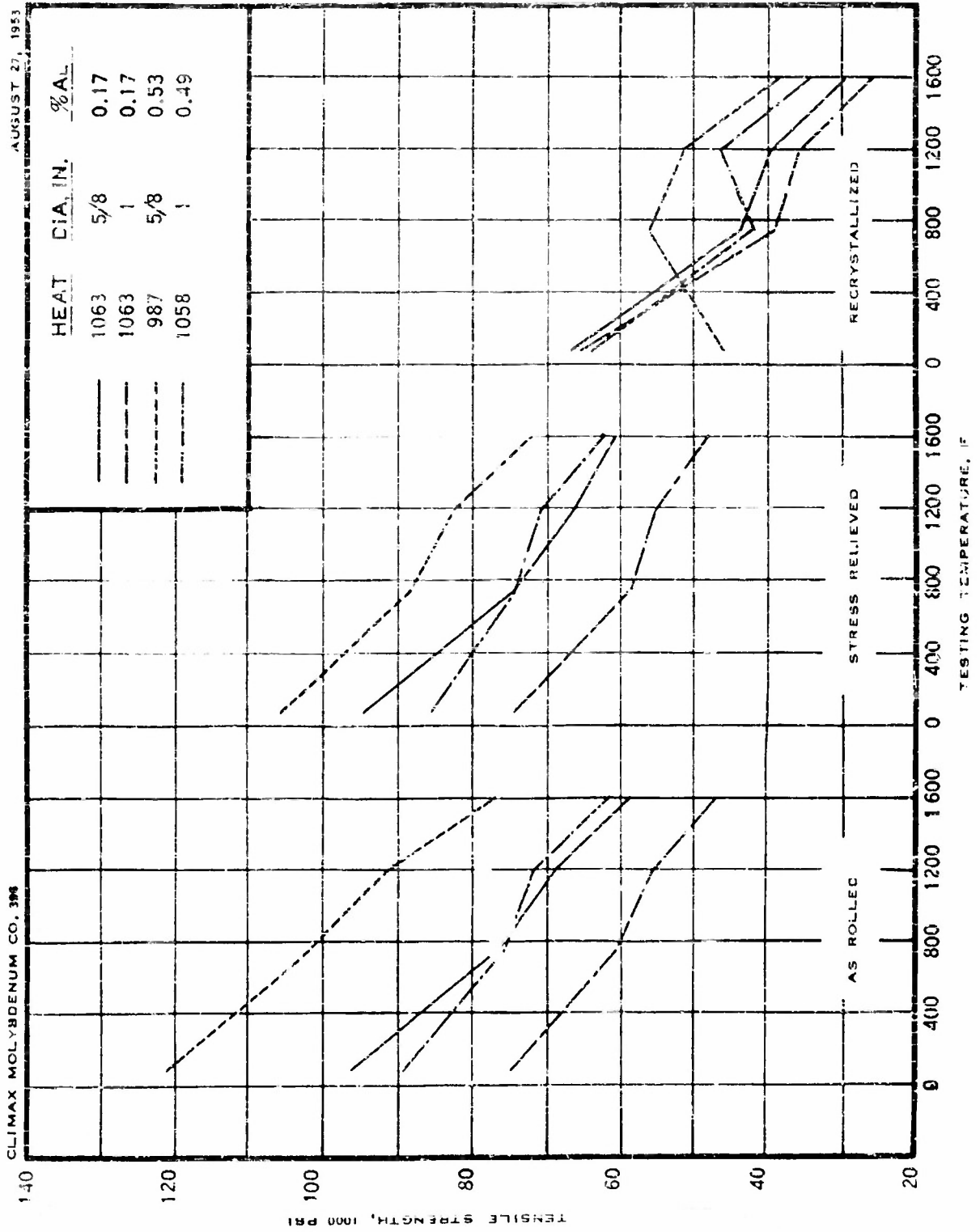


FIGURE C48-- TENSILE STRENGTH OF MOLYBDENUM-ALUMINUM ALLOY BARS

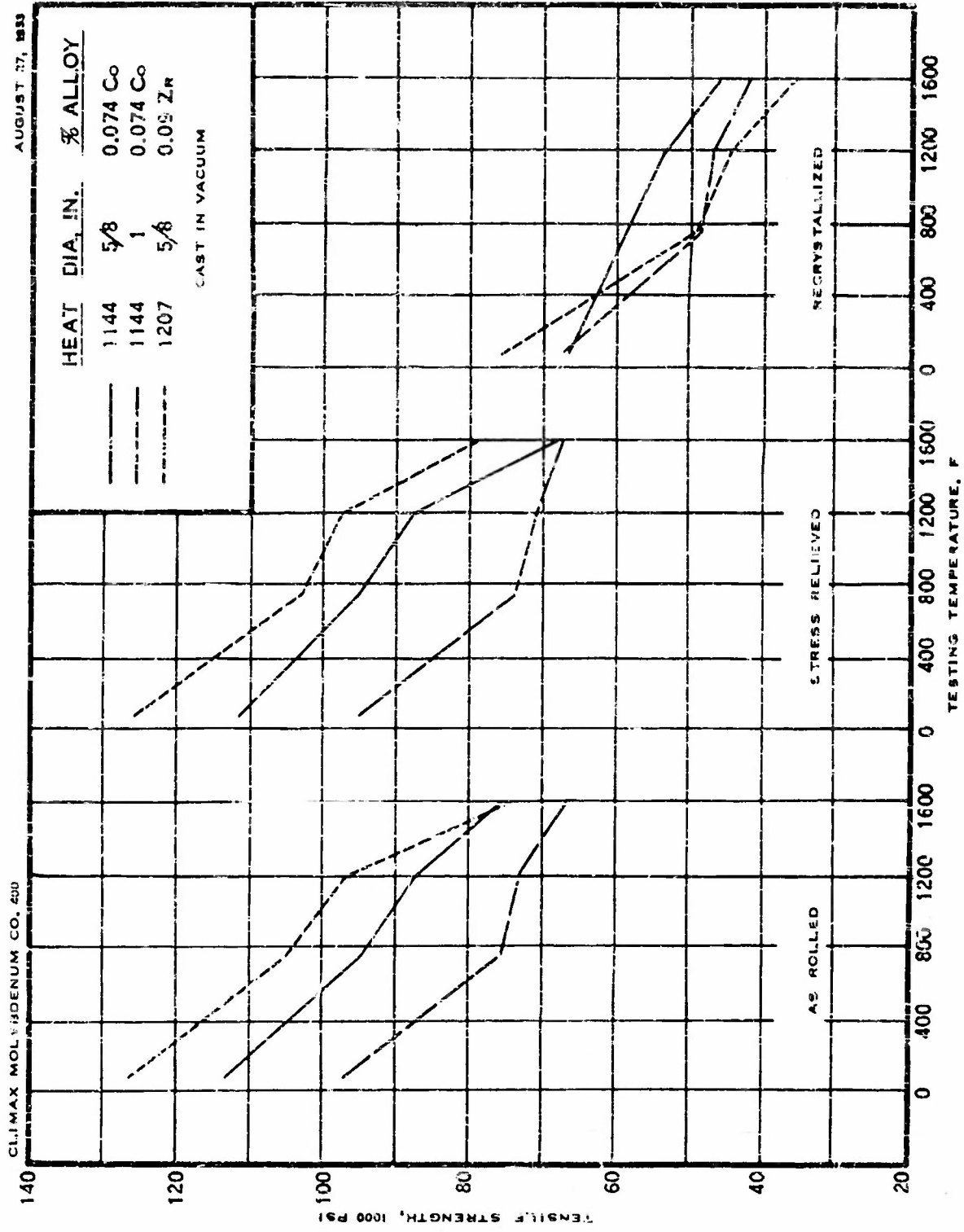


FIGURE C49 — TENSILE STRENGTH OF MOLYBDENUM-COBALT AND MOLYBDENUM-ZIRCONIUM ALLOY BARS

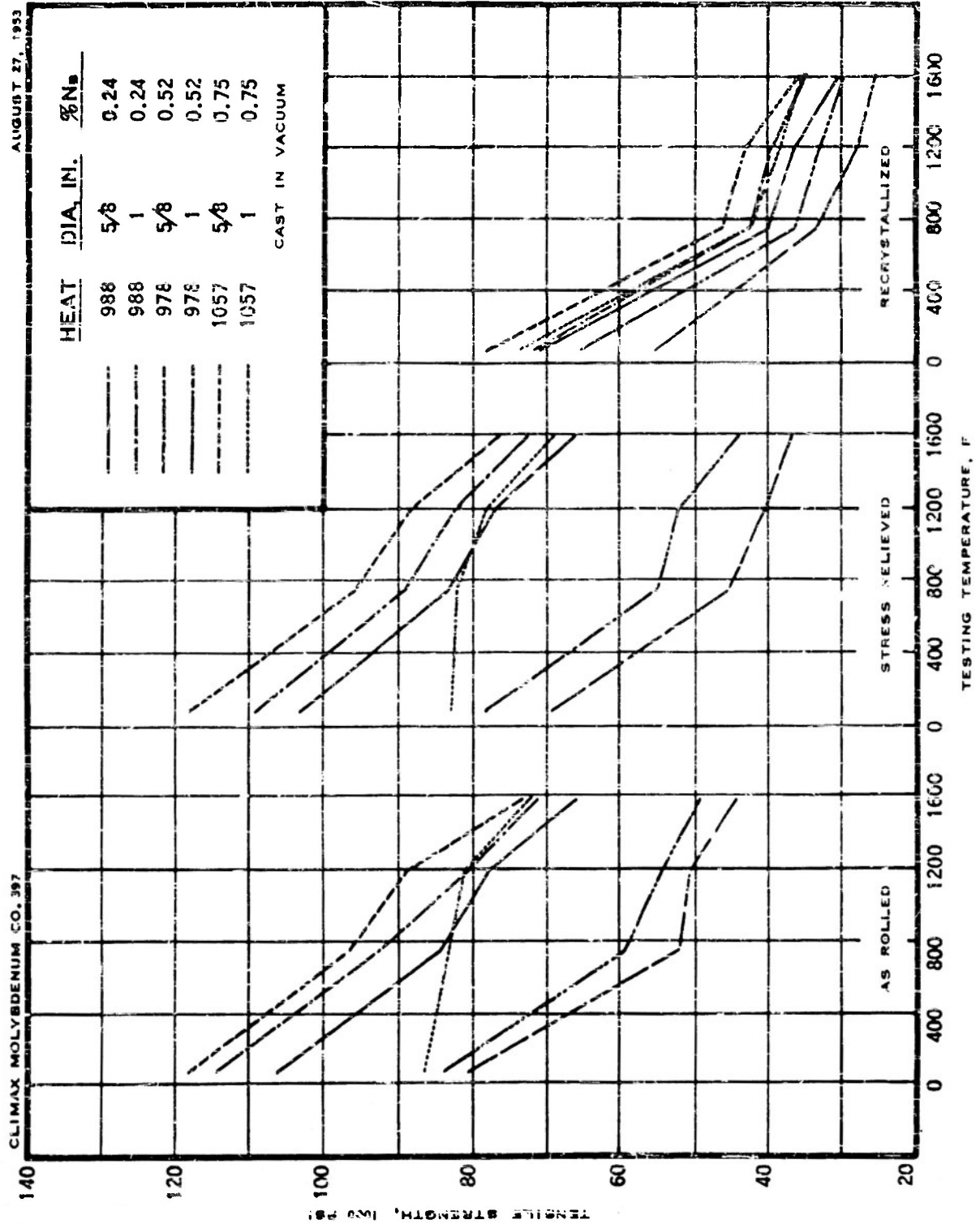


FIGURE C50 - TENSILE STRENGTH OF MOLYBDENUM-NIOBIUM ALLOY BARS

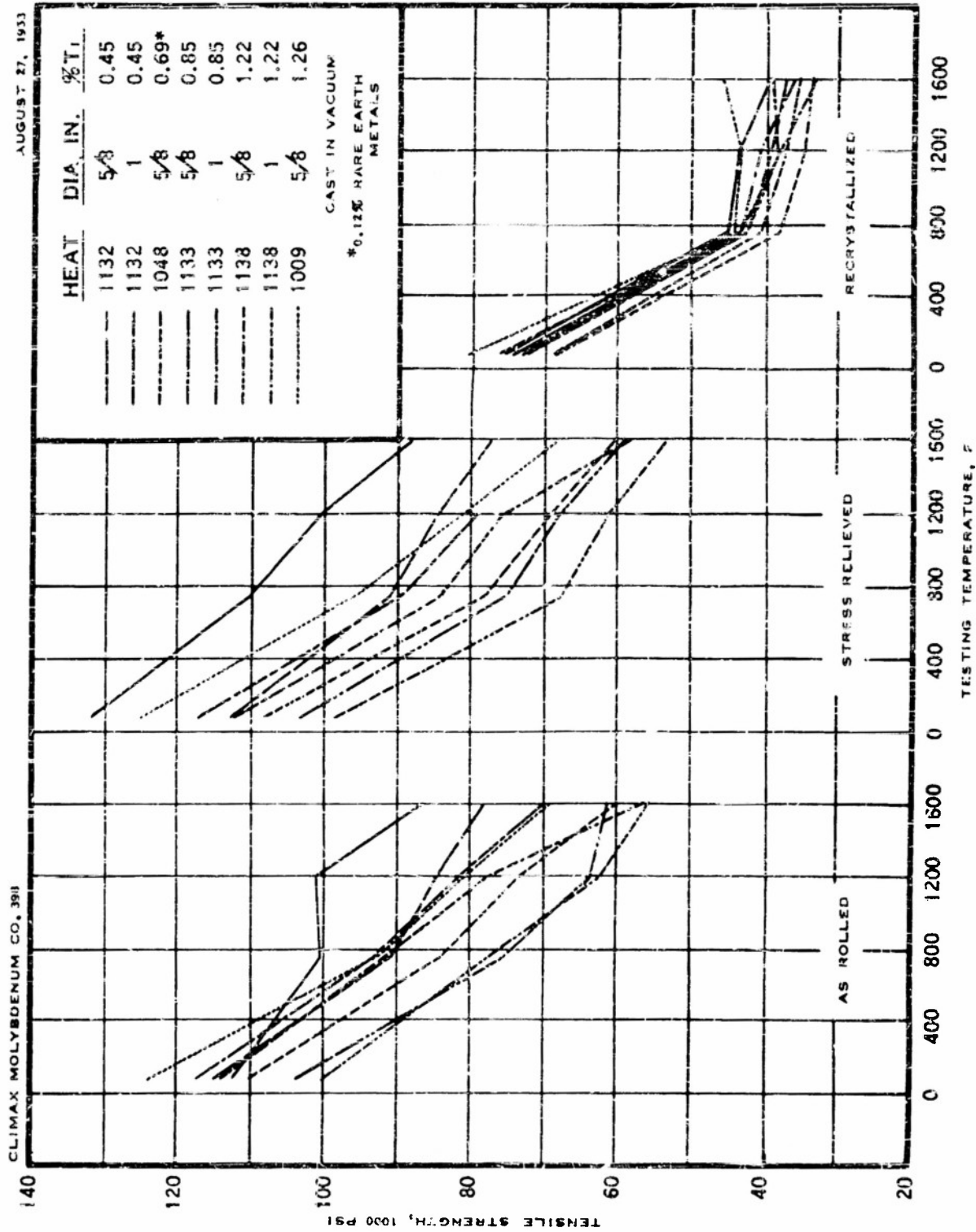


FIGURE C51— TENSILE STRENGTH OF MOLYBDENUM--TITANIUM ALLOY BARS

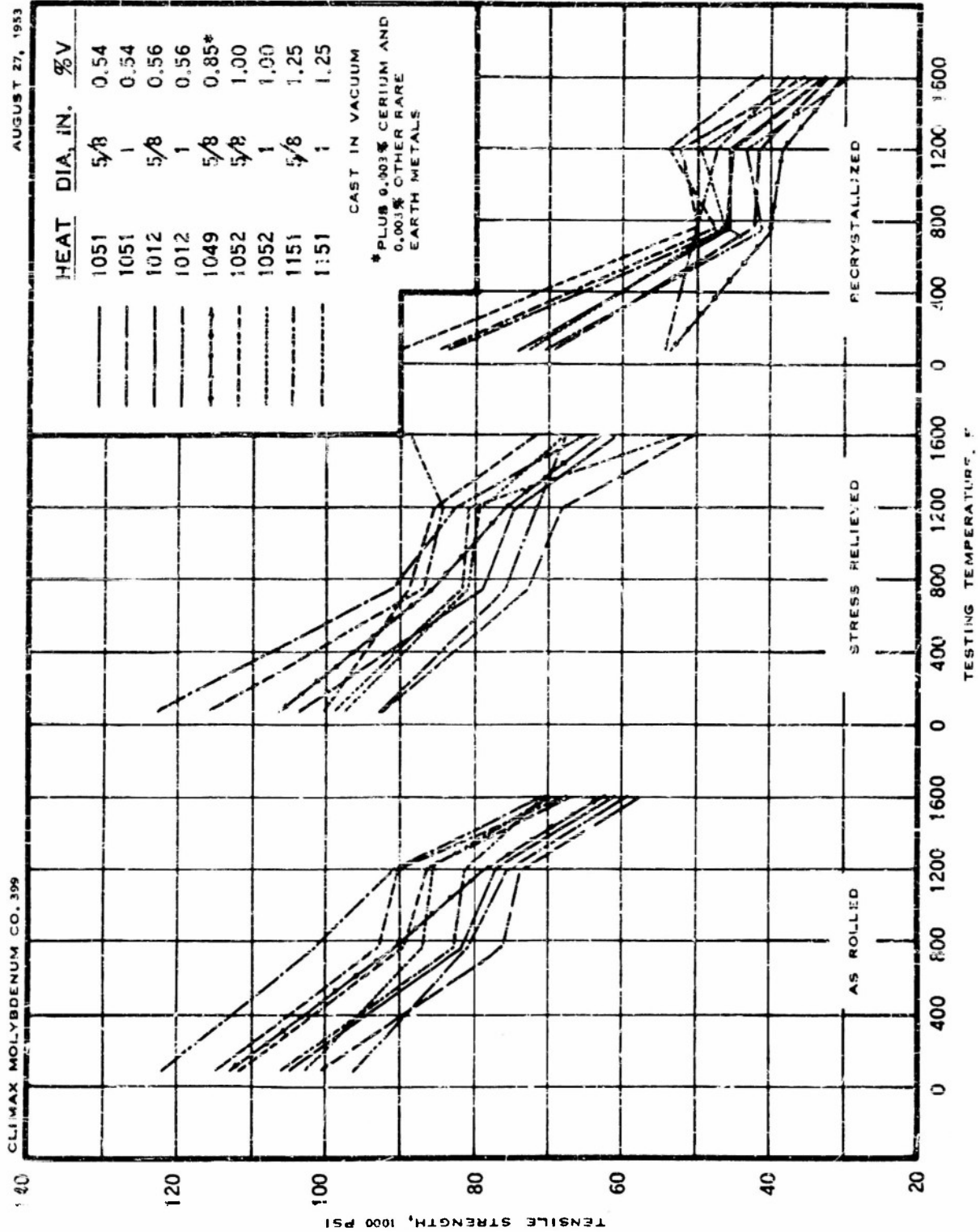


FIGURE C52— TENSILE STRENGTH OF MOLYBDENUM-VANADIUM ALLOY BARS

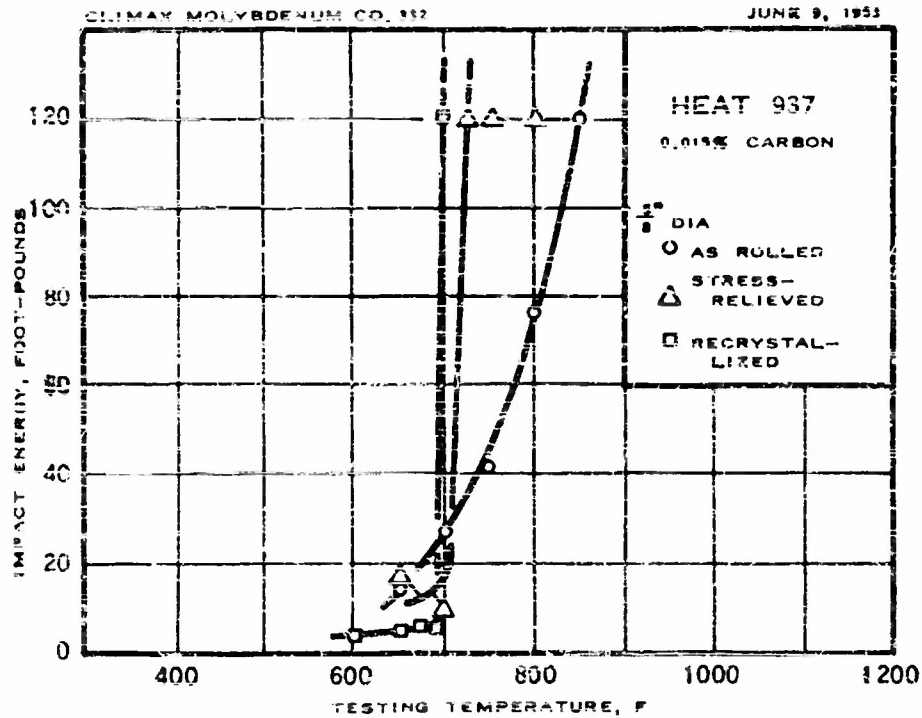


FIGURE C53 - IMPACT (V-NOTCH) TRANSITION FOR UNALLOYED MOLYBDENUM

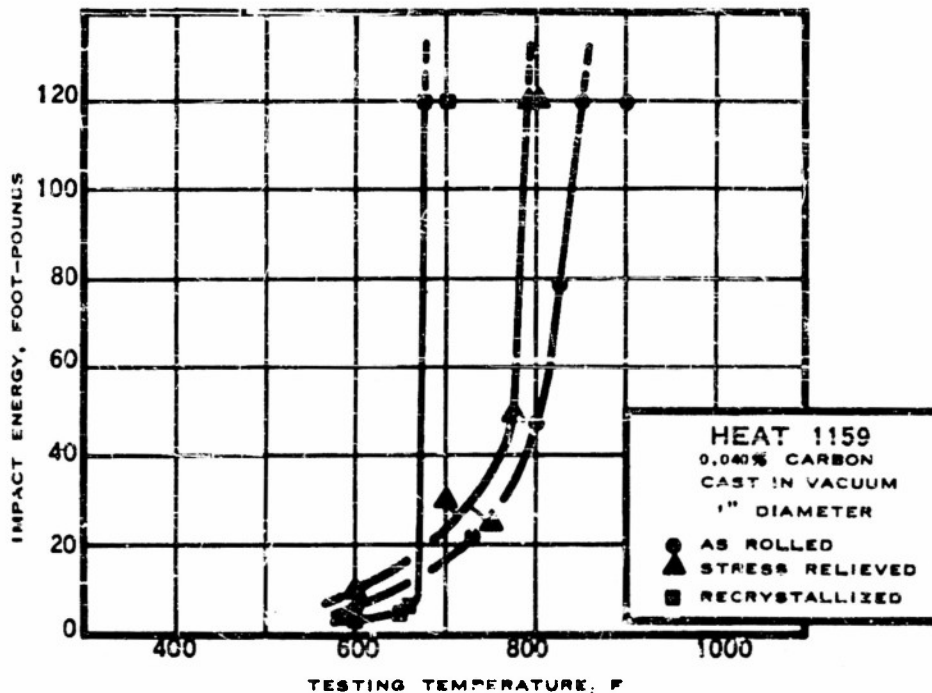


FIGURE C54- IMPACT (V-NOTCH) TRANSITION FOR UNALLOYED MOLYBDENUM

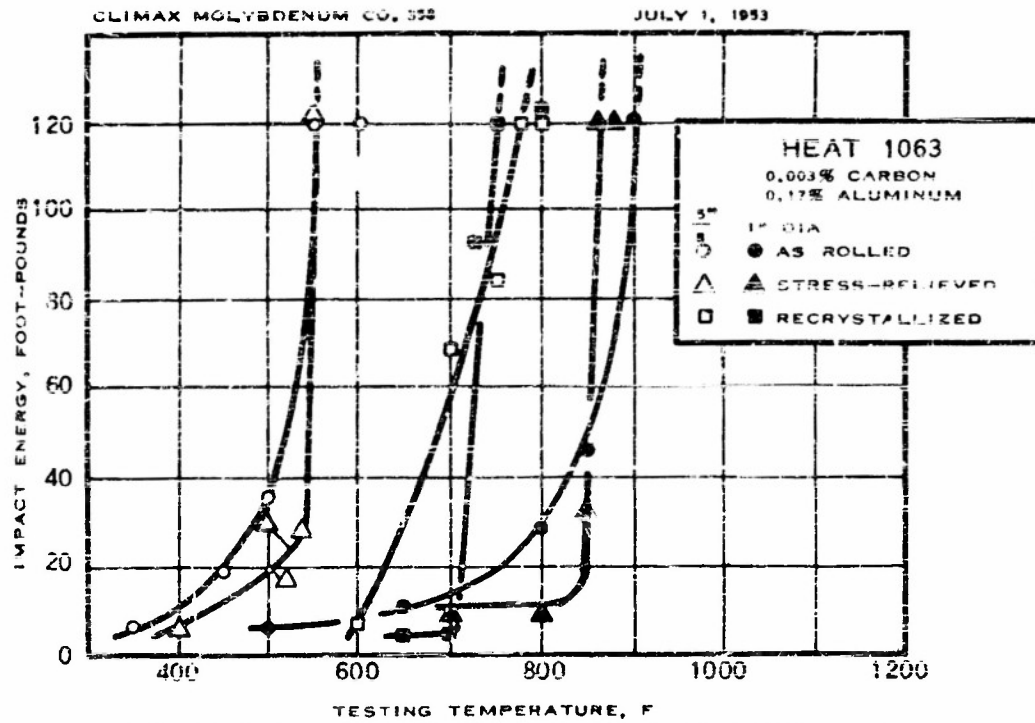


FIGURE C55 - IMPACT (V-NOTCH) TRANSITION FOR
0.17% ALUMINUM-MOLYBDENUM ALLOY

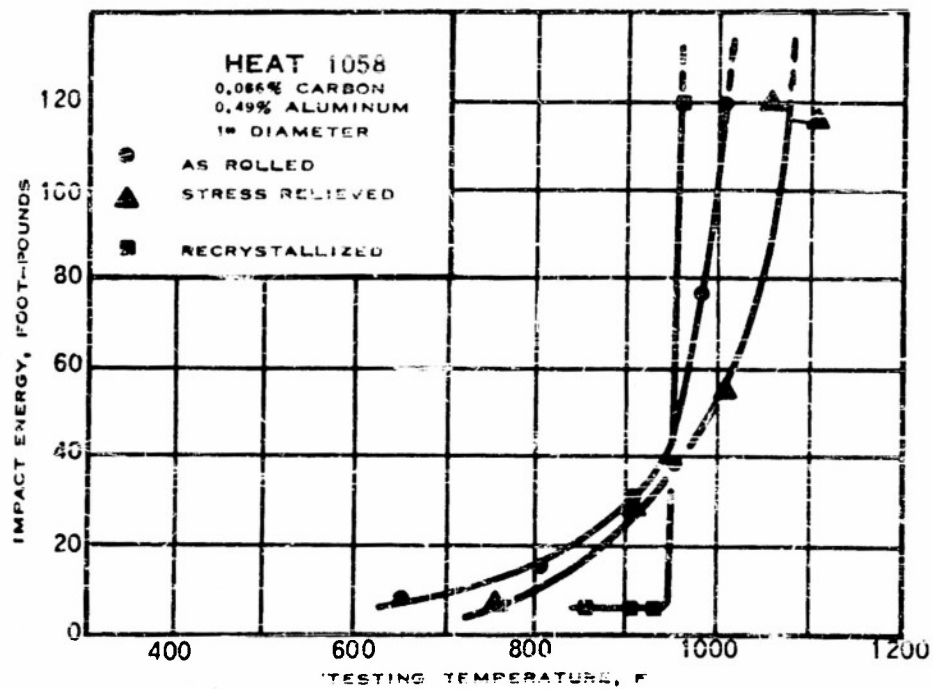


FIGURE C56 - IMPACT (V-NOTCH) TRANSITION FOR
0.49% ALUMINUM-MOLYBDENUM ALLOY

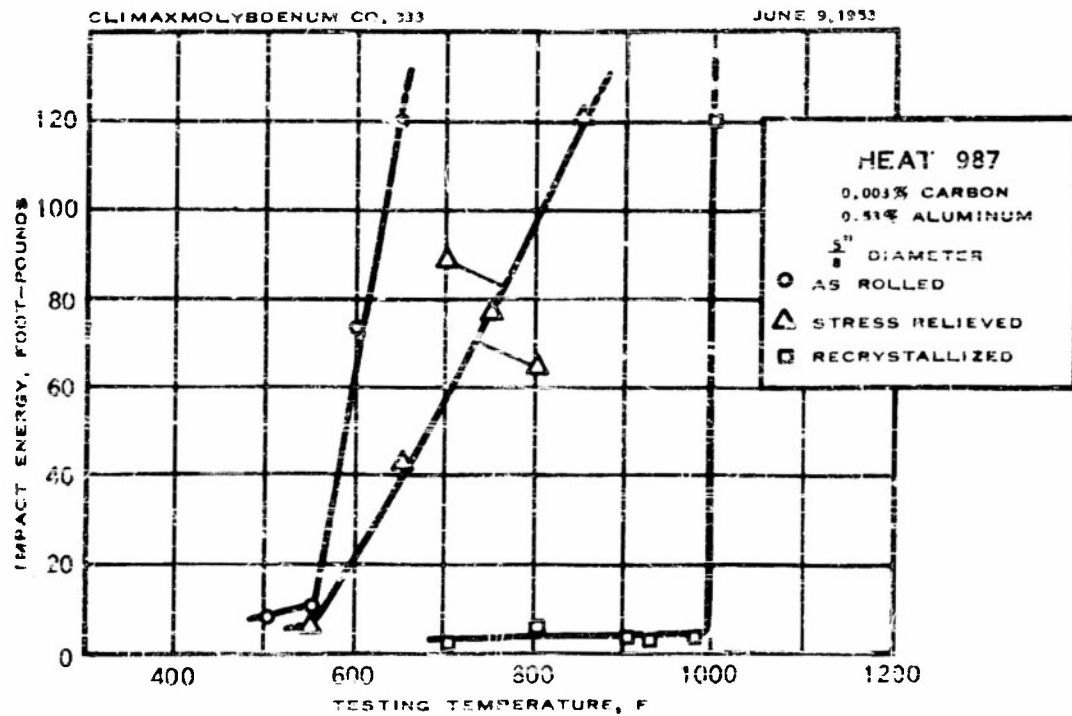


FIGURE C57 — IMPACT (V-NOTCH) TRANSITION FOR
 0.53% ALUMINUM—MOLYBDENUM ALLOY

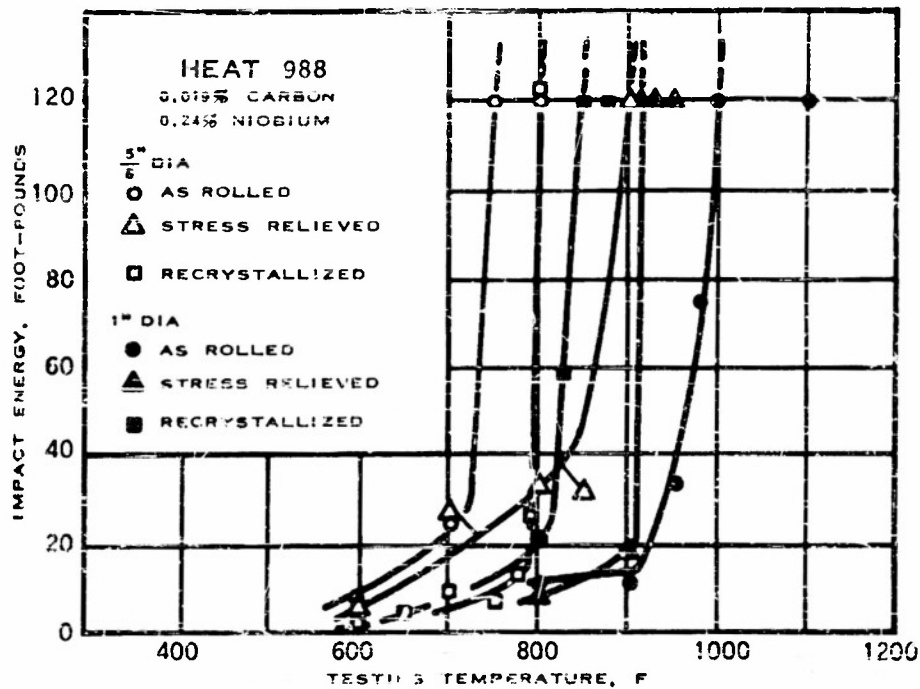


FIGURE C58 — IMPACT (V-NOTCH) TRANSITION FOR
 0.24% NIOBIUM—MOLYBDENUM ALLOY

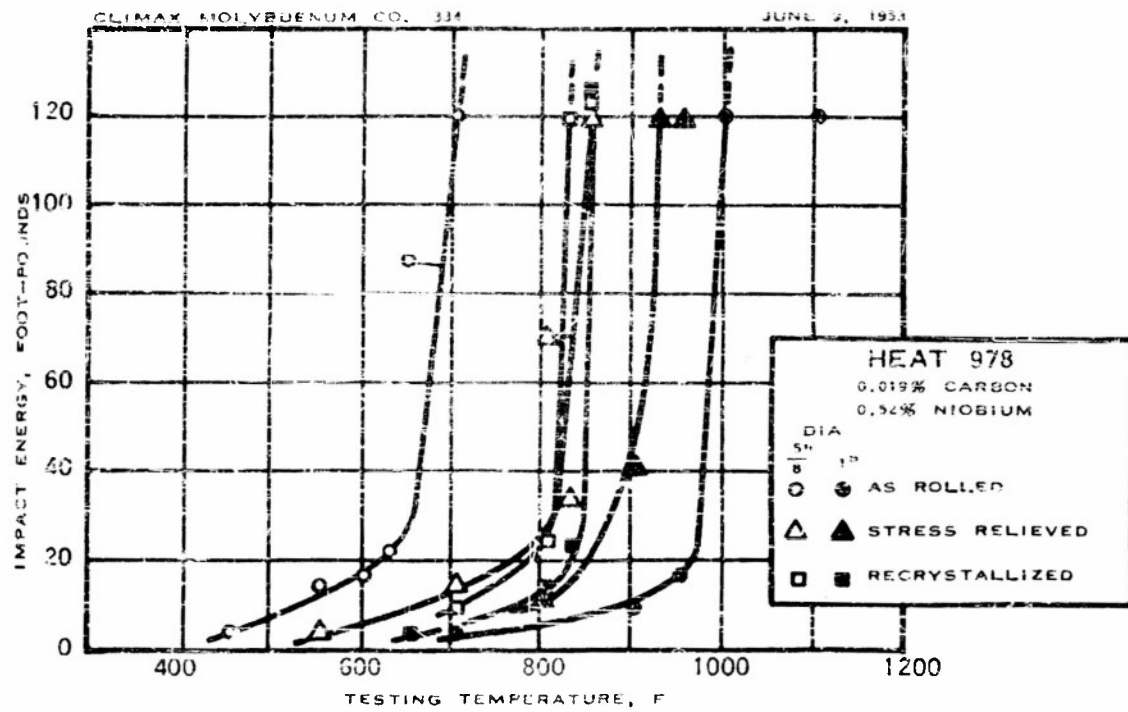


FIGURE C59 — IMPACT (V-NOTCH) TRANSITION FOR
0.52% NIOBIUM — MOLYBDENUM ALLOY

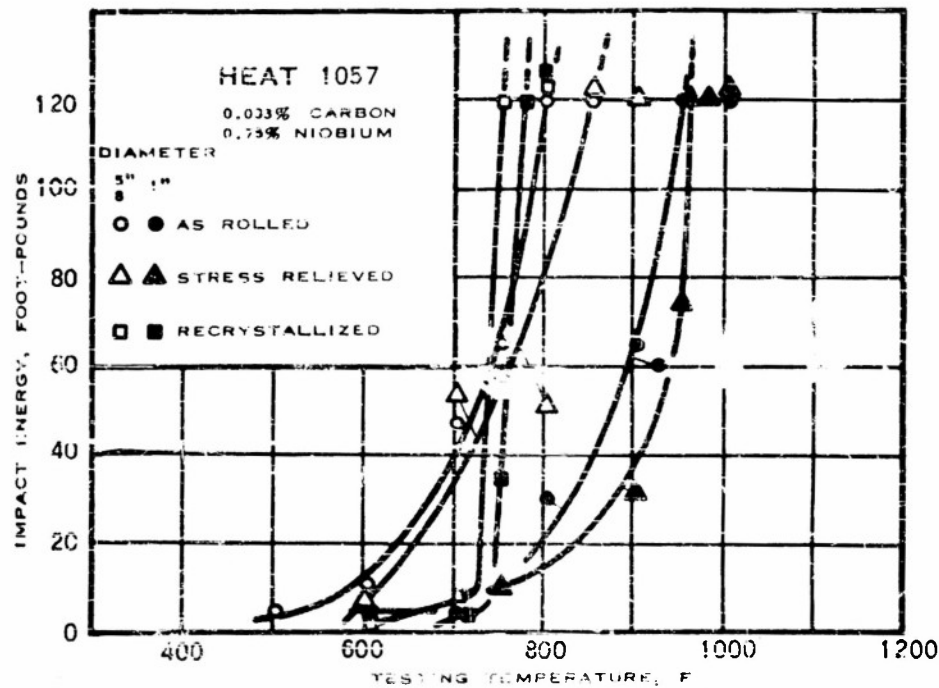


FIGURE C60 — IMPACT (V-NOTCH) TRANSITION FOR
0.75% NIOBIUM — MOLYBDENUM ALLOY

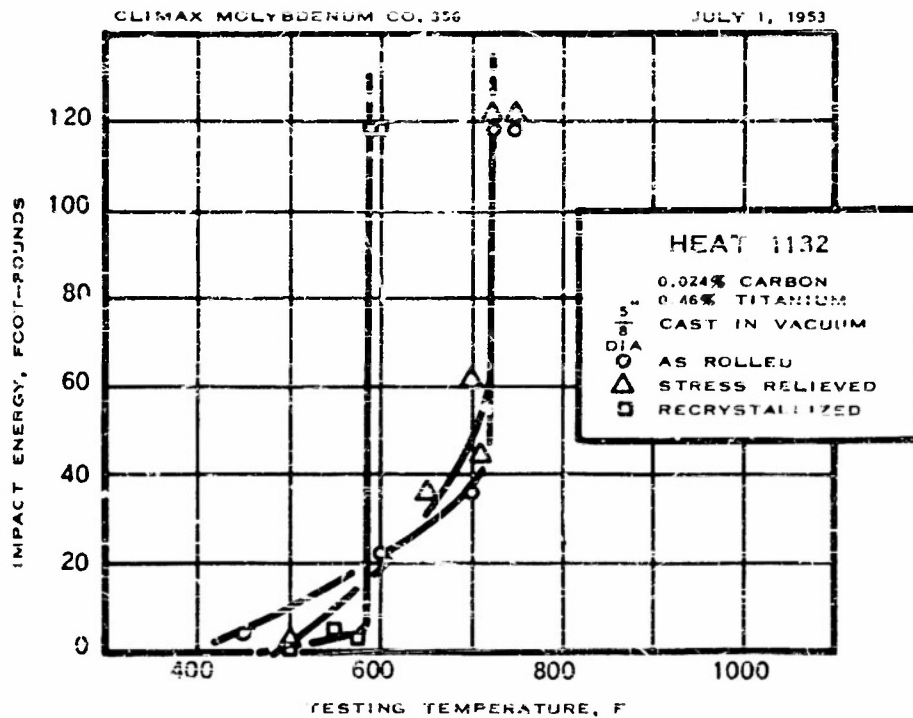


FIGURE C61 — IMPACT (V-NOTCH) TRANSITION FOR
0.46% TITANIUM-MOLYBDENUM ALLOY

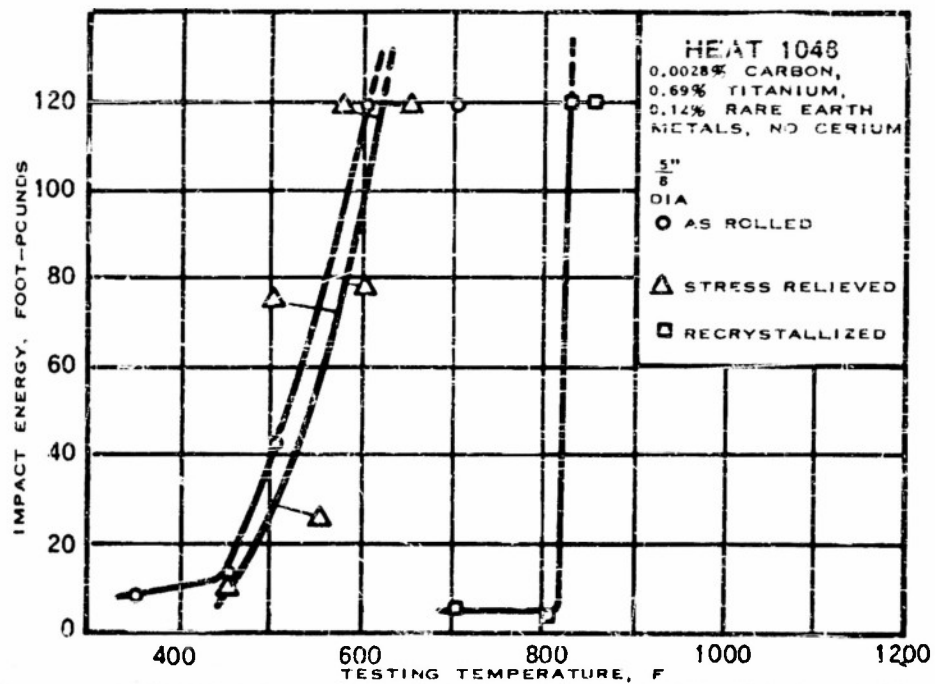


FIGURE C62 — IMPACT (V-NOTCH) TRANSITION FOR
0.69% TITANIUM-MOLYBDENUM ALLOY

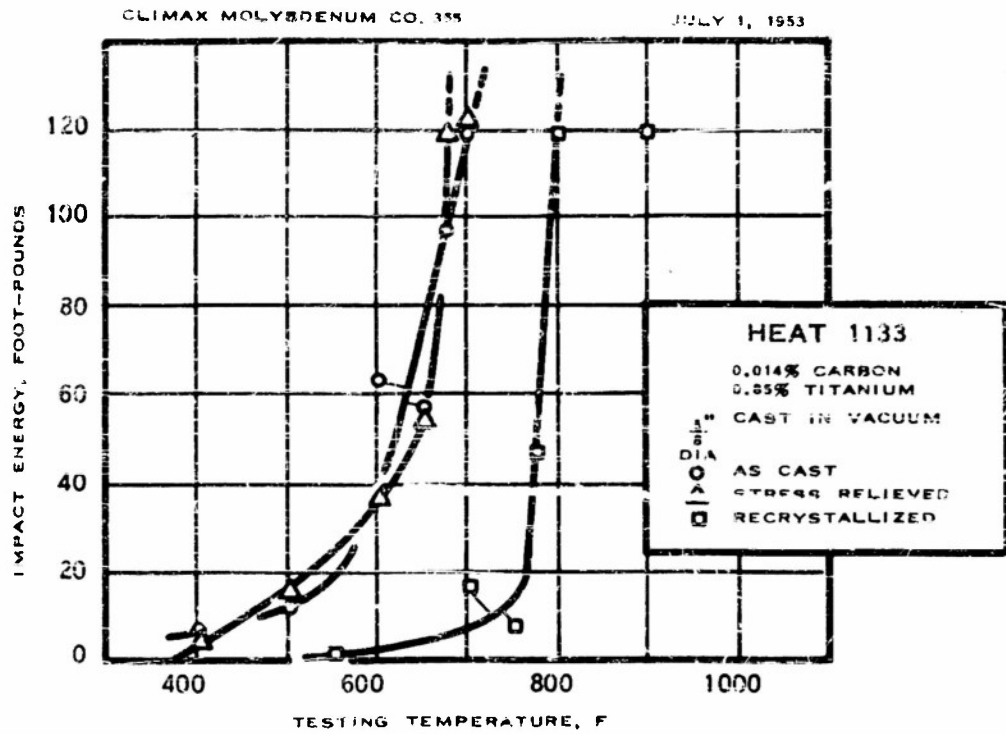


FIGURE C63— IMPACT (V-NOTCH) TRANSITION FOR
0.85% TITANIUM—MOLYBDENUM ALLOY

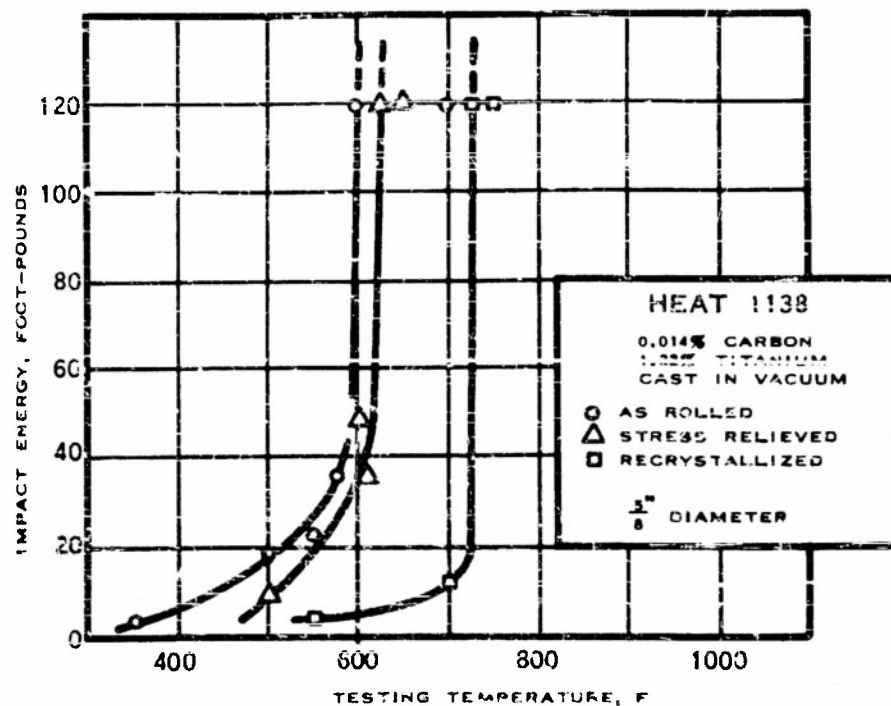


FIGURE C64— IMPACT (V-NOTCH) TRANSITION FOR
1.22% TITANIUM—MOLYBDENUM ALLOY

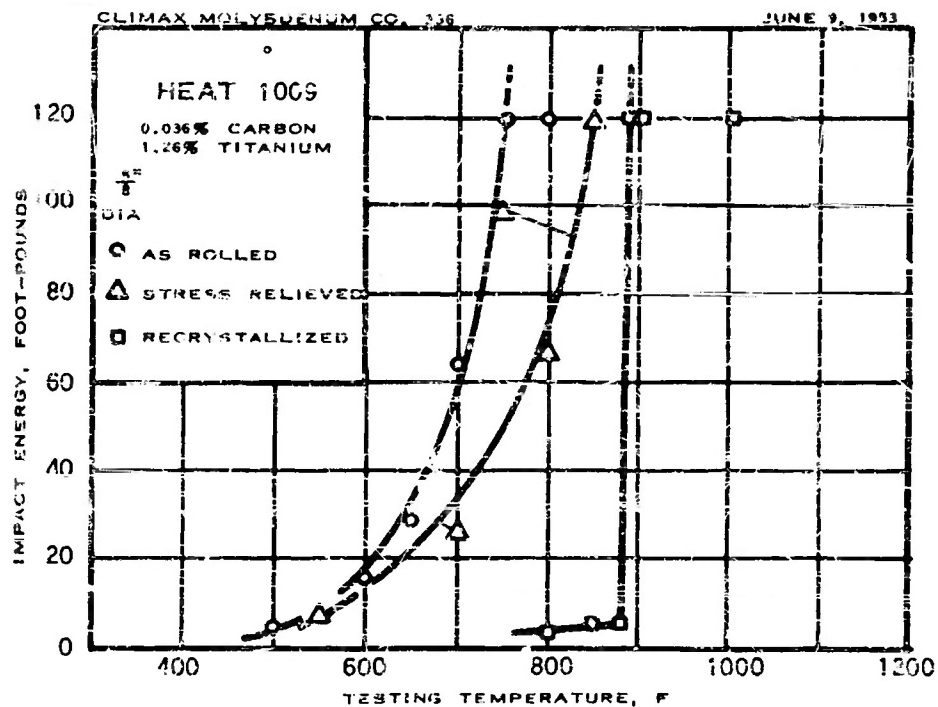


FIGURE C65— IMPACT (V-NOTCH) TRANSITION FOR
1.26% TITANIUM-MOLYBDENUM ALLOY

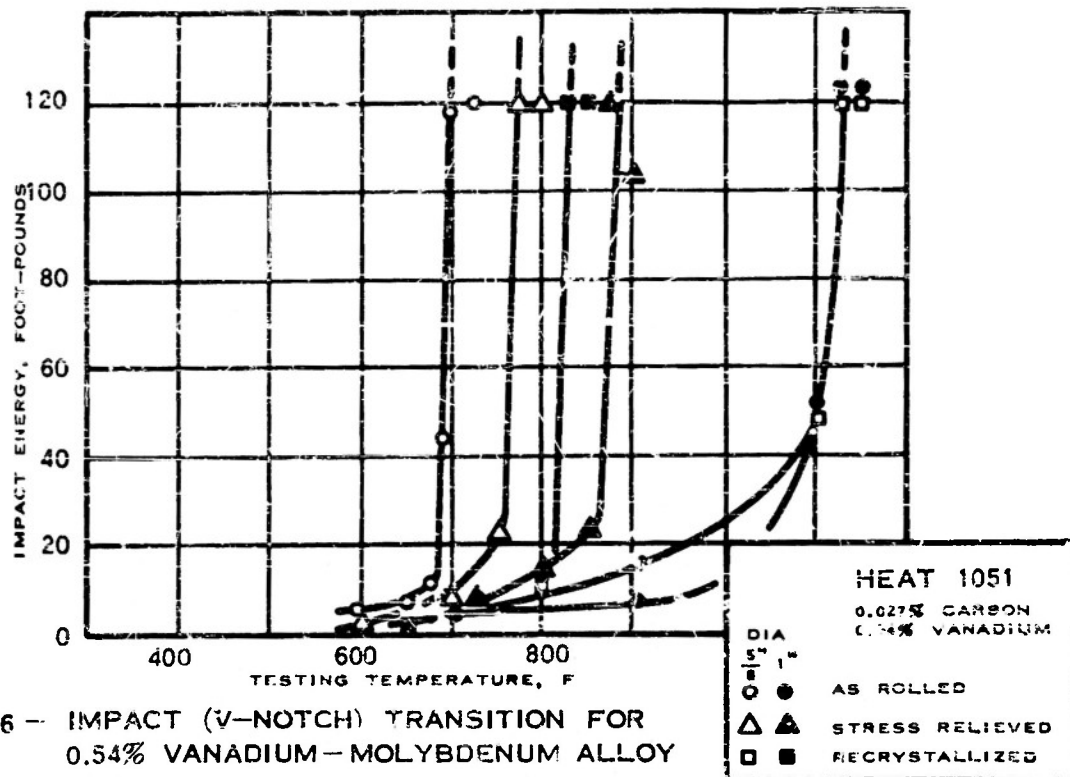


FIGURE C66 — IMPACT (V-NOTCH) TRANSITION FOR
0.54% VANADIUM-MOLYBDENUM ALLOY

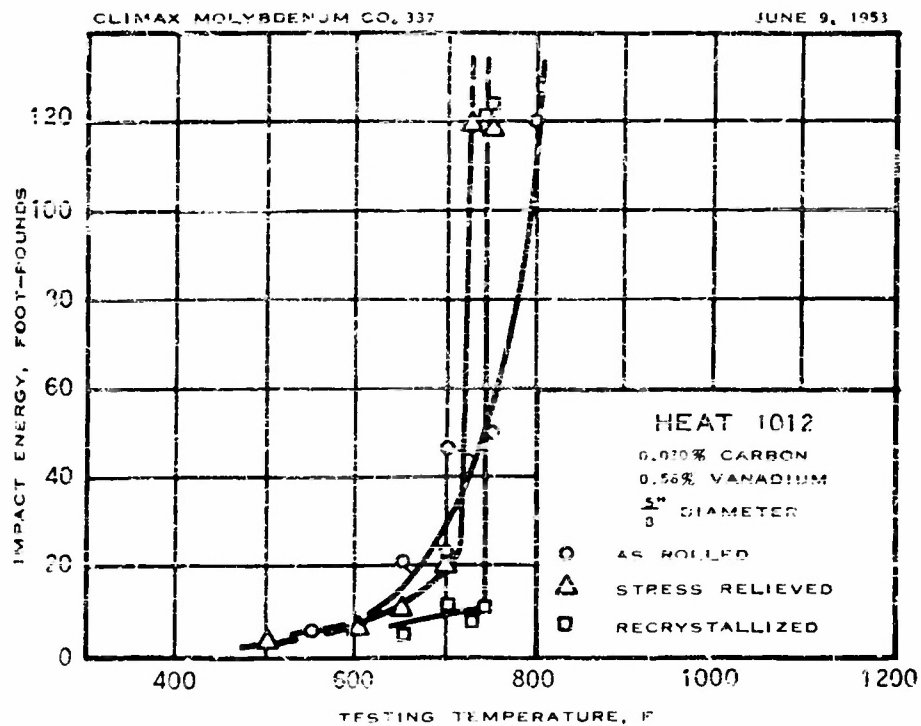


FIGURE C67—IMPACT (V-NOTCH) TRANSITION FOR
0.56% VANADIUM—MOLYBDENUM ALLOY

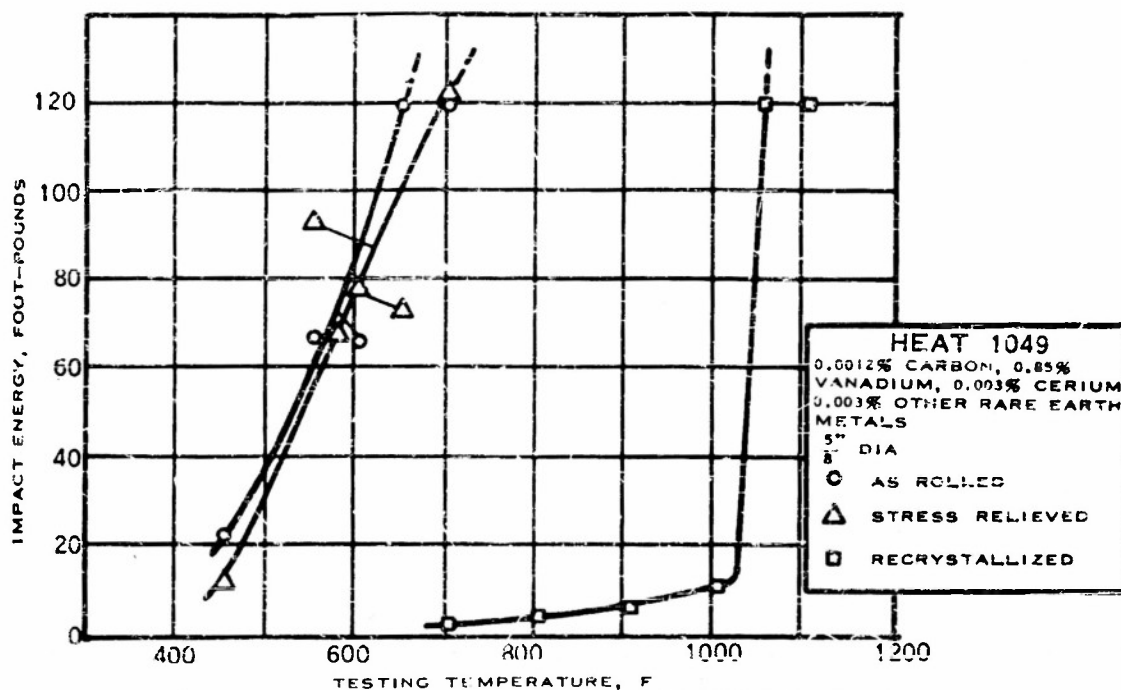


FIGURE C68—IMPACT (V-NOTCH) TRANSITION FOR
0.85% VANADIUM—MOLYBDENUM ALLOY

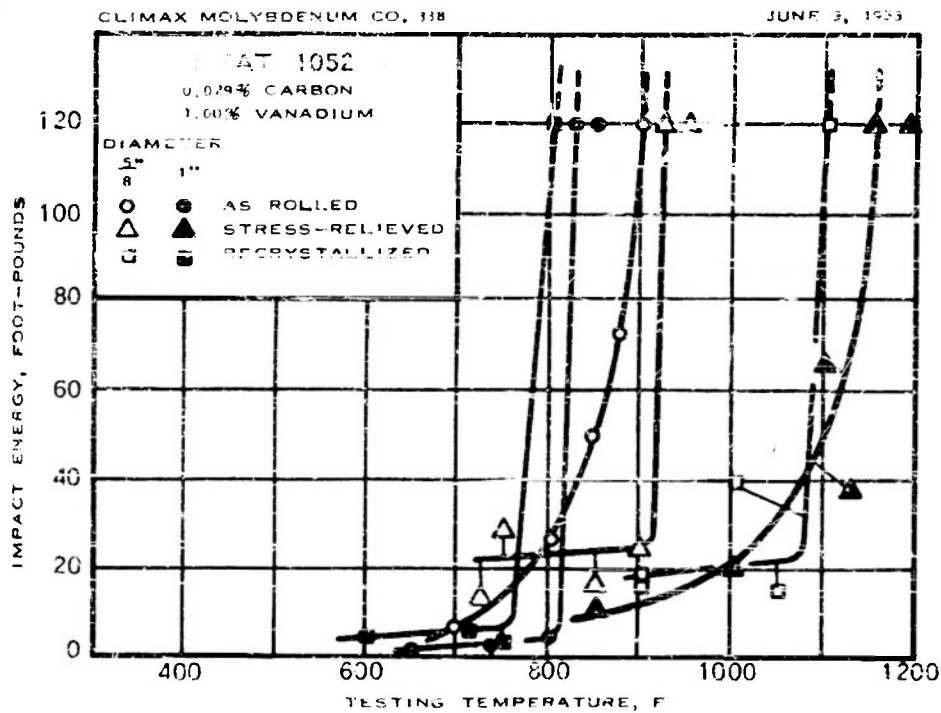


FIGURE C69 - IMPACT (V-NOTCH) TRANSITION FOR
1.00% VANADIUM--MOLYBDENUM ALLOY

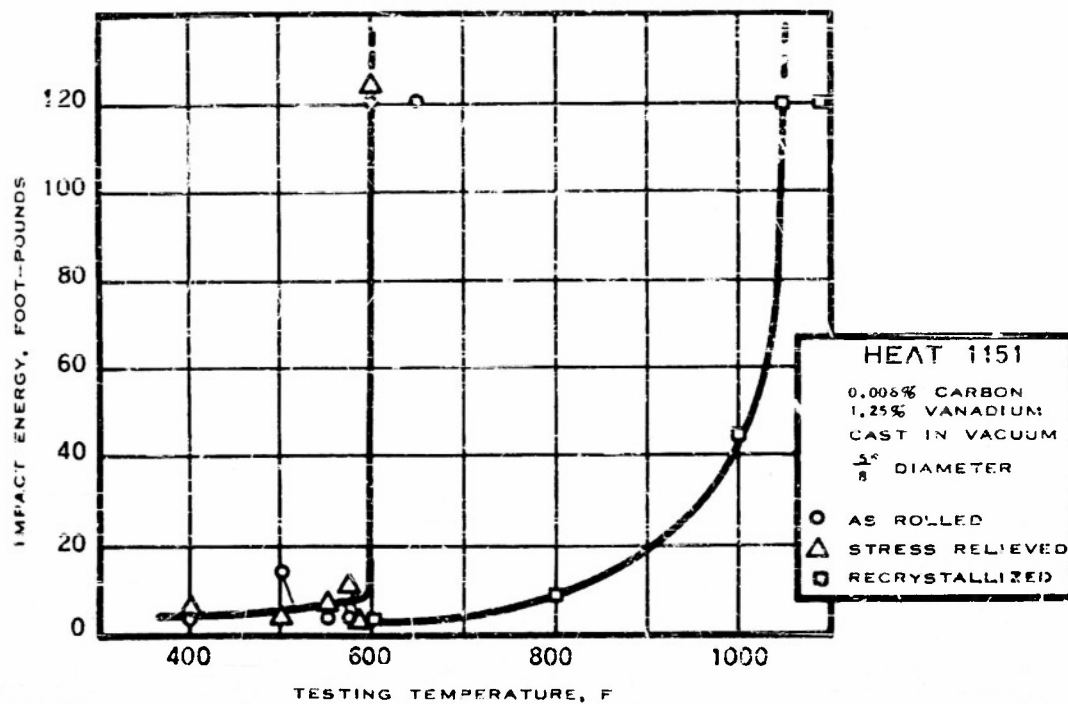


FIGURE C70 - IMPACT (V-NOTCH) TRANSITION FOR
1.25% VANADIUM--MOLYBDENUM ALLOY

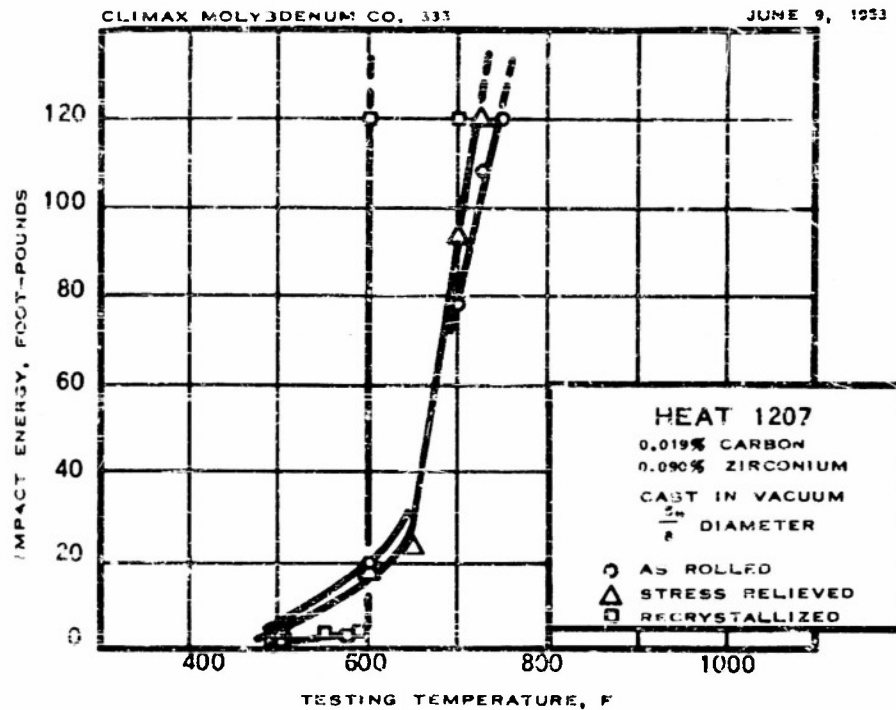


FIGURE C71— IMPACT (V-NOTCH) TRANSITION FOR
 0.090% ZIRCONIUM—MOLYBDENUM ALLOY

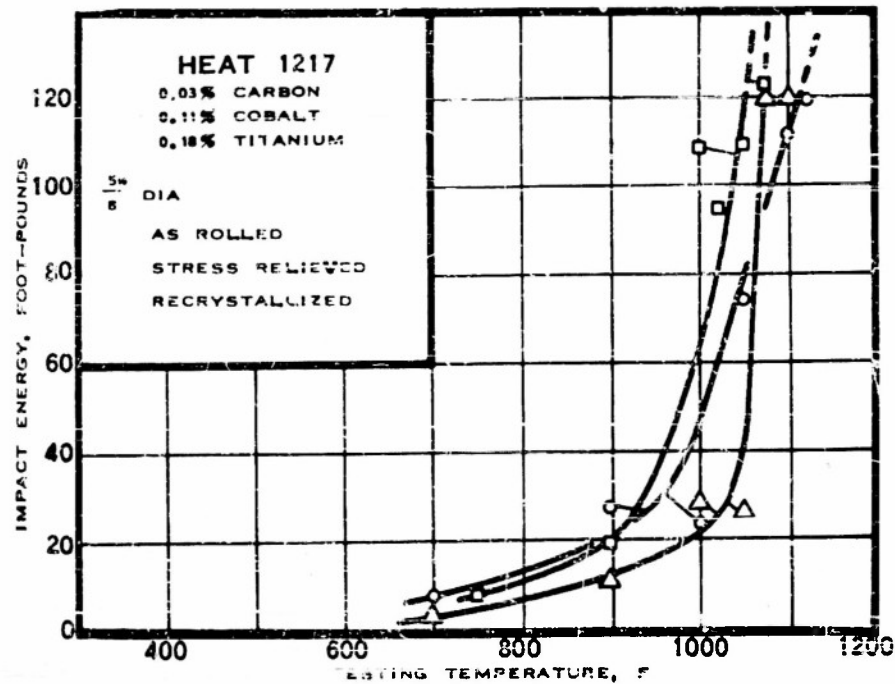


FIGURE C72— IMPACT (V-NOTCH) TRANSITION FOR
 0.11% COBALT—0.18% TITANIUM—
 MOLYBDENUM ALLOY

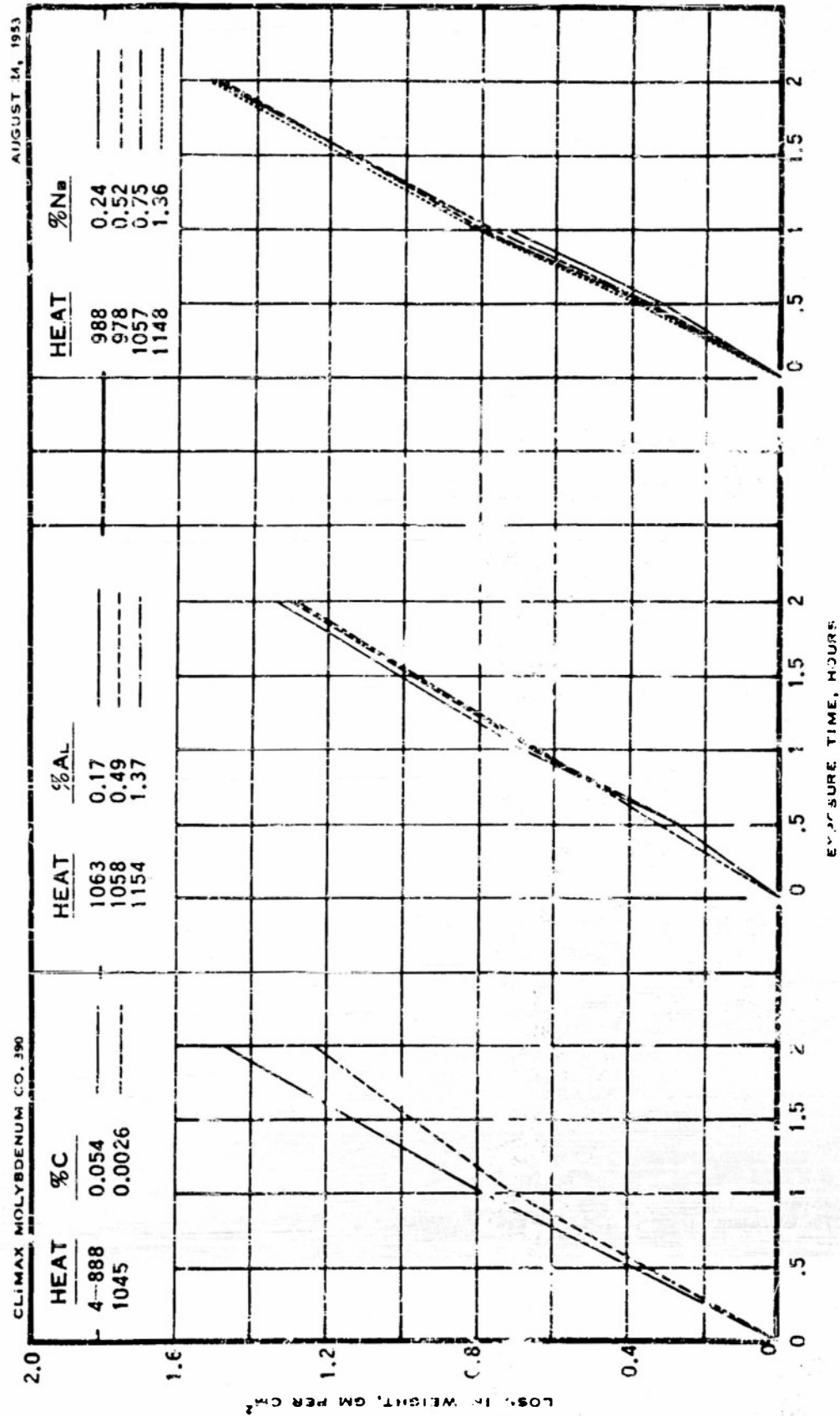


FIGURE C74 - OXIDATION OF UNALLOYED MOLYBDENUM, MOLYBDENUM-ALUMINUM,
AND MOLYBDENUM-NIOBIUM ALLOYS AT 1750 °F IN MOVING AIR

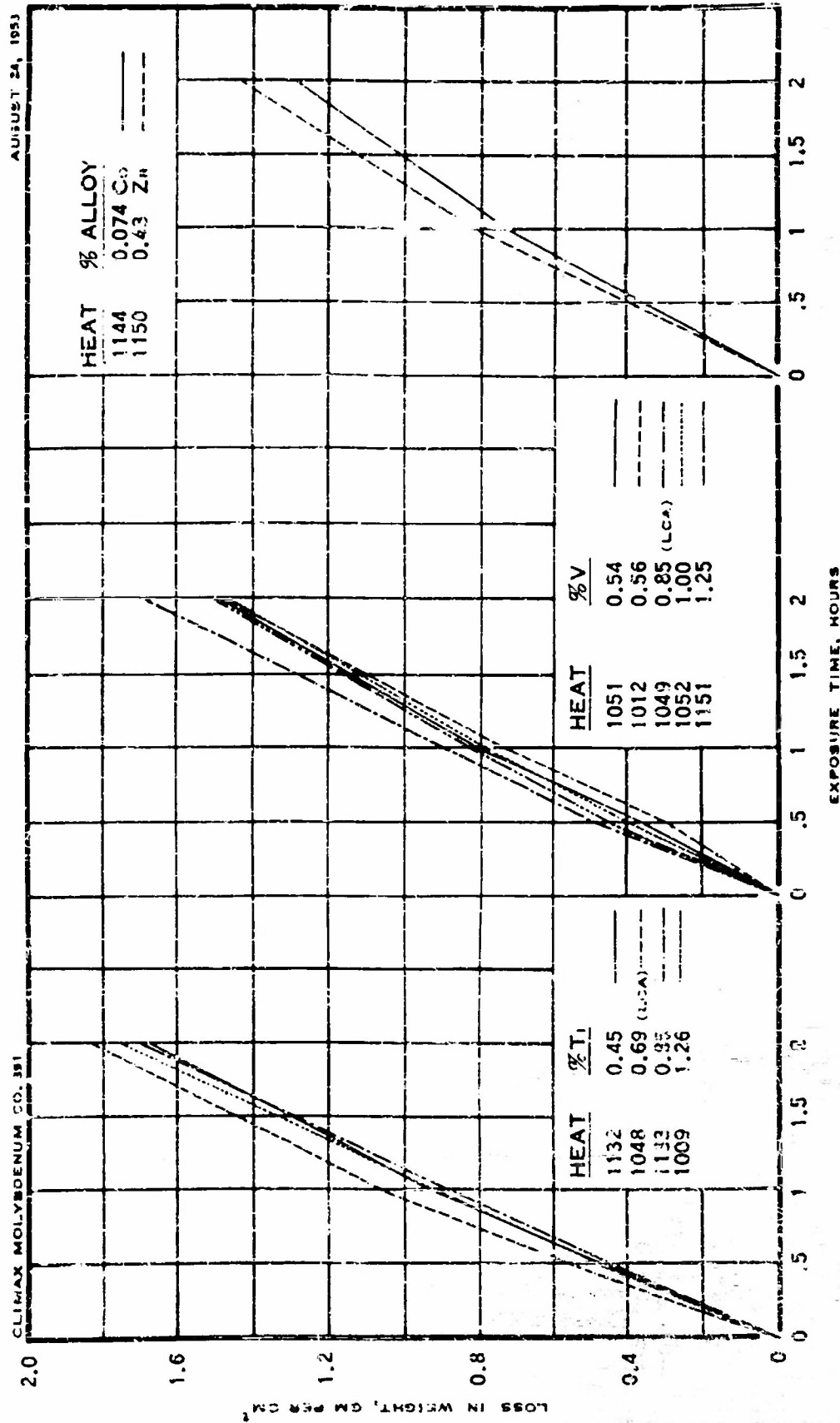


FIGURE C75 -- OXIDATION OF MOLYBDENUM-TITANIUM, MOLYBDENUM-VANADIUM, MOLYBDENUM-COBALT, AND MOLYBDENUM-ZIRCONIUM ALLOYS AT 1750 F IN MOVING AIR